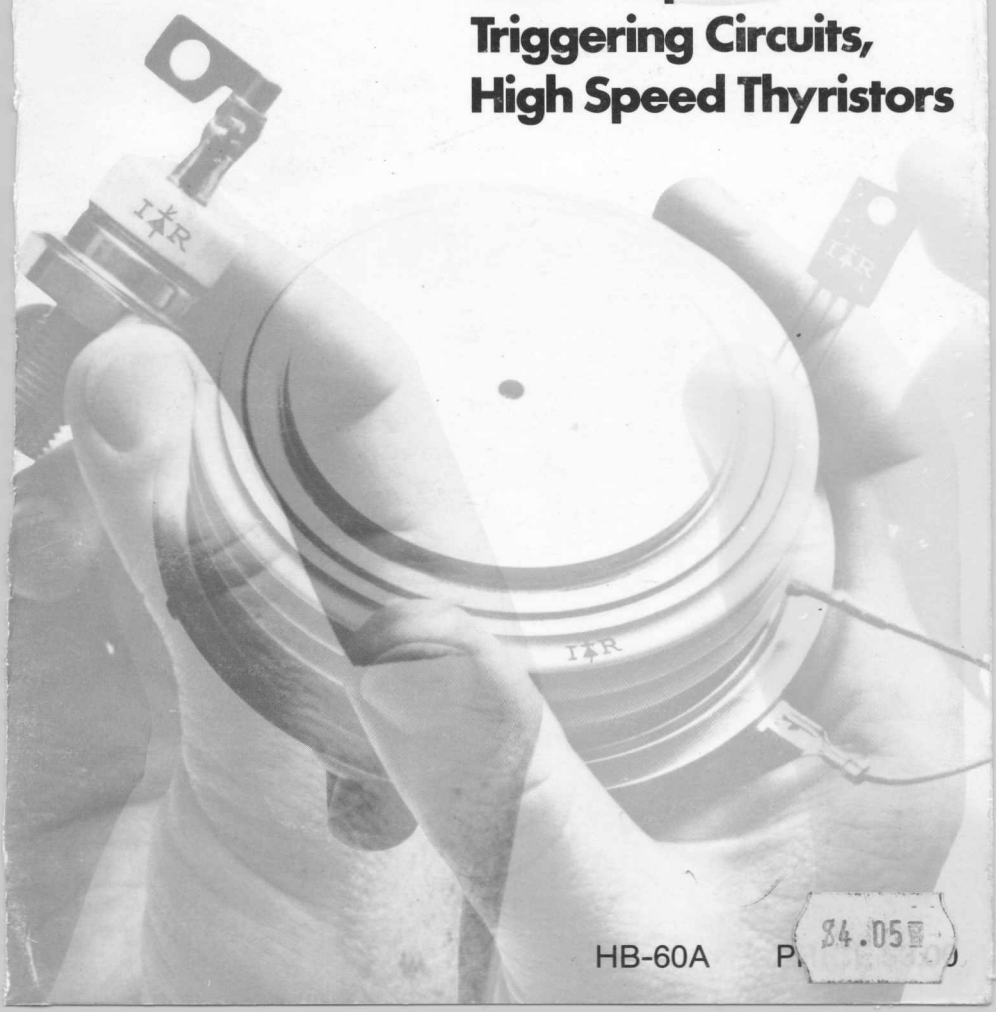


84.05

SCR applications handbook

New chapters on:
Triggering Circuits,
High Speed Thyristors



HB-60A

P 84.05

SCR Applications Handbook

Edited by
Dr. Richard G. Hoft
Professor of Electrical Engineering
University of Missouri at Columbia

Contributors: The Engineering Staff of International Rectifier

Bryan Bixby
David Borst
Larry Carver
Arthur Connolly

F.W. Parrish
Ralph Rosa

David Cooper
Frank Durnya
John Gault
M. Frank Gift

1st Printing; September 1974
2nd Printing, December 1977

ACKNOWLEDGEMENTS

This handbook is the result of the efforts of a dedicated group of engineers. Not only those at International Rectifier, but also in numerous laboratories and factories throughout the world — a group of people we commonly refer to as our customers. Without our customers, the insight into the broad range of applications discussed in this book would be impossible.

Although this handbook is primarily intended for circuit and systems engineers, we hope it will also be found useful by educators, students and others interested in the use of semiconductor devices.

Information furnished in this Applications Handbook is believed to be accurate and reliable. However, International Rectifier can assume no responsibility for its use; nor any infringement of patents, or other rights of third parties which may result from its use. No license is granted by implication or other use under any patent or patent rights of International Rectifier. No patent liability shall be incurred for the use of the circuits or devices described herein.

Copyright, International Rectifier Corp., Semiconductor Division, El Segundo, California, 1977. All Rights Reserved.

Contents

PREFACE	State of the Art	5
CHAPTER 1	DEVICE CHARACTERISTICS	27
	Reverse Blocking Triode Thyristor-SCR	27
	Bidirectional Triode Thyristor—Triac	82
	Hockey-Puk SCRs	90
	Passivated Assembled Circuit Elements	
	PACE/paks	95
	General Application Hints	102
CHAPTER 2	PARALLEL OPERATION	113
	Important Characteristics	113
	Turn-On Sensitivity and Delay Time	114
	Finger Voltage	123
	Latching and Holding Current	125
	Steady-State Condition	125
	Loop Inductance	126
CHAPTER 3	SERIES OPERATION	131
	Equalization	131
	Triggering Series-Operated SCRs	138
CHAPTER 4	AC PHASE CONTROL	149
	Phase Control Circuits	149
	Heater Control Circuits	167
	Ferroresonant Transformer Regulated AC	
	Power Supply	182
	Motor Control Circuits	193
	Welding Service Circuits	195
CHAPTER 5	SOLID-STATE RELAYS AND CONTRACTORS	203
	Solid-State Relays	203
	Solid-State Contactors	210
	Solid-State Switches	213
	Aircraft Power System	218
CHAPTER 6	DC POWER CONVERSION	231
	Biphase Circuits	231
	Single-Phase, Half-Wave Circuits	236
	Polyphase Rectifier Circuits	238
	Hybrid Circuits	241
	Triggering Pulses for Bridge Circuits	243
	DC Motor Drives	244
	Triac Reversing Drives	248
	PACE/pak Power Controls	250
CHAPTER 7	LINE-COMMUTATED INVERTERS	257
	Regenerative Phase-Controlled Rectifiers	257
	Brushless Motor Drives	262
	Cycloconverters	267

CHAPTER 8	FORCE-COMMUTATED INVERTERS	283
	Basic Circuits	283
	Frequency Multiplier	293
	DC Power Supplies	293
	Induction Heating Supply	301
	Variable Frequency Motor Drives	307
CHAPTER 9	CHOPPERS	313
	Switching Principles	313
	Commutation Circuits	315
	DC Motor Drives	320
	Battery Charger Design Example	339
CHAPTER 10	FAST RECOVERY DIODES	345
	High-Frequency Power Rectification	345
	Recovery Characteristics	349
	Schottky Barrier Diodes	359
CHAPTER 11	PROTECTION	367
	Protecting with Fuses	367
	Protecting by Limiting Peak Junction Temperature	384
CHAPTER 12	COOLING	393
	Thermal Considerations for Stud-Mounted Devices	393
	Thermal Considerations for Hockey-Puk Devices	397
	Cooling for Specific Applications	402
	Oil-Immersed Cooling	403
CHAPTER 13	TESTING	409
	Parameter 1: Blocking Voltage	409
	Parameter 2: On-State Voltage	411
	Parameter 3: DC Triggering Characteristics	414
	Parameter 4: Holding Current	416
	Parameter 5: Latching Current	422
	Parameter 6: Turn-On Time	428
	Parameter 7: Turn-On-Voltage	428
	Parameter 8: Turn-Off Time	429
	Parameter 9: Critical dv/dt	443
	Parameter 10: Critical di/dt	448
	Parameter 11: Thermal Resistance	450
	Testing Power Triacs	453
	Triggering Circuits	462
CHAPTER 14	TRIGGERING CIRCUITS	471
CHAPTER 15	HIGH SPEED THYRISTORS	481
APPENDIX I	SYMBOLS AND TERMS	489
APPENDIX II	DEVICE SPECIFICATIONS	501
APPENDIX III	CROSS REFERENCE	531
INDEX		543

State of the Art

A new era in electric power conversion began with the development of the silicon controlled rectifier (SCR) in late 1957. From the first 16 ampere average current rated unit, an entirely new family of semiconductor devices was created. Thyristors are now available with current ratings from milliamperes to over a thousand amperes and with voltage ratings up to 2,600 volts. It is estimated that nearly one thousand domestic manufacturers use thyristor devices.

A large number of disc type (hockey-puk) SCRs are manufactured; high dv/dt and di/dt devices with fast turn-off are available for inverter applications; many plastic packages are being produced; and several manufacturers provide unpackaged SCRs and triacs in chip form. The continuing developments in both linear and digital integrated circuit components have made very complex thyristor gating and control circuits much more feasible. International Rectifier now has a line of SCR devices rated up to 2,500 amperes RMS. These devices are produced in a wide variety of packages including plastic, press-fit, conventional stud-mounted, and hockey-puk.

The triac is widely used for ac voltage control. Although the majority of these bi-directional triode thyristors are rated at or below 40 amperes and at voltages up to 600 volts, International Rectifier produces 60, 100 and 200 ampere devices rated up to 1,000 volts.

The first thyristor applications involved simple phase control for lamp dimmers, heat controls, and ac motor voltage controls. As a wider range of triacs became available, they replaced the SCR in most of these applications. More advanced phase control circuits were pursued next including reversing dc motor drives with inversion to the ac system for regenerative braking of up to 6000 hp armature controlled motors for large mill drives.

A great variety of sophisticated static power conversion equipment is now being produced, ranging from small appliance controls to variable frequency 100 hp ac drives for a wide range of industrial applications.

In an electric power control system, the power converter is the critical link for matching the source to the load. The characteristics of both the source and the load and often the electrical and ambient environment determine the duty on the converter. It falls upon the circuit designer to choose the proper circuit arrangement for the specific application. However, he is often constrained by the capability of the available power switching devices. Recently, this device capability has become the major factor in determining the size and efficiency of a converter circuit, hence the optimum arrangement for the required duty. The most recent developments in thyristor characteristics have been to make this limiting factor in power system design less restrictive.

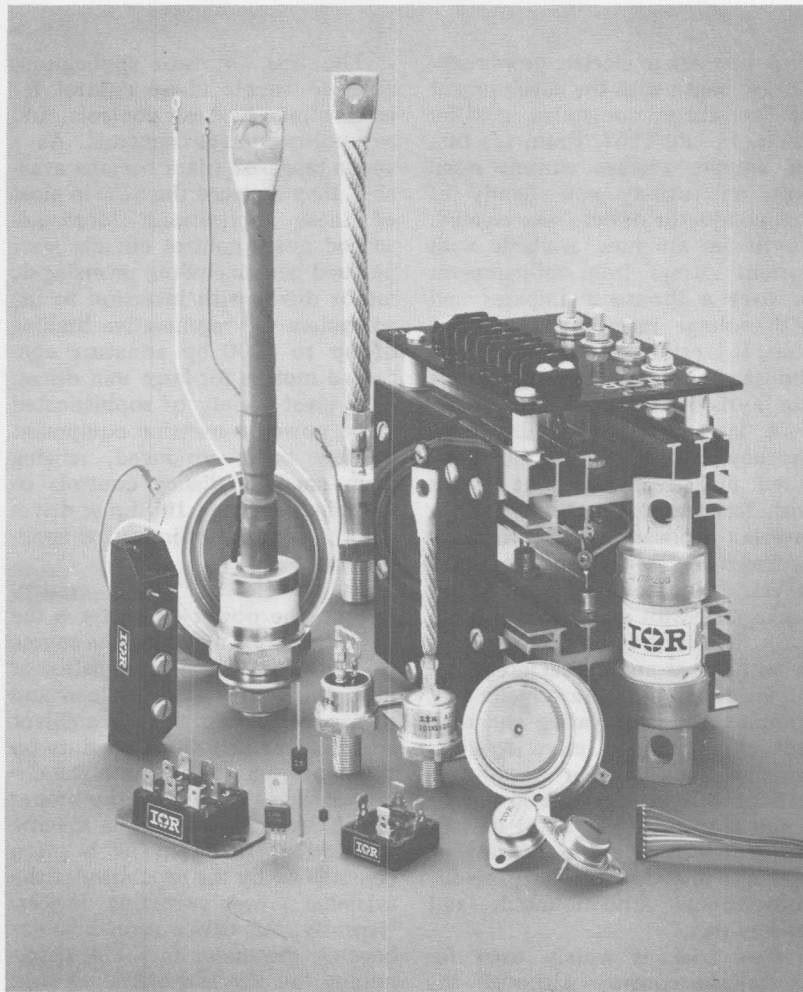


Figure 1. The International Rectifier thyristor line includes SCR devices rated from 1.6 amperes to 2,500 amperes of RMS current, peak reverse voltage ratings ranging from 50 to 1,700 volts, as well as power logic triacs, passivated assembled circuit elements, (PACE/paks), power assemblies and a wide variety of heat exchangers and mounting hardware.

The choice of power conversion systems can be divided into the four main categories shown in Figure 2. Figure 2(a) shows a dc source feeding a dc chopper which, in turn, converts the power and regulates it through a dc load. Figure 2(b) consists of an alternating current generator acting as a source for a cycloconverter. The load can require from the cycloconverter variable frequency and/or variable volt-seconds. Figure 2(c) shows a dc source feeding an inverter which feeds either an ac variable frequency load or a dc variable volt-second load. In this case the inverter may or may not be preceded by a variable dc source, depending upon the requirements of the load and the type of inverter used. The fourth system (Figure 2(d)) is the familiar alternating current generator phase controlled converter which could

instead be a zero cross-over voltage triggered, pulse burst modulated system feeding a dc load. The cycloconverter is a special case of this system. A fifth category is forced commutated cycloconverters. This type of system combines the requirements of a cycloconverter and some classes of inverter so that the characteristics required of the switching device in this type of application can be derived from the other categories.

The three most critical applications are the dc chopper with time-ratio control, the cycloconverter of a polyphase variety, and the inverter, whether in the chopping or pulse-modulated mode or in the alternating mode. In general, the dynamic requirements of the device in a cycloconverter application are greatly dependent upon high operating frequency. In other systems

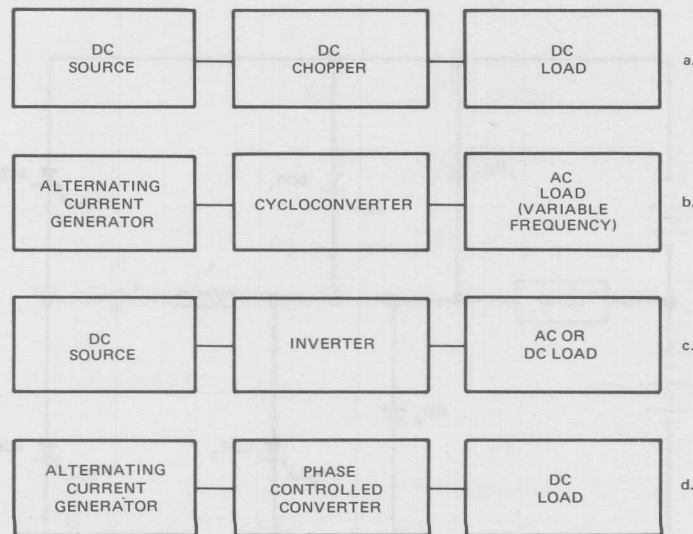


Figure 2. Four Basic Power Conversion Systems

this frequency is low, as in the alternating inverter. In both of these cases, neither the di/dt nor the dv/dt becomes an extreme limiting factor in the application of the device. In extreme cases where, for instance, a cycloconverter is employed as a variable speed, constant frequency drive in an aircraft application, where the designer attempts to limit the blanking time in the system in order to achieve the most usefulness from the devices and reduce the apparent output harmonic content, the cycloconverter takes on the characteristics of a pulse width modulated inverter. The semiconductor devices are required to operate conditions of high frequency operation, critical turn-off time under limited back bias conditions, and high reapplied dv/dt . The extreme case for the inverter is pulse width modulation or chopped-mode operation.

The forced commutation, pulse width modulation inverter has been thoroughly described in the literature by McMurray and Shattuck [1], and Bedford and Hoft [2]. The circuit shown in Figure 3 is a typical single-phase, half bridge version of this type and is useful here for the purpose of analysis.

Referring to Figure 3, SCR_1 and SCR_2 conduct load current from the center tapped dc supply. SCR_{1A} and SCR_{2A} provide for commutation in conjunction with a properly charged capacitor C_1 . SCR_1 and SCR_{2A} are triggered on simultaneously. Load current is conducted through SCR_1 . At the same time, the capacitor charges resonantly through the inductance L_1 , attaining voltage polarity as shown. SCR_{2A} will cease conduction when the capacitor becomes fully charged. The circuit is then prepared for commutating SCR_1

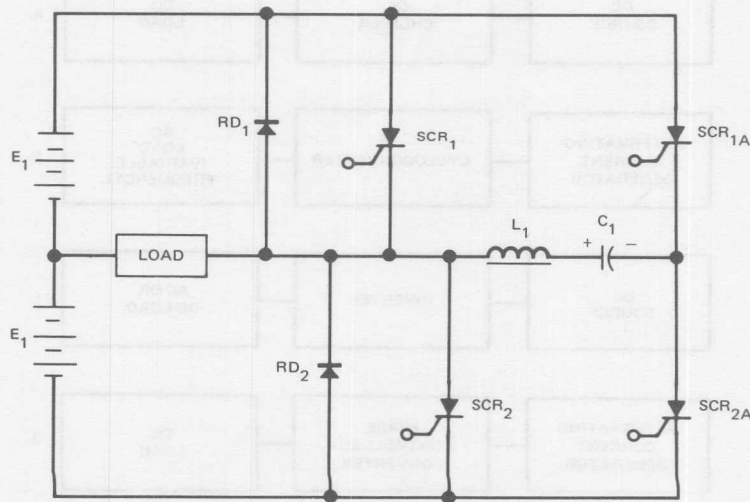


Figure 3. Impulse Commutated Inverter

off. When SCR_{1A} is triggered on, SCR₁ is back-biased through L₁ and C₁ and diode RD₁. The capacitor then supplies the sweepout energy of SCR₁ and the load current, and may discharge its excess commutation energy through RD₁. The capacitor C₁ will then charge in the opposite direction to that shown and SCR_{1A} will cease conduction when this capacitor reverses its charge.

In order to provide both voltage and frequency control to a load, for example an induction motor, this circuit can be used in a multiple-pulse modulation mode to be able to provide not only frequency control, but also volt-second control. However, this mode of operation necessitates several switching and commutation cycles during a single load half cycle. Typical waveshapes of current and voltage for SCR₁ are shown in Figure 4. Also shown are the current waveshapes of SCR_{2A}

and SCR_{1A}. The variation of these waveshapes with load and changes in circuit parameters are well explained in the references [1] [2]. In order to show distinctly the markedly different current conditions for the SCRs in the commutation and main portions of the power circuit, the duration of the commutation current has been extended with respect to the on-time of the main power circuit. In an actual case, these impulses of half sine wave current are generally much shorter in comparison to the on-time of the main SCRs. Using these waveshapes as a guide, optimum device characteristics may be extracted.

The main devices see very rapidly rising current flowing into the load. They also conduct the current required to charge the commutation capacitor. These devices switch from a very high voltage. Typically, on a rectified 460 V, 3-phase power

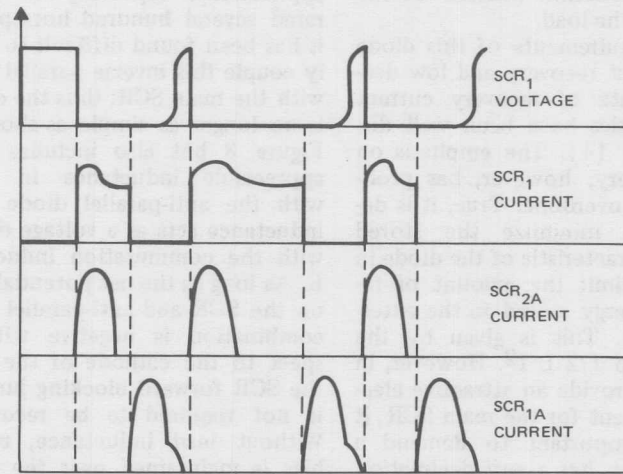


Figure 4. Typical Waveshapes for Impulse Commutated Inverter

line, they will switch from approximately 550 volts when used in the full bridge version and, without external suppression, rates of rise of on-state current will be in the order of 100 to 200 amperes/ μ sec. By employing limiting reactance in series with the main device, this current can be quite easily limited to 20 amperes/ μ sec, even including the discharge of the capacitor in the snubber network, which is connected in parallel with the SCR to provide dv/dt suppression in the circuit.

Using a circuit with a heavily inductive load, the purpose of the anti-parallel diode is obviously to provide a path for this reactive energy to flow. When the load is both active and reactive, such as a motor capable of regeneration into the system, the diode is necessary to provide a path for such regeneration without creating excess negative voltage on the main power devices. It is also useful in minimizing the harmonic content of the current in the load.

The requirements of this diode to have fast recovery and low declination rate of recovery current characteristics have been well discussed [3] [4]. The emphasis on fast recovery, however, has probably been overdone. True, it is desirable to minimize the stored charge characteristic of the diode in order to limit the amount of inductive energy stored in the external circuit. This is given by the relationship $1/2 L I^2$. However, in order to provide an attractive electrical ambient for the main SCR, it is most important to demand a diode which has a soft declination characteristic, that is, returns from its peak negative sweepout current

to zero in a relatively soft manner. This will minimize the di/dt in the circuit, therefore minimizing the $L di/dt$ in the external circuit. By this means the transient voltage and dv/dt to which SCR₁ and SCR₂ are subjected when the anti-parallel diode does recover will be limited.

The diode, no matter how soft and quick its recovery, creates several problems. Just at the time the main SCR is required to be back-biased by the commutation circuit, the diode minimizes this back-bias by providing essentially a one-volt drop in anti-parallel with the SCR during the discharge period of the commutation circuit. This is a disadvantage for most thyristors, especially large power devices, because low back-bias on the SCR tends to extend the necessary recovery time of the forward and reverse junctions, extending the time interval before the SCR is capable of withstanding reapplication of forward voltage. In some applications, especially in drives rated several hundred horsepower, it has been found difficult to closely couple this inverse parallel diode with the main SCR; thus the circuit is no longer as simple as shown in Figure 3 but also includes some appreciable inductance in series with the anti-parallel diode. This inductance acts as a voltage divider with the commutation inductance L . As long as the net potential drop on the SCR and anti-parallel diode combination is negative with respect to the cathode of the SCR, the SCR forward blocking junction is not required to be recovered. Without lead inductance, reverse bias is maintained over the entire conduction interval of the diode. However, with inductance, the co-

sinusoidal voltage generated by the reactive voltage division, can shrink the reverse bias time by as much as 50%, since the inductive potential drop is opposite to the forward drop of the diode at the midpoint of the commutation cycle. Thus, the effective commutation time is considerably reduced in the type of mechanical arrangement where the inductance in series with the anti-parallel device cannot be minimized. In some cases, circuit designers have purposely inserted an inductance in this portion of the circuit, thus reducing the effective commutation time by 2:1 but providing increased negative bias on the SCR during the initial portion of the commutation period. By this means, some of the lost commutation time is regained by optimizing the magnitude of the reverse bias.

Some further observations can be made, referring to the waveshapes in Figure 4. The main SCR must exhibit a superior (very short) turn-off time, in addition to low switching losses and high di/dt capability. Since it is required to be commutated several times during a half cycle, short turn-off times are necessary to minimize the commutation storage energy and therefore the size of the commutation components. Since the dv/dt in the system tends to be very high, it is also desirable that this SCR have a very short turn-off time with high reapplied dv/dt . In order to have successful pulse width modulation, it is necessary to recharge the commutation circuits before commutating the main SCR during a given half cycle to the load. Thus, for maximum utilization of the SCRs, it is desirable for the SCR charging the commutation circuit to recover

quickly, making it possible to turn on the next commutation SCR the earliest possible time after gating the main device. This provides maximum modulation in the system. The commutation device is required to have low switching losses under high sinusoidal current pulses at several times the pulse rate of the basic inverter circuitry in order to minimize its switching losses. Since the commutation circuit tends to ring, the auxiliary or commutation SCR is often required to have a high voltage rating unless an auxiliary resistor and an extra pair of feedback diodes are utilized from a common point of the commutation circuit to provide damping of the circuit resonance.

With these requirements in mind, International Rectifier designed an SCR capable of operation in a several hundred horsepower drive system which demanded all of the required attributes of the switching thyristors described. The accelerated cathode excitation (ACE gate) SCR with epitaxial emitter structure when tested using the circuit of Figure 5 exhibits rather low switching losses, as shown in Figures 6 and 7. Also shown in Figure 6 is a typical large junction alloy-diffused device without accelerated cathode excitation gating, tested under the same conditions. This device has considerably higher losses, namely 16,900 peak watts per pulse. Also shown in Figure 7 is a double diffused device tested under these conditions, having switching losses of 10,900 peak watts per pulse. The advantage, then, of the accelerated cathode excitation epitaxial emitter structure in terms of dynamic losses per pulse is as much as 7,300 peak watts. Using this

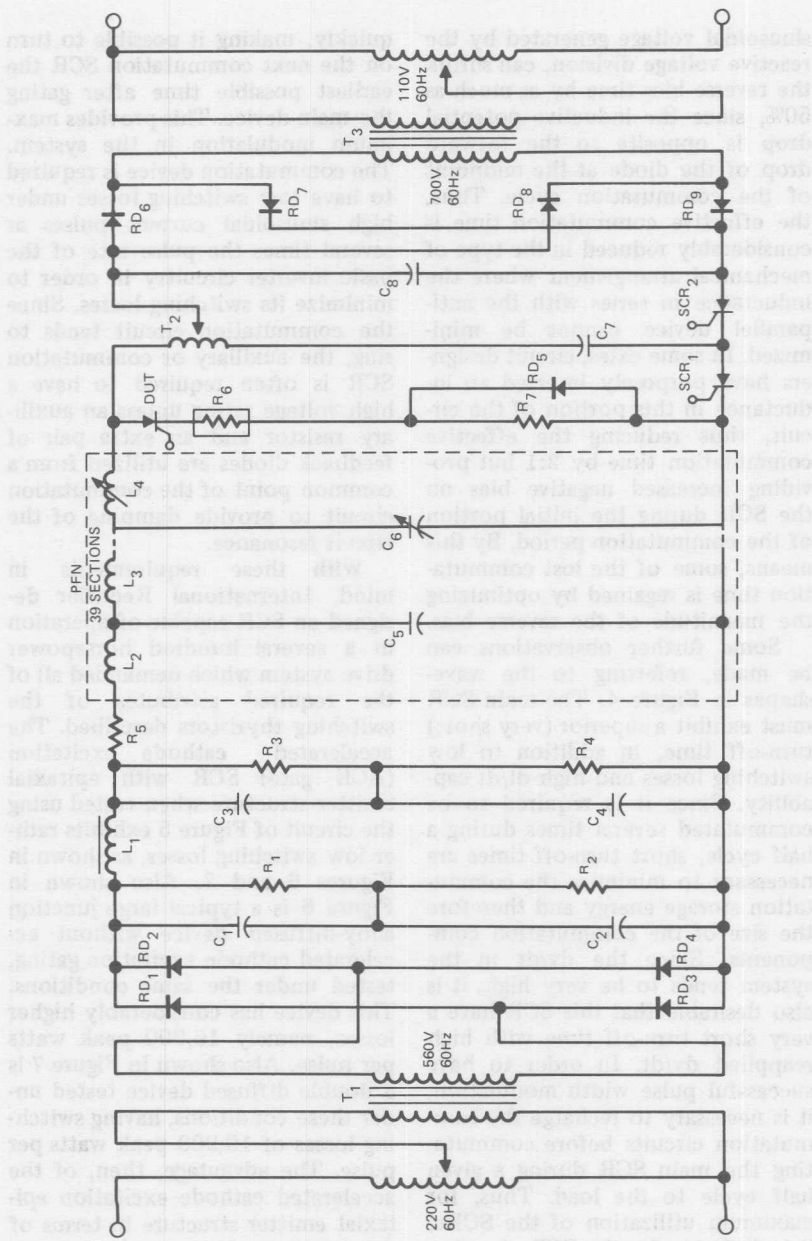


Figure 5. Pulse Forming Network Test Circuit

device in a typical 60 Hz inverter motor drive application, with pulse width modulation at five pulses per half cycle, results in a difference in switching losses of 500 watts; therefore increasing the effective rating of the ACE epitaxial device over

alloy-diffused and double diffused devices tested and compared under the same conditions by a factor of 41%.

Referring to the voltage fall shown on the turn-on waveshapes in Figure 8, it is obvious that with

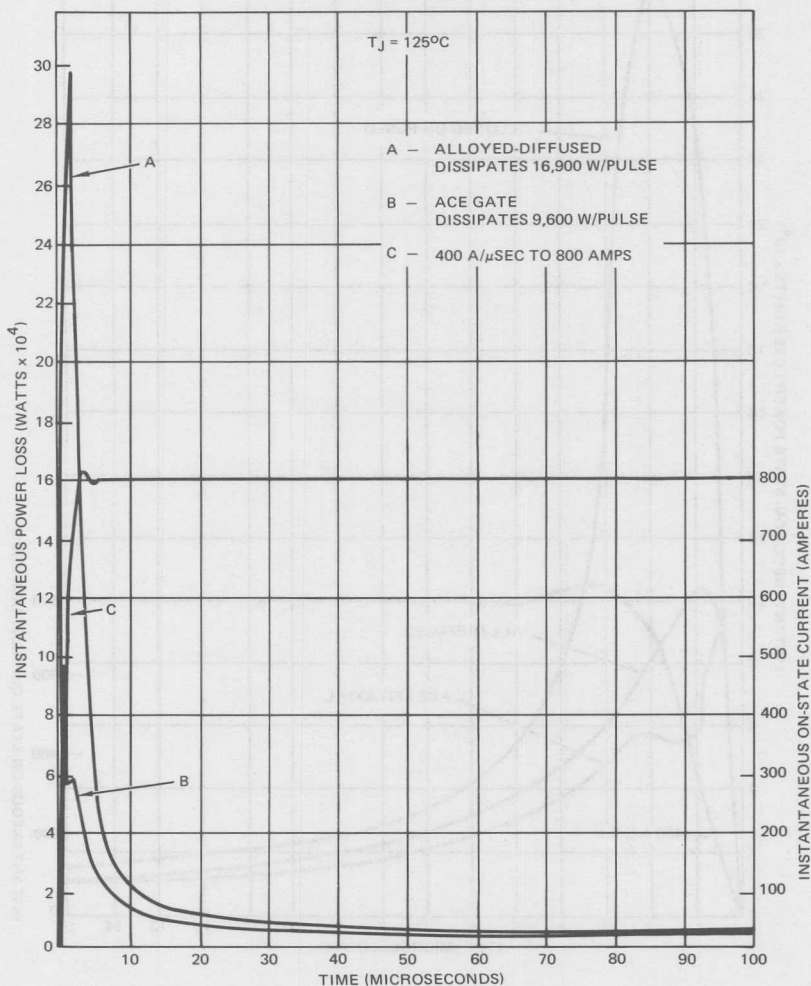


Figure 6. Instantaneous Power Loss vs. Time

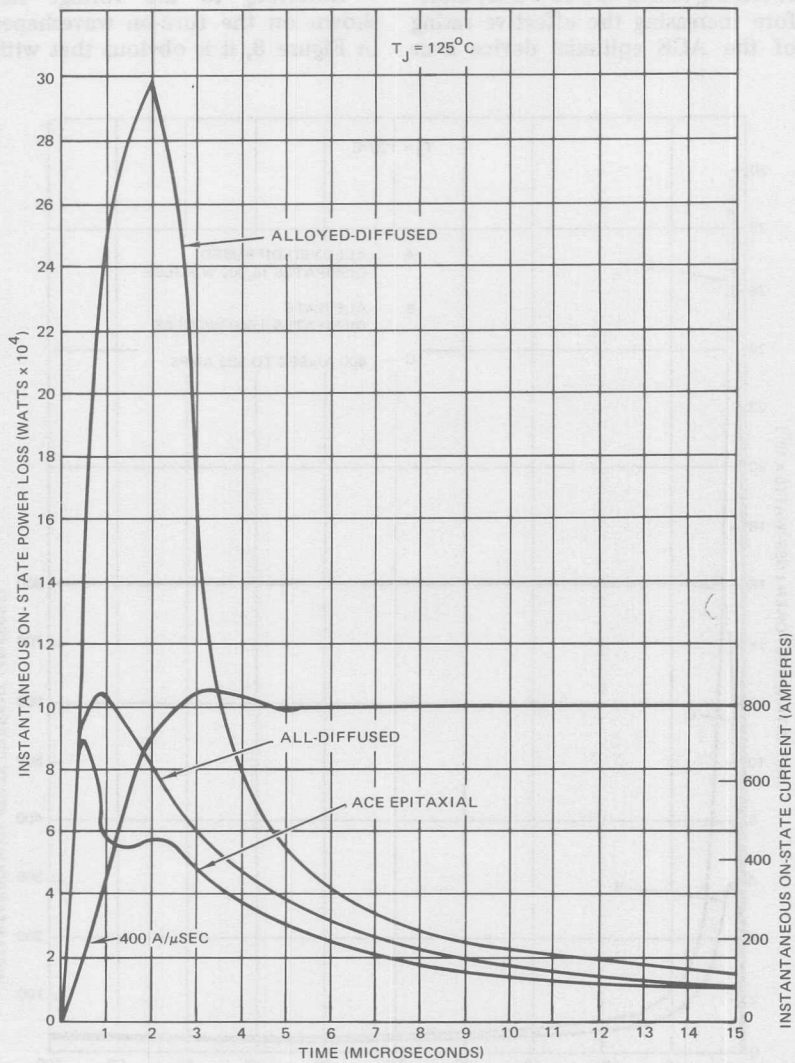


Figure 7. Detail of Instantaneous Power Loss vs. Time

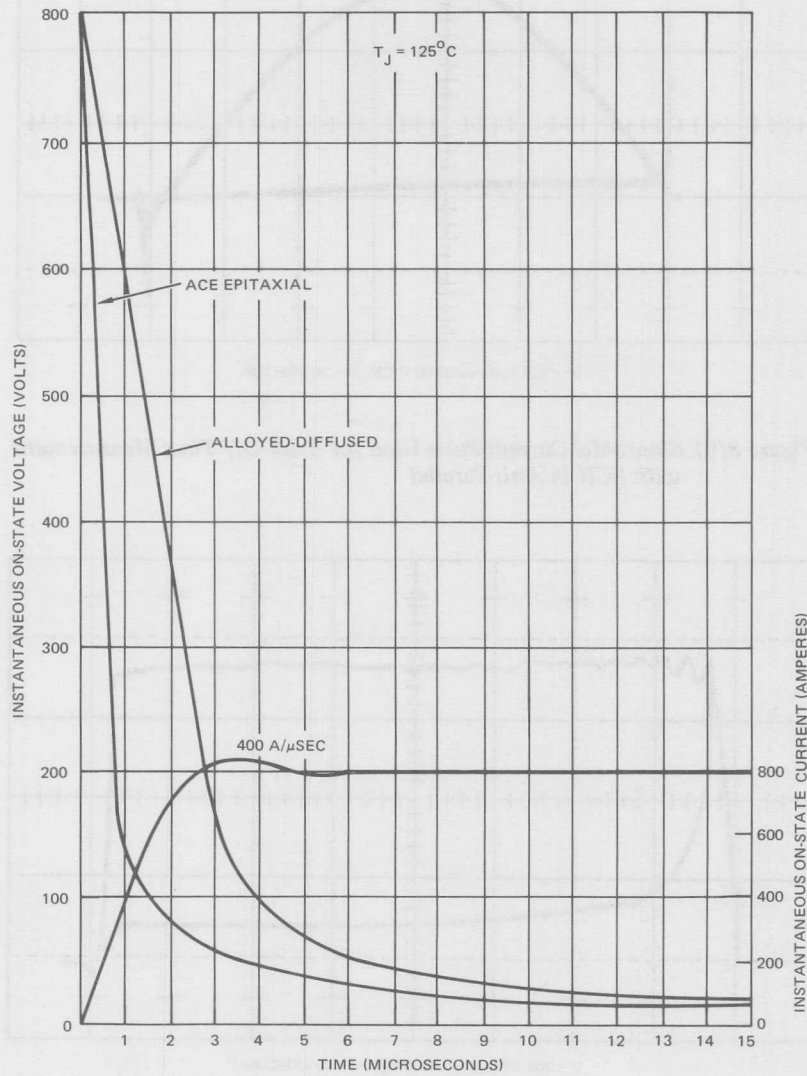
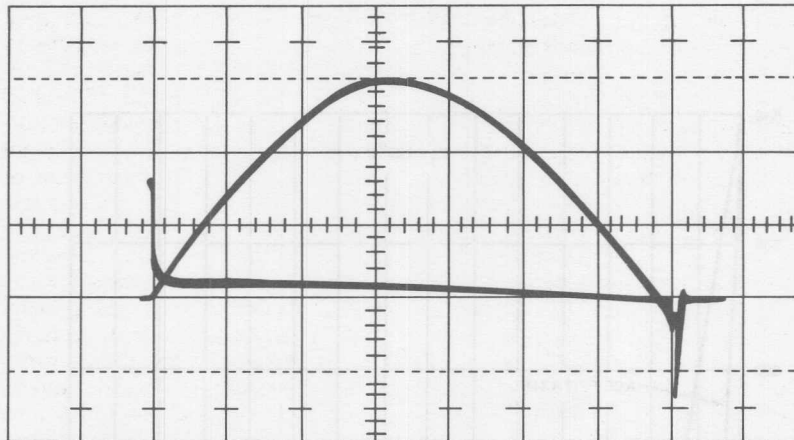
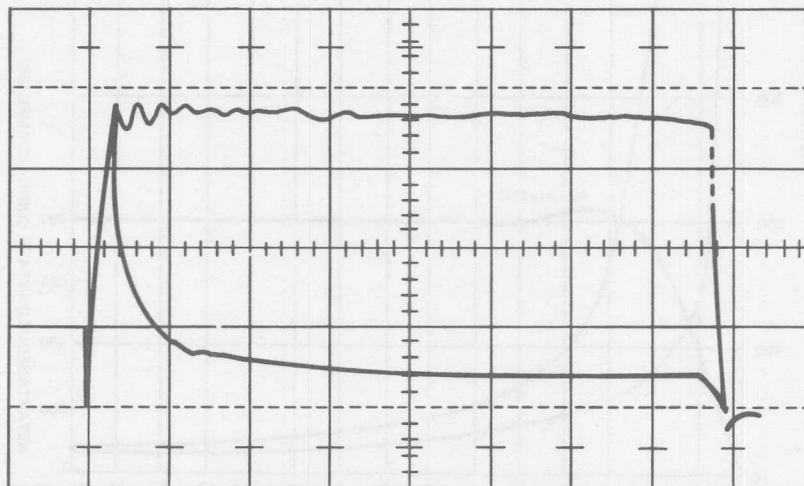


Figure 8(a). Instantaneous Turn-On Voltage vs. Time



V = 500 A/div AND 50 V/CM; H = 20 μ SEC/div

Figure 8(b). Sinusoidal Current Pulse Used for Turn-Off Time Measurement with SCR in Anti-Parallel



V = 200 A/div AND 10 V/CM; H = 25 μ SEC/div

Figure 8(c). Trapezoidal Current Pulse Used for Turn-On Power Loss Evaluation

this new emitter structure, the turn-on of the device is completed in a much shorter period of time than that obtained using more standard emitter structures. Another important feature is the turn-off time of the device using the anti-parallel diode arrangement shown in Figure 3. However, to be useful in an induction motor drive of several hundred horsepower capacity, this turn-off time must be minimized in the 1,500 to 2,000 ampere range with the forward current declining at a rate of 40 or 50 A/ μ sec. Test results with and without an anti-parallel diode at high and low currents are shown in Table I. Figure 9 shows the percent change in turn-off time versus peak current.

Since the diode recovery is of prime importance it is interesting to observe that the SCR developed with the new emitter structure also exhibits an inherently soft recovery characteristic. An assembly using two of these SCRs is an application of this theory. One of the devices is chosen to have very good dynamics in terms of turn-off time, dv/dt , and low switching losses with the ACE epitaxial emitter structure. The other device in the assembly is connected in anti-parallel with this SCR, but is arranged to be anode-triggered through a resistor-diode network so that when it becomes forward-biased it automatically turns on. By using Hockey-Puk devices, an assembly arrangement was made in which the stray inductance of the anti-parallel loop was minimized, thus reducing the voltage divider effect discussed earlier. The turn-off time of a typical assembly tested under the identical conditions previously described, was re-

duced by 50%, and the reapplied dv/dt on the main commutated SCR was minimized, since the anode-triggered anti-parallel SCR had an inherently soft recovery characteristic. The voltage impressed on the main SCR at the initiation of commutation in the circuit remained as a forcing voltage to sweep out the main SCR during the delay period of the anode-triggered device connected in anti-parallel with it. In order to further study the advantages of this combination, a more complicated anode-triggering circuit was inserted which provided an adjustable delay period (see Figure 10). Increasing this delay period did not appreciably decrease the turn-off time of the main SCR (See Table I). Thus it was possible to maintain a simple diode resistor combination for anode-triggering of the anti-parallel device and still obtain minimum commutation time for the main thyristor.

The third device required in the system is the commutation or auxiliary thyristor. This device is required to periodically carry a high amplitude half sine wave impulse of current, providing charging and discharging of the commutation capacitor through the commutation inductance L_1 . This device is also required to turn off in a reasonable time under these conditions. The peak of this commutation current has to exceed the current in the main SCR previous to the turn-off since in the impulse commutated circuit the anti-parallel diode is only back-biased when the commutation current exceeds the load current. In Figure 11, t_0 indicates the commutation time allowed for the main device (the time the main device is back-biased), I_{load} indi-

Table I. Turn-Off Time

DEVICE NO.	TURN-OFF TIME			
	WITH REVERSE BIAS $I_{TM} = 500A$	WITH ANTI-PARALLEL DIODE	WITH ANODE TRIGGERED ANTI-PARALLEL SCR (NO DELAY)	WITH ANODE TRIGGERED ANTI-PARALLEL SCR (10 μ SEC DELAY)
	μ sec	μ sec	μ sec	μ sec
X (1000V Rated)	28	105	50	50
Y (1000V Rated)	20	74	35	35

I_{TM} = 1500A Half Sine Wave

t_p = 150 μ sec

dv/dt reapplied = μ sec

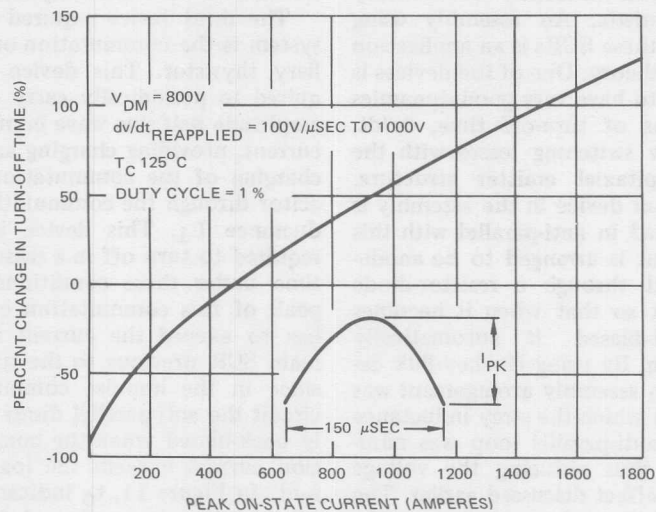
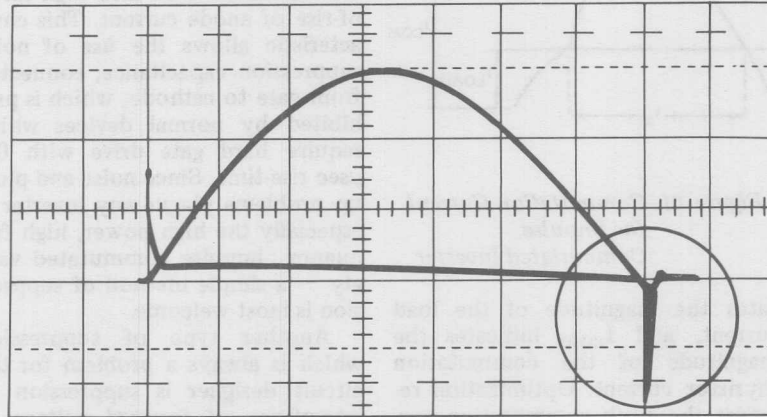
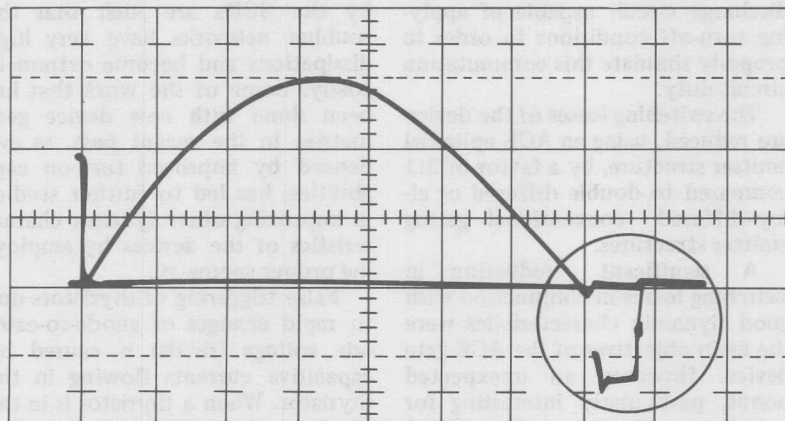


Figure 9. Percent Change in Turn-Off Time vs. Peak Current



V = 500 A/div AND 50 V/CM; H = 20 μ SEC/div

Figure 10(a). Reverse Voltage with Anode Triggered Anti-Parallel SCR



V = 500 A/div AND 200 V/CM; H = 20 μ SEC/div

Figure 10(b). Reverse Voltage with Anode Triggered Anti-Parallel SCR Delayed with R-C Combination

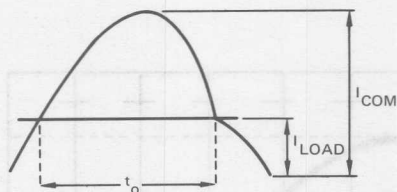


Figure 11. Commutation Current for Impulse Commutated Inverter

icates the magnitude of the load current, and I_{COM} indicates the magnitude of the commutation thyristor current. Optimization requires the peak commutation current to equal 1.5 times the load current. Thus, for a load current of 1,200 amperes, the commutation device should see a peak current of 1,800 amperes. The accelerated cathode excitation epitaxial emitter device has been tested in an LC discharge circuit capable of applying turn-off conditions in order to properly simulate this commutation circuit duty.

The switching losses of the device are reduced, using an ACE epitaxial emitter structure, by a factor of 2:1 compared to double diffused or alloy-diffused conventional gating emitter structures.

A significant reduction in switching losses in conjunction with good dynamic characteristics were the main objectives of the ACE gate device. However, an unexpected bonus, particularly interesting for inverter applications, is realized from the regenerative nature of the ACE gate. Once triggered into conduction, no matter how marginal the gate signal, the ACE structure

supersedes and expands the gating process. Consequently, 2 μ sec rise-time gate pulses do not impair device operation even into high rates-of-rise of anode current. This characteristic allows the use of noise suppression capacitance, connected from gate to cathode, which is prohibited by normal devices which require hard gate drive with 0.1 μ sec rise-time. Since noise and pick-up problems plague any inverter — especially the high power, high frequency, impulse commutated variety — a simple method of suppression is most welcome.

Another type of suppression which is always a problem for the circuit designer is suppression of rate-of-rise of forward voltage as seen by the thyristors in the power circuit. Even in low frequency circuits, dv/dt suppression is often necessary. In high frequency systems the values necessary for the snubber network components to effectively influence the dv/dt as seen by the SCRs are such that the snubber networks have very high dissipations and become extremely costly. Some of the work that has been done with new device geometries in the recent past, as evidenced by improved turn-on capabilities, has led to further studies in improving other dynamic characteristics of the devices by employing proper geometry.

False triggering of thyristors due to rapid changes of anode-to-cathode voltage (dv/dt) is caused by capacitive currents flowing in the thyristor. When a thyristor is in the blocking state, the center region supports the applied voltage, but this region has a certain junction capacitance as shown in Figure 12(a). The basic electrical equiva-

lent is shown in Figure 12(b). When the anode-to-cathode voltage is changing, a displacement current flows through this junction capacitance and into the gate cathode region. If this displacement current is sufficiently high, then the thyristor will become triggered into conduction by this dv/dt generated gate current.

There is a circuit technique which is very widely used in the application of thyristors to control the dv/dt applied to thyristors in operating circuits; this is shown in

Figure 13.

However, device manufacturers have been able to greatly improve the dv/dt capability of thyristors by modifying the semiconductor structure. This device structure modification evolved from the use of external resistors connected from gate to cathode to improve dv/dt capability (see Figure 14).

Obviously, this external resistor provides an alternate path for the displacement current, reducing the amount flowing through the gate cathode region. However, this re-

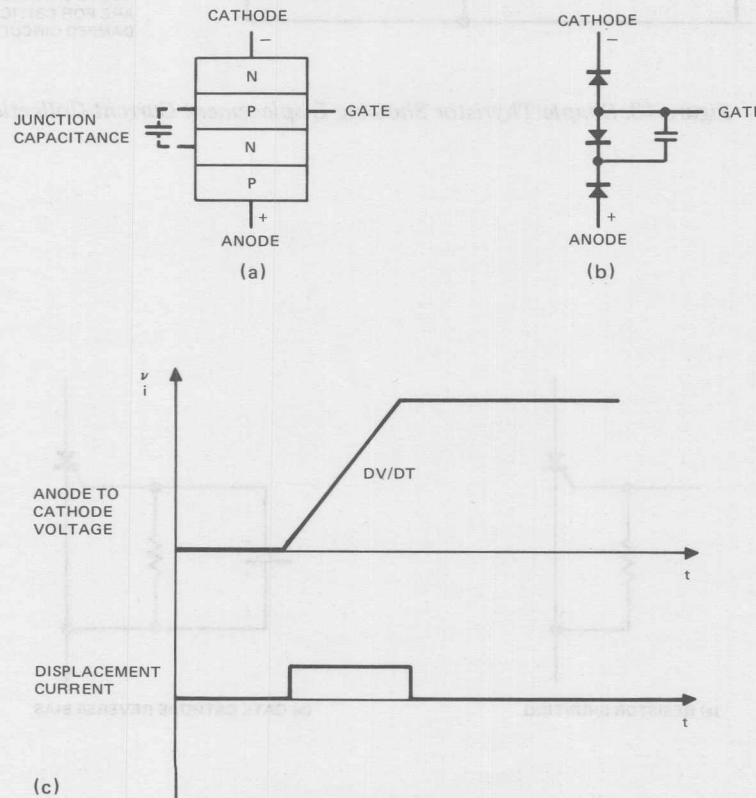


Figure 12. Current By-Passed by Low Impedance Negative Bias Gate Supply

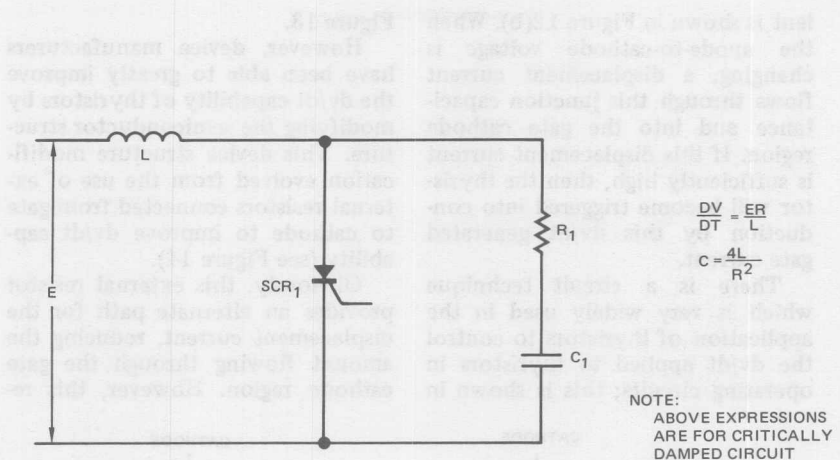


Figure 13. Simple Thyristor Showing Displacement Current Collection

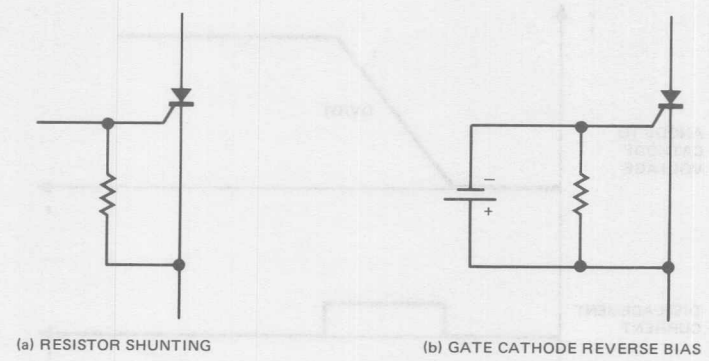


Figure 14. Theoretical Optimum Thyristor Geometry for External Gate Bias dv/dt Suppression

sistor provides maximum shunting of the gate to the cathode at the point where the internal gate wire is attached. At the opposite side of the silicon slice, the shunting is less efficient but with very small devices, the external resistor is useful in improving dv/dt capability. As the device area increases, a more efficient shunting (or emitter shorting) means is required. One way of achieving this is to extend the cathode metallization to cover part of the gate region as shown in Figure 15. This overlap provides an intern-

al resistor, which shunts the entire circumference of the gate cathode region, thus providing a more efficient shunt. Unfortunately, as thyristors become larger, this internal shunt becomes less efficient because of the effects of the internal lateral resistance of the gate region, as shown in Figure 16.

To provide the most efficient internal shunting, large area thyristors are fabricated with distributed internal shorts as shown in Figure 17. Small islands of gate (P) material are created which extend

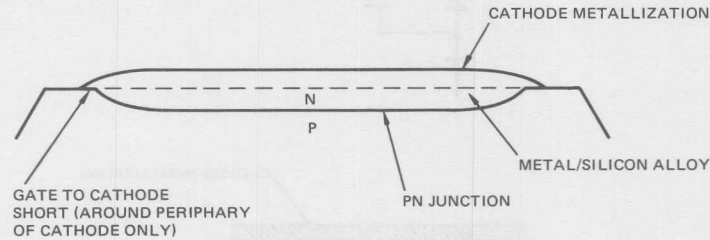


Figure 15. Gate-Cathode Region Showing Edge Shorting

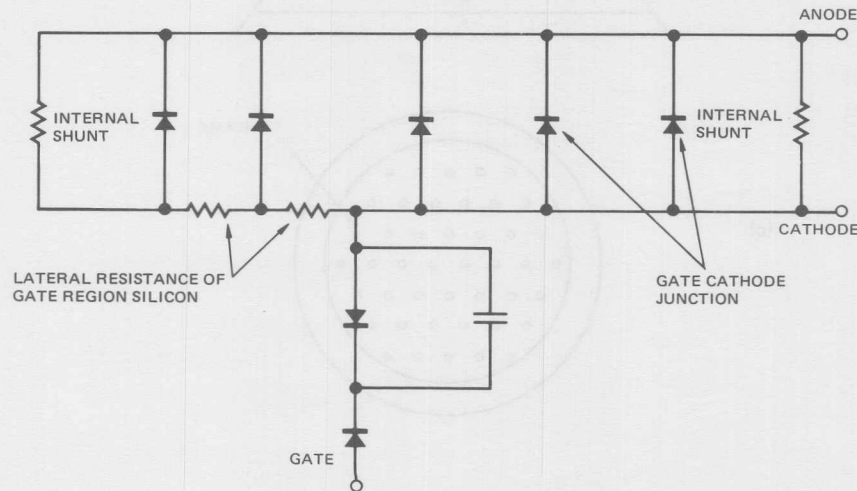


Figure 16. Simplified Circuit of Large Area Thyristor

through the cathode (N) region and are connected to the cathode metallization. Through the use of this technique, it is now possible to manufacture thyristors with dv/dt capability well in excess of $1500V/\mu\text{sec}$.

IR's ACE gate device illustrates the thyristor innovations that have made possible a new generation of sophisticated solid-state power control techniques.

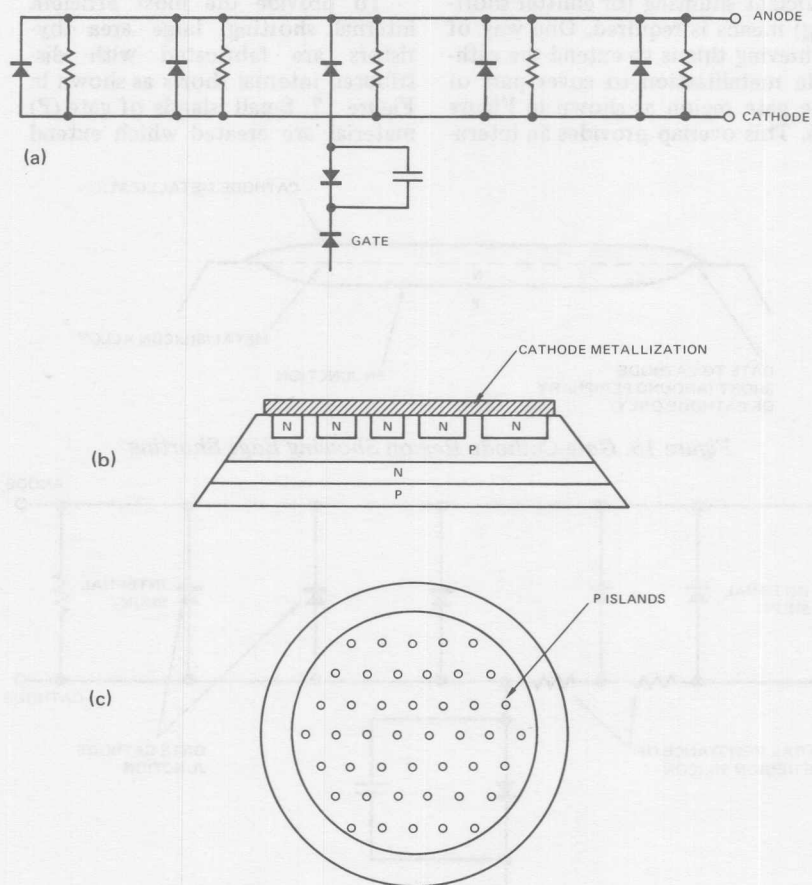


Figure 17. Thyristor Internal Shorts

References

1. W. McMurray and D.P. Shattuck, "A Silicon Controlled Rectifier Inverter with Improved Commutation," AIEE Transactions Vol. 80, Part I, 1961, pp. 531-542.
2. B.D. Bedford and R.G. Hoft, "Principles of Inverter Circuits," John Wiley & Sons, New York, 1964.
3. R.M. Crenshaw, "Application and Characterization of a 250 Ampere Fast Recovery Rectifier," International Rectifier Application Note AN-B-4.
4. D.W. Borst and D. Cooper. "Characterization and Application of a 250 Ampere Fast Recovery Rectifier." Proceedings of R & D Symposium on Power Semiconductor Technology, September 1967, Columbia, Missouri.



International Rectifier's custom-built test equipment is used to check the performance of each SCR before it is marked and shipped. This test is used to measure forward voltage drop, surge capability, gate characteristics and blocking voltage.

Device Characteristics

REVERSE BLOCKING TRIODE THYRISTOR—SCR

The most widely used member of the thyristor family of semiconductor devices is the reverse blocking triode thyristor or silicon controlled rectifier, the SCR. The SCR is a *rectifier* since it has a forward direction in which it may have a very low resistance and a reverse direction in which it has a very high resistance. It is *controlled*, since it can be switched from a high forward resistance (off-state) to a low forward resistance (on-state). Although the change in resistance is great (high voltages can be blocked, high currents can be conducted), it can be achieved with very small values of control voltage, current, and power. Also, once the SCR has been triggered on, it will remain on, even with the triggering signal removed.

The circuit symbol and block diagram of the silicon controlled rectifier are illustrated in Figure 1-1. Figure 1-2 shows the cross-

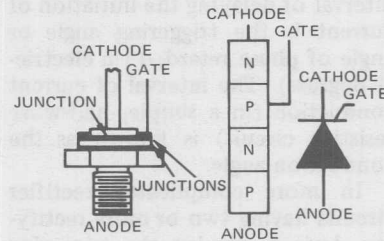


Figure 1-1. SCR Cross-Section, Block Diagram and Graphic Symbol

section of a typical silicon wafer used in an SCR.

As a circuit element, the silicon controlled rectifier can be used to block the normal flow of current for any length of time desired. To initiate conduction, a signal is applied to the gate to trigger the device on. When used in an ac circuit, conduction may be initiated at the beginning of any given positive half cycle, thus providing a

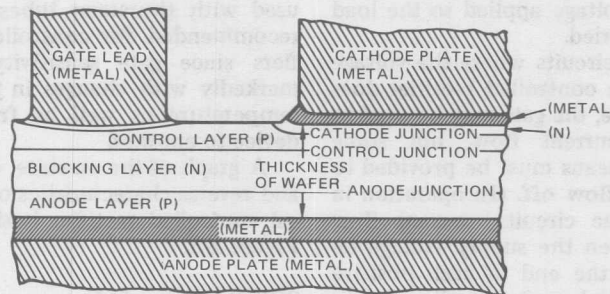


Figure 1-2. Cross-Section of SCR

simple on-off control. Or conduction may be initiated at some later time in the positive half cycle, thus varying the average voltage impressed upon the load. This process is known as phase control, and the interval of delaying the initiation of current is the triggering angle or angle of phase retard, α (in electrical degrees). The interval of current conduction (in a simple, half-wave resistive circuit) is known as the conduction angle.

In more complicated rectifier circuits having two or more rectifying devices, varying the triggering angle α reduces the average output voltage, but does not necessarily change the conduction angle, since this is determined primarily by the particular circuit used.

Controlled rectifiers may be used to control ac power by connecting them in an anti-parallel (inverse parallel) manner, so that one conducts load current in one direction while the other conducts in the opposite direction. (IR's logic-triac, discussed later in this Chapter, controls ac as well as dc, depending on gate signal characteristics.) The gate triggering signal may be used to switch the flow of current on and, by using phase control, the average voltage applied to the load may be varied.

In dc circuits where the voltage across the controlled rectifier does not reverse, the gate may be used to initiate current flow, but some specific means must be provided to turn the flow off. (In operation in resistive ac circuits, current flow ceases when the supply voltage reverses at the end of each positive half cycle.) In a dc circuit, a mechanical switch may be used to interrupt the current, or a more com-

plex circuit can be used in which triggering a second controlled rectifier causes a momentary flow of reverse current through the first controlled rectifier, causing it to turn off. This process is known as commutation, and is the basis of operation of the controlled rectifier inverter. Devices having a maximum rated turn-off time are useful for such applications.

Gate triggering circuits should provide a well-defined pulse of current which is several times greater than the maximum required dc gate current to trigger (at the minimum anticipated operating temperature) given for the particular device to be used. Curves in Product Data Bulletins show the range of gate voltage and current within which satisfactory operation can readily be achieved without exceeding the voltage, current, and power dissipation ratings of the gate. When conventional gate SCRs are used in applications where the initial anode current rises very steeply (high di/dt), gate pulses approaching the maximum permitted by the gate characteristic curve are most desirable to minimize device heating while it is first turning on. Triggering by varying a dc bias, commonly used with thyatron tubes, is not recommended for controlled rectifiers since gate sensitivity varies markedly with changes in junction temperature as well as from one device to another.

A graph of the on-state, off-state and reverse characteristics of a typical controlled rectifier is shown in Figure 1-3.

SCR Operation [1]

A relatively straightforward representation of the SCR that demon-

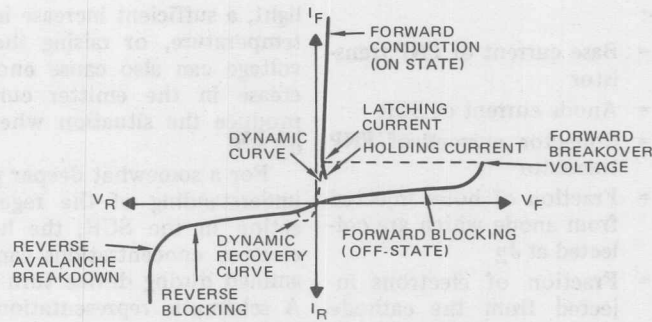


Figure 1-3. SCR Forward and Reverse Characteristics

strates its regenerative switching action is shown in Figure 1-4.

For this method of analysis, the SCR is considered as two transistors. The center N-P regions of the SCR are common to both the PNP and NPN transistors. For the PNP transistor, the base current is given by the relationship in Formula 1-A.

$$I_{B1} = I_A - I_{E1} = I_A - \alpha_1 I_A - I_{CO1} = (1 - \alpha_1) I_A - I_{CO1} \quad (1-A)$$

The collector current for the NPN transistor is given in Formula 1-B:

$$I_{C2} = \alpha_2 I_{B1} + I_{CO2} \quad (1-B)$$

Combining 1-A and 1-B gives Equation 1-C:

$$(1 - \alpha_1) I_A - I_{CO1} = \alpha_2 I_{C2} + I_{CO2} \quad (1-C)$$

Defining I_K gives Equation 1-D:

$$I_K = I_A + I_g \quad (1-D)$$

The final expression is given in Equation 1-E:

$$(1 - \alpha_1) I_A - I_{CO1} = \alpha_2 (I_A + I_g) + I_{CO2} \quad (1-E)$$

$$I_A (1 - \alpha_1 - \alpha_2) = \alpha_2 I_g + I_{CO1} + I_{CO2}$$

$$I_A = \frac{\alpha_2 I_g + I_{CO1} + I_{CO2}}{1 - \alpha_1 - \alpha_2}$$

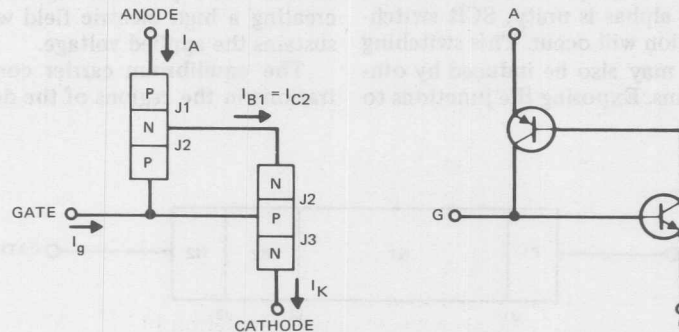


Figure 1-4. SCR - Transistor Analogy

Where:

- I_{B1} = Base current of PNP transistor
- I_A = Anode current of SCR
- I_{C1} = Collector current of PNP transistor
- a_1 = Fraction of holes injected from anode which are collected at J_2
- a_2 = Fraction of electrons injected from the cathode which are collected at J_2
- I_{CO1} = Leakage current of PNP transistor
- I_K = Cathode current of SCR
- I_{CO2} = Leakage current of PNP transistor
- I_g = Gate current of SCR

It is possible to obtain this same expression by equating the base drive current $I_G + I_{C1}$ to the base current of the NPN transistor.

Equation 1-E indicates that if $a_1 + a_2$ becomes equal to unity, the anode current can increase without bound, which results in a type of regenerative action. Since the current gains of transistors are effected by changes in the emitter current, if the gate drive raises the emitter current to the point where the sum of the alphas is unity, SCR switching action will occur. This switching action may also be induced by other means. Exposing the junctions to

light, a sufficient increase in device temperature, or raising the anode voltage can also cause enough increase in the emitter current to produce the situation where $a_1 + a_2 = 1$.

For a somewhat deeper physical understanding of the regenerative action in the SCR, the hole and electron concentrations can be examined during device turn-on [2]. A schematic representation of the SCR for this discussion is shown in Figure 1-5.

If a forward voltage less than the breakover voltage is slowly applied, the anode becomes positive with respect to the cathode, and junction J_2 becomes reverse-biased while junctions J_1 and J_3 are lightly forward-biased. The device remains in the off condition. Electrons near junction J_2 move toward the positively biased anode leaving behind donor impurities that are stripped of electrons; and in a similar fashion, holes in the P_2 side of J_2 move toward the cathode, leaving uncompensated acceptor impurities on the right side of J_2 . The result is that a depletion region composed of donors and acceptors uncompensated by mobile charge carriers develops in the region of J_2 creating a high electric field which sustains the applied voltage.

The equilibrium carrier concentrations in the regions of the device

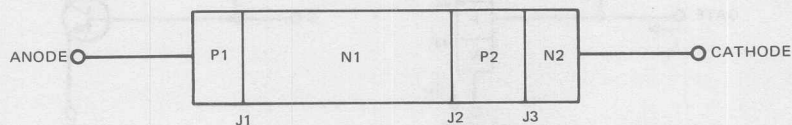


Figure 1-5. SCR Two Terminal Representation

of Figure 1-5 are assumed to be as follows:

- P_1 10^{19} acceptor/cm³
 N_1 10^{14} donor/cm³
 P_2 10^{16} acceptor/cm³
 N_2 10^{19} donors/cm³

These relative concentrations are typical of those required for desirable operation of practical devices.

When the forward voltage is raised to the breakover voltage level, the following events occur:

- A. The increased forward voltage produces a larger forward bias on J_1 . This means that more holes are injected from region P_1 to N_1 as in a normal forward-biased diode. Since the electron density in N_1 is much less than the hole density in region P_1 , electron injection from right to left across J_1 may be neglected.
- B. The holes injected from P_1 to N_1 diffuse across region N_1 and are then swept across J_2 because of the large electric field at J_2 . This junction had been reversed-biased by nearly the full anode-cathode applied voltage.
- C. The holes swept across J_2 increase the hole density in region P_2 . This produces a momentary build-up of positive charge in region P_2 , which raises the effective forward bias on J_3 .
- D. The greater forward bias on J_3 causes more electrons to be injected from N_2 to P_2 as in a normal forward conducting diode. Because of the relative carrier concentrations, hole injection from P_2 to N_2 is negligible compared to the increased electron injection from right to left across J_3 .
- E. The electrons injected into region P_2 diffuse across this region and are swept into the N_1 region by the electric field across J_2 .
- F. The additional electrons swept into the N_1 region momentarily raise the negative charge in this region, which results in greater forward bias on J_1 . This increased forward bias causes more holes to be injected from P_1 to N_1 . This is the beginning of event A above, and thus a regenerative switching action occurs.

The regenerative switching action continues until the anode-cathode voltage across the device drops to about one volt. This low value of voltage results because the electric field across J_2 continues to sweep holes from N_1 to P_2 and electrons from P_2 to N_1 until a sufficient number of the uncompensated donors and acceptors in the space charge region of J_2 have become compensated to forward bias this junction. In the steady-state forward conducting condition, the major carrier flow involves holes from left to right across J_1 and electrons from right to left across J_3 . Recombination in the relatively long N_1 and P_2 regions must occur to provide the necessary hole and electron current across J_2 to sustain the carrier flow at the terminals of the device.

Although the turn-on action has been discussed, assuming it was initiated by increasing the anode-cathode voltage to the breakover level, a similar action is initiated when gate current is applied. This increases the forward bias on junction J_3 , producing a sequence of events, starting with event D, which again produces the regenerative switching action.

The anode-cathode voltage across the device in the forward conducting condition is the sum of

the voltages on the three junctions as shown in Formula 1-F:

$$V_{AK} = V_{J1} - V_{J2} + V_{J3} \quad (1-F)$$

Since the "back-injection" on J_2 is not as great as the injection across the other two junctions, the forward voltage of the SCR, when it is on, is somewhat greater than the forward drop of a similar diode conducting the same current. For example, the corresponding diode and SCR drops might be typically 0.8 volt and 1.1 volts respectively.

An interesting feature of the "turned-on" condition of the SCR is that the middle junction, J_2 , is forward-biased, while the current flowing through it is a reverse current with respect to this junction [3]. Thus, junction J_2 in this condition is similar to the thermoelectric generator or the recovery state of a silicon rectifier.

However, the "generator" behavior of the plain rectifier is a short duration carrier recombination or clean-up period, while the "generator" character of junction J_2 is maintained continuously when the SCR is in its forward conducting state. Thus, the forward power loss is less than the sum of the theoretical losses in junctions J_1 and J_3 . It may be calculated from the observed terminal voltage drop vs. current characteristic as in a simple rectifier.

This has been a brief discussion of the operation of the SCR. For a more complete discussion of this subject, the reader may refer to a number of semiconductor texts and articles, including references [4], [5], and [6].

Static Characteristics

The characteristics of an SCR

are strongly influenced by temperature. Since there are two dependent variables (voltage and current) and four independent variables (conduction-state, gate current, time, and temperature), the presentation of the complete set of characteristics is impracticable, and only the most essential characteristics are discussed.

Off-State with No Gate Signal

In the off-state, with no gate signal applied, the controlled rectifier has the characteristics of two conventional silicon rectifier diodes connected in series, back-to-back. As seen in Figure 1-3, the off-state characteristic is essentially symmetrical and consists of a saturation current region where the current is substantially independent of applied voltage but is strongly temperature dependent, and an avalanche region where the current rises rapidly for only a small increase in applied voltage. In the reverse direction, the avalanche breakdown is similar to that in a silicon rectifier diode, where excessive avalanche current can destroy the device.

In the forward blocking, or off-state, region, avalanche current above a certain value will switch the device to the on-state and the off-state characteristic is terminated at the voltage where this occurs. This is known as the forward breakover voltage. Both the reverse breakdown voltage and the forward breakover voltage are temperature dependent. Devices are normally assigned the same voltage rating in both the off-state and reverse directions. However, most devices exhibit a slightly higher reverse avalanche voltage than off-state ava-

lanche voltage and, therefore, in practice, it is the off-state voltage rating that becomes the final rating of the device. The off-state and reverse power losses are small compared to the forward conduction and switching losses.

The breakover voltage and current are stable and reproducible for a particular device at a given temperature and the quoted breakover voltage is equal to, or greater than, rated peak repetitive voltage over the entire range of operating temperatures. The current to assure the device remaining in conduction after triggering but with gate current removed (the latching current) is of the same order of magnitude but is somewhat greater than the holding current, the minimum current at which the device will remain in the on-state, although there may be a considerable spread between devices.

At the point of breakover, the SCR suddenly switches to the on-state, where it exhibits a characteristic similar to a conventional silicon rectifier diode, having a very low forward voltage and a high current carrying capability.

The device will not return to the off-state until the anode-to-cathode current has been reduced by external means to a value below the holding current. The holding current is the minimum value that will continue to sustain the device in the on-state and any further reduction will cause the device to switch off.

The blocking currents are strongly temperature dependent. Figure 1-6 shows the variation of this leakage for a typical device over the temperature range from -65°C to $+130^{\circ}\text{C}$. This example is only typical, and there will be variations

among individual devices and among series of devices.

Of greater significance is the temperature dependence of the breakover voltage. This relation is shown in Figure 1-7. From this figure, it can be seen that the use of breakover as a means of controlling the device would be difficult since the operating temperature would have to be accurately controlled.

Off-State with Gate Signal

When gate current is present, an appreciable increase in both off-state and reverse current is observed. This results in additional power losses which could damage the device if not considered when determining the permissible on-state current.

When a small gate current is applied to an off-state biased device (anode positive with respect to cathode), in addition to an increase in off-state leakage current, the breakover voltage will be substantially reduced. Figure 1-8 shows the effect of increasing gate current on the off-state characteristic. To avoid the possibility of the device triggering on when it is not supposed to, most designers utilize pulse triggering techniques. The triggering pulses are then made large enough to insure positive triggering at all temperatures, thereby reducing the possibility of a triggering failure.

On-State

In the on-state, a controlled rectifier has a forward characteristic similar to that of a silicon rectifier diode. Average current turned on is independent of gate current, except at very low levels. The characteristic is dependent on temperature,

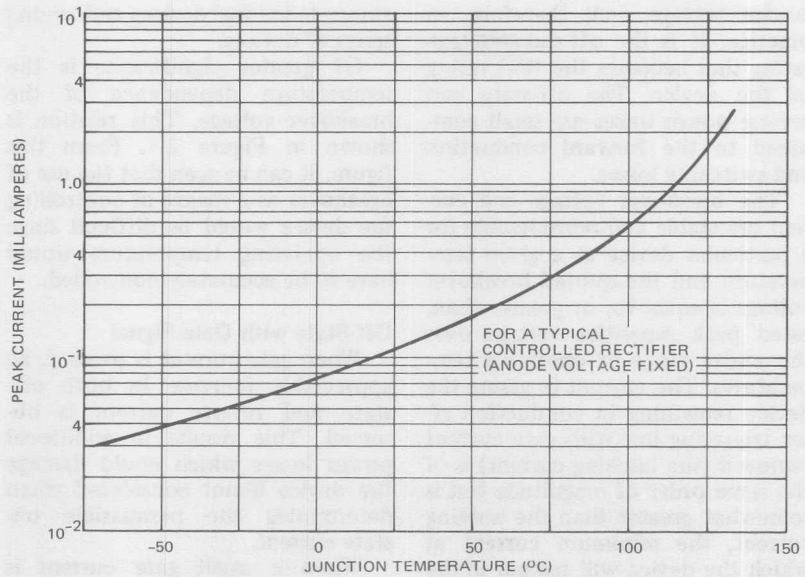


Figure 1-6. Typical SCR Blocking Current

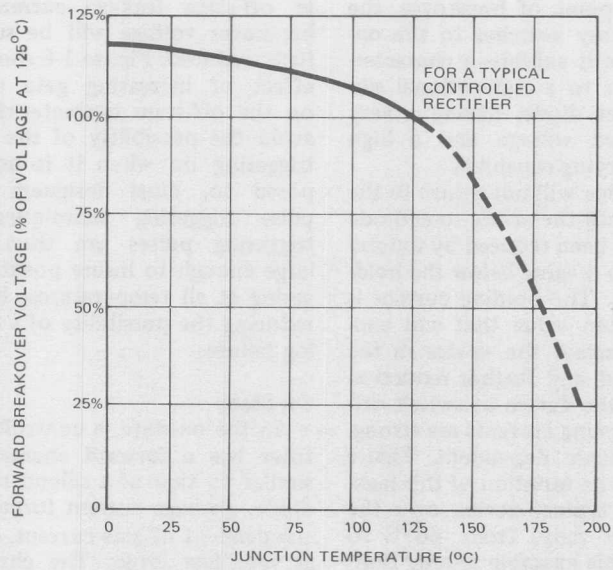


Figure 1-7. Typical SCR Breakover Voltage

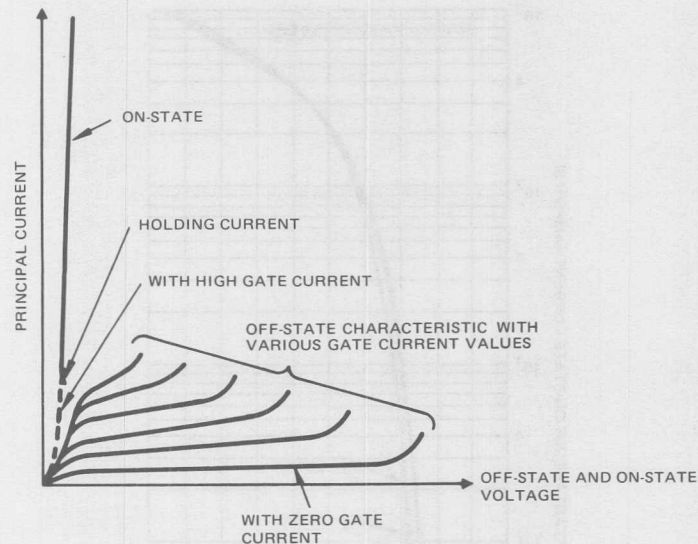


Figure 1-8. SCR Off-State and On-State Voltage

but the change in on-state voltage with temperature is small. Typical on-state voltage versus on-state current characteristics are shown in Figure 1-9.

The limiting factors for maximum permissible on-state current are power loss and current density. On the other hand, at low on-state currents approaching the holding current, the on-state characteristic becomes unstable. At levels below the holding current, the device turns off and reverts to the off-state, when the gate trigger pulse is removed. The value of the holding current decreases with increasing temperature as shown in Figure 1-10.

At low levels of on-state current, the on-state voltage increases with decreasing current and in this region, the device has a tendency to turn off. Over an appreciable range,

the on-state voltage is substantially constant, and at high current levels (above rated current), the device becomes primarily resistive, particularly at high temperatures. In this region, the resistances of the silicon-to-metal contacts and the internal conductors become significant and are of particular importance with regard to devices carrying high surge current pulses of short duration. The temperature dependence of the on-state voltage at high levels of current is such that a self-sustaining temperature rise is produced. The familiar loop observed on a volts-versus-current oscilloscope trace is caused in part by this transient heating hysteresis.

It is important to differentiate between holding current and latching current. Holding current is the current below which a controlled rectifier fails to conduct when the

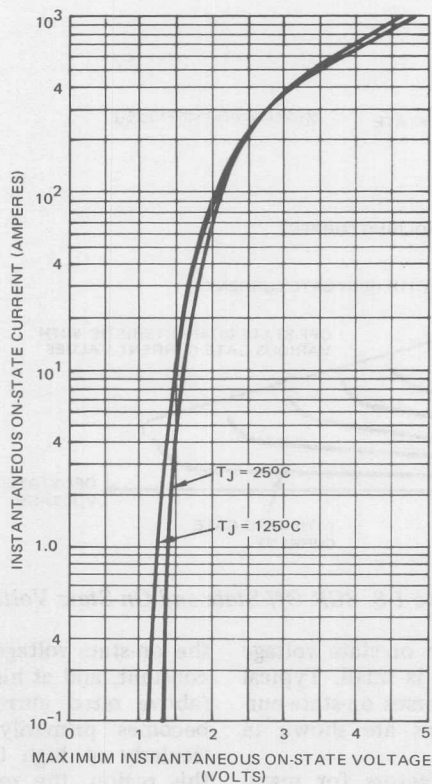


Figure 1-9. SCR On-State Voltage

anode current has been smoothly decreased. Latching current, on the other hand, is the minimum level of anode current at which the controlled rectifier will latch on and maintain itself in the on-state after an applied gate trigger current has been removed. Again, latching current occurs when the device is in the off-state and is being triggered on. The holding current occurs when the device is in the on-state, and current through the device is decreasing until the device turns off. Latching current may be sev-

eral times greater than holding current.

Voltage Rating

In selecting controlled rectifiers, the voltage and current ratings are the first considerations. The voltage rating should be high enough to withstand anticipated voltage transients, as well as the repetitive peak off-state and reverse blocking voltages that the device will see. In heavy industrial rectifier diode equipment, it is common practice to provide a margin of two and

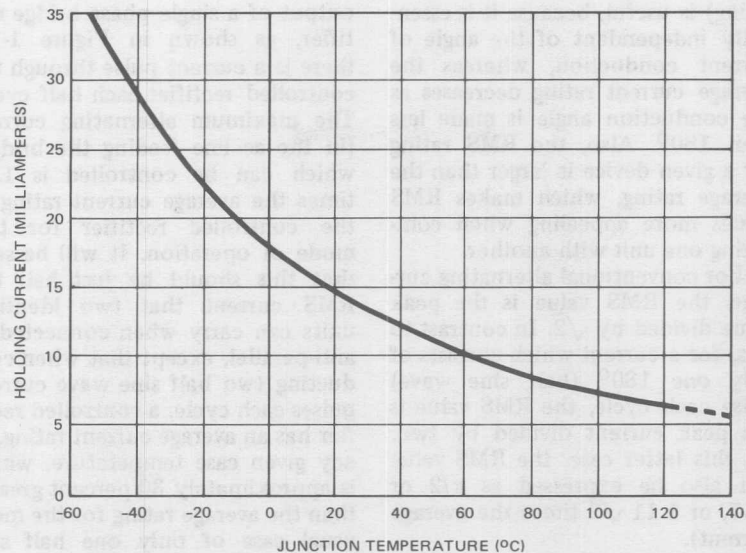


Figure 1-10. Typical SCR Holding Current

one-half times between the working peak reverse voltage applied by the circuit and the repetitive peak reverse voltage rating of the rectifier diodes.

In the case of controlled rectifiers, a somewhat smaller margin is quite often employed. This is the result of two factors. First, the maximum junction operating temperature for controlled rectifiers is usually lower than for rectifier diodes. Diodes usually may be operated up to 190° or 200°C. Most controlled rectifiers are limited to 125°C although a few may be operated at 150°C. At these lower temperatures, reverse leakage is less and there is reduced danger of a catastrophic failure due to a reverse voltage spike. Second, it is possible, by using selenium surge suppressors, such as IR's Klip-Sels, to engineer clamping circuits which prevent transients that appear across the

controlled rectifiers from exceeding about 1.7 times the device peak voltage rating (2.4 divided by $\sqrt{2}$). Thus, equipment designed for operation directly from a 480-volt power circuit under conditions of five percent high ac line voltage and protected with Klip-Sels, can make use of controlled rectifiers rated 1200 volts. (The ac supply voltage will be 505 volts under five percent high line conditions, and this will impose a working peak reverse voltage on the controlled rectifiers of 715 volts. Since 1.7 times 715 is 1215 volts, a 1200-volt device is suitable.)

Current Rating

Controlled rectifiers are assigned both an average current rating (based on 180° current conduction angle and averaged over a full cycle) and an RMS current rating. The RMS rating (which is also the dc

rating) is useful, because it is essentially independent of the angle of current conduction, whereas the average current rating decreases as the conduction angle is made less than 180° . Also, the RMS rating for a given device is larger than the average rating, which makes RMS values more appealing when comparing one unit with another.

For conventional alternating current, the RMS value is the peak value divided by $\sqrt{2}$. In contrast to this, for a current which consists of only *one* 180° (half sine wave) pulse each cycle, the RMS value is the peak current divided by two. (In this latter case, the RMS value can also be expressed as $\pi/2$ or 1.57, or $1.11\sqrt{2}$ times the average current).

The RMS value of two half sine wave current pulses in one cycle is $\sqrt{2}$ times the RMS value of one such pulse per cycle. Thus, when two identically rated controlled rectifiers are connected in anti-parallel (see Figure 1-11), they can handle 1.41 times the RMS current rating of either one (this is 2.22 times the average current rating of either one).

On the other hand, when one controlled rectifier is fed by the

output of a single phase bridge rectifier, as shown in Figure 1-12, there is a current pulse through the controlled rectifier each half cycle. The maximum alternating current (in the ac line feeding the bridge) which can be controlled is 1.11 times the average current rating of the controlled rectifier for this mode of operation. It will be seen that this should be just half the RMS current that two identical units can carry when connected in anti-parallel, except that when conducting two half sine wave current pulses each cycle, a controlled rectifier has an average current rating, at any given case temperature, which is approximately 30 percent greater than the average rating for the more usual case of only one half sine wave pulse per cycle. This is true, because the peak current that must be carried for a given average current, when there are two current pulses per cycle, is only half of what it would be if there were only one pulse per cycle, and this causes less heating of the semiconductor material for a given value of average current and permits higher current rating. These ratings are extended in Table I-I.

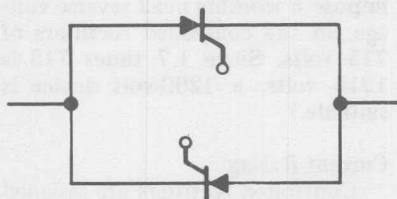


Figure 1-11. SCR Anti-Parallel Circuit

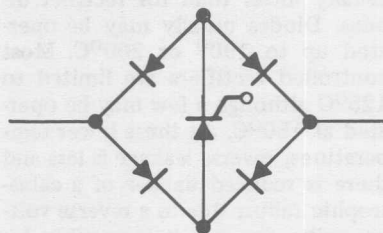


Figure 1-12. Hybrid Bridge Rectifier Circuit

Table I-I. RMS Values

$I_T(AV)$ MAX. AVERAGE ON-STATE CURRENT RATING (A)	$I_T(RMS)$ MAX. RMS ON-STATE CURRENT RATING (A) ($\pi/2 I_T(AV)$)	RMS RATINGS	
		ONE DEVICE, TWO PULSES PER CYCLE (A) (1.11×1.3 $I_T(AV)$)	TWO DEVICES IN ANTI- PARALLEL* (A) ($\sqrt{2}$ $\pi/2 I_T(AV)$)
3	4.7	4.3	6.7
4.7	7.4	6.8	10.4
10	16	14.4	22.2
16	25	23	35.5
22.3	35	32	49.5
35	55	51	78
40	63	58	89
50	80	72	111
70	110	101	156
80	125	115	178
100	160	144	222
150	235	216	333
250	400	361	555
300	470	433	666
350	550	505	777
420	660	606	933
500	785	722	1111
550	865	794	1222
700	1100	1010	1555
850	1350	1227	1888
1000	1600	1447	2221
1600	2500	2309	3554

Rounded off for ease of handling.

*Based on maximum allowable case temperature being the same as maximum allowed at rated half sine wave current.

The waveform of currents carried by inverter thyristors seldom is a simple half sine wave or rectangle. Yet, the designer needs to know the RMS value of this current when selecting the thyristor to be

used. The following procedure may be used to calculate the RMS value of any current waveform that can be broken up into segments for which the RMS value can be calculated individually.

The RMS value of the current wave is determined by dividing the waveform into segments, calculating the I^2t value for each segment, adding up these values and from this sum, determining the RMS value. Thus, it is possible to quickly determine the RMS value of current waveforms of any degree of complexity.

Figure 1-13 tabulates the I^2t values (more precisely the integral of i^2dt values) for a number of commonly encountered current waveforms. The mathematical expressions describing these waveforms are given under the heading "Function." In addition, a formula for I^2t is shown for each case. Both expressions are in terms of the peak value of the current wave in question, I_{cm} . The duration of time term, t , is defined in the waveshape sketches. Note, in the case of an exponentially decaying current wave, the time used is the value to the first time constant of the exponential curve.

Figure 1-14 illustrates how a complex wave may be split up into segments which are appropriate for this method of analysis. A waveshape can be found in Figure 1-13 which will match the shape of each segment of the complex wave. By inserting the peak value of each segment and the duration of each segment into the formula for the I^2t of a wave having the same waveform, the I^2t value of each segment can be obtained.

The RMS value of the complex current wave can then be calculated from Formula 1-G:

$$I_{RMS} = \sqrt{\frac{\sum t_1/t_0 I^2t}{t_1 - t_0}} \quad (1-G)$$

Where:

t_0 = Time at start of complex waveform.

t_1 = Time at end of the wave.

If the waveform being analyzed includes a period where current is zero, it is only necessary to include the duration of this period in the term $t_1 - t_0$.

This method may be used to calculate the RMS value of an alternating current wave, as well as of a rectified wave. This results from the fact that the current is squared in I^2t , so that I^2t is positive for either polarity of current.

Calculation of Rectangular Waveform

Current Rating of Thyristors

Most data sheets for power thyristors (silicon controlled rectifiers and triacs) give current ratings only for the case of a single phase (half wave) resistive load. These ratings are usually given in the form of curves showing the maximum allowable current vs. case temperature for various conduction angles such as 180, 120, 90, 60 and 30 degrees. These current waveforms are shown in Figure 1-15(a). In the case of stud-mounted thyristors, the highest value of average current given for any particular waveform has an RMS value equal to the maximum RMS rating of the thyristor in question.

The designer quickly finds that in a great many applications current flow is nearly rectangular so that the above published ratings do not apply. For a given conduction period and average current value, the heating effect of a rectangular current wave is less than that of a mutilated sine wave of equal con-

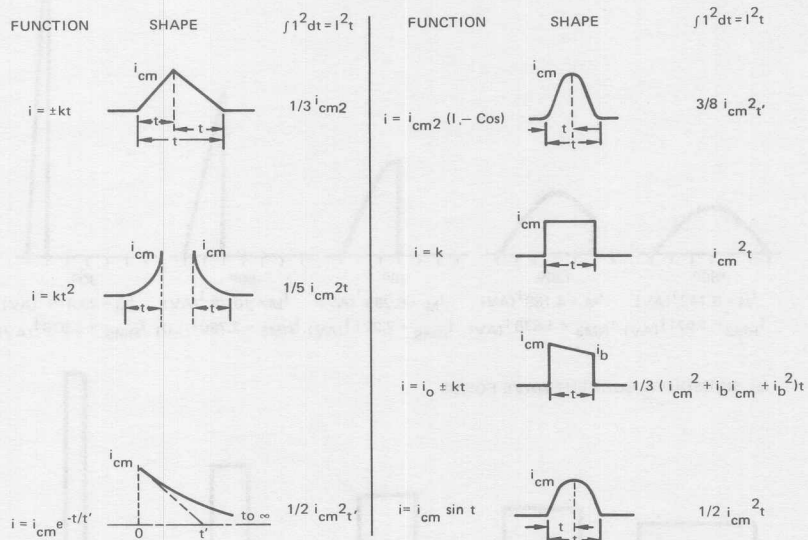
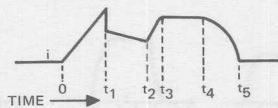
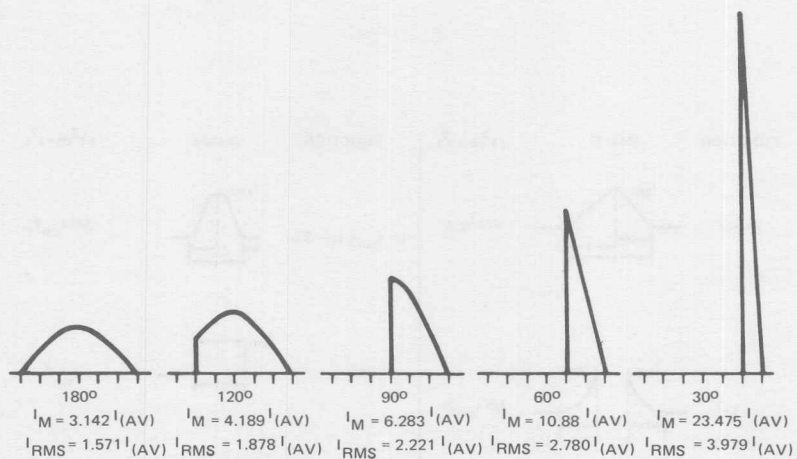


Figure 1-13. Evaluating Current Waveshapes

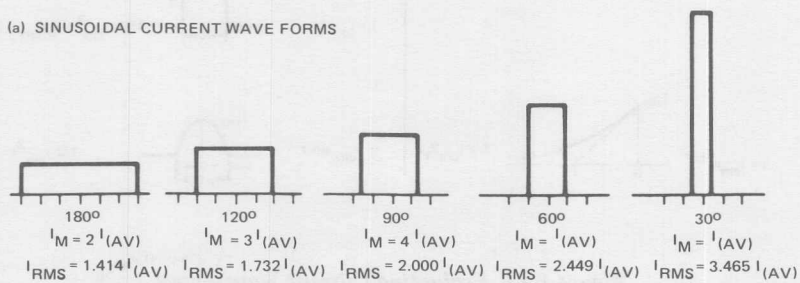


EXAGGERATED FOR CLARITY
 COMPLEX CURRENT WAVEFORM SUBDIVIDED
 INTO SECTIONS EACH CONFORMING TO ONE
 OF THE MORE COMMON WAVE SHAPES.

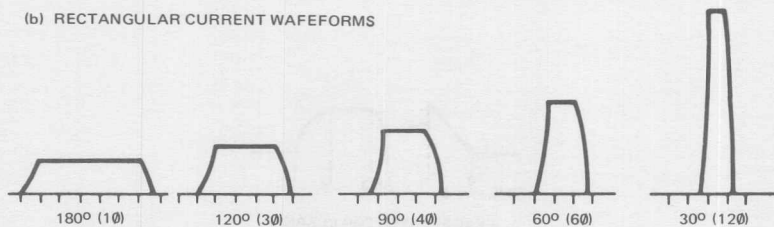
Figure 1-14. Analyzing Complex Waveshapes



(a) SINUSOIDAL CURRENT WAVE FORMS



(b) RECTANGULAR CURRENT WAVEFORMS



(c) RECTIFIER BRIDGE CURRENT WAVEFORMS

Figure 1-15. Comparison of Conduction Angle Waveforms

duction time, because the peak current is less. This can be seen from Figure 1-15(b). Thus, the thyristor current ratings for rectangular waveform current are greater for any given conduction period, and advantage should be taken of this.

The current waveshapes observed in single phase, full wave (bi-phase) and polyphase rectifier units usually are more rectangular than sinusoidal. Load inductance tends to prevent rapid variations in load current, making the current waves flat topped. On the other hand, inductance in the ac supply (including rectifier transformer reactance) prevents instantaneous transfer (commutation) of current from one rectifying element to the next, resulting in overlapping current flow through the circuit elements that are commutating. The resulting current waveforms are illustrated in Figure 1-15(c). When phase retard is used in such rectifier equipment to control the average

output voltage, the angle of current flow remains essentially fixed; the initiation of the current wave is simply delayed by the angle of phase retard, α , as can be seen from Figure 1-16. It is interesting to note that as α is increased, for a given value of load current, commutation takes less time so that the current waveform becomes more rectangular.

The duration of current flow (the conduction period) is determined by the rectifier circuit and not by the angle of phase retard. Conduction periods for common rectifier circuits are given in Table I-II.

The current flow through thyristors in many inverter circuits also tends to be rectangular. The current flows through an inductance from a source having a fixed direct voltage and the thyristors serve to switch the current from one load winding to another; thus, essentially rectangular current waves result.

Table I-II. Conductive Periods of Common Rectifier Circuits, Inductive and Resistive Loads

CIRCUIT	CONDUCTION PERIOD
Single-Phase, Center Tap (bi-phase, single-way)	180°
Single-Phase Bridge (double-way)	180°
Three-Phase Wye (single-way)	120°
Three-Phase, Double Wye with Interphase Transformer (single-way)	120°
Three-Phase Bridge (double-way)	120°
Six-Phase Star (single-way)	60°
Twelve-Phase Quadruple Zig-Zag (single-way)	30°

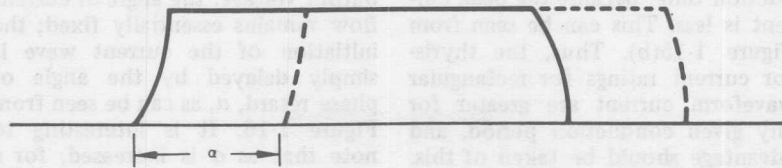


Figure 1-16. Effect of Phase Retard

Calculation Procedure

The calculation of thyristor current rating for rectangular waveform currents is not difficult. Basically, all the device data that are required is the on-state voltage curve at maximum rated junction temperature, the transient thermal impedance curve for times between 1 and 10 milliseconds, and the rated thermal resistance of the device, junction-to-case. If a curve of instantaneous on-state power loss vs. instantaneous on-state current is available, this will simplify the procedure, because it will not be necessary to calculate the instantaneous on-state power loss from the on-state voltage curve.

Junction temperature rise above case temperature can be calculated by formula 1-H.

$$\Delta T_{J(JC)} = \frac{t_p}{\tau} P_{TM} R_{\theta JC} + \left(P_{TM} - \frac{t_p}{\tau} P_{TM} \right) Z_{\theta}(t_p) = P_{TM} \left[\frac{t_p R_{\theta JC}}{\tau} + \left(1 - \frac{t_p}{\tau} \right) Z_{\theta}(t_p) \right] \quad (1-H)$$

Where:

- $T_{J(JC)}$ = Junction temperature rise above case temperature
 P_{TM} = Peak on-state (triggered) power loss at a given

peak anode current.

- t_p = Duration of one rectangular wave of current (conduction period).
 τ = Time interval between the start of one current pulse and the start of the next (the period, i.e., the reciprocal of the supply frequency).
 $R_{\theta JC}$ = Thermal resistance of the thyristor, junction-to-case.
 $Z_{\theta}(t_p)$ = Transient thermal impedance of the thyristor for the time duration of one current pulse.

In the above formula, the average junction temperature rise is calculated by the expression $t_p/\tau (P_{TM}) (R_{\theta JC})$ (average power dissipated times thermal resistance). To this is added a term which represents the temperature response of the junction in the final pulse of load current. This additional rise is calculated by multiplying the increment of power dissipated during the pulse which is greater than the average power dissipated $(1 - t_p/\tau) P_{TM}$, by the transient thermal impedance for the time of one current pulse, $Z_{\theta}(t_p)$. More complex expressions have been published for this temperature rise, but the above expression gives a conservative answer that is within a few degrees of the more precise value, and is far easier to calculate.

A further refinement is to allow for the heating effect of the losses during the reverse and off-state blocking periods. In power thyristors, these losses generally are only a few watts, and so cause only a small additional temperature rise of 1 to 2 degrees Celsius (Centigrade).

Temperature Rise Above Cooling Fluid Temperatures

The equipment designer must know junction temperature rise above cooling fluid temperature (temperature of incoming air, water, oil, etc.), not simply junction temperature rise above device case temperature. The additional rise of the case above the cooling fluid is calculated by multiplying the total average on-state, off-state and reverse blocking losses by the thermal resistance from case to cooling fluid.

There are usually two thermal drops in series in the path of heat flow from case to cooling fluid, these being:

- A. Thermal resistance from case to heat exchanger (often referred to as case to heat sink).
- B. Thermal resistance from heat exchanger to cooling fluid.

Thermal resistance from case to heat exchanger is a function of the size of the thyristor base and presence or absence of silicone grease on the mating surfaces. Representative values are given in Table I-III.

Thermal resistance from heat exchanger to cooling fluid must be determined from the configuration and size of the heat exchanger used, the velocity of the cooling fluid, the surface finish of the heat exchanger, etc. The thermal resistance, device-mounting-surface-to-coolant, of the heat exchanger can be obtained from the heat ex-

changer manufacturer or from tests.

An expression for calculating junction temperature rise above cooling fluid temperature can now be written, taking into account the factors just discussed (see Formula 1-J):

$$\Delta T_{J(JA)} = \left(\frac{t_p}{\tau} P_{TM} + P_{B(AV)} \right) (R_{\theta JC} + R_{\theta CH} + R_{\theta HA}) + P_{TM} \left(1 - \frac{t_p}{\tau} \right) Z_{\theta}(t_p) \quad (1-J)$$

Where:

- $T_{J(JA)}$ = Junction temperature rise above ambient cooling fluid temperature.
- $R_{\theta CH}$ = Thermal resistance, case-to-heat exchanger.
- $R_{\theta HA}$ = Thermal resistance, heat-exchanger-to-ambient.
- $P_{B(AV)}$ = Average power losses during reverse and off-state blocking periods.

(The other terms are the same as those for Formula 1-H).

The RMS value of the current rating calculated by the above procedures should not exceed the RMS current rating of the thyristor being considered.

Example:

To illustrate the principles discussed above, consider a 70 ampere (average), 110 ampere (RMS) stud-mounted thyristor operating in a three-phase bridge rectifier circuit with inductive load. The on-state voltage and the transient thermal impedance curves for this device are given in Figures 1-17 and 1-18, respectively. Maximum thermal re-

Table I-III. Thermal Resistance, Case to Heat Exchanger

SIZE OF THYRISTOR CASE			$R_{\theta CS}$ THERMAL RESISTANCE TO HEAT EXCHANGER ($^{\circ}\text{C}/\text{W}$)	
HEX BASE (INCH)	THREADED STUD	JEDEC NO.	DRY	GREASED
7/16	10-32	TO-64	0.90	0.60
9/16	1/4-28	TO-48	0.50	0.35
11/16	1/4-28	TO-65	0.35	0.25
1- 1/16	1/2-20	TO-49, 83, 94	0.15	0.10
1- 1/4	3/4-16	TO-93	0.10	0.08
1-11/16	3/4-16	—	0.05	0.04

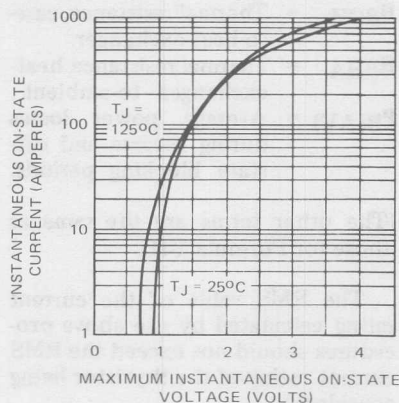


Figure 1-17. Maximum Instantaneous On-State Voltage

sistance, junction to case, is $0.30^{\circ}\text{C}/\text{watt}$, and maximum rated junction operating temperature is 125°C . The device is mounted on an air-cooled heat exchanger having a thermal resistance to ambient air of $0.30^{\circ}\text{C}/\text{watt}$ at a cooling air

velocity of 1000 lf/min. The maximum ambient air temperature in which the device is to operate is 45°C . The supply frequency is 60 Hz and therefore the supply period, τ , is $1/60 = 0.0167$ seconds. From Table I-II, the conduction period is 120 deg., or $0.0167 \times 120/360 = 5.6 \times 10^{-3}$ seconds, and from Figure 1-18, the transient thermal impedance for a square wave pulse of this duration is found to be $3.6 \times 10^{-2}^{\circ}\text{C}/\text{watt}$.

From Table I-III, the thermal resistance from case to heat exchanger is $0.10^{\circ}\text{C}/\text{watt}$ (greased). The average power loss during the reverse and off-state blocking periods can be calculated from the maximum leakage current for the thyristor, 5 mA. A conservative, worst-case estimate is 3 watts, full cycle average.

The above data may be used in Formula 1-J to solve for the peak power loss required to raise the peak junction temperature to 125°C :

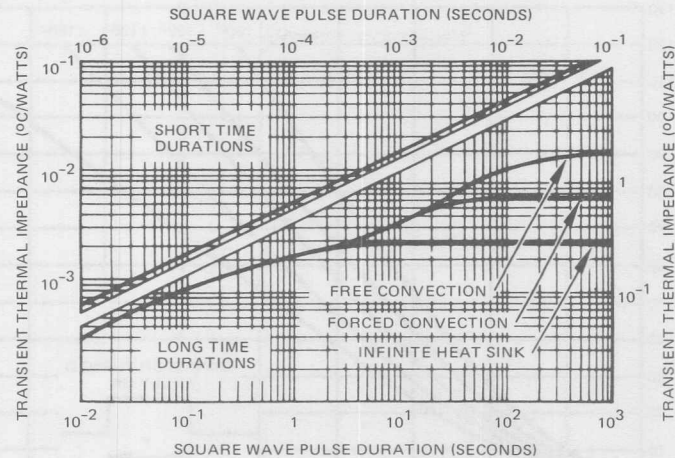


Figure 1-18. Maximum Transient Thermal Impedance, Junction-to-Case

$$\begin{aligned} & (1/3 P_{TM} + 3) (0.30 + 0.10 + 0.30) \\ & + P_{TM} (1 - 1/3) 0.036 = 125 - 45 \\ & 0.257 P_{TM} = 77.9 \\ & P_{TM} = 303W \end{aligned}$$

From the on-state voltage curve for 125°C junction temperature, the peak current producing this amount of power loss can be found (by successive approximations) to be: $303/1.68 = 180$ amperes. The maximum permissible average current is then $180/3 = 60.0$ amperes.

Referring to Figure 1-15(b), the RMS value of this current is $180/1.732 = 104A$, which is within the 110A RMS rating of the thyristor in this example.

The manufacturer will usually publish a curve of on-state power loss vs. direct current, such as the dc curves shown in Figures 1-19 and 1-20. Such curves permit reading the value of permissible peak amperes directly without the need for calculating them from the on-state voltage curve.

If the manufacturer has provided curves of average on-state power loss for rectangular current wave operation, such as shown in Figures 1-19 and 1-20, the average current may be read directly by converting the peak power to average power. In the example, the average power is 101 watts, which is one-third the peak power, since the conduction period is one-third of a cycle (120 degrees). From the 120 degree curve in Figure 1-19, the average current is found to be 59 amperes.

Using Rectangular Current Waveform Rating Curve

When the manufacturer provides curves of average on-state current vs. maximum allowable case temperature for rectangular current waves, such as the curves in Figure 1-21, calculations can be simplified even more. In this case, the main step in determining the current rating is to calculate the temperature rise of the case above ambient due to the on-state losses, which is the

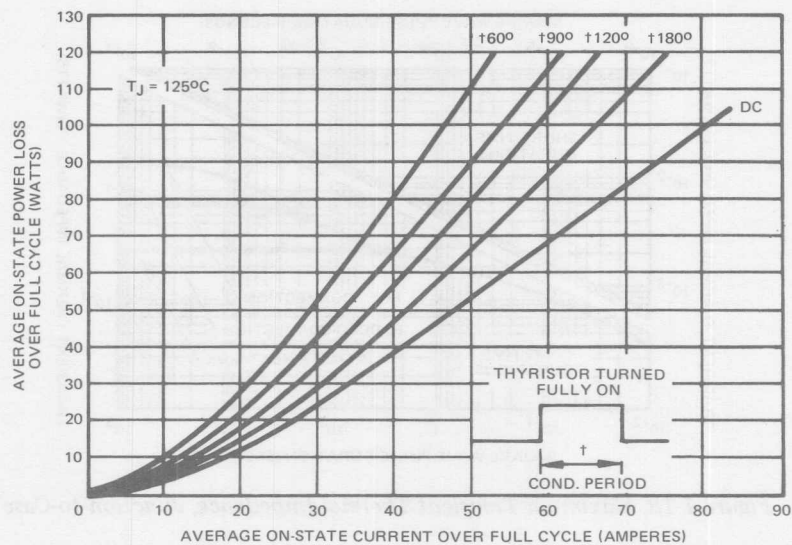


Figure 1-19. Average Low Current Level On-State Power Loss, Rectangular Current Waveform

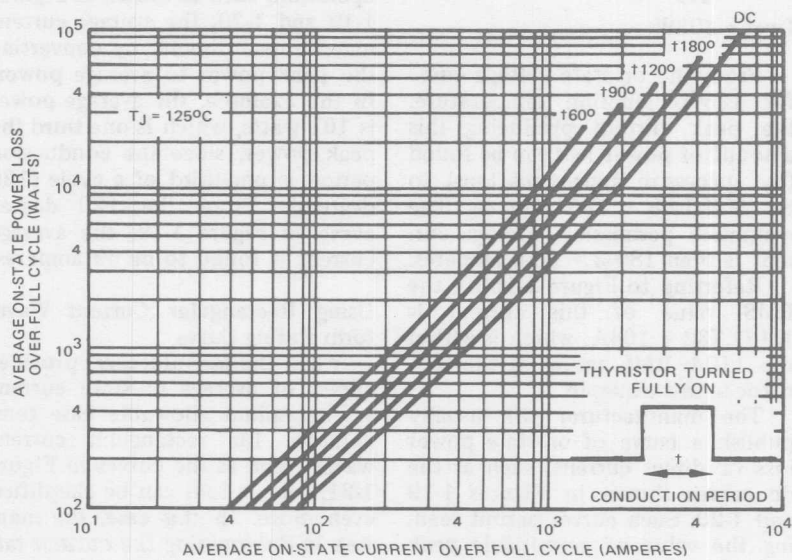


Figure 1-20. Average High Current Level On-State Power Loss, Rectangular Current Waveform

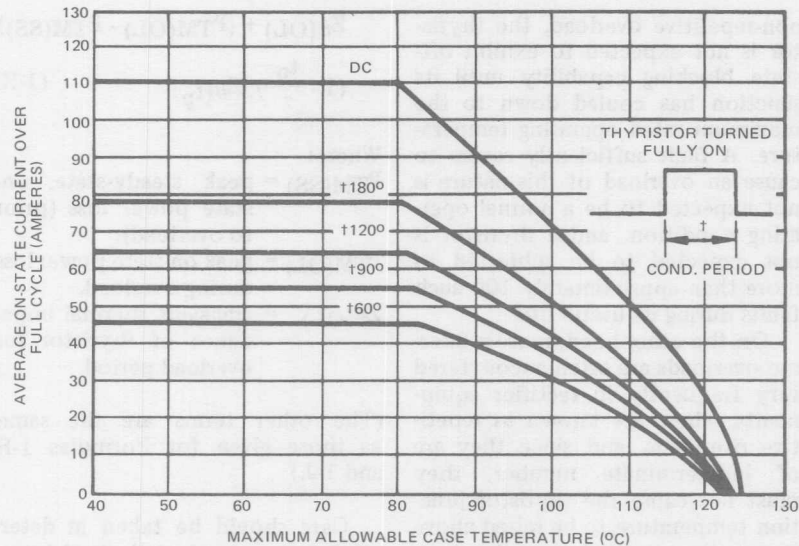


Figure 1-21. Average On-State Current vs. Case Temperature, Rectangular Current Waveform

product of these losses and the thermal resistance from case to ambient. Taking the example, this thermal resistance is $0.40^{\circ}\text{C}/\text{watt}$. The average reverse and off-state blocking power losses are 3 watts, and the temperature rise from case to ambient caused by these losses is 1.2°C . In effect, this raises the maximum allowable ambient temperature to 46.2°C . A current must now be found for which the maximum allowable thyristor case temperature, as read from Figure 1-21, will be just high enough to permit the average power generated in the thyristor to be dissipated to the cooling medium by the heat exchanger. This value of on-state current must be found by successive approximations. Since the answer in this case, 59 amperes, has previously been calculated, the procedure can be illustrated by a single calculation:

Maximum case temperature permitted at 59 amperes:

$$86.0^{\circ}\text{C} \text{ (from Figure 1-21)}$$

Maximum temperature rise permitted between ambient and case at 59 amperes:

$$86.0 - [45 + (3 \times 0.40)] = 86.0 - 46.2 = 39.8^{\circ}\text{C}$$

Maximum average on-state power loss permitted:

$$39.8/0.40 = 99.5 \text{ watts}$$

Maximum average on-state current permitted:

$$58.5 \text{ amperes (from Figure 1-19)}$$

This is essentially the same as the 59 amperes used at the start of the calculation.

The manufacturer's data sheet provides a non-repetitive surge current rating, which may be imposed on the thyristor when it is operating at maximum rated current, voltage, and temperature conditions in a half-wave circuit. Following rated

non-repetitive overload, the thyristor is not expected to exhibit off-state blocking capability until its junction has cooled down to the maximum rated operating temperature. A fault sufficiently severe to cause an overload of this nature is not expected to be a normal operating condition, and a thyristor is not expected to be subjected to more than approximately 100 such faults during its useful life.

On the other hand, more moderate overloads are often encountered very frequently in rectifier equipments. These are known as repetitive overloads, and since they are of indeterminate number, they must not cause the thyristor junction temperature to be raised above the maximum rated operating temperature, if long thyristor life is to be assured. Consequently, a reduction in the continuous loading on the thyristor is required, to provide an additional temperature rise which can take place during the overload.

The required amount of this temperature rise margin depends upon the severity of the overloads and their durations.

Of the many possible overload schedules, one of the most common is that of a short overload following continuous loading. The following simplified formula, 1-K, an extension of Formula 1-J, may be used to calculate the junction temperature rise at the end of the overload:

$$\Delta T_{J(JA)} = \left(\frac{t_p}{\tau} P_{TM(SS)} + P_{B(AV)}\right) + (R_{\theta JC} + R_{\theta CH} + R_{\theta HA}) + P_{TM(SS)} \left(1 - \frac{t_p}{\tau}\right) Z_{\theta}(t_p) + \frac{t_p}{\tau} (P_{TM(OL)} - P_{TM(SS)})$$

$$Z_{\theta}(OL) + (P_{TM(OL)} - P_{TM(SS)}) \left(1 - \frac{t_p}{\tau}\right) Z_{\theta}(t_p) \quad (1-K)$$

Where:

$P_{TM(SS)}$ = peak steady-state, on-state power loss (prior to overload).

$P_{TM(OL)}$ = peak on-state power loss during overload.

$Z_{\theta}(OL)$ = transient thermal impedance of thyristor for overload period.

(The other terms are the same as those given for Formulas 1-H and 1-J.)

Care should be taken in determining the transient thermal impedance for the overload period. A transient thermal impedance curve for the thyristor mounted on an infinite heat sink may be used only over the range where the transient thermal impedance is no more than ninety percent of the maximum value given on the curve. For longer overloads, a transient thermal impedance curve for the device mounted on the heat exchanger actually being used is required. Two such curves are given in Figure 1-18 for the thyristor used in the example.

If a temperature rise margin, $\Delta T_{J(OL)}$, is provided for overloads when determining the steady-state current loading of the thyristor, the repetitive overload which can be imposed can be found by solving Formula 1-L for $P_{TM(OL)}$, the peak on-state power loss during the overload period.

$$\Delta T_{J(OL)} = (P_{TM(OL)} - P_{TM(SS)}) \left[\frac{t_p}{\tau} Z_{\theta}(OL) + 1 - \frac{t_p}{\tau} Z_{\theta}(t_p) \right] \quad (1-L)$$

Having found the maximum peak on-state power loss permitted during the overload period, the average current which can be carried during the overload period may be calculated as before.

SCR Dynamic Characteristics

Triggering

The simplest means for triggering a controlled rectifier is to apply a positive dc potential between gate and cathode. This is the operating condition used to determine compliance with published specifications for maximum gate current and voltage required to trigger all units of a given type. The designer quickly learns that there are a number of considerations which require the application of greater current and voltage to the gate in order to achieve successful device operation in a practical piece of equipment.

Fortunately, in modern devices, the maximum gate current and voltage which may be applied greatly exceed the values required to trigger under dc conditions. This is illustrated in Figure 1-22, which shows the gate characteristics for a 70 ampere (average) device. It can be seen that the designer has a large region within which to operate where the gate can be driven harder than the amount barely required to turn the device on and yet not be driven beyond its maximum peak power rating. In order to avoid exceeding the maximum continuous power rating of the gate when applying a high peak signal, it must be applied as a pulse and not continuously.

For reasons of economy, both to reduce the size of components used to build the gate excitation circuit and to reduce the power consumed

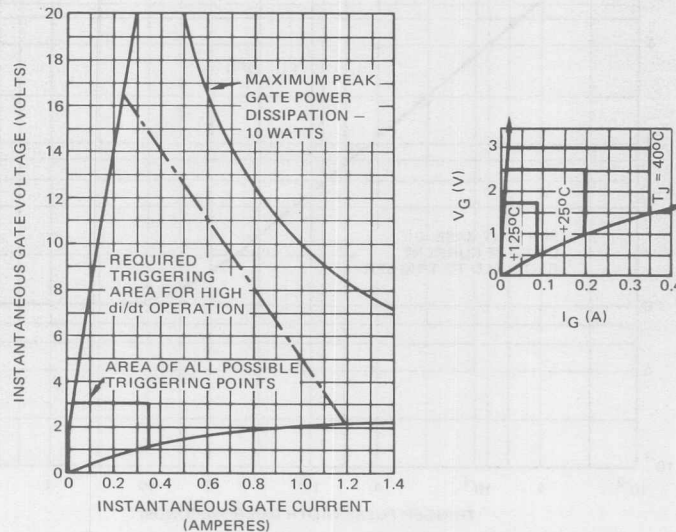


Figure 1-22. Gate Characteristics

by this circuit, a relatively short pulse is often applied to the gate, rather than a long pulse or a continuous dc signal. As pulse width is reduced, it is found that the peak current and voltage required to trigger a given device becomes greater. This effect is most noticeable for pulse widths shorter than 15 microseconds, as shown in Figure 1-23. For such short pulses, it can be seen that essentially a fixed electrical charge is required to trigger the controlled rectifier.

A controlled rectifier does not turn on "all at once." When first the gate is pulsed, there appears to be no increase in current flow. This period is known as the delay time, (t_d), and usually is shorter than one microsecond. Current then starts to flow through the wafer in a small region near the gate lead, then spreads throughout the silicon wa-

fer. This second period, during which the current through the device increases, from 10% to 90%, is known as the rise time (t_r). It varies from a few to more than 10 microseconds, being longer for the larger controlled rectifiers.

This action is sufficiently fast so that any controlled rectifier will be turned fully on long before a sine wave of current at a conventional power frequency (up to 400 Hz) has reached its peak. On the other hand, when a controlled rectifier is used to switch high amplitude current pulses, large currents can flow before turn-on is complete. With the current confined to a small portion of the total semiconductor volume, the forward voltage will be greater than the published value, and the additional heat generated by large currents flowing at that time has been known to cause a

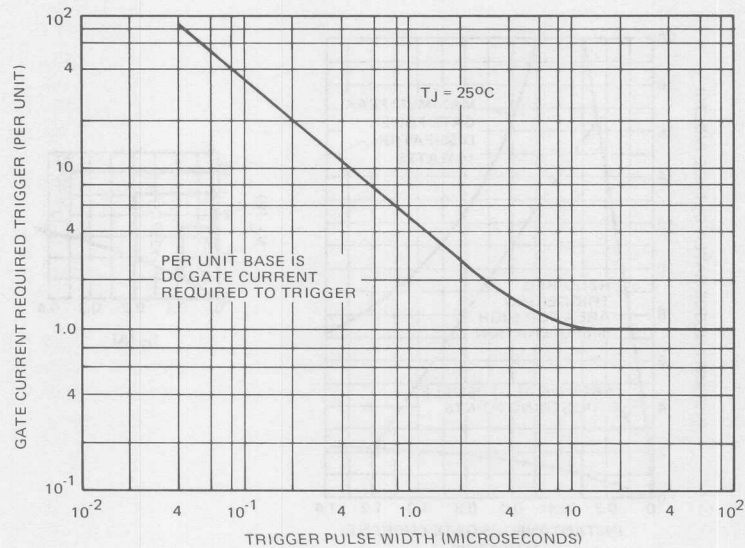


Figure 1-23. Gate Current to Trigger

local failure of the semiconductor material near the gate terminal.

There are several remedial steps which the circuit designer can take in overcoming these limitations:

- A. Increase the magnitude of the current pulse carried by the gate. This increases the number of carriers injected into the semiconductor material. But published gate current and voltage limits must not be exceeded.
- B. Add a self-saturating inductor in series with the controlled rectifier. This should require from 10 to 50 microseconds to saturate, during which time the controlled rectifier is being turned on by the small current which flows through the reactor before it saturates.
- C. Select controlled rectifiers which are comparatively fast in turn-on action. (IR's ACE gate SCRs fall into this category.)
- D. Use several smaller controlled rectifiers in place of one larger one, in one of two arrangements:
 - 1) Several controlled rectifiers connected in parallel.
 - 2) Several controlled rectifiers connected in series.

In the arrangement described in D1 all the controlled rectifiers would be triggered from a single gate pulse generator, each through a "ballast" resistor in series with its gate. In D2, the circuit would have to be redesigned to operate at a higher voltage and a lower current. All gates could be triggered simultaneously using a multi-secondary pulse transformer, or opto-electronic gating technique. A "sympathetic" ("slave") arrangement could also be used, so that triggering one controlled rectifier would cause the others to be triggered with a minimum of delay.

For most controlled rectifier types only a typical value of turn-on time (the sum of $t_d + t_r$) is given. If units having a specified maximum turn-on time are required, standards for measuring this time are needed. Turn-on time is affected by the magnitude of the triggering pulse, the magnitude of the voltage applied between anode and cathode, the junction temperature, and the inductance in the test circuit.

A check on the magnitude of the inductance in the test circuit can be made by simultaneously observing anode-to-cathode current and inverted anode-to-cathode voltage on a fast-writing cathode ray oscilloscope. When the two traces are adjusted to overlap at beginning and end, they will overlap throughout the turn-on interval if the circuit is purely resistive. The effect of the inductance is to delay the rise of current, and speed up the fall of voltage. From this it is evident that turn-on time should not be measured by observing the fall in voltage, as this can give times which are too short.

It is difficult to eliminate circuit inductance completely; on the other hand, a small amount should not seriously impair the accuracy of the turn-on time measurement.

di/dt

When an SCR is triggered, it does not immediately go into full conduction, as discussed in the section on Triggering. Current flow begins in a relatively small area; how small depends upon how the SCR is made, and in many units, how strong a signal is applied to the gate.

In a conventional SCR having a single gate, on-state current is initi-

ated in a small spot near the gate and turn-on action spreads, as indicated in Figure 1-24, at a rate which is roughly 0.1 mm per microsecond. Using this value, the time required to fully switch on SCRs of various current ratings can be calculated (Figure 1-25).

The time required to turn high current rated SCRs fully on is far longer than the published "turn-on time" of most devices, which is usually in the order of five microseconds. This is the result of the definition of turn-on time, which is specified as the length of time after

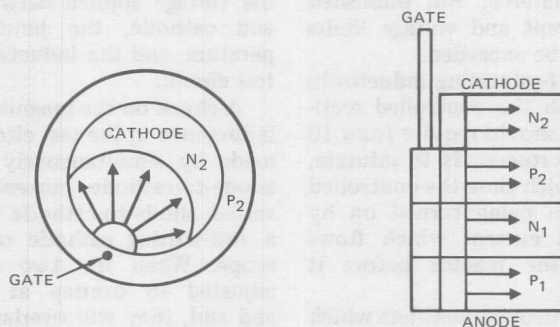


Figure 1-24. Turn-On Action

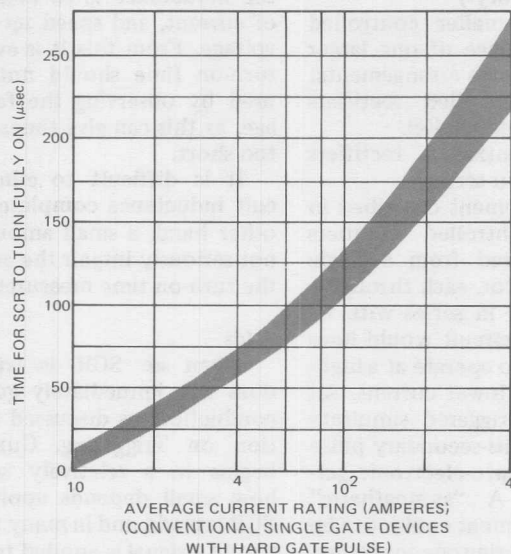


Figure 1-25. Time to Turn-On

the appearance of the gate trigger pulse that is required for the voltage across the SCR to decrease to ten percent of its initial value. If the SCR is switched on with 500 volts, it will only partially be turned on when this voltage drops to 50 volts, since when fully turned on, its on-state voltage will be in the order of two volts. Thus, the turn-on time rating of a power SCR gives very little information about performance throughout the entire turn-on interval.

The stress on an SCR is particularly severe during the first few microseconds of current flow. An excessive rate-of-rise of on-state current (di/dt) will cause device failure.

Two di/dt ratings exist in the industry; the non-repetitive rating, determined from a test lasting 300 pulses, and the repetitive rating, which is based on results of a 1000-hour life test. The repetitive di/dt rating will often be about 33 percent of the non-repetitive rating.

In a conventional gate SCR, the di/dt rating is affected by the magnitude of the gate drive; trigger pulses of over one ampere in amplitude and with rise times of $0.1 \mu\text{sec}$ and less result in an improvement in di/dt capability.

A typical triggering circuit is shown in Figure 1-26. In many cases, where the load is inductive and most certainly when the load consists of a dc or ac motor, it is necessary to apply a gate signal for the full time the SCR is to remain in the conducting state. For low frequency operation of thyristors, this requirement can be very difficult to achieve without incorporating considerable complexity and high cost in the triggering circuit. For instance, in the case of a large power supply constructed as a magnetic supply for a plasma arc generator, it was necessary to drive six SCRs in parallel per leg in a three-phase, full converter (bridge) configuration. Since the load was inductive, it was necessary to supply

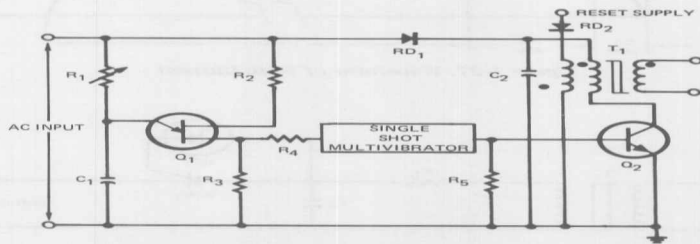


Figure 1-26. Typical Triggering Circuit

the gating signals over about 140° of the half cycle. Since this type of load also subjects the SCR to high inrush currents, it was necessary to provide the gating signals with a sharply rising leading edge to a relatively high level. The desired short circuit gate current is shown in Figure 1-27.

Since these gate signals had to be electrically isolated, the master driving circuit contained a gating transformer. To design such a transformer capable of the leading edge rise time shown in Figure 1-27, and yet with sufficient volt-second capacity to support the gate signal for 10 msec, is extremely difficult. The circuit shown in Figure 1-28 was incorporated in order to accomplish the desired gate signal.

The cost involved in producing the leading edge of the pulse was moderate. Even with this added cost and complexity, the allowable di/dt in the circuit was less than 150 amperes per microsecond. The power SCR with IR's ACE geometry makes this circuit complexity unnecessary. This type of thyristor is capable of withstanding non-repetitive inrush currents of 800 amperes per microsecond with a gate current requirement of 100 mA and a gate current rise time of 2 μ sec. If one uses the suggested figure of merit for turn-on capability of an SCR (as given in Formula 1-M) and compares conventional SCRs to the ACE type of device, the ACE device is found to be more than 1000 times superior to conventional types of power thyristors.

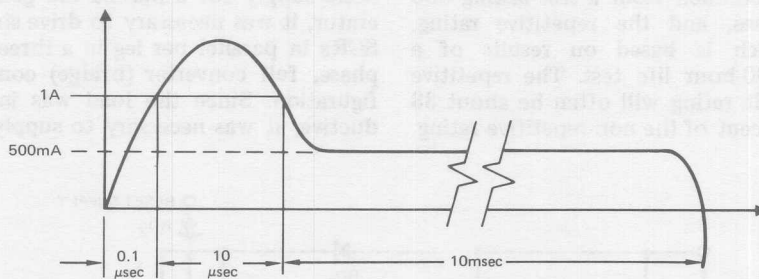


Figure 1-27. Waveform of Gate Current

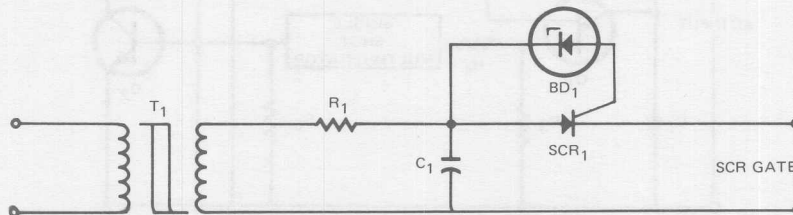


Figure 1-28. Addition to Triggering Circuit

$$\text{F.M.} = \frac{di/dt \cdot t_r}{IGM} \quad (1-M)$$

Where:

di/dt = Maximum allowable rate-of-rise of inrush current.

t_r = Required gate signal rise time.

IGM = Required gate current for high di/dt capability.

In the past, the ability of a thyristor to turn on rapidly has been limited not only by the gate drive requirements, but also by the necessary trade-offs used to achieve the other desirable characteristics in the device. Making a high voltage device demanded the use of high resistivity silicon, which decreased the spreading velocity of the turn-on action. The requirement for high dv/dt dictated the use of emitter shorting, which diminished the effectiveness of the gate to turn the device on efficiently. Now with the geometry available in the ACE family of thyristors, these trade-offs are no longer a consideration. It is possible to incorporate all of these desirable features in a single thyristor with high manufacturing yields and ultimately low cost to the user. Considering the cost savings realizable by reduction in driving circuit complexity and di/dt suppression components in the power circuit, and the availability of full-parameter production devices, the economic practicality of many circuits is accomplished, where it was strictly conjecture before.

The di/dt rating is also affected by the magnitude of the off-state voltage prior to switching the device on. More power will be dissipated in the silicon wafer when the device is switched on from a higher

voltage. In addition, devices made for the higher voltage ratings will be made with thicker silicon of higher resistivity, which means more losses.

Throughout the time an SCR is turning fully on, internal losses will be greater than stipulated by the published power loss curves for the device (which are based on fully turned-on operation), due to the higher current density in the portion of the silicon wafer which is turned on at any instant. In addition to being the cause of failure during initial turn-on (di/dt failure), extra losses during the entire turn-on period contribute to average junction heating and require that the device be operated at a lower current level than would otherwise be expected.

This effect becomes more pronounced as operating frequency is increased, because the device is turned on more frequently in a given period of time. It is also more pronounced as the current rating of the SCR is increased, if this is done by increasing the size of the silicon wafer, since the time required for current flow to equalize throughout the wafer becomes greater.

The action of a conventional thyristor during turn-on may be seen in Figure 1-29. Here, the thyristor is conducting an essentially rectangular current wave. The curve of instantaneous power loss shows the internal power being dissipated, which is, at any instant, the product of the current through the device and the voltage across it.

Turn-on losses in a conventional thyristor can be reduced by using a "soaking reactor," which delays the appearance of the main power pulse for a short time, such as 10 microseconds, following the gate trigger

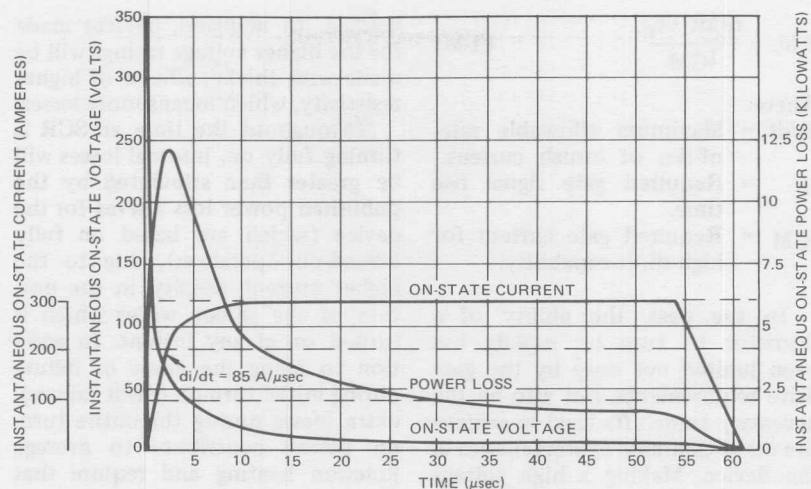


Figure 1-29. Values During Turn-On

pulse. During this time, the reactor, and possibly a resistor in parallel with it, permits enough anode current to flow to cause propagation of the turn-on action within the thyristor. When the reactor saturates, permitting full load current to flow, the power loss is reduced because of the larger area of the silicon wafer that is at that instant turned on. Figure 1-30 shows how turn-on losses in one thyristor were reduced as soaking time was increased.

Very often, snubber circuits, consisting of a resistor and a capacitor in series, are used across the thyristor to absorb transient voltages. Because of the low inductance in a typical snubber circuit, severe di/dt can be imposed at the very instant of turn-on. This can cause additional switching losses and even a thyristor failure. The effect of changing the value of R in a snubber across one particular thyristor is shown in Figure 1-31. A value of R

must be used that is high enough to prevent excessive di/dt in the thyristor, but at the same time, will not nullify the effect of the capacitor, rendering the snubber network useless.

Turn-on of large area devices can be speeded up by simultaneously triggering the device at more than one point. The calculated effect of adding a second gate to a device rated 110 amperes RMS is shown in Figure 1-32. Complete turn-on is seen to occur in 75 microseconds instead of in 105. In addition, since current flow is initiated at two points instead of one, the di/dt capability of the device is improved by a factor of two. Substitution of this device for one having a single gate, but otherwise the same, in an inverter operating at several thousand hertz, will permit a significant increase in output power at the same case temperature.

This discussion of turn-on losses has been concerned with thyristors

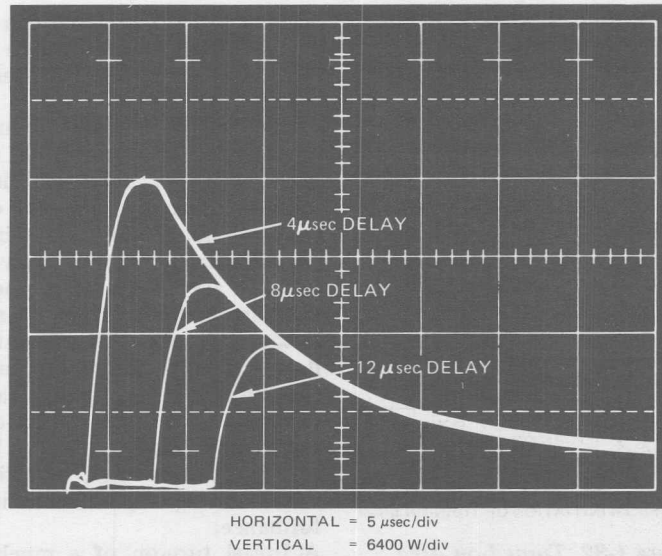


Figure 1-30. Power Loss During Turn-On

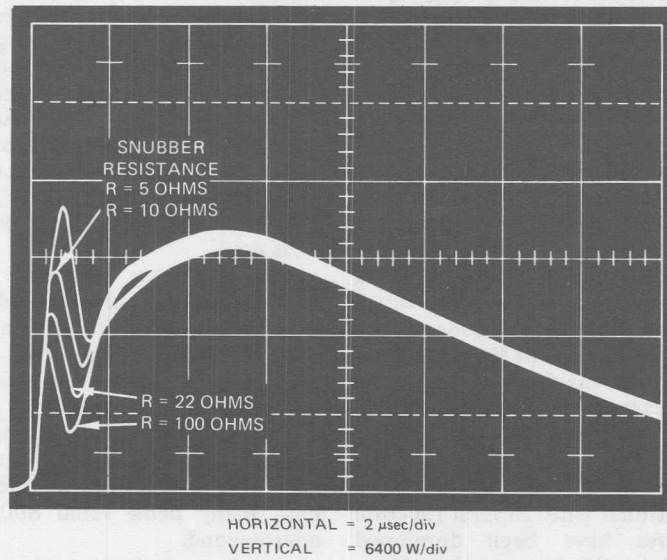


Figure 1-31. Turn-On Power Loss Snubber Resistance

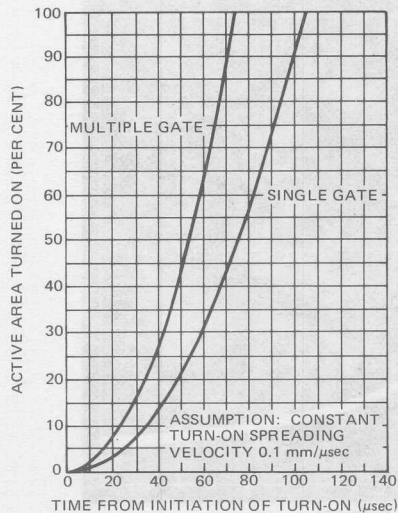


Figure 1-32. Turned-on Area

having one or two conventional gates located at the periphery of the junction assembly. A single gate located at the center of the junction assembly is sometimes used. This configuration would appear to offer superior initial turn-on performance and a shorter propagation time to full conduction. In actual practice, devices made this way behave about the same as those having one gate located at the edge of the wafer because of slight non-uniformities in the junctions favoring current propagation in some directions from the center over others.

The ACE class of thyristors employs a mechanism whereby the anode current is caused to flow in a special geometry during turn-on, which results in an enhancement of the turn-on action initiated by a conventional gate. Several junction structures have been developed which have this regenerative effect, whereby the load current, when it

begins to flow, causes a much larger region to be turned on than could be turned on by one or even two conventional gates.

This action can be understood by referring to Figure 1-33, which shows the geometry used in one such thyristor. A single gate of the conventional type is seen to initiate current through an auxiliary cathode. To accomplish this, since the auxiliary cathode is not connected to the external circuit, current must flow across the narrow gap between the auxiliary and main cathode regions. This causes turn-on of the main cathode along the length of the narrow gap, resulting in the following improvement in performance:

- A. Initial turn-on of a much larger portion of the junction than even a multiple gate is able to turn on, even with high gate drive.
- B. Reduction in time required for the total junction of a large area thyristor to enter into conduction of the principal current.
- C. Reduction in gate drive needed, because the above action takes place, even though a gate trigger pulse of moderate current amplitude and relatively long rise time is used.

Thyristors are available which make use of the main cathode current to initiate gating action along straight or circular segments of the main cathode region, or at a large (10 or more) number of points around the main cathode periphery. They are all capable of providing very high non-repetitive di/dt ratings, many being rated 800A per microsecond.

As all such devices rely on the regenerative effect caused by a rap-

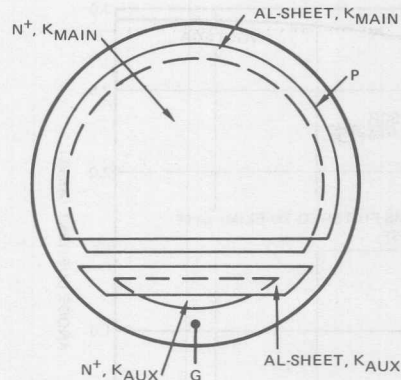


Figure 1-33. Auxiliary Cathode Structure

idly rising load current flowing through special geometries, their performance is not improved by the addition of a soaking reactor. They are able to handle higher snubber currents and to control more usable amounts of power than conventional single gate or multiple gate thyristors when switching from high blocking voltages and at high repetition rates.

There is a small penalty to pay for the improved turn-on action of these devices with special cathode geometries. The active main cathode area is not as large as it is in a conventional thyristor having the same size junction assembly. Except in the case of devices having very complex cathode geometries, designed for operation well above 10 kHz, this reduction in active area is small. It does result in a slight reduction in the low frequency current rating. This is more than offset by the considerable increase in current rating at frequencies of 1 kHz and above, that these special thyristors exhibit as compared with conventional gate units.

dv/dt

Silicon controlled rectifiers exhibit a tendency to switch from the off-state to the on-state when the anode-to-cathode voltage is abruptly increased. This tendency is a function of the rate-of-rise of the voltage. The rate which switches the controlled rectifier into conduction is known as the critical rate-of-rise, or more simply, " dv/dt ."

The mechanism for this phenomena can be explained in terms of the internal capacitance which the controlled rectifier exhibits. When the voltage across the controlled rectifier is increased, charges flow through the controlled rectifier in a manner analogous to the charging current of a capacitor. The greater the rate-of-rise of the applied voltage, the greater will be this flow of charges. As the rate-of-rise is increased, sufficient charges will eventually flow to act in the same manner as the charges which are injected when the gate is energized with a positive potential with respect to the cathode, and the controlled rectifier will turn on. Figure 1-34 shows the rate-effect-caused current due to a sharply rising voltage on a 740A RMS SCR.

The magnitude of rate-effect-caused current should not be confused with latching and holding currents, more familiar on SCR data sheets. At first glance, one might wonder how a device would remain in the blocking state with 2.1A flowing anode-to-cathode, since latching currents are typically less than a single ampere. The important difference lies in the relative current densities involved. Rate effect currents are rather uniformly distributed over the entire semiconductor wafer, as is the blocking

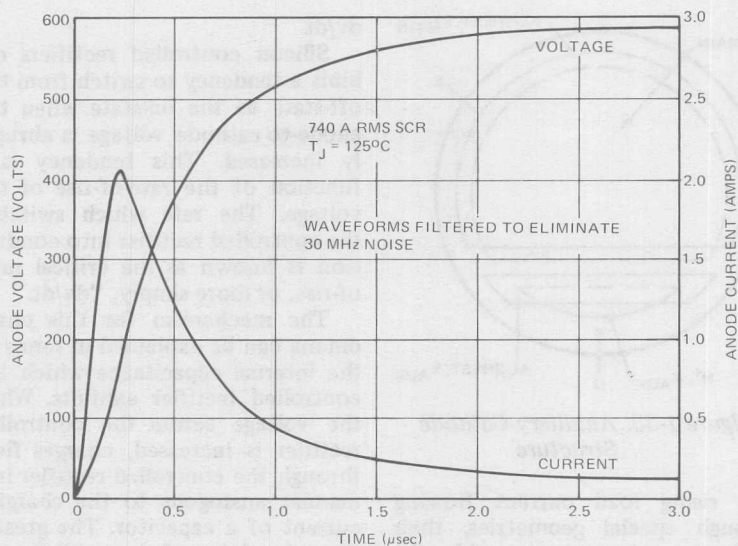


Figure 1-34. Rate Effect Current

junction capacitance, while latching and holding currents are subject to low level injection phenomena, where only limited crystal domains are involved in conduction. Since internal device gain is a function of active region current densities, internal gain during dv/dt excursions will be held below unity even though total currents are in excess of conventional latching currents.

A quantitative specification of a controlled rectifier's ability to resist rate effect turn-on is the dv/dt rating. A convenient definition employs an exponentially rising off-state voltage waveform. Definitions of terms are presented in Appendix I. The dv/dt is defined as shown in Formula 1-N.

$$dv/dt = \frac{(0.632) V_{DM}}{\tau} \quad (1-N)$$

Where:

τ = time constant of the exponential (equals RC)

V_{DM} = peak anode voltage.

In the testing of controlled rectifiers, the critical rate-of-rise of principal voltage is encountered under two different conditions. It is important to keep these two considerations distinctly separated to avoid ambiguity when discussing or specifying controlled rectifier characteristics.

The first test condition is with the controlled rectifier deenergized, and the off-state voltage is abruptly applied to it. This is the test condition for what is known as the critical rate-of-rise of applied off-state voltage (dv/dt).

There was, at one time, considerable discussion in the industry as to whether this voltage should be applied in a straight line or in an

exponential manner, and if it is applied in an exponential manner, whether the rate-of-rise should be defined as the initial rate-of-rise or some other, lower value. This lower value would take into account the fact that the voltage curve is exponential, and, therefore, the initial rate-of-rise does not exist throughout the entire time that the voltage is rising to its ultimate value.

The major controlled rectifier manufacturers have accepted as standard conditions that the applied off-state voltage should rise exponentially to a value equal to the minimum breakover voltage rating (V_{BO}) or repetitive peak off-state voltage rating (V_{DM}) of the device under test, and that the rate-of-rise shall be defined as the average rate-of-rise during the first time constant of the exponential voltage curve (τ). This situation is obtained by charging a capacitor, C , through a resistor, R , and is depicted in Figure 1-35. It can be seen that the voltage at the end of the first time constant is 63.2% of the total voltage applied to the device. The rate-of-rise of applied forward voltage, dv/dt , is defined in Formula 1-N.

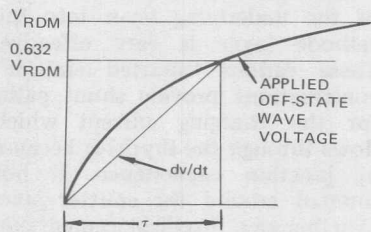


Figure 1-35. Critical dv/dt Test Waveforms

The second test condition where the rate-of-rise of off-state voltage is encountered is in the test for turn-off time of a controlled rectifier. The turn-off time of a controlled rectifier depends in part upon the rate at which the off-state voltage is reapplied after the principal current has been interrupted and a time has elapsed during which the controlled rectifier regains its blocking ability. If the principal voltage is reapplied in a gradual manner, it may be reapplied sooner than if it is applied in a steeply rising manner. Of course, there is a limit to how rapidly the voltage can be reapplied, because the controlled rectifier cannot withstand a rate-of-rise greater than that which it can handle when the voltage is applied with the rectifier initially de-energized. Thus, the rate-of-rise of reapplied off-state voltage, which is a condition of the turn-off time test, is generally considerably less than the critical rate-of-rise of applied off-state voltage for the device under test.

In the test procedure which has been adopted by the industry for measuring the turn-off time of controlled rectifiers, the reapplied off-state voltage is forced to rise in a linear fashion until rated repetitive peak off-state voltage or some stated portion of it is reached. In this case, the rate-of-rise is defined as the slope of the voltage, since it is a straight line.

To summarize, for controlled rectifiers, two critical rates of application of principal voltage exist. One is the critical rate-of-rise of applied off-state voltage with the device initially de-energized. The other is the rate-of-rise of reapplied off-state voltage which defines the

end of the turn-off period and hence is a parameter in the measurement of turn-off time.

When a capacitor is charged from an infinite dc source through a resistor, the voltage across the capacitor will reach 63.2% of the source voltage in one time constant (the product of the capacitance being charged and the series resistance). This is derived from the Formula 1-P.

$$V = V_O (1 - e^{-\frac{t}{RC}}) \quad (1-P)$$

Where:

V_O = voltage to which the capacitor ultimately charges (the source voltage).

At the end of the first time constant $t = RC$ and therefore, $-t/RC = -1$. The equation becomes Formula 1-Pa.

$$V = V_O (1 - e^{-1}) = V_O (1 - 1/e) \quad (1-Pa)$$

Since $e = 2.718$, $1/e = 0.368$ and $1 - 1/e = 0.632$.

Thus, the average rate-of-rise at the end of the first time constant = $0.632 V_O/RC$.

The rate-of-rise, at the first instant the voltage is applied to the circuit, can be found by differentiating the basic equation given above at $t = 0$. This calculation reveals that the initial rate-of-rise is V_O/RC , which is $1/0.632$ or 1.58 times the average rate-of-rise at the end of the first time constant.

In many practical circuits using SCRs, they are subjected to a steady potential upon which the rising voltage pulse is superimposed. Such an initial bias will enhance the critical dv/dt capability of the device, as compared with its perform-

ance when subjected to a voltage pulse having the same dv/dt , but rising from zero.

The ability of a given part to withstand an exponential dv/dt pulse is enhanced by reducing the junction temperature and also by reducing the voltage applied at the end of the exponential ramp. The general effect of varying these two parameters on critical applied dv/dt is shown in Figure 1-36, based on the observed behavior of a 470 ampere RMS, 1300 volt, epitaxial SCR. This part exhibited a fairly low dv/dt at maximum rated voltage and junction temperature, so that the higher dv/dt ratings observed at reduced voltage and current levels were not so high that they could not be measured.

It is also possible to improve the ability of an SCR not to trigger when the anode voltage is suddenly increased by providing a conducting path between the cathode (or emitter) layer of the device and the layer immediately below it. (These layers can be identified in the exaggerated thyristor cross section shown in Figures 1-2 and 1-24.) This conducting path can readily be provided around the outside of the cathode region. In high current devices which have large cathode areas, a pattern of small intrusions of the underlying layer into the cathode layer is very effective. These various "shorted emitter" constructions provide shunt paths for the charging current which flows through the thyristor because of junction capacitance. If not shunted around the emitter junction this way, this displacement current will very likely trigger the SCR on when the anode voltage suddenly increases in the positive direction.

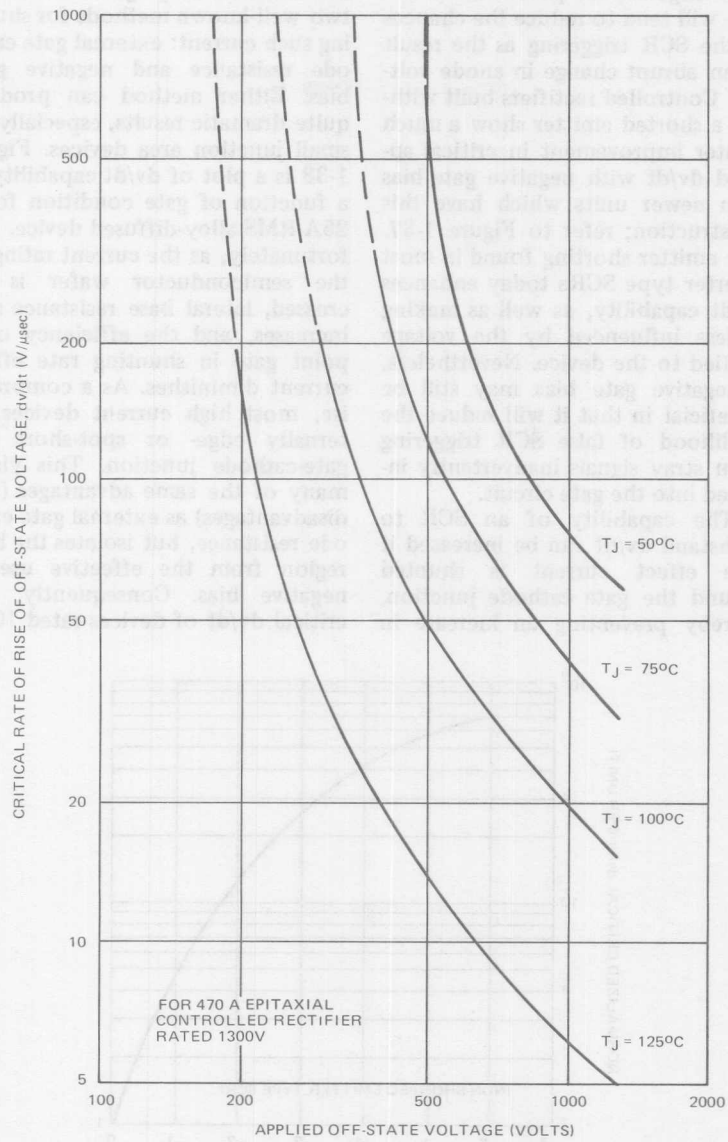


Figure 1-36. Critical Rate-of-Rise of Applied Off-State Voltage Vs. Applied Off-State Voltage

A negative dc potential on the gate will tend to reduce the chances of the SCR triggering as the result of an abrupt change in anode voltage. Controlled rectifiers built without a shorted emitter show a much greater improvement in critical applied dv/dt with negative gate bias than newer units which have this construction; refer to Figure 1-37. The emitter shorting found in most inverter type SCRs today enhances dv/dt capability, as well as making it less influenced by the voltage applied to the device. Nevertheless, a negative gate bias may still be beneficial in that it will reduce the likelihood of false SCR triggering from stray signals inadvertently induced into the gate circuit.

The capability of an SCR to withstand dv/dt can be increased if rate effect current is shunted around the gate cathode junction, thereby preventing an increase in

the internal loop gain. There are two well-known methods for shunting such current: external gate cathode resistance and negative gate bias. Either method can produce quite dramatic results, especially on small junction area devices. Figure 1-38 is a plot of dv/dt capability as a function of gate condition for a 25A RMS alloy-diffused device. Unfortunately, as the current rating of the semiconductor wafer is increased, lateral base resistance also increases, and the efficiency of a point gate in shunting rate effect current diminishes. As a compromise, most high current devices internally edge- or spot-short the gate-cathode junction. This yields many of the same advantages (and disadvantages) as external gate cathode resistance, but isolates the base region from the effective use of negative bias. Consequently, the critical dv/dt of devices rated 100A

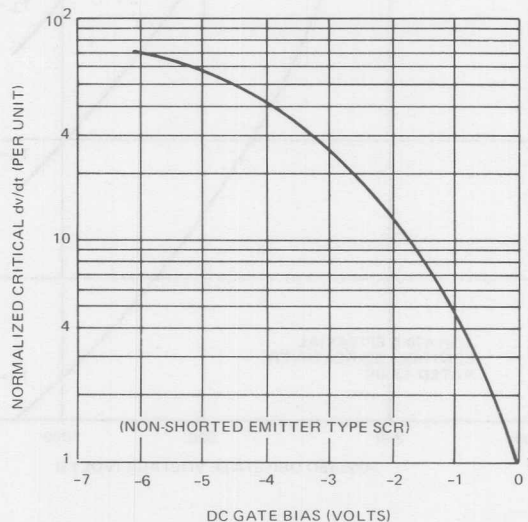
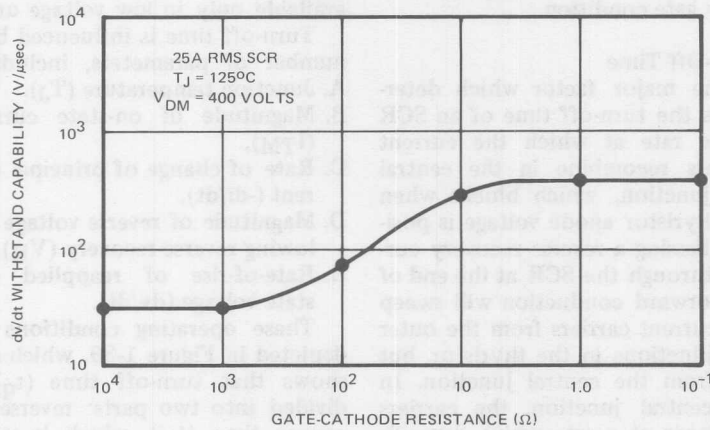
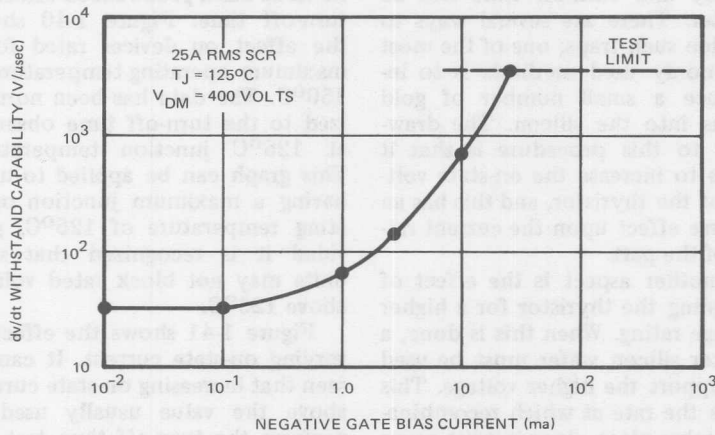


Figure 1-37. Critical Applied dv/dt Vs. Gate Bias



(a) GATE-CATHODE RESISTANCE



(b) NEGATIVE GATE CURRENT

Figure 1-38. Improvement of dv/dt of 25A RMS SCR with Application of Gate Bias Resistance and Current

RMS and above is largely unaffected by gate condition.

Turn-Off Time

The major factor which determines the turn-off time of an SCR is the rate at which the current carriers recombine in the central P-N junction, which blocks when the thyristor anode voltage is positive. Passing a reverse recovery current through the SCR at the end of the forward conduction will sweep out current carriers from the outer two junctions in the thyristor, but not from the central junction. In the central junction, the carriers disappear at a rate which depends upon the characteristics of the silicon. If this silicon contains dopants or dislocation centers which can serve as "traps" for the carriers, recombination will proceed more rapidly and turn-off time will be shorter. There are several ways to provide such traps; one of the most commonly used methods is to introduce a small number of gold atoms into the silicon. The drawback to this procedure is that it tends to increase the on-state voltage of the thyristor, and this has an adverse effect upon the current rating of the part.

Another aspect is the effect of designing the thyristor for a higher voltage rating. When this is done, a thicker silicon wafer must be used to support the higher voltage. This slows the rate at which recombination takes place, since it must occur in a larger volume of silicon. Thus, it is much easier to build very fast low voltage thyristors in the range of 600 volts and below, than it is to build units having the same turn-off time but able to block 1000 or 1200 volts. It is generally found

that very fast turn-off times are available only in low voltage units.

Turn-off time is influenced by a number of parameters, including:

- A. Junction temperature (T_J).
- B. Magnitude of on-state current (I_{TM}).
- C. Rate of change of principal current ($-di/dt$).
- D. Magnitude of reverse voltage following reverse recovery (V_R).
- E. Rate-of-rise of reapplied off-state voltage (dv/dt).

These operating conditions are depicted in Figure 1-39, which also shows that turn-off time (t_q) is divided into two parts: reverse recovery time (t_{rr}), which is much the same as reverse recovery time of a rectifier diode, and gate recovery time (t_{gr}).

Varying junction temperature above and below the maximum rated value has a pronounced effect on turn-off time. Figure 1-40 shows the effect on devices rated for a maximum operating temperature of 150°C. The data has been normalized to the turn-off time observed at 125°C junction temperature. This graph can be applied to units having a maximum junction operating temperature of 125°C, provided it is recognized that such units may not block rated voltage above 125°C.

Figure 1-41 shows the effect of varying on-state current. It can be seen that increasing on-state current above the value usually used to perform the turn-off time test has only a minor effect on turn-off time. This curve is for the condition of constant junction temperature. At high current levels, the accompanying heating of the junction will cause an apparent increase in turn-off time.

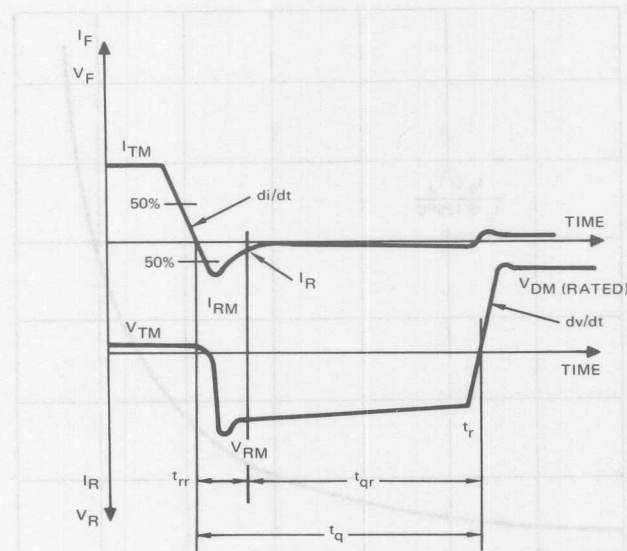


Figure 1-39. SCR Turn-Off Time Waveforms

The rate-of-change of principal current at the end of the on-state current pulse affects turn-off time, because of its effect on reverse recovery time. The higher the rate of change, the shorter the reverse recovery time. Turn-off time is shortened to the same extent that reverse recovery time is reduced.

The magnitude of reverse voltage applied to the SCR during the turn-off interval will influence turn-off time. A reverse voltage is required to produce reverse recovery current. Varying the reverse voltage will vary the rate of change of this current, which affects turn-off time as noted above. In addition, increasing the reverse voltage during the period following recovery will cause turn-off time to be reduced. This effect is most noticeable for reverse voltages up to 25 to 30 volts. Greater reverse voltage causes no appreciable further reduction in turn-off time.

In some inverter circuits, a diode is connected in anti-parallel with the SCR. This has the effect of clamping the reverse voltage to the forward voltage of the diode. Turn-off time under this condition may be considerably longer than under standard test conditions, where considerably more reverse voltage is applied. The amount that turn-off time changes as a result of the diode clamp is not a fixed percentage of standard turn-off time. To assure obtaining devices with the desired maximum turn-off time under this condition, they should be individually tested with an appropriate rectifier diode connected in anti-parallel, which can be done quite readily. During this test, the leads to the diode should be kept very short, to prevent lead inductance from delaying the clamping effect of the diode and nullifying its effect on the turn-off time.

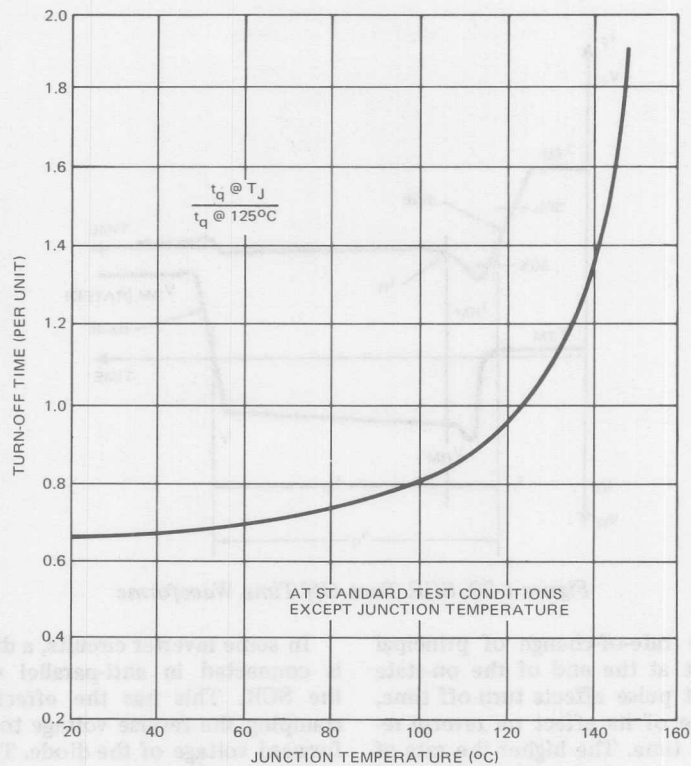


Figure 1-40. Temperature Turn-Off Time Vs. Junction

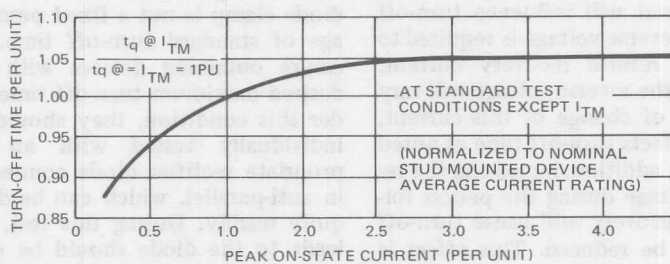


Figure 1-41. Turn-Off Time Vs. On-State Current

Increasing the rate-of-rise of re-applied off-state voltage also has an adverse effect on turn-off time. This is shown in Figure 1-42. Re-applied dv/dt must be less than the critical applied dv/dt capability of the SCR, or else the SCR will be triggered by dv/dt alone and will appear never to turn off.

SWITCHING LOSSES

Throughout the time an SCR is turning fully on, internal losses will be greater than stipulated in the published power loss curves for the device, which are based on fully turned on operation. In addition to being the cause of failure during initial turn-on (di/dt failure), losses during the turn-on period contribute to average junction heating and require that the device be operated at a lower current level than would otherwise be expected.

This effect becomes more pronounced as operating frequency is increased, because the device is turned on more frequently in a

given period of time. It is also more pronounced as the current rating of the SCR is increased, if this is done by increasing the size of the silicon wafer, since the time required for current flow to equalize throughout the wafer will increase. Reduction of turned-on area due to propagation rate limitations increases current densities and, therefore, power losses. Figure 1-29 shows waveforms during turn-on of a controlled rectifier switching from 400 volts. The maximum anode current is 300 amperes, with the leading edge rising at a rate of 85 A/ μ sec. Superimposed on this figure is the instantaneous power loss. The energy dissipation is approximately 180 kW- μ sec per pulse. Compare this to 76 kW- μ sec per pulse if the device were initially fully turned on. At high frequencies and short on-state current pulses, the power dissipation of a device can be 3 to 10 times the 60 to 400 Hz catalog values. Therefore, the turn-on losses of devices intended for high fre-

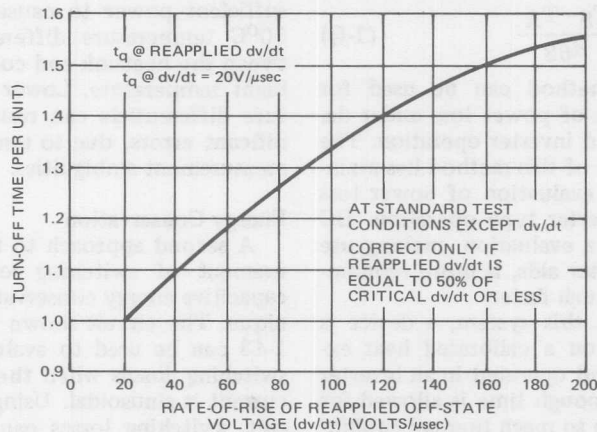


Figure 1-42. Turn-Off Time Vs. Reapplied dv/dt

quency applications are of paramount importance when trying to design a practical system.

There are several methods by which switching losses may be measured:

- A. Comparison of case temperatures under dc and switching test conditions.
- B. Energy conservation.
- C. Visual readout of current and voltage followed by mechanical integration of V and I vs. time plot.
- D. Electronic analog multiplier.

DC Method

Turn-on losses may be evaluated thermally using a direct current comparison method. The method depends upon the linear relation between device case temperature, average power loss, and properly chosen system thermal impedance. Mounting a device on a heat exchanger (sink) of known thermal resistance at a known cooling rate allows the calculation of device power dissipation by Formula 1-Q.

$$P_{(AV)} = \frac{T_S - T_A}{R\theta_S} \quad (1-Q)$$

This method can be used for evaluation of power loss under dc, 60 Hz, and inverter operation. The usefulness of this method lies mainly in the evaluation of power loss under inverter type operation. DC and 60 Hz evaluation, making use of computer aids, is more economical and much faster.

To use this system, a device is mounted on a calibrated heat exchanger and operated in an inverter system. Enough time is allowed for the system to reach thermal equilibrium. The average power dissipation is then calculated using Formula

1-Q. In using this equation, it must be kept in mind that the *average* power loss includes turn-on, blocking, recovery, and gate losses. However, for devices rated 70 amperes and larger, blocking and gate losses are a minor portion of total losses. The average total switching loss (including recovery loss) then becomes Formula 1-R.

$$P_{(AV)} \text{ (total switching) } = P_{\text{Turn-on}} + P_{\text{Recovery}} + (P_{\text{Gate}} + P_{\text{Blocking}}) \quad (1-R)$$

Then, using (1-Q) and (1-R), and considering gate and blocking losses as being very small, Formula 1-T is the result.

$$P_{(AV)} \text{ (total switching) } = \frac{P_{\text{Turn-on}} + P_{\text{Recovery}}}{R\theta_S} \quad (1-T)$$

This method of determining total switching losses requires an inverter to simulate operating conditions and a dc current source of sufficient power to cause a 35 to 50°C temperature differential between the heatsink and coolant ambient temperature. Lower temperature differentials can result in significant errors, due to temperature measurement ambiguities.

Energy Conservation

A second approach to the measurement of switching losses is a capacitive energy conservation technique. The circuit shown in Figure 1-43 can be used to evaluate SCR switching losses when the on-state current is sinusoidal. Using this circuit, switching losses can be evaluated at low repetition rates. The circuit operates in the following

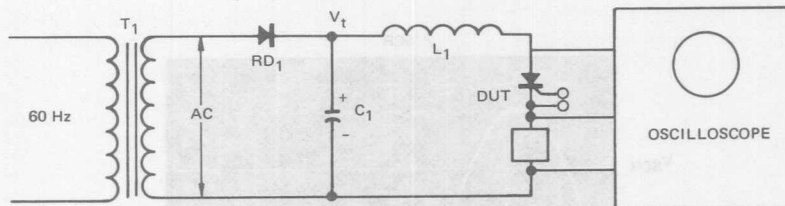


Figure 1-43. Energy Conservation Test Circuit

manner: capacitor C_1 is charged through rectifier RD_1 to test Voltage V_T ; the test SCR is then gated while the ac source is negative, isolating the charging supply from the test circuit. A sine wave of on-state current passes through the test device. Ringback of current is prevented by the rectifying action of the SCR. If the circuit has a high Q , the circuit losses are mainly SCR switching losses. Figure 1-44 illustrates actual circuit waveforms. The capacitor stored energy is shown in Formula 1-U.

$$\text{Stored energy (watt-seconds)} = \frac{1}{2}C(V_1)^2 \quad (1-U)$$

Assuming a lossless circuit, the peak voltage after the first current pulse (if the current cannot reverse) would be equal to the initial capacitor voltage, but of opposite sign. In a circuit with an SCR and components that do have losses, the reverse voltage across the capacitor will be less than the initial capacitor voltage (see Figure 1-44.)

The stored energy after one-half period of conduction is shown in Formula 1-Ua.

$$\text{Stored energy (Watt-Seconds)} = \frac{1}{2}C(V_2)^2 \quad (1-Ua)$$

Combining Equations 1-U and 1-Ua results in Formula 1-Ub.

$$\begin{aligned} \text{Total circuit losses (Watt-Seconds)} \\ &= \frac{1}{2}C(V_1)^2 - \frac{1}{2}C(V_2)^2 \quad (1-Ub) \\ &= \frac{1}{2}C(V_1^2 - V_2^2) \end{aligned}$$

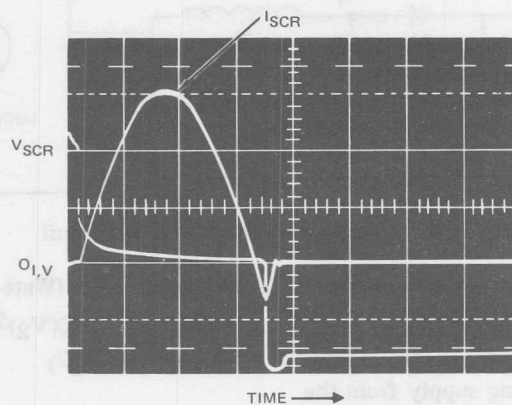
Unfortunately, the losses calculated in this manner include the losses in L_1 and C_1 . Evaluation of circuit losses can be performed by operating the circuit at some higher frequency than 60 Hz and thermally measuring the SCR losses and comparing these losses with those calculated using 1-Ub. The difference between the two will be circuit component losses. There are other methods existing which allow the calculation of circuit losses [7]. Once the circuit losses have been determined, use Formula 1-V to find the SCR switching losses.

$$\text{SCR Switching Losses (watt-seconds)} = \frac{1}{2}C(V_1^2 - V_2^2) - (1-V) \text{ circuit losses.}$$

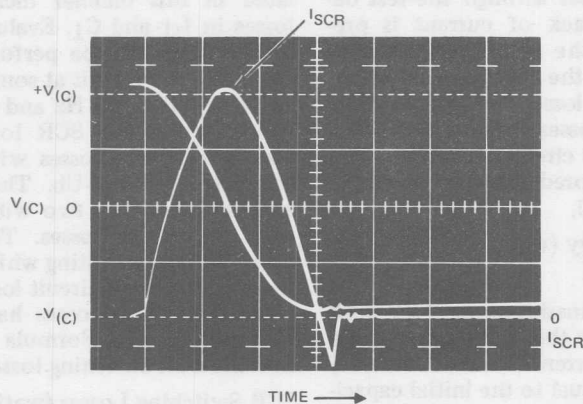
This technique of determining SCR switching losses is extremely useful in applications where on-state current waveforms are sinusoidal. It is not easily adapted to trapezoidal or other non-sinusoidal current waveforms.

Mechanical Integration

Evaluation of switching losses by mechanical integration is self-



(a) SCR ON-STATE CURRENT AND VOLTAGE



(b) SCR ON-STATE CURRENT AND CAPACITOR VOLTAGE

Figure 1-44. Waveforms for Energy Conservation Circuit

explanatory. Oscillograms of the on-state voltage and current vs. time are used to obtain the instantaneous power loss by multiplication. The instantaneous power loss plotted vs. time can then be integrated using a computer or mechanical means. This method, while time consuming and accurate to only $\pm 5\%$ due to oscilloscope line

widths, is applicable to all current waveforms.

Electronic Analog Multiplier

The evaluation of SCR switching losses, using the previously discussed methods, is not always practical when considering the complexity of most current waveforms and the complications of testing. A

study was initiated at IR to determine the feasibility of using electronic analog multipliers to calculate controlled rectifier switching losses.

The concept was enticingly simple: real-time waveforms in, multiplied power losses out. The SCR voltage and current waveforms would be appropriately scaled, of course, to conform to the input requirements of a given multiplier. With such scaling, input slopes could approach $-100\text{V}/\mu\text{sec}$ due to voltage fall times and $5\text{V}/\mu\text{sec}$ due to current rise times. To be meticulously accurate, a multiplier processing such signals should respond at a $105\text{V}/\mu\text{sec}$ slewing rate. This is a difficult constraint on the analog multiplier. However, for a moderately accurate ($\pm 10\%$) system, this requirement may be relaxed. Ultra high frequency components of the actual power loss are small when compared to total switching losses. For instance, Figure 1-45(a) shows the on-state voltage and current waveforms for a current pulse rising at $50\text{A}/\mu\text{sec}$. The rate of fall of voltage is 5000V per $1/2 \mu\text{sec}$. At the end of the first $1/2 \mu\text{sec}$, current has risen to only 1% of its peak value. The loss contribution in this first moment is negligible, as the power loss curves in the figure demonstrate. An actual output slew rate of 5 to $10\text{V}/\mu\text{sec}$ would yield reasonable results.

Figure 1-45(a) is also a comparison of power loss via manual and electronic multiplication. The analog multiplier used was fairly inexpensive (less than \$100) and had a maximum guaranteed slew rate of $10\text{V}/\mu\text{sec}$. While there is a difference between waveforms from $t = 0$ to $t = 0.75$, the multiplier does

recover fast enough to faithfully display the instantaneous power loss over the remaining length of the pulse. Figure 1-45(b) is the oscillogram of the instantaneous power loss using the electronic multiplier. (The oscillatory reverse recovery losses at the tail of the pulse are real and faithfully represented.) The multiplier indicated a power loss 8% lower than the manual calculation. Experimental error and bias probably accounts for a significant portion of this 8% figure.

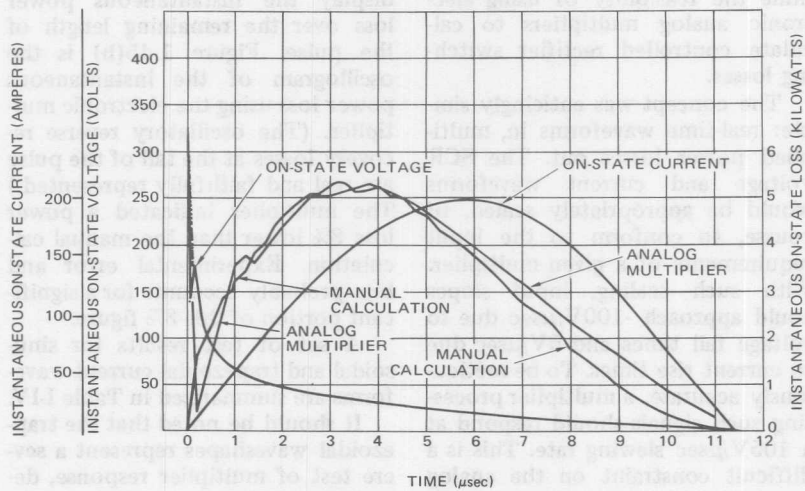
A set of test results for sinusoidal and trapezoidal current waveforms are summarized in Table I-IV.

It should be noted that the trapezoidal waveshapes represent a severe test of multiplier response, demanding an account of losses due to very steep current wavefronts. This observation seems to be reflected in the percentage difference column of Table I-IV. Electronic multiplier losses lag manual losses by 6 to 9%. Figure 1-46 presents a corroborating opinion by visual comparison of trapezoidal losses. In the first microsecond, the electronic multiplier lags the "actual" power loss by 25%. Recovery is complete by the third microsecond.

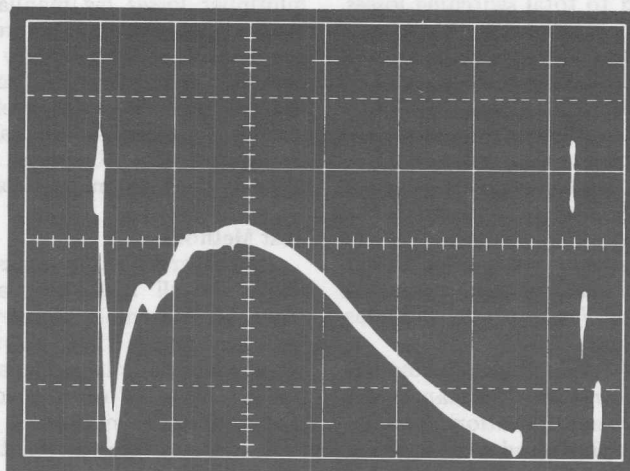
Test Methods

The several techniques presented above are all reasonably accurate from an experimental viewpoint. Vast differences exist, however, in versatility, maintainability, and simplicity. Table I-V offers a comparative summary of methods.

It is reasonable to class the various techniques by defining suitable applications. For instance, incoming inspection testing and general production testing might well be handled by energy conservation



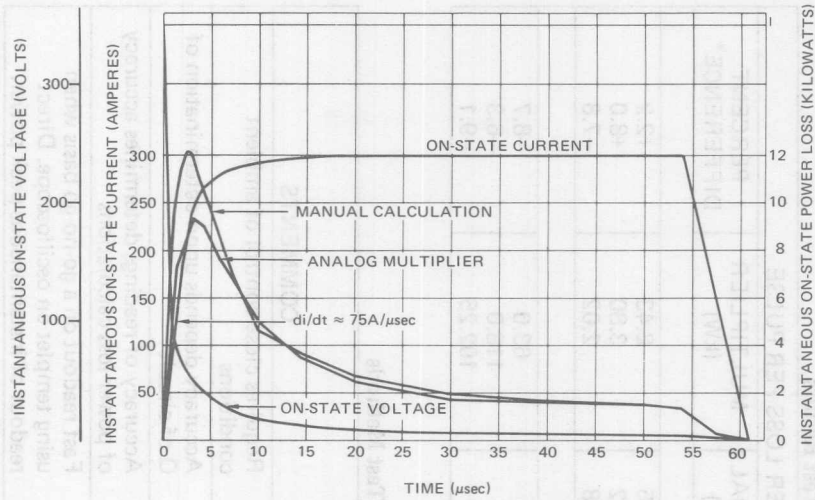
(a) ON-STATE CURRENT AND VOLTAGE



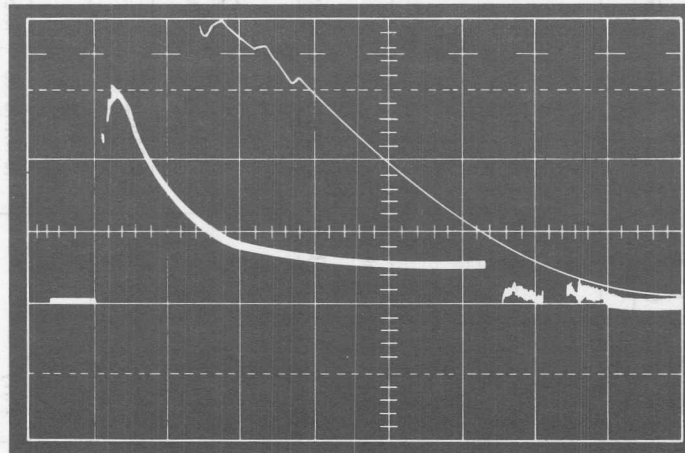
HORIZONTAL = 2 μ sec/div
 VERTICAL = 1700 W/div

(b) POWER LOSS

Figure 1-45. Measurement of Turn-On Losses



(a) GRAPHIC COMPARISON



(b) OSCILLOGRAM COMPARISON

Figure 1-46. Comparison of Trapezoidal Losses

Table I-IV. Summary of Switch Loss Test Results

DEVICE NO.	PULSE WIDTH (μ SEC)	PEAK CURRENT (AMPERES)	POWER LOSS PER PULSE			
			di/dt A/ μ SEC	MANUAL (kW)	MULTIPLIER (kW)	PERCENT DIFFERENCE*
Sinusoidal						
1	4.6	175	90	8.25	8.43	+2.2
2	11.5	200	50	3.52	3.80	+8.0
3	18.5	175	25	2.18	2.02	-7.8
Trapezoidal						
4	50	200	150	69.0	63.0	-8.7
5	50	200	100	126.4	118.0	-6.3
6	50	200	75	112.3	102.25	-9.1

*Assumes manual calculation is correct.

Table I-V. Summary of Switching Loss Test Methods

METHOD	ON-STATE CURRENT WAVEFORM	TIME TEST POINT	ACCURACY	COMMENTS
DC	Any	½ Hour	Medium High	Requires close control of ambient conditions
Energy Conservation	Most suitable for sine wave	2 Minutes	High	Accuracy depends upon determination of Q of circuit
Manual Integration	Any	½ Hour	High	Accuracy of readings determines accuracy of power loss calculations
Analog Multiplier	Any	½ Minutes	Medium High	Fast readout on a go-no-go basis when using templet on oscilloscope. Direct readout of instantaneous peak power.

power loss techniques. All parts could be given a specification based on a standard sine current pulse generated by simple apparatus. However, for infrequent laboratory testing, where waveshapes may vary considerably from a sinewave, the thermal calculation or manual integration methods are most suitable. Tedious experimentation and calculation are offset by a low initial investment.

The final technique, analog multiplication, is the most versatile, accepting any waveform and displaying power losses as a function of time. An initial investment of parts and time, coupled with a continuous investment in calibration time, represents the cost of analog multiplication. The electronic multiplier then becomes valuable to engineering groups with significant interest in power semiconductor design and application.

PARAMETER TRADE-OFFS

As semiconductor manufacturing processes have been developed and refined, manufacturers are able to produce devices with desirable sets of characteristics by simply trading off one characteristic against the other. For instance, the turn-off time of a thyristor can be shortened in the case of an alloy-diffused device by using a gold doping technique. At the same time, however, as turn-off time is reduced, the forward voltage of the device increases. This limits the steady-state operating current under an allowable ambient condition and reduces the surge capability of the device.

In other words, one can take, for instance, a silicon chip of large enough diameter which, with rela-

tively long enough turn-off time, could handle, say, 470 amperes in a pressure-assembled case and by doping the silicon heavily enough in the proper manner, cause the turn-off time to be reduced to tens of microseconds, at the same time increasing the forward voltage to lower the useful current handling capability of the device to 250 or 300 amperes.

By applying a shorting technique between the emitter and the underlying P-layer of a four-layer device, thus producing one or more low impedance paths around this P-N junction, the dv/dt capability of the SCR can be improved considerably. This technique, known as emitter shorting, however, also affects the triggering capability of the SCR. The inrush current capacity of the thyristor during the turn-on interval is also affected.

Blocking voltage capability of a thyristor in both the forward and reverse directions is affected by the resistivity of the basic silicon material used in producing the device and the thickness of the silicon used. This resistivity, however, also affects the propagation rate of the device as it is being turned on. This is another parameter of importance to consider in determining the inrush capabilities of a thyristor during the turn-on interval. A summary of parameter trade-offs for conventional SCR devices is shown in Table I-VI.

SCR GEOMETRY

The original process used to manufacture silicon controlled rectifiers was the alloy-diffused process. In this process, after the original PNP sandwich is produced by diffusion methods, the final P-N

Table I-VI. SCR Parameter Trade-Offs

SCR PARAMETER	VOLTAGE RATING	CURRENT RATING	I_{GT}	CRITICAL dv/dt	t_q	V_{TO}	di/dt RATING	\$
Edge Contouring	↑							↑
Emitter Shorting		↓	↑	↑				↑
Gold Doping (1)	↓	↓	↑	↑	↓	↑	↓	↑
Thinner N-Base	↓	↑			↓	↓	↑	
Multiple Gates			↑			↓	↑	↑
Better Cooling		↑		↑	↓			↑
Reduced Voltage Operation				↑				↑

(1) In addition to gold doping, other means of reducing minority carrier lifetime will have the same effect on the listed parameters except voltage rating may not be adversely affected by other methods.

junction is formed by using a gold antimony disc weighted down on the surface of the PNP sandwich and passing these parts through an alloying furnace, thus causing the gold antimony to alloy into the silicon, producing a final N region. It became obvious that if the dynamic characteristics of a 4-layer device were to be controlled carefully by the manufacturer, a new, more exact process of forming this last N region was necessary.

International Rectifier developed a new SCR series which incorporated an epitaxial emitter region. Instead of alloying a disc for the last N layer, a window was created in which the N layer was grown, thus producing the emitter in a much more exact geometry. With this new capability of control of large areas of the silicon, the trade-off ability of the device designer and process engineer became much more predictable. Larger and larger devices of higher and higher current

capability became available with all of the necessary dynamic requirements for inverter application.

One of the most important limitations soon made itself even more evident in these large area devices. This limitation was the ability of the device to turn on non-destructively into high inrush (high di/dt) currents. When one of the SCRs in question did fail on di/dt, it was generally observed that a small burnt area appeared in proximity with the gate in the general vicinity of or at the edge of the shorting disc.

One of the approaches to a solution to this problem was to produce devices with a center-triggered gate construction, in order to propagate conduction throughout the device more rapidly at the beginning of the turn-on interval. Since the spreading rate of propagation in the silicon is a physical constant for given current and resistivity conditions, it is necessary to produce a

large initially turned-on area in order to cause a larger area to conduct in a given amount of time. However, the center-triggered gate will propagate more rapidly than an edge-triggered unit only if the gate is concentrically located with respect to the edge of the main cathode N region. This, of course, is physically impossible in production with a large number of units, so that any center-triggered configuration will yield a wide variation in turn-on capabilities over a number of production units, determined solely by the ability of the manufacturer to build perfectly concentric circles on the surface of the device.

Manufacturers then began to produce new geometries in order to help the turn-on capabilities and other dynamic properties of the device. The internal feed-back in SCRs of early edge-triggered and center-triggered constructions caused gate current starvation during the initial turn-on interval. This has been used in new geometries in order to produce an amplification or regeneration of a low level gating signal externally applied. What the manufacturer does with the geometry of the device in order to take advantage of this available energy determines 1) whether the device will propagate rapidly and, therefore, switch on efficiently, thus having high di/dt capability and low repetitive switching losses and 2) whether this geometry is or is not made independent of the main cathode N region resistivity and depth in order to make the device turn-on capabilities independent of turn-off time, dv/dt , voltage rating, etc. This geometry control arrangement, used in the ACE family

of devices, not only uses the internal amplification inherent in the thyristor, but also tends to cause a linear spreading action over the main cathode, thus minimizing any hot spots that can occur during the turn-on interval, at the same time leaving the delay time of the device unaffected.

The aluminum deposition or metallic contact also makes it possible for the device to operate at very high frequencies. Some early versions using wire connections, under high di/dt conditions, had such high internally amplified currents that at several kilohertz the wires tended to fuse, thus opening the gate connections in the device. Although the devices would still turn on in most cases, the amplified or regenerative turn-on action was no longer present. Thus, in order to produce a device which can be successfully manufactured in large quantities with reproducible inverter type characteristics, it is necessary to separate the N regions used for the main cathode and the amplified or regenerative gating completely so that the resistivity of one region can be made independent of the other; thus, short turn-off time, high dv/dt and high voltage capability can be produced in the device independently of its turn-on characteristics.

Prior to techniques utilizing the shorted emitter to achieve high dv/dt ratings, it was observed that by using an inverse bias on the gate of a thyristor during its off period, it was possible to increase its dv/dt rating considerably over the unbiased gate condition. The results, however, were rather spotty in that some devices appeared to improve much more than others. It was also

observed that in using a shorted emitter technique, this increased dv/dt capability with negative gate bias was much less apparent.

BIDIRECTIONAL TRIODE THYRISTOR—TRIACS

In the years that followed the advent of the first thyristor devices, it became obvious that as the inherent limitations in accuracy and response of the control elements were removed the industrial user became willing, in fact anxious, to include more sophistication in his equipment in order to reduce his maintenance requirements and increase productivity. At first, the engineer was able to satisfy these requirements with good assurance of reliability and a reasonable degree of complexity. As the demand for larger and more complex systems increased, however, it became apparent that a new limitation began to present itself. With more and more components required to make up a control system, both in the power control and in the logic and command circuitry, the maximum achievable reliability began to be a limiting factor in producing a system which would prove attractive economically to the user. The cost of packaging components began to approach and, in some extreme cases, exceed that of the components being packaged. The semiconductor designers' solution to the problem was, of course, the use of microcircuit techniques. Thick films, thin films, monolithics, hybrids and, most recently, large scale integration have extended the range of application for the most imaginative and resourceful circuit and system designers.

In the midst of this new tech-

nological revolution, the power semiconductor designers also began to respond. The design of the first triac marked a new departure for power device technology. By incorporating the functions of two SCRs into a single chip device — both functions controlled by one gate — the way was opened for simplification in the power circuitry, as well as in the low power level control and logic circuits.

An examination of the construction of International Rectifier's triac indicates that except for a modification of the gating in one portion of the device, the triac can be viewed as two anti-parallel connected silicon controlled rectifiers constructed in one wafer of silicon. This similarity is illustrated by Figure 1-47(a), a block diagram of two SCRs connected in anti-parallel, and Figure 1-47(b), a block diagram of a triac. If the gating on the right-hand SCR were changed and the control PNP regions connected as illustrated in Figure 1-47(c), the similarity would be complete.

Gating

The gating characteristics of the triac are very different from those of two anti-parallel SCRs. For the anti-parallel SCRs, a positive gate signal is applied between Gate 1 and Main Terminal 1 when Main Terminal 1 is negative, and between Gate 2 and Main Terminal 2 when Main Terminal 2 is negative. This method of operation requires two separate gate circuits.

In the triac, Gate 1 and Gate 2 are connected together and operated from a single gate circuit connected between the gates and Main Terminal 1. The easiest triggering

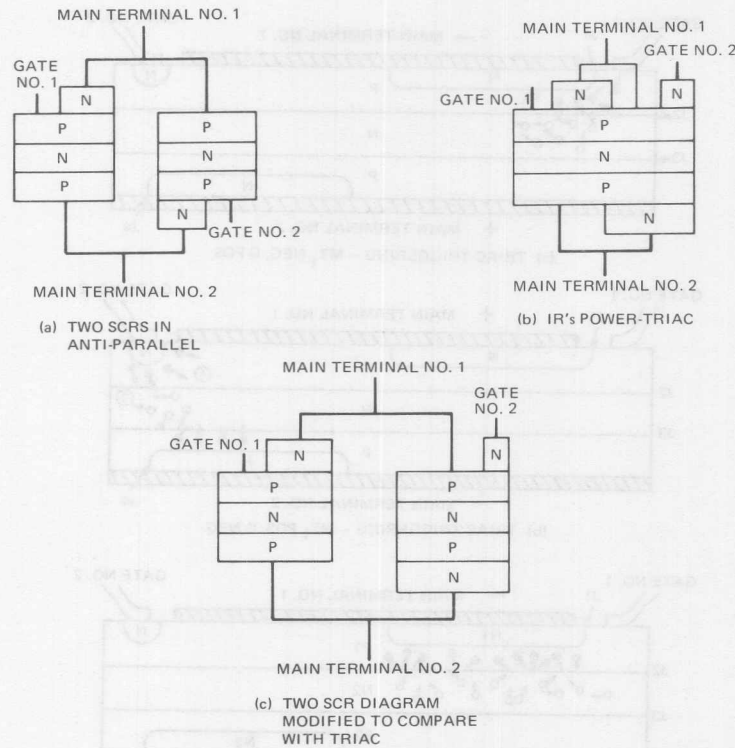


Figure 1-47. Triac Block Diagrams

mode for ac control is achieved by biasing the gates positive when Main Terminal 1 is negative, and negative when Main Terminal 1 is positive. Triggering for ac control is also possible with negative bias on the gates during both half cycles. For dc control, a positive gate bias will result in operation similar to an SCR. This type of operation was made possible by a design in which a positive gate bias will not trigger the device when Main Terminal 1 is positive.

When Main Terminal 1 is negative, triggering takes place in the same manner as in an SCR. The

positive bias at Gate 1 with respect to the top N type cathode, causes injection of electrons from this cathode into the P type region as shown in Figure 1-48(a). A large percentage of these injected electrons are collected by junction J2 which is reverse biased. This collector current in turn induces a forward bias across junction J3, which results in injection of holes into the central N type region. Some of these holes recombine with electrons, but a small percentage of them are collected by reverse biased junction J2. This hole injection occurs over a larger area of

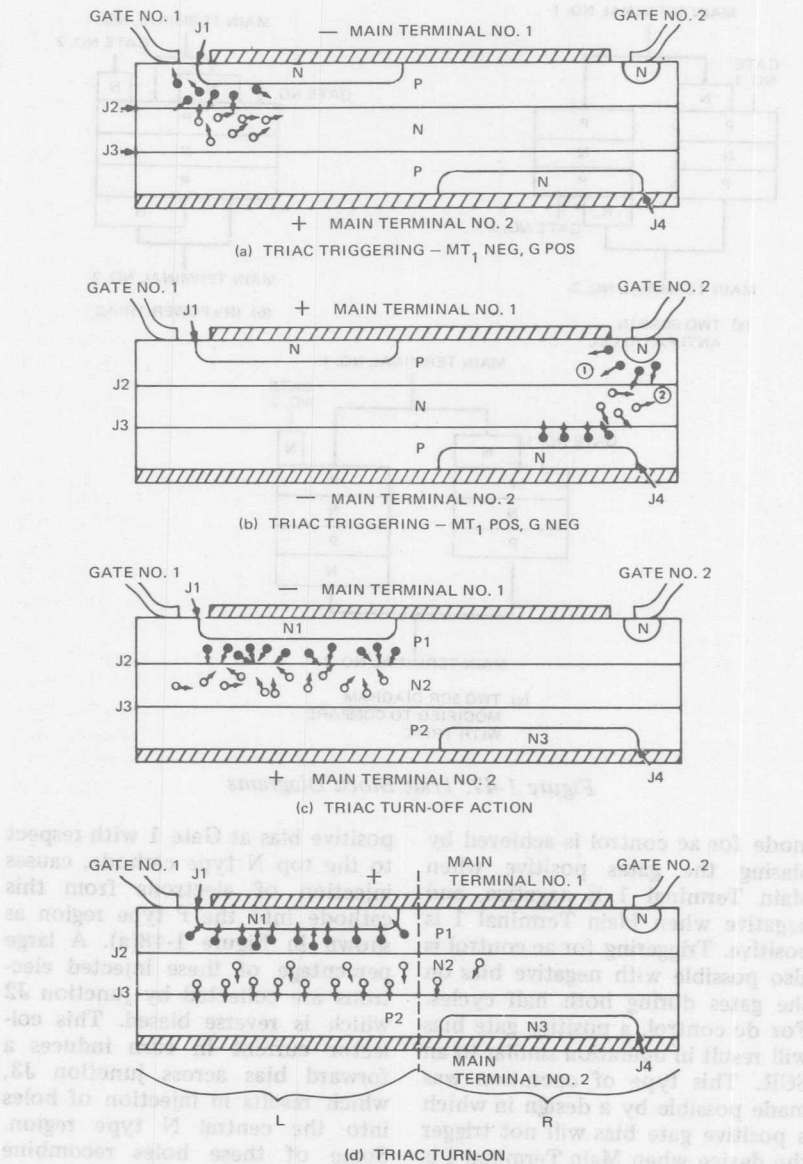


Figure 1-48. Triac Internal Operations

junction J3 than the area of the initial electron injection from J2. The ratio of the areas is a function of the diffusion length of electrons in the upper P region and the resistivity of the central N region.

The collected holes induce an additional injection of electrons from J1 over an even larger area than the hole injection area. This counter injection continues until the entire area under the upper N type region or cathode is conducting and the reverse bias across J2 has collapsed. Although the counter injection has been described as a stepwise process, since collection is not an abrupt occurrence, the growth of the conduction area is a fairly smooth, continuous process.

Since Main Terminal 1 is also connected to the upper P type region, some shunting of the gate signal will occur. This shunt current is, however, minimized by judicious placement of Gate 1. The same type of shunting occurs in an SCR with a shorted emitter construction.

As shown in Figure 1-48(b), when Main Terminal 1 is positive, a negative bias on Gate 2 will cause injection from the N type gate region. Many of these injected electrons will recombine with holes. This current can be considered to be as a parasitic diode current between Gate 2 and Main Terminal 1, since it has no useful function. Some of the injected electrons, however, will be collected by J2 in the vicinity of Gate 2 and cause J2 to become forward biased. Since Main Terminal 1 is positive with respect to Gate 2, J2 at point (1) will have a greater forward bias than at point (2). This forward bias will cause an injection of holes primarily at point (1) into the central

N type region. Some of these injected holes will be collected by junction J3, which is now reverse biased. This will induce injection of electrons from J4 into the lower P type region, which, in turn, will be collected by J3. Here again, the counter injection will continue until the entire area over the lower N type region or cathode is turned on.

As long as the current through the device is maintained above a certain minimum level (holding current), this positive feedback will continue and the device will continue to conduct.

Turn-Off Time

Except for gating, the triac is a symmetrical device. The turn-off mechanism, when the device has been conducting in one direction is virtually the same as turn-off in the other direction.

Consider the case depicted in Figure 1-48(c), where Main Terminal 1 is negative with respect to Main Terminal 2, and the left-hand portion of the device is conducting. Regions P1 and N2 in the left-hand portion are flooded with minority carriers. Majority carriers are not shown.

When the polarity of the device is reversed, some of these minority carriers will recombine with majority carriers, and most of the others will be collected by junctions J1 and J3. The collection of these stored minority carriers results in reverse recovery current. This current causes the injection of additional minority carriers from junction J2. Both electrons are injected into P1 and holes are injected into N2 by junction J2. The primary effect is the injection of holes into N2. This additional injection pro-

longs the recovery process, but since the α of the P1, N2, P2 section is quite low at these current densities, only a small percentage of them ever reach J3.

If a sufficient number of holes are collected at section R of J3 to induce injection of electrons by J4 into P2 section R (see Figure 1-48(d)), the device will turn on. This can only occur if a large number of holes have diffused into section R from section L of N2 or if a sufficient number of holes are injected into section R of N2 by J2 during the recovery phase of section L.

This problem is minimized by constructing the device with a horizontal separation between N1 and N3 of several minority carrier diffusion lengths and obtaining a high enough sheet resistance of N2 to minimize injection of carriers from J2 into section R of N2.

dv/dt

The load circuit in many applications will have a somewhat lagging power factor. This may result in appreciable reapplied dv/dt of opposite polarity. Consider a single phase circuit shown in Figure 1-49,

controlled by a pair of anti-parallel connected SCRs. The resulting waveshapes when these two SCRs are triggered symmetrically (that is, if the respective triggering angles of their anode-cathode voltages are equal), are illustrated in Figure 1-50. Figure 1-51 illustrates instances when the triggering angle α is less than or greater than the circuit power factor angle ϕ .

Examining the waveshapes shown in Figure 1-51(b) in a qualitative manner is most useful in determining the characteristics required of a control device used in this type of circuit. It becomes apparent that the control device will be subjected to sudden applications of off-state voltage (e_S) because of the inductive nature of the load. (i_L lags e_{AC}). A device incapable of remaining in a blocking state during this type of operation will cause full conduction to occur and loss of control to the load will result.

A pair of SCRs in anti-parallel, as in Figure 1-49, connected to a lagging power factor load will repeatedly be required to withstand high dv/dt stresses (as seen in Figure 1-51). However, since the de-

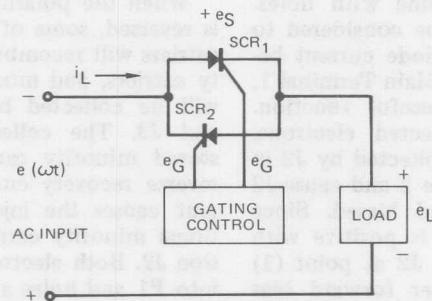


Figure 1-49. Single-Phase AC Controller Circuit

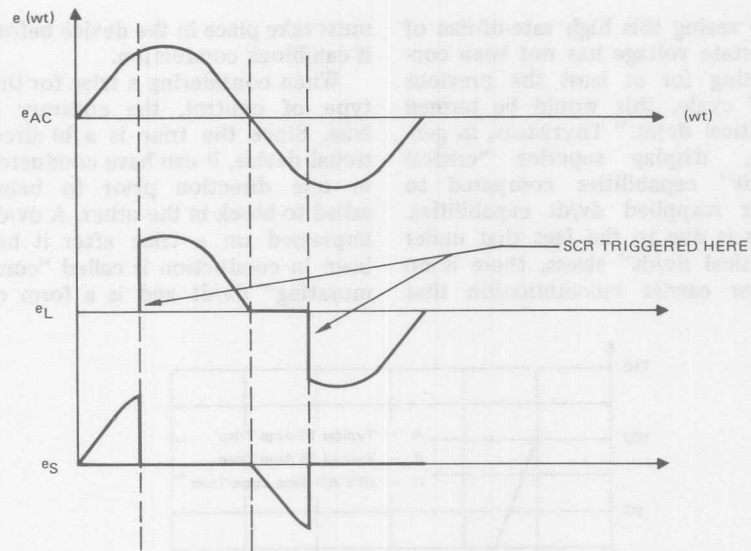
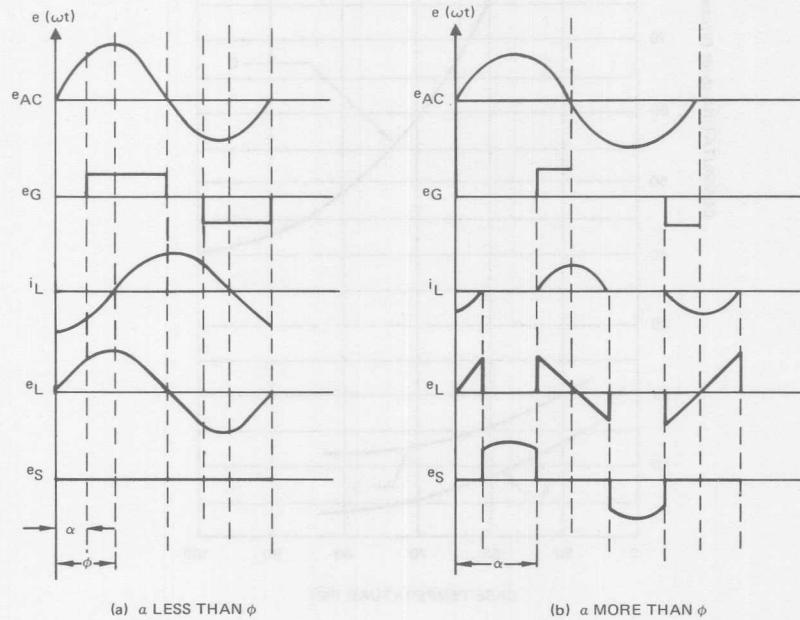


Figure 1-50. Characteristics of Anti-Parallel Connected SCRs



(a) α LESS THAN ϕ

(b) α MORE THAN ϕ

Figure 1-51. Characteristics of AC Controller Circuit

vice seeing this high rate-of-rise of off-state voltage has not been conducting for at least the previous half cycle, this would be termed "critical dv/dt ." Thyristors, in general, display superior "critical dv/dt " capabilities compared to their reapplied dv/dt capabilities. This is due to the fact that under "critical dv/dt " stress, there is no major carrier recombination that

must take place in the device before it can block conduction.

When considering a triac for this type of control, the contrary is true. Since the triac is a bi-directional device, it can have conducted in one direction prior to being asked to block in the other. A dv/dt impressed on a triac after it has been in conduction is called "commutating" dv/dt and is a form of

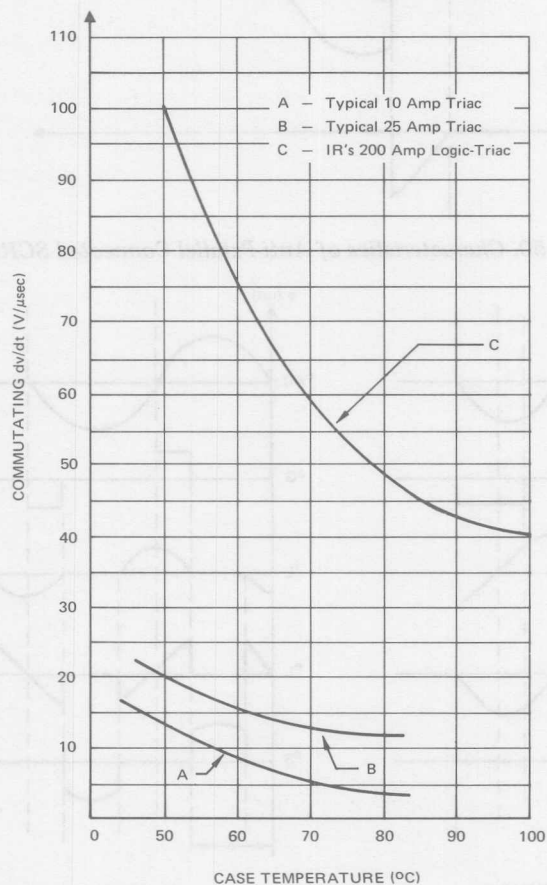


Figure 1-52. Triac Commutating dv/dt

“reapplied” dv/dt . The choice between using a triac for the control element in Figure 1-49 or a pair of anti-parallel SCRs is determined by the inductive nature of the load and the availability of triacs with high “commutating” dv/dt ratings versus the availability of SCRs with high “critical” dv/dt ratings.

A comparison of typical commutating dv/dt ratings for various triacs and their dependence on temperature is shown in Figure 1-52. It remains with the designer to determine the dv/dt conditions existing in the circuit and to choose the proper device accordingly. Fortunately, snubber circuits may be used to reduce the dv/dt stress on a triac when the device is used in conjunction with a highly inductive circuit. By using an R-C network connected across the device, as shown in Figure 1-53, it is possible to suppress the rate-of-rise of voltage (dv/dt) seen by the device.

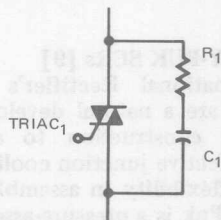


Figure 1-53. Triac with Snubber Circuit

Choice of a triac vs. two anti-parallel SCRs from the consideration of di/dt limitations is rarely a determining factor. For some extreme cases, the designer may want to use devices which are designed to have extremely fast turn-on characteristics to minimize the di/dt

suppression necessary. Since triacs now available are not specifically designed for very high inrush rates a pair of fast turn-on SCRs with special gate structures would be the best choice in such cases.

Dissipation Characteristics

Since the triac is characterized as a bi-directional control device, its ratings are also characterized in this fashion. It is relatively easy, then, for the design engineer to determine the required heat dissipator for a given circuit application. Knowing the required RMS current which the device will be subjected to, one can consult a curve of RMS on-state current vs. maximum allowable case temperature. As in Figure 1-54, this is represented by one curve for all conduction angles. We shall label this maximum allowable case temperature as T_C . The next step is to consult the curves for device dissipation vs. RMS current for the proper conduction angle. Representative curves are shown in Figure 1-55. This dissipation may be called W_T . Knowing the maximum ambient temperature T_A and the interface thermal resistance between the heat sink and the device case ($R_{\theta CS}$), we can now calculate the necessary heat exchanger efficiency for the application ($R_{\theta S}$) using Formula 1-W.

$$R_{\theta S} = \frac{[T_A + R_{\theta CS} \times W_T(AV)]}{W_T(AV)} \quad (1-W)$$

Where:

- $R_{\theta S}$ = Heat exchanger efficiency
- T_C = Case temperature
- T_A = Ambient temperature
- $R_{\theta CS}$ = Thermal resistance,

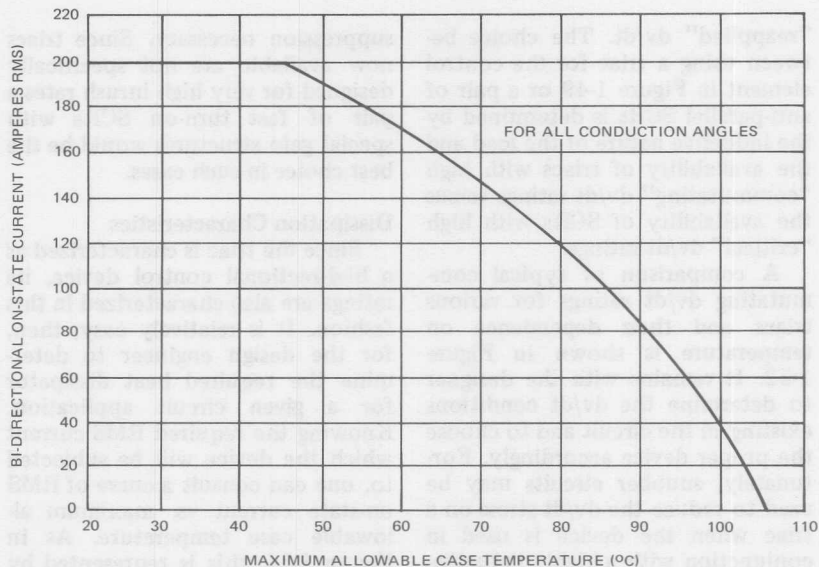


Figure 1-54. Triac On-State Current vs. Maximum Allowable Case Temperature

heat exchanger to device
 $WT(AV) =$ Device power loss

The dissipation in the triac is considerably greater than that of a single SCR for a given RMS line current. This, of course, is to be expected, since the triac conducts during both half cycles. It is often more practical to use high power triacs when either forced air cooling or liquid cooling is available. These cooling means provide high thermal efficiency and allow the use of relatively small heat exchangers to keep the triac below its maximum allowable case temperature. If natural convection cooling is the only means available, a rather large heat exchanger will generally be required as compared to one needed for each

SCR in an equivalent anti-parallel configuration.

HOCKEY-PUK SCRs [9]

International Rectifier's Hockey-Puks are a natural development in SCR construction to achieve more effective junction cooling and greater flexibility in assembly. The Hockey-Puk is a pressure-assembled device designed to maximize the benefits of double-side cooling using air-cooled or liquid-cooled heat exchangers. This double-side cooling is accomplished by constructing the device so that the anode and cathode connections are large area contacts. These copper pole pieces maximize heat transfer to the heat exchangers while retaining compactness.

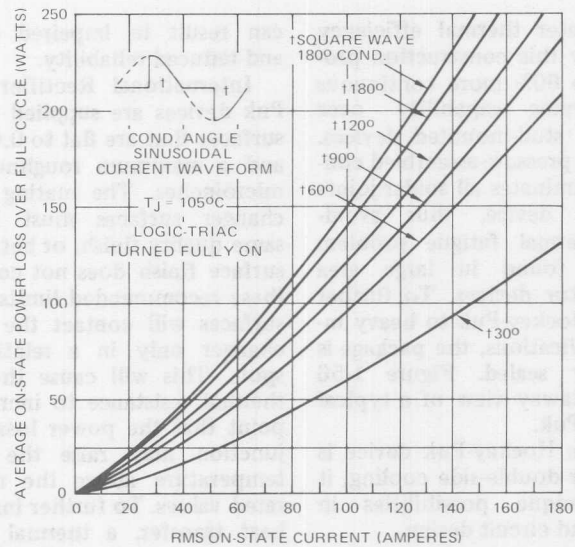


Figure 1-55(a). Low-Level On-State Power Loss vs. Current

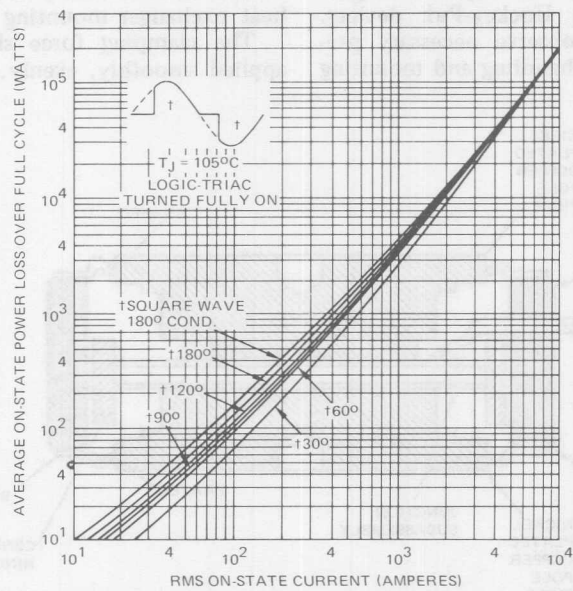


Figure 1-55(b). High-Level On-State Power Loss vs. Current

The greater thermal efficiency achieved by this construction provides up to 60% more continuous current-carrying capability over comparable stud-mounted devices. In addition, pressure-assembled construction eliminates all solder joints within the device, thus avoiding the thermal fatigue problem sometimes found in large area semiconductor devices. To further adapt the Hockey-Puk to heavy industrial applications, the package is hermetically sealed. Figure 1-56 shows a cutaway view of a typical IR Hockey-Puk.

Since the Hockey-Puk device is designed for double-side cooling, it presents unique possibilities in mounting and circuit design.

Mounting the Hockey-Puk

Mounting is an important aspect in applying Hockey-Puk devices. Failure to observe necessary precautions in handling and mounting

can result in impaired operation and reduced reliability.

International Rectifier Hockey-Puk devices are supplied with pole surfaces that are flat to 0.0015 TIR and a maximum roughness of 32 microinches. The mating heat exchanger surfaces must have the same quality finish, or better. If the surface finish does not conform to these recommended limits, the pole surfaces will contact the heat exchanger only in a relatively few spots. This will cause the contact thermal resistance to increase to a point that the power losses of the junction may raise the junction temperature above the maximum rated values. To further insure good heat transfer, a thermal interface compound, such as Penetrox "A", (Burdny Corp.), or equivalent, should be used between the pole piece and heat exchanger mounting surfaces.

The clamping force should be applied smoothly, evenly, and per-

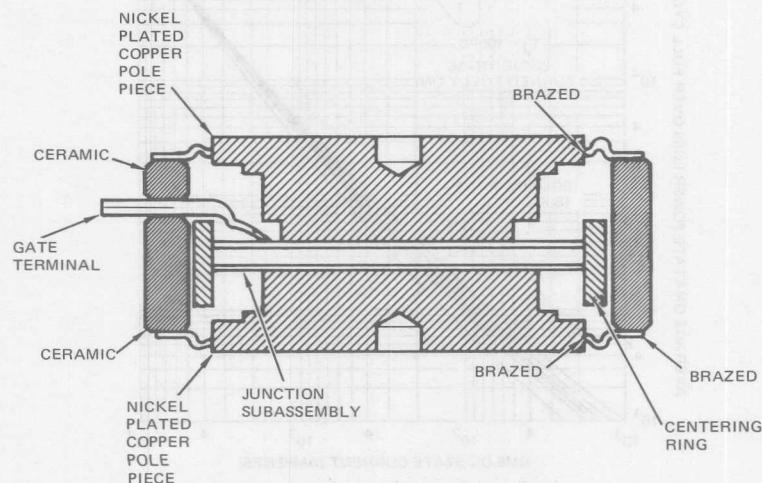


Figure 1-56. Typical Hockey-Puk Structure

pendicularly to the Hockey-Puk to insure that there is no deformation of either the pole faces or heat exchanger during mounting. The amount of clamping force is important. The clamping force required on IR Hockey-Puks is listed in Table I-VII. Figures 1-57 and 1-58 show the effect that varying the clamping force (applied force in pounds) has on thermal resistance and on-state voltage on a device rated to have 900 to 1100 pounds applied.

The clamp shown in Figure 1-59 was designed to apply the clamping force in a smooth, even manner, perpendicular to the Hockey-Puk pole face. Figure 1-60 shows the effect of non-perpendicular application of force. Note the resultant

hot spot and pole deformation. This type of mounting drastically reduces device capability.

Mounting Hockey-Puk Assembly

When the Hockey-Puk is assembled, one more precaution must be taken. If the assembly is mounted with both heat exchangers immovable as shown in Figure 1-61(a), the thermal expansion due to normal operation can place stresses on the assembly, causing catastrophic failure. Figure 1-61(b) shows a better method of mounting a single Hockey-Puk assembly. The same principle would apply for two or more devices on a common heat exchanger.

Versatility

Stud-mounted controlled recti-

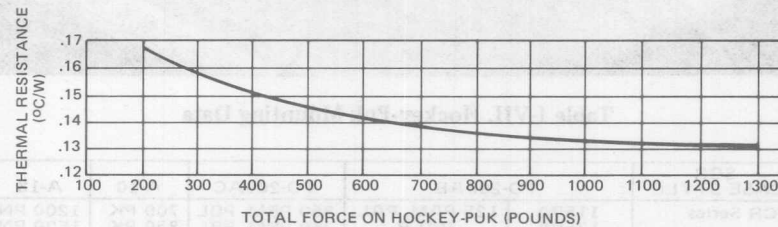


Figure 1-57. Hockey-Puk Thermal Resistance vs. Applied Force

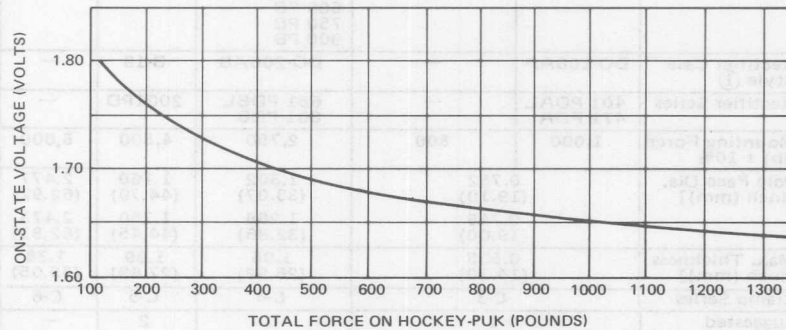


Figure 1-58. Hockey-Puk On-State Voltage vs. Applied Force

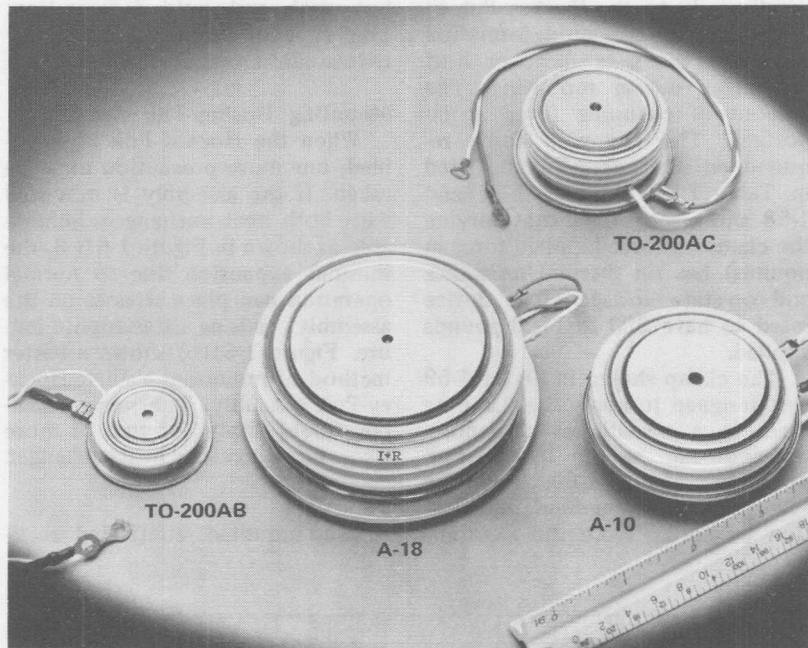


Table I-VII. Hockey-Puk Mounting Data

SCR CASE STYLE	TO-200AB		TO-200AC	A-10	A-18
SCR Series	115PA 175PA 250PA 300PA	125 PAM, PAL, PALB 140 PAM, PAL	350 PBM, PBL 360 PBM, PBL 420 PB, PBM 430 PBM, PBL 470 PB 500 PBQ 550 PB, PBQ 600 PB 750 PB 900 PB	700 PK 850 PK 1000 PK	1200 PN 1600 PN
Rectifier Case Style ①	DO-200AA	—	DO-200AB	B-19	—
Rectifier Series	401 PDAL 471 PDA	—	651 PDBL 801 PDB	2001PD	—
Mounting Force (lb) ± 10%	1,000	800	2,750	4,500	8,000
Pole Face Dia. [inch (mm)]		0.752 (19.10)	1.302 (33.07)	1.760 (44.70)	2.477 (62.92)
		0.748 (19.00)	1.298 (32.96)	1.750 (44.45)	2.473 (62.81)
Max. Thickness [inch (mm)]		0.555 (14.10)	1.06 (26.92)	1.09 (27.69)	1.38 (35.05)
Clamp Series		C-3	C-4	C-5	C-6
Suggested Springs		1	3	2	—

① Similar to SCR types, but without gate and auxiliary cathode terminals.

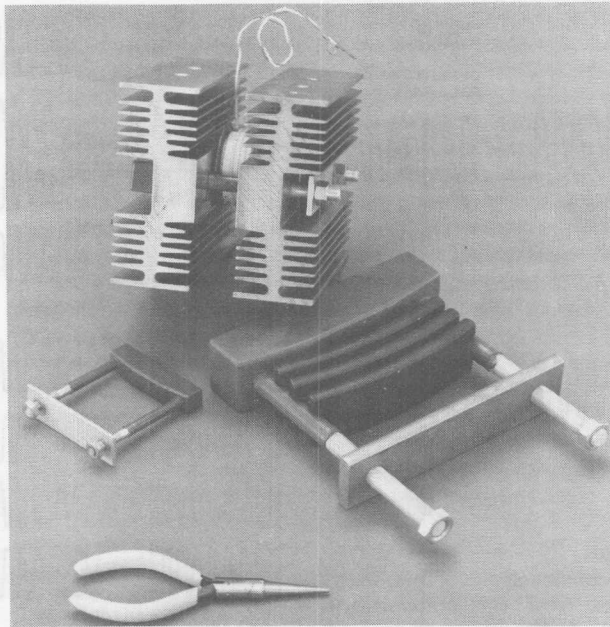


Figure 1-59. Typical Hockey-Puk Mounting Clamp

fiers are not available in the forward polarity configuration (cathode to base). The Hockey-Puk configuration permits overcoming this limitation by merely turning the Hockey-Puk over in the assembly. Having this versatility, the Hockey-Puk allows the design engineer much more freedom in parallel and series designs. Some of these possibilities are illustrated in Figure 1-62.

PASSIVATED ASSEMBLED CIRCUIT ELEMENTS — PACE/paks [10, 11]

IR uses improved passivation techniques for power semiconductors, and has employed some of the technology from the microelectronics industry to manufacture high power thyristor and rectifier hybrid circuits. The circuits generally util-

ize thyristor or diode junctions mounted on an electrically isolating, thermally-conductive substrate, which is, in turn, mounted to a copper or aluminum plate that can be attached to a heat dissipator. The active components of the device are encapsulated with high temperature, moisture-resistant epoxy. The junctions are isolated from the copper plate by means of a beryllium oxide, or, in the case of lower power applications, an alumina substrate. Then, depending upon the amount of current to be handled, the devices are interconnected by a wire frame or by thick film techniques. The power and control leads can then be brought out of the epoxy encapsulation by means of fast-on terminals or lugs.

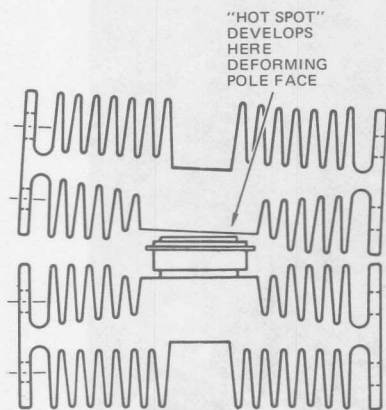


Figure 1-60. Hockey-Puk with Uneven Force

Advantages

This construction offers many advantages over the conventional packaging techniques. These advantages include: 1) The user's engineering design time is better utilized because only one device must be specified instead of as many as five for single-phase applications and seven for three-phase applications. 2) Assembly labor costs are reduced, as only one device must be mounted and interconnected for the entire power section. 3) Visual keys by either color coding or mechanical asymmetries can be used to aid in making the assembly installation foolproof. 4) Isolated heat dissipators are eliminated because the single copper plate is isolated from the circuit. 5) Thermal efficiencies are better than with individual devices. 6) In many applications, the smaller size of the power circuit assembly can be utilized to advantage. For example, a single-phase full wave controlled bridge assembly, designed for a 2

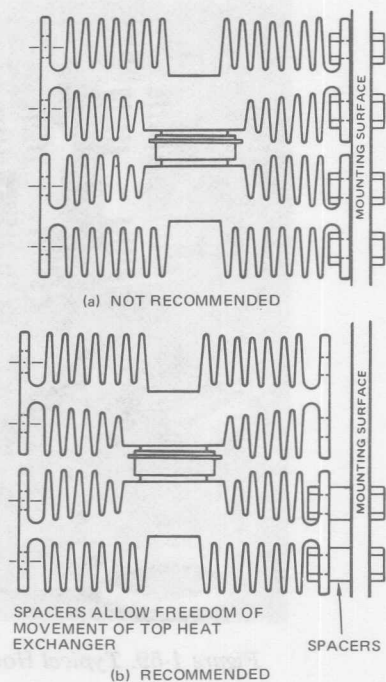


Figure 1-61. Mounting a Hockey-Puk Assembly

hp dc motor, is only 1.25" x 2.5" x 0.9" (31.75 x 63.5 x 22.86 mm) and could be mounted directly on the bell housing of the motor itself. 7) There is a savings in the parts inventory required for a product using the PACE/pak; this parts count savings can be as high as 7 to 1, not counting hardware and wire. 8) An increase in rating over the equivalent junction when mounted in the standard junction-soldered-to-stud case is obtained. This was noted during the earliest testing and evaluation of the PACE/pak; there was a large reduction of the thermal impedance, junction-to-case of the thyristors (the "case" being the

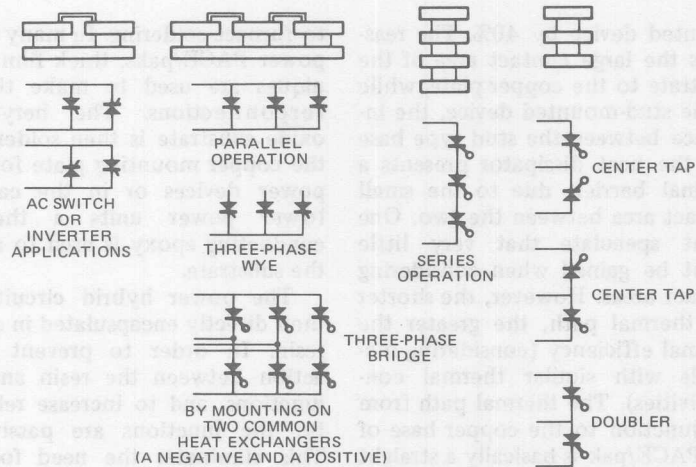


Figure 1-62. Hockey-Puk Mechanical Configurations

copper base plate) when compared to the same junction soldered to a copper stud.

From the rating sheets of IR's 25 ampere, standard, stud-mounted SCR series, the thermal impedance of a 16RC is $1.5^{\circ}\text{C}/\text{W}$. However, referring to Figure 1-63, the SCR

and the diode together in the hybrid assembly have a thermal impedance of $0.9^{\circ}\text{C}/\text{W}$. Mounting the devices on the beryllium substrate directly has increased the heat removal capacity (reduced the thermal impedance) of the hybrid assembly over that of the stud-

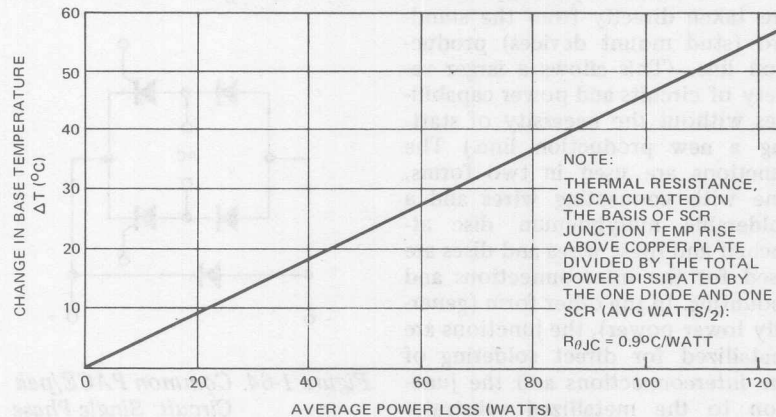


Figure 1-63. PACE/pak Estimated Power Loss

mounted device by 40%. The reason is the large contact area of the substrate to the copper plate, while in the stud-mounted device, the interface between the stud type base and the heat dissipator presents a thermal barrier, due to the small contact area between the two. One might speculate that very little might be gained when considering contact areas. However, the shorter the thermal path, the greater the thermal efficiency (considering materials with similar thermal conductivities). The thermal path from the junction to the copper base of the PACE/pak is basically a straight line, while the thermal path of the stud-mounted device is at best a 20° line around the stud of the device. This principle also holds true for the diodes in these assemblies.

Construction

The construction of the PACE/pak is straightforward; however, there are some variations in the techniques used, depending on the power level to be handled by the device.

Diode and/or thyristor junctions are taken directly from the standard (stud mount devices) production line. (This allows a larger variety of circuits and power capabilities without the necessity of starting a new production line.) The junctions are used in two forms, one with connecting wires and a solderable molybdenum disc attached and these wires and discs are used for the interconnections and mounting. In the other form (generally lower power), the junctions are metallized for direct soldering of the interconnections and the junction to the metallized substrate. This latter form of junction is particularly suited, with proper jigging,

to furnace soldering. In many lower power PACE/paks, thick film techniques are used to make the interconnections. The beryllium-oxide substrate is then soldered to the copper mounting plate for high power devices or in the case of lower power units a thermal-conducting epoxy is used to attach the substrate.

The power hybrid circuits are then directly encapsulated in epoxy resin. In order to prevent interaction between the resin and the junctions, and to increase reliability, the junctions are passivated. This eliminates the need for any intermediate encapsulation of the junctions, with the consequent advantage of better heat flow and less bulk and cost. The method used is the same as that used in the production of some microelectronic circuits.

Rating and Application

To give more insight into the use of these new encapsulated devices, consider the circuit configuration shown in Figure 1-64. This circuit

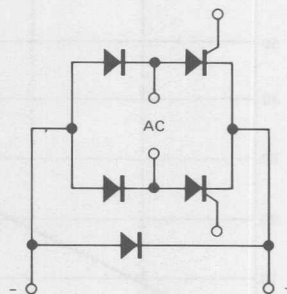


Figure 1-64. Common PACE/pak Circuit: Single-Phase Hybrid Bridge with Free-Wheeling Diode

would be used in low power dc motor drives or without the free-wheeling diode as a power supply. Further, for purposes of this discussion, let us assume that the devices used are in the 25 ampere RMS rating category.

Figure 1-65 defines the maximum allowable base plate (case) temperature vs. conduction angle and dc output current. Knowing the worst case conditions of the user's application, the maximum allowable base plate (case) temperature can be determined. Then, taking Figure 1-66, which shows power loss vs. conduction angle and output current, and knowing the maximum allowable base plate temperature, it is possible to determine the heat dissipator requirements. Assuming a 1.5" (38.1 mm) surface

area, a good thermal compound and smooth contact surface, the thermal resistance of the base plate to dissipator, $R_{\theta CS}$, is in the neighborhood of $0.1^{\circ}\text{C}/\text{W}$.

Using these design graphs, it is possible to characterize this power hybrid assembly in a fashion very similar to that used for a discrete device. There are some interesting variations from this rule, because this is a complete circuit, not a single device. Consider working into a highly inductive load with the circuit shown in Figure 1-64. The permissible output current into an inductive load can actually be greater than that permitted for a resistive load, during a phase-back condition. Figure 1-67 shows this for the 25 amp PACE/pak working into a theoretically perfect inductor at a

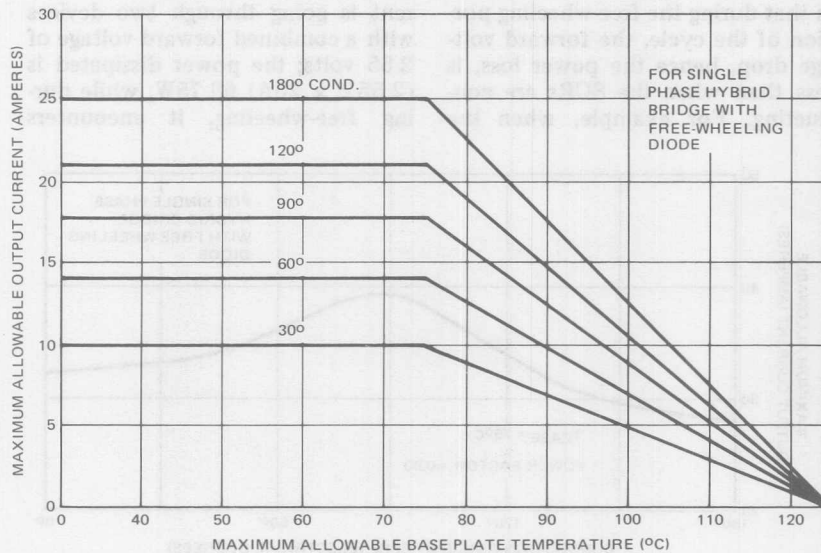


Figure 1-65. PACE/pak Output Current vs. Base Plate Temperature and SCR Conduction Angle

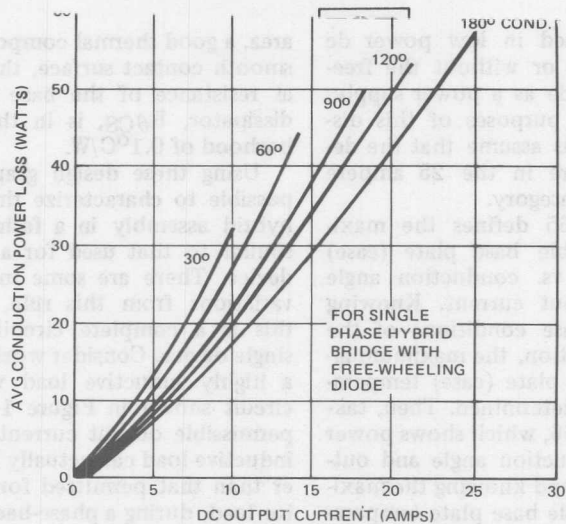


Figure 1-66. PACE/pak Actual Power Loss vs. Output Current and SCR Conduction Angle

75°C case temperature. The reason is that during the free-wheeling portion of the cycle, the forward voltage drop, hence the power loss, is less than when the SCRs are conducting. For example, when the

bridge is conducting 25A, the current is going through two devices with a combined forward voltage of 2.55 volts; the power dissipated is (2.55V x 25A) 63.75W, while during free-wheeling, it encounters

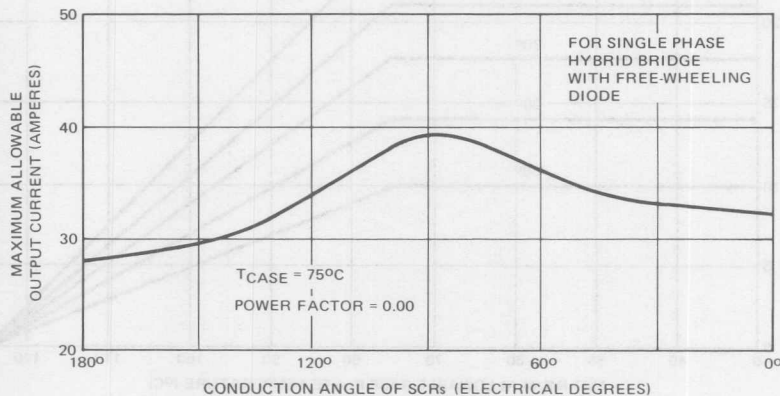


Figure 1-67. Maximum Allowable Output Current vs. SCR Conduction Angle

only one diode voltage drop, 0.9 volts, and the power dissipated is $(0.9V \times 25A)$ 22.5W. The final downturn in current at about 90° is caused by having reached the free-wheeling diode's current capability.

Circuits

The use of PACE/paks is similar to using integrated circuits, in that the designer is no longer selecting an individual component, but he selects the circuit which will meet his functional job requirement. However, similarly to the integrated circuit industry, it is expensive to generate an infinite variety of specialized circuits to satisfy each application. As with the integrated circuit industry, it is better for a designer to select a standard circuit, rather than a special design, and take advantage of volume production and the resultant lower costs.

Some of the variations which are available and relatively easy to generate are shown in the following figures.

Several common SCR bridge control circuits can be seen in Figure 1-68 with (c) being the most common. Both circuit (c) and (d) can be supplied with or without a free-wheeling diode. Circuit (a) can be used for generator exciters, dc motor drives and power supplies. It also has the advantage of not requiring a free-wheeling diode. Circuit (b) can be used as a dc motor drive with the added advantage of being able to provide regeneration during braking. Circuits (c) and (d) are commonly used as dc motor drives. The most popular power levels to date have been in the one to five horsepower range. It might be noted that by shorting the positive to negative output of these

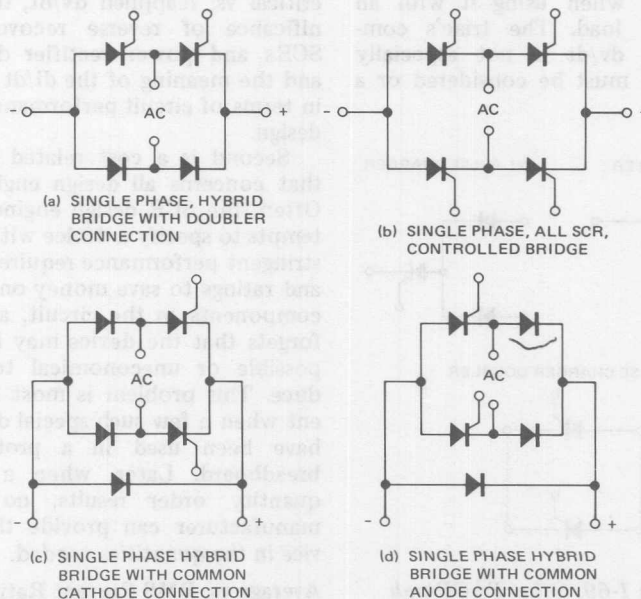


Figure 1-68. PACE/pak Bridge Configuration Circuits

circuits, an ac switch configuration is obtained.

Figure 1-69 shows a miscellany of circuits that have been built using a common substrate. Circuit (a) has been used as a field excited in a generator, a half wave dc power supply, as well as a dc relay/contact driver. Circuit (b) is a universal configuration. It can be used as a positive or negative center tap circuit, pulse charger, doubler, ac switch or with selected devices even an inverter leg. Circuit (c) is an inexpensive pulse charger for leading power factor loads.

A variety of ac switches are shown in Figure 1-70; these can be used for lighting controls, heating controls and motor starters. The triac is especially well-suited to these jobs and has the advantage of being only one control element. However, some caution must be exercised when using it with an inductive load. The triac's commutating dv/dt is not especially high and must be considered or a

loss of control may be experienced during a phase-back condition. The circuit using the diode in anti-parallel is used mostly in three-phase circuits; however, it could be used in a limited range single-phase light dimmer application.

A new area where PACE/paks are being applied is three-phase power circuits as shown in Figure 1-71. Three phase diode bridge circuits can be delivered with voltage ratings of up to 600 volts and current levels to 150 amps.

Various other circuit configurations are under development, with new standard building blocks being introduced regularly.

GENERAL APPLICATION HINTS

One of the most common difficulties in the application of thyristors is a misunderstanding of SCR specifications and ratings, such as critical vs. reapplied dv/dt , the significance of reverse recovery in SCRs and power rectifier diodes, and the meaning of the di/dt rating in terms of circuit performance and design.

Second is a cost related factor that concerns all design engineers. Often, the SCR design engineer attempts to specify a device with very stringent performance requirements and ratings to save money on other components in the circuit, and he forgets that the device may be impossible or uneconomical to produce. This problem is most apparent when a few such special devices have been used in a prototype breadboard. Later, when a large quantity order results, no SCR manufacturer can provide the device in the quantities needed.

Average vs. RMS Current Ratings

A problem with "simple" con-

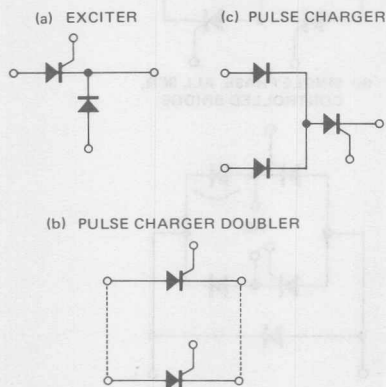


Figure 1-69. Other PACE/pak Circuits

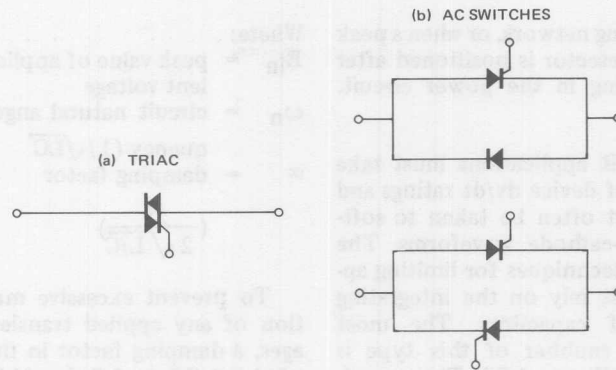


Figure 1-70. PACE/pak AC Switch Circuits

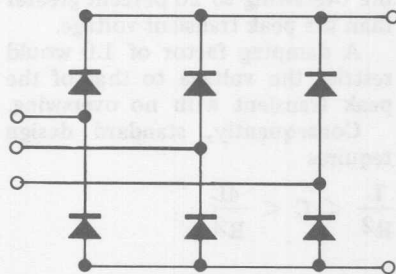


Figure 1-71. PACE/pak Three-Phase Rectifier Circuit

trolled bridge rectifier circuits often overlooked is that output voltage cannot be decreased to near zero while maintaining the same average output current. In this case, the device may be kept well within its average current rating, but will be operating many times beyond maximum RMS current rating.

This is true because the different form factors associated with the average and RMS currents cause the RMS value to greatly exceed the average at low conduction angles. The limiting factor is that RMS current (heating) flows through the

resistive portion of the leads and internal assembly parts, and adds heat to the junction rather than carrying it away. Table I-VIII shows the various form factors vs. the conduction angle (θ_C).

Table I-VIII. Form Factor vs. Conduction Angle (Sine Wave)

θ_C	I_{RMS}/I_{AVG}
15°	5.653
30°	3.979
45°	3.233
60°	2.780
90°	2.221
120°	1.878
180°	1.571

It is important for the designer to keep these concepts in mind, because the average current may look extremely low, yet the RMS currents may be high enough to cause device destruction. It is possible to fall into this trap when selecting a current detection circuit or locating it in the main circuit. The problem exists, for example, when current is detected through

an averaging network, or when a peak current detector is positioned after the filtering in the power circuit.

Snubbers

All SCR applications must take account of device dv/dt ratings and steps must often be taken to soften anode-cathode waveforms. The standard techniques for limiting applied dv/dt rely on the integrating ability of capacitors. The most primitive snubber of this type is shown in Figure 1-72. The capacitor absorbs excess transient energy, while the resistor defines the applied dv/dt in conjunction with the external system inductance.

An informative analysis studies the response of this snubber to a step function voltage. If an infinitely sharp voltage, of magnitude E , is impressed across the entire R,L,C combination, the waveform applied to the protected SCR will be considerably softened, due to the high transient impedance of the inductor. The maximum SCR dv/dt will then be given by Formula 1-X.

Maximum device $dv/dt =$

$$2 \alpha \omega_n E_{in} = \frac{ER}{L} \quad (1-X)$$

Where:

E_{in} = peak value of applied transient voltage

ω_n = circuit natural angular frequency ($1/\sqrt{LC}$)

α = damping factor

$$\left(\frac{R}{2\sqrt{L/C}} \right)$$

To prevent excessive magnification of any applied transient voltages, a damping factor in the range of about 0.5 to 1.0 should be chosen for the LRC suppressor network. A damping factor of 0.7 restricts the overshoot to 20 percent greater than the peak transient voltage.

A damping factor of 1.0 would restrict the voltage to that of the peak transient with no overshoot.

Consequently, standard design requires

$$\frac{L}{R^2} < C < \frac{4L}{R^2}$$

Going over the upper limit overdamps the circuit and requires excessively large capacitors and dissipation.

In practical situations, it is usually necessary to choose R quite

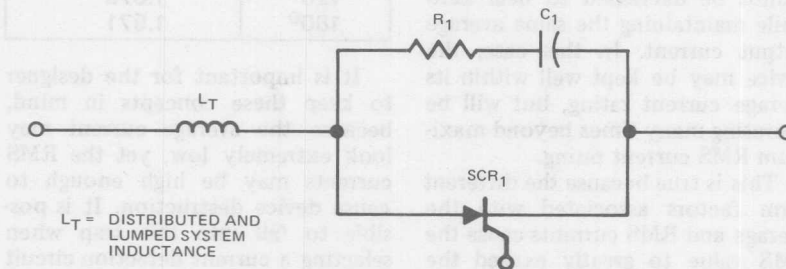


Figure 1-72. SCR Snubber Circuit

small (10 to 200 ohm) but even so, for higher frequency operation, the snubber dissipation can be quite significant, increasing system cost and impairing system efficiency.

However, these are the trade-offs that the design engineer must decide for himself.

Hybrid Bridge

Two systems may be used to provide controllable three-phase bridge rectifiers, one utilizing 6 SCRs (the full converter circuit) and the other 3 SCRs and 3 conventional rectifiers (the hybrid or semi-converter circuit). (See Figures 1-73 and 1-74.)

Figure 1-73 shows the 6 SCR 3-phase bridge circuit. This circuit provides full control of output power as the thyristors receive independent gate triggering signals and does not lose control of the output voltage. On the other hand, the bridge circuit shown in Figure 1-74 consists of only 3 SCRs together with 3 diodes and requires only 3 gate drive circuits. Consequently it is much less expensive to build.

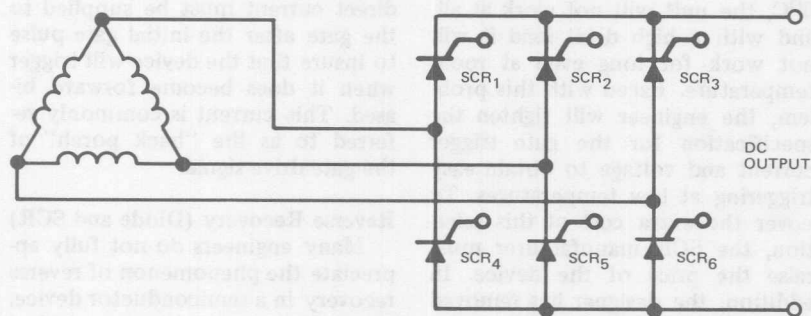


Figure 1-73. Three-Phase, All-SCR (Full Converter) Bridge Circuit

On inductive loads, in hybrid assemblies, it is important to avoid sudden removal of the gate pulses, as the inductance prevents the output current from immediately dropping to zero and the conducting SCR will not turn-off. Current will be drawn from the supply under these conditions for 240° of the full cycle, and, providing the inductance of the load is sufficiently high, current will circulate for the remaining 120° (via the rectifier in series with the conducting thyristor).

The above condition can remain in effect indefinitely, and will generally result in serious overloading of the conducting SCR. Two solutions are available for this difficulty:

- A. Never remove gate pulses unless the output current has previously been maintained at a low level for a period of time well in excess of the load time constant.
- B. Provide a free-wheeling diode across the load.

Gate Drive

One of the most frequent causes of trouble for a designer is the SCR

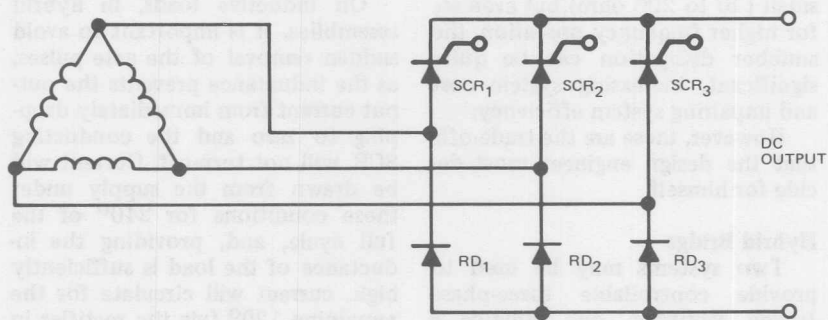


Figure 1-74. Three-Phase, Hybrid (Semi-Converter) Bridge Circuit

gate drive. The problem usually involves providing sufficient power gain between the logic and the SCR gate; arriving at the SCR gate with adequate drive and isolation seems to be a stumbling block for many SCR design engineers.

The design engineer would like to trigger a 740 ampere RMS SCR with a unijunction transistor pulse circuit through a 10 volt-microsecond pulse transformer for isolation.

The problem exists because, under the above conditions, many large SCRs will turn on and operate successfully at room temperature and with a low di/dt load, but at 0°C , the unit will not work at all, and with a high di/dt load it will not work for long even at room temperature. Faced with this problem, the engineer will tighten the specification for the gate trigger current and voltage to obtain easy triggering at low temperatures. To cover the extra cost of this selection, the SCR manufacturer must raise the price of the device. In addition, the designer has removed some much needed noise immunity and performance with a high di/dt load may still be marginal.

The designer, in this case, should reconsider his drive circuits to decide if, in the long run, it would not be less expensive to meet the gate drive conditions specified in the catalog data sheet for a standard device.

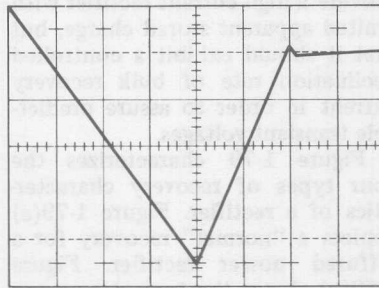
There is another problem surrounding a lagging power factor load. In many inverter designs, the power SCR in the circuit may not be forward biased until well into the half-cycle. At the same time, the reactive current is flowing through the free-wheeling diode. In this case, it is clear that a pulse gating scheme cannot be used. A direct current must be supplied to the gate after the initial gate pulse to insure that the device will trigger when it does become forward biased. This current is commonly referred to as the "back porch" of the gate drive signal.

Reverse Recovery (Diode and SCR)

Many engineers do not fully appreciate the phenomenon of reverse recovery in a semiconductor device. They tend to view them as perfect switches. At low frequency (60 Hz) and low current, this is a valid

assumption with respect to reverse recovery. However, at high frequency (repetition rates) and large currents, reverse recovery takes on considerable importance.

Consider, for instance, the wave-shape for the diode designated as a normal diffused rectifier shown in Figure 1-75. Let us assume the diode is to be applied in a typical inverter power supply (Figure 1-76). Figures 1-75, 1-77, and 1-78 show that the average losses during recovery can be calculated by Formula 1-Y.



NORMAL DIFFUSED RECTIFIER
DIODE, 250A
FORWARD CURRENT: 785A PEAK
di/dt: -25A/ μ sec t_a : 4.1 μ sec
 t_{rr} : 5.8 μ sec t_b : 1.7 μ sec
 $I_{R(REC)}$: 95A

Figure 1-75. Diode Reverse Recovery

$$W_R = \frac{V_F I_{R(REC)} t_a/2 + V_{RWM} I_{R(REC)} t_b/2}{t_a + t_b} \quad (1-Y)$$

Where:

W_R = Recovery power
 V_f = Diode forward voltage at the proper current level during t_a .

$I_{R(REC)}$ = 95A
 t_a = 4.1×10^{-6} sec
 t_b = 1.7×10^{-6} sec
 V_{RWM} = Peak reverse voltage applied to rectifier during operation.

Assume:

$$V_F = 2V$$

Therefore:

the losses, $W_R =$

$$\frac{2V \cdot 95A \cdot 4.1 \times 10^{-6} \text{ sec}/2 + 4.1 \times 10^{-6} \text{ sec} + 1.7 \times 10^{-6} \text{ sec}}$$

$$\frac{600V \cdot 95A \cdot 1.7 \times 10^{-6} \text{ sec}/w}{4.1 \times 10^{-6} \text{ sec} + 1.7 \times 10^{-6} \text{ sec}}$$

Averaging this dissipation over the full cycle period for the inverter determines the contribution of the recovery losses to the total diode

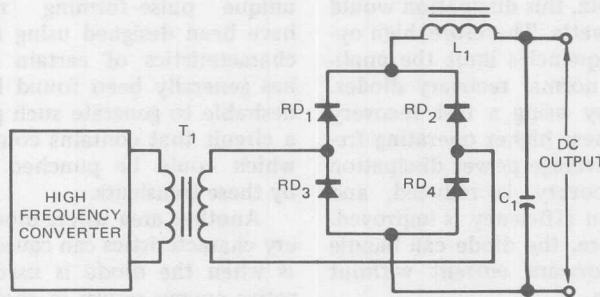


Figure 1-76. High Frequency Inverted Bridge Circuit

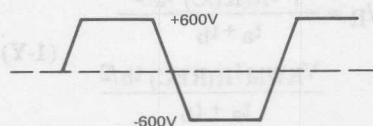


Figure 1-77. Output Waveshape of T_1 Inverter Bridge

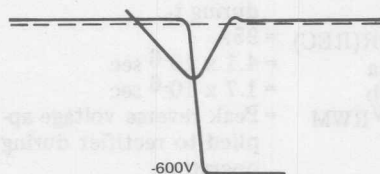


Figure 1-78. Inverter Bridge Rectifier Recovery Characteristics

dissipation. This contribution is given in Formula 1-Z.

$$W_a = fW_R (t_a + t_b) \quad (1-Z)$$

Where:

W_a = Average recovery power

f = Inverter operating frequency

Assume:

$$f = 1 \text{ kHz}$$

Therefore:

$$W_a = 48.8 \text{ W}$$

At 3 KHz, this dissipation would be 146.4 watts. Therefore, high operating frequencies limit the application of normal recovery diodes.

Thus, by using a fast recovery diode at these higher operating frequencies, average power dissipation during recovery is reduced, and rectification efficiency is improved. Furthermore, the diode can handle a larger forward current without overheating.

It has also been found, especially in some of the higher current dif-

fused rectifiers, that the sweep-out characteristic can display a rather dismaying property. The declination rate (time for decay of the bulk recovery current) can be very fast. This sudden decrease of current generates a rather high apparent di/dt in the distributed inductance of the circuit and the resultant voltage ($e = L di/dt$), generated by this "snap-off" characteristic, has often attained a peak value several times the circuit voltage. Consequently, it is important not only to provide a high current rectifier with limited apparent stored charge, but that it should exhibit a controlled declination rate of bulk recovery current in order to assure predictable transient voltages.

Figure 1-79 characterizes the four types of recovery characteristics of a rectifier. Figure 1-79(a) depicts a "normal" recovery for a diffused power rectifier. Figure 1-79(b) shows the typical recovery current of a rectifier with a snap-off characteristic. Figure 1-79(c) shows recovery current of a "soft" recovery rectifier, and Figure 1-79(d) shows recovery current of a fast recovery rectifier. The snap-off diode characteristic has been found to be so rapid that some rather unique pulse-forming networks have been designed using the snap characteristics of certain units. It has generally been found less than desirable to generate such pulses in a circuit that contains components which could be punched through by these transients.

Another area where diode recovery characteristics can cause trouble is when the diode is used for reactive energy return in choppers. If the load is reactive enough to conduct during the whole off period

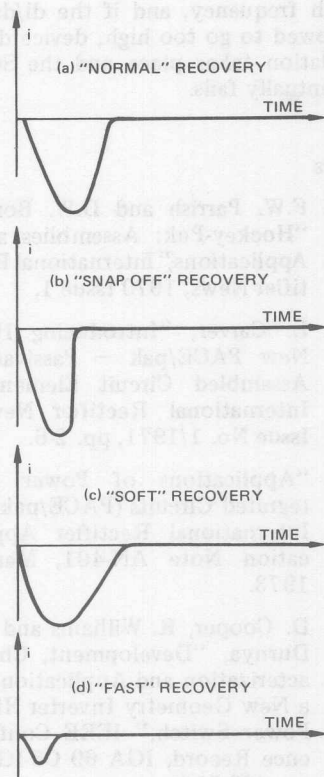


Figure 1-79. Rectifier Recovery Characteristics

for the SCR, when the SCR is again triggered, it sees essentially a short circuit until the diode recovers. Generally, unless some means is used to limit the initial current through the SCR and diode (or a fast recovery diode is used), there will be excessive di/dt through the SCR. This is a particularly insidious problem, because di/dt can manifest itself as a slow deterioration causing the SCR to fail many months later.

The SCR itself also has a reverse recovery interval, which can give rise to similar difficulties if it is not fully appreciated during design.

di/dt

If the current in an SCR is allowed to build up too rapidly at turn-on, there is a current crowding effect in the area where gate current is flowing. The device switches on progressively across the junction, starting at the point where the gate current is injected at about $0.1 \text{ mm}/\mu\text{sec}$. (This turn-on increase in current is called di/dt .) This current crowding causes local overheating, which may or may not destroy the device immediately. There can, however, be a degradation in device characteristics which will eventually lead to a failure. Therefore, it is important that if the basic external circuits will allow the current in the device to rise at above a certain critical rate, then the external circuit has to be modified by the introduction of sufficient inductance, to reduce the maximum possible rate of change of current to within a defined value.

The most obvious area where this can happen is in resistive or capacitive circuits, where the SCR must switch on into such a load. The designer must be cautious when dealing with these loads.

Another trap exists where the load is an incandescent lamp. In this case, the load is not only resistive, but the initial current, when the lamp is cold, can be ten times the rated running current.

Another area that must be considered is the R-C snubber network, where the SCR is expected to discharge the snubber capacitor each time it turns on. This discharge

current increases the di/dt required of the device.

Also, high di/dt in a circuit can lead to higher switching losses, which is especially important at

high frequency, and if the di/dt is allowed to go too high, device degradation takes place and the SCR eventually fails.

References

1. F.E. Gentry, et. al., "Semiconductor Controlled Rectifiers," Prentice-Hall, Inc., Englewood Cliffs, New Jersey, 1964, pp. 65-68.
2. Ibid, pp. 68-77.
3. I. Somos, "Switching Characteristics of Silicon Power Controlled Rectifiers, I — Turn-on Action," Transactions of AIEE, Part 1, Volume 80, July 1961.
4. I.M. Mackintosh, "The Electrical Characteristics of Silicon P-N-P-N Triodes," Proceedings of the IRE, Volume 40, June 1958, pp. 1229-1235.
5. R.W. Aldrich and N. Holonyak, Jr., "Multiterminal P-N-P-N Switches," Proceedings of the IRE, Volume 46, June 1958, pp. 1236-1239.
6. D.R. Muss and C. Goldberg, "Switching Mechanism in the N-P-N-P Silicon Controlled Rectifier," IEEE Transactions on Electron Devices, Volume ED-10, May 1963, pp. 113-120.
7. F.B. Golden, "Measure SCR Switching Losses the Easy Way," GE Seminar Application Information, March 1970.
8. J. Gault, "Power Logic-Triac... The Inside Story," International Rectifier, "Rectifier News," Fall 1967, pp. 2-3.
9. F.W. Parrish and D.W. Borst, "Hockey-Puk: Assemblies and Applications," International Rectifier News, 1970 Issue 1.
10. L. Carver, "Introducing IR's New PACE/pak — Passivated Assembled Circuit Element," International Rectifier News, Issue No. 1/1971, pp. 2-6.
11. "Applications of Power Integrated Circuits (PACE/pak)," International Rectifier Application Note AN-401, March 1973.
12. D. Cooper, R. Williams and F. Durnya, "Development, Characterization and Application of a New Geometry Inverter High Power Switch," IEEE Conference Record, IGA 69 C5-IGA, pp. 499-506.
13. A.S. Grove, "Physics and Technology of Semiconductor Devices," John Wiley and Sons, New York, 1967.
14. I. Somos, "Switching Characteristics of Silicon Power Controlled Rectifiers II — Turn-Off Action and dv/dt Self-Switching," Conference Paper for IEEE Summer General Meeting and Nuclear Radiation Effects Conference, Toronto, Ont., Canada, June 16-21, 1963.
15. N. Mapham, "Overcoming Turn-On Effects in Silicon

- Controlled Rectifiers," *Electronics*, August 17, 1962.
16. J.S. Read and R.F. Dyer, "Power Thyristor Rating Practices," *Proceedings of the IEEE*, Vol. 55, No. 8, August, 1967, pp. 1312-1317.
 17. D.W. Borst, "Turn-On Action in Large-Area Controlled Rectifiers," *Proceedings of the IEEE*, (Proceedings Letters) August 1967.
 18. R.L. Longini and J. Malngailis, "Gated - Turn-On of Four Layer Switch," *IEEE Transactions on Electron Devices*, Volume ED-10, May 1963.
 19. N. Mapham, "The Rating of SCRs When Switching into High Currents," *IEEE CP* 63-1091, 1963.
 20. K. Aaland, "Pulse Current Limits of Silicon Controlled Rectifiers," *IEEE CP*-1236, 1963.
 21. D.E. Burke and G.W. Albrecht, "RCA 40216 Silicon Controlled Rectifier Design Considerations and Device Data for Use in High-Current Pulse Application," *RCA Application Note SMA-29*, 1963.
 22. R.F. Dyer, "Concurrent Characterization of SCR Switching Parameters for Inverter Applications," *Semiconductor Products and Solid-State Technology*, April 1965.
 23. J. Warren and R. Wagner, "Applying Silicon Controlled Rectifiers, Part 1, SCR Protection and Gate Firing Circuits," *Automation*, 1965.
 24. J.C. Hey, "Triggering SCRs into High di/dt ," *EDN*, Nov., 1965.
 25. R.F. Dyer, "The Rating and Application of SCRs Designed for Power Switching at High Frequencies," *IEEE Conference Record of the Industrial Static Power Conversion Conference*, Nov., 1965.
 26. I. Somos and D.E. Piccone, "Behavior of Power Semiconductor Devices Under Transient Conditions in Power Circuits," *IEEE Conference Record of the Industrial Static Power Conversion Conference*, November, 1965.
 27. R. Wechsler, "Reducing (di/dt)-Effect Failures in Silicon Controlled Rectifiers," *Motorola Tech. Inform. Note AN-173*, 1966.
 28. W.H. Dodson and R.L. Longini, "Probed Determination of Turn-On Spread of Large Area Thyristors," *IEEE Transactions on Electron Devices*, Vol. ED-13, No. 5, May 1966.
 29. J.B. Rice, "Design of Snubber Circuits for Thyristor Converters," *IEEE Conference Record of Fourth Annual Meeting of Industry and Applications Group*, 1969.
 30. J.B. Rice and L.E. Nickels, "Commutating dv/dt Effects in Thyristors Three-Phase Bridge Converters," *IEEE Transactions on Industry and General Applications*, November/December 1968.

31. W. McMurray, "Optimum Snubbers for Power Semiconductors," IEEE Conference Record of Sixth Annual Meeting of Industry and General Applications Group, 1971.
32. J.D. Harnden, Jr., and F.B. Golden, "Power Semiconductor Applications, Volume I: General Considerations," IEEE Press, New York, 1972.
33. N. Mapham, "The Ratings of SCRs when Switching into High Currents," IEEE CP-63 498, Winter General Meeting New York, January 29, 1963.
34. R.F. Dyer, "The Rating and Application of SCRs Designed for Switching at High Frequency," IEEE Transactions on Industry and General Applications, January/February 1966.
35. J.D. Harnden, Jr., "Present Day Solid-State Switches," IEEE Spectrum, September 1965.
36. H.F. Storm, "Solid-State Power Electronics in the U.S.A.," IEEE Spectrum, Oct. 1969, pp. 49-59.

Parallel Operation

Important Characteristics

The following characteristics of thyristors are of importance in achieving an optimum design in a large power, high current converter using devices in parallel: 1) Turn-on sensitivity, 2) Delay time, 3) Finger voltage, 4) Turn-on propagation characteristics, 5) Latching and holding current, 6) On-state voltage, 7) Thermal resistance, and 8) Loop Inductance.

The relative importance of these characteristics depends upon the system that is being designed in terms of whether it is a single-phase converter, multiple phase converter, chopper, inverter, etc. This is important because of the theoretical rise time possible of the device currents due to the external circuit limitations. We can discuss some of

the system characteristics and their relation to each other and some of the solutions commonly used to help to control or match the characteristics of the devices. The solutions used by the circuit designer will depend upon his particular application.

Of the eight listed characteristics, turn-on sensitivity, delay time, and turn-on propagation characteristics are interrelated. Turn-on propagation was discussed in detail in Chapter 1 and will not be discussed here. Figure 2-1 shows the delay times of two thyristors manufactured by different methods. Curve A is typical of the characteristic of an alloy diffused SCR. Curve B is typical of either an epitaxial diffused thyristor or a double-diffused thyristor.

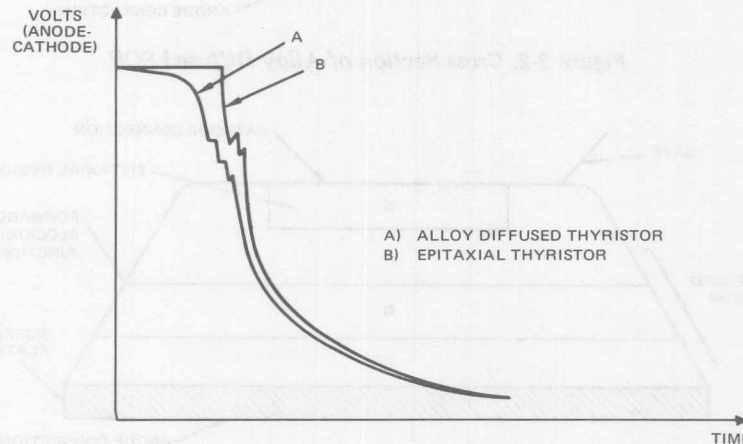


Figure 2-1. Turn-On Characteristics of Two Thyristors

Turn-On Sensitivity and Delay Time

In order to understand why these characteristics are inherently different, one must understand a little about the construction of each type of device and how the cathode regions are formed in them. In the case of an alloy diffused thyristor, after the initial diffusion sandwich forming a PNP wafer is achieved, the final junction is formed by alloying a gold antimony disc into the top of the silicon wafer as shown in Figure 2-2. This forms an N-region and forms the final PN junction. Because this

is a relatively imprecise means of forming a junction, this region has a rather feathered boundary and therefore provides somewhat of a nonuniform turn-on characteristic as is seen in Figure 2-1.

Figure 2-3 shows the construction of an epitaxial diffused device which is formed in terms of the PNP sandwich in a similar manner to that of the alloy diffused device, but when the final N region is added, a well-defined window is cut into the silicon and intrinsic silicon is mixed in a gaseous form with an N dopant and deposited into this

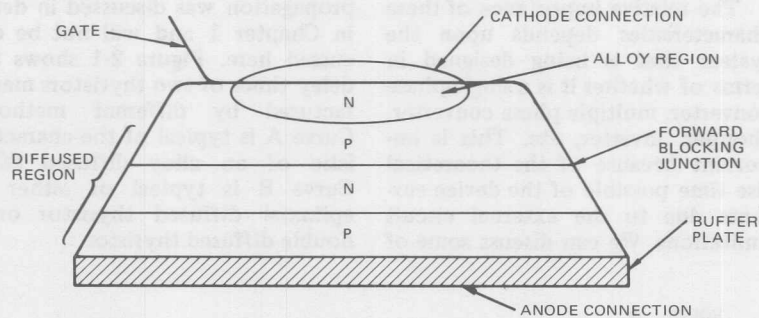


Figure 2-2. Cross Section of Alloy Diffused SCR

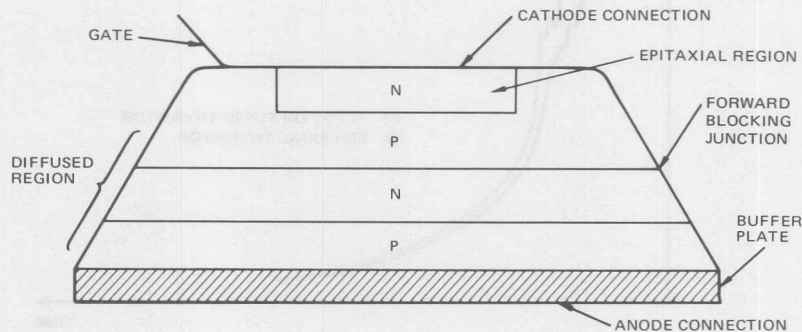


Figure 2-3. Cross Section of Epitaxial Diffused SCR

window forming a much more sharply defined PN junction. This junction, which can be considered hyperabrupt, exhibits a much more uniform turn-on characteristic and a much more uniform delay time characteristic as is shown in Figure 2-1.

In many applications, this type of characteristic is not important. Where the devices are to be paralleled, the turn-on characteristic of the device, including the triggering sensitivity and the delay time, become important. For example, consider two SCRs to be connected in parallel; first two devices having an alloy diffused structure, and then two devices having an epitaxial diffused structure, and consider their various characteristics and what might happen if these characteristics were not in some way taken into consideration in the circuit design.

Figure 2-4 illustrates one of the sets of conditions for alloy diffused devices that may result in this case. The turn-on characteristic of device A, shown in the top of Figure 2-4, indicates that the anode-to-cathode voltage begins to fall more quickly because the triggering sensitivity of that device, as shown in the second part of Figure 2-4, is slightly greater than that of device B. Since the devices have no well-defined delay time, they begin to turn on as soon as gate current is applied and then the voltage across device A begins to fall more rapidly as both devices go into the regenerative turn-on mode.

The anode current as shown in the third part of Figure 2-4 begins to rise sooner in device A than in device B, and even if the devices had been matched in forward voltage at some high current, they

would never achieve that current level equally because of the unequal turn-on characteristics. Figure 2-4 is somewhat optimistic in the fact that anode current of device B is shown rising at all. If indeed device A turned on and there were no appreciable inductance in the loop which includes device A, device B might never turn on if the anode-to-cathode voltage of A fell below the finger voltage of B before it triggered.

One of the things that affects the degree of importance of this characteristic is the amount of inductance in each SCR loop. This loop inductance can be built in by the construction of the equipment, or may be inserted in the form of a saturable or a nonsaturating inductance, whichever is more economic and more feasible for the circuit designer in order to force this type of sharing.

One method of equalizing this turn-on characteristic of alloy diffused devices is to choose a resistor to be put in series with each gate of the devices to be paralleled. By adjusting the turn-on sensitivity of the device under a given anode-to-cathode voltage and triggering characteristic, this resistor can force better uniformity in the devices. This technique is not necessary if a device with a hyper-abrupt junction is used as in the case of an epitaxial diffused device.

Let's consider a similar idealized example of the turn-on characteristics of the epitaxial diffused device shown in Figure 2-5. Figure 2-5 shows the anode-to-cathode voltage vs. time characteristic, the gate triggering current characteristics, and the anode current resulting from paralleling two epitaxial diffused

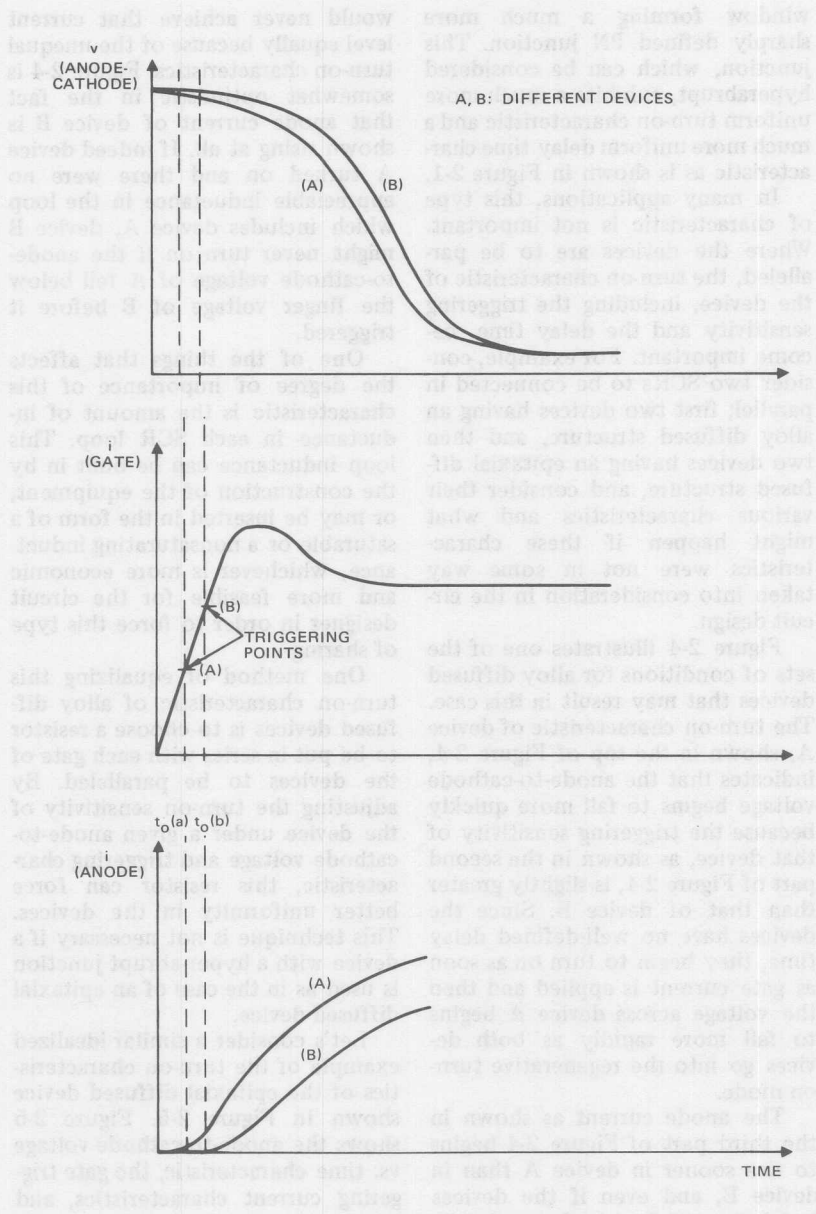


Figure 2-4. Alloy Diffused SCR Turn-On Characteristics

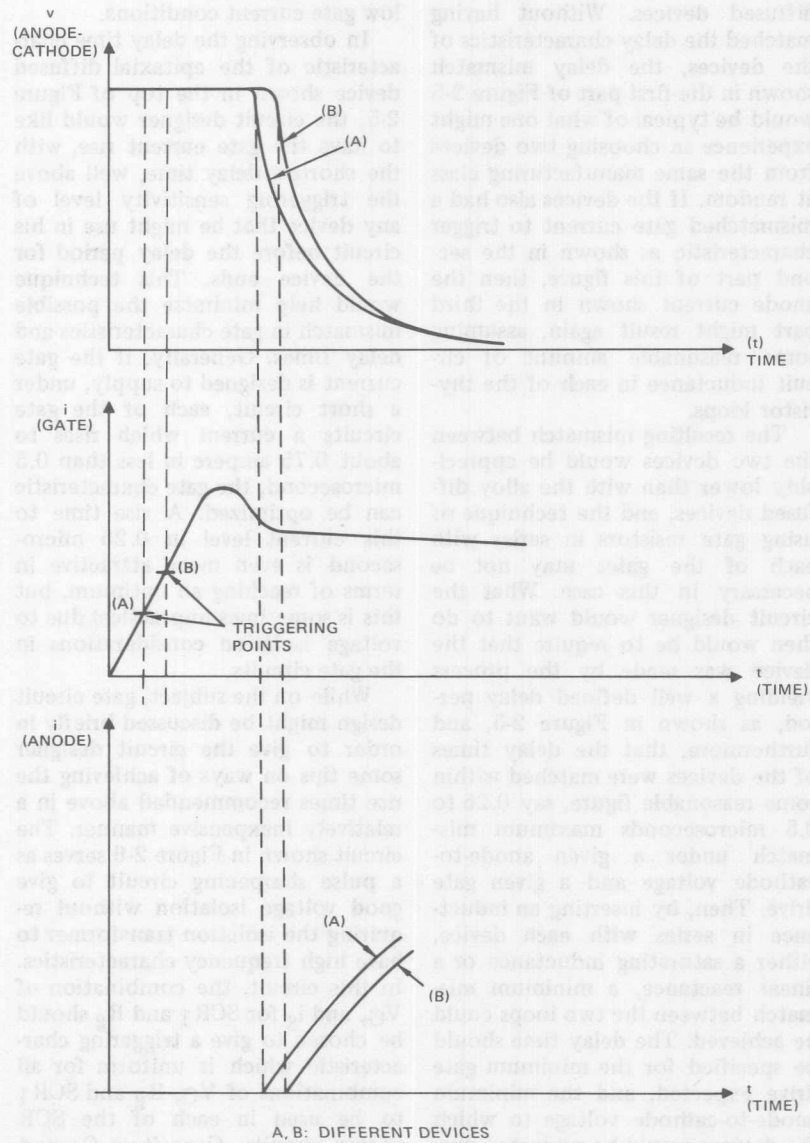


Figure 2-5. Epitaxial Diffused SCR Turn-On Characteristics

thyristors in a similar fashion to that used in Figure 2-4 for the alloy diffused devices. Without having matched the delay characteristics of the devices, the delay mismatch shown in the first part of Figure 2-5 would be typical of what one might experience in choosing two devices from the same manufacturing class at random. If the devices also had a mismatched gate current to trigger characteristic as shown in the second part of this figure, then the anode current shown in the third part might result again, assuming some reasonable amount of circuit inductance in each of the thyristor loops.

The resulting mismatch between the two devices would be appreciably lower than with the alloy diffused devices, and the technique of using gate resistors in series with each of the gates may not be necessary in this case. What the circuit designer would want to do then would be to require that the device was made by the process yielding a well defined delay period, as shown in Figure 2-5, and furthermore, that the delay times of the devices were matched within some reasonable figure, say 0.25 to 0.5 microseconds maximum mismatch under a given anode-to-cathode voltage and a given gate drive. Then, by inserting an inductance in series with each device, either a saturating inductance or a linear reactance, a minimum mismatch between the two loops could be achieved. The delay time should be specified for the minimum gate drive expected, and the minimum anode-to-cathode voltage to which the devices would be subjected during turn-on for current sharing, because delay time of a device will

lengthen under low anode to cathode forcing voltages and also under low gate current conditions.

In observing the delay time characteristic of the epitaxial diffused device shown in the top of Figure 2-5, the circuit designer would like to have the gate current rise, with the shortest delay time, well above the triggering sensitivity level of any device that he might use in his circuit before the delay period for the device ends. This technique would help minimize the possible mismatch in gate characteristics and delay times. Generally, if the gate current is designed to supply, under a short circuit, each of the gate circuits a current which rises to about 0.75 ampere in less than 0.5 microsecond, the gate characteristic can be optimized. A rise time to this current level in 0.25 microsecond is even more attractive in terms of reaching an optimum, but this is sometimes impractical due to voltage isolation considerations in the gate circuits.

While on the subject, gate circuit design might be discussed briefly in order to give the circuit designer some tips on ways of achieving the rise times recommended above in a relatively inexpensive manner. The circuit shown in Figure 2-6 serves as a pulse sharpening circuit to give good voltage isolation without requiring the isolation transformer to have high frequency characteristics. In this circuit, the combination of V_G , and i_g for SCR₁ and R_g should be chosen to give a triggering characteristic which is uniform for all combinations of V_G , R_g and SCR₁ to be used in each of the SCR trigger circuits. Capacitors C_1 and resistors R_1 act not only as delay circuits to square up the collector

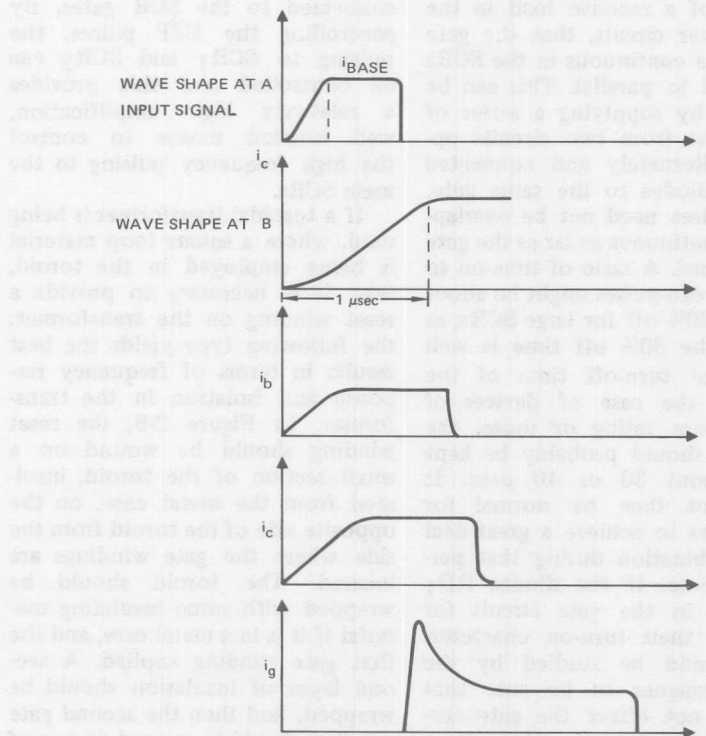
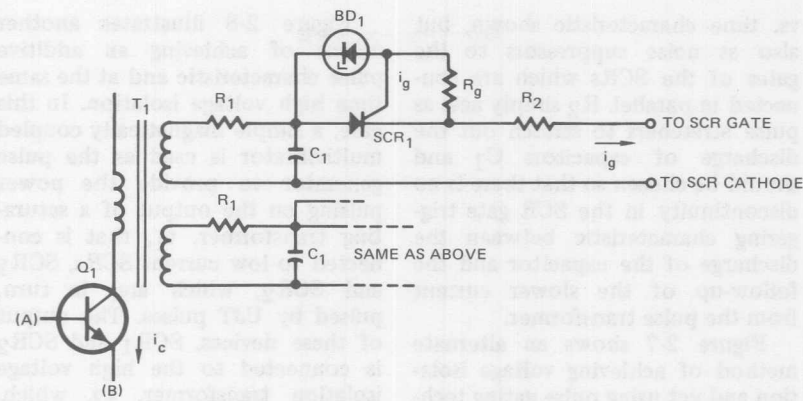


Figure 2-6. Pulse Sharpener Circuit

vs. time characteristic shown, but also as noise suppressors to the gates of the SCRs which are connected in parallel. R_2 simply acts as pulse stretchers to stretch out the discharge of capacitors C_1 and should be chosen so that there is no discontinuity in the SCR gate triggering characteristic between the discharge of the capacitor and the follow-up of the slower current from the pulse transformer.

Figure 2-7 shows an alternate method of achieving voltage isolation and yet using pulse gating techniques where it may be important, because of a reactive load in the main power circuit, that the gate current be continuous in the SCRs connected in parallel. This can be achieved by supplying a series of gate pulses from two circuits operating alternately and connected through diodes to the same gate. These pulses need not be overlapping or continuous as far as the gate is concerned. A ratio of time-on to time-between-pulses might be about 70% on, 30% off for large SCRs, as long as the 30% off time is well below the turn-off time of the SCR. In the case of devices of 300 ampere rating or more, the off time should probably be kept below about 30 or 40 μsec . It would not then be normal for the devices to achieve a great deal of recombination during that period of time. If the diodes RD_1 are used in the gate circuit for isolation, their turn-on characteristics should be studied by the circuit designer to be sure that they do not effect the gate current rise characteristic. Normally a device doped for fast recovery characteristics will serve well in this type of application.

Figure 2-8 illustrates another means of achieving an additive pulse characteristic and at the same time high voltage isolation. In this case, a simple magnetically coupled multivibrator is used as the pulse generator to provide the power pulsing on the output of a saturating transformer, t_1 , that is connected to low current SCRs, SCR_1 and SCR_2 , which are, in turn, pulsed by UJT pulses. The output of these devices, SCR_1 and SCR_2 is connected to the high voltage isolation transformer, t_2 , which, through two squaring networks, is connected to the SCR gates. By controlling the UJT pulses, the pulsing to SCR_1 and SCR_2 can be controlled and this provides a relatively high amplification, well isolated means to control the high frequency pulsing to the main SCRs.

If a toroidal transformer is being used, where a square loop material is being employed in the toroid, then it is necessary to provide a reset winding on the transformer; the following type yields the best results in terms of frequency response and isolation in the transformer. In Figure 2-9, the reset winding should be wound on a small section of the toroid, insulated from the metal case, on the opposite side of the toroid from the side where the gate windings are located. The toroid should be wrapped with some insulating material if it is in a metal case, and the first gate winding applied. A second layer of insulation should be wrapped, and then the second gate winding should be wound on top of the first one. The primary winding should then be wound on top of the gate windings with the neces-

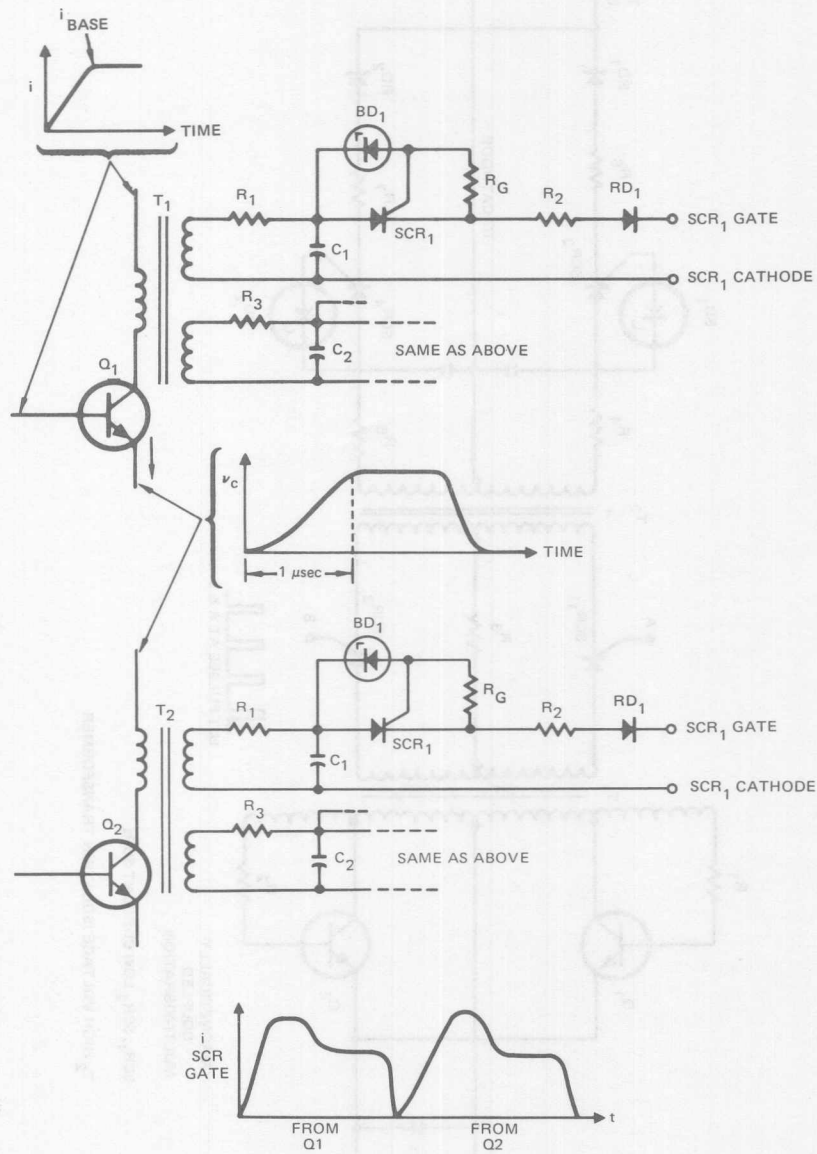
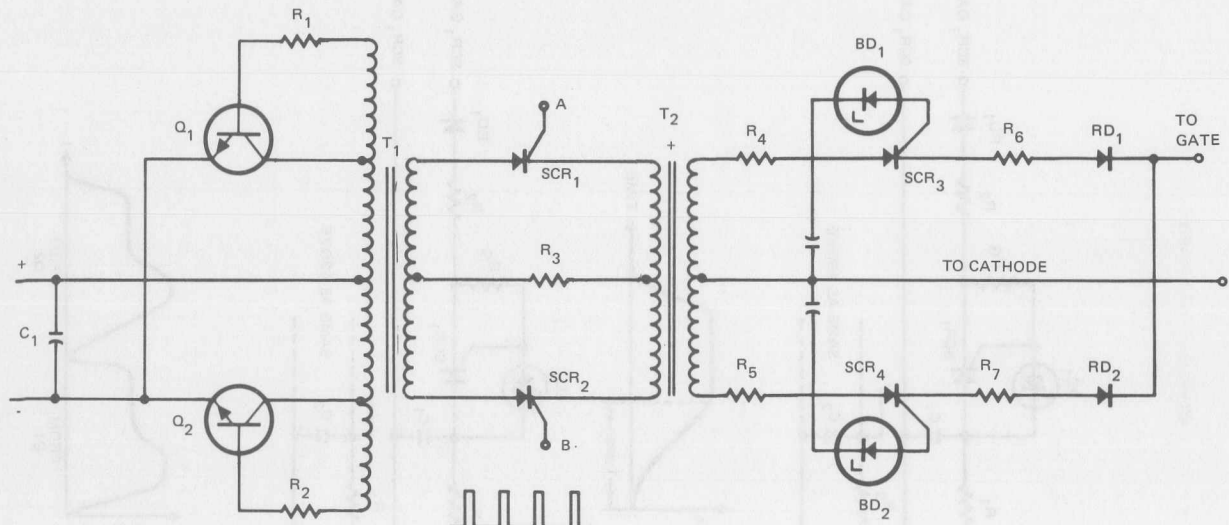


Figure 2-7. Multiple Gate Circuits to Achieve Continuous Pulsing



MAGNETICALLY
COUPLED
MULTI-VIBRATION

SCR₁, SCR₂ LOW CURRENT SURs

T₂ HIGH VOLTAGE ISOLATION TRANSFORMER



Figure 2-8. Multi-Vibrator Pulse Generator Circuit

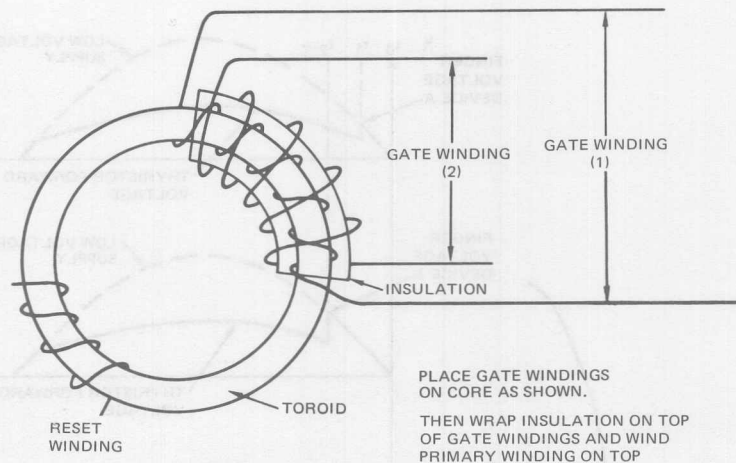


Figure 2-9. Toroidal Transformer with Reset Winding

sary insulation material in-between. This gives an optimum coupling between the gate windings in terms of equalization to the main or primary winding.

Finger Voltage

Probably the least understood characteristic and certainly one of major importance in high frequency thyristor applications is the finger voltage of the device. The finger voltage characteristic of a thyristor can be seen by observing the trace of the anode-to-cathode voltage vs. time during the operation of the device under a given applied time varying anode voltage and gate drive condition, as in Figure 2-10(b). All thyristors require some minimum anode to cathode voltage (greater than the normal on-state voltage) before they can be triggered into conduction. The reason for this is not fully understood, but it can be explained in terms of the low current, low voltage, saturated gain of the PNP transistor in

the two transistor model which is used to explain the operation of thyristors.

Unless this minimum anode-to-cathode voltage (finger voltage) is actually applied to the thyristor, it will not turn on. Figure 2-10(a) shows the V-I characteristic for two thyristors which are perfectly matched except for finger voltage, device A having a lower finger voltage than device B. Forward voltage waveshapes applying to the two devices are shown in Figure 2-10(b). At time " t_0 ," the thyristors become forward biased and the gate current is applied. However, thyristor A does not begin to conduct until time " t_1 ," and thyristor B conducts later at time " t_2 ." Therefore, if thyristors A and B are connected directly in parallel, thyristor B will never see a high enough voltage to turn on. From this, it can be seen that the specification of finger voltage is a critical requirement in very low voltage applications.

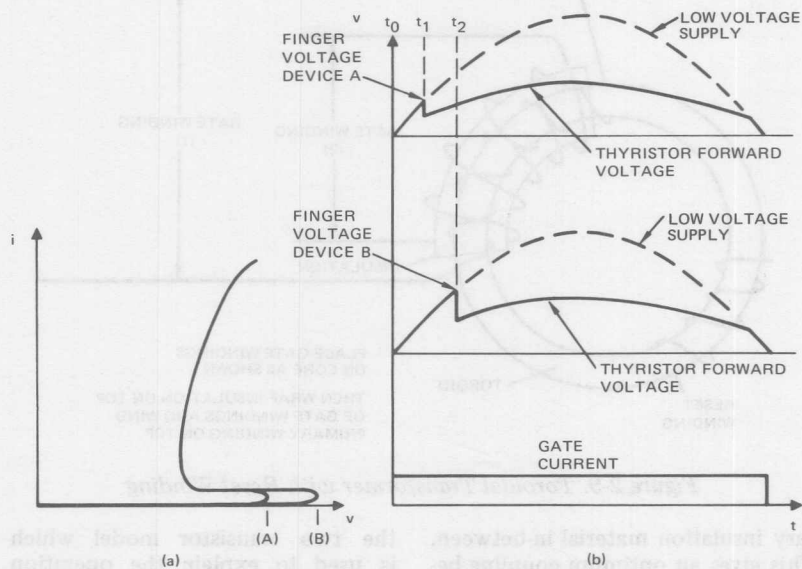


Figure 2-10. Finger Voltage

In higher voltage applications, finger voltage can be an important parameter where parallel thyristors are to be gated just before, or at the time, the thyristor becomes forward-biased. It is possible to minimize the effects of finger voltage in two ways. First, by ensuring that gate current is not applied to the thyristors until the supply (anode-to-cathode) voltage has risen above the maximum finger voltage level. Second, by including an inductor in series with each thyristor, with sufficient voltsecond capability to ensure that all thyristors have more than the finger voltage before the inductors saturate.

This finger voltage characteristic is most pronounced in high voltage devices (thyristors processed from high resistivity silicon with wide base regions). If this characteristic were not measured and matched for

a group of thyristors to be connected in parallel, and should one device possess a much higher finger voltage than another, the device with the high finger voltage might never turn on fully.

All major manufacturers of devices understand this characteristic well enough to measure it under given anode-to-cathode voltage and gate drive conditions and to specify a match so that the circuit designer can then include sufficient loop inductance in the individual thyristor loops to equalize the voltage under a worst match condition. Usually any linear or nonlinear inductance used in the individual thyristor loops to help equalize the turn-on characteristics, the mismatch due to delay mismatch, and to minimize the turn-on inrush of anode current differences due to equalization characteristic differences, is suffi-

cient to equalize the finger voltages between devices, so long as this voltage has been tested and reasonably well matched among the individual thyristors.

Latching and Holding Current

The next characteristic, "Latching and Holding Current," is important to understand, because the two are not the same, and also they are important in terms of successful turn-on of a thyristor with a given gate drive. The "holding current" is that minimum on-state current that sustains the device current conduction following operation at some nominal level of conduction current. The "latching current" is the minimum on-state current needed to keep the device in the on-state after the trigger pulse has been removed. Generally, the latching current is two to four times the holding current for a given device. The holding current is important in an inductive circuit where, after a gate pulse is applied to a device and it has turned on successfully, some disturbance in the load temporarily diminishes the anode current of the thyristor. If this anode current should fall below the holding current the device may turn off. If subsequently the load demands more current, the load current will be found to have been discontinued, unless an additional gate pulse is supplied to the thyristor to turn it on again.

It is important that a thyristor reach the latching current level before the initial gate pulse is removed from the thyristor or else it may turn back off again and never reach full conduction. In a circuit where devices are being paralleled and their gates are being supplied

with gate pulses, this latching current level is important to know for a given set of devices to insure that all of the devices will turn on and stay on, once the gate pulses are removed. This characteristic is also important where an inductance is being inserted with each thyristor in a parallel circuit, so that with a given anode-to-cathode voltage supplied to the device, the required duration of the gate pulse can be obtained by the following simple relationship:

Latching current and holding current decreases with temperature increase, as the gate current increases, and as the applied anode voltage increases. Therefore, the measurements chosen for a given circuit should be chosen carefully to match up with the worst case device characteristics in terms of the circuit conditions to which the device will be subjected.

Steady-State Conditions

Once all of the transient sharing conditions mentioned to this point are satisfied, the matter of steady-state conditions must be considered in terms of paralleling the devices. The primary consideration is the on-state voltage of the device. In order for devices to equally share load current, the drops across parallel paths must be equal. Even if an inductance is inserted in series with the thyristor, a mismatch in the steady-state equalized on-state voltages of the thyristors could cause a mismatch of current.

It is important to specify the maximum anode current expected in the thyristor under the worst operating condition at which the devices are expected to share equal-

ly and also the maximum temperature at which this current can occur. This, then, will guarantee that once the devices are matched at this level, they will be matched under the worst case condition.

An additional consideration, when considering Hockey-Puk type devices, is the thermal resistance of the device. When Hockey-Puks are connected for parallel operation, they should be mounted using the maximum allowable mounting force in order to minimize the thermal resistance differences from one device to another. If the thermal resistances between the internal pole pieces and the junctions are different, even if the on-state voltages are closely matched at a given junction temperature, the junction temperatures from one device to another could vary because of different abilities to transmit heat and therefore the desired match in on-state characteristics might never be obtained.

Loop Inductance

With all of these device characteristics taken into consideration, the last item to consider (but by far not the least) is the loop inductance in the thyristor arrangement. Obviously, any time a group of large devices is to be connected in parallel, it is difficult to get the current in and out of the thyristor packages and equalize the inductances in each current carrying loop. Proximity of ferrous materials or other conductors to the bus-bars coming to and from the individual thyristors can affect the magnetic fields and therefore can change the apparent inductance. Differences in spacing between conductors and incoming and outgoing bus-bars can also

change this inductance. Various methods have been used in the past to provide forcing of current in this type of loop. One method is shown in Figure 2-11, and discussed in Reference [1]. In this case, a series of current balancing reactors are connected as shown, in order to force current sharing during the initial period of conduction in each circuit. This method is used infrequently in today's circuit designs, because of the high cost of the core material and the expense involved in paralleling multiple devices.

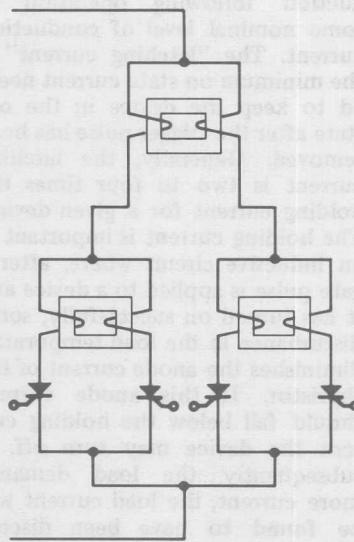


Figure 2-11. Thyristor Assembly [1]

A second approach is to use a linear reactor in series with each device and to go through the exercise of specifying the devices under the limitations previously discussed in this section and choosing the magnitude of the inductance to satisfy those conditions outlined.

A third system which is used quite effectively is to use a delay reactor in series with each thyristor to provide the same sort of inductive function as mentioned above but to minimize the size of the reactor by minimizing its volt-second capacity.

Of equal importance with the choice of type of magnetic device used for equalization is the mechanical arrangement of the thyristors in the system. For instance, two possible mechanical configurations are shown in Figures 2-12 and 2-13 with the expected current sharing per leg in each thyristor branch shown on the accompanying graphs [2]. The contrast between a straight-through, bus-bar assembly as shown in Figure 2-12, with the resulting 20% mismatch between the maximum and nominal current per device and that in Figure 2-13

shows how some slight variations in bus-bar configuration can have significant effect upon the number of devices necessary to carry a given amount of current or on the maximum expected mismatch between parallel connected devices. In this case, the ac bus-bar loops shown in Figure 2-13 change the inductance in the center of the construction, thus varying the amount of mismatch across the assembly.

Another technique that has been used successfully to minimize this mismatch in inductance per diode path is shown in Figure 2-14. If the system can be connected in a cylindrical manner, then, theoretically, the inductance becomes more nearly equalized until finally there would be no apparent mismatch due to construction variations or mismatch in inductive loops from one device to another. The degree

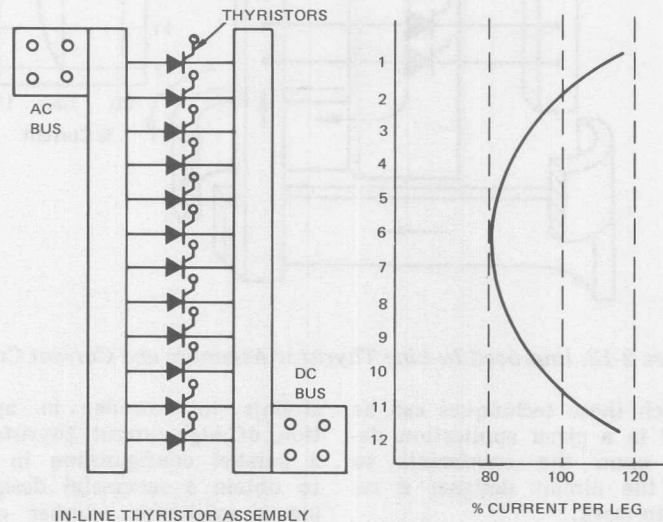


Figure 2-12. In-Line Thyristor Assembly and Current Curve

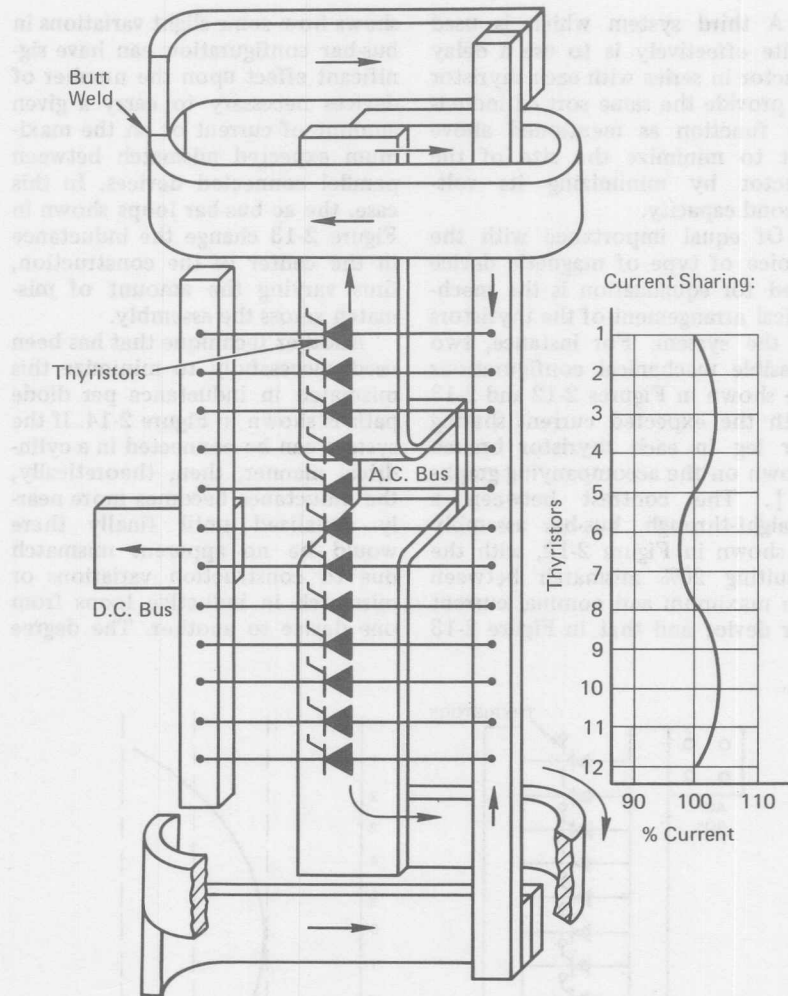


Figure 2-13. Improved In-Line Thyristor Assembly and Current Curve

to which these techniques can be applied in a given application depends upon the constraints to which the circuit designer is required to work.

It has been the aim of this chapter to point out the various con-

straints to consider in application of high-current thyristors in a parallel configuration in order to obtain a successful design using a minimum number of devices with the maximum expected reliability.

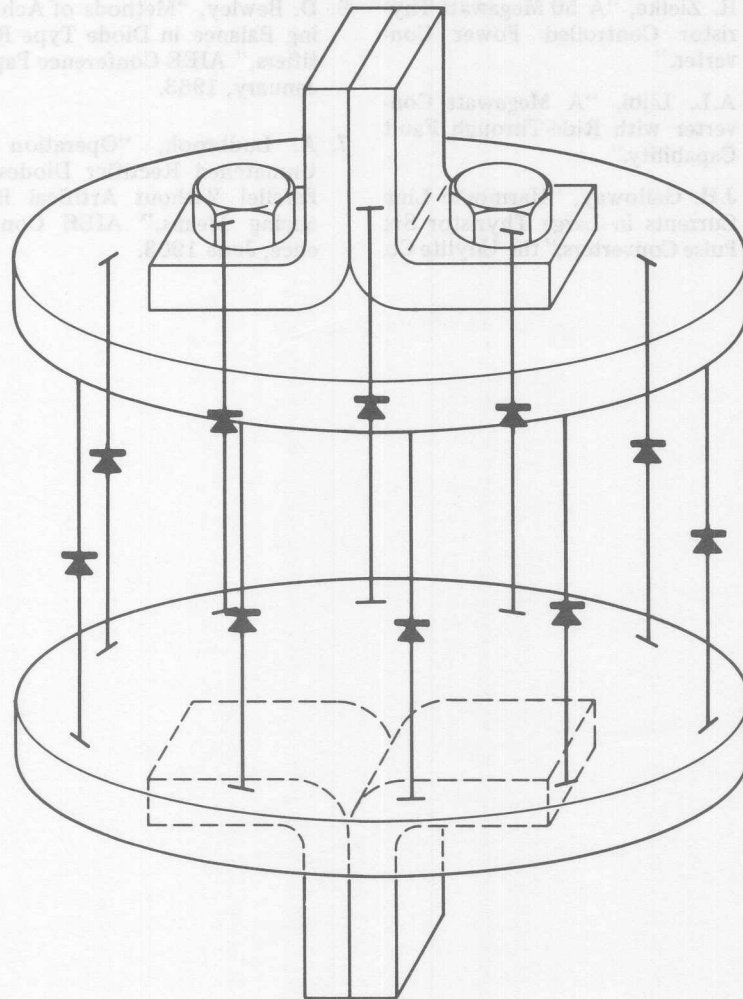


Figure 2-14. Cylindrical Paralleling Assembly

References

1. Dortort, Patent 2994028, dated July, 1961.
2. R. Zielke, "A 50 Megawatt Thyristor Controlled Power Converter."
3. A.L. Lijoi, "A Megawatt Converter with Ride-Through Fault Capability."
4. J.H. Galloway, "Harmonic Line Currents in Large Thyristor Six Pulse Converters," the Udylite Co.
5. "SCR Handbook," Second Edition, International Rectifier.
6. D. Bewley, "Methods of Achieving Balance in Diode Type Rectifiers," AIEE Conference Paper, January, 1963.
7. A. Ludbrook, "Operation of Unmatched Rectifier Diodes in Parallel Without Artificial Balancing Means," AIEE Conference, June 1963.

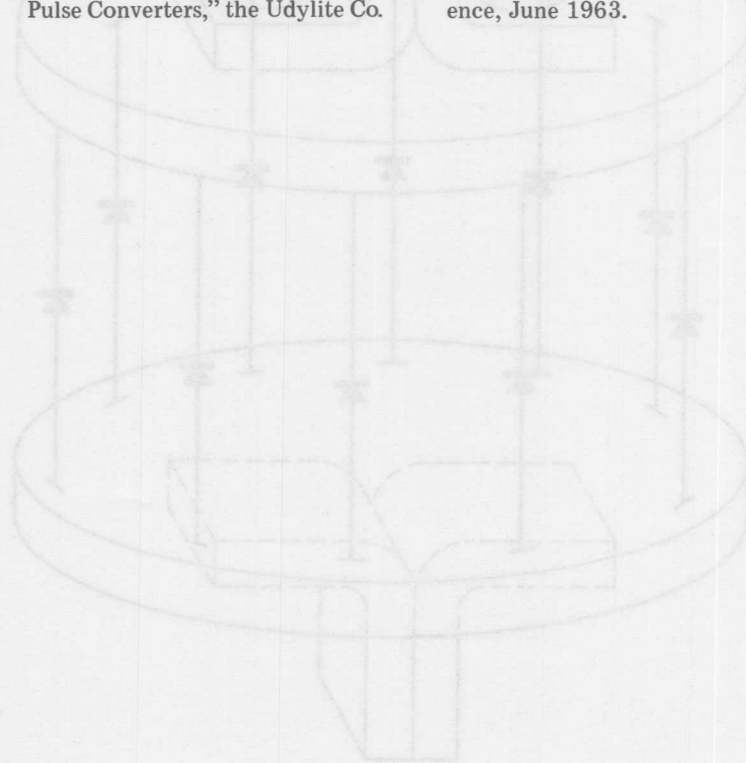


Figure 2. Six-Pulse Thyristor Converter

Series Operation

Although SCRs are available in voltage ratings in thousands of volts, it is often necessary to connect them in series in order to block higher voltages than any available individual SCR can handle. In such cases, there are several requirements to take into account in order to assure proper and safe operation of the semiconductor devices. The general topics to be considered, and which are covered in the following sections are equalization and triggering. Equalization of off-state and reverse (leakage) current of the devices will be taken into account as will equalization of the recovered charge. Reliable triggering of devices connected in series will be discussed. This section will consider the delay time differences in devices and the differences between the various capacitances to ground, or neutral. Also, some general triggering methods will be considered which can lead to an easy solution of series triggering problems.

Equalization

The two characteristics to take into consideration under this heading are elevated temperature blocking characteristics of the SCRs and their recovery characteristics. In each case, the difference in characteristics from one device to another must be considered.

If we were to examine two oscilloscope traces of anode blocking current vs. anode voltage for two different SCRs of the same family

at a given junction temperature, we might observe traces similar to those shown in Figure 3-1. For either a positive or a negative voltage applied to the SCRs, the leakage currents at a given temperature at that voltage are somewhat different. Obviously, if we were to connect these two devices in series and begin to apply voltage either in the reverse or off-state direction on the series combination, SCR₂ would begin to take the majority of the applied voltage, since its leakage at any applied voltage in either direction is lower than that of SCR₁. Although the voltage-current characteristics are nonlinear for these devices, they would, at any given condition, divide voltage in inverse proportion to their leakage currents. Therefore, if we were to try to connect these devices in series and at the same time force them to more equally share the applied voltage, a method to force this sharing would be to connect a resistor in parallel with each device as shown in Figure 3-2.

One method for equalization would be to vary the value of the resistance dependent upon whether the SCR was a high or low leakage device. We would, therefore, have unequal resistances down the string of a number of SCRs connected in series. However, this is in general not a practical approach to circuit design, and, therefore, one would like to determine some value of resistance that would be suitable for connection in parallel with any

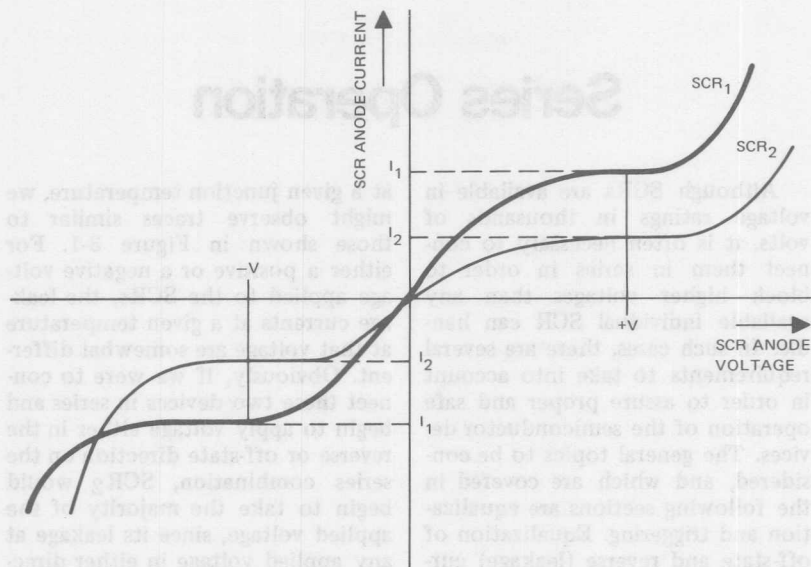


Figure 3-1. SCR Blocking Characteristics

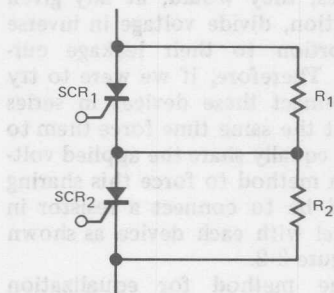


Figure 3-2. Resistor Equalization of Blocking Voltage

SCR of a given family. In order to do this, it's necessary to know certain characteristics of both the application and the devices to be used.

The first thing to know is what is the maximum voltage to be applied to the circuit; the second is

what is the maximum allowable voltage for any given device; the third is the minimum applied voltage for any given device. In other words, what is the maximum mismatch that the circuit designer wishes to see as he checks voltage across the series string with full voltage applied to it.

For instance, let's say we have a 4000V supply voltage and we would like to have a 2:1 redundancy or safety factor in the voltage rating of the devices. Therefore, we would choose devices whose total voltage capability equaled 8000V. Let's also say that we have 2200V SCRs available for the application. We would, therefore, decide that nominally we would want to connect four 2200V devices in series. Let's also assume we've decided that the maximum voltage we want

any device to see is 2100V, and the minimum voltage we want any device to see is 1900V. Therefore, the difference between the maximum and minimum applied voltage on any given cell is 200V. In addition, we look at leakage current at the maximum allowable operating junction temperature for the devices (in general, this is given as 125°C) and find that the maximum peak blocking current at 2000V is 20 mA.

The minimum peak blocking current for any given device of this family is not a characteristic generally given by SCR manufacturers. To be safe, one could assume that this value of blocking current was zero; however, this would lead to an extremely conservative design. The best way to determine this value is to contact the manufacturer, describe the application and ask for some minimum blocking current value at the maximum temperature that could be expected or guaranteed by that manufacturer in any devices delivered. Let's assume that this value is 5 mA. The difference then, between the maximum blocking current and the minimum blocking current at a given temperature with approximately the designed applied voltage is 15 mA. We then have enough information to calculate the required equalization resistance.

A derivation of the relationship between this difference in blocking current, allowable difference in voltage, and equalization resistance is given in Formula 3-A and Figure 3-3.

Assume:

$$E_1 + E_2 + E_3 = E_T$$

$$E_1 < E_{MAX}$$

$$E_2 = E_{MAX}$$

$$E_3 < E_{MAX}$$

$$\Delta E = E_2 - E_1$$

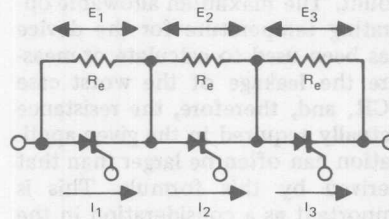


Figure 3-3. Voltage Equalization Network

Therefore:

$$I_1 - I_2 = \text{Maximum Leakage Difference} = \Delta I$$

$$\frac{E_1}{R_E} + I_1 = \frac{E_2}{R_E} + I_2 = \frac{E_3}{R_E} + I_3$$

$$\frac{E_1}{R_E} + I_1 = \frac{E_2}{R_E} + I_2$$

$$\frac{E_1}{R_E} + \Delta I = \frac{E_2}{R_E}$$

$$\Delta I R_E = E_2 - E_1$$

Therefore:

$$R_E = \frac{E_2 - E_1}{\Delta I} = \frac{\Delta E}{\Delta I} \quad (3-A)$$

Where:

E_T = Voltage to be blocked by String

E_{MAX} = Maximum Voltage Allowed per Device

R_E = Equalization Resistance

Using this derived formula, the equalization resistance for the previous example, with $\Delta E = 200$ volts and $\Delta I = 15$ mA, is $200 \div 15 \times 10^{-3}$ or 13.3 thousand ohms. This is unquestionably a conservative figure for equalization resistance. A worst case example for leakage differences has been taken into ac-

count. The maximum allowable operating temperature for the device has been used to calculate or measure the leakage of the worst case SCR, and, therefore, the resistance actually required in the given application can often be larger than that derived by this formula. This is important as a consideration in the circuit design, because dissipation in this resistor in very high voltage applications can be extremely high and, therefore, costly and limiting in the design.

Another point worth noting in considering this simple approach to choosing the equalization resistance is that unidirectional conducting thyristors have a slightly higher blocking current at a given blocking voltage and temperature in the off-state direction than in the reverse direction. Stating it another way, they have a higher blocking capability in the reverse direction than in the off-state direction. In certain applications, this can be taken into account in designing equalizing networks for series SCR strings if the application is such that the reverse voltage applied to the system is higher than the forward voltage applied.

The next consideration is to determine the power dissipated in the equalization resistor. This is given

by the expression shown in Formula 3-B. Although this seems to be a very simple relationship, for some applications it can be misleading.

$$W = \frac{(E_{MAX RMS})^2}{R_E} \quad (3-B)$$

For single phase applications, the applied voltage vs. time on a given equalizing resistor may be very close to being sinusoidal and, therefore, the maximum RMS voltage is easily determined and the power dissipated in the resistor can be calculated. However, in applications where the reverse voltage is not sinusoidal, the circuit designer should be careful to determine the maximum RMS voltage applied to any of the equalization resistors. For a rectangular voltage waveshape, as shown in Figure 3-4(a), Formula 3-C states that the RMS voltage is equal to the square root of the duty cycle times the peak voltage. This, then, reduces Formula 3-B to the expression shown as Formula 3-D.

$$E_{RMS} = \sqrt{\text{Duty Cycle} \times E_{MAX}} \quad (3-C)$$

Where:

$$\text{Duty Cycle} = \frac{t_1}{t_1 + t_2}$$

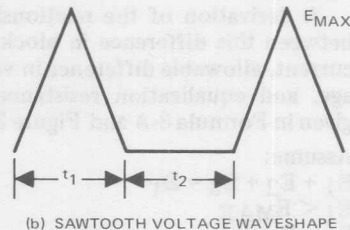
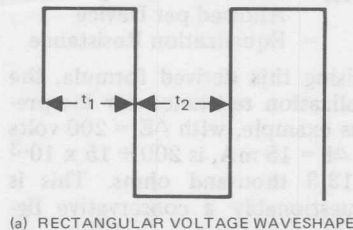


Figure 3-4. Voltage Waveshapes

$$W = \frac{\text{Duty Cycle} \times (E_{\text{MAX}})^2}{R_E} \quad (3-D)$$

Formulas 3-C and 3-D apply only in the square wave case. Similar expressions can be derived for other waveshapes; for instance, for a sine wave application of varying duty cycle, the dissipation is given by Formula 3-E.

$$W = \frac{\text{Duty Cycle} \times (E_{\text{MAX}})^2}{2 R_E} \quad (3-E)$$

For a sawtooth application as shown in Figure 3-4(b), Formula 3-F gives the expression for the dissipation.

$$W = \frac{\text{Duty Cycle} \times (E_{\text{MAX}})^2}{3 R_E} \quad (3-F)$$

Where:

$$\text{Duty Cycle} = \frac{t_1}{t_1 + t_2}$$

Another point in choosing the equalization resistor is to be careful about the type of resistor used. In the case where the voltage applied rises very sharply and the voltage per resistor is rather high, it is often wise to consider the crowding effects that can take place in a resistor. For these applications, bulk type resistors, for instance some of the noninductive bulk types, are advisable for reducing to a minimum difficulties with corona discharge in the resistor or nonlinear resistance characteristics with time. Another type of resistor that can be used here is a film type wound on a stable type of mandrel, such as glass. In most phase control applications, normal wirewound, vitreous enamel, power-type resistors are generally acceptable.

In general, when using an SCR or a triac, the circuit designer will connect a series RC combination in parallel with the SCR or triac to minimize the dv/dt applied to the device and therefore to prevent turn-on of the SCR during high rates of rise of applied circuit voltage. In the case of series connected SCRs, however, this network accomplishes a dual purpose. Because of carrier recombination in a semiconductor after on-state (forward) conduction, the semiconductor exhibits a reverse recovery phenomenon. If an SCR has been conducting forward current and then at some period later it is back-biased, it will exhibit a recovery characteristic similar to that shown in Figure 3-5. There is, then, a period of time between the application of the reverse voltage to the SCR and the ability of the SCR to block that reverse voltage. This characteristic varies somewhat as a result of varying the peak current through the

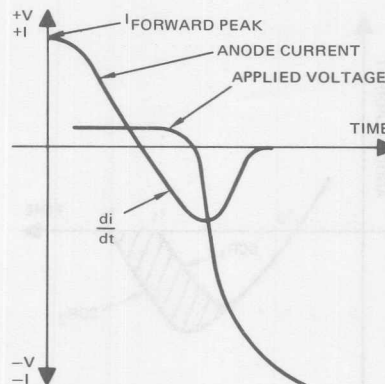


Figure 3-5. SCR Recovery Characteristics

device during conduction, the declination rate of that current (the declination di/dt), and the junction temperature of the device.

The recovery characteristic also varies from one device to another, even in a manufacturing process. Two devices from a given manufacturing lot with the same rating might show recovery characteristics as shown in Figure 3-6. If we were to integrate this recovery current over the recovery time, we would get the expression for recovered charge, Q . Subtracting the integrals for Q for the two devices, we would get an expression for the difference in stored charge of the two SCRs, ΔQ . This is shown in Formula 3-G.

$$\begin{aligned}
 Q_{SCR1} &= t_0 \int^{t_1} i_{SCR1} dt \\
 Q_{SCR2} &= t_0 \int^{t_2} i_{SCR2} dt \\
 \Delta Q &= Q_{SCR2} - Q_{SCR1} \\
 &= t_0 \int^{t_2} i_{SCR2} dt - \\
 &= t_0 \int^{t_1} i_{SCR1} dt
 \end{aligned}
 \tag{3-G}$$

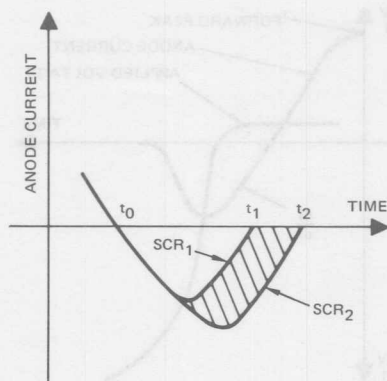


Figure 3-6. Recovery Characteristics of two Similar SCRs

Shown in Figure 3-7(a) is a series connection of the two SCRs used in the derivation of Formula 3-G, together with their steady-state equalization resistances and some series impedance in the circuit shown as "L". If a voltage were applied to this combination, the two devices would share voltage in a fashion similar to that shown in Figure 3-7(b). The resultant voltage sharing under these conditions with no external means of forcing equalization of the recovery characteristics may not be acceptable.

A means of forced sharing of the blocking voltage is to connect a series combination of a resistor, R_S , and capacitor, C_S , across each device as shown in Figure 3-8. In this way, the recovered charge of the parallel combination of R_S , C_S , and SCR is equivalent to all other parallel combinations in the series string. The size of R_S and C_S in this network is generally determined by the amount of dv/dt suppression to be accomplished for the device as well as the needed equalization of recovered charge to force voltage sharing. The size of R_S is also determined by series impedance, the type of application, and the allowable inrush current imposed on the SCR during turn-on. The size of the capacitor, C_S , is determined by the required ΔQ equalization of the two devices. If additional capacitance is required for dv/dt suppression, the capacitor can be increased in size, with no harmful effect on the sharing of blocking voltage.

The relationship between ΔQ , the difference in recovered charge from one device to another, ΔV , the allowable difference in sharing voltage during the reverse recovery of the devices and C_S , the capacitance

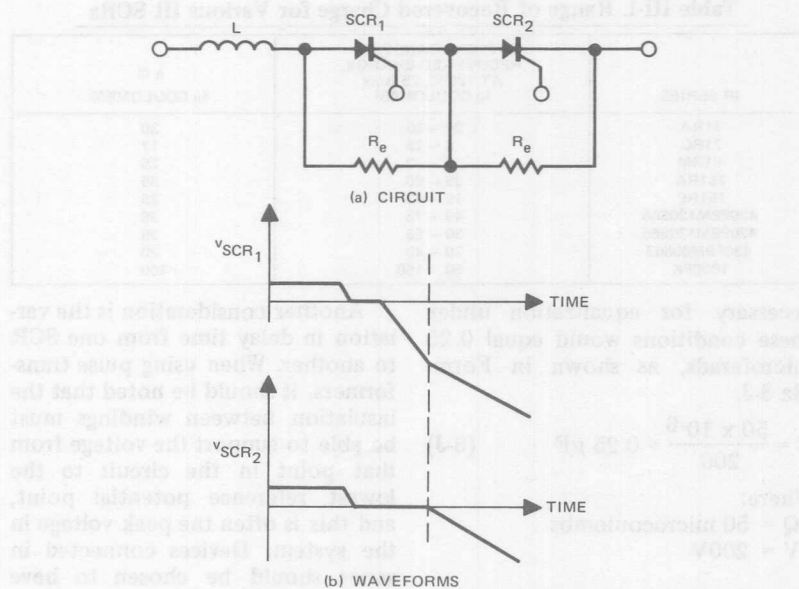


Figure 3-7. Series Connection with No Equalization Capacitor

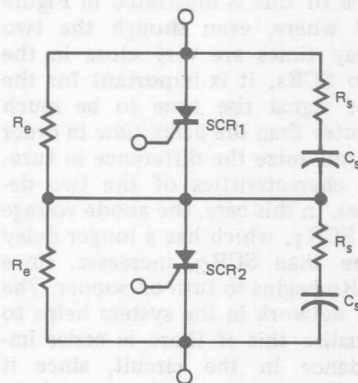


Figure 3-8. Series Connection with R-C Equalization

needed for equalization, is given in Formula 3-H. The capacity selected should be able to operate on alternating voltage without overheating.

Capacitors should also be a type, such as extended foil, having minimum inductance.

$$C = \frac{\Delta Q}{\Delta V} \quad (3-H)$$

Where:

ΔQ = Difference in recovered charge

ΔV = Allowable blocking voltage differences

C = Equalization capacitor

Table III-I gives typical recovered charge for a number of types of SCRs. As an example, if the series string of devices used in the previous example had a ΔQ of 50 microcoulombs and the allowable difference in sharing voltage was given as 200V, then the capacitance

Table III-I. Range of Recovered Charge for Various IR SCRs

IR SERIES	TYPICAL RANGE OF RECOVERED CHARGE, AT 125°C, 25 A/μs (μ COULOMBS)	Δ Q (μ COULOMBS)
71RA	20 - 50	30
71RC	8 - 25	17
81RM	5 - 30	25
151RA	25 - 60	35
151RC	15 - 40	25
420PBM120S68	45 - 75	30
420PBM120S66	30 - 55	25
430PBM60S63	20 - 40	20
1000PK	50 - 150	100

necessary for equalization under these conditions would equal 0.25 microfarads, as shown in Formula 3-J.

$$C = \frac{50 \times 10^{-6}}{200} = 0.25 \mu F \quad (3-J)$$

Where:

$$\Delta Q = 50 \text{ microcoulombs}$$

$$\Delta V = 200V$$

In high dv/dt circuits, the resistor should be chosen so that the RC circuit is overdamped. In this way, the capacitor will not charge to a voltage above its proper sharing voltage. Again, the resistor should be chosen to be of a bulk type or of a film type wound on a stable core such as glass. The capacitor should have minimum inductance in this type of circuit and therefore should be of extended foil construction and, since there can be a considerable amount of power dissipation in the capacitor, it should be oil-filled.

Triggering Series-Operated SCRs

Under series operation, the gates of the various devices will be at considerable potential above neutral or ground in the circuit. Most triggering circuits are low voltage, low energy-level circuitry and the capacitance to ground or to neutral in these circuits may vary widely from one SCR to another.

Another consideration is the variation in delay time from one SCR to another. When using pulse transformers, it should be noted that the insulation between windings must be able to support the voltage from that point in the circuit to the lowest reference potential point, and this is often the peak voltage in the system. Devices connected in series should be chosen to have delay times closely matched so that differences in the turn-on characteristics are minimized. The importance of this is illustrated in Figure 3-9 where, even though the two delay times are very close in the two SCRs, it is important for the gate signal rise time to be much shorter than the delay time in order to minimize the difference in turn-on characteristics of the two devices. In this case, the anode voltage of SCR₁, which has a longer delay time than SCR₂, increases, since SCR₂ begins to turn on sooner. The RC network in the system helps to equalize this if there is series impedance in the circuit, since it tends to minimize the rate-of-rise of applied voltage on any part of the circuit.

The gate circuit of Figure 3-10 can be used to minimize difference in turn-on characteristics of SCRs in a series string. This gate circuit will transform a slow rising square

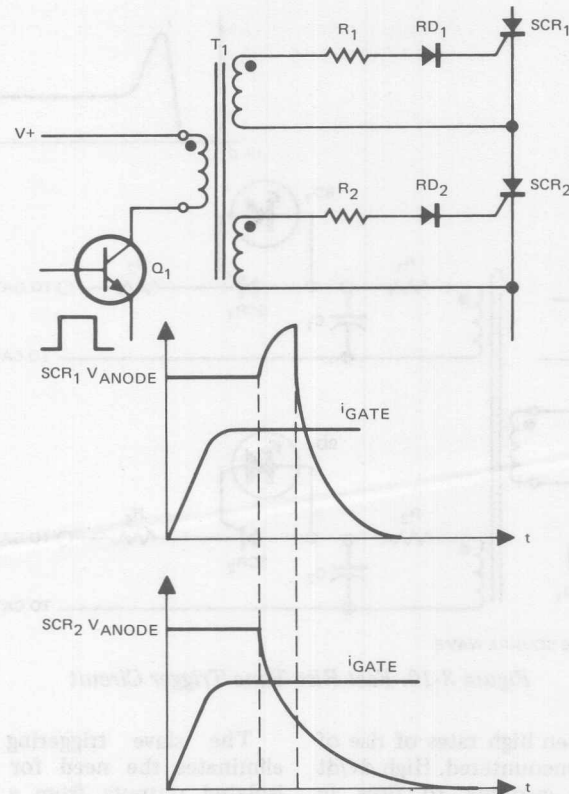


Figure 3-9. Delay Time Effect on Series SCRs

wave into a trigger signal with both a fast rise time and a current overshoot on the leading edge, both desirable qualities for triggering series SCRs.

It is often necessary, because the load is either an active load or an inductive load, to make the trigger pulse to the SCRs either continuous over a 180° conduction angle of the supply voltage or a series of pulses which are spaced so no appreciable recovery in the SCR takes place between pulses. A suitable gate circuit for this type of opera-

tion is shown in Figure 3-11. In this gate circuit, a blocking oscillator is triggered by a high frequency clock. The resultant series of pulses is then amplified by a power transistor and used to trigger the series string of SCRs.

The gate circuit of Figure 3-12 combines the qualities of a fast rise time gate current to minimize delay time effects and a wide pulse for inductive loads.

Interwinding capacitance of conventional pulse transformers may be prohibitive for series operation

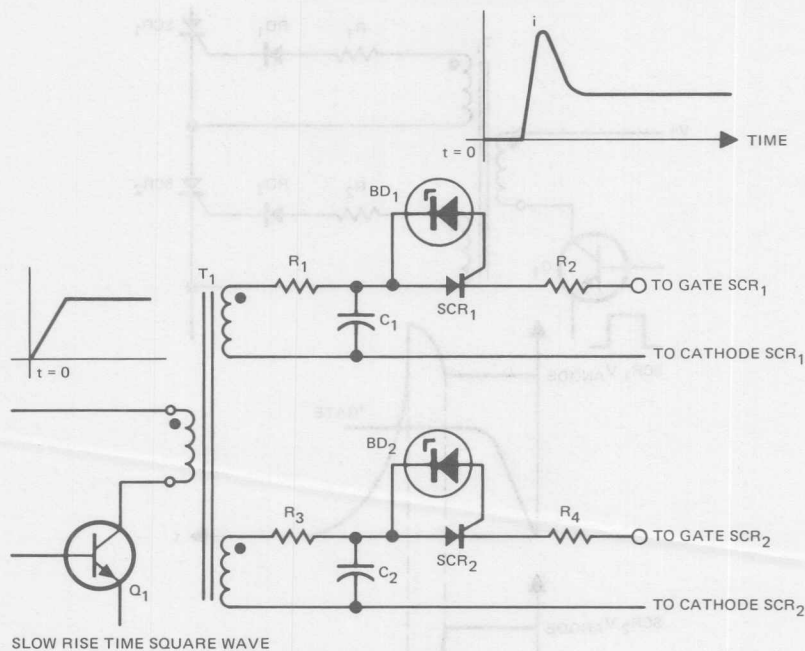


Figure 3-10. Fast Rise Time Trigger Circuit

of SCRs when high rates of rise of voltage are encountered. High dv/dt can induce currents to flow in the interwinding capacitance, which may falsely trigger an SCR. This problem can be avoided by the use of optical couplers to provide extremely high voltage isolation between trigger circuits of series connected SCRs. The gate circuit of Figure 3-13 uses a light emitting diode (LED) and photo-sensitive SCR to provide optical isolation for each main SCR.

Another method for triggering series-connected SCRs is to trigger one gate and arrange for the other gates to trigger "sympathetically" by use of a slave triggering circuit arrangement.

The slave triggering method eliminates the need for multiple, isolated outputs from a powerful triggering circuit. One such method is shown in Figure 3-14. Resistors R_1 and R_2 are voltage equalizing resistors. Capacitors C_1 and C_2 , with their damping resistors R_3 and R_4 , provide additional voltage equalizing under ac conditions, and also provide transient suppression.

When the controlled rectifier SCR₂ is triggered, its anode-to-cathode voltage drops abruptly to a low value. This results in a surge of charging current into capacitor C_3 and through the gate of controlled rectifier SCR₁, which is turned-on. Resistor R_5 should be about ten times the gate-to-cathode resistance of the controlled rectifier.

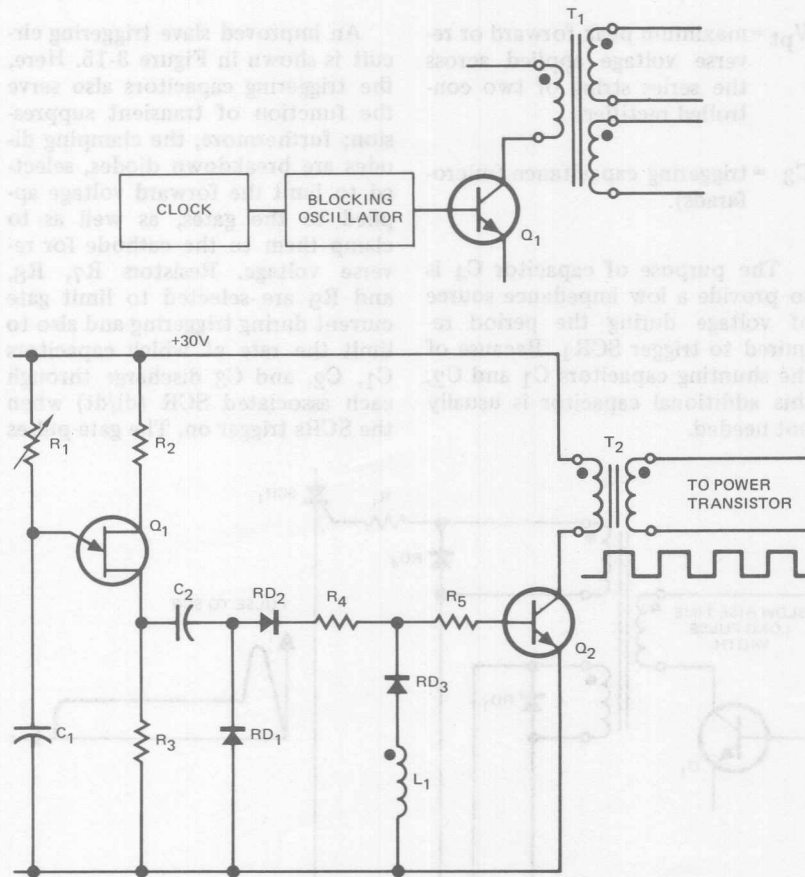


Figure 3-11. Pulse Train Trigger Circuit

The rectifier diode RD₁ acts as a clamp to prevent the gate of its controlled rectifier from being made negative during the negative half cycles when the gate capacitor is charged in the reverse direction. Capacitor, C₃, must be large enough to assure reliable triggering, but if it is made too large, it may cause turn-on as a result of its charging current, due to the forward voltage. Hence, the size of this

capacitor must fall between two limits given by Formula 3-K.

$$\frac{10^6}{12.6 \times f \times R_S \times V_{pt}} > C_3 \quad (3-K)$$

$$> \frac{I_{GT}}{10^7}$$

Where:

f = frequency of ac supply
 I_{GT} = maximum gate current required to trigger

V_{pt} = maximum peak forward or reverse voltage applied across the series string of two controlled rectifiers

C_3 = triggering capacitance (microfarads).

The purpose of capacitor C_4 is to provide a low impedance source of voltage during the period required to trigger SCR₁. Because of the shunting capacitors C_1 and C_2 , this additional capacitor is usually not needed.

An improved slave triggering circuit is shown in Figure 3-15. Here, the triggering capacitors also serve the function of transient suppression; furthermore, the clamping diodes are breakdown diodes, selected to limit the forward voltage applied to the gates, as well as to clamp them to the cathode for reverse voltage. Resistors R_7 , R_8 , and R_9 are selected to limit gate current during triggering and also to limit the rate at which capacitors C_1 , C_2 , and C_3 discharge through each associated SCR (di/dt) when the SCRs trigger on. The gate pulses

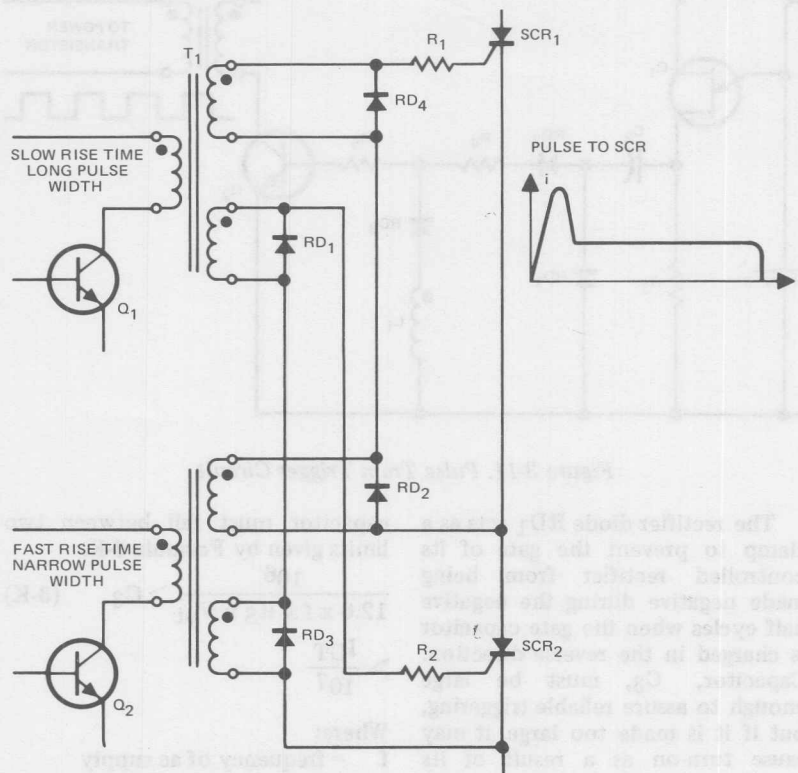


Figure 3-12. Combined Fast Rise Time and Wide Pulse Trigger Circuit

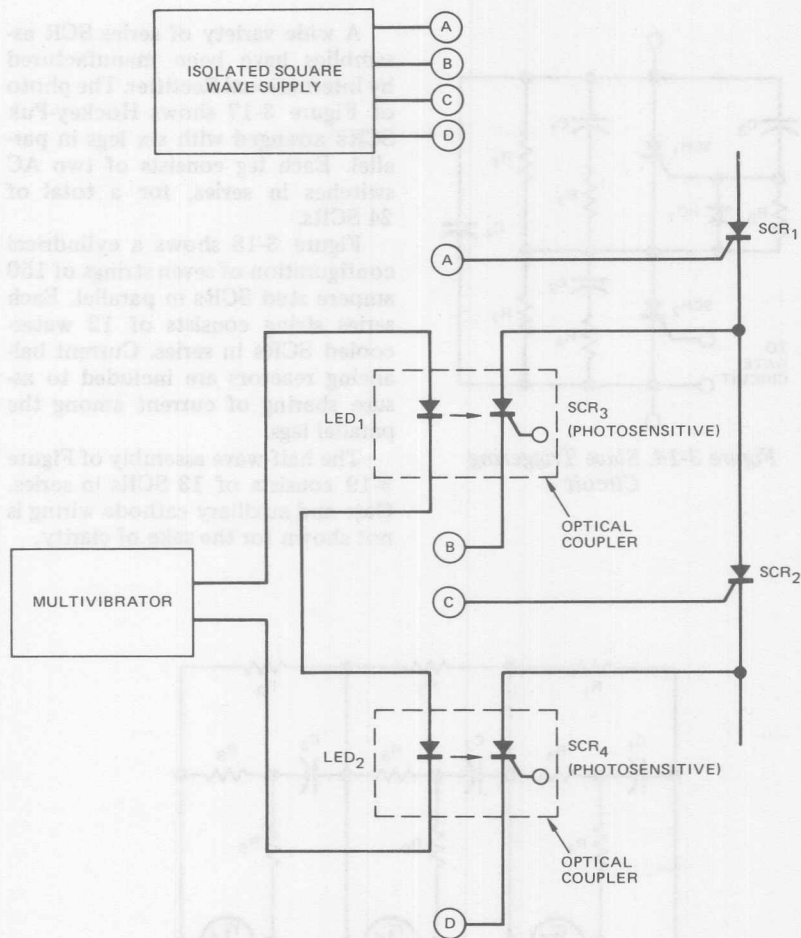


Figure 3-13. Optically Coupled Series SCRs

may be applied between any gate and cathode, and all the controlled rectifiers will turn on; usually it is most convenient to apply the pulses in the manner shown.

Another slave triggering circuit is shown in Figure 3-16. This circuit is very simple, but selection of the resistor and capacitor is much more critical, since no protection is pro-

vided against applying excessive voltage, current or power to the gate of the "slave" controlled rectifier. Whereas the circuit of Figure 3-15 operates satisfactorily under many different circumstances, the circuit of Figure 3-16 must be tuned to a narrow range of favorable conditions with the probability of failure when these conditions are not maintained.

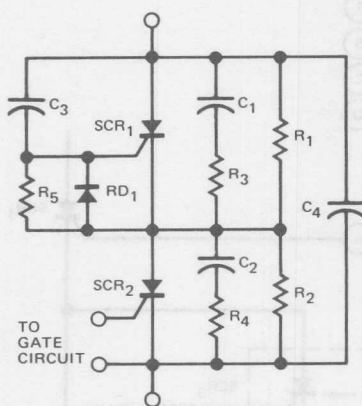


Figure 3-14. Slave Triggering Circuit

A wide variety of series SCR assemblies have been manufactured by International Rectifier. The photo of Figure 3-17 shows Hockey-Puk SCRs arranged with six legs in parallel. Each leg consists of two AC switches in series, for a total of 24 SCRs.

Figure 3-18 shows a cylindrical configuration of seven strings of 150 ampere stud SCRs in parallel. Each series string consists of 12 water-cooled SCRs in series. Current balancing reactors are included to assure sharing of current among the parallel legs.

The half-wave assembly of Figure 3-19 consists of 13 SCRs in series. Gate and auxiliary cathode wiring is not shown for the sake of clarity.

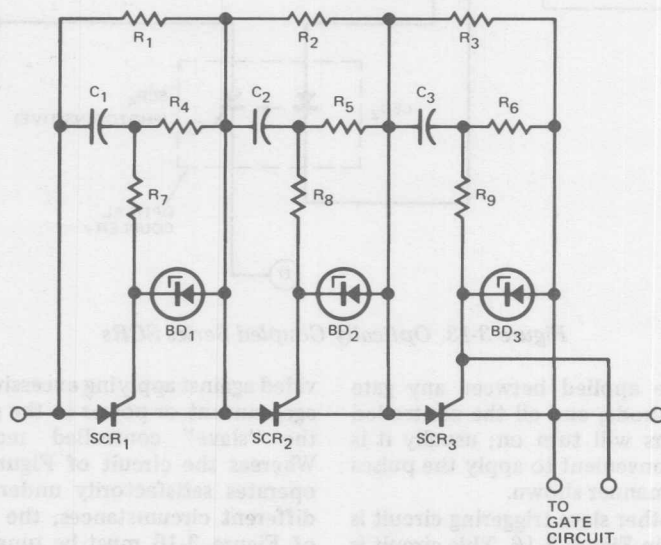


Figure 3-15. Improved Slave Trigger Circuit

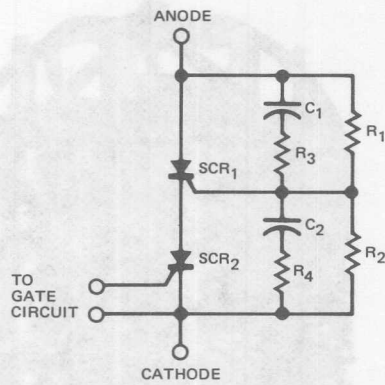


Figure 3-16. Economical Slave Trigger Circuit

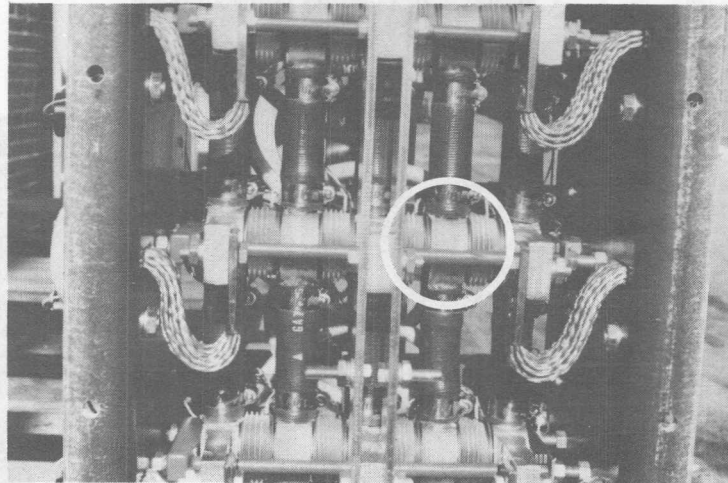


Figure 3-17. Series-Connected Hockey-Puk SCRs in Liquid-Cooled Assembly

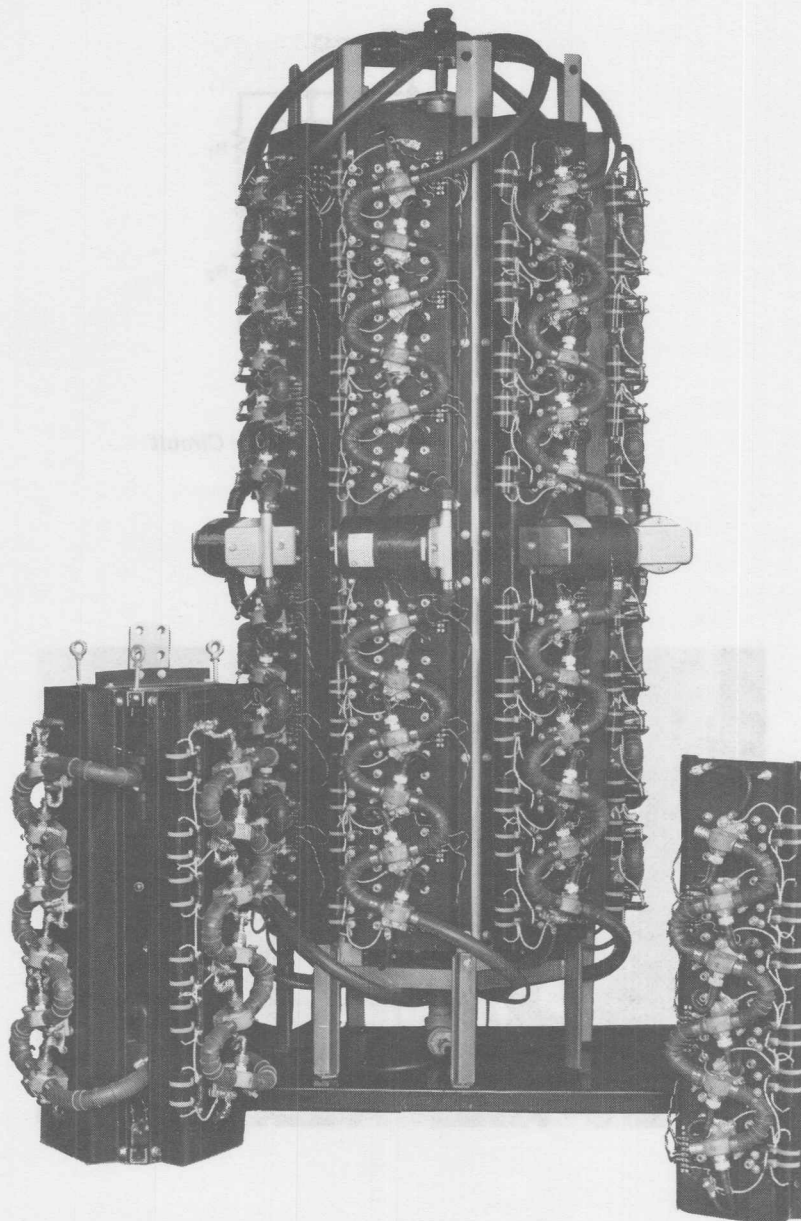


Figure 3-18. Series-Connected, Stud-Mounted SCRs in Liquid-Cooled Assembly

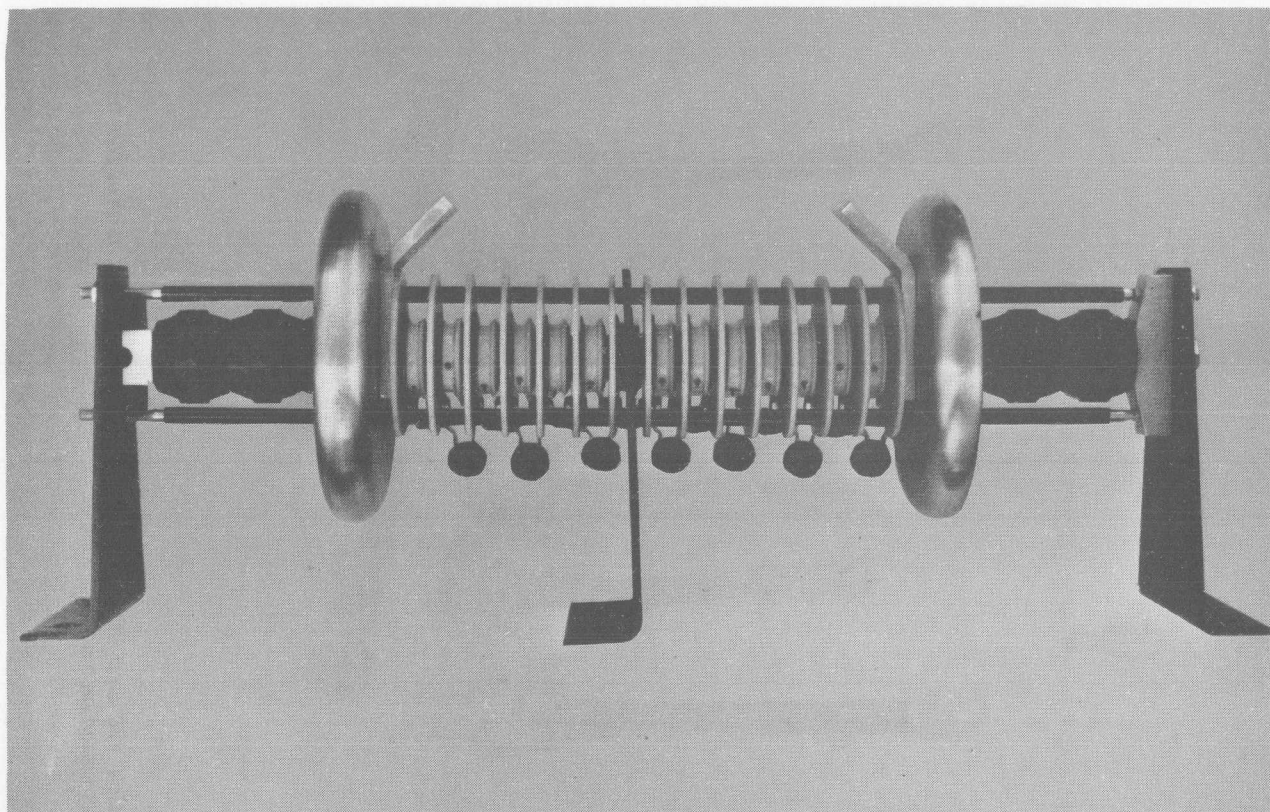
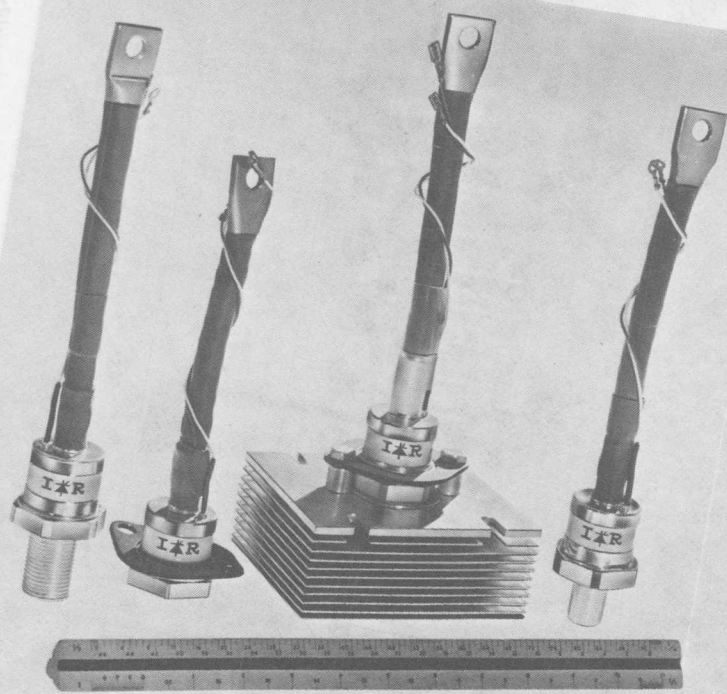


Figure 3-19. Series-Connected, Hockey-Puk SCRs in Half-Wave Assembly

IR's 470 amp SCR is available in two stud sizes, with a flat base, and mounted on a heat exchanger.



IR's 470 amp SCR is available in two stud sizes, with a flat base, and mounted on a heat exchanger.

AC Phase Control

Solid-state ac controllers take many forms. They may be used simply for on-off switching, in which case triggering the semiconductor device(s) at essentially zero voltage on the ac wave will minimize radio frequency interference (RFI). On the other hand, by employing phase controlled triggering the ac controller may be used to adjust the voltage applied to the load and so perform such functions as ac motor speed control or adjusting the direct voltage output from a rectifier fed by a transformer having a solid-state controller on the primary.

A number of circuit configurations are possible; two popular ones for single-phase applications are two SCRs connected in anti-parallel, or a single triac, which functionally replaces two SCRs.

Mechanical configuration requirements differ greatly for various controller applications. In the smaller current ratings, PACE/pak assemblies which simplify installation and cooling may be considered. For larger ratings, assemblies in which the rectifying devices are mounted on extruded aluminum heat exchangers are popular. For some industries, notably the resistance welding industry, where cooling water is readily available and space and weight limitations are severe, water-cooled assemblies are popular.

PHASE CONTROL CIRCUITS

A number of circuits are available for controlling alternating volt-

age with thyristors. Reverse blocking thyristors may be connected in anti-parallel, or a single-phase bridge may be used to rectify the ac line current, so that one thyristor can control both halves of the ac wave; this is accomplished by replacing the dc load on the single phase bridge with a short circuit and locating the load in the ac line. In some polyphase circuits, essentially the same control of voltage can be obtained when one thyristor is replaced with a rectifier diode. This arrangement is more economical. A number of possible circuit configurations are shown in Table IV-1.

In addition, the same kind of control can be provided by a triac, since it can be triggered into conduction during either half of the ac wave. In Table IV-1, a triac may be used in place of many of the all-thyristor and thyristor-diode control circuits shown, within the current ratings available.

When the load is inductive, current flows as a sine wave which lags the supply voltage by the angle θ , the angle which is a measure of the power factor. If each thyristor is triggered at this angle, load current will be unaffected. If the triggering angle is made to lag behind θ , the load current will flow as a series of nonsinusoidal pulses of less than 180 electrical degrees duration.

As the angle of phase retard is increased, these pulses become increasingly shorter until, at 180 degrees retard, they cease to exist, and the voltage across the load is

Table IV-I. Thyristor Circuit to Control AC Loads

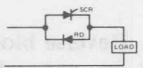
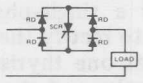
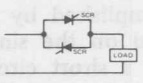
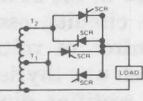
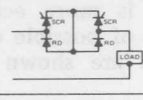
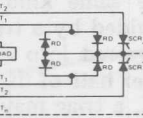
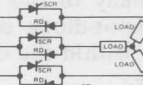
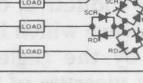
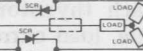
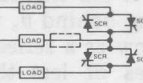
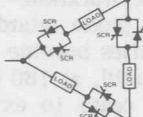
CIRCUIT	RELATIVE POWER OUTPUT	TYPE OF LOAD	CONTROL RANGE %	TYPICAL USES	APPLICABLE MODES OF CONTROL	SEE NOTES
1A 	1	Resistive only	50 to 100	Low Power Heater Loads Lamp Intensity Control	SWC PC PBM	1 2 3 4
2A 	0.7	Resistive or with low inductance	0 to 100	Heater Control Lamp Intensity Control Motor Speed Control (Induction or Universal)	SWC PC PBM	2 3 4
3A 	1	Resistive or Inductive	0 to 100	Heater Control Lamp Intensity Control Motor Speed Control (Induction or Universal) Transformer Primary Control Solenoid Pull Control AC Magnet Control	SWC PC PBM	3 4
4A 	1	Resistive or Inductive	% T ₁ to 100	Heater Control Lamp Intensity Control Motor Speed Control (Induction or Universal) Solenoid Pull Control AC Magnet Control On Load Tap Changing	SWC PC PBM	3 4 5 6
5A 	1	Resistive or Inductive	0 to 100	Heater Control Lamp Intensity Control Motor Speed Control (Induction or Universal) Transformer Primary Control Solenoid Pull Control AC Magnet Control	SWC PC PBM	3 4
6A 	1	Resistive or Inductive	% T ₁ to 100	Heater Control Lamp Intensity Control Motor Speed Control (Induction or Universal) Solenoid Pull Control AC Magnet Control On Load Tap Changing	SWC PC PBM	3 4 5 6
7A 	1.73	Resistive or Inductive	0 to 100	Heater Control Lamp Intensity Control Motor Speed Control (Induction) Transformer Primary Control Solenoid Pull Control AC Magnet Control	SWC PC PBM	3 4 7
8A 	1.73					
9A 	1.73	Resistive or Inductive	0 to 100	Heater Control Lamp Intensity Control Motor Speed Control (Induction) Transformer Primary Control Solenoid Pull Control AC Magnet Control	SWC PC PBM	2 3 4 7 8
10A 	1.73					
11A 	3	Resistive or Inductive	0 to 100	Heater Control Lamp Intensity Control Motor Speed Control (Induction) Transformer Primary Control Solenoid Pull Control AC Magnet Control	SWC PC PBM	3 4 10

Table IV-I. Thyristor Circuits to Control AC Loads (Continued)

CIRCUIT	RELATIVE POWER OUTPUT	TYPE OF LOAD	CONTROL RANGE %	TYPICAL USES	APPLICABLE MODES OF CONTROL	SEE NOTES
12A 	1.21	Resistive or Slightly Inductive	0 to 100	Heater Control Lamp Intensity Control Transformer Primary Control (when load has high power factor) Note: If load is connected Δ , a third diode-thyristor control unit is required in the third line.	SWC PC PBM	3 4 8 11
13A 	1.21	Resistive or Slightly Inductive	0 to 100	Heater Control Lamp Intensity Control Transformer Primary Control (when load has high power factor) Note: If load is connected Δ , a third diode-thyristor control unit is required in the third line.	SWC PC PBM	3 4 8 11
14A 	2.1	Resistive or Slightly Inductive	0 to 100	Heater Control Lamp Intensity Control Transformer Primary Control (when load has high power factor)	SWC PC PBM	3 4 10
15A 	2.1	Resistive or Inductive	% T_1 to 100	Heater Control Motor Speed Control (Induction) On Load Tap Changing	SWC PC PBM	3 4 5 6 10 for Y Conn. Load 7 11 12
16A 	1	Resistive or Inductive (Inductance in R_A only)	Depends on Ratio $R_A:R_B$	Heater Control Lamp Intensity Control Transformer Primary Control (Transf. Winding replaces R_A) Induction Motor Speed Control	SWC PC PBM	3 4 13
17A 	3	Resistive or Inductive (Inductance in R_A only)	Depends on Ratio $R_A:R_B$	Heater Control Lamp Intensity Control Transformer Primary Control (Transf. Winding replaces R_A) Induction Motor Speed Control Wound Rotor Induction Motor Speed Control	SWC PC PBM	3 4 11 13
18A 	1.73	Resistive or Inductive	0 to 100	Heater Control Lamp Intensity Control Motor Speed Control (Induction) Transformer Primary Control Solenoid Pull Control AC Magnet Control	SWC PC PBM	1 2 14

Table IV-I. Thyristor Circuits to Control AC Loads (Continued)

1) All Circuits

Pulse burst modulation is applicable only to the control of heating element loads where substantial thermal inertia exists.

2) All Circuits

Zero voltage switching may be employed advantageously to supplement pulse burst modulation control and eliminate RFI resulting from steep wavefronts common to phase control modes.

3) Circuit 1A

Used only for low power loads, operating directly from distribution systems where unbalance between positive and negative half cycles is not detrimental.

4) Circuit 1A

Can be used also to control the speed of small universal motors.

5) Circuits 4A, 6A, 14A

The switching mode between two transformer taps is useful for both phase control and pulse burst modulation control, especially for heating elements. Tap T_1 is selected to provide slightly less than the minimum required power input; then, either phase control or pulse burst modulation can be used to add the necessary incremental extra power to obtain fine control and with a minimum fluctuation of heater element temperature, resulting in longer element life. In addition, less waveform distortion is introduced than when either type of control switches from zero to full voltage (as in Circuits 2A, 3A, 4A, and 6A through 12A).

6) Circuits 4A, 6A, 14A

In circuits similar to 4A, additional taps between T_1 and T_2 also may be used provided that an anti-parallel pair of thyristors is added for each tap. This mode of operation permits tap changing under load, either by switching from tap to tap or, when phase control is also provided, to provide a smooth variation of voltage between each pair of taps.

7) Circuits 7A, 8A

In Circuits 7A and 8A, where an anti-parallel diode-thyristor pair is used, either in each line or between load and neutral of a polyphase Y connected circuit, it is NOT permissible to connect the neutral to a 4-wire system. Where a 4-wire system is necessary, see Circuits 9A, 10A and 12A.

8) Circuits 9A, 10A, 12A, 13A

In circuits 9A, 10A, 12A, and 13A, the 3-phase Y connected circuits will operate with full control in a 3-wire system with only two anti-parallel thyristor sets, or bridge-thyristor sets. When 4-wire systems are necessary, a third set of either type is required in the location indicated by the phantom box.

9) Circuits 9A, 10A

For 3-phase delta connected circuits, it is practical to use circuits 9A, 10A, 12A, and 13A with only two anti-parallel thyristor sets, or two bridge-

Table IV-I. Thyristor Circuits to Control AC Loads (Continued)

thyristor sets, in two of the three supply lines. The addition of the third set, however, provides added insurance against false triggering due to a voltage transient, since with three sets the transient must trigger two devices before conduction can commence.

10) Circuits 11A, 14A, 15A

Placing the two thyristor sets or the bridge-thyristor sets inside the delta instead of in the line always requires three sets. However, this location of the sets results in the ability to control 73 percent higher line current for the same thyristor rating. It also requires that the semiconductors have a 73 percent higher peak reverse voltage/forward breakover voltage rating as compared to the Y connected circuits with three semiconductor device sets.

11) Circuits 9A, 10A, 12A, 13A

In all Y connected circuits, it is necessary to provide a gate triggering supply which supplies either: a) double pulsing at 60 degree phase displacement, instead of 120 degrees, or b) a square-wave triggering pulse, that is maintained for a time interval which exceeds 60 degrees, to assure that the two thyristors, which are in cascade line-to-line, conduct at the same time.

12) Circuits 4A, 6A

Where definite maximum and minimum duty cycles are known or are determinable for the circuits which switch from one voltage level to another (as opposed to zero to full voltage switching), it may be practical to utilize devices with lower rated current (thyristors and/or diodes) than where phase control of the thyristors is the only control means.

13) Circuits 16A, 17A

The shunt control circuits 16A and 17A provide a similar mode of control to those of the transformer tap switching control (circuits 4A, 6A, 14A, and 15A), and are useful where transformers with taps are not available, but where taps can be obtained on heater elements, or they are useful to control a resistor in the rotor circuit of a wound-rotor motor.

14) Circuit 18A

The delta assembly of thyristors connected in the wye of heater loads, transformer primary windings, or induction motor yields results similar to 7A, 8A, 9A, 10A, 12A, and 13A.

LEGEND OF ABBREVIATIONS:

SCR = Silicon Controlled Rectifier

RD = Rectifier Diode

FWD = Free Wheeling (By-Pass) Diode

SWC = Switching Control

PC = Phase Control

PBM = Pulse Burst Modulation

RFI = Radio Frequency Interference

ZVS = Zero Voltage Switching

zero. Thus, the voltage across the load will be reduced by phase retard in much the same manner as with a resistive load, except that voltage control will take place over a narrower range of triggering angles; from θ to 180 degrees. At all triggering angles, the power factor of the load does not depart significantly from the value observed with no phase control [2], [3].

The typical transfer characteristics of ac phase control circuits are shown in Figures 4-1, 4-2, and 4-3.

Triggering Thyristors

When thyristors are used to control resistive loads, almost any of the varied forms of triggering circuits may be used with satisfactory results. Synchronization of the triggering pulses may be accomplished from either the line voltage or the voltage across the thyristor.

However, when the load is inductive, several precautions must be observed in order to achieve optimum performance.

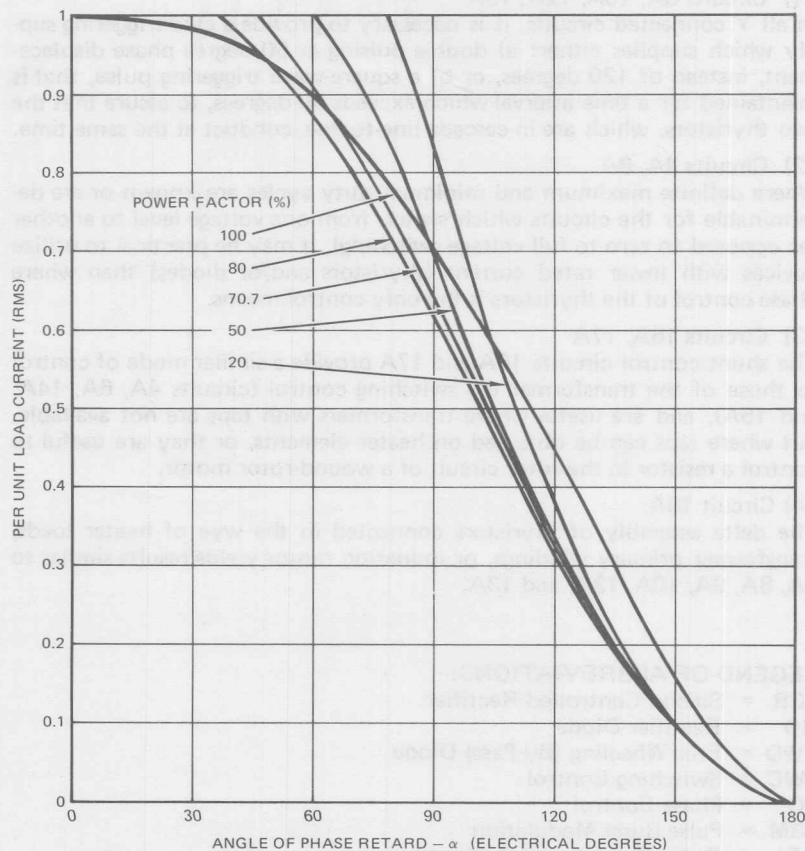


Figure 4-1. Load Current vs. Angle of Phase Retard

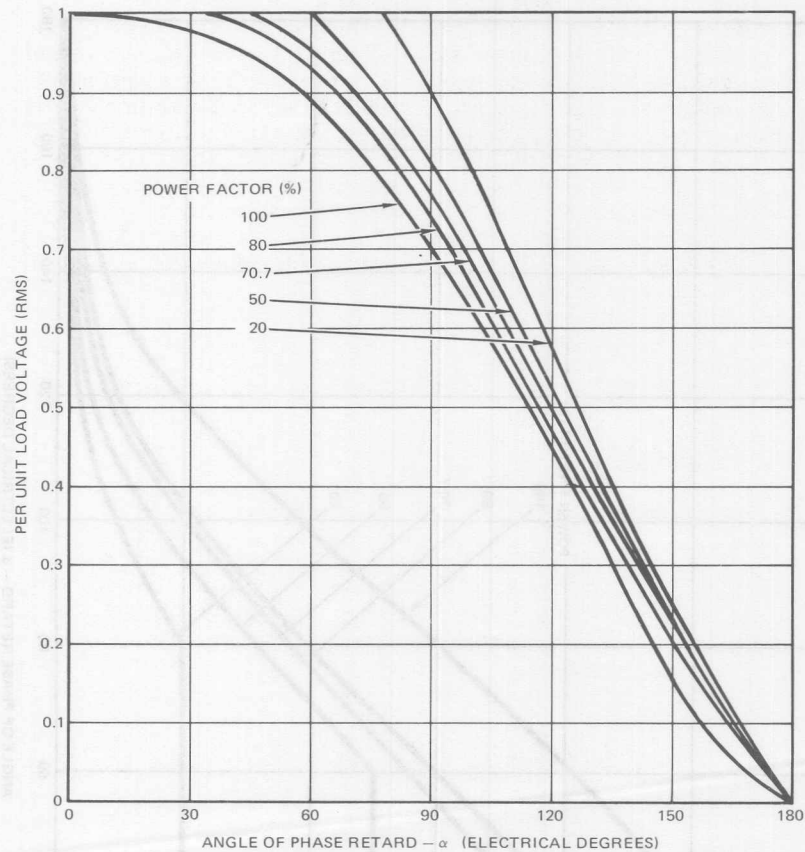


Figure 4-2. Load Voltage vs. Angle of Phase Retard

A. If a triggering circuit is used which produces a narrow spike of gate signal, the charge injected into the thyristor may not be sufficient to maintain the thyristor in the conducting state until the load current has built up to a magnitude larger than the latching current. This may result in mistriggering and erratic control, or no load current whatever. One solution is to shunt the inductive load with a small resistive load drawing a current some-

what larger than the maximum value of thyristor latching current. An alternate (and usually more satisfactory) solution is to provide a triggering circuit which produces a square-wave gate signal which lasts from the time at which triggering is initiated until the time when the thyristor conducts a significant amount of current.

B. For inductive loads, it is mandatory to obtain line synchronization for the triggering circuit from

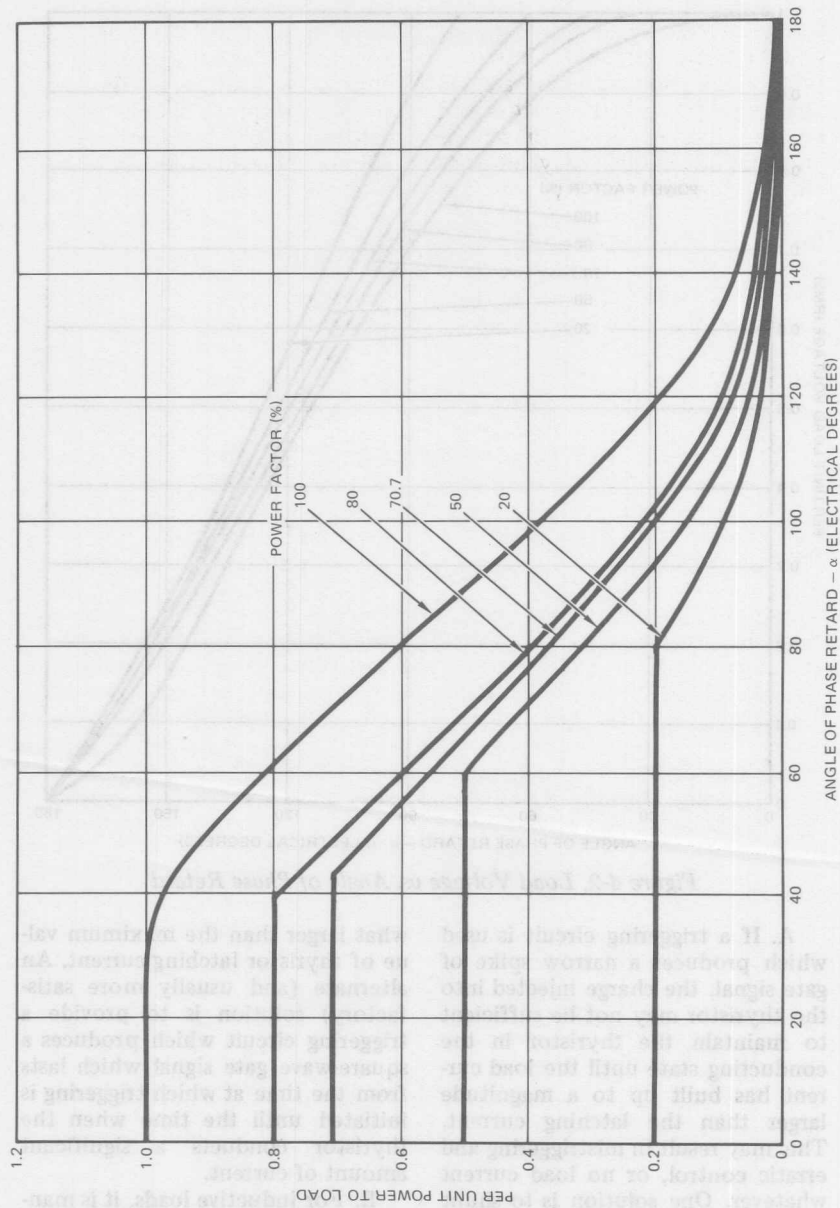


Figure 4-3. Angle of Phase Retard vs. Power

the line voltage, *NOT* from the voltage across the thyristor. If the synchronizing signal is obtained from across the thyristor, a large unbalance between the positive and negative half cycles of current is probable. The result may be overloading of one thyristor, saturation of a transformer core (if a transformer is being controlled), and unstable control. (See Figure 4-4.)

For highly inductive loads, triggering the thyristor full on can result in no output if the triggering pulse is so short that it disappears and the thyristor regains its off-state blocking ability before current can flow in the load circuit. To avoid this, it is necessary to make the triggering pulses long enough so that the thyristor will always be able to conduct whenever circuit conditions are right for conduction, once it has been triggered. Figure 4-5 defines the necessary triggering pulse duration as a function of the load power factor, when the pulse is initiated with zero phase retard.

Other Means of AC Voltage Control

There are numerous types of equipment or systems which can be controlled readily and advantageously by the use of thyristors as switches (as opposed to using them in the phase control mode for continuous variability of voltage). Of

course, many of the switching mode circuits may be readily modified so that they incorporate phase control to provide a fine voltage adjustment to supplement the switching mode of control.

Some of the advantages of the switching mode of operation of thyristors for controlling voltage are as follows:

A. Switching of load voltage (either from zero to full voltage or from partial to full voltage) is accomplished without mechanical contacts, thus eliminating common maintenance problems which result from burning, pitting, and welding of contacts. "Contact bounce" is also eliminated, thereby reducing radio frequency interference (RFI) caused by the repetitive shock excitation of reactive circuit elements.

B. "Zero voltage switching" may be used to essentially eliminate radio frequency interference (RFI) often encountered when voltage is controlled by phase control.

C. The use of the switching mode of voltage control eliminates the reduction in power factor which inherently occurs when voltage is reduced by phase control.

Many of these switching control circuits will find use in controlling heating elements for ovens, furnaces, hot plates, crucibles, and space heaters. Of equal importance,

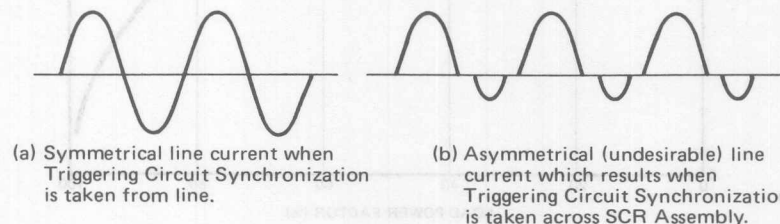


Figure 4-4. Triggering Circuit Synchronization

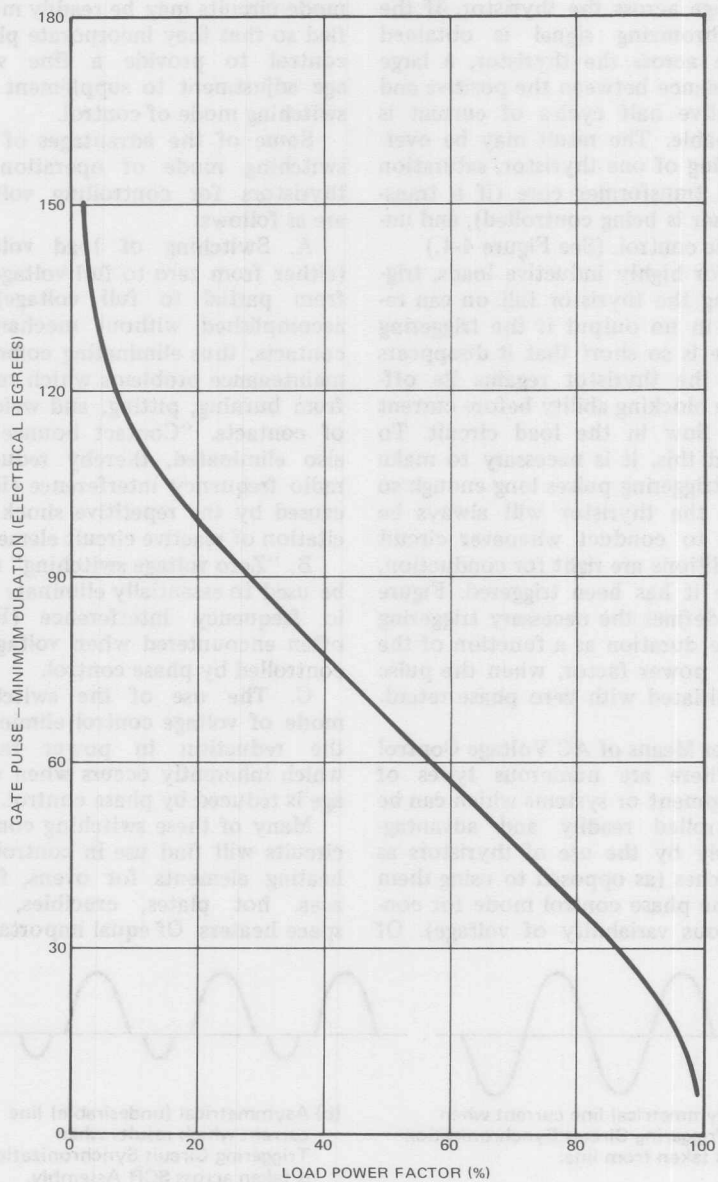


Figure 4-5. Pulse Duration vs. Load Power Factor

they may also be used for speed controls of squirrel cage and wound rotor induction motors where the motor and/or load inertia is high. Still other types of load, for example; 1) resistance welders, 2) stud welders, 3) flashers and flashing beacons, and 4) magnetic hammers or pulsers, demand this type of control as an inherent element in their mode of operation.

Most heating elements have a high thermal inertia and are easily adaptable to control by the switching mode, either by being switched from zero to full voltage (Circuits 1A, 2A, 3A, 5A, 7A, 14A and 18A of Table IV-I) or from a low voltage tap to full voltage (Circuits 4A, 6A, 15A). Where the heating elements can be tapped at a midpoint, the circuits of 16A and 17A are also useful.

When the circuits with a tapped transformer winding are compared to those with a tapped load, it will be seen that the final control result is very similar. However, where the transformer is tapped, the load voltage is initially low and is switched to a higher value. In the tapped load circuit, the initial voltage is high across one section of the load and zero across the other section. After switching, the voltage decreases across one section while increasing across the other. This tapped load "shunt controller" performs equally well for resistive loads (such as heating elements) and for speed control of wound rotor induction motors, by varying the resistance in the rotor circuit.

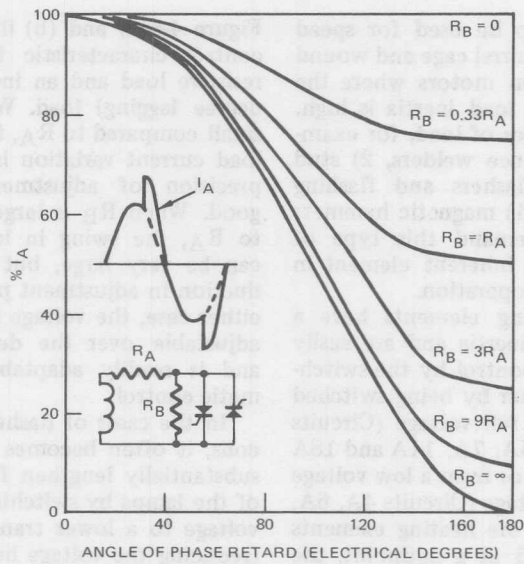
Phase control is also very effective with circuits 16A and 17A (although radio frequency interference filtering may be necessary) using the shunt mode of control.

Figure 4-6(a) and (b) illustrate the control characteristic for both a resistive load and an inductive (70 degree lagging) load. When R_B is small compared to R_A , the range of load current variation is small, but precision of adjustment is very good. When R_B is large compared to R_A , the swing in load current can be very large, but with a reduction in adjustment precision. In either case, the voltage is smoothly adjustable over the design range, and is readily adaptable to automatic control.

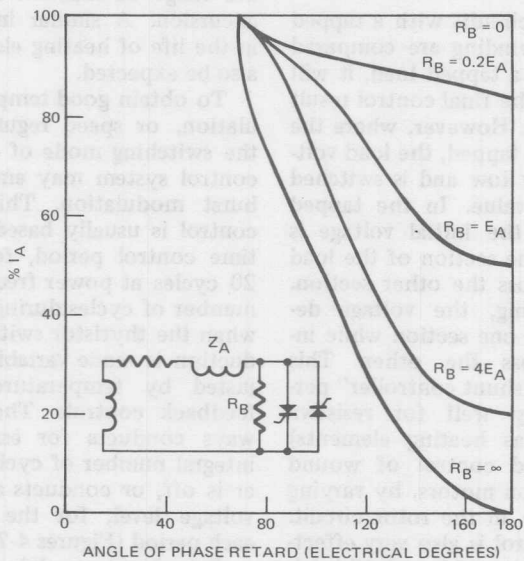
In the cases of flashers and beacons, it often becomes possible to substantially lengthen filament life of the lamps by switching from full voltage to a lower transformer tap (reducing the voltage below the incandescence level), thus minimizing the range of filament temperature excursion. A similar improvement in the life of heating elements may also be expected.

To obtain good temperature regulation, or speed regulation, with the switching mode of control, the control system may employ pulse-burst modulation. This mode of control is usually based on a fixed time control period, for example, 20 cycles at power frequency. The number of cycles during this period when the thyristor switch is in conduction is made variable and is adjusted by temperature or speed feedback controls. The switch always conducts for essentially an integral number of cycles, and either is off, or conducts at a reduced voltage level, for the balance of each period (Figures 4-7 and 4-8).

Pulse-burst modulation can be applied to the control of most heating systems and motor drives due to the high thermal or mechanical in-

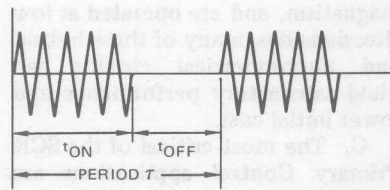


(a) RESISTIVE LOAD



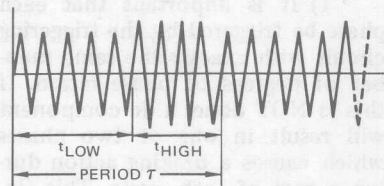
(b) INDUCTIVE LOAD

Figure 4-6. Thyristor Shunt Mode of AC Control



CONTROL OF AC LOAD
(CIRCUITS 1A, 2A, 3A, 5A,
AND 7A THROUGH 13A)

Figure 4-7. Pulse Burst Modulation
Voltage Control —
Full On/Off



CONTROL OF AC LOAD
(CIRCUITS 4A, 6A, AND 15A)

Figure 4-8. Pulse Burst Modulation
Voltage Control —
Transformer Tap
Switching

ertia of these systems. Systems with very high inertia can tolerate relatively long control periods, whereas systems with lower inertia, or requiring a fine control resolution, will demand a short control period.

As mentioned earlier, the use of pulse burst modulation with thyristor switches will minimize radio frequency interference, but this, by itself, will not completely eliminate it. The fast turn-on of a thyristor when the supply voltage is at any value other than zero, still causes one pulse of shock excitation each time the thyristor is turned on to carry a burst of pulses. However,

with thyristor switches, it is possible and often desirable to incorporate zero voltage switching. When controlled in this mode, the thyristors are always turned on at zero voltage (they turn off at zero current), thus eliminating the interference caused by fast switching of heavy currents.

All of the circuits which switch from one tap to another (either tapped transformer or tapped load) may incorporate phase control to supplement the switching type of control to obtain voltage or current regulation of power supplies. Methods of applying phase control have been discussed earlier in this chapter. It is possible to achieve such regulation by phase control alone and eliminate the taps. However, where only a limited range of adjustability is required, the combination of phase control with switching mode operation greatly reduces the peak-to-RMS current ratio in ac power supplies. For instance, output voltage can be smoothly varied between the voltages obtained from any two transformer taps by first gating a thyristor connected to the lower voltage tap, and then later in the cycle gating a thyristor connected to the higher voltage tap. This type of voltage control reduces the peak-to-average current ratio. It also minimizes the change in power-factor as voltage is varied.

Application of Specific Circuits

Circuits to control resistive loads (heater, lighting, etc.) are very tolerant of variable supply conditions, such as waveform distortion, phase unbalance (either magnitude or phase shift distortion) and variations in switching rate, as long as

the switching period is small when compared to the thermal time constant of the load. Any of the Table IV-I circuits may be utilized when properly matched to the application requirements. Triggering synchronization may be taken from either the line, or across the power control device or assembly.

The control of power into the primary of a transformer becomes slightly more critical. The following procedures should be observed to assure good operation:

A. The load is now inductive. Therefore, triggering synchronization must come from the supply line (NOT from across the SCR assembly) to insure equal positive and negative half cycles of power (see Figure 4-4(a) and (b)).

B. If the transformer iron is worked near saturation, or if it has a high residual magnetism, the triggering circuit should be designed to insure that conduction always starts on a positive half cycle and ends on a negative half cycle. If this is not done, a transformer core may become partially saturated and draw excessive magnetizing current on one-half cycle and very little on the opposite polarity half cycle. (This is particularly true of resistance welding transformers.)

1) Polyphase circuits using SCRs to control both half cycles (Circuits 11A, 14A, 15A, 17A and 18A) are recommended because both positive and negative half cycles are balanced in both waveform and area. Hybrid circuits (7A, 8A and 14A) and unsymmetrical circuits (9A, 10A, 12A and 13A) can result in asymmetrical distortions (see Figures 4-9(a) and (b)).

2) However, where transformers have relatively low residual

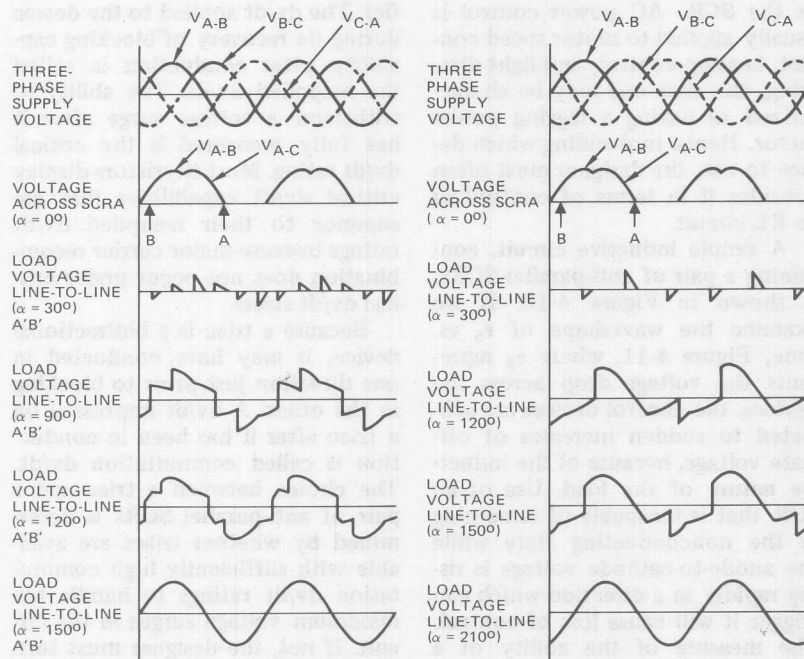
magnetism, and are operated at low flux densities, many of these hybrid and unsymmetrical circuits can yield satisfactory performance and lower initial cost.

C. The most critical of the SCR Primary Control applications are probably those involving induction motor control (either squirrel cage or wound rotor). It is highly recommended that "all SCR" control circuits be used for all motor controls (Circuits 11A, 12A, 14A, 15A, 17A or 18A). The reasons for this are as follows:

1) It is important that each phase be triggered by the triggering circuit with exactly the same number of degrees of phase retard. If this is NOT done, a dc component will result in one or two phases which causes a braking action during a part of each cycle. This (internal) fighting to accelerate and brake during each cycle can cause damaging overheating of rotor bars or windings.

2) Figure 4-9(b) illustrates an unbalanced voltage waveform typical of hybrid circuits. Since flux is proportional to voltage (below saturation), a rotor voltage and current may be induced which is different for positive and negative half cycles. This can again result in overheating of the rotor, and poor speed control.

3) When thyristors are used to control squirrel cage motor speed (by increasing the slip), selection of the motor and type of load is very important. The motor load should be one for which the load varies approximately as (speed)³, i.e., such as a fan, a squirrel cage blower or a centrifugal pump, but never one requiring constant torque. The motor should be of a high torque,



WAVEFORMS FOR CIRCUITS 11A, & 14A, ALSO FOR 9A, 10A, 12A AND 13A WHEN THREE SCR SETS ARE USED WITH RESISTIVE LOAD. NOTE THAT WAVEFORMS ARE SYMMETRICAL EVEN THOUGH SHAPE IS DISTORTED.

WAVEFORMS FOR CIRCUITS 7A & 8A. NOTE THAT WAVEFORMS ARE BOTH ASYMMETRICAL AND DISTORTED. (THESE WAVEFORMS PROBABLY ARE SOMEWHAT TYPICAL FOR CIRCUITS 9A, 10A, 12A & 13A WHEN ONLY TWO SCR SETS ARE USED.)

(a) Symmetrical SCR Primary Controller (b) Hybrid SCR Primary Controller

Figure 4-9. Waveforms of SCR Primary Controller

high slip design (similar to NEMA Class D). It is usually found that the slip must be greater than 8 percent. Careful system tests should be made with the motor and load to ensure that operating motor current over the desired control range does not exceed rated current limits or temperature rise limits (cooling efficiency is reduced as the speed is reduced).

The Triac vs. the SCR [4]

For ac power control, anti-parallel (inverse parallel) connection of a pair of SCRs has been troublesome because SCR anodes are generally grounded to the case. This necessitates insulating the case of at least one of the devices from ground, using an insulator that also is a good thermal conductor, if a grounded heat dissipator is used.

One question facing the circuit designer is whether to use the triac or the SCR. AC power control is usually applied to motor speed control, heating control, and light dimming, the first one may be characterized as having a lagging power factor. Hence in deciding which device to use, the designer must often consider it in terms of controlling an RL circuit.

A simple inductive circuit, containing a pair of anti-parallel SCRs, is shown in Figure 4-10. If we examine the waveshape of e_s vs. time, Figure 4-11, where e_s represents the voltage drop across the devices, the control devices are subjected to sudden increases of off-state voltage, because of the inductive nature of the load. Use of an SCR that is incapable of remaining in the nonconducting state while the anode-to-cathode voltage is rising rapidly in a direction which can trigger it will cause loss of control. The measure of the ability of a device to withstand rapid application of off-state voltage without losing its blocking capacity is its dv/dt rating.

There are two types of dv/dt ratings for a silicon controlled rectifier. The dv/dt applied to the device during its recovery of blocking capability after conduction is called the reapplied dv/dt . The ability to withstand a voltage surge after it has fully recovered is the critical dv/dt rating. Most thyristors display critical dv/dt capabilities that are superior to their reapplied dv/dt ratings because major carrier recombination does not occur under critical dv/dt stress.

Because a triac is a bidirectional device, it may have conducted in one direction just prior to blocking in the other. A dv/dt impressed on a triac after it has been in conduction is called commutation dv/dt . The choice between a triac and a pair of anti-parallel SCRs is determined by whether triacs are available with sufficiently high commutation dv/dt ratings to handle the maximum voltage surges in the circuit. If not, the designer must turn to anti-parallel SCRs.

By using an RC snubber connected across the device, as shown in Figure 4-12, the rate of voltage

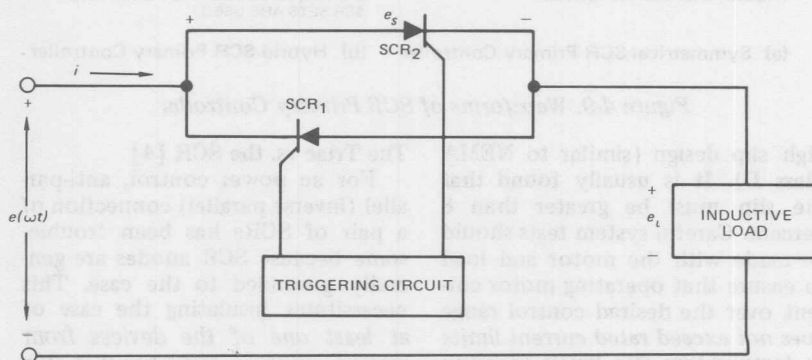


Figure 4-10. Single-Phase AC Controller

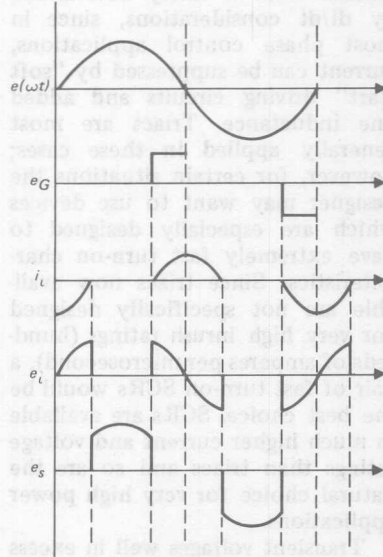


Figure 4-11. Waveforms for Triggering Angle α Greater than Phase Angle θ

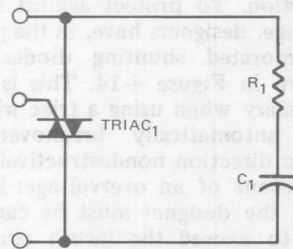


Figure 4-12. Triac with Snubber Network

rise can be suppressed. Analysis of this circuit leads to the expression in Formula 4-A.

$$C = \frac{4 (V_M)^2}{(dv/dt \text{ max.})^2 L} \quad (4-A)$$

Where:

V_M = Peak applied voltage
 L = Total inductance of the circuit

The resistance of the circuit should be chosen so that the capacitor discharge does not damage the device from an inrush current standpoint.

During device turn-on, rapid current buildups in limited areas can cause excessively high temperatures which may damage an SCR or triac. Following initial injection of carriers at the gate, a short period of time is required for current to flow across the whole cross-section of the device. If the carriers cannot disperse rapidly enough, the device will be damaged.

Voltage fall and current rise vs. time are plotted in Figure 4-13. As can be seen by multiplying instantaneous values of current and voltage, a curve of watts dissipated vs. time can be obtained. Note that the power curve reaches a sharp peak during turn-on.

A load having a leading power factor or a nonlinear resistance, such as a bank of incandescent lamps (very low cold resistance and high hot resistance) is prone to high inrush currents. Insertion of a choke in series with this type of load reduces inrush currents. The proper value of this choke can be calculated by considering the relationship in Formula 4-B.

$$L = \frac{e}{di/dt} \quad (4-B)$$

Where:

e = Choke forcing voltage
 di/dt = The maximum allowable rate of change of current

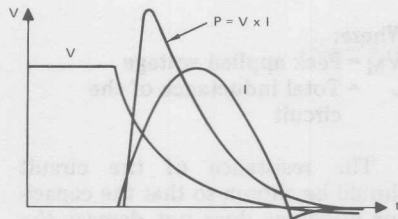


Figure 4-13. Power Dissipation Curve During High di/dt Turn-On Action

specified for the semiconductor device during switching.

It is useful to consider the use of a self-saturating choke in the circuit, which has an inductance that decreases with increasing current. This would limit current flow during turn-on of the device. Equation 4-C gives the voltage drop across a coil, which serves as the basic equation for the design of this reactor.

$$edt = Nd\phi \quad (4-C)$$

Where:

- e = Circuit forcing voltage
- dt = Delay time
- $d\phi$ = Saturation level of choke
- N = Number of turns

Knowing the delay time (dt) introduced by the choke and the circuit forcing voltage (e), it is possible to equate this to the saturation level of the choke ($d\phi$) and the number of turns necessary (N). By selecting a ϕ vs I relationship for the choke, it is possible to design for a nonlinear case (saturating choke) or use an idealized B-H loop for an approximate solution [5],[6].

The choice of triac or anti-parallel SCR is rarely determined by di/dt considerations, since in most phase control applications, current can be suppressed by "soft start" driving circuits and added line inductance. Triacs are most generally applied in these cases; however, for certain situations the designer may want to use devices which are especially designed to have extremely fast turn-on characteristics. Since triacs now available are not specifically designed for very high inrush ratings (hundreds of amperes per microsecond), a pair of fast turn-on SCRs would be the best choice. SCRs are available in much higher current and voltage ratings than triacs and so are the natural choice for very high power applications.

Transient voltages well in excess of normal supply potentials are common on commercial power lines. There are SCRs that will break-over nondestructively in the off-state direction but may be damaged by overvoltage in the reverse direction. To protect against such damage, designers have, in the past, incorporated shunting diodes, as shown in Figure 4-14. This is unnecessary when using a triac which will automatically breakover in either direction nondestructively in the event of an overvoltage; however, the designer must be careful not to exceed the inrush current rating of the device when the triac is triggered by a sharp transient.

Since the triac is a bidirectional device, its characteristics are given for both positive and negative excursions. For the designer to determine the heat sinking needed for correct heat dissipation, he must first find the RMS current to which

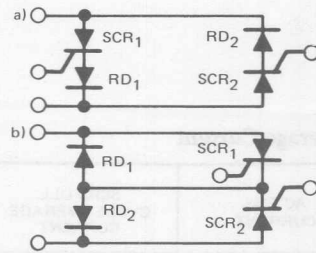


Figure 4-14. Inverse Voltage Protection Circuits

the device will be subjected. He then consults a curve of RMS current vs. allowable case dissipation for the selected device to obtain the maximum allowable case temperature T_C . The next step is to check the curves for device dissipation vs. RMS current for the proper conduction angle. This dissipation, called average on-state power loss, is designated W_T . Knowing the maximum ambient temperature T_A and the interface thermal impedance between the heat dissipator and the device case ($R_{\theta CS}$), the heat dissipator thermal resistance ($R_{\theta SA}$) is calculated using Equation 4-D.

$$R_{\theta SA} = \frac{T_C - (T_A + R_{\theta CS} (W_T))}{W_T} \quad (4-D)$$

Where:

- $R_{\theta SA}$ = Heat dissipator (sink to ambient) thermal resistance
- T_C = Maximum allowable case temperature
- T_A = Maximum ambient temperature
- $R_{\theta CS}$ = Interface (case to sink) thermal resistance
- W_T = Average on-state power loss

In the case of anti-parallel SCRs, determination of the allowable case temperature is not as straight forward. Generally, when applying anti-parallel SCRs to an ac controller, the load RMS current is known; however, since most SCR ratings are in terms of full cycle average current, it is necessary to convert the RMS current to the full cycle average current for each device. A list of such conversions for various triggering points is given in Table IV-II. If the load is inductive, one must solve a lengthy transcendental equation [3].

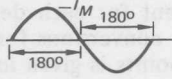
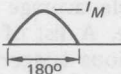
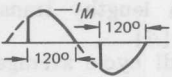
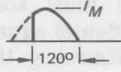
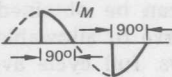
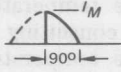
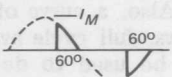
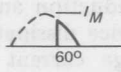
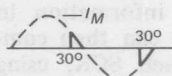
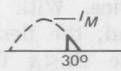
Knowing the full cycle average current in each SCR, the allowable case temperature can be obtained by consulting a curve of allowable case temperature vs. full cycle average current for the appropriate conduction angle. Also, a curve of device dissipation vs. full cycle average current can be used to determine the power dissipated in the device. With this information in hand, the designer can then compute $R_{\theta SA}$ for each SCR, using Formula 4-D.

The dissipation in a triac is considerably greater than that of a single SCR. Therefore, it is often advantageous when using high power triacs to employ either forced air or liquid cooling. These cooling means provide high thermal efficiency, yet require relatively small heat sinks.

HEATER CONTROL CIRCUITS

Perhaps one of the most obvious applications of an ac control device is in heating control. Since a heating load by nature has a long thermal time constant, it is not responsive to instantaneous current changes. This characteristic makes it adapt-

Table IV-II. RMS vs. Average Current

AC WAVESHAPES	SCR CURRENT WAVESHAPES	AC RMS CURRENT	SCR FULL CYCLE AVERAGE CURRENT
		$0.5 I_M$	$0.318 I_M$
		$0.448 I_M$	$0.239 I_M$
		$0.354 I_M$	$0.159 I_M$
		$0.223 I_M$	$0.080 I_M$
		$0.085 I_M$	$0.021 I_M$

able to zero voltage triggering techniques using pulse burst modulation in conjunction with power triacs. Instead of applying ordinary phase control means with its inherent sharply rising circuit voltages and resulting radio frequency interference, the triggering control for a triac can be arranged to trigger the device only when the supply voltage is going through zero.

The waveshapes of Figure 4-15 are an illustration of this type of control with unity power factor load. With a three-phase 460V line, using three power triacs at 143 amps RMS each, as illustrated in

Figure 4-16, a heating load capacity of $(\sqrt{3})$ (143 amps RMS) (460V RMS) = 114KW can be controlled.

Examining the steady-state rating of a suitable device as shown in Figure 4-17(a) (curve of RMS current vs case temperature), the maximum allowable case temperature is 70°C and the 143A rating can be achieved, for instance, by using a water-cooled heat dissipator. At 143 amperes, 180° conduction (bidirectional), the curve of dissipation vs. RMS current (Figure 4-17(b)) shows that the device will dissipate 225 watts. If we use a water-cooled heat exchanger with a

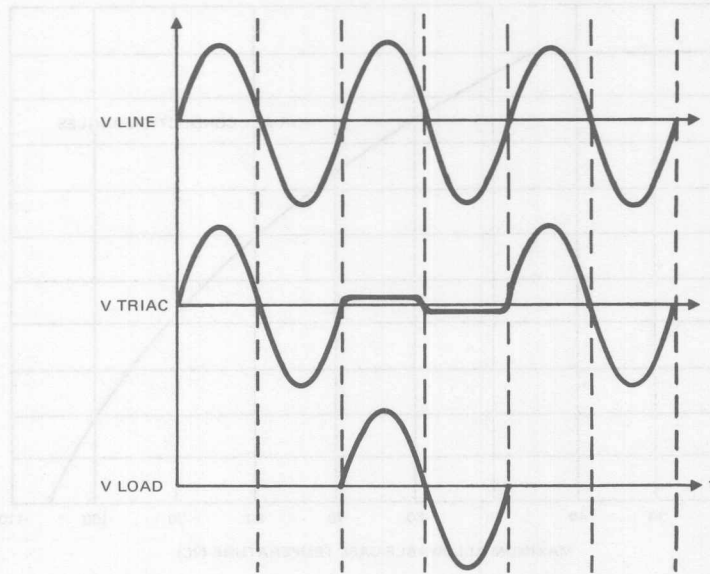


Figure 4-15. Voltage Waveforms for Zero Voltage Control of an AC Load

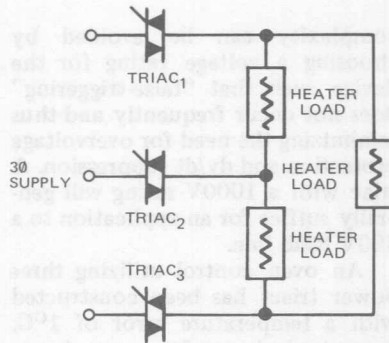


Figure 4-16. Triac Three-Phase Heater Power Control Circuit

thermal efficiency of $0.0425^{\circ}\text{C}/\text{W}$ at $3.5 \text{ gal}/\text{min}$ flow rate as shown in Figure 4-18, we can keep the exchanger rise below 9.6°C . With a $0.08^{\circ}\text{C}/\text{W}$ efficiency between heat

exchanger and case, the total temperature rise between the cooling water and the triac case is 27.6°C . Thus, with 42°C cooling water, the maximum allowable junction temperature of the triac will not be exceeded and the load of 114KW can be controlled.

An interesting extension of the application of a triac to this type of load can be achieved by using the gate characteristic of the IR power logic triac. If the triacs controlling an ac heater load were to be triggered with a negative dc gate signal, the full ac supply would be conducted to the heater load. By simply reversing the gate potential, half wave rectification of the supply to the load will take place. Thus, by using a simple gate signal reversal, the supply to the load can be reduced appreciably.

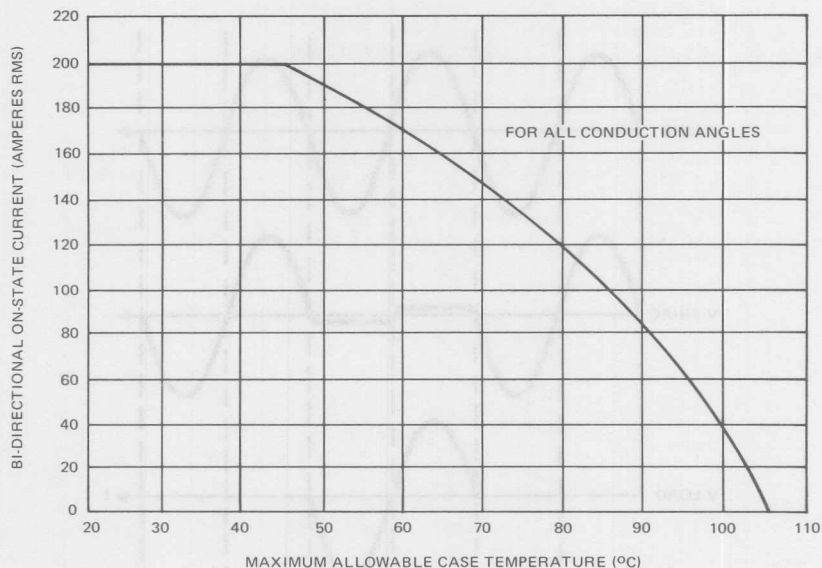


Figure 4-17(a). RMS Current vs Case Temperature

There are many types of triggering circuits which are useful for zero voltage triggering. Three of these are illustrated in Figures 4-19, 4-20, and 4-21. In addition, there are now a number of integrated circuit zero voltage switches which can be used in zero voltage triggering circuits.

In heating applications, transients tending to cause the triacs to trigger, due to high rates of rise of main terminal voltage (dv/dt) or by exceeding the break-over voltage rating of the devices (V_{BO}), are not generally worrisome to the circuit designer. An occasional power pulse to the load not called for by the control circuitry is generally of little consequence. By using a device with known avalanche and break-over capability, considerable circuit

complexity can be avoided by choosing a voltage rating for the device such that "false-triggering" does not occur frequently and thus minimizing the need for overvoltage protection and dv/dt suppression. A triac with a 1000V rating will generally suffice for an application to a 460V RMS line.

An oven control utilizing three power triacs has been constructed with a temperature error of 1°C . Some typical waveforms are shown in Figure 4-22.

Zero Voltage Triggering Circuits

In Figure 4-19, transistor Q_1 and zener diode BD_1 comprise the reference amplifier which establishes an error signal. If the measured quantity is greater than the reference established by BD_1 , Q_2 will

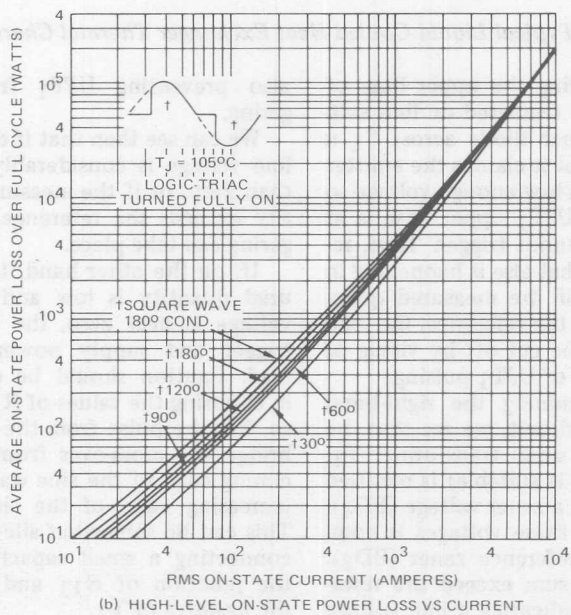
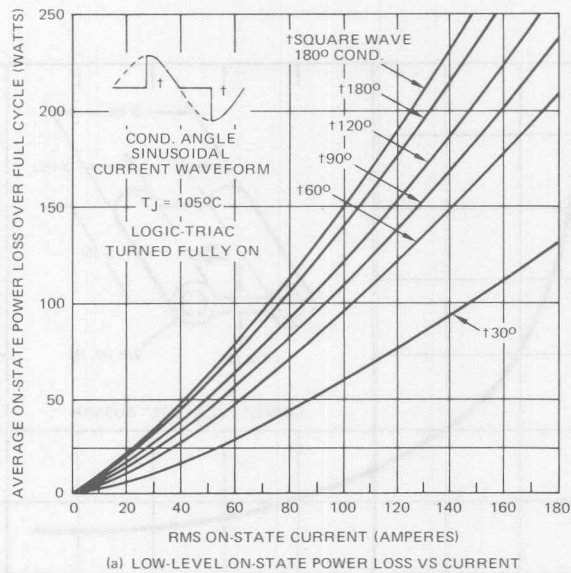


Figure 4-17(b). Allowable Power Dissipation

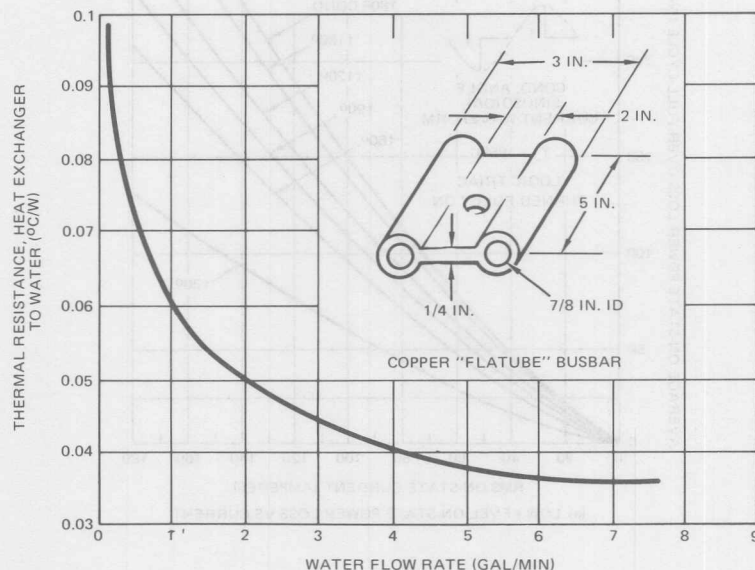


Figure 4-18. Typical Liquid-Cooled Heat Exchanger Thermal Characteristic

turn on pulling the upper base of UJT₁ to the regulated dc line voltage. The zener diode across C₁ is chosen so that it clamps the emitter of UJT₁ to a low enough voltage so that if the UJT₁ upper base is at V₁, UJT₁ cannot trigger. Thus, regardless of what else is happening in the circuit, if the measured quantity is above the reference, the load current will be cut off by virtue of the cessation of UJT₁ pulsing.

Now examining the right-hand side of the circuit, we see that the output of a small transformer T₁, (12V output is suitable) is rectified and added to a zener voltage (BD₄), the sum of these voltages is compared to a reference zener (BD₃). Should this sum exceed the reference level (indicating a line voltage far from cross-over), transistors Q₄ and Q₃ are turned on, pulling the upper base of UJT₁ to V₁ and

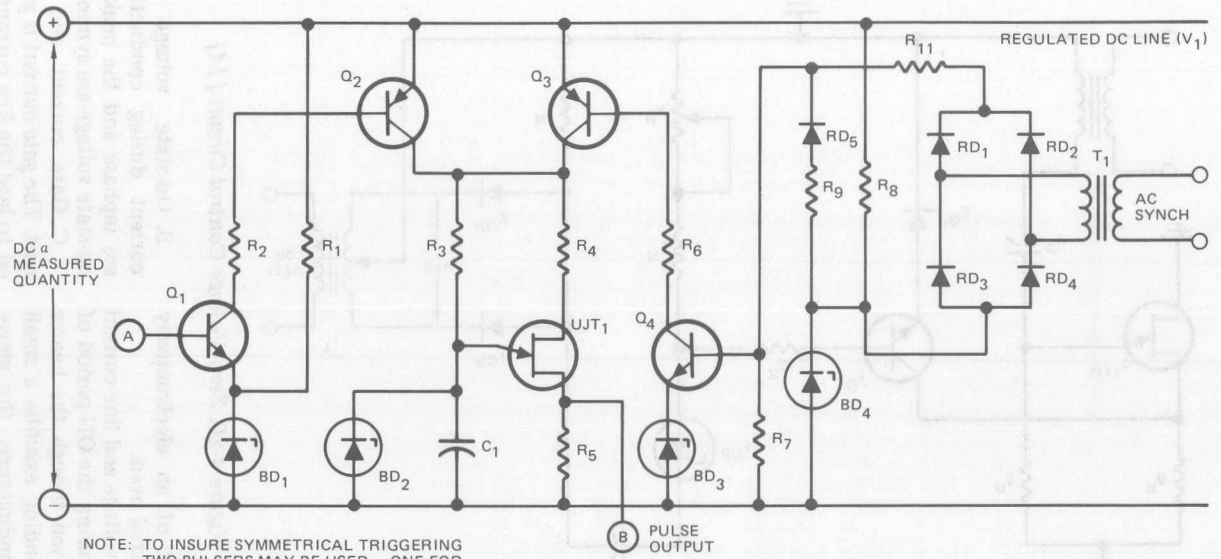
also preventing UJT₁ from triggering.

We can see then that if either the line voltage is considerably greater than zero, or if the measured quantity exceeds the reference, no triggering can take place.

If, on the other hand, the measured quantity is low and the line voltage is near zero, the UJT will trigger and supply power to the load. Caution should be exercised in choosing the values of R₃ and C₁ so that the pulse from the UJT will bridge the cross-over from the declining edge of the sine wave to the increasing edge of the sine wave. This can be somewhat alleviated by connecting a small capacitor from the junction of R₁₁ and RD₅ to the negative of V₁.

Notes Relative to Figure 4-22

Operational waveforms of power



NOTE: TO INSURE SYMMETRICAL TRIGGERING
TWO PULSERS MAY BE USED - ONE FOR
EACH HALF CYCLE

Figure 4-19. Zero Voltage Triggering Circuit

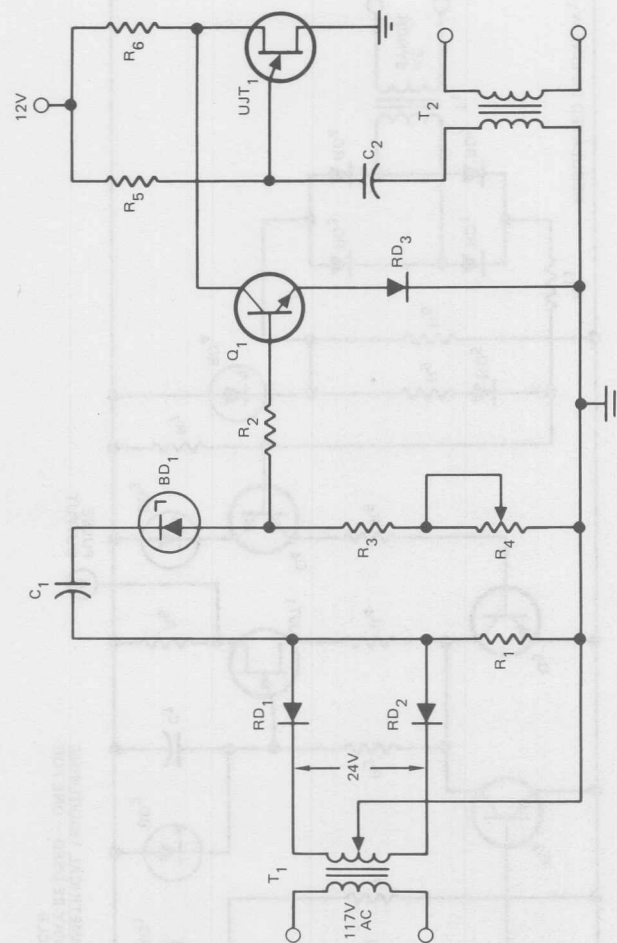


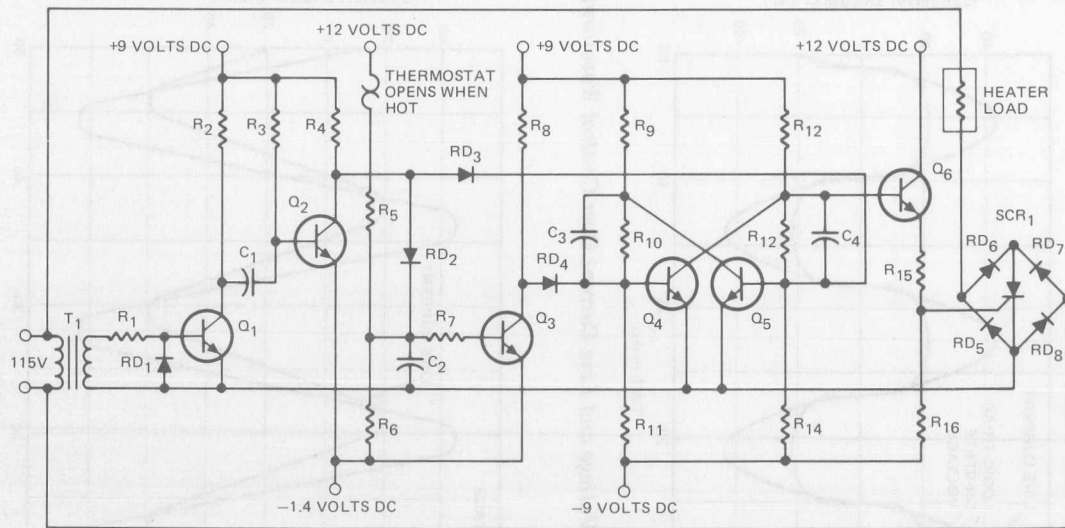
Figure 4-20. Zero Voltage Control Circuit [14]

triac control of an electronically heated industrial oven.

A. Line voltage and line current waveforms during the ON period of operation. Even though the heater resistance winding exhibits a small amount of inductance, the waveforms are symmetrically sinusoidal and undistorted by the triac control.

B. On-state voltage and line current during conduction. They are inphase and the peak values of on-state voltage are symmetrical.

C. Gate current and line current. The gate current is phase-shifted to lead the line current such that it will be driving the triac gate hard at the time it starts to conduct current.



FILAMENT TRANSFORMER STEPS DOWN AC SUPPLY TO GIVE CONTROL SIGNAL FOR SCR₁'S TRIGGERING CIRCUIT.

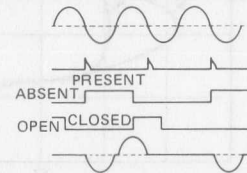
SUPPLY VOLTAGE

TURN-ON PULSES FOR Q₅

TRIGGER SIGNAL FOR SCR₁

THERMOSTAT STATE

LOAD CURRENT



WAVEFORM PATTERNS DEMONSTRATE THE ACTION OF THE ZERO-CROSSING DETECTOR CIRCUIT.

Figure 4-21. Zero Voltage Control Circuit [15]

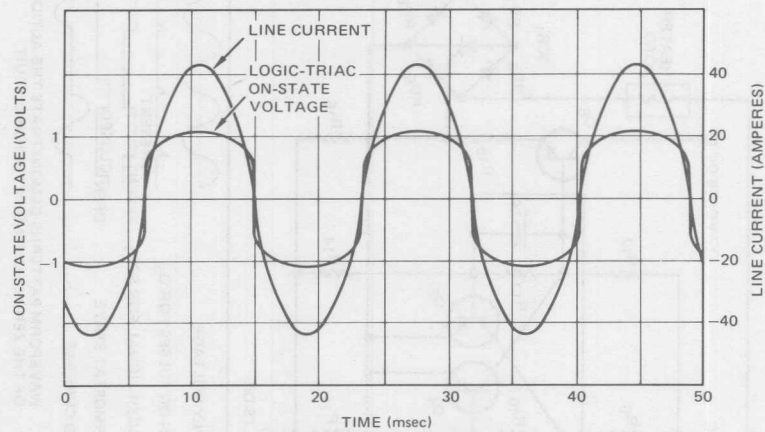


Figure 4-22(a). Line Voltage and Line Current Over Control Waveforms

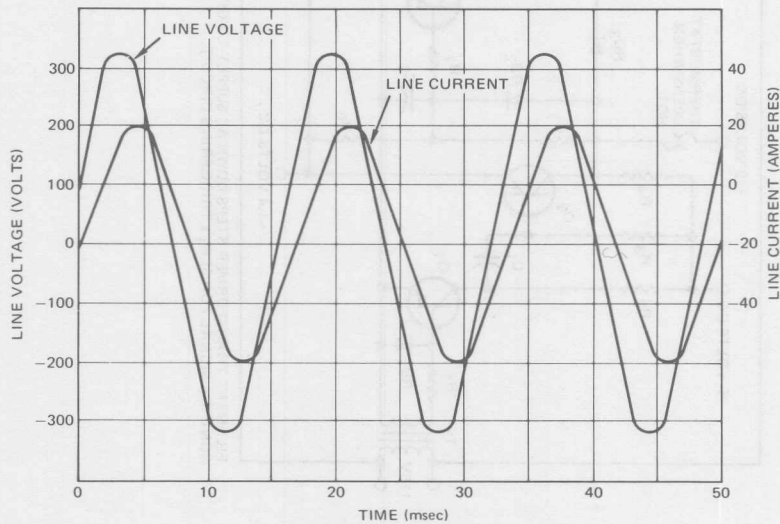


Figure 4-22(b). On-State Voltage and Line Current

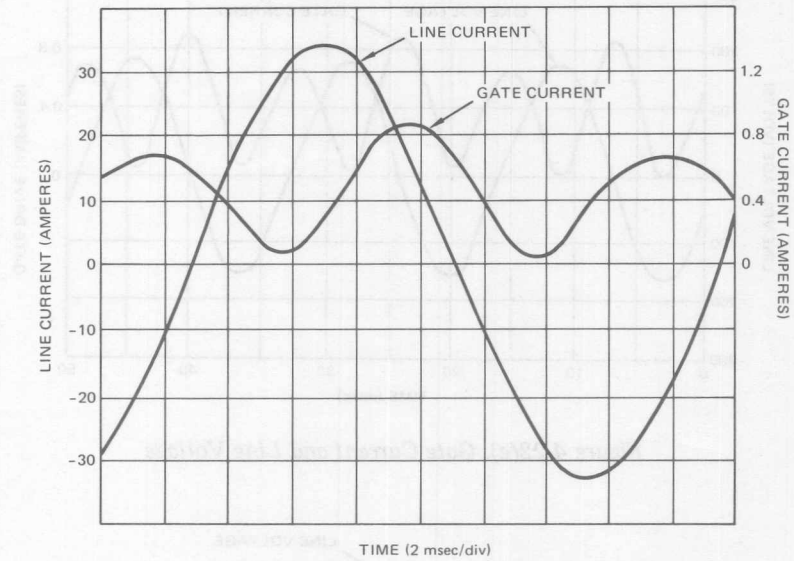


Figure 4-22(c). Gate Current and Line Current Waveform

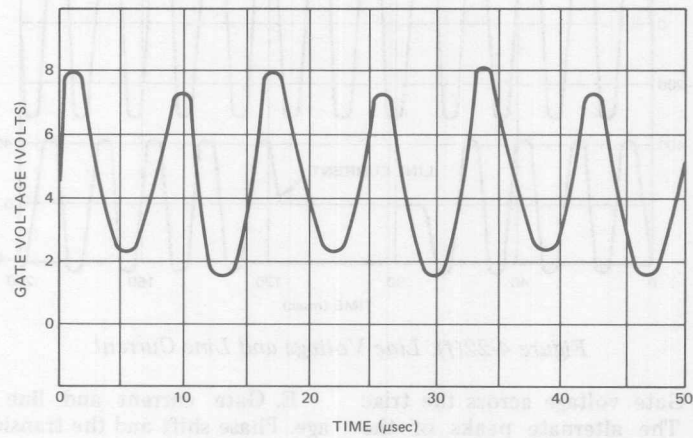


Figure 4-22(d). Gate Voltage

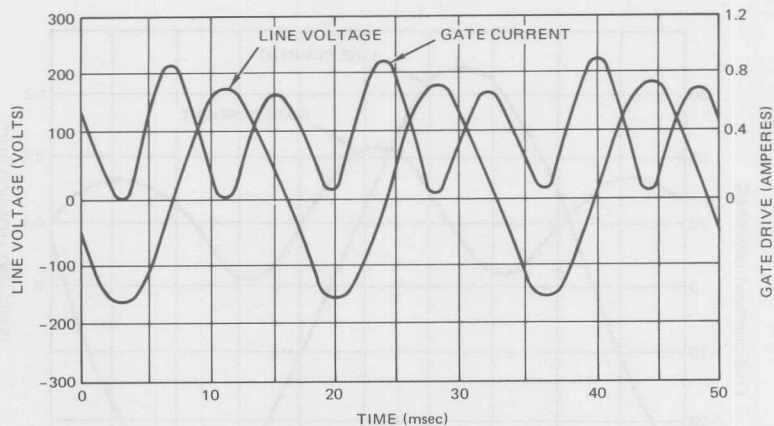


Figure 4-22(e). Gate Current and Line Voltage

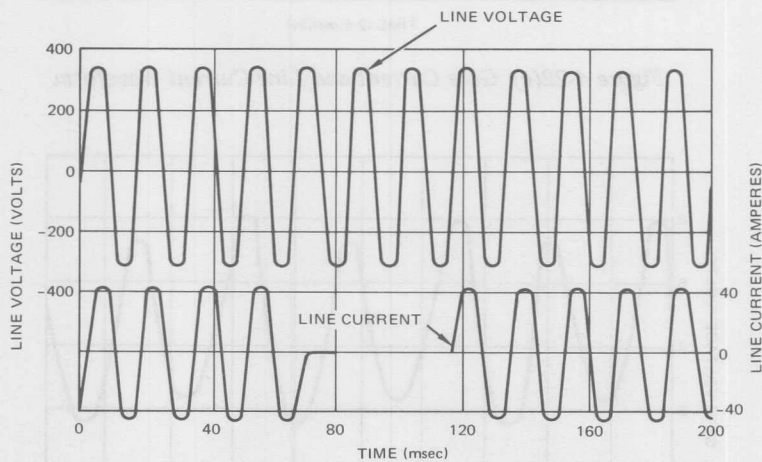


Figure 4-22(f). Line Voltage and Line Current

D. Gate voltage across the triac gate. The alternate peaks of the waveform shows the small influence in voltage magnitude that the direction of flow of line current imposes on the gate signal.

E. Gate current and line voltage. Phase shift and the transient in the gate current are obvious as line current changes polarity.

F. Line voltage and line current showing zero-voltage switching.

Note the line voltage is a continuous sine wave, while the line current starts and stops at the zero axis. The triac operating temperature also influences the starting load current at the zero cross-over point.

Lighting Circuits [7], [8]

A lamp dimmer is an example of one of the basic uses of phase control. There are many different types of triac circuits designed for lamp dimming. However, most of these differ only in the method of triggering the triac. Among the components used for triggers are UJTs, PUTs, neon bulbs, silicon unilateral switches, asymmetrical switches, reed switches, and diacs. The diac offers the advantage of needing fewer components for a trigger circuit. Its characteristics also make it an ideal trigger for a triac. The main disadvantage of the diac is that it takes approximately 32 volts to break over, thus limiting the portion of the wave that can be controlled.

One of the more simple circuits using a diac-triac combination to dim incandescent lamps is the single

time constant phase control shown in Figure 4-23. This circuit has as its major disadvantages a limited control range and hysteresis. For a more thorough description of hysteresis see reference [9]. For the single time constant circuit, the voltage on the capacitor charges up to the breakover voltage of the diac and discharges through the diac to trigger the triac. This enables the triac to conduct for the remaining portion of the half cycle of the input wave. When the input goes to zero, the triac turns off and the charge on the capacitor, since the diac has already recovered, begins to build up with the opposite polarity until the same events occur again. Figure 4-24 shows waveforms for this single time constant circuit when operating with a large phase control angle.

A slightly more complex circuit is the double time constant circuit, shown in Figure 4-25. This circuit was designed and built for both a 3600 and a 7200 watt load.

The double time constant circuit operates in a similar fashion to the single time constant circuit with the exception of capacitor C_1 recharg-

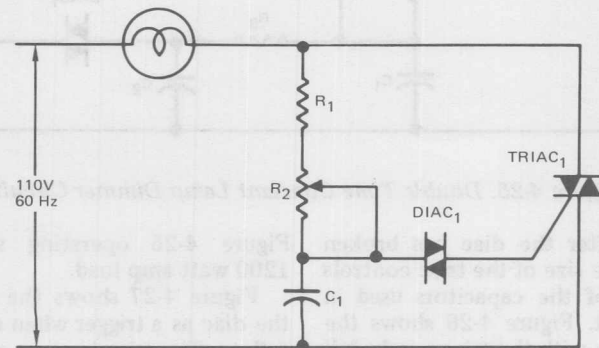
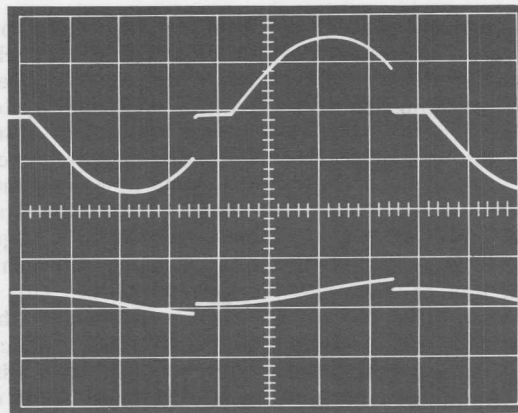


Figure 4-23. Single Time Constant Lamp Dimmer Circuit



UPPER: VOLTAGE ACROSS TRIAC

LOWER: VOLTAGE ACROSS C_2

100 V/DIV; 10 MSEC/DIV

Figure 4-24. Waveforms for Single Time Constant Lamp Dimmer Circuit
(Operating with Large Phase-Control Angle)

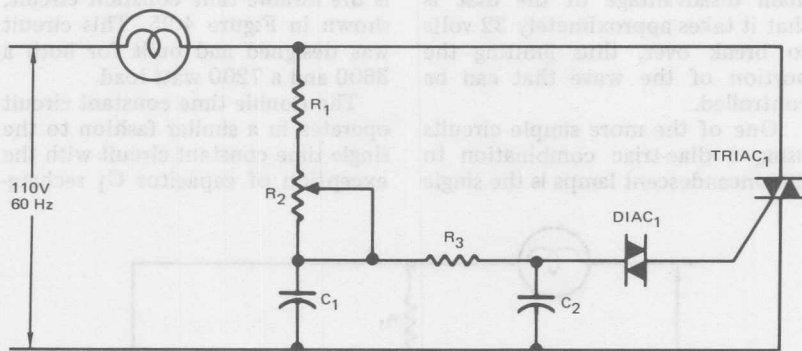
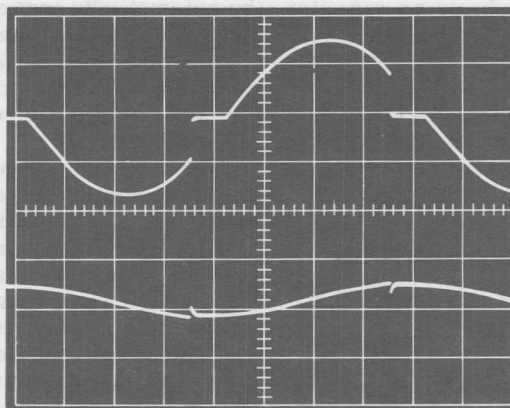


Figure 4-25. Double Time Constant Lamp Dimmer Circuit

ing C_2 after the diac has broken down. The size of the triac controls the size of the capacitors used in the circuit. Figure 4-26 shows the waveforms with the triac nearly full on for the 3600 watt circuit of

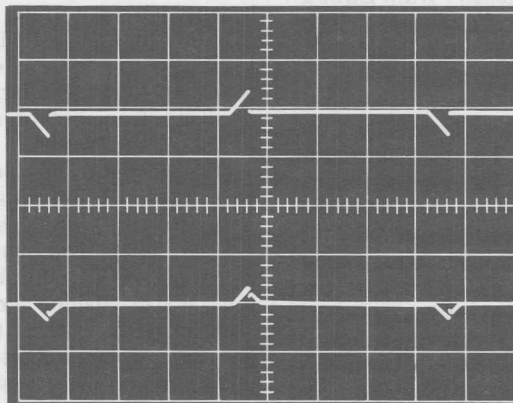
Figure 4-25 operating with the 1200 watt amp load.

Figure 4-27 shows the effect of the diac as a trigger when operating full on. The triac is never on for the full period of the input wave, but



UPPER: VOLTAGE ACROSS TRIAC
100 V/DIV 10 MSEC/DIV
LOWER: VOLTAGE ACROSS CAPACITOR
100 V/DIV 10 MSEC/DIV

**Figure 4-26. Waveforms for Double Time Constant Lamp Dimmer
(Near Full On)**



UPPER: VOLTAGE ACROSS TRIAC
100 V/DIV 10 MSEC/DIV
LOWER: VOLTAGE ACROSS C_2
100 V/DIV 10 MSEC/DIV

**Figure 4-27. Waveforms for Double Time Constant Lamp Dimmer
(Full-On Operation)**

only after the charge on capacitor C₂ has reached 32 volts.

The relative light intensity of the circuit in Figure 4-25 as measured with a light meter held two feet away from a circular concentration of the 1200 watt lamp load is shown in Figure 4-28.

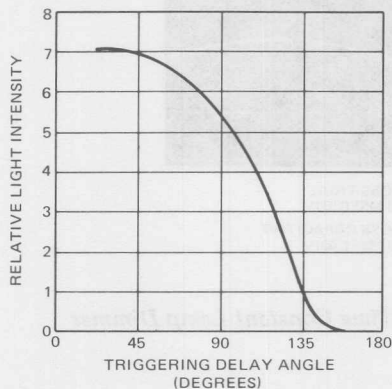


Figure 4-28. Relative Light Intensity from Double Time Constant Triggering Circuit Lamp Dimmer

A configuration for a light flasher is shown in Figure 4-29, requiring two triacs and one heat sink, rather than the four SCRs and three heat sinks previously required.

When motor loads are switched on to an ac line which is also supplying fluorescent lamps there is often a visible flicker in the lamps due to the surge loading of the line. This can often be objectionable, especially when the motor starting is frequent. For example, compressor motors are often required to start frequently and run a relatively short time. One method of minimizing the effect of such flicker is

by automatically correcting the line voltage during high surge currents. This is done by inserting a section of a step-up transformer to boost the line voltage temporarily until the surge disappears.

The triac is an excellent device for this purpose because of the simplicity of the driving function and the ease of heat sinking. A tap changer similar to that shown in Figure 4-30 can be used as a line compensator. Line compensation can also be accomplished by using a triac and an autotransformer as shown in Figure 4-31. As the starting contactor, K₁, in series with the motor load, is closed, the motor surge current begins to flow. This current is generally three to six times the running current of the machine. The surge causes a voltage drop on the line inductance and transient inductance of the supply alternator which causes the line voltage, as seen by the fluorescent lamps, to drop. If the surge current is sensed by a current transformer as shown in Figure 4-31 and caused to trigger the triac into a compensating auto-transformer, the flicker resulting from motor starting can be greatly minimized.

The degree of compensation can be adjusted by the resistor in series with the triac, while the surge current at which compensation takes place can be changed by adjusting the resistor divider across the secondary of the current transformer. By utilizing this circuit across each line, a three-phase system can be automatically compensated.

FERRORESONANT TRANSFORMER REGULATED AC POWER SUPPLY

A ferroresonant voltage regulator may be used for line voltage

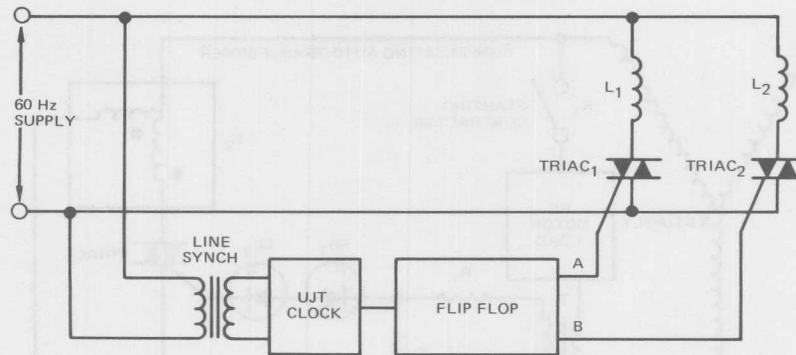


Figure 4-29. Light Flasher Circuit

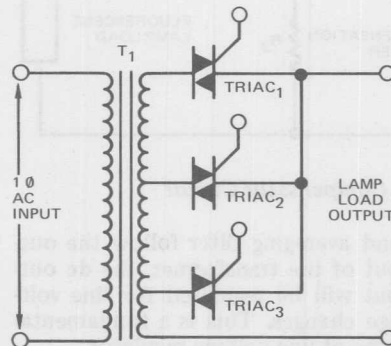


Figure 4-30. Static Tap Changer Circuit

regulation. This is inherent in the device, since it is composed of a high leakage transformer which serves as a saturable reactor and an inductance in series. The half cycle average output voltage of the ferroresonant regulator is given in Formula 4-E.

$$V_O = 4N \phi_S f \times 10^{-8} \quad (4-E)$$

Where:

V_O = Average output voltage

N = Number of turns

ϕ_S = Saturation flux
 f = Input frequency [10]

Since the saturation flux, ϕ_s is fixed as long as the input frequency remains constant, the output voltage will remain the same. This equation points out the main difficulty of the ferroresonant regulator, in that the output voltage is frequency sensitive. Some of the other disadvantages include: (1) Since the core operates in saturation, the core losses are high and the external magnetic field is high; (2) Since the output varies directly with the cross-sectional area of the core, normal core tolerances cause unit-to-unit output voltage differences; (3) Since the core is the regulating element, the output voltage varies with load current changes due to voltage drop in the secondary resistance.

One method of eliminating these disadvantages is to simulate saturation of the transformer. This can be done by using a transformer with additional magnetic shunts and an additional winding, or by adding inductance in series with the primary winding of a transformer with two secondary windings. This in-

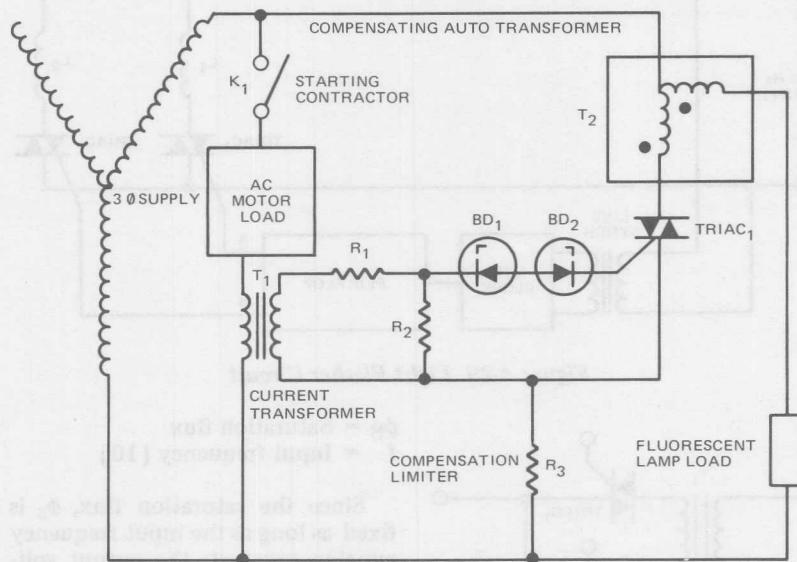


Figure 4-31. Line Voltage Compensator Circuit

ductance must be sufficiently large to produce the voltage drop required to regulate the output voltage.

The conventional ferroresonant regulator may be described in several ways. One simplified explanation is to consider it similar to the circuit of Figure 4-32. Assume the input voltage is sufficiently large so that the core of T_1 is driven from $-\phi$ to $+\phi_s$ in less than a half cycle. Thus, the half cyclic average voltage induced in any winding on T_1 is a constant as long as the core saturates and the frequency is fixed. This is true, regardless of the magnitude or waveform of the input voltage. Also, regardless of the number of turns on the primary winding, as long as the core is driven into saturation, the output voltage follows the number of turns on the secondary winding. If a rectifier

and averaging filter follow the output of the transformer, the dc output will be regulated for line voltage changes. This is a fundamental type of line voltage regulator.

A more efficient line voltage regulator would use an inductor, L_1 , in series with T_1 , rather than a resistor to eliminate the power losses (see Figure 4-33). This circuit also regulates the half cyclic average of the output voltage, regardless of the magnitude or waveform of the input voltage. If a rectifier and averaging filter follow the output of T_1 , again the output voltage will be regulated for line voltage variations.

The circuit of Figure 4-34(a), called a ferroresonant regulator, is a more effective and efficient technique of regulating the output voltage. This circuit uses a capacitor C_1 in parallel with T_1 . C_1 and L_1 are

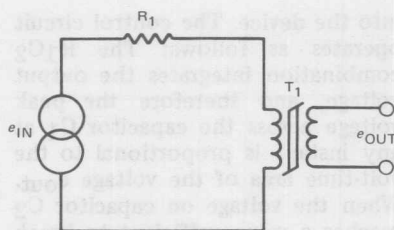


Figure 4-32. Saturating Transformer Regulator

tuned near the input frequency. This arrangement provides almost unity power factor and efficient power transfer. Figure 4-34(b) shows the schematic for a ferroresonant transformer. Here the magnetic functions of L_1 and T_1 are combined on a single core structure. The leakage inductance provided by the shunts takes the place of L_1 . Figure 4-35 shows a typical output voltage waveform from either arrangement.

Because of the near square waveform of the output voltage, and since for a square wave $V_{PK} = V(AV) = V_{RMS}$, this circuit regulates all three values. Therefore, with this circuit, the filter may be either capacitor input or inductor

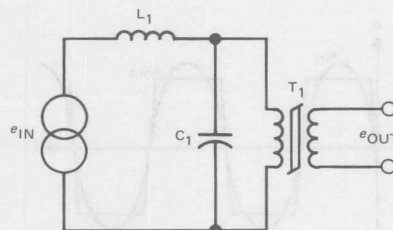


Figure 4-33. Improved Saturating Transformer Regulator

input — it does not matter — the dc output will be the same and will be regulated for line voltage changes. In practice, a capacitor terminated rectifier is usually used because the filter capacitance is reflected in parallel with C_1 , reducing the value of C_1 required to resonate with L_1 .

Another advantage of this circuit is that the tuning of L_1 and C_1 provides a low pass filter between the input and the output. Thus, harmonics in the input waveform are attenuated by ferroresonant regulator circuits.

Shown in Figure 4-36, is a circuit which consists of a ferroresonant regulator, a control circuit, and a rectifier and filter [10]. In the control circuit the R_1C_2 combina-

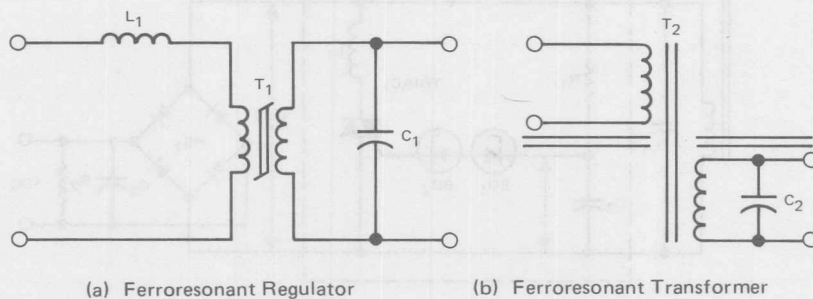


Figure 4-34. Secondary Resonance, Saturating Transformer Regulators

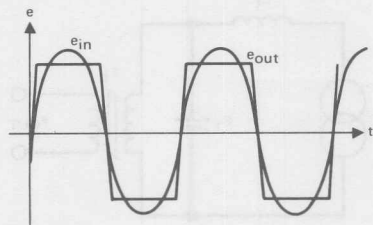


Figure 4-35. Waveshapes of Ferro-Resonant Regulator on Transformer

tion is an integrator used to measure the volt-time area of the output voltage. L_1 is an inductor chosen to have a value approximately equal to the value of the saturated inductance of the secondary of the ferroresonant transformer. The triac acts as a switch which closes when there is sufficient gate current flowing

into the device. The control circuit operates as follows: The R_1C_2 combination integrates the output voltage, and therefore the peak voltage across the capacitor C_1 at any instant is proportional to the volt-time area of the voltage e_{out} . When the voltage on capacitor C_2 reaches a value sufficient to break over the zener diode, BD_1 or BD_2 , on alternate half cycles, gate current flows and the triac conducts current. This causes the capacitor C_1 to rapidly discharge and recharge in the opposite direction through the inductor L_1 . At this time, the voltage across the triac and the current through it are reversed, causing the triac to come out of conduction, thus completing the half cycle. The same action occurs the next half cycle with the opposite polarity. Clearly this ac-

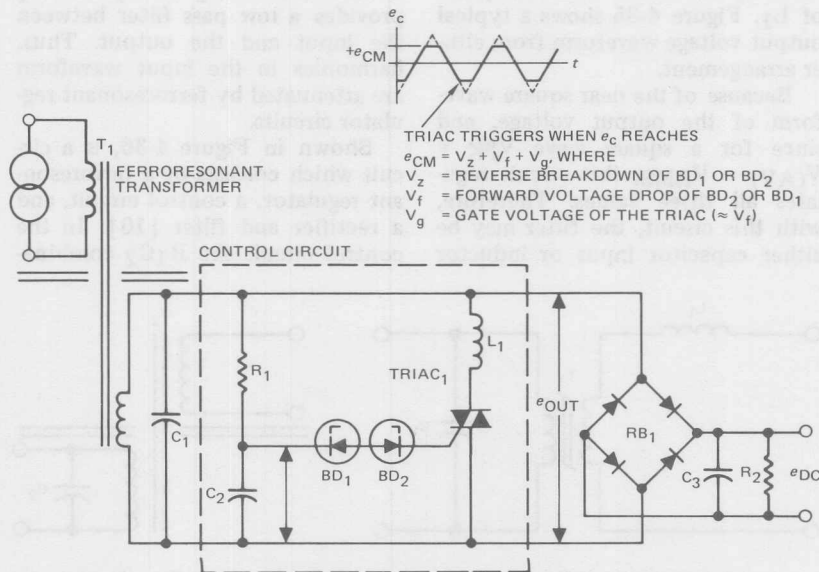


Figure 4-36. Ferroresonant - Triac Regulator

tion cannot occur if the core saturates since the necessary volt-time area to trigger the triac cannot be obtained.

Specifically, the output voltage, e_{out} in this figure is approximately a square wave. However, in this case, the output voltage is still frequency-dependent.

Figure 4-37 is a schematic of the ferroresonant circuit incorporating feedback. Here the control circuit has been placed across an isolated winding of the transformer. This is necessary to obtain the isolation required for the feedback circuit. The integrating resistor consists of

R_4 , R_5 , and R_0 , where R_0 is the impedance seen looking into a $-a'$. The zener diode BD_3 is the reference, and the transistor Q_1 is the error detector and amplifier. The diode bridge, RB_2 , is added to keep the current flow through Q_1 unidirectional. In this arrangement, R_0 is an impedance whose value is decreased by the feedback circuit as e_{DC} tries to increase. Thus, the regulating function is taken by sampling the actual filtered dc output voltage rather than by monitoring the intermediate square wave voltage. Therefore, the regulator is no longer frequency dependent. As

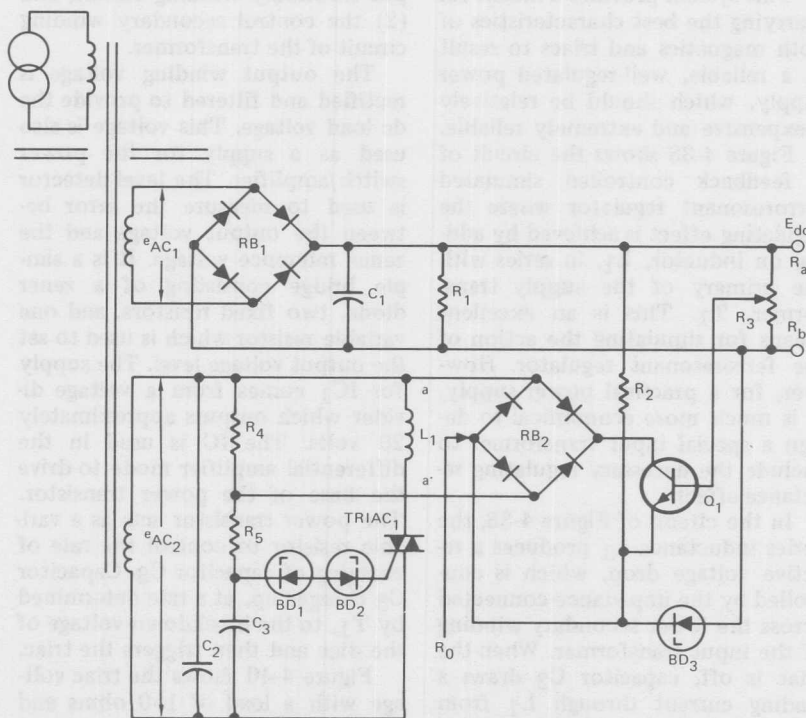


Figure 4-37. Ferroresonant-Triac Regulator with Isolated Output Regulation

can be seen from Figure 4-37, the output voltage is regulated by controlling the amplitude of the ac voltage feeding the rectifier bridge and filter. Another advantage of this circuit is that L_1 can be made very small, causing the voltage across the triac to reverse more rapidly, making $e(t)$ a squarer wave, and reducing the required filter capacitance. Since the transformer core does not saturate, core losses are reduced and the circuit is more efficient. The half cycle response of the ferroresonant regulator is retained, and the stray magnetic field is reduced.

This system provides a means for marrying the best characteristics of both magnetics and triacs to result in a reliable, well-regulated power supply, which should be relatively inexpensive and extremely reliable.

Figure 4-38 shows the circuit of a feedback controlled simulated ferroresonant regulator where the regulating effect is achieved by adding on inductor, L_1 , in series with the primary of the supply transformer, T_1 . This is an excellent means for simulating the action of the ferroresonant regulator. However, for a practical power supply, it is much more economical to design a special input transformer to include the necessary regulating reactance effect.

In the circuit of Figure 4-38, the series inductance L_1 produces a reactive voltage drop, which is controlled by the impedance connected across the lower secondary winding of the input transformer. When the triac is off, capacitor C_2 draws a leading current through L_1 from the ac supply. This leading current produces a voltage across L_1 , which adds to the source voltage. Thus,

the transformer secondary voltages are highest when the triac is off. If inductor L_2 is such that its reactance is one-half that of capacitor C_2 , a lagging current, equal in magnitude to the leading current drawn by C_2 alone, will flow through inductor L_1 when the triac is on for the entire cycle. Thus, the triac can be phase controlled to adjust the voltage across L_1 , thereby regulating the transformer secondary voltages. Figure 4-39 includes phasor diagrams to illustrate this regulating principle.

The circuit in Figure 4-39 is divided into two parts: (1) the output secondary winding circuit, and (2) the control secondary winding circuit of the transformer.

The output winding voltage is rectified and filtered to provide the dc load voltage. This voltage is also used as a supply for the power switch/amplifier. The level detector is used to measure the error between the output voltage and the zener reference voltage. It is a simple bridge consisting of a zener diode, two fixed resistors, and one variable resistor which is used to set the output voltage level. The supply for IC_1 comes from a voltage divider which outputs approximately 20 volts. The IC is used in the differential amplifier mode to drive the base of the power transistor. The power transistor acts as a variable resistor to control the rate of charging of capacitor C_3 . Capacitor C_3 charges up, at a rate determined by T_1 , to the breakdown voltage of the diac and then triggers the triac.

Figure 4-40 shows the triac voltage with a load of 150 ohms and the output adjusted to 75 volts. It can be seen that the triac is on for an appreciable part of each cycle.

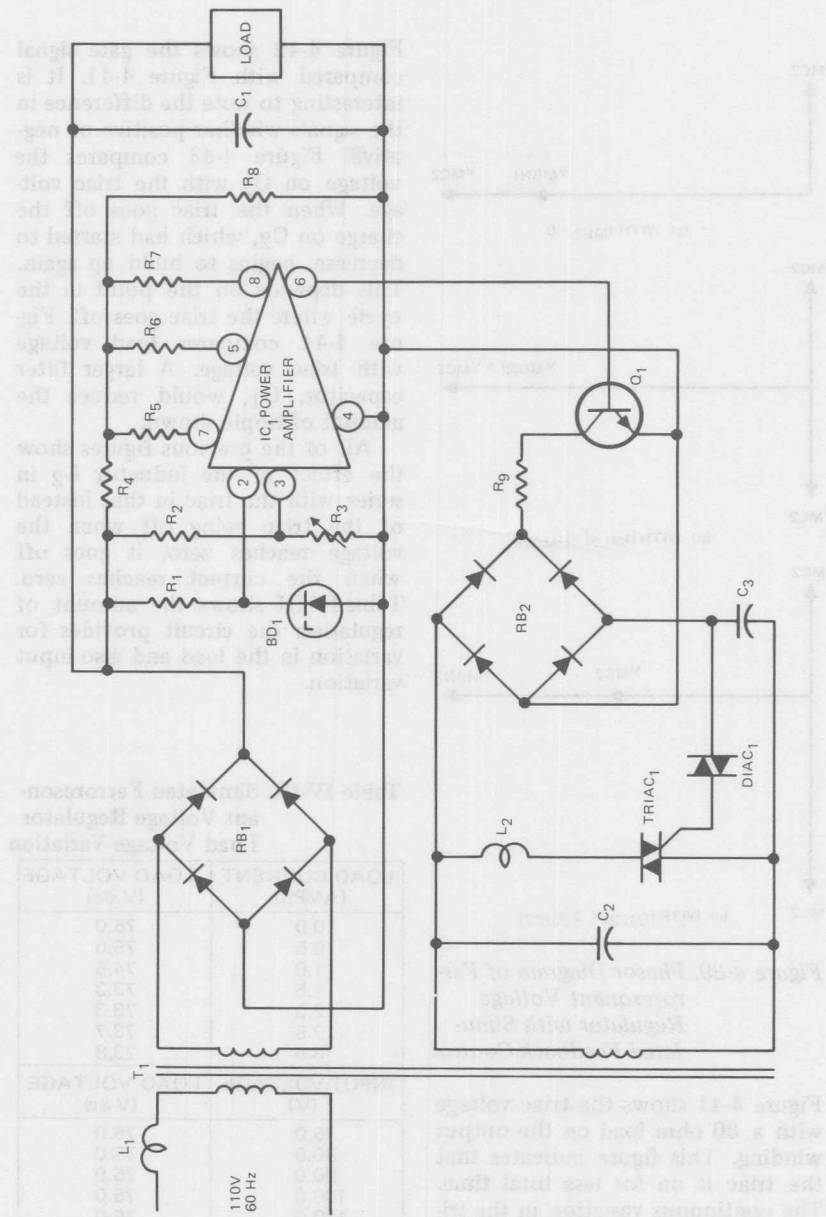


Figure 4-38. Ferroresonant Voltage Regulator with Simulated Feedback Control

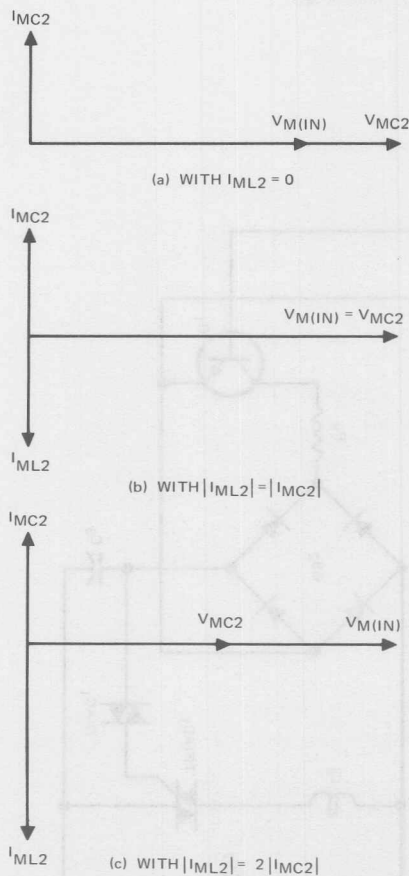


Figure 4-39. Phasor Diagram of Ferroresonant Voltage Regulator with Simulated Feedback Control

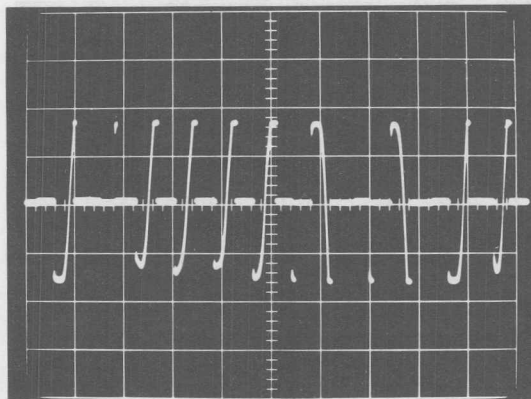
Figure 4-41 shows the triac voltage with a 30 ohm load on the output winding. This figure indicates that the triac is on for less total time. The continuous variation in the triac triggering angle is believed to be caused by the system attempting to regulate the ripple in the output.

Figure 4-42 shows the gate signal compared with Figure 4-41. It is interesting to note the difference in the signals whether positive or negative. Figure 4-43 compares the voltage on C_2 with the triac voltage. When the triac goes off the charge on C_2 , which had started to decrease, begins to build up again. This depends on the point in the cycle where the triac goes off. Figure 4-44 compares load voltage with triac voltage. A larger filter capacitor, C_1 , would reduce the amount of ripple shown.

All of the previous figures show the effect of the inductor L_2 in series with the triac in that instead of the triac going off when the voltage reaches zero, it goes off when the current reaches zero. Table IV-III shows the amount of regulation the circuit provides for variation in the load and also input variation.

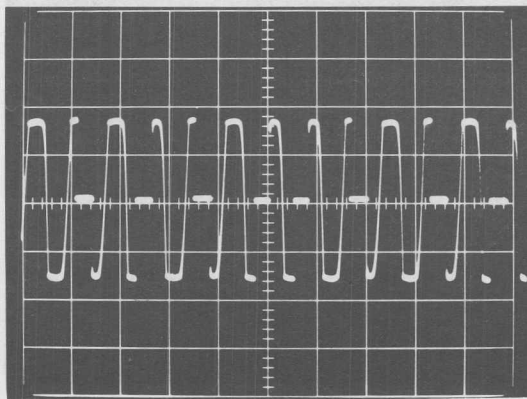
Table IV-III. Simulated Ferroresonant Voltage Regulator Load Voltage Variation

LOAD CURRENT (AMPS)	LOAD VOLTAGE (V dc)
0.0	75.0
0.5	75.0
1.0	74.6
1.5	73.3
2.0	73.3
2.5	73.7
3.0	73.8
INPUT VOLTAGE (V)	LOAD VOLTAGE (V dc)
75.0	75.0
80.0	75.0
90.0	75.0
100.0	75.0
110.0	75.0
120.0	75.0
130.0	75.4
140.0	75.8



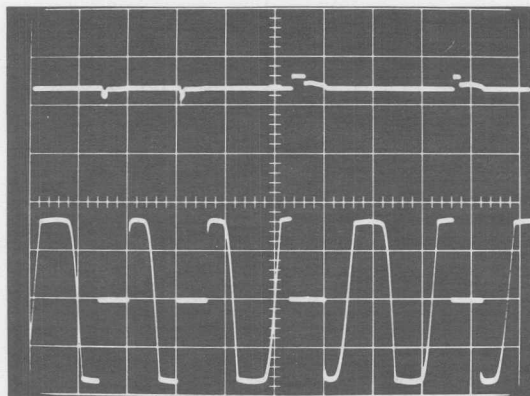
50 V/DIV; 20 MSEC/DIV

Figure 4-40. Ferroresonant Voltage Regulator Triac Voltage with 150 Ohm Load



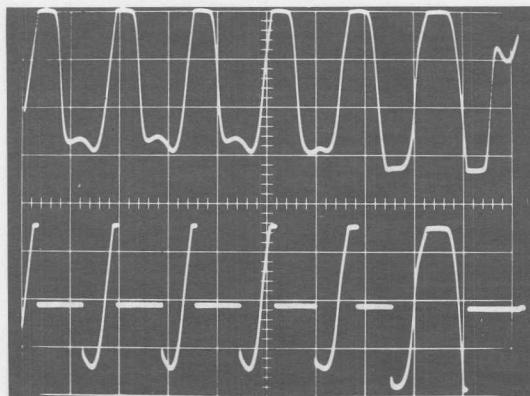
50 V/DIV; 20 MSEC/DIV

Figure 4-41. Ferroresonant Voltage Regulator Triac Voltage with



UPPER: 5 V/DIV; 10 MSEC/DIV
 LOWER: 50 V/DIV; 20 MSEC/DIV

Figure 4-42. Ferroresonant Voltage Regulator Gate Signal and Triac Voltage



50 V/DIV; 10 MSEC/DIV

Figure 4-43. Ferroresonant Voltage Regulator Capacitor Voltage and Triac Voltage

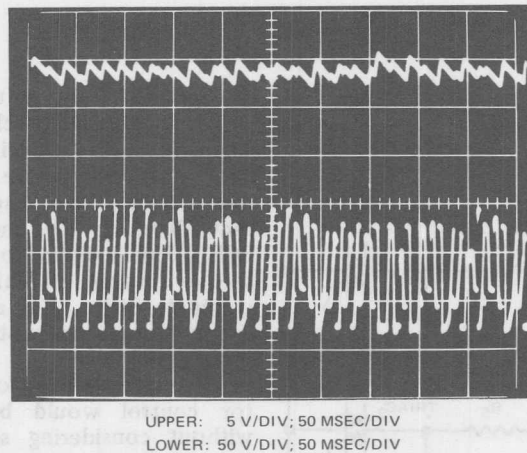


Figure 4-44. Ferroresonant Voltage Regulator Load Voltage and Triac Voltage

MOTOR CONTROL

For many years, induction motors were considered to be constant speed machines which provided a cost reduction and improvement in reliability.

These factors, together with the possible simplification of starting controls, have favored the use of induction motors over other types of machines. Wound rotor machines with secondary resistance and shorting means (contactors) have provided limited speed control. However, the disadvantages of finite step speed control, with its inherently poor speed regulation and incompatibility with closed-loop speed regulator operation, have eliminated this drive from consideration in most variable-speed drive applications.

With the availability of the power SCR and power triac, these limitations have been circumvented, providing an expanded field of application for induction machines. For

high performance applications, variable-frequency, constant volt-second supplies have been constructed using cycloconverters and dc link inverters which minimize the power losses in the machine compatible with the greatest possible controllable speed range. However, due to the relative complexity of these drives and the resulting cost, there is an economic lower limit of horsepower when applying them. Consequently, there is a need in the power level below about 25 HP for a reduced cost speed control system. The statically controlled wound rotor induction machine can meet these requirements.

Figure 4-45 illustrates a triac phase controlled system. The control of the triacs is simply a phase control problem and has been discussed for inductive loads.

When the starting duty of a synchronous motor is such that a rotor resistor is required, the circuit

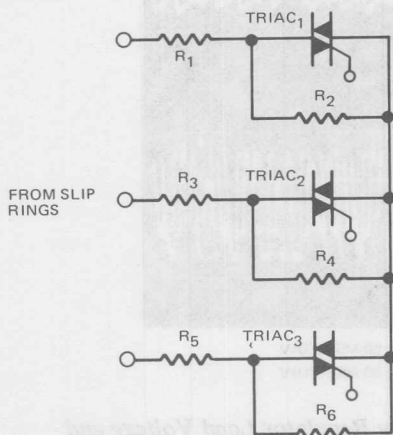


Figure 4-45. Triac Speed Control

of Figure 4-46 can be used. During starting, SCR₁ is blocking and remains so until the exciter field supply is energized and dc flows to the motor field circuit, whereupon current flows in R₂ and turns on SCR₁. This is similar to low starting torque starters, in which one can eliminate SCR₁, R₁, and R₂ and simply short the motor field on starting [11].

No discussion of polyphase motor control would be complete without considering static motor starters. For example, a simple static motor starter is shown in Figure 4-47. The current transformer feedback level will reduce until the

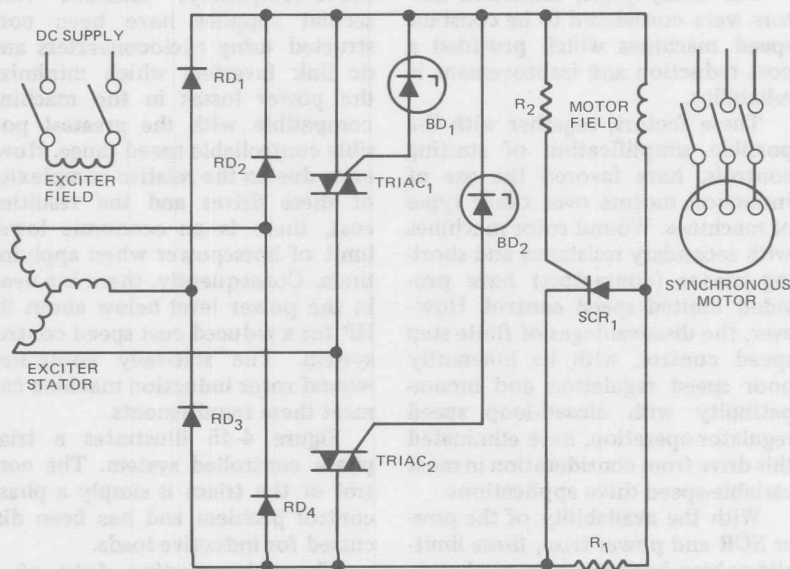


Figure 4-46. Triac Synchronous Motor Starter

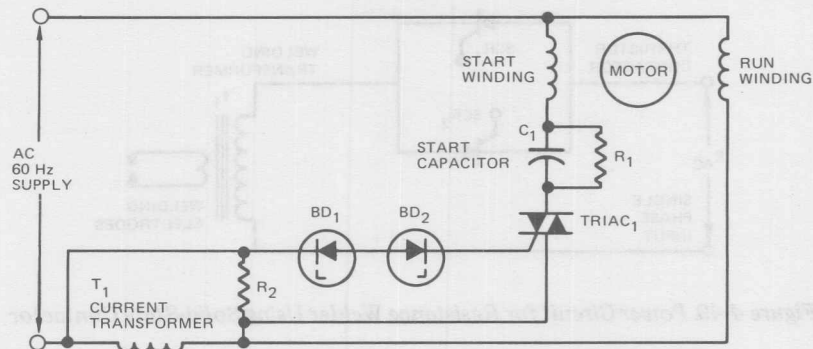


Figure 4-47. Triac Static Motor Starter

starting winding is de-energized as the motor comes to speed. Perhaps a more straight forward application is shown in Figure 4-48 which is for a polyphase motor contactor. An interesting by-product of this type of static starter is that the motor can be easily plugged by using a triac with a "logic" gate and simply reversing the gate signal polarity, thereby applying dc to the motor ac line terminals.

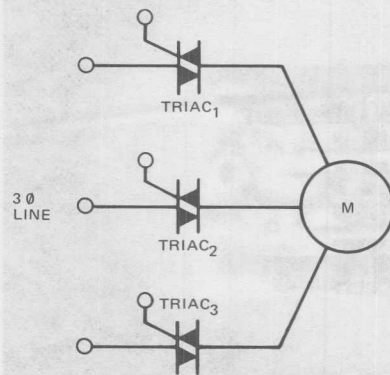


Figure 4-48. Triac Three-Phase Motor Starter Circuit

WELDING SERVICE CIRCUITS [16]

The basic circuit configuration for an AC resistance welder is shown in Fig. 4-49.

SCRs in anti-parallel (or "back-to-back") configuration are used to control the power applied to the transformer primary. By precisely controlling the phase angle and number of pulses applied to the gates, a very precise control of welding power ("heat") may be obtained.

Water cooling is almost exclusively used in this service. In addition, it has become common also to water-cool the welding transformer and welding electrodes.

The Hockey-Puk method of constructing the power thyristors is the ideal configuration to use in building an assembly of two thyristors in anti-parallel for welding service. Full load on the welding transformer amounts to a virtual short circuit on the secondary. In addition, welding transformers generally have a high leakage reactance which limits short circuit current. Therefore, if current surges due to transformer

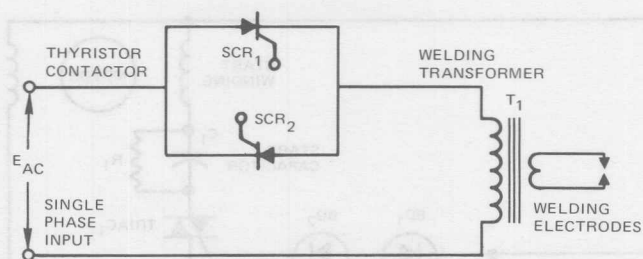


Figure 4-49. Power Circuit for Resistance Welder Using Solid-State Contactor

saturation can be avoided, there is no need to provide a reserve for overloads when determining the current the thyristors may have to handle. Thus, by cooling the Hockey-Puks on both sides, they may be operated at a high current density without concern for the possibility of damage due to a current overload. In addition, their pressure-assembled construction eliminates the possibility of device degrada-

tion due to deterioration of internal solder bonds. This degradation is caused by repeated heating and cooling resulting from the cyclical welding load.

Hockey-Puk Assembly for Welder Service

A representative water-cooled assembly of two large thyristor Hockey-Puks is shown in Fig. 4-50. It will be seen that a water-cooled pad

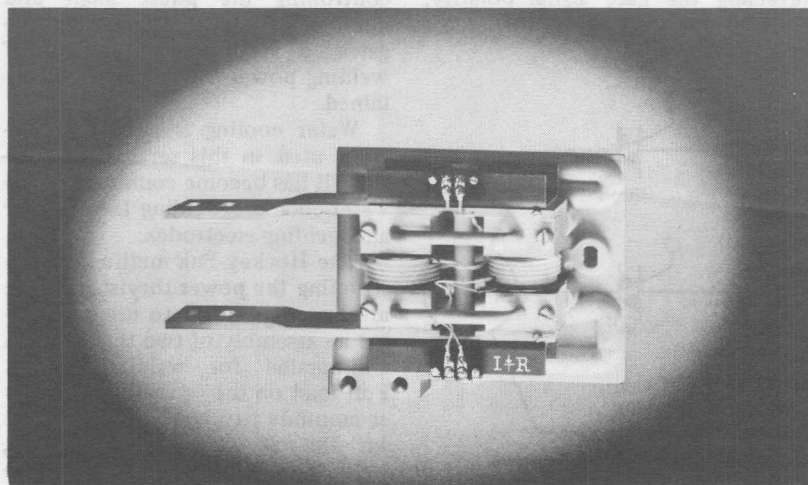


Figure 4-50. Water-Cooled, Hockey-Puk SCR AC Switch On a Coolant Manifold

is provided next to each Hockey-Puk pole piece. These remove the heat and, together with the copper tubing which joins each pair of pads, provide the means to bring the electric current into and out of the assembly. Terminations for electrical cables and inlet and outlet water connections are provided. A sufficient length of non-conductive tubing to permit connecting the water paths of the two pairs of water-cooled pads in series is incorporated in the manifold which also serves as a base for the assembly.

When two 470 ampere average Hockey-Puk SCRs are used in this assembly, the highest ac line current that may be handled continuously is 1200A RMS. This is under conditions of 40°C maximum inlet water temperature at a flow of at least 1.2 gallons per minute.

Welding Service Rating Curves

In welding service current is required in trains of pulses as shown in Fig. 4-51. Frequently these trains have a longer off than on period. (Duty cycle less than 50 percent.) Advantage can be taken of this operating condition to control greater amounts of current than 1200A during the on periods. Current carrying capability during such operation is enhanced by the water cooling system, which tends

to rapidly carry heat away from the semi-conductor devices. Thus, the junction cools down rapidly between power applications.

Fig. 4-52 gives the rating of a variety of AC switches shown in Fig. 4-50 for various duty cycles. The conditions covered by the curves in Fig. 4-52 embrace those usually found in welding service. Two variables are considered; percent duty cycle and number of conducting cycles in each pulse train. For example, consider an application requiring a train of 36 cycles for each weld at a rate of ten welds in one minute. This represents a duty cycle of 10 percent (36 cycles of current flow out of every 360 cycles of the 60 Hz power source). Reading from Fig. 4-50 (by interpolating between 20 and 50 conducting cycles), it is seen that the solid state contractor can handle up to 2000 amperes RMS, under these conditions.

The curves shown in Figure 4-52 demonstrate that with the variety of Hockey-Puk thyristors available, a wide range of welding applications is suitable for thyristor control.

Protection Considerations

It was mentioned that current surges due to transformer saturation should be avoided. Some of the steps which can be taken in

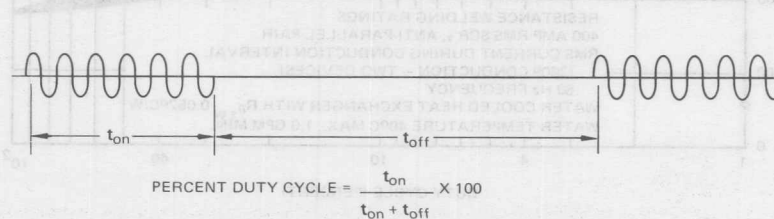


Figure 4-51. Typical Welding Current Waveform

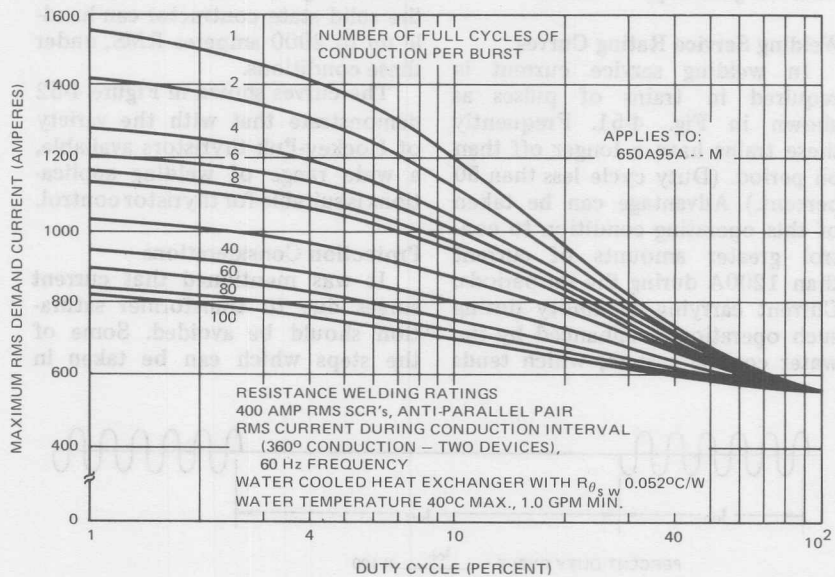
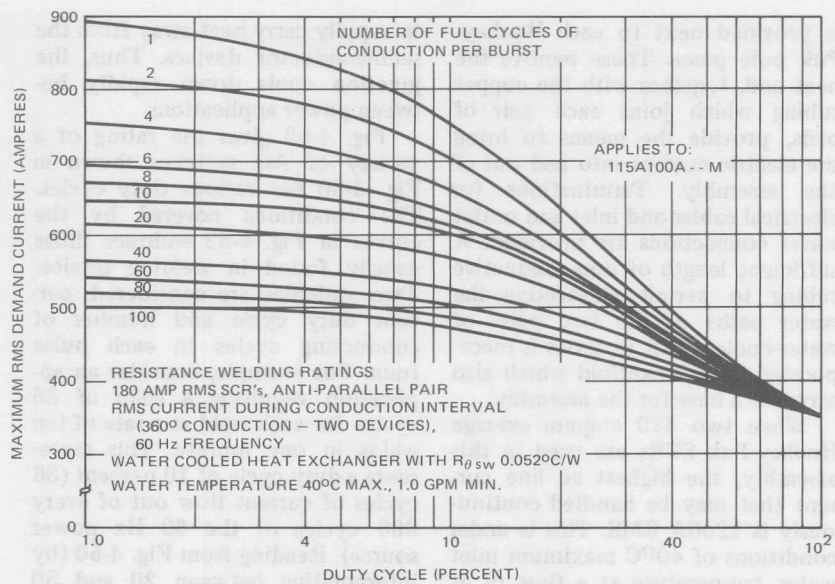


Figure 4-25(a) and (b). Welder Service Rating Curves for Thyristor AC Switch (Type 470A95A)

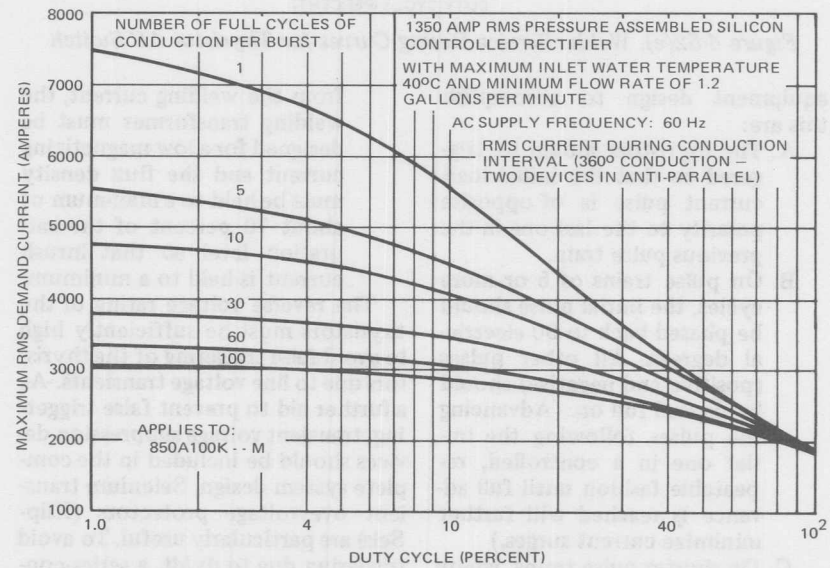
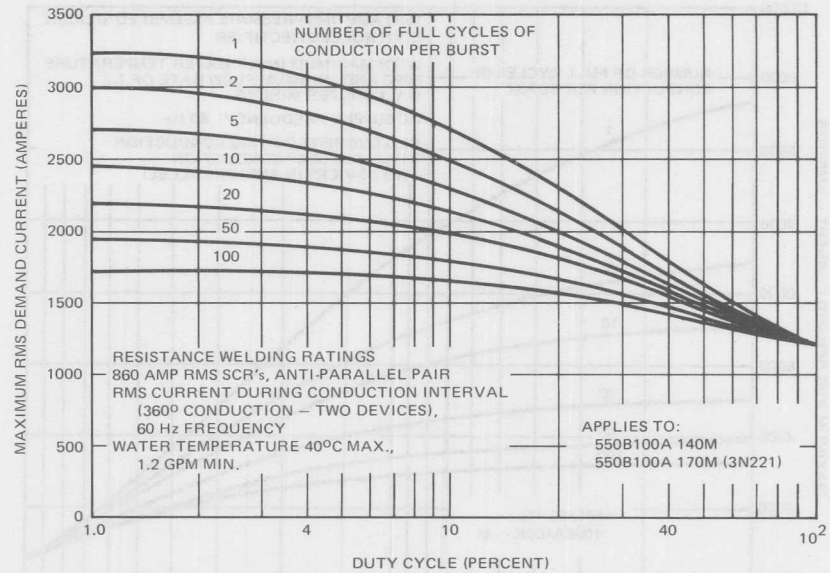


Figure 4-52(c) and (d). Welder Service Rating Curves for Thyristor AC Switch (Type 470A95A)

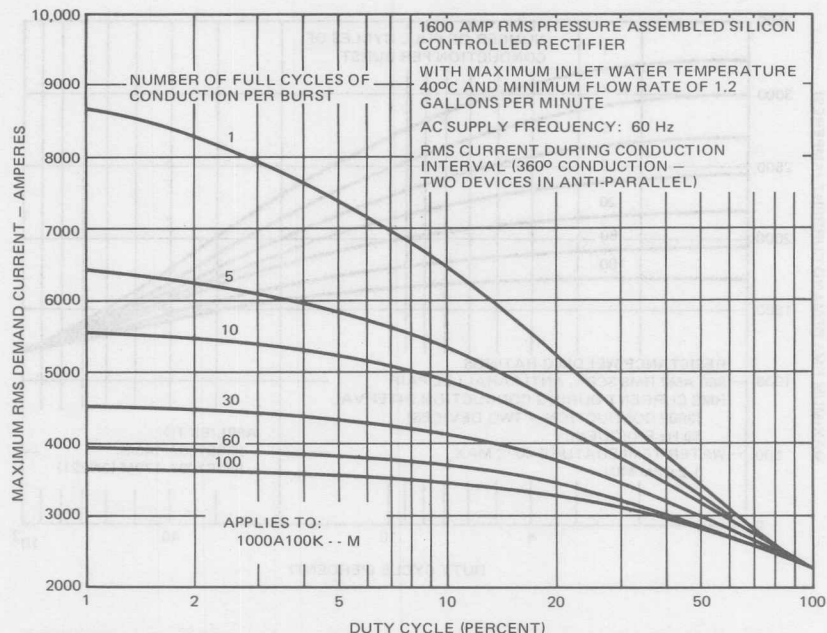


Figure 4-52(e). Welder Service Rating Curves for Thyristor AC Switch

equipment design to accomplish this are:

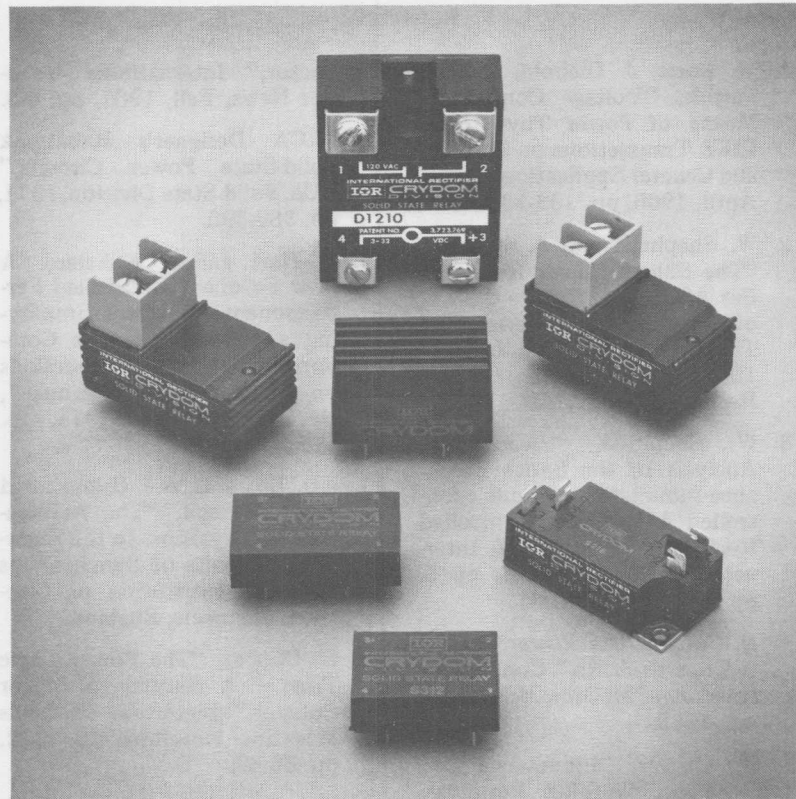
- A. The thyristors should be triggered so that the initial load current pulse is of opposite polarity to the last one in the previous pulse train.
- B. On pulse trains of 5 or more cycles, the initial pulse should be phased back to 90 electrical degrees. All other pulses (positive and negative) should be phased full on. (Advancing the pulses following the initial one in a controlled, repeatable fashion until full advance is reached will further minimize current surges.)
- C. On shorter pulse trains, where all current pulses must be phased full on in order to obtain the desired amount of heat

from the welding current, the welding transformer must be designed for a low magnetizing current and the flux density must be held to a maximum of about 70 percent of the saturation level so that inrush current is held to a minimum.

The reverse voltage rating of the thyristors must be sufficiently high to avoid false triggering of the thyristors due to line voltage transients. As a further aid to prevent false triggering, transient voltage suppression devices should be included in the complete system design. Selenium transient overvoltage protectors (Klip-Sels) are particularly useful. To avoid triggering due to dv/dt , a series-connected capacitor-resistor, "snubber network" should be connected across anti-parallel thyristors.

References

1. W. Borst, J. Diebold, and W. Parrish, "Voltage Control by Means of Power Thyristors," IEEE Transactions on Industry and General Applications, Mar. / April, 1966, pp. 102-124.
2. W. Shepherd and J. Stanway, "The Silicon Controlled Rectifier AC Switch for the Control of Single Phase Series and Transformer Coupled Loads," 1964 IEEE International Conv. Record, pt. 4, pp. 155-163.
3. W. Shepherd, "Steady-State Analysis of the Series Resistance-Inductance Circuit Controlled by Silicon Controlled Rectifier," 1965 IEEE International Conv. Record, pt. 8, pp. 183-193.
4. D. Cooper, "AC Power Control — Triac or SCRs," Control Engineering, McGraw-Hill, August, 1968.
5. W. Grover, "Inductance Calculations, Working Formulas, and Tables," Dover, New York, 1946.
6. J.G. Truxal, "Control Engineer's Handbook," McGraw-Hill, New York, 1958, Section 7.
7. R.G. Hoft and G.N. Vogelgesang, "Solid-State Power Control Program, Progress Report #2," University of Missouri, Columbia, August 21, 1973, Part C.
8. D. Cooper, "AC & DC Power Control with a Single Semiconductor," International Rectifier News, Fall, 1967, pp. 4-8.
9. "RCA Designer's Handbook Solid-State Power Circuits," RCA, Solid-State Division, 1971, pp. 380-390.
10. P. Hart and J. Kakalec, "A New Feedback Controlled Ferroresonant Regulator Employing a Unique Magnetic Component," IEEE Transactions on Magnetics, Vol. mag-7, No. 3, September 1971, pp. 571-574.
11. J.D. Edwards, A.J. Gilbert, and E.H. Harrison, "The Application of Thyristors to the Excitation Circuits of Synchronous Motors," Institution of Electrical Engineers, England.
12. D. Cooper, "The Power Logic Triac — A Natural for Motor Control," Electronic Products Magazine, November 20, 1972, pp. 66-69.
13. "Applications of Power Integrated Circuits (PACE/pak)," International Rectifier Application Note AN-401, March, 1973.
14. J.D. Reed, University of Georgia, Athens, Georgia.
15. Nairn & D.A. Thalimer, Consolidated Electrodynamics Corp.
16. D.W. Borst, "Hockey-Puk Assemblies in Resistance Welding Service," International Rectifier News, 1970, issue 1, pp. 5-7.



Crydom was the originator of the solid state relay. The product line now includes photo-isolated SSR's ranging from 2 Amp, PC-board mounted units to 40 Amp SSR's. Several series employ integral heat radiators to increase ratings. Newer products include input/output switches (extreme left, and right of picture) which are used to interface microprocessors and micro-computers with the higher power equipment they control.

Solid State Relays and Contactors

Widespread use of Solid State Relays (SSR's) in standard packages has developed in recent years. Although SSR's are still usually more expensive than the equivalent electro-mechanical relays, they have several distinct operational characteristics which give them overall advantage in difficult applications.

SSR's are used in applications which require long life, smooth (RFI free) switching characteristics, ability to be driven directly from low level integrated circuit signals, or extreme shock and vibration resistance. These applications include both the replacement of electro-mechanical relays and discrete component solid state switch-

ing circuits for control of motors, heaters, lamps, transformers, contactors, valves, and solenoids.

Solid-State Relays

A solid-state relay, in terms of its function in a circuit, is identical to an electro-mechanical relay. It has input or control terminals and output or power terminals with a certain electrical isolation between input and output circuits. However, this is a superficial similarity. The differences in the principles of operation are shown in Figure 5-1. In the electro-mechanical relay, the coupling is achieved magnetically and in the very common type of

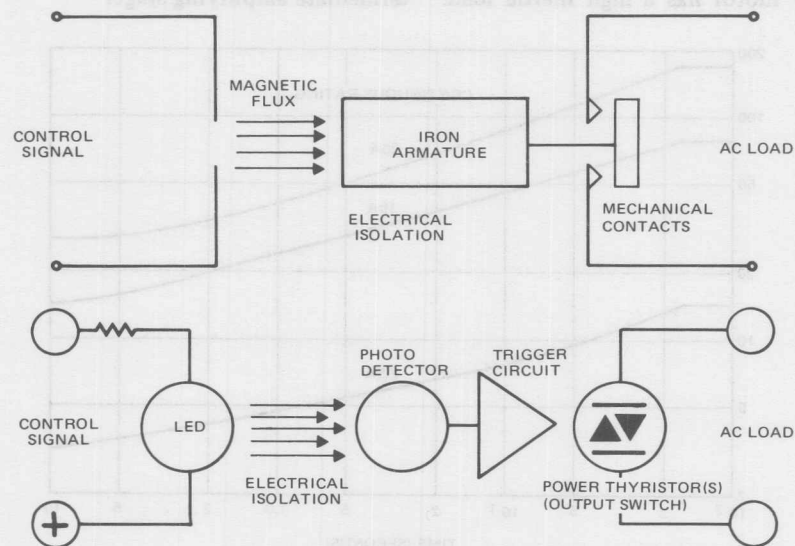


Figure 5-1. Solid-State Relay Block Diagram

solid-state relay shown, the coupling is achieved by light.

In general, solid-state relays provide only single-pole operation, because most of the cost is in the output pole, not in the control, and little economy can be achieved by using extra power semiconductors with a single control. The solid-state relays described here have normally open contacts, but because of the easy interface with low level controls, a normally closed function can easily be achieved in the control circuits by the use of a single inverting stage in the input circuit.

Figure 5-2 shows the RMS surge current rating of three series of solid-state relays, as a function of time. This is very important when the relays are being used to control high inrush current loads such as motors, particularly when the motor has a high inertia load.

The solid-state relay is more complex than the electro-mechanical relay, but this complexity allows the solid-state relay to perform more sophisticated functions, particularly with respect to a well-defined closing angle, delay time, and total closed time. However, before discussing the specific uses of a solid-state relay, the characteristics of this type of device will be reviewed. Typical input and output characteristics are shown in Figures 5-3 and 5-4. Table V-I lists the specifications for three typical series of solid-state relays.

Solid-state relays are available in a wide combination of output currents and voltages with ac or dc control. The types with dc control can be selected for low (3 to 32V dc) or high (80 to 140V dc) voltage operation. The low voltage types can be operated directly from low level logic circuits without an intermediate amplifying stage.

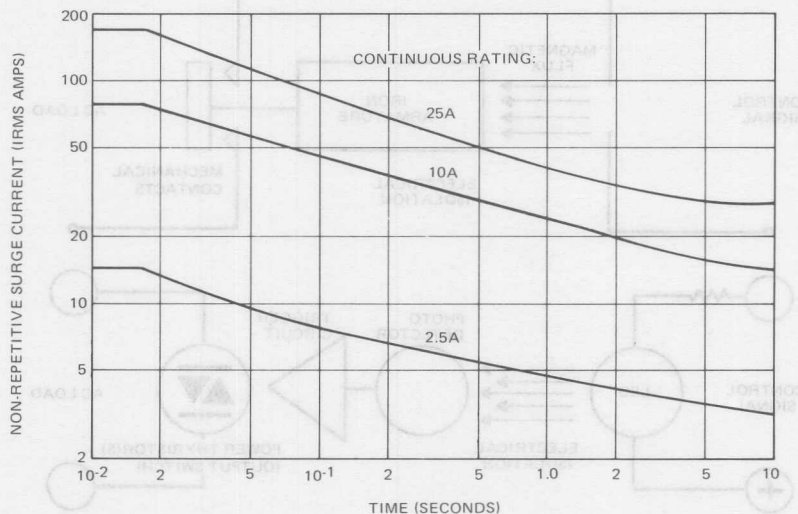


Figure 5-2. Solid-State Relay Surge Current Ratings

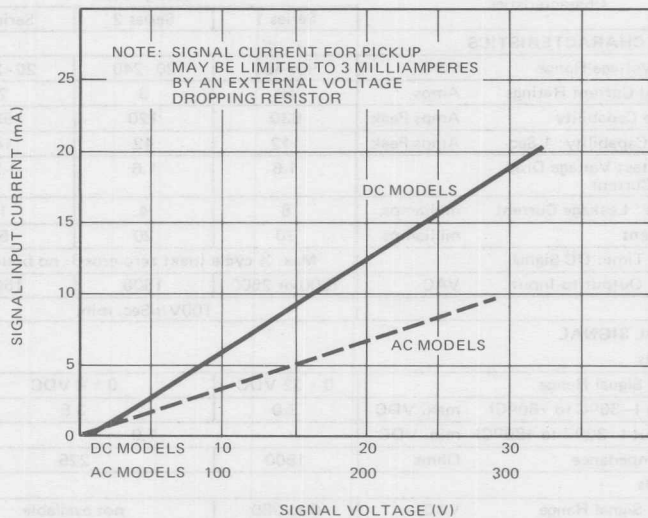


Figure 5-3. Solid-State Relay Signal Current Drain

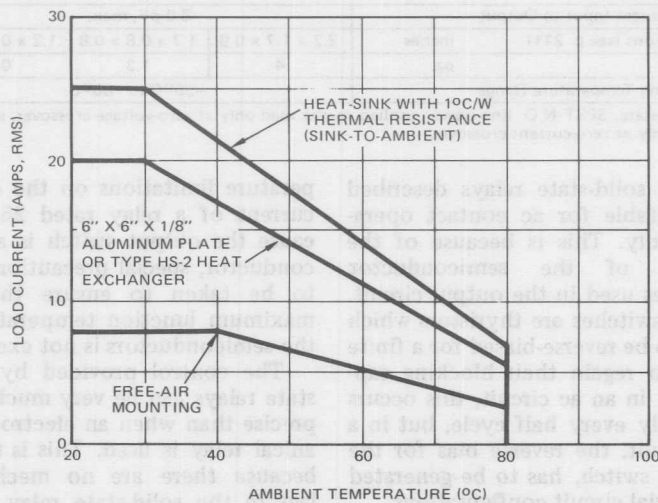


Figure 5-4. Solid-State Relay Load Current Rating

Table V-I. Typical Solid-State Relay Electrical Specifications

Characteristics		Package Style		
		Series 1	Series 2	Series 3
OUTPUT CHARACTERISTICS				
AC Line Voltage Range	VAC	90-480	20-240	20-240
Max. Load Current Ratings	Amps	40	8	2
One-Cycle Capability	Amps Peak	630	120	55
Overload Capability: 1 Sec	Amps Peak	112	42	14
Max. Contact Voltage Drop @ Rated Current		1.6	1.6	1.2
"Off-state" Leakage Current	milliamps	8	4	1
Min. Current	milliamps	20	20	5
Response Time: DC Signal		Max. ½ cycle (next zero cross): no bounce		
Isolation: Output-to-Input	VAC	1500 or 2500	1500	1500
dv/dt		100V/μSec. min.		
CONTROL SIGNAL				
DC Models				
Control Signal Range		0 ± 32 VDC	0 ± 8 VDC	
Pick-Up (-30°C to +80°C)	max. VDC	3.0	3.5	
Drop-Out (-30°C to +80°C)	min. VDC		1.0	
Input Impedance	Ohms	1500	225	
AC Models				
Control Signal Range	VAC	0 to 280	not available	
Pick-Up (-30°C to +80°C)			not available	
Drop-Out (-30°C to +80°C)			not available	
Input Impedance			not available	
Isolation: Input-to-Output; Input-to-Base		Opto-isolated, 1500 VAC, 10 ¹⁰ ohms DC		
Capacitance: Input-to-Output		8.0 pF, max.		
Dimensions (see p. 211)	inches	2.2 x 1.7 x 0.9	1.7 x 0.8 x 0.8	1.2 x 0.8 x 0.4
Weight	oz.	4	1.3	0.6
Operating Temperature Range		-30°C to +80°C		

All solid-state, SPST-N.O. line power applied to the load only at zero-voltage crossover, and interrupted only at zero-current crossover.

The solid-state relays described are suitable for ac contact operation only. This is because of the nature of the semiconductor switches used in the output circuit. These switches are thyristors which have to be reverse-biased for a finite time to regain their blocking capability; in an ac circuit, this occurs naturally every half cycle, but in a dc circuit, the reverse bias for the output switch, has to be generated by special circuit configurations.

Figures 5-3 and 5-4 describe the input characteristics and the tem-

perature limitations on the output current of a relay rated 25A. Because the output switch is a semiconductor, special precautions have to be taken to ensure that the maximum junction temperature of the semiconductors is not exceeded.

The control provided by solid-state relays can be very much more precise than when an electro-mechanical relay is used. This is mainly because there are no mechanical lags in the solid-state relay. Also, because there is no movement of contacts, there is absolutely no con-

tact bounce. In addition, because semiconductor switches react instantaneously to a trigger signal, there need be no significant delay between the application of a trigger signal and the operation of the output switch.

On the other hand, by the proper configuration of internal control circuits, the application of a trigger signal to the output switch, can be delayed relative to the application of an input signal. In the solid-state relays discussed here, this feature has been included so there is a variable delay between the input and trigger signals which ensures that the output switch always closes at voltage zero (zero voltage switching control). This is a very important and desirable feature. Not only is the closing angle totally defined, but by switching on at voltage zero, radio frequency interference (RFI) is eliminated. This is a very important consideration

when the relay is associated with equipment such as computers and on-line process controls, which can be very sensitive to electrical noise. This feature is shown in Figure 5-5.

The control signal is applied, but the load voltage does not appear until the next voltage crossover. When the control signal is removed, the output switch remains closed until the next current zero. For this example, the load is resistive, and the switch opens at voltage zero because the current and voltage are in phase. However, if the load is reactive, then the switch (because the semiconductors remain on until the current reverses) remains closed until current zero, as shown in Figure 5-6, once again eliminating RFI caused by rapidly changing currents. Examination of the contact voltage waveshapes shows that when the contacts open, with reactive load, the contact voltage steps up to the supply voltage very

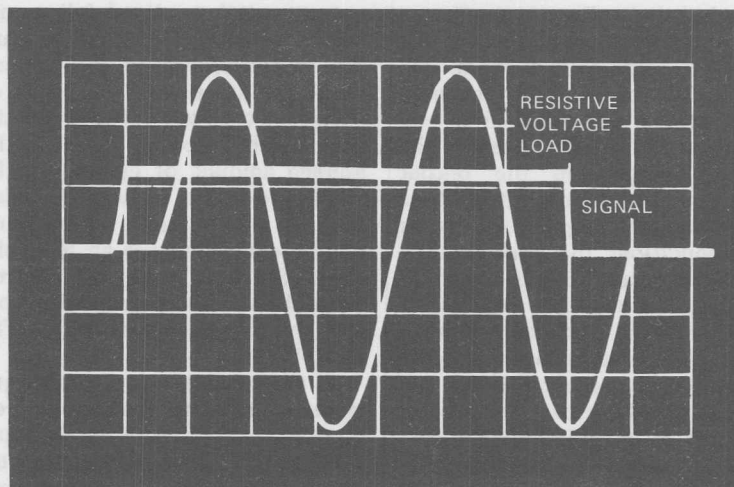


Figure 5-5. Solid-State Relay DC Control Signal and Resulting AC Load Voltage

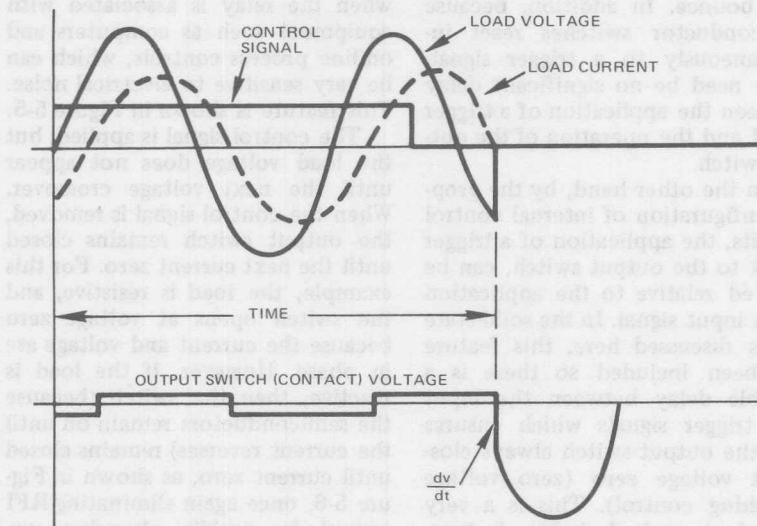


Figure 5-6. Waveforms for Solid-State Relay Controlling Inductive Load

rapidly, imposing a high dv/dt on the output switch.

The output switch is rated for a critical dv/dt of $100V/\mu\text{sec}$ minimum to rated voltage at maximum junction temperature. For the majority of applications with the power factors normally encountered, the voltage switched to will be less than half the peak of the supply voltage and the output switch will be operating at less than rated junction temperature. Under these conditions, the dv/dt capability will generally be in excess of $400V/\mu\text{sec}$. In very few applications will the circuit dv/dt be this high. In those applications where dv/dt is a problem, a snubber network can be connected across the output terminals as shown in Figure 5-7.

One application for the solid-state relay is energy control for heating loads such as furnaces and commercial heating. To control this

type of load, which has a fairly high thermal inertia, the pulse burst modulation technique is used. In pulse burst modulation when the output switch is closed full supply voltage is applied to the load until the switch is opened. By varying either the duration of the 'burst' of energy or the time between 'bursts' or a combination of the two, the average amount of energy can be controlled. The solid-state relay with its zero voltage switching and precise control makes an ideal element for this type of control. Typical pulse burst modulation control waveshapes are shown in Figure 5-8.

A very simple control technique would be to allow the load temperature to fluctuate between an upper and lower limit by closing the output switch at the lower limit and opening it at the upper limit. The absolute limits would be a function

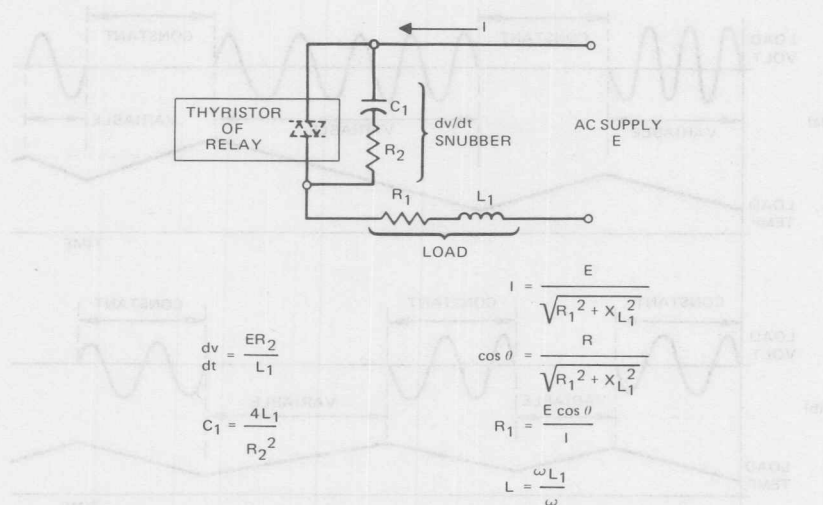


Figure 5-7. Solid-State Relay with Snubber Network

of the heating and cooling rates of the load relative to the possible nearly half cycle delay and extension of the conduction period (if the load is inductive) due to the zero voltage turn on and zero current turn off of the solid-state relay.

Fig. 5-9a shows 3 package styles which form an SSR product line suitable for a vast range of applications.

Solid-state relays are being widely used in traffic signal controls, where the reliability of the relays and the zero voltage turn-on makes them ideal. A typical three-relay module for traffic signal control is shown in Figure 5-9b, with the relays mounted directly to a heat dissipator. This is possible because the relay base plate is isolated from the internal control and power circuits.

These relays are very well suited to computer, machine control, and process applications. The compatibility of the relays with logic circuit outputs allows them to be driven

directly from low level circuits and the absence of RFI generation eliminates the possibility of cross-talk between power and control circuits. Along with the precise control of output voltage duration, sophisticated timing and sequencing of power switching can be achieved, taking the guesswork out of the operation of many machine tool and process control systems.

Because they do not create arcs, solid-state relays are especially well suited for application in explosive environments and hospital operating rooms, although in this particular case, it must be recognized that in the off condition, the solid-state relay can have leakage currents of 4 or 5 mA (depending on the voltage classification). If necessary, relays can be selected to have significantly lower leakage currents, particularly if the junction temperature is limited to some level below its rated value.

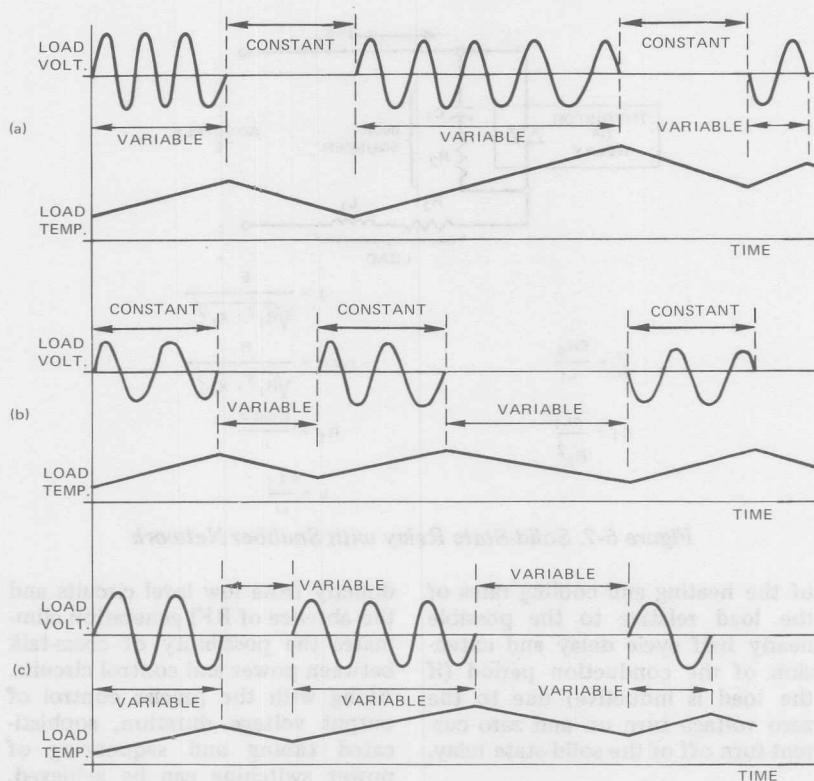


Figure 5-8. Waveforms for Pulse Burst Modulation Operation of Solid-State Relays

Solid-State Contactors

Basically a solid-state contactor can be described as an extension of a solid-state relay. However, due to the higher ratings provided, contactors are constructed with discrete components rather than junctions contained in a single package. In one type the main power switching components are electrically isolated from the frame of the contactor. The insulating material used to accomplish this has excellent thermal properties ensuring good heat transfer to the main heat dissi-

pators. The construction of a typical solid-state contactor is shown in Figure 5-10.

The solid-state contactor has excellent surge capability for those types of loads which require high starting currents (e.g., induction motor starters which draw high currents until the machine is running close to its normal speed). The rated surge current/time characteristics of a range of solid-state contactors are shown in Figure 5-11.

Like the solid-state relay, the solid-state contactor is designed to

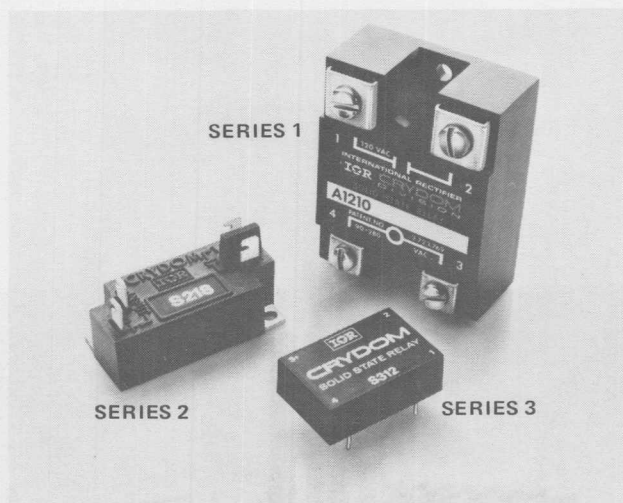


Figure 5-9a. Solid-State Relay Product Line

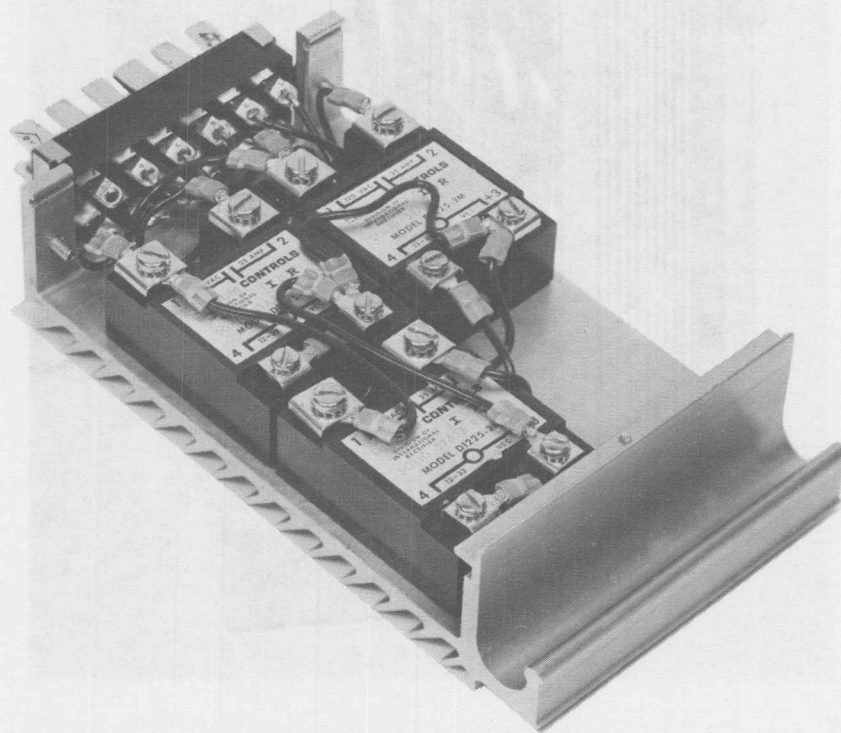


Figure 5-9b. Typical Three Solid-State Relay Assembly

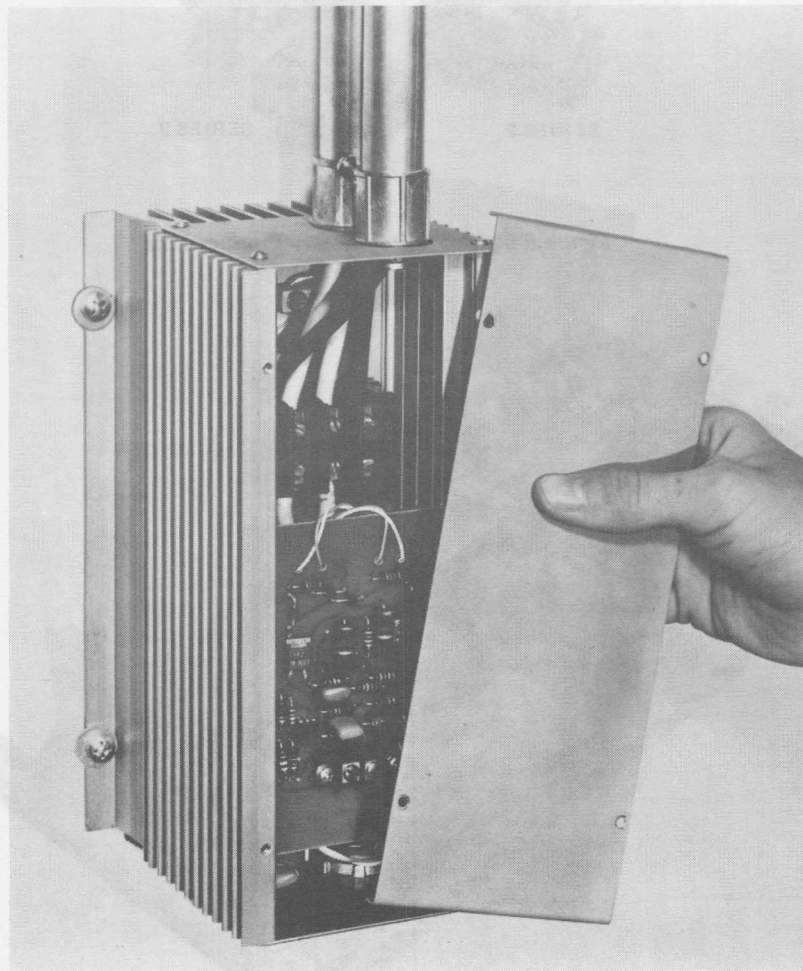


Figure 5-10. Typical Solid-State Contactor

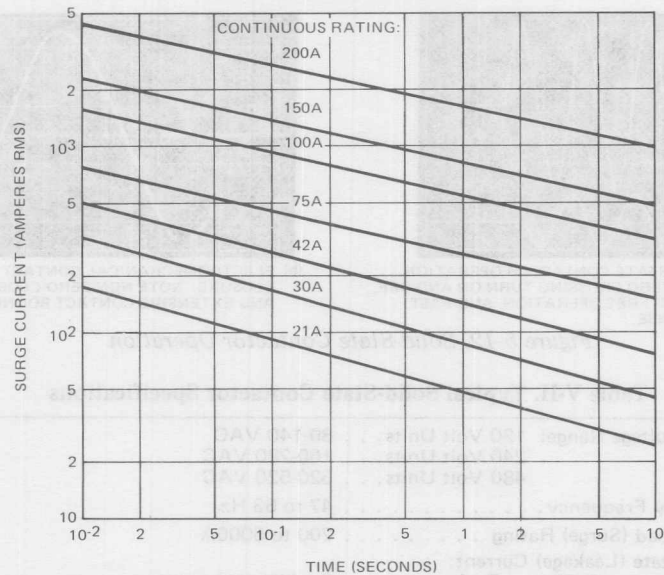


Figure 5-11. Solid-State Contactor Surge Current Ratings

close at a voltage crossover and, because of the output thyristors, to open at a current zero. An excellent example of the difference in operation between solid-state and electro-mechanical contactors is shown by the oscillograms in Figure 5-12.

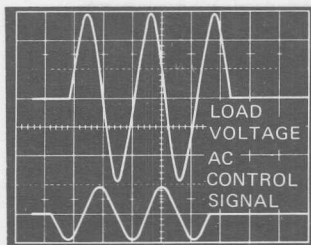
The general specifications for a range of solid-state contactors are shown in Table V-II. Three typical applications of solid-state contactors are shown in Figures 5-13, 5-14 and 5-15.

There are many other applications for solid-state contactors, but most of these are extensions of the three described in Figures 5-13, 5-14 and 5-15. In many systems, where the source impedance is sufficient to limit the available fault current to within the capabilities of the contactor, it can be used with no back-up protection (fuses or

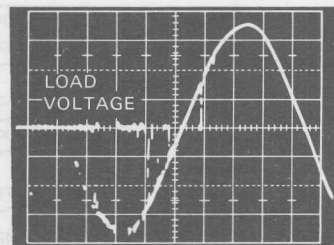
mechanical contacts). In this instance, a detection system is provided which consists of a di/dt detector and an absolute current amplitude detector. This combination allows the system to anticipate a fault without reacting to sudden load changes (as a di/dt detector alone might). The control signal to the contactor is removed only when the detector recognizes that both the di/dt and the current amplitude have exceeded allowable limits. When this condition is reached, the control signal is removed and at the next current zero, the switch opens allowing just the initial half cycle of fault current to flow. A typical sequence is shown in Figure 5-16.

Solid-State Switches

One application for solid-state switches is in a system for vehicle



(a) SOLID STATE CONTACTOR OPERATION. NOTE ZERO CROSSING TURN ON AND OFF, BOUNCE FREE OPERATION, AND FAST RESPONSE.

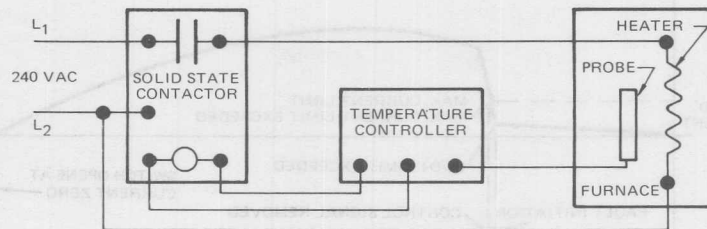


(b) ELECTROMECHANICAL CONTACTOR CLOSURE. NOTE NON-ZERO CLOSURE AND EXTENSIVE CONTACT BOUNCE.

Figure 5-12. Solid-State Contactor Operation

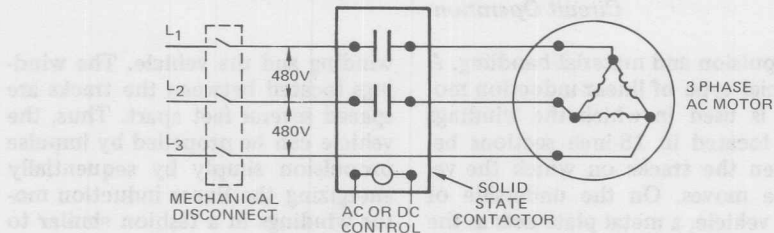
Table V-II. Typical Solid-State Contactor Specifications

AC Voltage Range:	120 Volt Units . . .	80-140 VAC
	240 Volt Units . . .	160-280 VAC
	480 Volt Units . . .	320-520 VAC
Supply Frequency		47 to 63 Hz
Overload (Surge) Rating		200 to 5000A
Off-State (Leakage) Current:		
21 through 75 amp Ratings		5 milliamperes max.
Over 75 amp Ratings		20 milliamperes max.
Minimum Applied Load:		
21 through 75 amp Ratings		200 milliamperes
Over 75 amp Ratings		500 milliamperes
Output Switch (Contact) Voltage Drop		1.6 Volts max. at rated current
Response Time:		
DC Control		0 to 1/2 cycle max. (next zero crossing)
AC Control		0 to 1-1/2 cycle max.
Isolation:		
Terminals to case		5000 VAC min.
Signal to output		1500 VAC min.
Critical dv/dt		100 volts per microsecond min.
Control Signal		The standard 21 and 30 ampere units operate from DC control only. For AC control of the 21 and 30 ampere models, add the letter "A" to the part no. All higher current models have a universal input for AC or DC control.
AC Control: Signal Range		90 to 280 VAC (use 50,000 ohms, 3W dropping resistor for 480V operation)
Pick-up		90 VAC max.
Drop-out		10 VAC min.
Input Impedance		Single pole: 30,000 ohms Two pole: 15,000 ohms
DC Control: Signal Range		3 to 32 VDC, reverse polarity protection
Pick-up		3.0 VDC max.
Drop-out		1.0 VDC min.
Input Impedance		21A and 30A ratings: Single pole: 1,500 ohms; Two-pole: 750 ohms Over 30A ratings: Single pole: 680 ohms; Two-pole: 340 ohms
Operating Ambient Temp. Range		-30°C to 75°C



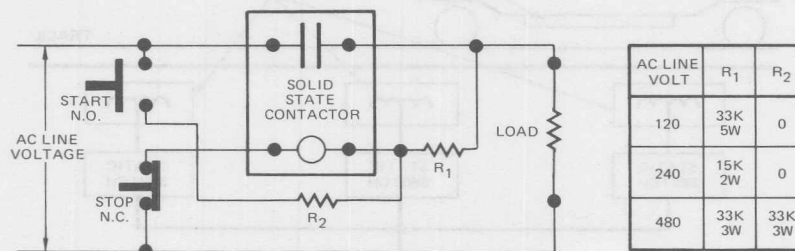
THE CONTACTOR PROVIDES ELECTRICALLY AND ACOUSTICALLY NOISE-FREE OPERATION IN AN ON-OFF OR TIME PROPORTIONING MANNER WITH A TIME BASE AS SHORT AS ONE SECOND.

Figure 5-13. Solid-State Contactor Temperature Control System



THE TWO-POLE CONTACTOR SERVES AS A LONG LIFE MOTOR STARTER CONTROLLED FROM ANY LOW POWER, REMOTE SOURCE. A MECHANICAL DISCONNECT IS NORMALLY USED IN ALL THREE LINES AS A SAFETY DISCONNECT. TWO LEG SWITCHING IN THE CONTACTOR WORKS WELL FOR ALL DELTA AND FLOATING NEUTRAL WYE LOADS. THREE SINGLE POLES MUST BE USED FOR A GROUNDED NEUTRAL WYE LOAD.

Figure 5-14. Solid-State Contactor Three-Phase Motor Starter Circuit



THE ADDITION OF ONE OR TWO EXTERNAL RESISTORS ALLOWS CONTACTORS TO BE CONTROLLED BY MOMENTARY PUSH-BUTTONS.

Figure 5-15. Solid-State Contactor with Pushbutton Control

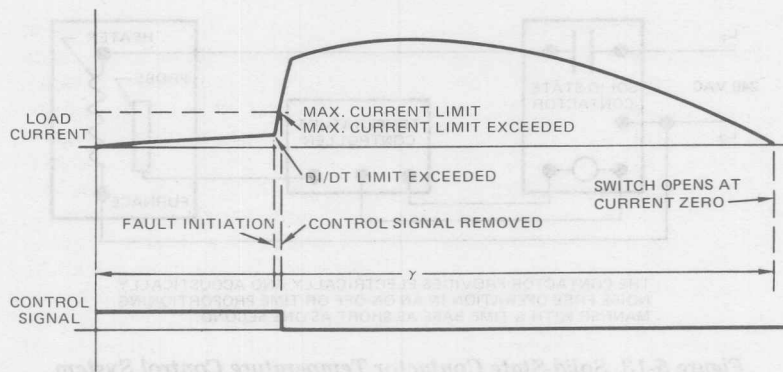


Figure 5-16. Waveforms of Solid-State Contactor Fault Detection Circuit Operation

propulsion and material handling. A special type of linear induction motor is used in which the windings are located in 18-inch sections between the tracks on which the vehicle moves. On the underside of the vehicle, a metal plate acts as the member in which current can be induced to provide linear induction motor action between an excited

winding and the vehicle. The windings located between the tracks are spaced several feet apart. Thus, the vehicle can be propelled by impulse propulsion simply by sequentially energizing the linear induction motor windings in a fashion similar to that shown in Figure 5-17.

The advantage of this type of switching is the minimizing of

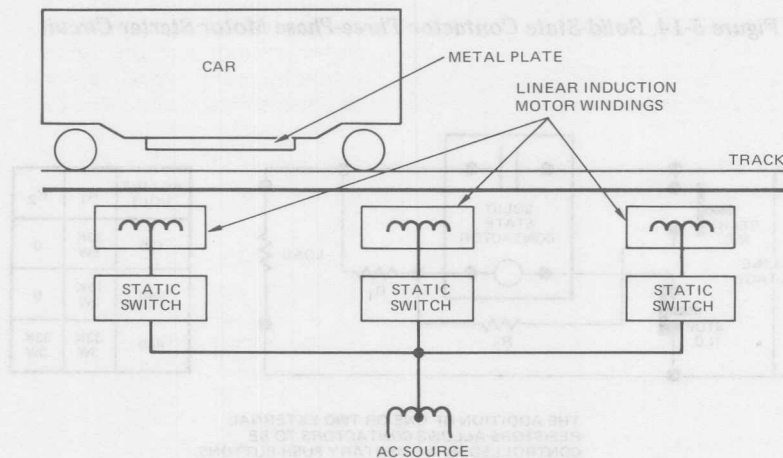


Figure 5-17. Linear Induction Motor System

power demand from the ac source, since the majority of the induction motors need not be energized simultaneously. This tends to average out the power demand and reduce the overall installation cost and operating cost of the system. The requirements for the static switch needed to energize the system are interesting.

A. It must be capable of being operated remotely from a centralized computer which senses the position and the destination of the cars and dispatches them by energizing the proper motors.

B. The signaling must be isolated from the power circuit to prevent transients.

C. The switch must be low cost because of the considerable number of switches required in a large system. For instance, when using the system in a large airport baggage handling unit, up to 50,000 switches might be required.

D. The switch must employ a zero voltage triggering system to minimize radio interference and the filtering cost of the system.

E. The switch must be small to enable it to be located remotely with the motor winding.

F. It must be completely sealed, since it will not be packaged in an electronic rack or equipment cabinet.

G. This switch must be able to operate in a high ambient temperature, because it will be located thermally close to the motor winding.

A typical single-phase switch, which meets the above requirements, is shown in Figure 5-18. The simple solid-state power switch consists of a triac, TRIAC₁, a gate drive source, R₁, C₁, and an on-off switch, S₁. With S₁ closed, the triac gate is shorted to main terminal 1, and the solid-state switch is off. With S₁ open, power line voltage is applied through R₁ and C₁ to the triac gate, triggering TRIAC₁ into conduction. S₁ may be any bi-directional switch, mechanical or solid-state, with an on-state voltage drop less than the minimum gate-voltage-to-trigger of TRIAC₁.

An additional requirement of the single-phase switch is that it must have its power components electrically isolated from the heat sink. For instance, it might be possible to package the linear induction motor winding and the switch in a common heavy metal case to be imbedded between the rails, the

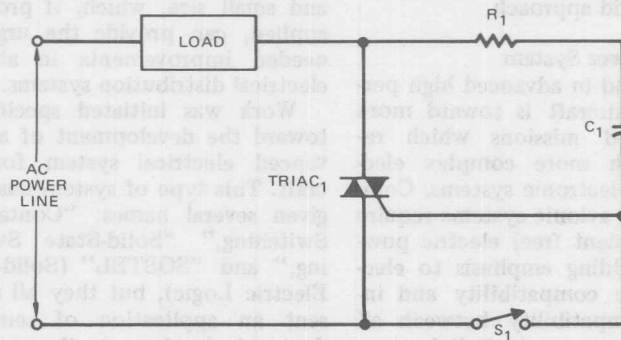


Figure 5-18. Solid-State AC Switch Circuit

case acting as the heat sink for the electronic switch. It would not be allowable from a safety standpoint to have the case electrically hot.

These requirements suggest the applicability of the PACE/pak hybrid circuit techniques for this type of application. Certainly alumina, beryllium oxide, and boron nitride substrates are economically feasible in large quantities for hybrid circuits of a given type. Also passivation techniques for SCR junctions make their applicability to such hybrid circuit constructions quite feasible. Since these substrates are readily available with moly-manganese metallization for connection purposes, and since the moly-manganese provides the proper thermal co-efficient of expansion to interface with the silicon of the semiconductor, thermal fatigue difficulties can easily be overcome. The requirements for this type of application are not far from the requirements for electric heating control. The applicability of triacs in this type of control is also evident. Other applications of the same techniques take advantage of the common circuitry capability and the large volume, low cost of such a hybrid approach.

Aircraft Power System

The trend in advanced high performance aircraft is toward more sophisticated missions which require much more complex electrical and electronic systems. Complex digital avionic systems require clean (transient free) electric power, thus adding emphasis to electromagnetic compatibility and interface compatibility between all signal systems and digital computers.

The approach must simplify circuitry, combine functions, separate signal and power switching requirements, and eliminate any unreliable features of switching control and protective devices used in circuit techniques. The application of semiconductor technology to aircraft electrical distribution systems, however, has been slow to catch on. Some of this can be attributed to the application approach that has generally been made. A number of solid-state devices have been placed on the market with the idea of providing a solid-state device to replace an electro-mechanical device on a part-for-part basis. This approach has some obvious drawbacks since in most aircraft electric control circuits the switching logic is performed at the power level. Because of the voltage drop and power dissipation characteristics of semiconductor devices, this approach results in a very inefficient system and makes it impossible to meet the voltage drop requirements of Military Specification MIL-W-5088 for Aircraft Electric Distribution Systems. However, semiconductor devices have advantages such as high reliability, long life, and small size, which, if properly applied, can provide the urgently needed improvements in aircraft electrical distribution systems.

Work was initiated specifically toward the development of an advanced electrical system for aircraft. This type of system has been given several names: "Contactless Switching," "Solid-State Switching," and "SOSTEL" (Solid-State Electric Logic), but they all represent an application of semiconductor technology to the management and control of aircraft electric

systems. Figure 5-19 is a block diagram of an aircraft electrical system. Figure 5-20 is representative of conventional aircraft electrical circuits and is presented to highlight the fact that logic functions are performed at the power level. In the advanced system, emphasis is placed on separating power switching from signal switching and on switching power through a minimum number of semiconductor devices (see Figure 5-21). This not only minimizes the voltage drop between the source of power and utilization equipment, but also provides efficient power control, since power dissipation is held to a minimum. Lower power dissipation means that less heat sinking is required, and therefore size and weight are reduced.

A concept is required which separates power and signal switching

and utilizes solid-state devices to perform all of the switching and circuit protection functions normally performed by electro-mechanical switches, relays, and circuit breakers. The system is composed of three basic building blocks: 1) signal sources, 2) control logic, including bus monitoring and built-in testing, and 3) power controllers. Signal sources are transducers which provide a digital output. They are used to sense controlling functions such as temperature, pressure, mechanical motion, etc. Their output signals are fed into the control logic unit where they are correlated in a prescribed manner to provide signals to control the power controllers. The logic switching is performed by standard integrated circuit NAND/NOR gates to provide maximum reliability with minimum space and weight. The fan-out cap-

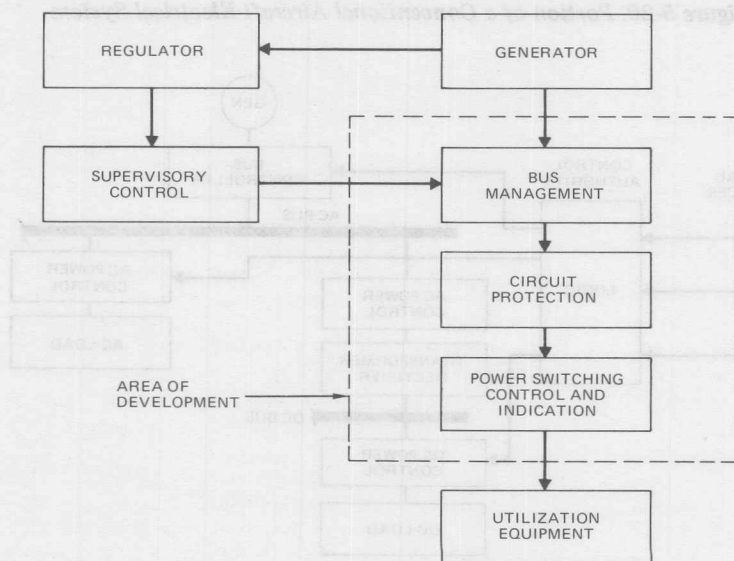


Figure 5-19. Aircraft Electrical System Block Diagram

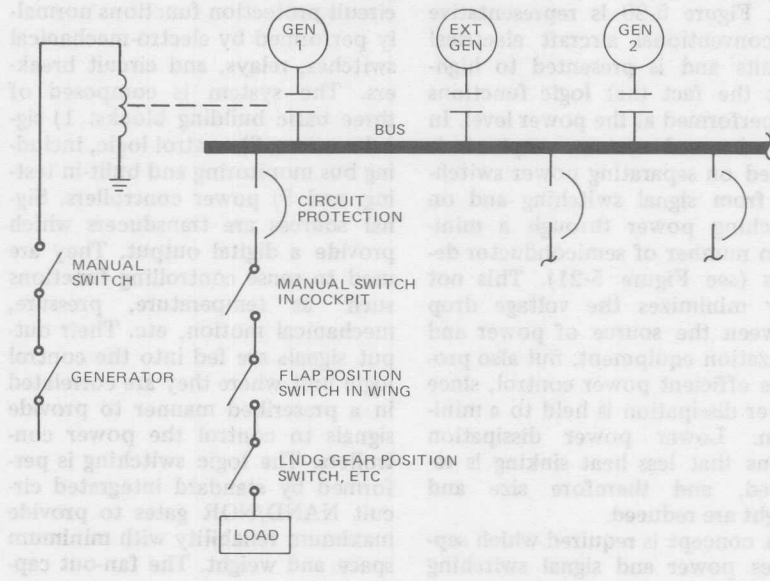


Figure 5-20. Portion of a Conventional Aircraft Electrical System

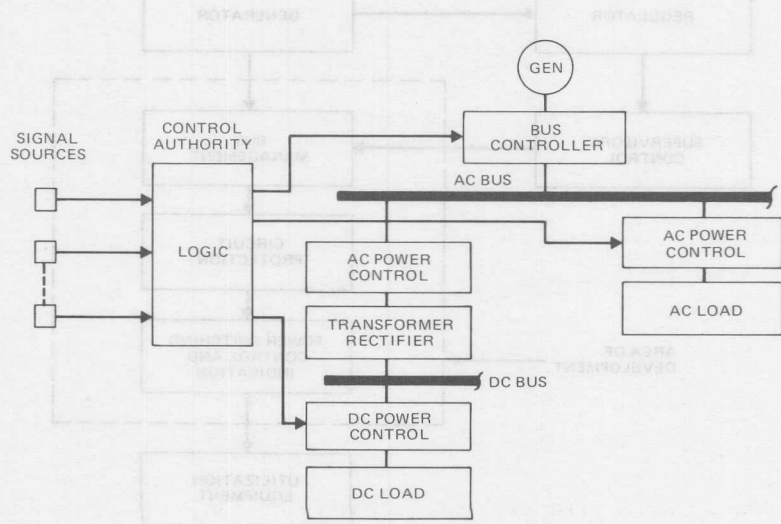


Figure 5-21. Portion of a Solid-State Aircraft Electrical System

ability provided by multiple-phase switches and relays is provided by the integrated circuit and is performed at the signal level instead of at the power level. This reduces considerably the number and size of wires needed to gather intelligence from the various controlling functions.

The flow of power from the power sources to the bus and from the bus to the loads is controlled by power controllers. Separation of power switching and signal switching provides high system efficiency and makes it possible to meet the voltage drop requirements of the MIL Specs. The flexibility of the system permits the incorporation of an automatic bus monitoring system which permits optimum loading on the source supplying power. By assigning priorities to various loads in the airplane, it becomes possible to operate the emergency source at its optimum capacity. A technique is included to perform preflight go-no-go tests on the low level portions of the system which are made up of signal sources and data handling equipment. Bus controllers and power controllers are not checked by the built-in test circuitry and are actually inhibited while the built-in test feature is in operation. However, they are checked as part of subsystem functional checks. A digital indicator indicates a faulty signal source during the short and open test and a faulty input buffer card during the input buffer test. A typical solid-state electrical system of this type is shown in Figure 5-21.

An alternative and even more advanced solid-state electrical system is shown in Figure 5-22. In this system, the control signal sensing

and the power switching approach remain essentially unchanged. The change occurs in the method of handling and processing the control data which is by remote multiplexing the input terminals located in close vicinity to large groups of signal sources, thus allowing a significant reduction in the length of wires required to gather control information. These terminals monitor each signal source and upon command from the Master Control Unit (MCU), code and serially transmit the status of each signal source through the multiplex transmission data line. The MCU decodes the data from the input terminals, solves the switching equations, and according to instructions permanently stored within its memory, transmits coded output data over the multiplex data transmission line to the properly addressed output terminal. The MCU contains a non-destructable read only memory in which are stored all control instructions and the switching equation associated with the control of power to each individual load. Changes in control logic can be accomplished by reprogramming the MCU with a paper or magnetic tape, thereby eliminating the need to make any wiring changes in the aircraft. Upon malfunctioning of the operating unit, the standby MCU is automatically switched into operation. The two MCUs are interchangeable. The power controllers for these systems must be capable of switching electric power in a system exhibiting characteristics described below and controlled by a 5V, 10 mA dc signal supplied by the control logic unit.

The load switching power controllers are used between the bus

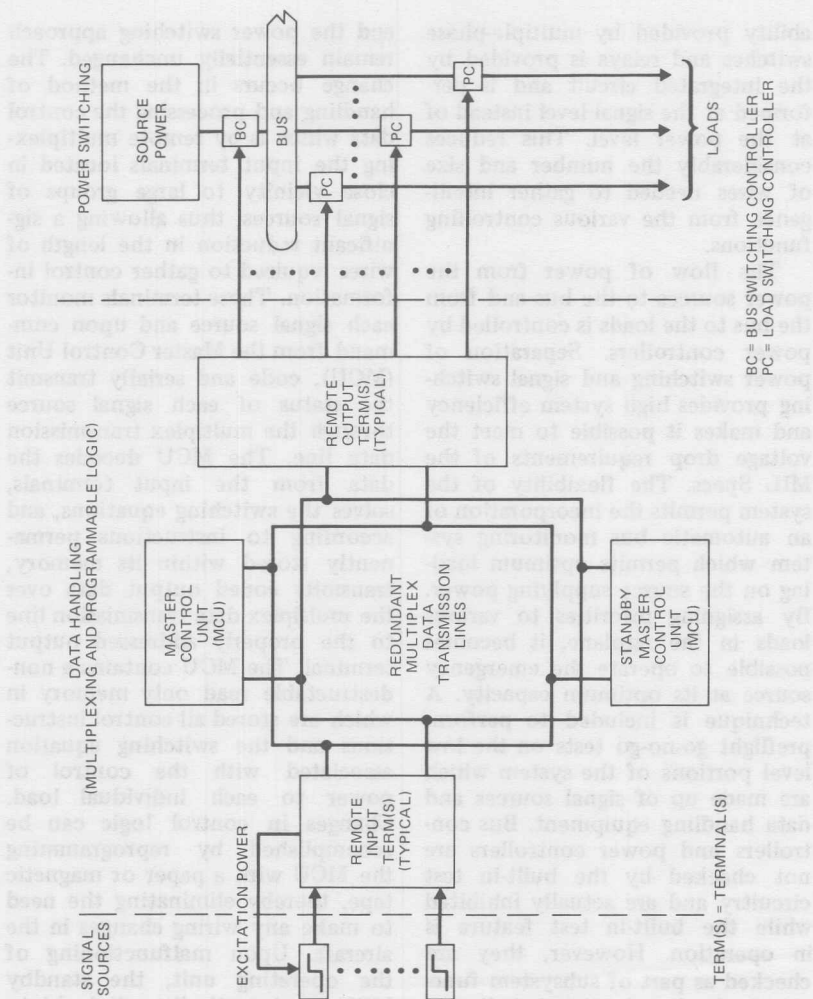


Figure 5-22. Portion of an Advanced Solid-State Aircraft Electrical System

and the utilization equipment to provide control current limiting and circuit protection, while the bus switching controllers are used only to connect power sources to the bus. The requirements for these power controllers are isolation be-

tween the control and the power circuits, operating efficiency of 95% minimum, voltage drop of 0.5V max dc (1.5V max ac), leakage current of less than 10^{-4} amperes at maximum temperature, operating ambient temperature

range of -54°C to 85°C , and no external power supply to be required. The ac voltage is allowed to swing between 60V RMS and 180V RMS. The ac units must also control loads exhibiting a power factor between 0 lagging and 0.4 leading. In the dc power switches, the power switching element is an N-P-N silicon power transistor. The ac power controller contains a thyristor power switch, power supply, driver, circuitry for zero-cross-over turn-on, current sensing, and circuit protection. This is shown in block diagram form in Figure 5-23 and in more detail in Figure 5-24. The anti-parallel connected SCRs could also be a triac with the proper electrical characteristics.

The bus switching controller performs the function of a relay only. The ac bus switching power controller block diagram is identical to

that shown in Figure 5-24, except it does not contain the current limiting and the circuit protection circuitry, but it does include a lockout feature that is not included in the ac load controller.

In either case, the overload requirement for the ac controllers can be high compared to the steady-state rating. As an example, in a typical 20 KVA system, fault currents of 350 amperes per phase have been recorded. Therefore, very large semiconductor chips must be used in the units. The required ac power controller trip characteristics are shown in Figure 5-25.

Although packaging efficiency is an important factor in determining the size of the power controller module, the power dissipated within the module is of utmost importance. To prevent the junction temperature of the devices within the

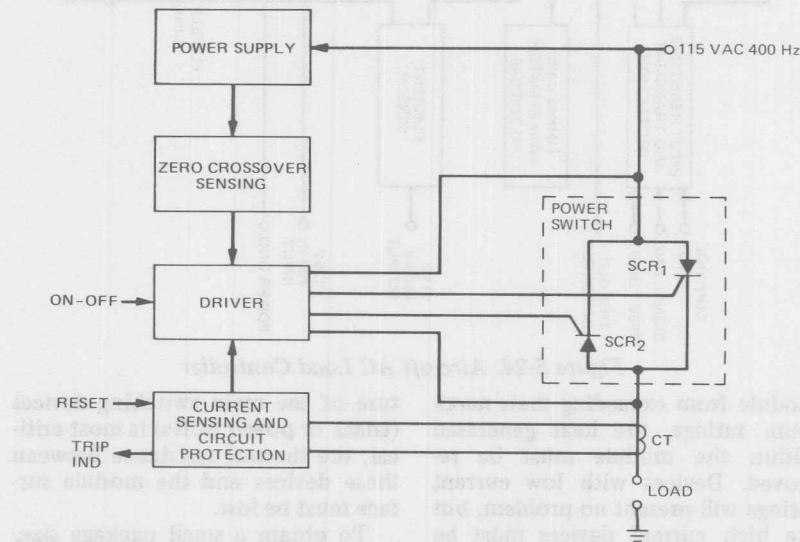


Figure 5-23. Aircraft AC Power Switch and Control Circuit

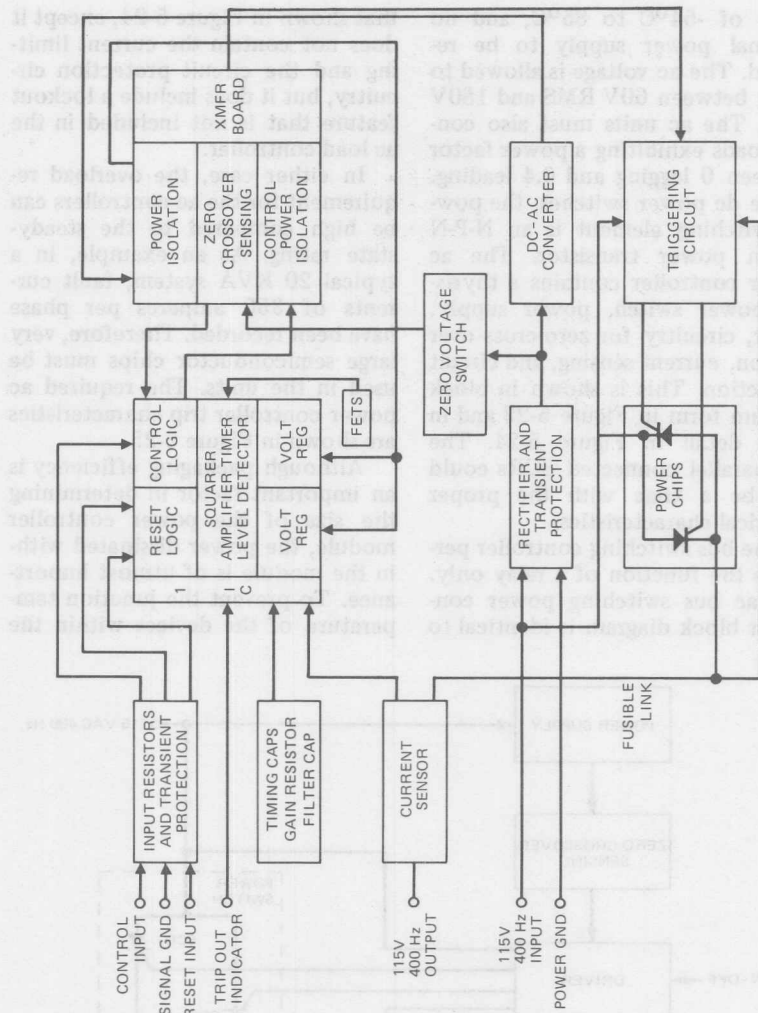


Figure 5-24. Aircraft AC Load Controller

module from exceeding their maximum ratings, the heat generated within the module must be removed. Devices with low current ratings will present no problem, but the high current devices must be attached to an external heat dissipator. Since the junction tempera-

ture of the main switching devices (triacs or power SCRs) is most critical, the thermal resistance between these devices and the module surface must be low.

To obtain a small package size, integrated circuits, transistor, SCR and triac wafers, and thin film tech-

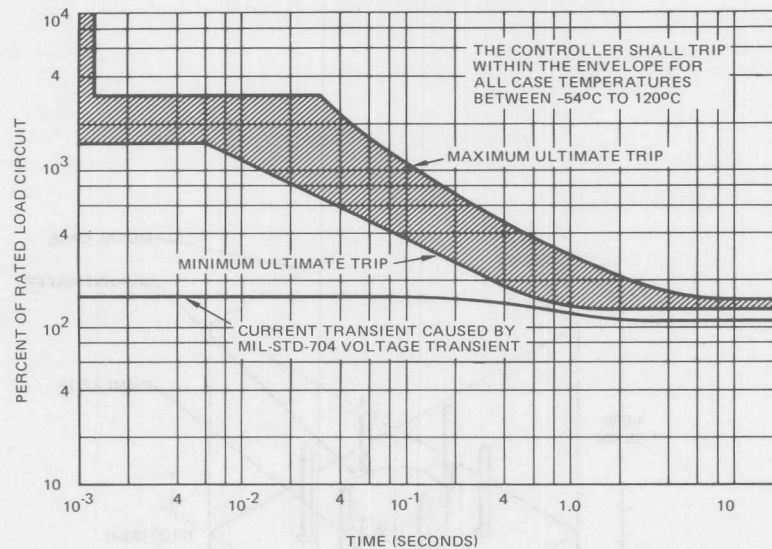


Figure 5-25. Aircraft AC Power Controller Characteristics

niques must be used, as shown in Figure 5-26. In this package, the logic elements are located toward the top of the package, and the large, vertical internal connection posts are available to support and connect the logic to the power functions. A more detailed outline of the internal assemblies is shown in Figure 5-27. A function requiring both isolation and current sensing for the desired trip characteristics can be rather space-limiting. The overall outside dimension of this cube (Figure 5-28) is approximately one inch (25.4 mm) square. The thermal considerations and the effect of the temperatures on the power chip can be limiting in the design. Table V-III lists required thermal resistances for various current ratings of controllers. In examining this data, it should be apparent that one of the assumptions for determining the required thermal

resistances is a maximum allowable junction temperature approaching 170°C. But many logic-triacs are advertised at a maximum allowable junction temperature of 125°C. However, by modifying the process and geometry of the junction assembly devices have been made which actually will operate quite reliably and satisfactorily at 175°C junction temperature with an allowable reapplied dv/dt up to 100 volts/ μs . This not only permits the small size of the package as seen in the previous figures, but also permits operation under the extreme power factor conditions described. An extreme case for this design in terms of power rating might require a power device even larger than the 200 ampere power logic triac chip size — in this case, two power SCRs are used.

Since reliability was so heavily stressed in the earlier discussion of

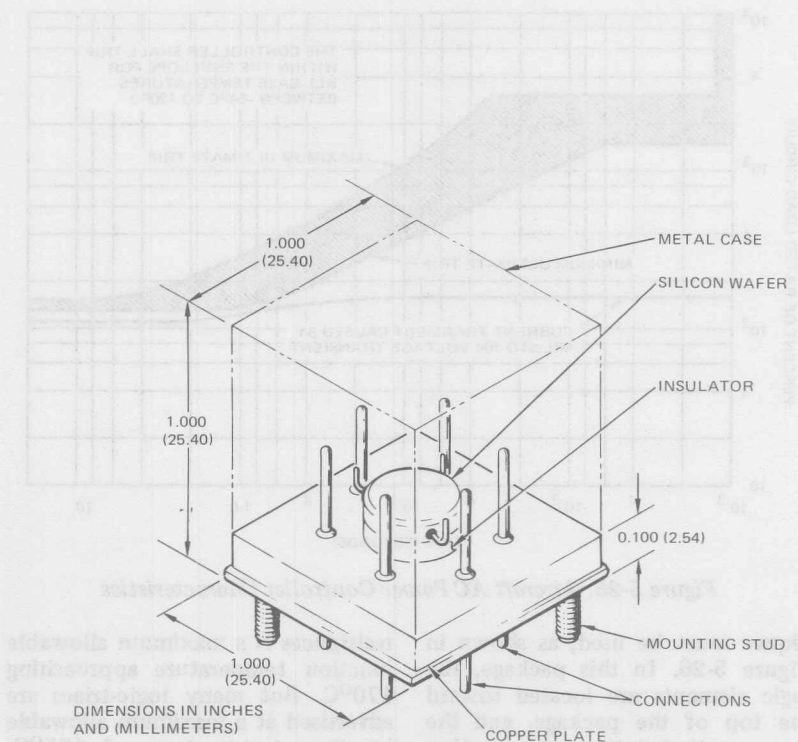


Figure 5-26. Aircraft AC Power Controller Module

the system requirements, it is certainly of interest to show a reliability study of a typical ac controller with estimated failure rates (see Table V-IV). The inordinately high failure rate of the SCRs shown is estimated on a very conservative basis because no transient suppression was involved or associated with the circuitry, and also because of the many unknowns associated with a very new type of packaging. However, even with these conservative figures, it can be seen that the failure rate of the devices and of the overall system is very low.

The marriage of power devices and low level solid-state logic elements in hybrid circuitry for reliable, small, efficient power control opens a new era in the field of power control development. Where circuits can be designed for high volume usage or common circuits can be used for several smaller volume applications, the cost of present systems can be greatly reduced. Where low level logic hybrid circuitry is marginally economically feasible, high power level hybrid circuitry is, without question, economically feasible.

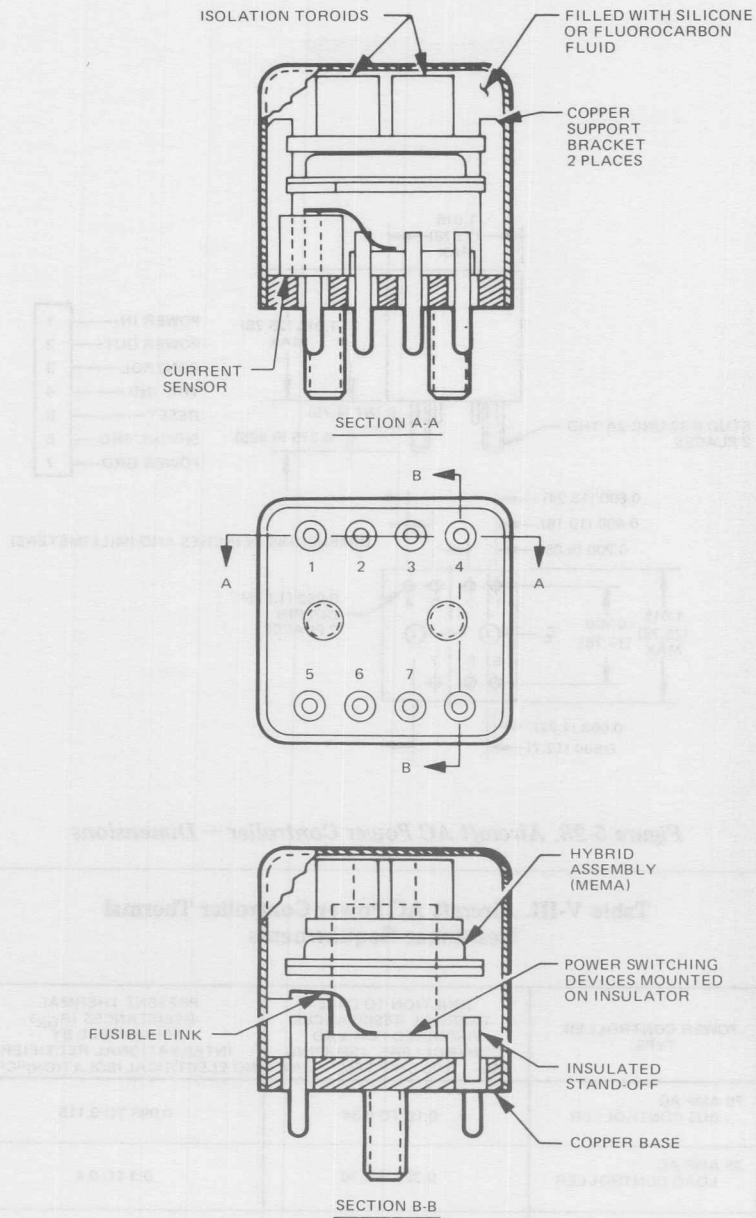


Figure 5-27. Aircraft AC Power Controller — Internal Details

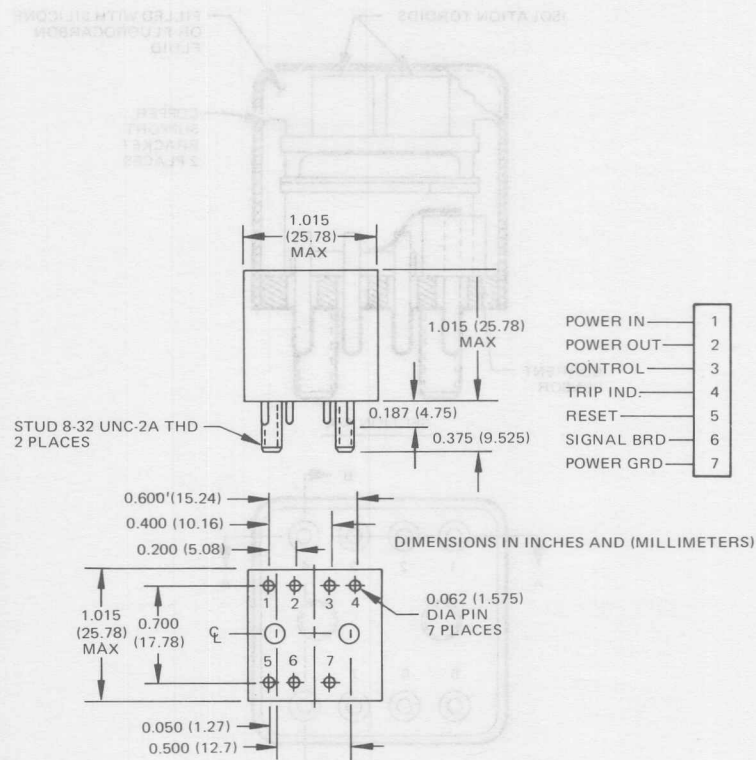


Figure 5-28. Aircraft AC Power Controller — Dimensions

Table V-III. Aircraft AC Power Controller Thermal Resistance Requirements

POWER CONTROLLER TYPE	JUNCTION TO CASE THERMAL RESISTANCES REQUIRED FOR VAD CONTROLLERS, ASSUMING 150 - 170°C CHIP TEMP. °C/W	PRESENT THERMAL RESISTANCES (R _{Gjc}) ACHIEVABLE BY INTERNATIONAL RECTIFIER (NO ELECTRICAL ISOLATION) °C/W
75 AMP AC BUS CONTROLLER	0.16 TO 0.34	0.095 TO 0.115
35 AMP AC LOAD CONTROLLER	0.32 TO 0.70	0.3 TO 0.4
10 AMP AC LOAD CONTROLLER	1.5 TO 2.8	1.0 TO 1.5

Table V-IV. Aircraft AC Power Controller Failure Rate Data

QTY	COMPONENT	FAILURE RATE SOURCE	FAILURE RATE
3	INTEGRATED CIRCUITS @ 0.020	1	0.060
14	RESISTOR, FILM @ 0.007	2	0.098
2	CAPACITOR, CERAMIC @ 0.038	2	0.076
2	SCR @ 0.102	2	0.204
2	DIODES, GP @ 0.005	2	0.010
6	TRANSISTOR @ 0.010	2	0.060
2	SCR @ 1.3	6	2.600
4	TRANSFORMERS @ 0.2	2	0.800
1	RECTIFIER (BRIDGE) @ 0.020	2	0.020
100	LEAD BOND @ 0.00007	3	0.007
	SUBSTRATE, FRAME & COVER	4	0.0035
24	EXTERNAL LEADS @ 0.00005	5	0.0012
TOTAL FAILURE RATE			4.886

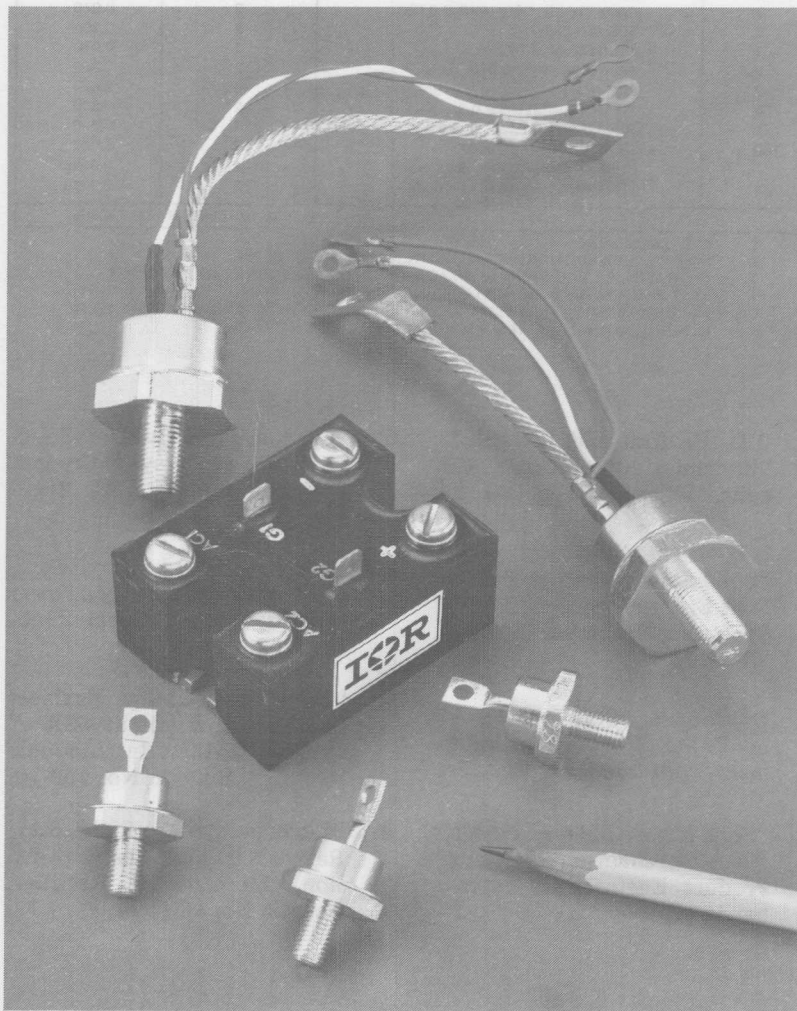
1. SEE DISCUSSION
2. NORMALIZED MIL-HDBK-217A MINUTEMAN LEVEL, FAILURE RATES.
3. ULTRASONIC LEAD BOND ESTIMATE BASED ON TELEDYNE INDUSTRY DATA
4. BEST ENGINEERING ESTIMATE.
5. WELDED TERMINATION ESTIMATE BASED ON TELEDYNE AND INDUSTRY DATA
6. INTERNATIONAL RECTIFIER NORMALIZED LIFE TEST DATA.

References

1. B.D. Bedford and R.G. Hoft, "Principles of Inverter Circuits," Wiley, 1964, p. 364.
2. L.D. Dickey and C.M. Jones, "Solid-State Switching for Aircraft Electrical Systems," IEEE Spectrum, November 1970, pp. 73-79.
3. D. Cooper, "State of the Art in Power Conversion Equipment," International Rectifier.
4. "Solid-State Relays Nudging Electromechanical Relays," Product Engineering, September 1971.
5. "Crydom Photo-Isolated Solid-State Power Relays," Crydom Division, International Rectifier, 1971.
6. B. Bixby, "Solid-State Relays, Contactors and Packaged Power Circuits," International Rectifier, 1973.
7. "Facts Every Design Engineer Should Know About SSR's." Crydom Division, International Rectifier, Bulletin No. 400-70.
8. "Introduction to Solid State Relays," R. Fox, Crydom Division, International Rectifier, Bulletin No. 300-100.

Table V-IV. Aircraft AC Power Controller Failure Rate Data

FAILURE RATE	FAILURE RATE SOURCE	COMPONENT	REF
0.000	1	INTEGRATED CIRCUITS BRIDGE	2
0.000	2	RECTIFIER IN BRIDGE	3



International Rectifier PACE/pak (Passivated Assembled Circuit Elements) are packaged circuit functions which replace discrete devices. For example, the unit above (center) is a 42.5 Amp single phase hybrid bridge with free wheeling diode. It is used in place of a separate assembly requiring the three SCR's and three diodes shown, plus additional heat sinking.

DC Power Conversion

Probably the most common method of adjusting direct voltage by phase control is by using reverse blocking thyristors in a conventional rectifier circuit and delaying the start of current conduction through them. By this means, the direct voltage can be reduced from the value obtained without phase control to some other desired value. If the start of conduction is delayed sufficiently, the average output voltage will be reduced to zero.

The average voltage which will appear across the load for a given phase control angle depends upon the rectifier circuit and the type of load. Performance with a purely resistive and also with a highly inductive load can easily be analyzed, and in this way, insight is provided with respect to circuit performance when the load is partly resistive and partly inductive. It is also useful to consider performance when the load is capacitive, has a large counter-EMF, or is provided with a free-wheeling diode. Table VI-1 shows a number of typical circuits.

In some circuits, half of the thyristors are replaced by rectifier diodes which cannot be phase controlled. In these hybrid or half-controlled circuits, the voltage reduction for a given phase control angle, or angle of retard, will be different than in conventional circuits where all the rectifying devices are thyristors [1].

Biphase Circuits

As a simple example of a phase controlled rectifier circuit, consider

the single-phase, full-wave, center-tap circuit (more correctly known as the biphasic circuit) shown in Figure 6-1. Output direct voltage waveforms for several angles of delay, or phase retard, α , are shown in Figure 6-2 for the cases of resistive load and highly inductive load. Angle of phase retard α is measured from the point where current conduction through the rectifying device would naturally begin if a device with no forward blocking capability (i.e., a rectifier diode) were being used. A thyristor may be made to operate in the same manner as a diode by pulsing the gate so that the thyristor conducts the instant that anode voltage becomes positive with respect to the cathode (anode is forward biased). By delaying the triggering pulse, the thyristor blocks the more positive ac phase so that the preceding phase, although it is at a lower potential, remains connected to the load. When the delayed triggering pulse finally appears, load current is commutated (or switched) to the thyristor triggered, and this connects the load to the ac phase having the highest voltage at that instant. However, during the time when the triggering pulse is delayed by the angle α , the voltage across the load is less than if conduction had occurred at the earliest possible moment. In this way, the average voltage across the load is reduced by phase control.

When the load is purely resistive, load current will be a faithful reproduction of load voltage, as illus-

Table VI-I. Circuits for DC Loads

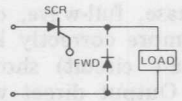
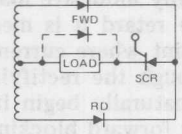
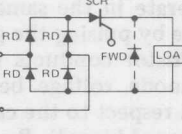
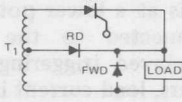
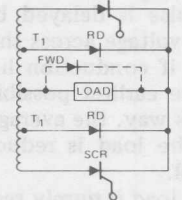
CIRCUIT	RELATIVE POWER OUTPUT	TYPE OF LOAD	CONTROL RANGE %	TYPICAL USES
	1	Resistive or Capacitive Inductive if free wheeling diode is used.	0 to 100	Heating Element (small) Battery Charging (small) Universal Motor Speed Control
	1.4	Resistive or Capacitive Inductive if free wheeling diode is used.	0 to 100	Heating Elements Lamp Intensity Control Adjustable & Regulated Power Supplies Motor Speed Controls
	1.4	Resistive or Capacitive Inductive if free wheeling diode is used.	0 to 100	Heating Elements Lamp Intensity Control Adjustable & Regulated Power Supplies Motor Speed Controls
	1	Resistive or Capacitive Inductive if free wheeling diode is used.	% T_1 to 100	Heating Element (small) Lamp Intensity Control (limited range) Battery Charging Universal Motor Speed Control
	2	All	% T_1 to 100	Heating Elements Lamp Intensity Control Adjustable & Regulated Power Supplies Motor Speed Controls Magnet Strength Control

Table VI-I. Circuits for DC Loads (Continued)

CIRCUIT	RELATIVE POWER OUTPUT	TYPE OF LOAD	CONTROL RANGE %	TYPICAL USES
	2	All	% T_1 to 100	Heating Elements Lamp Intensity Control Adjustable & Regulated Power Supplies Motor Speed Controls Magnet Strength Control
	2	All	% T_1 to 100	Heating Elements Lamp Intensity Control Adjustable & Regulated Power Supplies Motor Speed Controls Magnet Strength Control
	2.7	All	% T_1 to 100	Heating Elements Lamp Intensity Control Adjustable & Regulated Power Supplies Motor Speed Controls Magnet Strength Control
	2.7	All	% T_1 to 100	Heating Elements Lamp Intensity Control Adjustable & Regulated Power Supplies Motor Speed Controls Magnet Strength Control

NOTE: FWD = FREE WHEELING DIODE (BYPASS DIODE).

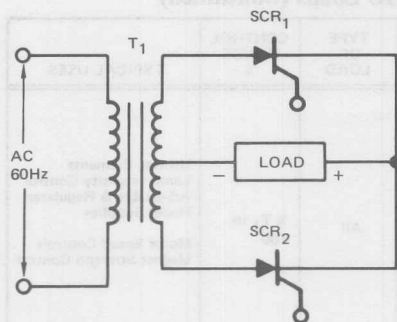


Figure 6-1. Biphas Circuit

trated in Figure 6-2(a). When phase control is introduced, the voltage across the load is seen to be discontinuous, and current flows through the thyristor for some interval less than the full 180 electrical degrees that it flows when there is no phase control. The time current flows under these conditions is

known as the conduction angle. Energy is stored in the inductance of the transformer each time current increases and is returned to the load as current decreases, so there is essentially no reactive voltage drop with a purely resistive load, as long as load current is discontinuous.

On the other hand, when the load is highly inductive, the load current remains continuous for all angles of phase retard. In this case, the duration of current flow through the rectifying devices remains the same as the phase retard angle is varied, but it is displaced with respect to the alternating supply voltage wave by the phase retard angle α as shown in Figure 6-2(b). With an inductive load, the angle of conduction is determined by the circuit used and not by the angle of phase retard, and is often referred to as the conduction period.

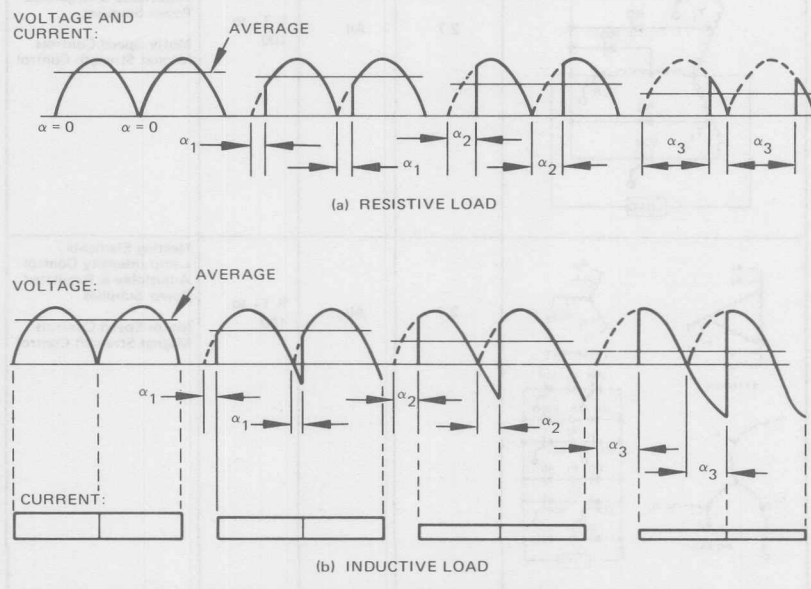


Figure 6-2. Biphas Circuit Waveforms

With an inductive load, the flow of current through each thyristor is essentially rectangular, assuming negligible ripple in the load current. Inductance in the ac supply (due to transformer leakage reactance, ac supply reactance, etc.) prevents the load current from commutating instantaneously from one thyristor to the next thyristor when the latter is triggered. For a brief interval, both thyristors conduct, one dropping current and the other picking it up. This interval is known as the angle of overlap, μ .

The currents through two thyristors which are under-going commutation are shown in Figure 6-3. It can be seen that the total current remains constant, due to the inductive nature of the load. The length of the angle of overlap μ depends upon the magnitude of the ac supply voltage, the load current, and the inductive reactance of the circuit which carries that commutating current (the circuit comprising the two diodes and the transformer windings which feed them).

The inductive reactance of this circuit is known as the commutating reactance.

During the angle of overlap, the direct output voltage of the rectifier is the average of the voltage applied to each thyristor by the transformer windings which feed them. This is a lower voltage than would be present if the angle of overlap were zero, and so the overlap phenomenon introduces a voltage drop E_x , which is a function of the angle of overlap. Hence, in a given rectifier unit, it is a function of load current, proportional to $I_C X_C$, the product of current commutated and commutating reactance.

In a thyristor feeding an inductive load and operated with phase retard, the angle of overlap will be present immediately following the angle of phase retard. As phase retard is increased, the angle of overlap μ will decrease, because there is a greater voltage difference between phases when commutation begins, and this speeds up the trans-

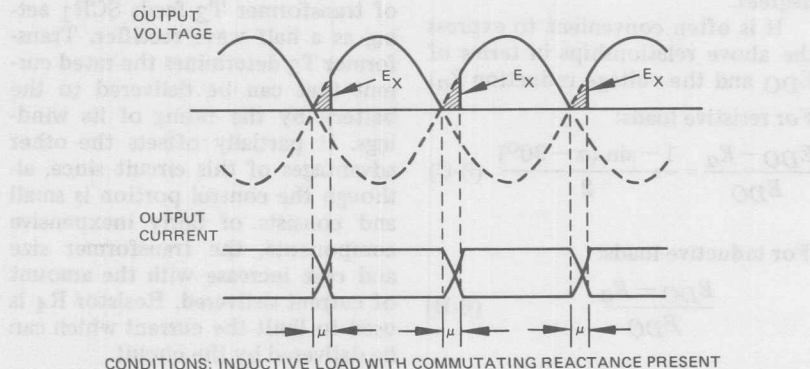


Figure 6-3. Biphasic Circuit Output Waveforms

fer of current from one phase to the next. However, the voltage drop due to overlap remains the same whether phase control is present or not.

In the inductive load case, although the alternating component of voltage appears across the load at large angles of phase retard, the average voltage can be reduced to zero. Zero average output voltage is obtained when α is 90 degrees. In order to obtain zero voltage across the load when it is resistive, the angle of phase retard must be 180 degrees.

Expressions that give the output voltage at no load for any angle of phase retard are:

For resistive loads:

$$E_D = E_{DO} \frac{1 - \sin(\alpha - 90^\circ)}{2} \quad (6-A)$$

For inductive loads:

$$E_D = E_{DO} \cos \alpha \quad (6-B)$$

In these expressions, E_D is the direct output voltage, E_{DO} is the output voltage without phase control (rectifying devices operated without constraint), and α is the angle of phase retard in electrical degrees.

It is often convenient to express the above relationships in terms of E_{DO} and the voltage reduction E_α .

For resistive loads:

$$\frac{E_{DO} - E_\alpha}{E_{DO}} = \frac{1 - \sin(\alpha - 90^\circ)}{2} \quad (6-C)$$

For inductive loads:

$$\frac{E_{DO} - E_\alpha}{E_{DO}} \quad (6-D)$$

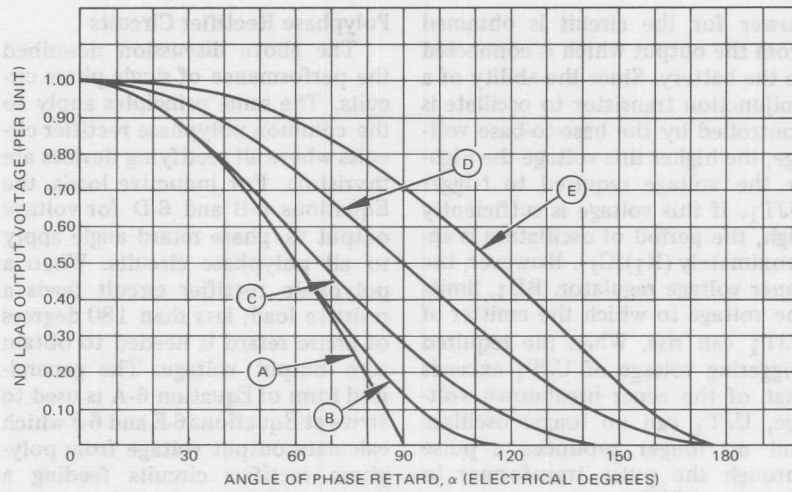
These two expressions are plotted on linear coordinates in Figure 6-4 as curves D and A, respectively.

Single-Phase, Half-Wave Circuits

The single-phase, center-tap circuit is actually a biphasic circuit, since it is two single-phase circuits displaced by 180 degrees. The single-phase, half-wave circuit, where the number of phases is one, was not considered in the previous discussion. Where it is used to feed a resistive load (equations 6-A and 6-B apply), recognizing that for a given alternating supply voltage, the direct voltage will be one-half of that obtained with the biphasic circuit, since load current flows only during every other half cycle. The half-wave circuit is not suitable for feeding an inductive load, because the inductance demands a continuous current source; the half-wave circuit can be used successfully with an inductive load shunted by a free-wheeling diode, in which case its performance with phase control is the same as when the load is resistive.

A half-wave phase control circuit for use as a very simple battery charger is shown in Figure 6-5[2]. Transformer T_2 is used to step down the input voltage. The output of transformer T_2 feeds SCR₁ acting as a half wave rectifier. Transformer T_2 determines the rated current that can be delivered to the battery by the rating of its windings. It partially offsets the other advantages of this circuit since, although the control portion is small and consists of fairly inexpensive components, the transformer size and cost increase with the amount of current delivered. Resistor R_4 is used to limit the current which can be delivered by the circuit.

The trigger circuit consists of a voltage sensor, a relaxation oscillator, and a pulse transformer. The



Per-unit no-load output voltage vs. angle of phase retard α . (A) Average values for all rectifier circuits when all rectifying devices are phase controlled and load is inductive. (B) Average values for 6-phase rectifier circuits when all rectifying devices are phase controlled and load is resistive or is provided with free wheeling diodes. (C) Average values for 3-phase rectifier circuits under same conditions as in (B). (D) Average values for biphaser rectifier circuits under same conditions as in (B) and (C). Also for single-phase and 3-phase hybrid bridge circuits, resistive or inductive load. (E) The RMS values for phase control of alternating voltage.

Figure 6-4. Output Voltage Vs. Angle of Phase Retard

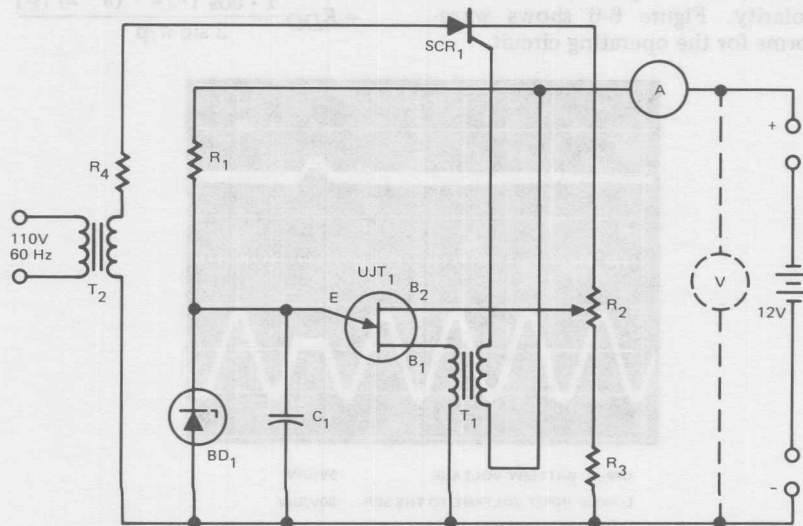


Figure 6-5. Half-Wave Battery Charger Circuit

power for the circuit is obtained from the output which is connected to the battery. Since the ability of a unijunction transistor to oscillate is controlled by the base-to-base voltage, the higher this voltage the higher the voltage required to trigger UJT₁. If this voltage is sufficiently high, the period of oscillation is approximately $(R_1)(C_1)$. However, the zener voltage regulator, BD₁, limits the voltage to which the emitter of UJT₁ can rise. When the required triggering voltage of UJT₁ exceeds that of the zener breakdown voltage, UJT₁ can no longer oscillate and no longer produces a pulse through the pulse transformer to the gate of SCR₁.

This circuit cannot oscillate unless a voltage between three volts and the cutoff voltage is present between the output terminals. Thus, it prevents SCR₁ from triggering into a short circuit, an open circuit, and the presence of reverse polarity. Figure 6-6 shows waveforms for the operating circuit.

Polyphase Rectifier Circuits

The above discussion described the performance of single phase circuits. The same principles apply to the common polyphase rectifier circuits where all rectifying devices are thyristors. For inductive loads, the Equations 6-B and 6-D for voltage output vs. phase retard angle apply to all polyphase circuits. When a polyphase rectifier circuit feeds a resistive load, less than 180 degrees of phase retard is needed to obtain zero output voltage. The generalized form of Equation 6-A is used to arrive at Equations 6-E and 6-F which calculate output voltage from polyphase rectifier circuits feeding a purely resistive load as phase retard angle α is varied.

$$E_D = E_{DO} \frac{1 - \sin(\alpha - \pi/p)}{a \sin \pi/p} \quad (6-E)$$

$$= E_{DO} \frac{1 - \cos[\pi/2 + (\pi - 2)/p]}{2 \sin \pi/p}$$

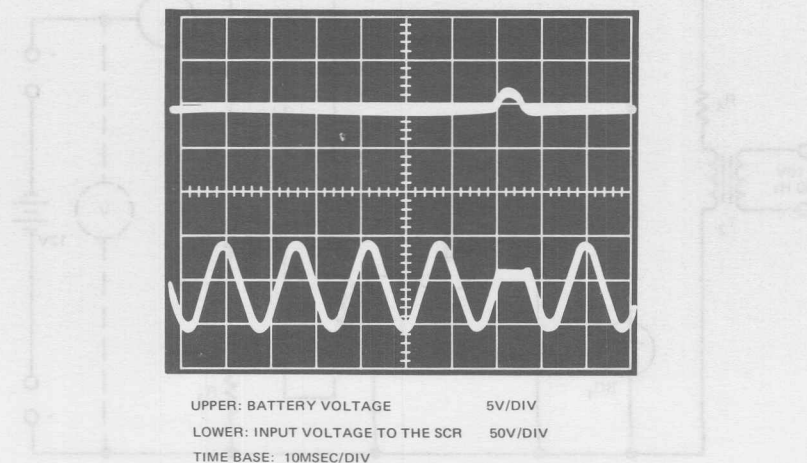


Figure 6-6. Oscilloscope of Half-Wave Battery Charger Circuit

$$\frac{E_{DO} - E_a}{E_{DO}} = \frac{1 - \sin(a - \frac{\pi}{p})}{2 \sin \frac{\pi}{p}} \quad (6-F)$$

$$\frac{1 - \cos(\frac{\pi}{2} + \frac{\pi - a}{p})}{2 \sin \frac{\pi}{p}}$$

In these expressions p is the number of rectifier phases. (For the biphasic circuit previously discussed, $p = 2$, since the circuit is actually two single-phase circuits 180 degrees out-of-phase.)

Curves B and C of Figure 6-4 show equation 6-F plotted for all 6-phase and 3-phase rectifier circuits, respectively. In each case, the curves are seen initially to follow the inductive load curve. The angle at which they depart from this curve, a_1 , is given in Formula 6-G.

$$a_1 = \frac{\pi}{2} - \frac{\pi}{p} \quad (6-G)$$

At this angle, the load current becomes discontinuous. The output voltage E_D becomes zero at φ_2 in each case, as shown in Formula 6-H.

$$a_2 = \frac{\pi}{2} + \frac{\pi}{p} \quad (6-H)$$

Table VI-II gives a_1 and a_2 for various numbers of phases p :

Table VI-II. Values for Angles of Phase Retard

p	2	3	4	6	12	∞
a_1	0	30	45	60	75	90
a_2	180	150	135	120	105	90

If the load includes both resistance and inductance, load current

will become discontinuous at some angle of phase retard greater than a_1 (from Table VI-II) and at this angle the voltage characteristic will no longer follow the inductive load ($\cos a$) curve, but will follow a line which goes through zero output voltage at a_2 . If the inductance of the circuit is fairly high, the change in slope of the output can be quite pronounced. This can lead to instability when the rectifier is provided with an automatic regulating system [3].

Operation With Free-Wheeling Diode

Where the load is inductive, and the large amount of ripple obtained in the usual circuits with a large angle of phase retard is not desired, one or more rectifier diodes may be used as free-wheeling diodes and placed across the load in the direction to block the flow of current from the rectifier, but to provide a path for the current flowing in the load inductance during the intervals when the rectifier output voltage is negative, as shown in Figure 6-7. This occurs at angles of a between a_1 and a_2 ; the values for these are given for several rectifier circuits in Table VI-II. The action of the free-wheeling diode reduces the ripple voltage across the load; it also causes the rectifier output current to become discontinuous although the load current is continuous.

When a free-wheeling diode is present, a rectifier behaves very much as if it were supplying a resistive load, and the curve of output voltage vs. angle of phase retard is the one shown in Figure 6-4 for the same rectifier circuit when it is feeding a resistive load.

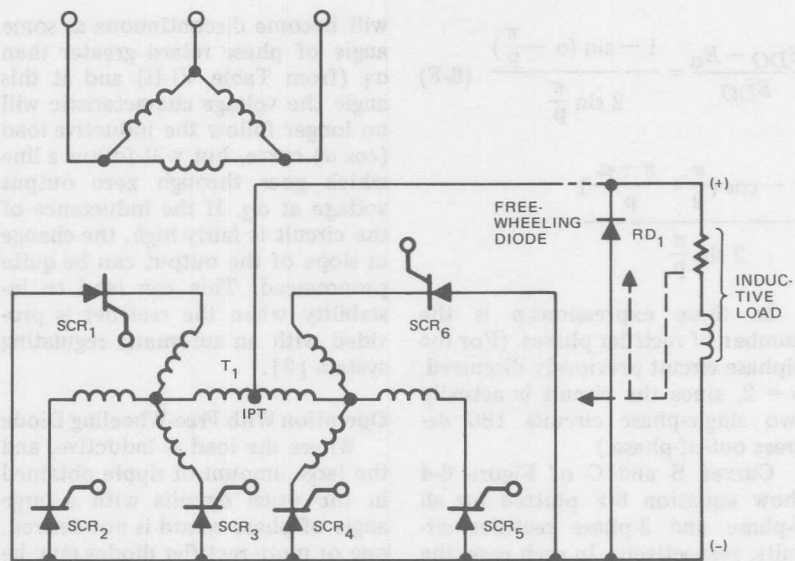


Figure 6-7. Six-Phase Double-Y Rectifier Circuit

Operation with Capacitive or Counter-EMF Load

A rectifier, when supplying either a capacitive or a counter-EMF load, will tend to deliver output current in a discontinuous manner, because current can flow only near the peak of each ac wave. For current to flow, the rectifier output voltage must exceed the voltage across the capacitor, which will be more or less fully charged, depending upon the magnitude of the resistive component of the load. Other loads presenting a counter-EMF, such as electrolytic cells, batteries, and lightly loaded dc motors, will cause the same circuit action.

If the load includes some inductance, which is usually the case, this inductance will store energy while the current is rising to its peak value, and current will continue to flow until this stored energy is de-

livered to the load. This means that the rectifier output current will persist for a longer time than just the interval when rectifier voltage exceeds the counter-EMF, which is the case when there is no inductance. Waveforms to illustrate current flow with and without load circuit inductance are shown in Figure 6-8.

When phase control is applied, the output voltage will be reduced if the thyristors are triggered at some instant later than when the rectifier phase voltage exceeds the counter-EMF. At the same time, the energy absorbed in the inductance of the load will be less, so that the conduction angle is further reduced, causing the additional loss in voltage output. Because of this interaction, there is no simple relationship between angle of phase retard and reduction of output voltage.

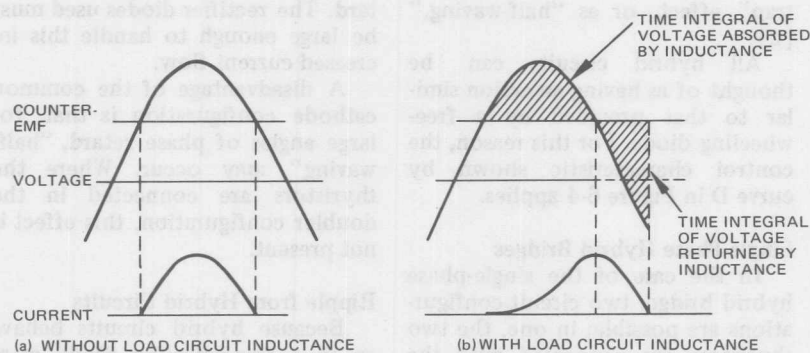


Figure 6-8. Waveforms of Biphasic Circuit Feeding Counter-EMF Load

When the load exhibits a counter-EMF, the earliest instant a given rectifying device can be triggered depends upon the ratio of the load voltage to the peak voltage supplied by the transformer. This ratio will vary with changes in load current, which could be caused by changes in load resistance; or it will vary because of changes in the alternating supply voltage. In the designing of the triggering circuit, this effect must be recognized; long triggering pulses are desirable, so that if the thyristor is triggered before load current can flow, it will remain turned ON by the triggering pulse until some instant later when current can flow to the load. If this is not done, the rectifier may fail to deliver any power to the load when it is phased ahead in an effort to obtain maximum output.

Hybrid Circuits

In the single-phase and poly-phase bridge circuits, half the rectifying devices can be made rectifier diodes, the others remaining thyristors, and the output voltage can be controlled by phase shifting the triggering pulses for the thyristors.

The performance of these hybrid or half-controlled circuits, where the thyristors have a common cathode (or common anode) connection, can be analyzed by considering them as a phase-controlled rectifier in series with one which is not. In this group of bridge circuits (including all hybrid circuits except one of the single-phase bridge circuits), when the angle of retard at which the thyristors are operated exceeds 90 degrees, the thyristors must invert or pump back some of the power delivered by the rectifier diodes. It is theoretically possible for this action to take place all the way down to zero voltage output, at which point the angle of phase retard required is 180 degrees. In practice, it will be found that with a large amount of phase retard, the current may not completely commute to the next phase before the phase which is commutating out becomes positive again. In this event, the thyristor which was supposed to commute to the next phase will instead conduct full ON, and control of output by phase control will be lost. This is sometimes referred to as the "mouse

trap" effect, or as "half-waving." [2].

All hybrid circuits can be thought of as having an action similar to that provided by a free-wheeling diode. For this reason, the control characteristic shown by curve D in Figure 6-4 applies.

Single-Phase Hybrid Bridges

In the case of the single-phase hybrid bridge, two circuit configurations are possible; in one, the two thyristors are connected with the cathodes (or anodes) tied to a common point, as in the center-tap rectifier circuit, and in the other configuration, the two thyristors are connected in series, as in the doubler rectifier circuit, (see Figure 6-9). Circuit action is similar, but not the same, in both cases.

With the common cathode configuration (Figure 6-9(a)), the conduction angle through all the rectifying devices remains the same as the angle of phase retard is increased. With the doubler circuit (Figure 6-9(b)), the conduction angle through the rectifier diodes increases with increasing phase re-

tard. The rectifier diodes used must be large enough to handle this increased current flow.

A disadvantage of the common cathode configuration is that, for large angles of phase retard, "half-waving" may occur. Where the thyristors are connected in the doubler configuration, this effect is not present.

Ripple from Hybrid Circuits

Because hybrid circuits behave as if a free-wheeling diode were present, the ripple voltage they exhibit, as output voltage is reduced by phase control, is less than in a bridge circuit using four thyristors. This can be illustrated by comparing the action of the single-phase bridge having four thyristors with that of the hybrid single-phase bridge. In the first circuit, with an inductive load, zero output voltage will be obtained with a phase retard angle of 90 degrees. Under this condition, the peak of the alternating input voltage will appear across the load (see Figure 6-2(b), waveforms for a_3), although the average voltage across the load will be zero.

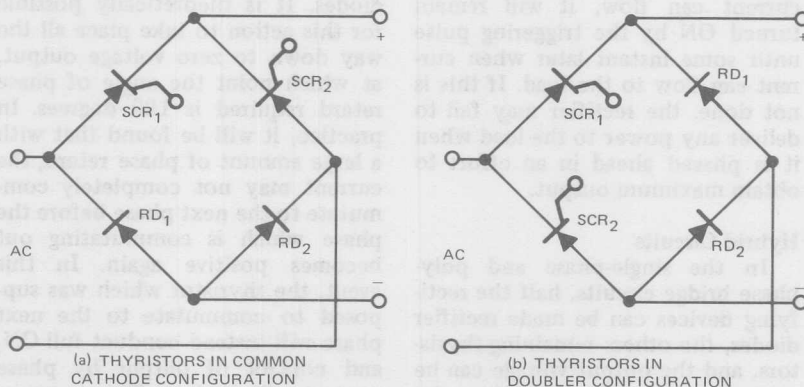


Figure 6-9. Single-Phase Hybrid Bridge Circuits

On the other hand, with the hybrid circuit phased back 180 degrees, the average and peak voltage both will be essentially zero. This difference in ripple voltage can be significant if part of the load is purely resistive, since with the hybrid circuit there will be less power dissipated in the resistive part of the load when the voltage is reduced by phase retard. For instance, with the hybrid circuit, an indicating lamp across the load will give a measure of the average voltage across the load; with the regular circuit having four thyristors, the lamp intensity will hardly change over the full range of average output voltage.

On the other hand, in the poly-phase hybrid bridge circuits, the ripple frequency will assume a lower value as phase retard is introduced. For instance, in the regular 3-phase bridge circuit, the fundamental ripple frequency is six times the supply frequency for all values of phase retard. In the hybrid 3-phase bridge circuit, a ripple frequency component three times the line frequency appears when phase retard is introduced. This action must be considered when the load is adversely affected by lower ripple frequencies; for example, in some dc motors.

Inversion of Inductive Energy

If it is desired to quickly reduce the voltage across an inductive load, this can be done by operating the rectifier as an inverter and pumping the energy stored in the load inductance back into the ac system. This is done by adjusting the angle of phase retard to be greater than 90 degrees. When a hybrid rectifier circuit is used, this mode of voltage control cannot be used, since the

half of the rectifier circuit which is made up of diodes cannot be made to function as an inverter.

Triggering Pulses for Bridge Circuits

In certain bridge rectifier circuits, precautions must be taken when designing the thyristor triggering circuit to be certain that the desired rectifier circuit action can take place. For example, in the conventional 3-phase bridge circuit having six thyristors, current flow through the load will not start if each thyristor is simply given a short gate pulse at the instant when current flow in each thyristor normally would start, since this circuit behaves as two 3-phase circuits in cascade and displaced by 30 degrees. To initiate current flow, thyristors in both halves of the circuit must be pulsed simultaneously. Under operating conditions where current flow becomes discontinuous, the simultaneous pulsing must occur six times a cycle.

Two solutions are possible. One is to provide each thyristor with a long gate pulse, more than 60 degrees in duration. The other solution is to double pulse each thyristor; one, when initiation of current flow is desired, and once again 60 degrees later.

In hybrid bridge circuits, where circuit action similar to that provided by a free-wheeling diode is obtained (and also in all-thyristor circuits which feed a load having a free-wheeling diode), the discontinuous nature of the current through the thyristors must be considered when designing the triggering circuit. Since the interval of current discontinuity varies with load current and also with angle of phase retard, a triggering circuit

which provides a long triggering pulse is desirable to assure proper action from the thyristors.

Full-Wave Control of Output of Single-Phase Diode Bridge

A circuit of particular interest for use with thyristors is the single-phase bridge rectifier with a thyristor in series in the dc output. If the thyristor can regain forward blocking ability at the end of each voltage pulse on the output of the bridge rectifier, phase control may be applied to the thyristor and it will control the average voltage applied to the load. This circuit is most successful when the load has a counter-EMF, as with a storage battery. It also can be made to work successfully with a resistive load and with a dc motor armature as the load when a free-wheeling diode is connected across the armature.

In this circuit, the diodes in the single-phase bridge help to provide a short interval at the end of each half-cycle when flow is zero and during which the thyristor can turn off. Nevertheless, when feeding a resistive load or a dc motor, thyristors which have fast turn-off times are needed. This is the major reason this circuit has never been used

with thyatron tubes. Conventional mercury vapor thyatrons simply do not turn off (deionize) fast enough to operate in this circuit at supply frequencies of 50 or 60 Hz.

If the load is resistive or is provided with a free-wheeling diode, the voltage output will follow curve D of Figure 6-4 as a is varied. It should be understood that a in this case is the angle of retard of each pulse applied to the thyristor in series with the load.

DC Motor Drives

The circuit in Figure 6-10 is a full-wave bridge, feeding the armature of a dc motor through a single controlled rectifier. The speed of the motor is controlled by appropriate triggering of the controlled rectifier at various angles with respect to the applied voltage which results in phase control of forward current through the controlled rectifier. [4],[5]

After every half cycle of forward current, the controlled rectifier must recover its forward blocking state. This means that the device must turn off during the time interval between the cessation of for-

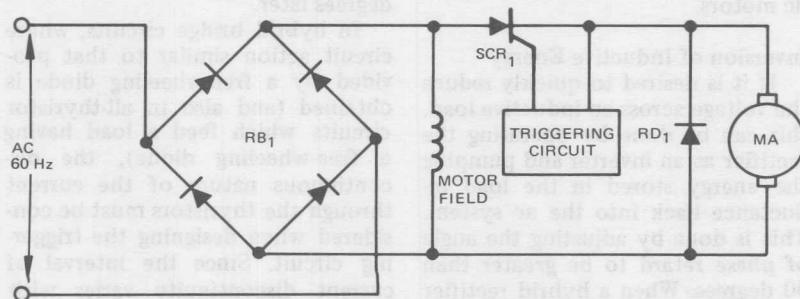


Figure 6-10. DC Motor Control Circuit

ward current and reapplication of forward voltage. A quick analysis of the applied voltage waveshapes would lead one to believe that the time interval between forward current cessation and reapplication of forward voltage is zero. However, in analyzing the circuit, one can see that the time required for the voltage to overcome the threshold voltage of two diodes and the controlled rectifier in series, is the time during which the device can recover to its blocking state. Threshold voltage is that voltage required across the diode or controlled rectifier to cause substantial forward current to flow. Threshold voltage is approximately 0.5 volts.

With an input of 230 volts, it would appear that the time interval provided by the threshold voltages

should be approximately 23 microseconds, as seen in Figure 6-11. There are three semiconductor devices in series with the motor when current is flowing so that the total threshold voltage is approximately 1.5 volts.

Voltages and waveshapes observed in laboratory tests of this circuit, as illustrated in Figure 6-12, show that in one case, from the time the forward current dropped to zero (indicated by zero forward voltage drop) to the time of the voltage transient, there is approximately 17 microseconds. This time interval is less than the anticipated 23 microseconds. We can see that with this circuit, one critical SCR parameter requiring careful definition is turn-off time.

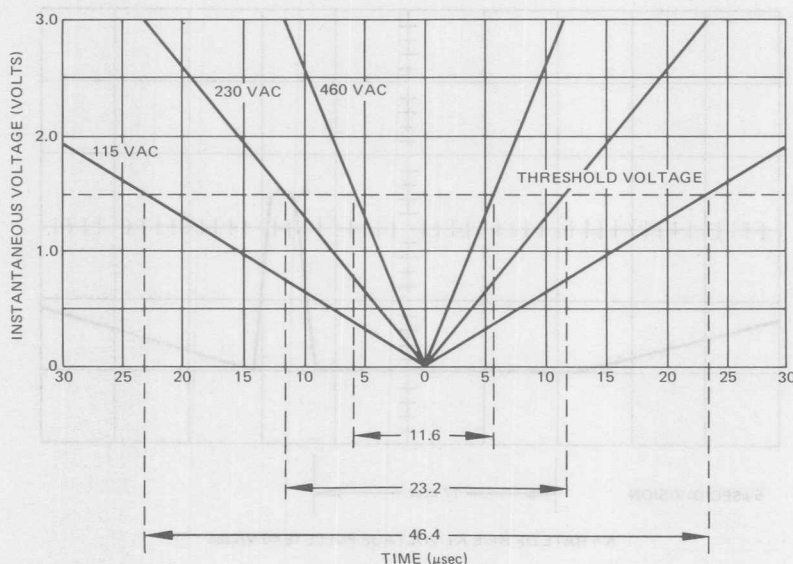


Figure 6-11. Interval of Zero Current Flow

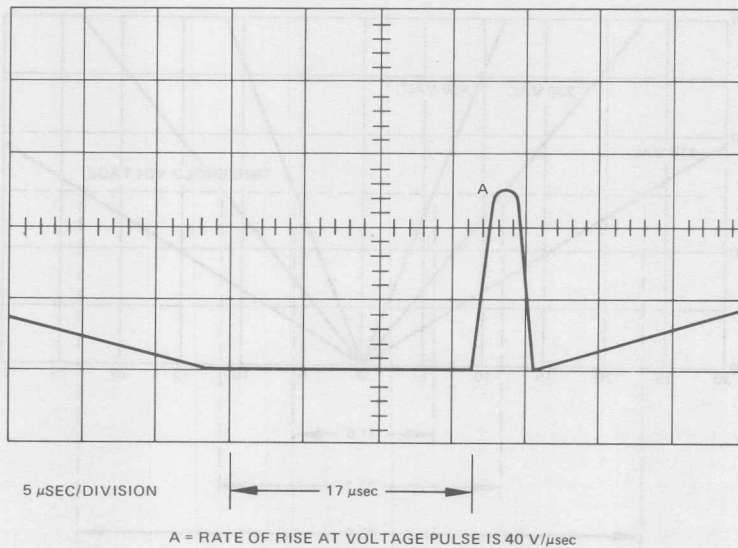
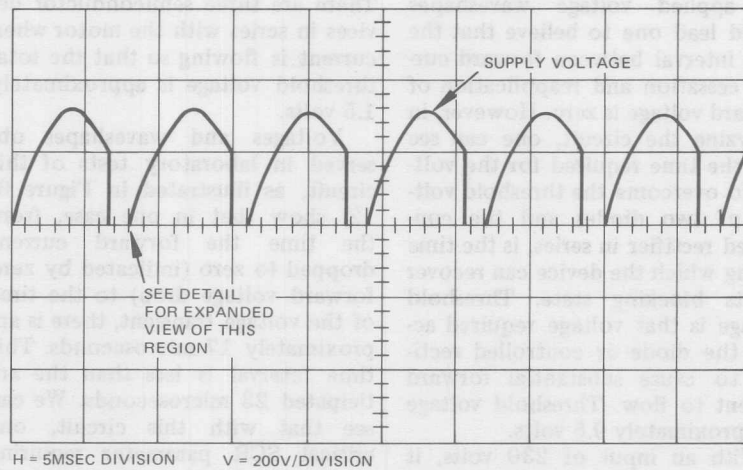


Figure 6-12. DC Motor Control Circuit Voltage Waveforms

The voltage transient (in Figure 6-12(b)) is 30% of the peak supply voltage, is five microseconds wide, and the rate-of-rise of the leading edge is 40 volts per microsecond. This particular voltage transient was seen for both resistive and inductive loads. It is caused by the recovery transient of the free-wheeling diode.

Thus, we see that instead of 23 microseconds allowed for turn-off, we have only 17 microseconds, a much more stringent requirement on the controlled rectifier. To select devices which will work reliably in the circuit of Figure 6-10, they should be tested for reverse recovery time with no reverse voltage, and also for circuit commutated turn-off time. A practical way to do this on many turn-off time testers is to select units which turn off fast, even when essentially zero reverse voltage is applied during the turn-off time interval.

Another approach which has been used successfully is the testing of devices by operating them in the circuit shown in Figure 6-10. Testing time can be minimized by providing the device under test with a very small heat exchanger, so that an elevated junction temperature (where turn-off and recovery times are the longest) will be reached in seconds. Torque is applied to the motor so that a specified motor current is drawn, and the device under test must not lose control of the motor at the end of a specified time period.

Another characteristic which devices should have in order to work well in this circuit is relatively high holding current. However, it is more important to have fast turn-off characteristics under the condi-

tions described above, than to have relatively high holding current, since the additional time during which the controlled rectifier may turn off that is gained by having a high holding current is only a few microseconds.

The controlled rectifier will be aided in turning off if one or more rectifier diodes are connected in series with it. Doing this will increase the threshold voltage mentioned earlier. In many cases, it may be found more economical to do this than to attempt to select extremely fast units, or to use another circuit configuration where turn-off time is not critical. For instance, the turn-off time of the controlled rectifiers in Figure 6-13 is not critical. However, it is quite possible that it would be more economical to add one or two diodes in series with the controlled rectifier in the circuit of Figure 6-10 than to use a completely different circuit.

A physical arrangement illustrating how two diodes may be connected in series with the controlled rectifier, at the same time mounting all the rectifying devices on three heat exchangers, is shown in Figure 6-14.

The single phase dc motor drive circuit using one controlled rectifier is an attractive and practical circuit to use with fractional and small integral horsepower rated motors when operation is from a 115 volt line. The required silicon controlled rectifier must be selected for maximum turn-off time under the special test condition of essentially no reverse voltage during the turn-off interval. The maximum permissible value of turn-off time under these conditions is long enough so there

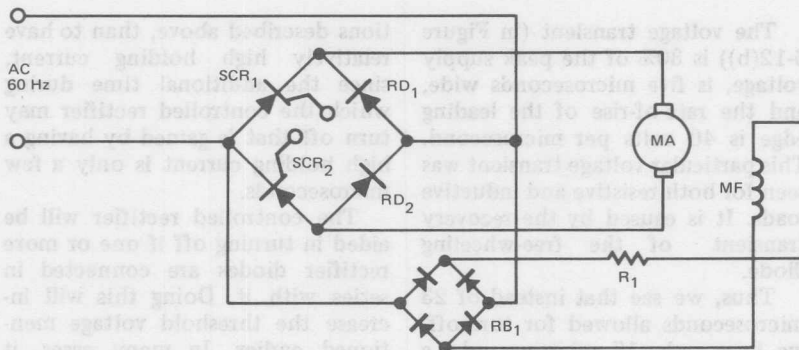


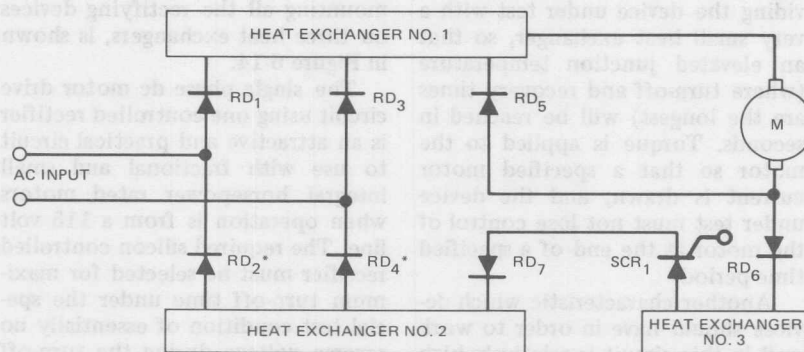
Figure 6-13. Single-Phase DC Motor Drive

usually is no great difficulty in selecting satisfactory parts from normal production. Selection of parts for operation from a 230-volt line is more difficult because of the shorter turn-off time required. The circuit can be modified to enable parts with longer turn-off times to operate satisfactorily. If this circuit is to be operated from a 460-volt line, circuit modifications are, in general, mandatory. In addition, consideration should be given to using a completely different motor drive

circuit, such as a hybrid single-phase bridge, having two diodes and two controlled rectifiers.

Triac Reversing Drives [6][7]

An application which lends itself ideally to use of the triac is a full-wave reversing drive for a dc motor. The basic power circuit is shown in Figure 6-15. If the gates of the triacs are synchronized as shown, the motor will have the polarity as shown in the diagram. If the phase relationships of the triac



* REVERSE POLARITY RECTIFIERS

Figure 6-14. Physical Arrangement for DC Motor Control Circuit

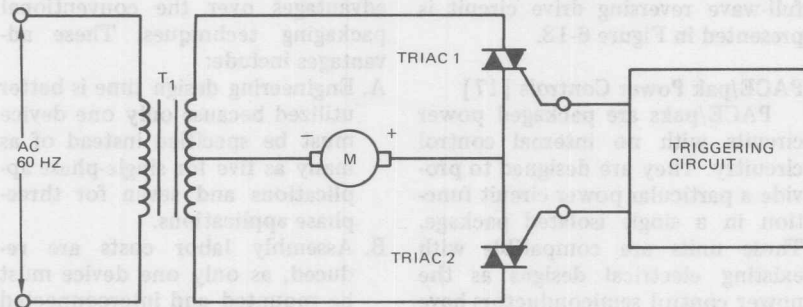


Figure 6-15. Full Wave Triac Reversing Drive Circuit

gate signals are reversed, the opposite polarity will be impressed on the motor. Figure 6-16 shows the waveforms for this circuit. The dv/dt as seen by the triac in this circuit can be reduced by placing an R-C snubber across the device. In some cases, it may also be necessary to place an inductance in series with the triac to reduce di/dt .

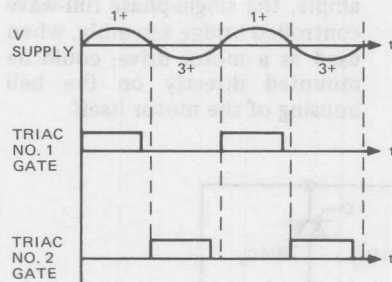


Figure 6-16. Waveforms for Triac Reversing Drive

A full-wave drive can be accomplished without a center-tapped transformer using the circuit shown in Figure 6-17. By properly phasing the signals to the gates of TRIACS 1, 2, 3, and 4, the motor can be made to run in either direction. We

can also plug the motor by gating the opposite pair of triacs.

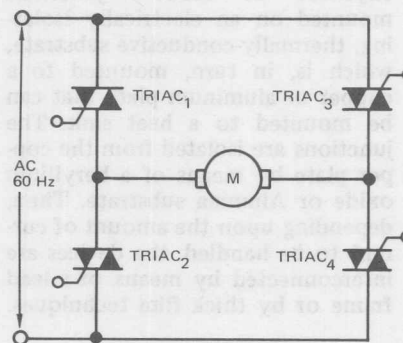


Figure 6-17. Circuit for Full-Wave Triac Reversing Drive Without Transformer

This dynamic braking action can also be achieved by simply providing positive gate bias on all the triacs. This will prevent the power supply from being connected to the motor, but will allow dynamic braking action of the machine. Of course, to limit the armature current, an impedance should be supplied in the armature circuit and/or field weakening should be incorporated.

A three-phase version of the full-wave reversing drive circuit is presented in Figure 6-18.

PACE/pak Power Controls [17]

PACE/paks are packaged power circuits with no internal control circuitry. They are designed to provide a particular power circuit function in a single isolated package. These units are compatible with existing electrical designs as the power control semiconductors have just been combined in a single package. PACE/paks are available in current ratings from 10 to 42.5 amps at 115 or 230 volt ratings.

The circuits generally utilize thyristor or diode junctions mounted on an electrically isolating, thermally-conductive substrate, which is, in turn, mounted to a copper or aluminum plate that can be mounted to a heat sink. The junctions are isolated from the copper plate by means of a beryllium oxide or Alumina substrate. Then, depending upon the amount of current to be handled, the devices are interconnected by means of a lead frame or by thick film techniques.

This construction offers many advantages over the conventional packaging techniques. These advantages include:

- A. Engineering design time is better utilized because only one device must be specified instead of as many as five for single-phase applications and seven for three-phase applications.
- B. Assembly labor costs are reduced, as only one device must be mounted and interconnected for the entire power section.
- C. Visual keys by either color coding or mechanical asymmetries can be used to aid in making the assembly operation foolproof.
- D. Isolated heat sinks are eliminated because the single copper plate is isolated from the circuit. Thermal efficiencies are better than with individual devices.
- E. In many applications, the smaller size of the power circuit assembly can be utilized. For example, the single-phase full-wave controlled bridge assembly, when used as a motor drive, could be mounted directly on the bell housing of the motor itself.

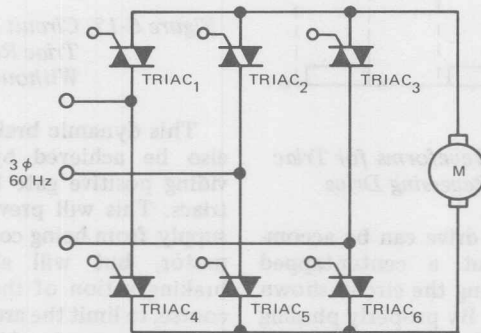


Figure 6-18. Three-Phase Triac Reversing Drive Circuit

One very useful circuit configuration is shown in Figure 6-19. This circuit would be used in low power dc motor drives or without the free-wheeling diode as a power supply. For purposes of this discussion, it is assumed that the devices used are in the 25 ampere RMS rating category.

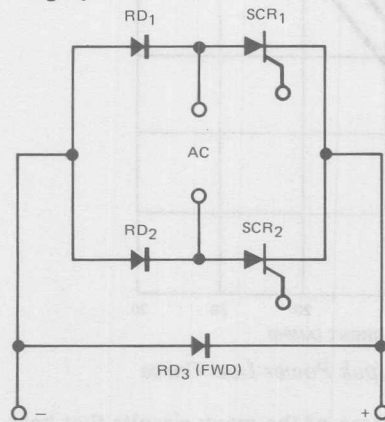


Figure 6-19. PACE/pak Hybrid Bridge

Figure 6-20 defines the maximum allowable base plate temperature vs. conduction angle and dc output current. Knowing the worst case application conditions, the maximum allowable base plate (case) temperature can be determined. Then, with Figure 6-21, which is for watts loss vs. conduction angle and output current, and knowing the maximum allowable base plate temperature, it is possible to determine the heat dissipator requirements. The thermal resistance of the base plate to sink, $R_{\theta CS}$, assuming a 1.5-inch (38.1 mm) square surface area, a good thermal compound and smooth contact surface, is in the neighborhood of $0.1^{\circ}\text{C}/\text{W}$. It can be seen that using these design graphs, it is possible to characterize this power hybrid assembly in a fashion very similar to that used for a discrete device.

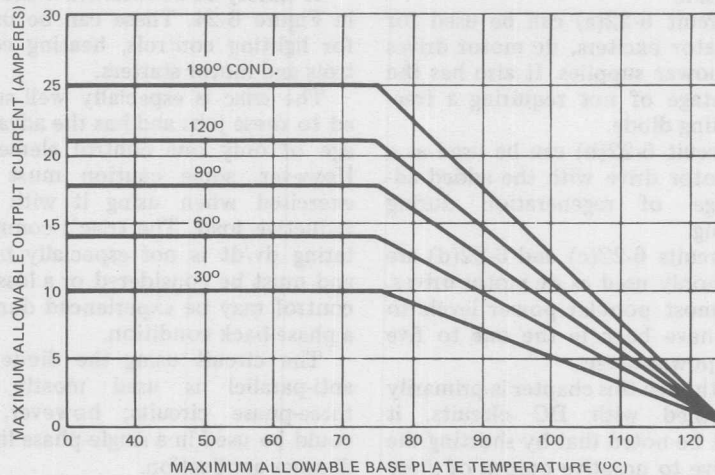


Figure 6-20. Typical PACE/pak Temperature Vs. Current Curve

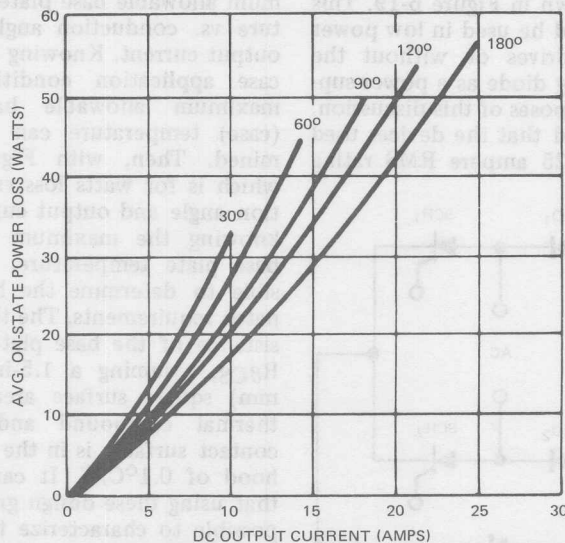


Figure 6-21. Typical PACE/pak Power Loss Curve

Several common SCR bridge control circuits are shown in Figure 6-22, with 6-22(c) being the most common.

Circuit 6-22(a) can be used for generator exciters, dc motor drives and power supplies. It also has the advantage of not requiring a free-wheeling diode.

Circuit 6-22(b) can be used as a dc motor drive with the added advantage of regeneration during braking.

Circuits 6-22(c) and 6-22(d) are commonly used as dc motor drives. The most popular power levels to date have been in the one to five horsepower range.

Although this chapter is primarily concerned with DC circuits, it might be noted that by shorting the positive to negative output of these circuits, an ac switch configuration is obtained. Figure 6-23 shows

three of the many circuits that have been built using a common substrate.

A variety of ac switches is shown in Figure 6-24. These can be used for lighting controls, heating controls and motor starters.

The triac is especially well suited to these jobs and has the advantage of only one control element. However, some caution must be exercised when using it with an inductive load. The triac's commutating dv/dt is not especially high and must be considered or a loss of control may be experienced during a phase-back condition.

The circuit using the diode in anti-parallel is used mostly in three-phase circuits; however, it could be used in a single-phase light dimmer application.

A new area where PACE/paks are being applied is three-phase

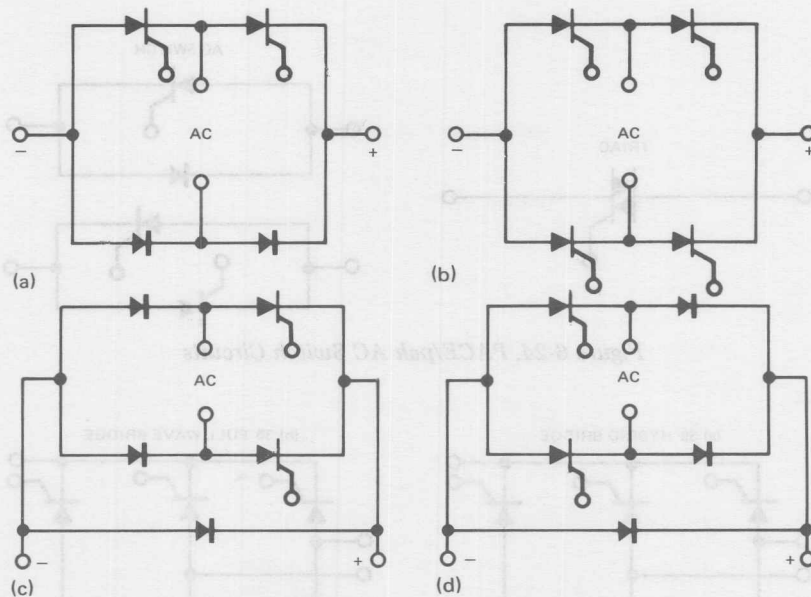


Figure 6-22. Popular PACE/pak Circuits

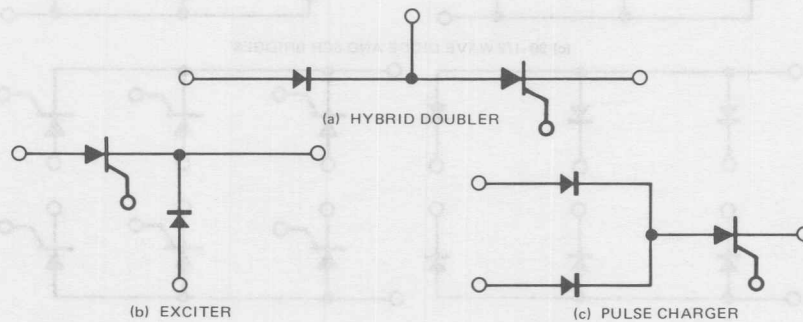


Figure 6-23. Other PACE/pak Circuits

power circuits as shown in Figure 6-25. Circuits can be delivered with voltages up to 1200 volts and current levels to 150 amps. Circuits 6-25(a) and 6-25(b) are standard three-phase controlled bridges.

Circuit 6-25(a) requires fewer gate control circuits and is excellent

for resistive and capacitive loads; however, some caution must be exercised on inductive loads. Unless some provision is made to handle the reactive current at phased-back conditions (a free-wheeling diode is one method), the bridge can lose control.

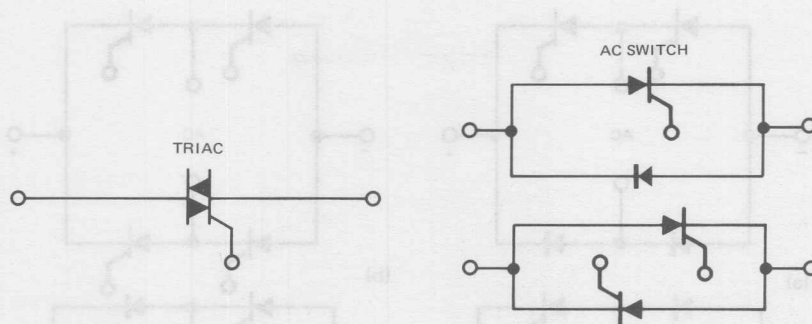


Figure 6-24. PACE/pak AC Switch Circuits

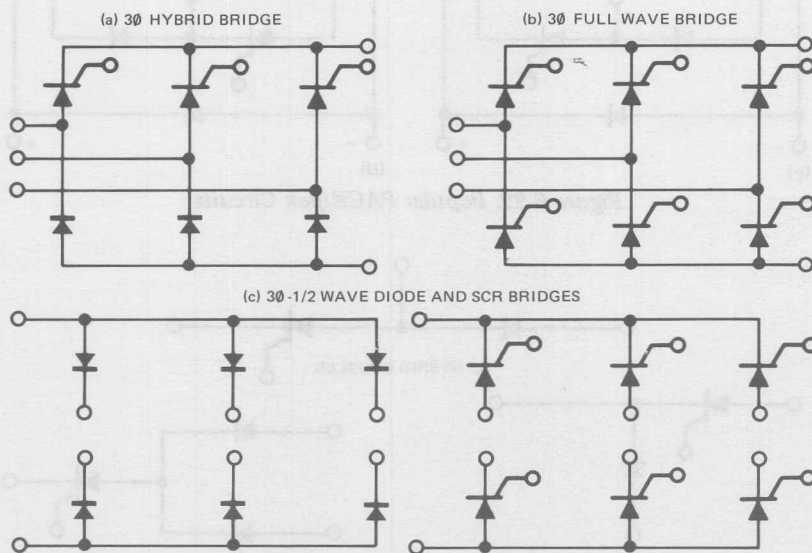


Figure 6-25. PACE/pak Three-Phase Circuits

Circuit 6-25(b) does not suffer from the above problem, but requires six gate control circuits.

The circuits shown in Figure 6-25(c) are usable as half-wave, three-phase circuits or can be combined to make various full-wave configurations.

Finally, an inverter module is shown in Figure 6-26. This array of devices can be interconnected with inductors and capacitors to form many of the basic force-commutated inverter circuits. These modules are very useful in many applications where size, weight and thermal considerations are important.

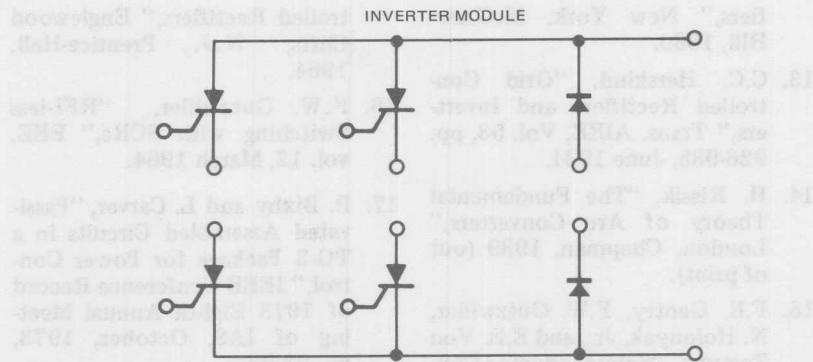


Figure 6-26. PACE/pak Inverter Circuit

References

1. D.W. Borst, E.J. Diebold, and F.W. Parrish, "Voltage Control by Means of Power Thyristors," *IEEE Transactions on Industry and General Applications*, March/April, 1966, pp. 102-124.
2. R.G. Hoft and G.N. Vogelgesang, "Solid-State Power Control Program Progress Report #2," University of Missouri, Columbia, August 21, 1974, Part C.
3. A. Ludbrook and R.M. Murray, "A Simplified Technique for Analyzing the Three-Phase Bridge Rectifier Circuit," 1965 IEEE IGA International Conv. Rec., pt. 8, pp. 121-127.
4. D.W. Borst, "Selection of Controlled Rectifiers for Single-Phase DC Motor Drives using One Controlled Rectifier," *International Rectifier News*, Winter/1966, pp. 4-6.
5. F. Durnya, "Selection of SCRs for Single-Phase DC Motor Drives," *International Rectifier News*, Summer/1968, pp. 5-6.
6. D. Cooper, "The 200 Amp Logic Triac — A New Breakthrough in Power Control," *International Rectifier Application Note AN-A-13*.
7. D. Cooper, "The Power Logic Triac — A Natural for Motor Control," *Electronic Products Magazine*, November 20, 1972, p. 67.
8. B.D. Bedford and R.G. Hoft, "Principles of Inverter Circuits," Wiley, 1964, Chapter 3.
9. B.R. Pelly, "Thyristor Phase-Controlled Converters and Cycloconverters," Wiley, 1971.
10. J. Schaefer, "Rectifier Circuits, Theory and Design," New York: Wiley, 1964.
11. W. Shepherd, "Steady-State Analysis of the Series Resistance-Inductance Circuit, Controlled by Silicon Controlled Rectifiers," 1965 IEEE IGA International Conv. Rec., pt. 8, pp. 183-193.
12. O.K. Marti and H. Winograd, "Mercury Arc Power Recti-

- fiers," New York, McGraw-Hill, 1930.
13. C.C. Herskind, "Grid Controlled Rectifiers and Inverters," Trans. AIEE, Vol. 53, pp. 926-935, June 1934.
 14. H. Rissik, "The Fundamental Theory of Arc Converters," London, Chapman, 1939 (out of print).
 15. F.E. Gentry, F.W. Gutzwiller, N. Holonyak, Jr., and E.E. Von Zastrow, "Semiconductor Controlled Rectifiers," Englewood Cliffs, N.J., Prentice-Hall, 1964.
 16. F.W. Gutzwiller, "RFI-less Switching with SCRs," EEE, vol. 12, March 1964.
 17. B. Bixby and L. Carver, "Passivated Assembled Circuits in a TO-3 Package for Power Control," IEEE Conference Record of 1973 Eighth Annual Meeting of IAS, October, 1973, pp. 93-98.

Line Commutated Inverters

Most phase-controlled rectifier circuits, comprised entirely of SCRs, can be operated as ac line voltage commutated inverters [1]. With a gradual variation in the thyristor triggering angle, a circuit will change from rectifier to inverter operation with a corresponding reversal of power flow. Inverter commutation is accomplished automatically by the instantaneous relationships existing between the applied ac line voltages. Thus, no added components are required to achieve reliable commutation. However, as commutation is provided by the line voltage, this type of inverter can only operate into an ac system where the ac voltage is maintained relatively independent of the circuit operation. Of course, it is also necessary to have a source of dc power on the dc side of the circuit to deliver power to the ac system.

Regenerative braking of dc motor drives is one common application of phase-controlled rectifiers as line commutated inverters. The cycloconverter is a second important type of line commutated inverter. Work is just beginning in a third very large application area — high voltage dc (HVDC) power transmission systems.

REGENERATIVE PHASE-CONTROLLED RECTIFIERS

In systems using solid-state power control, the load often stores a significant amount of energy [2]. Preferably, the control circuit should be designed to recover this

energy rather than leaving it to be dissipated unproductively. Energy recovery, of course, improves circuit efficiency and reduces the dissipation requirements of the equipment.

A regenerative technique, to return power from the load to the source, can recover the stored energy. This technique may or may not prove worthwhile, depending on the specific application. The design decision will depend on the following factors:

- A. The efficiency of the load when acting as a generator.
- B. The over-all system efficiency improvement that can be obtained, compared with the increased cost and complexity of the system.
- C. The ability of the source to accept energy.

Once the decision is made to use regeneration, the simplest energy-recovery scheme compatible with the type of control circuit should be chosen.

Four Possible Operating Quadrants

Any electrical control system can operate in any of the four quadrants. The number of quadrants in a design depends on the circuit configuration and the control elements. There is a forward power flow from source to load, if the equipment is operating in quadrants I or III (voltage and current are of the same polarity). If in quadrants II or IV (voltage and current are of opposite polarity), there is a reverse power flow from load to source. In many systems the equipment operates

partly in quadrants I or III and partly in quadrants II or IV; the net power flow in this case depends on the relative magnitudes of the "positive" and "negative" flow.

One of the simplest power-conversion systems is the three-phase, full-wave-bridge rectifier in Figure 7-1. This circuit operates in quadrant I — power can flow only from the source to the load. Thus a simple diode-rectifier system cannot be used to recover energy.

As an example of operation in more than one quadrant, consider

the controlled rectifier circuit of Figure 7-2. This circuit differs from the simple diode rectifier in one important aspect: the SCR can support voltage in both directions. Now, if the load and source characteristics are suitable, the circuit can operate in quadrant II and return energy to the source.

Typical waveforms for the SCR circuit are shown in Figure 7-3. The load in this case could be a dc electromagnet, which needs a large amount of charging energy. After charging is complete, the converter

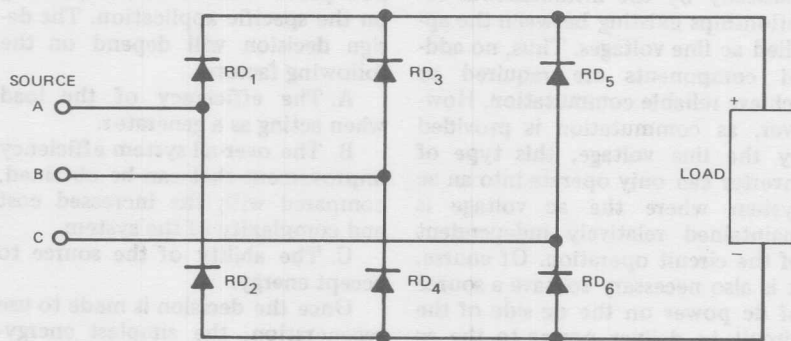


Figure 7-1. Three-phase Full-Wave Bridge Rectifier Circuit

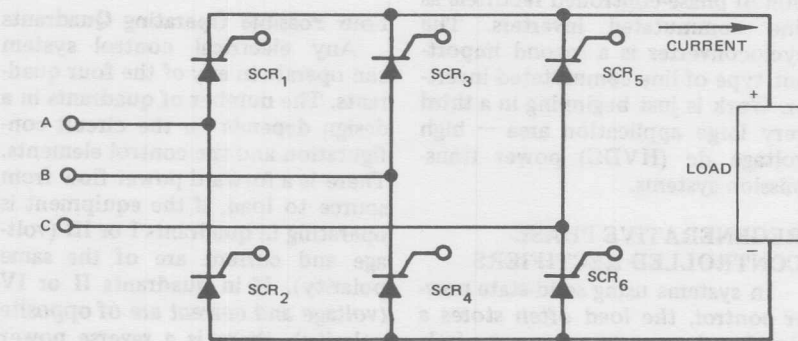


Figure 7-2. Three-phase Full-Wave, All-SCR Bridge Circuit

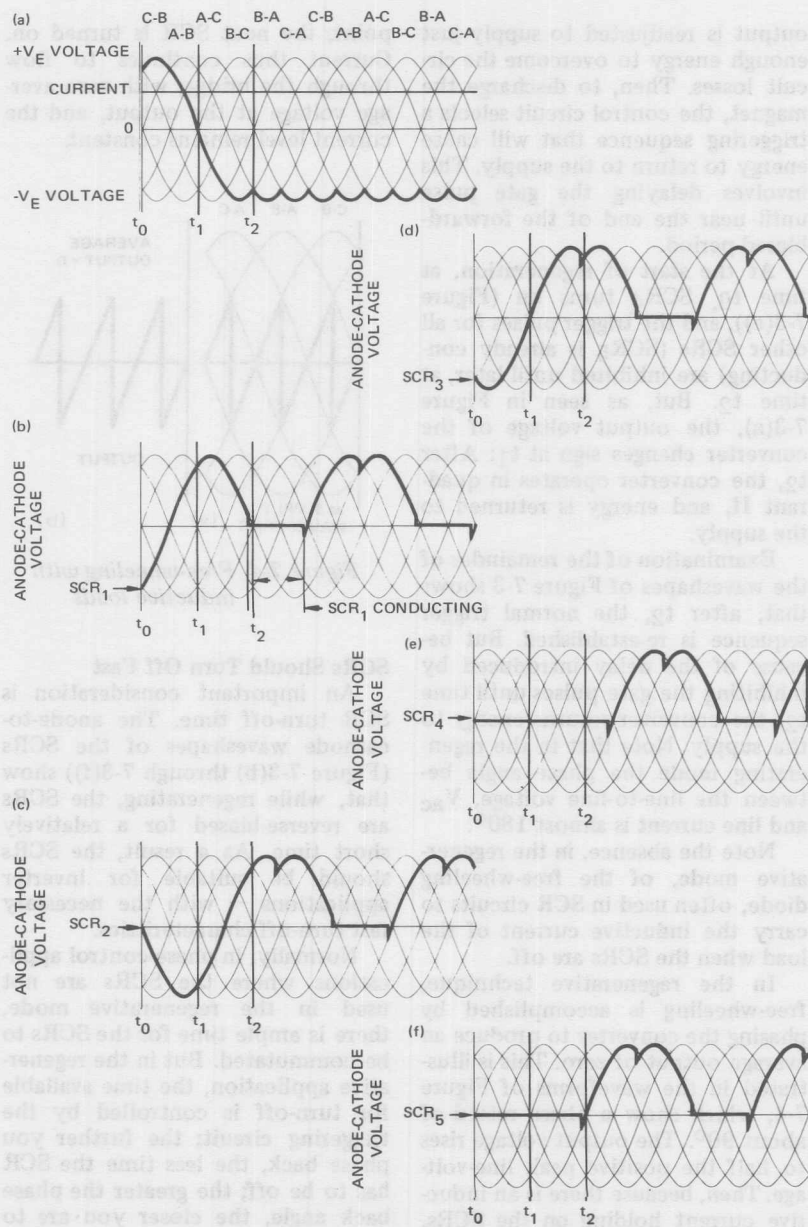


Figure 7-3. Waveforms for SCR Bridge during Regeneration

output is readjusted to supply just enough energy to overcome the circuit losses. Then, to discharge the magnet, the control circuit selects a triggering sequence that will cause energy to return to the supply. This involves delaying the gate pulse until near the end of the forward-biased period.

At the start of regeneration, at time t_0 , SCR₄ turns on (Figure 7-3(e)), and the trigger pulses for all other SCRs (SCR₅ is already conducting) are inhibited until later, at time t_2 . But, as seen in Figure 7-3(a), the output voltage of the converter changes sign at t_1 : After t_2 , the converter operates in quadrant II, and energy is returned to the supply.

Examination of the remainder of the waveshapes of Figure 7-3 shows that, after t_2 , the normal trigger sequence is re-established. But because of the delay introduced by inhibiting the gate pulses until time t_2 , the converter returns energy to the supply. Note that in the regenerative mode the phase angle between the line-to-line voltage, V_{ac} and line current is almost 180° .

Note the absence, in the regenerative mode, of the free-wheeling diode, often used in SCR circuits to carry the inductive current of the load when the SCRs are off.

In the regenerative technique, free-wheeling is accomplished by phasing the converter to produce an average output of zero. This is illustrated in the waveforms of Figure 7-4, which show a phase retard of about 90° . The output voltage rises to half the positive peak line-voltage. Then, because there is an inductive current holding on the SCRs, the output follows the ac line down to half the negative peak. At this

point, the next SCR is turned on. Current thus continues to flow through the bridge, with zero average voltage at the output, and the current level remains constant.

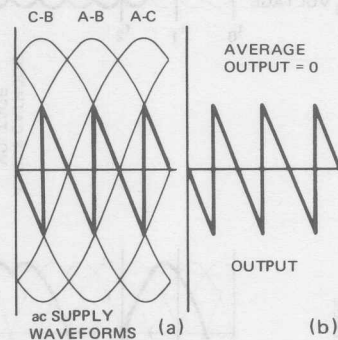


Figure 7-4. Free-wheeling with inductive loads

SCRs Should Turn Off Fast

An important consideration is SCR turn-off time. The anode-to-cathode waveshapes of the SCRs (Figure 7-3(b) through 7-3(f)) show that, while regenerating, the SCRs are reverse-biased for a relatively short time. As a result, the SCRs should be suitable for inverter applications — with the necessary fast turn-off characteristics.

Normally, in phase-control applications where the SCRs are not used in the regenerative mode, there is ample time for the SCRs to be commutated. But in the regenerative application, the time available for turn-off is controlled by the triggering circuit; the further you phase back, the less time the SCR has to be off; the greater the phase back angle, the closer you are to turning the SCR on before it becomes reverse-biased. This also

means that you are much closer to commutating off, under forward biased conditions, the SCR that is about to become forward-biased. But an SCR will not turn off when it is forward-biased; it will keep conducting. The turn-off time therefore defines the maximum "reverse" voltage applied to the load by fixing the minimum time before zero crossing at which the SCRs can be gated; also called, "margin angle."

The dual converter in Figure 7-5 is an example of a circuit that can be operated in all four quadrants. By selection of the R or F bank of SCRs, the direction of the load current can be chosen. The extra cost of this circuit is justified only where regeneration is economically advantageous and voltage reversal is not feasible — that is, load current alone must be reversed to recover the stored energy.

An example of this is a shunt motor that, for some reason, cannot have its field winding voltage reversed. Thus, the machine-generated emf does not change polarity, but current flows out of the machine during regeneration. The amplitude of the generated current is controlled by field strength up to the maximum and then by armature voltage control as the speed is reduced.

Once again, it must be recognized that the power factor of the system varies as a function of triggering angle. Figure 7-6 shows how both output voltage and input power factor vary as a function of triggering angle.

It is important to note that triac dc motor drives may all be operated in regenerative modes, provided the proper gating signals are applied.

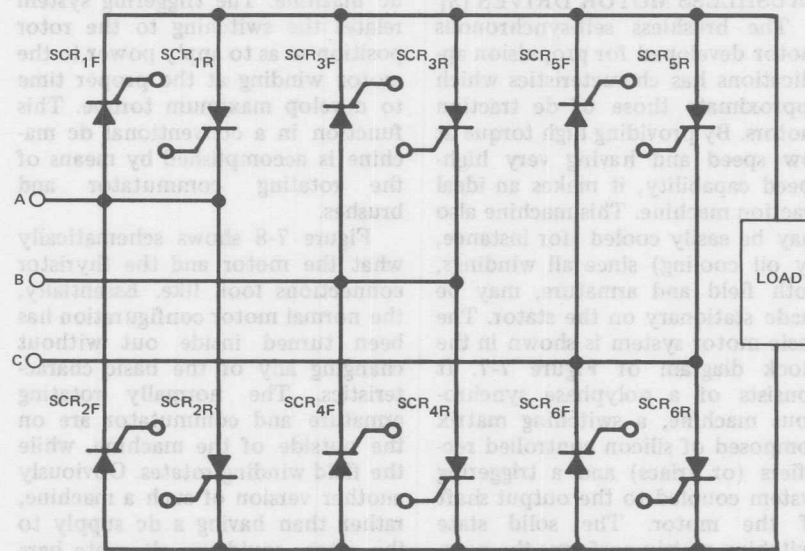


Figure 7-5. Dual Converter Circuit

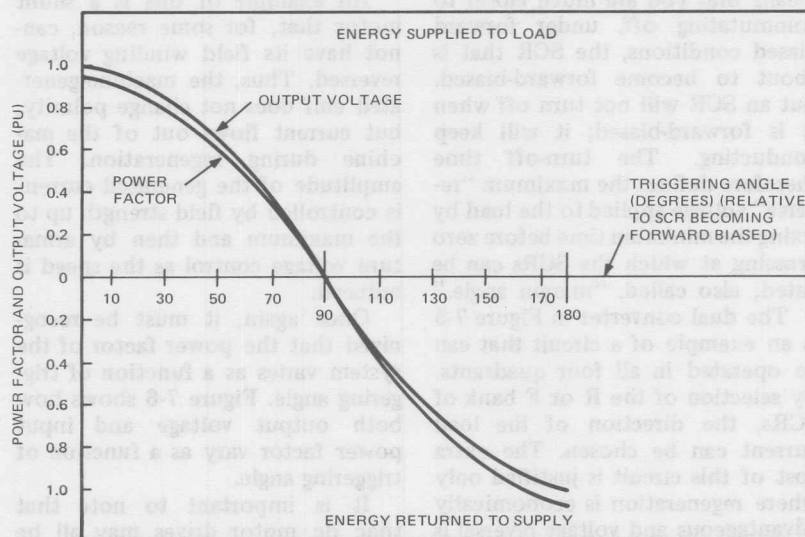


Figure 7-6. Power Factor vs. Triggering Angle

BRUSHLESS MOTOR DRIVES [3]

The brushless self-synchronous motor developed for propulsion applications has characteristics which approximate those of dc traction motors. By providing high torque at low speed and having very high-speed capability, it makes an ideal traction machine. This machine also may be easily cooled (for instance, by oil cooling) since all windings, both field and armature, may be made stationary on the stator. The basic motor system is shown in the block diagram of Figure 7-7. It consists of a polyphase synchronous machine, a switching matrix composed of silicon controlled rectifiers (or triacs) and a triggering system coupled to the output shaft of the motor. The solid state switching matrix performs the power switching function normally accomplished by the commutator of a

dc machine. The triggering system relates the switching to the rotor position so as to apply power to the motor winding at the proper time to develop maximum torque. This function in a conventional dc machine is accomplished by means of the rotating commutator and brushes.

Figure 7-8 shows schematically what the motor and the thyristor connections look like. Essentially, the normal motor configuration has been turned inside out without changing any of the basic characteristics. The normally rotating armature and commutator are on the outside of the machine, while the field winding rotates. Obviously another version of such a machine, rather than having a dc supply to the rotor, could use alternate bars of magnetic material and non-magnetic material to produce the same

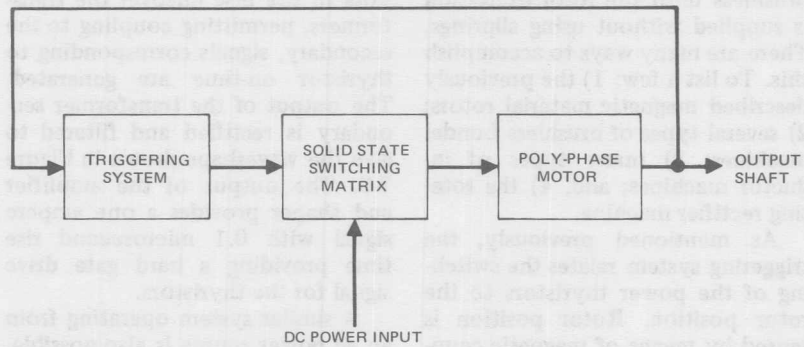


Figure 7-7. Basic Brushless Motor Drive System

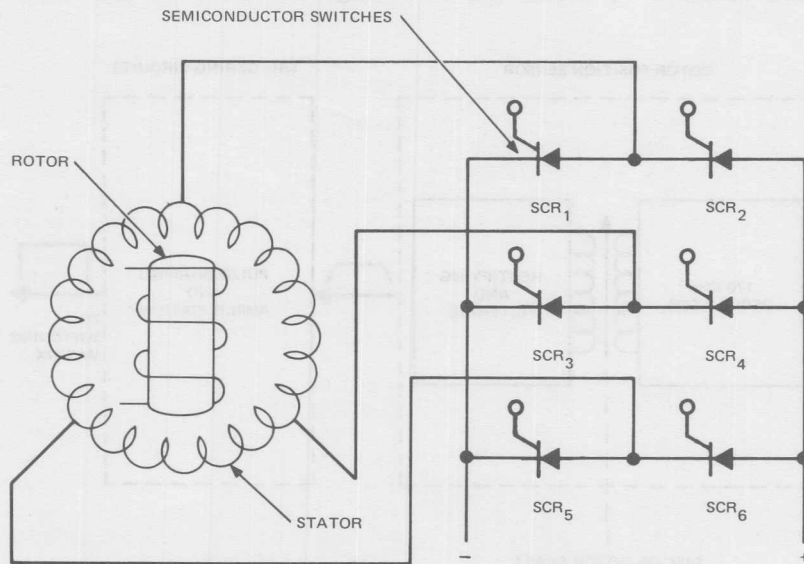


Figure 7-8. Motor and Thyristor Connections

effect. However, the motor input windings are now stationary, and the rotor or rotating field is the torque producing member. This motor configuration is not strictly brushless until the rotor excitation is supplied without using sliprings. There are many ways to accomplish this. To list a few: 1) the previously described magnetic material rotors; 2) several types of brushless Lundel machines; 3) many types of inductor machines; and, 4) the rotating rectifier machine.

As mentioned previously, the triggering system relates the switching of the power thyristors to the rotor position. Rotor position is sensed by means of magnetic coupling in six small cup core transformers. The primaries of these transformers are energized by a 170 kHz oscillator. A slotted disc at-

tached to the rotor rotates in such a way as to make and break the magnetic coupling in the primary and secondary of each of these small cup core transformers. As the slots in the disc uncover the transformers, permitting coupling to the secondary, signals corresponding to thyristor on-time are generated. The output of the transformer secondary is rectified and filtered to give the waveshape shown in Figure 7-9. The output of the amplifier and shaper provides a one ampere signal with 0.1 microsecond rise time providing a hard gate drive signal for the thyristors.

A similar system operating from an ac power source is also possible. This system is shown in Figure 7-10. Notice that in the ac system, there is essentially a full wave bridge connected to each motor

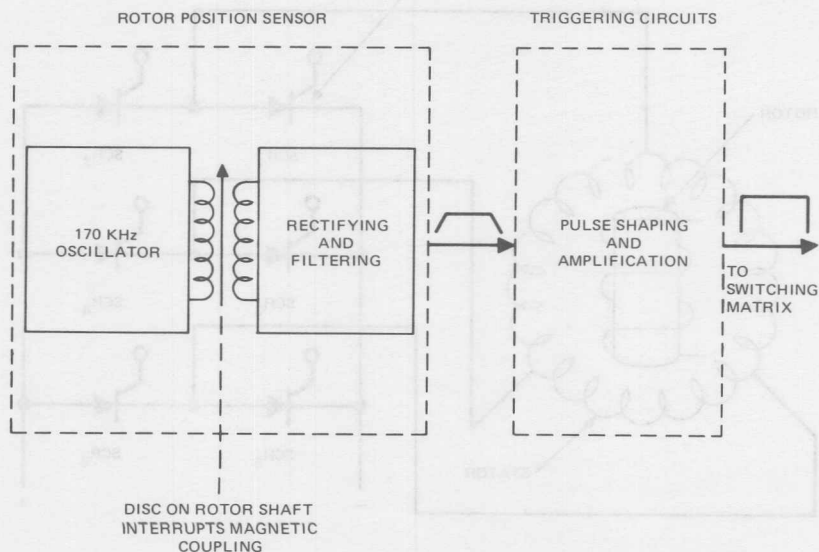
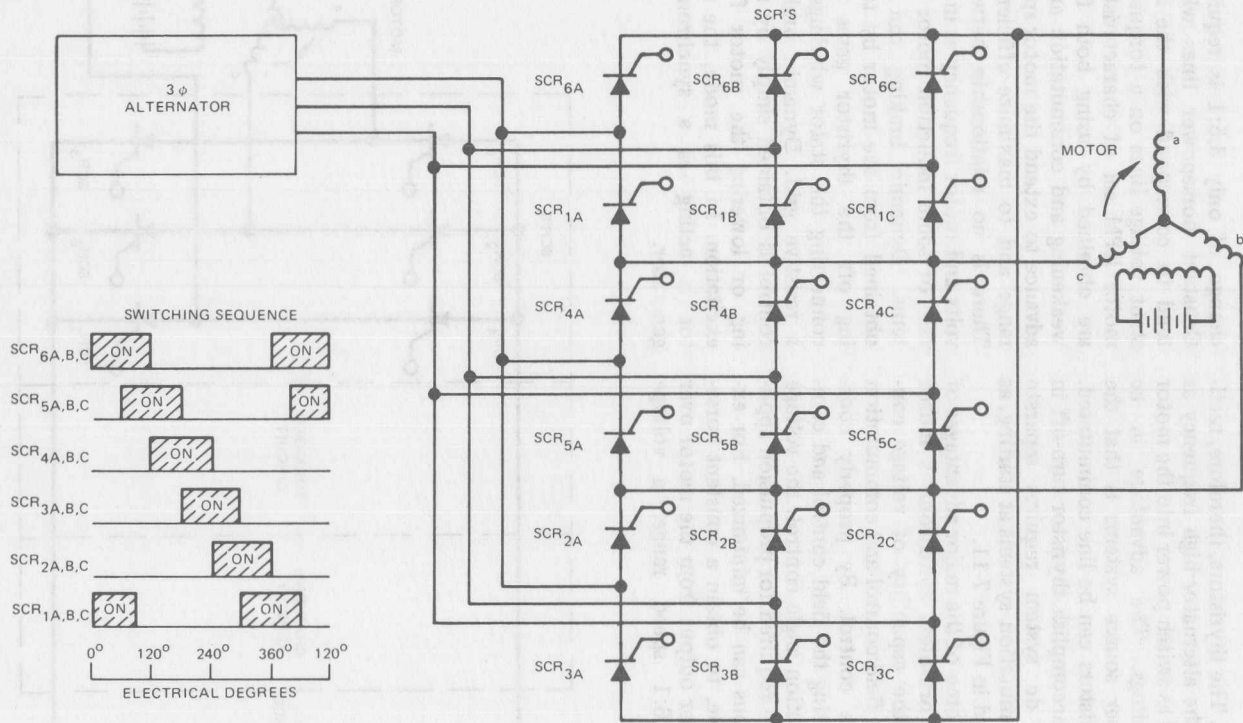


Figure 7-9. Position Sensor and Triggering Circuits

Figure 7-10. AC Input Brushless Motor



line. The thyristors, therefore, rectify the alternator high frequency as well as switch power into the motor windings. The advantage in ac power source systems is that the thyristors can be line commutated. To accomplish thyristor turn-off in the dc system requires separate commutation systems at starting, as noted in Figure 7-11.

Some of the major advantages of the brushless synchronous motor are the capability of voltage control, field control and commutation angle control. By properly coordinating the field control and commutation angle control, the voltage range required for propulsion applications can be minimized. For example, to obtain a constant horsepower output from the motor over a 16:1 speed range, a voltage

change of only 3.5:1 is required. Constant horsepower lines which tend to correspond with the constant voltage lines on a torque vs. motor RPM set of characteristics, are obtained by using both field weakening and commutation angle advance to extend the motor speed range and to maximize efficiency. There is no relationship between volts and motor frequency as in the case of some induction motor systems. Dynamic braking can be obtained from the motor by turning off the thyristor gates and connecting the stator windings to a resistive grid. Dynamic braking control is obtained simply by raising or lowering the motor field excitation. In this mode, the motor is acting as a synchronous generator.

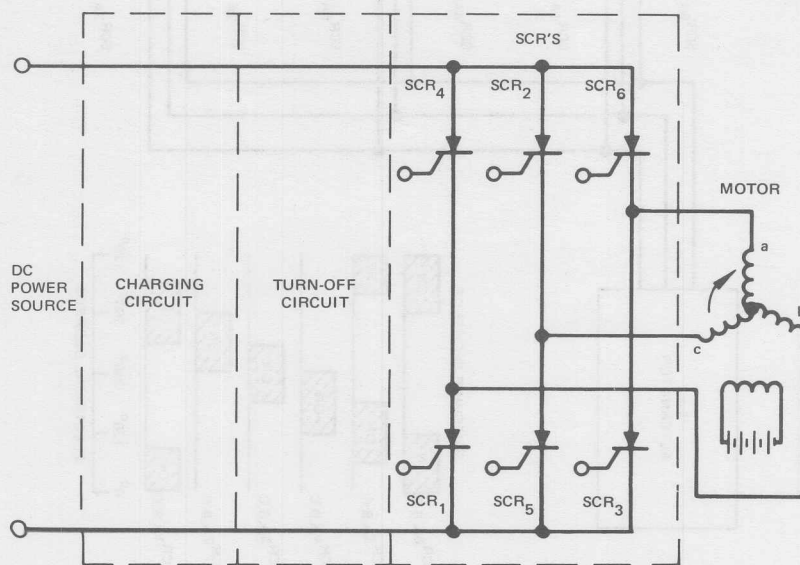


Figure 7-11. DC Input Brushless Motor

CYCLOCONVERTERS

Basic Systems

For years, cycloconverters were built with grid-controlled mercury arc rectifiers. The use of cycloconverters to transform a higher frequency to a lower frequency gradually fell from popularity because of the limited power inversion capability of mercury arc rectifiers at that time and because of the bulk and relative complexity of the cycloconverter systems. With the advent of thyristors, interest in the circuit sprang forth again. The first use of the system to any degree was for VSCF applications — variable speed, constant frequency supplies for aircraft. Closed loop, controlled slip, variable frequency induction motor drives were the next important application although, of course, the VSCF system also required the unit to drive induction motors. A

number of manufacturers began to develop circulating current-free reversing dc armature supplies which were essentially three-phase to single-phase cycloconverters. Three basic cycloconverter circuits are shown in Figure 7-12.

The advent of integrated circuits for the solid state control circuitry has made the use of the cycloconverter much more practical. The basic bias shift method of phase control is used to obtain a linear transfer characteristic between input control voltage and average cycloconverter output voltage. This method basically consists, for any given thyristor, of electronically summing a cosine wave voltage of line frequency and the dc control or bias voltage. A level detector is used to trigger a single shot multivibrator at the instant of the positive going zero-crossing of the out-

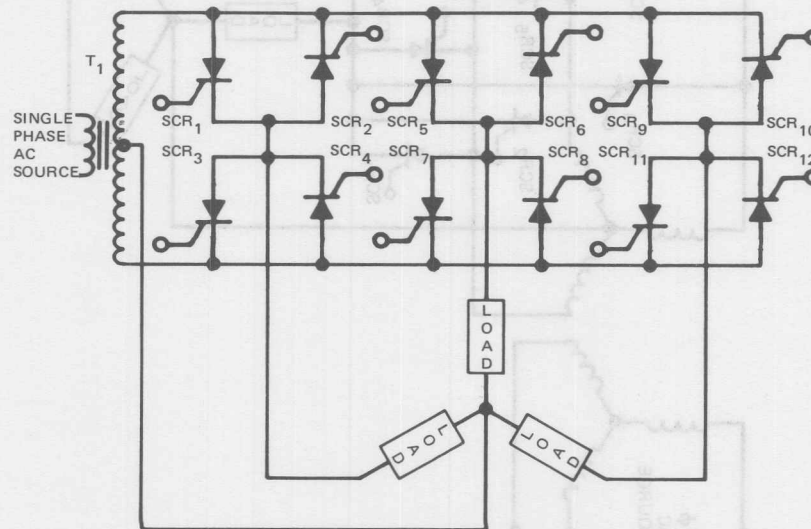


Figure 7-12(a). Cycloconverter Circuit: Single Way with Single Phase Input and Three-Phase Output

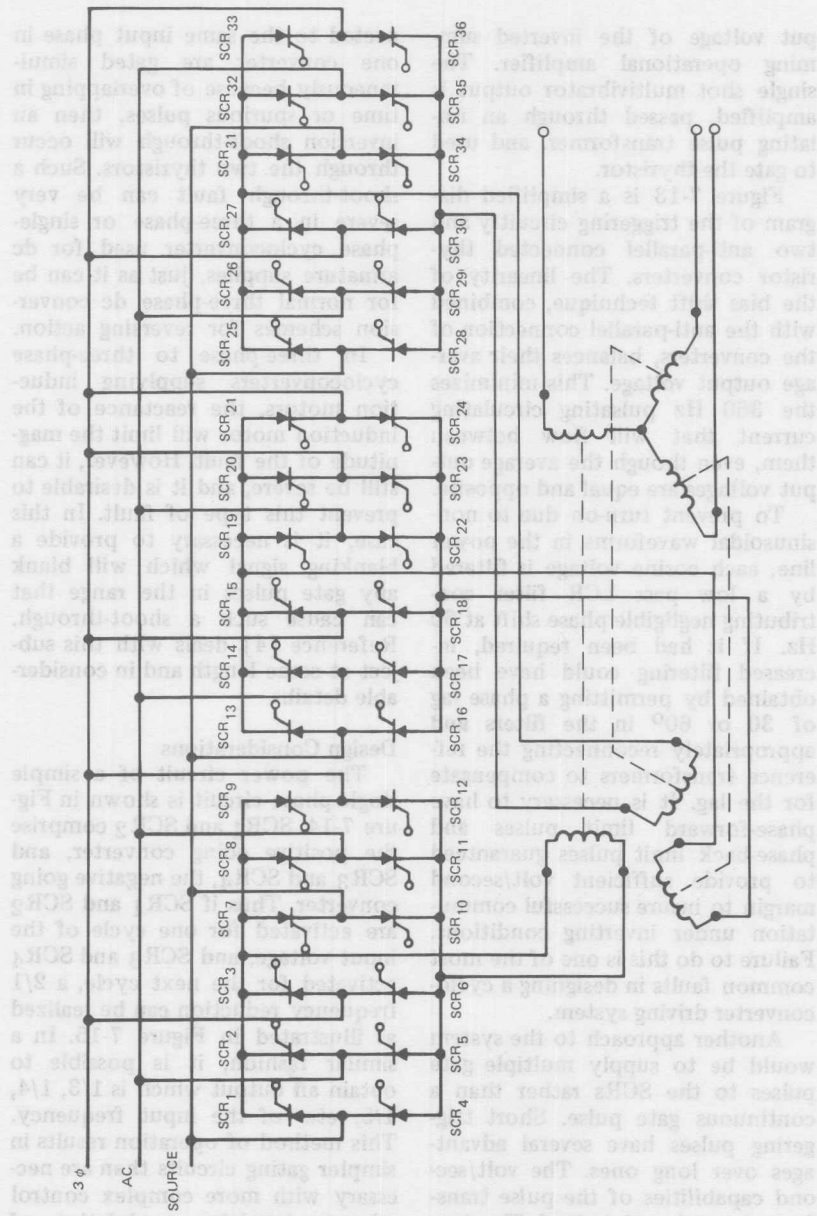


Figure 7-12(c). Cycloconverter Circuit: Double Way, with Three-Phase Input and Three-Phase Output

put voltage of the inverted summing operational amplifier. The single shot multivibrator output is amplified, passed through an isolating pulse transformer, and used to gate the thyristor.

Figure 7-13 is a simplified diagram of the triggering circuitry and two anti-parallel connected thyristor converters. The linearity of the bias shift technique, combined with the anti-parallel connection of the converters, balances their average output voltage. This minimizes the 360 Hz pulsating circulating current that will flow between them, even though the average output voltages are equal and opposite.

To prevent turn-on due to non-sinusoidal waveforms in the power line, each cosine voltage is filtered by a low pass LCR filter contributing negligible phase shift at 60 Hz. If it had been required, increased filtering could have been obtained by permitting a phase lag of 30 or 60° in the filters and appropriately reconnecting the reference transformers to compensate for the lag. It is necessary to have phase-forward limit pulses and phase-back limit pulses guaranteed to provide sufficient volt/second margin to insure successful commutation under inverting conditions. Failure to do this is one of the most common faults in designing a cycloconverter driving system.

Another approach to the system would be to supply multiple gate pulses to the SCRs rather than a continuous gate pulse. Short triggering pulses have several advantages over long ones. The volt/second capabilities of the pulse transformers can be minimized. The danger of overlap of gating can be minimized. If two thyristors con-

nected to the same input phase in one converter are gated simultaneously because of overlapping in time or spurious pulses, then an inversion shoot-through will occur through the two thyristors. Such a shoot-through fault can be very severe in a three-phase or single-phase cycloconverter used for dc armature supplies, just as it can be for normal three-phase dc conversion schemes for reversing action.

In three-phase to three-phase cycloconverters supplying induction motors, the reactance of the induction motor will limit the magnitude of the fault. However, it can still be severe, and it is desirable to prevent this type of fault. In this case, it is necessary to provide a blanking signal which will blank any gate pulses in the range that can cause such a shoot-through. Reference [4] deals with this subject at some length and in considerable detail.

Design Considerations

The power circuit of a simple single-phase circuit is shown in Figure 7-14. SCR₁ and SCR₂ comprise the positive going converter, and SCR₃ and SCR₄, the negative going converter. Thus if SCR₁ and SCR₂ are activated for one cycle of the input voltage, and SCR₃ and SCR₄ activated for the next cycle, a 2/1 frequency reduction can be realized as illustrated in Figure 7-15. In a similar fashion, it is possible to obtain an output which is 1/3, 1/4, 1/5, etc. of the input frequency. This method of operation results in simpler gating circuits than are necessary with more complex control schemes involving modulation of triggering angles. With large frequency ratios, the advantage of the

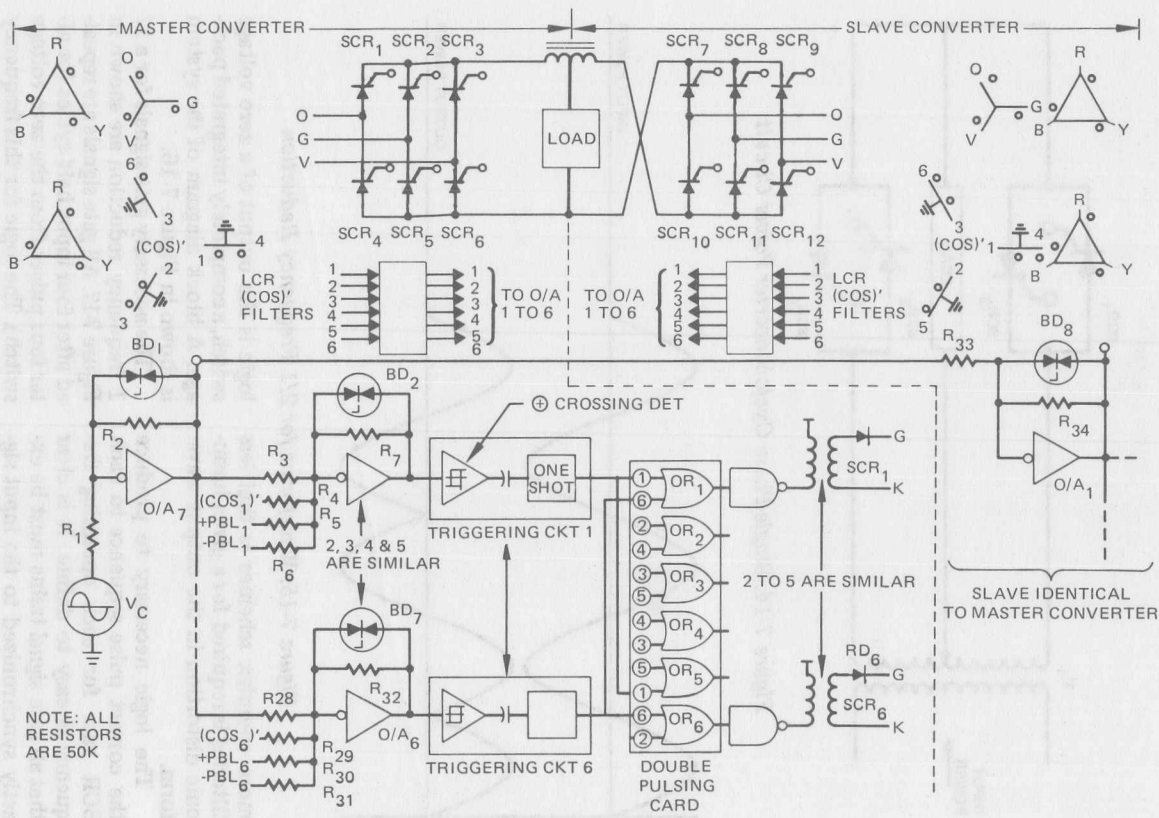


Figure 7-13. Single-Phase Output Cycloconverter

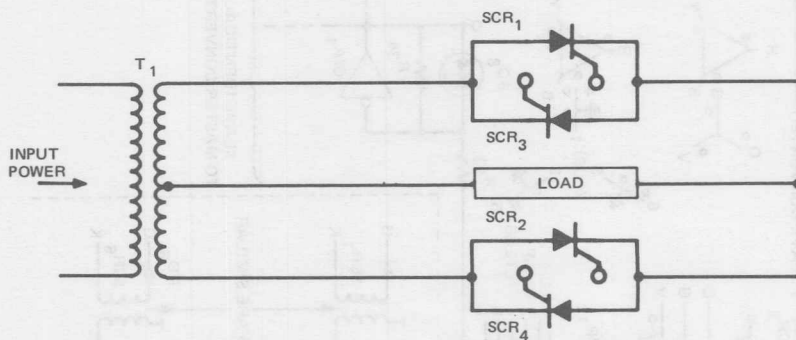


Figure 7-14. Single-Phase Cycloconverter Power Circuit

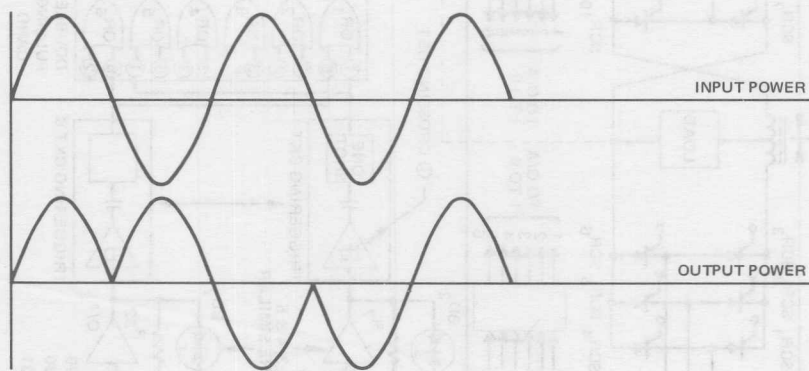


Figure 7-15. Waveforms for 2/1 Frequency Reduction

more complex schemes is that less filtering is required for a given harmonic distortion in the output waveform.

The logic necessary to produce the correct pulse sequence to each SCR gate for each operating frequency is easy to define. It is clear that all gate signal trains must be exactly synchronized to the input signal and also that each gate signal should appear at approximately the zero crossing of the input signal. Thus, a natural starting point for the

logic is the output of a zero voltage switch, a completely integrated package. A block diagram of the system is shown in Figure 7-16.

The necessary gate signals for a 2/1 frequency reduction are shown in Figure 7-17. All gate signals are repeated after four input half-cycles (or after four pulses from the zero voltage switch). The logic for this frequency should be driven by a synchronous divide-by-four counter using the zero voltage switch as the clock signal. The logic for this frequency follows:

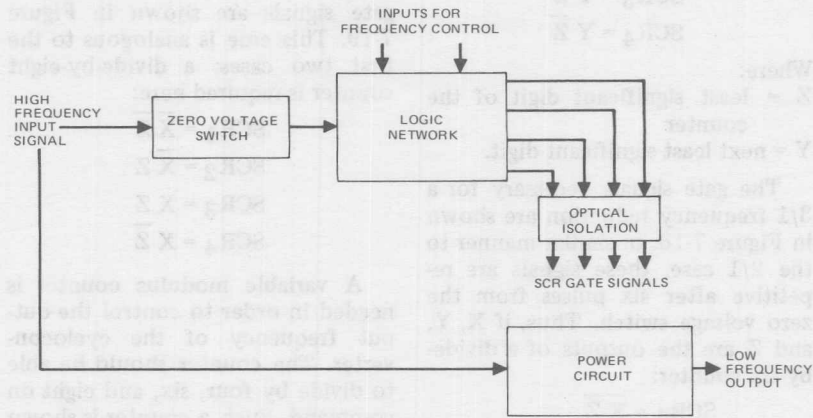


Figure 7-16. System Block Diagram

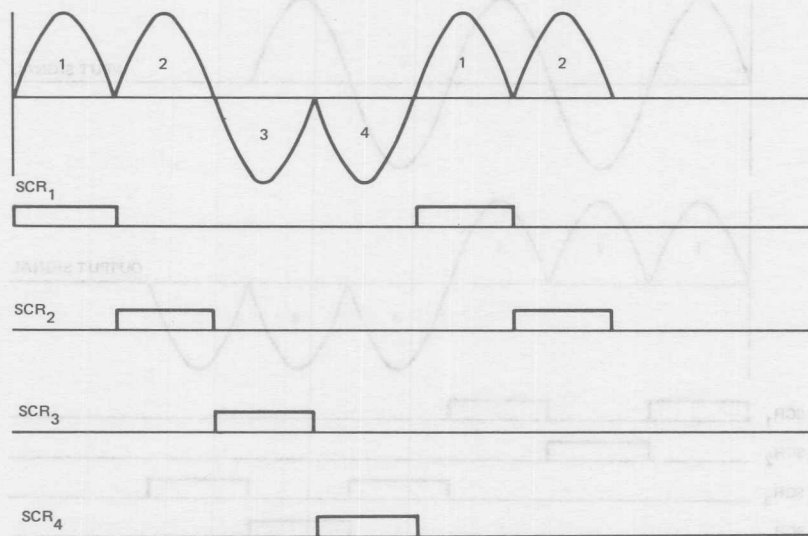


Figure 7-17. Gate Signals for 2/1 Frequency Reduction

$$\text{SCR}_1 = \overline{Y} \overline{Z}$$

$$\text{SCR}_2 = \overline{Y} Z$$

$$\text{SCR}_3 = Y \overline{Z}$$

$$\text{SCR}_4 = Y Z$$

Where:

Z = least significant digit of the counter

Y = next least significant digit.

The gate signals necessary for a 3/1 frequency reduction are shown in Figure 7-18. In similar manner to the 2/1 case, these signals are repetitive after six pulses from the zero voltage switch. Thus, if X, Y, and Z are the outputs of a divide-by-six counter:

$$\text{SCR}_1 = \overline{X} \overline{Z}$$

$$\text{SCR}_2 = \overline{X} \overline{Y} Z$$

$$\text{SCR}_3 = Y Z + X Z$$

$$\text{SCR}_4 = X \overline{Z}$$

Where:

X = third least significant digit.

For the 4/1 case, the required gate signals are shown in Figure 7-19. This case is analogous to the first two cases; a divide-by-eight counter is required here:

$$\text{SCR}_1 = \overline{X} \overline{Z}$$

$$\text{SCR}_2 = \overline{X} Z$$

$$\text{SCR}_3 = X \overline{Z}$$

$$\text{SCR}_4 = X Z$$

A variable modulus counter is needed in order to control the output frequency of the cycloconverter. The counter should be able to divide by four, six, and eight on command. Such a counter is shown in Figure 7-20. Its functions are listed in Table VII-I.

As can be seen from the power circuit, all four SCRs do not have

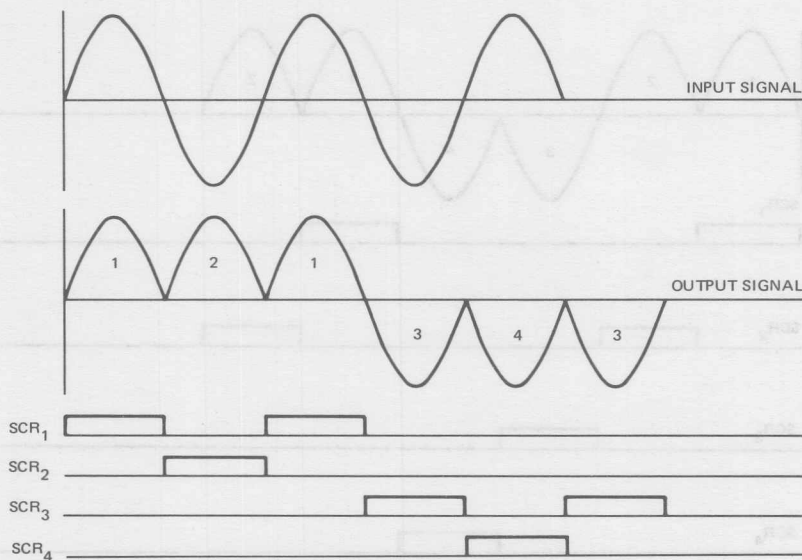


Figure 7-18. Gate Signals for 3/1 Frequency Reduction

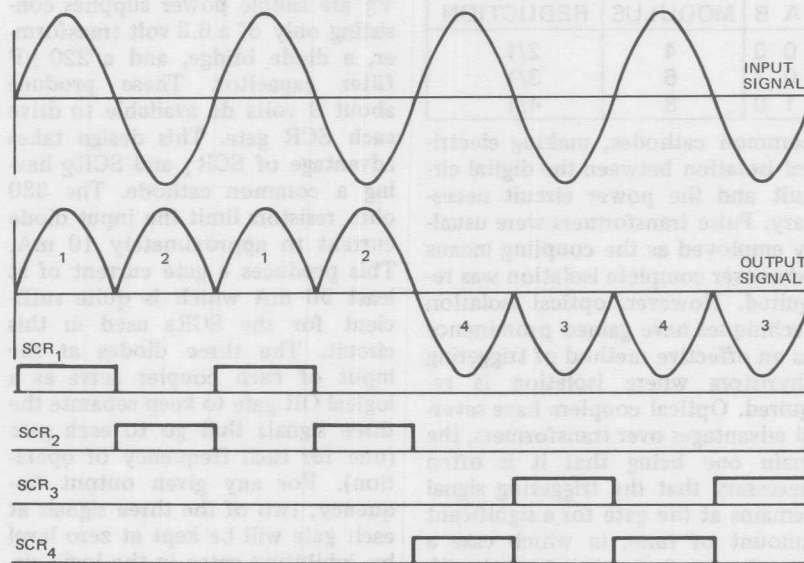


Figure 7-19. Gate Signals for 4/1 Frequency Reduction

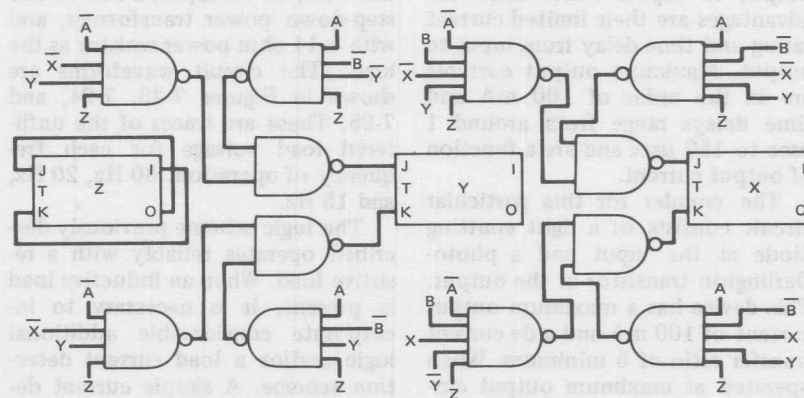


Figure 7-20. Variable Modulus Counter

Table VII-I. Functions of Modulus Counter

A	B	MODULUS	FREQUENCY REDUCTION
0	0	4	2/1
0	1	6	3/1
1	0	8	4/1

common cathodes, making electrical isolation between the digital circuit and the power circuit necessary. Pulse transformers were usually employed as the coupling means whenever complete isolation was required. However, optical isolation techniques have gained prominence as an effective method of triggering thyristors where isolation is required. Optical couplers have several advantages over transformers, the main one being that it is often necessary that the triggering signal remains at the gate for a significant amount of time, in which case a transformer design is extremely difficult. Optical couplers also have a higher frequency response, no inductance, and no feedback from output to input. Their main disadvantages are their limited current rating and time delay from input to output. Maximum output currents are in the order of 100 mA and time delays range from around 1 μ sec to 150 μ sec and are a function of output current.

The coupler for this particular circuit consists of a light emitting diode at the input and a photo-Darlington transistor at the output. This device has a maximum output current of 100 mA and a dc current transfer ratio of 5 minimum. When operated at maximum output current, it has a time delay of approximately 10 μ sec. A coupler is placed at the gate of each SCR yielding the

power and triggering circuits shown in Figure 7-21.

The voltage sources V_1 , V_2 , and V_3 are simple power supplies consisting only of a 6.3 volt transformer, a diode bridge, and a 220 μ F filter capacitor. These produce about 9 volts dc available to drive each SCR gate. This design takes advantage of SCR₁ and SCR₂ having a common cathode. The 330 ohm resistors limit the input diode current to approximately 10 mA. This produces a gate current of at least 50 mA which is quite sufficient for the SCRs used in this circuit. The three diodes at the input of each coupler serve as a logical OR gate to keep separate the three signals that go to each gate (one for each frequency of operation). For any given output frequency, two of the three signals at each gate will be kept at zero level by inhibiting gates in the logic circuit. The complete logic circuit is shown in Figure 7-22.

The circuit was operated from a 120 volt, 60 Hz input, a two-to-one step-down power transformer, and with a 14 ohm power resistor as the load. The circuit waveforms are shown in Figures 7-23, 7-24, and 7-25. These are traces of the unfiltered load voltage for each frequency of operation: 30 Hz, 20 Hz, and 15 Hz.

The logic scheme previously described operates reliably with a resistive load. When an inductive load is present, it is necessary to incorporate considerable additional logic and/or a load current detection scheme. A simple current detector is shown in Figure 7-26.

With an inductive load, the current through the positive SCR con-

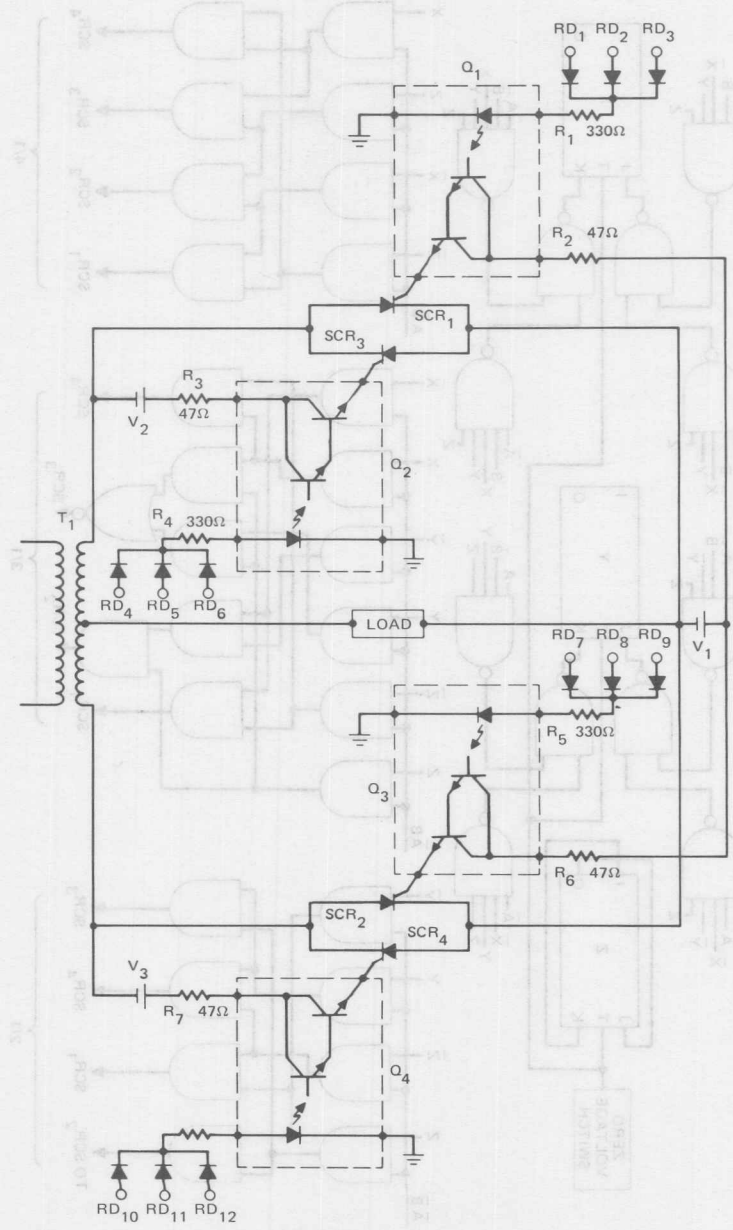


Figure 7-21. Cycloconverter Circuit Showing Optical Isolation

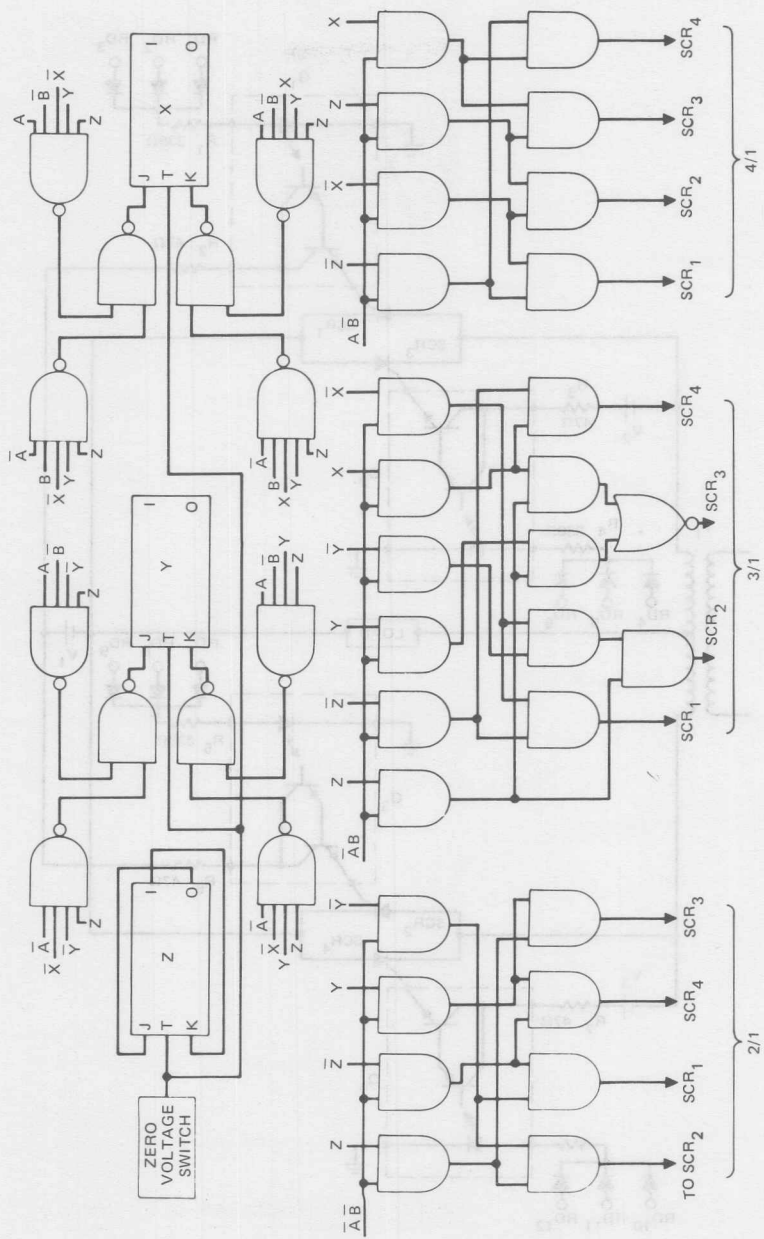


Figure 7-22. Complete Cycloconverter Logic Circuit for Resistive Load

30 Hz OUTPUT (20v/div) AND SCR₁
GATE SIGNAL (2v/div), FOR
RESISTIVE LOAD

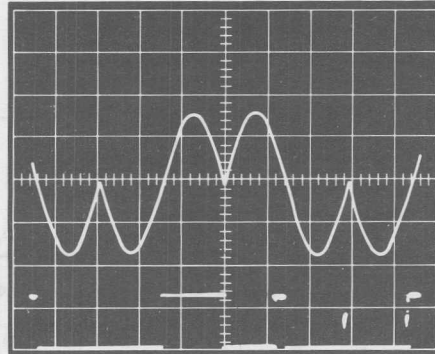


Figure 7-23. 30 Hz Output Cycloconverter Waveform

20 Hz OUTPUT (20v/div) AND SCR₂
GATE SIGNAL (2v/div) FOR
RESISTIVE LOAD

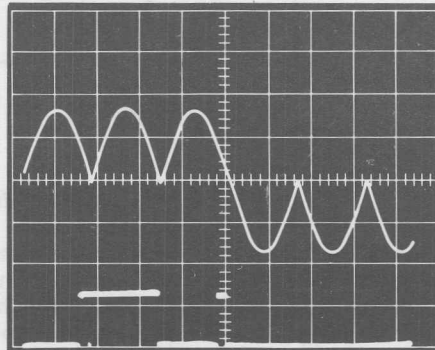


Figure 7-24. 20 Hz Output Cycloconverter Waveform

15 Hz OUTPUT (20v/div) AND SCR₁
GATE SIGNAL (2v/div) FOR
RESISTIVE LOAD

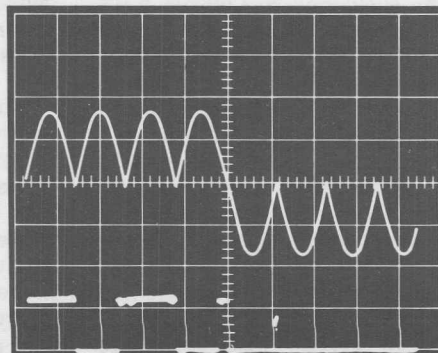


Figure 7-25. 15 Hz Output Cycloconverter Waveform

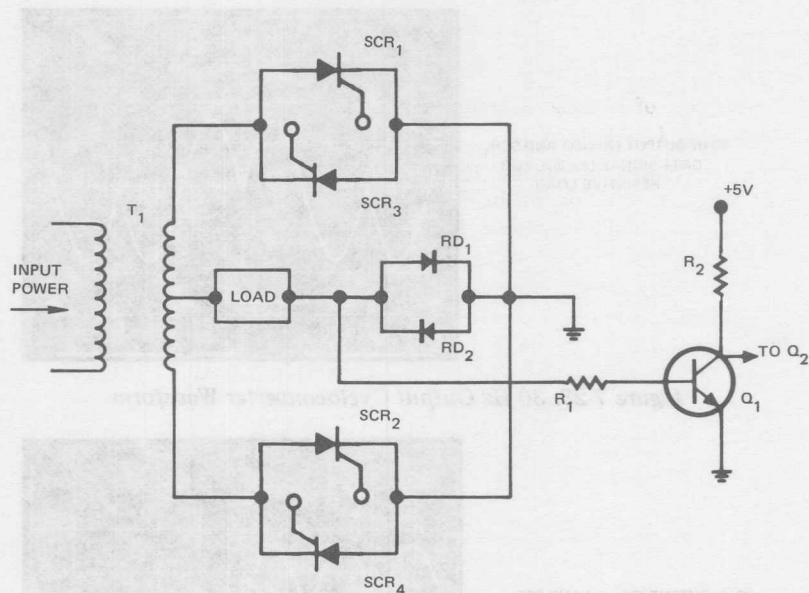


Figure 7-26. Power Circuit Showing Current Detector

verter may not go to zero for some time after the negative bank of SCRs is to begin conducting. This will cause a type of commutation failure which results in momentarily shorting the ac source voltage and which also produces distortion in the cycloconverter output waveform. Such a commutation failure can be avoided if the gate signals are inhibited until the load current goes to zero. It is also possible to operate with a circulating current using a reactor between the positive and negative SCR converters in the cycloconverter. In this mode of operation, gating signals are always applied to both the positive and negative banks of SCRs. The gate signals are such as to produce the same average load voltage regardless of which converter is conducting.

Three-Phase Cycloconverter

The gating logic is very similar for the three-phase and single-phase cycloconverters. Of course, many more SCRs are involved in poly-phase systems, and the proper phase relationship must be maintained for all SCRs in a given converter. Several typical gating schemes are illustrated in reference [4].

The SCR voltage ratings should be determined in the same fashion as for a phase controlled rectifier. However, the RMS current ratings may be reduced by $\sqrt{2}$, since each converter in a cycloconverter is conducting for only half the time. If the cycloconverter is operated at a very low frequency, the SCR current ratings should be the same as that for a simple phase controlled rectifier of the same configuration.

References

1. B.D. Bedford and R.C. Hoft, "Principles of Inverter Circuits," Wiley, 1964, Chapter 3.
2. Bryan Bixby, "Improve Efficiency in Power Control by Returning the Load Energy to the Source," *Electronic Design* 15, July 20, 1972, pp. 54-57.
3. D. Cooper, "State of the Art in Power Conversion Equipment," International Rectifier, 1969.
4. T.M. Hamblin and T.H. Barton, "Cycloconverter Control Circuits," *IEEE Transactions on Industry Applications*, July/August, 1972, pp. 443-453.
5. William McMonroy, "The Theory and Design of Cycloconverters," MIT Press, 1972.
6. B.R. Pelly, "Thyristor Phase-Controlled Converters and Cycloconverters," Wiley, 1971.



A vacuum evaporator used during the epitaxial growth of SCR junctions.

Forced Commutated Inverters

Modern thyristors make it feasible to produce power conversion systems with a variety of outputs, greater efficiency, higher reliability, and extremely fast response to control signals. Although all areas of the power conversion technology have been enhanced, dc-ac inverters have received the greatest boost from the application of power semiconductors. The solid-state inverter is one of the most sophisticated thyristor application areas. It is most demanding in terms of device characteristics, including short turn-off time, low switching loss, high dv/dt capability, and the ability to withstand rapid increases in on-state current. A great variety of circuit techniques are now available for the design of inversion equipment.

BASIC CIRCUITS

Parallel Inverter

The parallel capacitor-commutated inverter is one of the oldest

forced commutated inverters. It is described at length in reference [1] and in the additional literature cited in [1]. It is briefly described here to illustrate its important features compared with other forced commutated inverters. A basic circuit is shown in Figure 8-1.

SCR_1 and SCR_2 are alternately turned on to connect the dc source voltage to one-half of the transformer primary and then the other, producing a square wave voltage on the load. Assuming that SCR_1 is on, the commutating capacitor C_1 is also charged to a voltage which would equal twice the source voltage E_{DC} , neglecting the influence of inductor L_1 . SCR_1 is commutated when SCR_2 is triggered as this connects the charged commutating capacitor C_1 across SCR_1 to reverse bias this SCR causing it to turn off. During the SCR_2 conducting period, the capacitor is charged to the opposite polarity, ready to commutate off SCR_2 when SCR_1 is

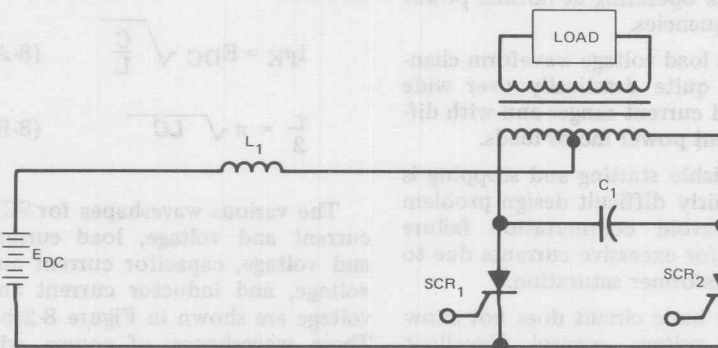


Figure 8-1. Parallel Inverter Circuit

triggered. The major purpose of L_1 is to limit the commutating capacitor charging current during switching. In fact, often a relatively large L_1 is used such that the dc source current is almost constant. This ensures commutation over a reasonable load range and minimizes oscillations in the commutating capacitor voltage.

There are many variations in the basic circuit shown in Figure 8-1 for single phase and polyphase systems. However, it does illustrate the important features of this class of forced commutated inverters. Summarizing the advantages and disadvantages of the parallel capacitor-commutated inverter:

- A. It is one of the simplest forced commutated inverters and it is a feasible approach where the load power factor is near unity and where the magnitude of the load is relatively constant.
- B. A reasonably sinusoidal load voltage can be produced with the use of an output filter.
- C. Gradually, the dc inductor L_1 , and the commutating capacitor C_1 are relatively large for circuits operating at normal power frequencies.
- D. The load voltage waveform changes quite drastically over wide load current ranges and with different power factor loads.
- E. Reliable starting and stopping is a fairly difficult design problem to avoid commutation failure and/or excessive currents due to transformer saturation.
- F. The basic circuit does not allow for voltage control. Excellent control can be achieved with the

addition of phase controlled SCRs on the transformer secondary.

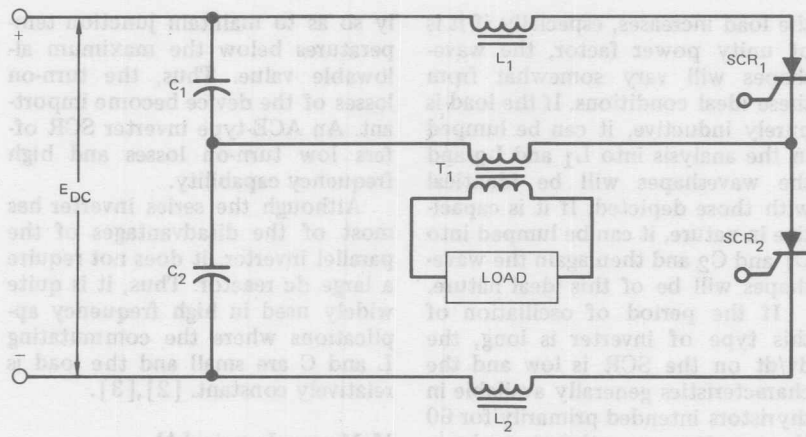
Series Inverter

Another forced commutated circuit is the series capacitor-commutated inverter. This inverter was developed using mercury arc valves. Figure 8-2 illustrates a series inverter. Assuming C_1 and C_2 are of equal magnitude and that the inductors L_1 and L_2 are also equivalent, SCR₁ switches on, resonantly discharging C_1 through L_1 and through the load which is transformer coupled to the main inverter circuit. At the same time, C_2 will charge resonantly towards the dc line potential. At the end of this conduction period then, SCR₁ will shut off when the current tries to reverse in this half of the circuit. SCR₂ is then turned on, discharging C_2 resonantly through the load and also through L_2 . During this time C_1 will resonantly charge toward the dc line potential as C_2 discharges. This will result in a peak current through the SCR given by equation 8-A and a half period of time in the circuit given by equation 8-B.

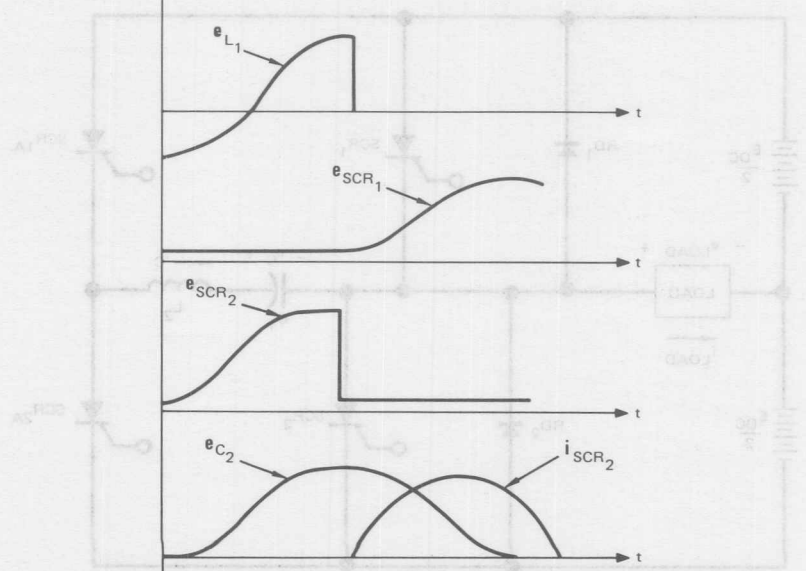
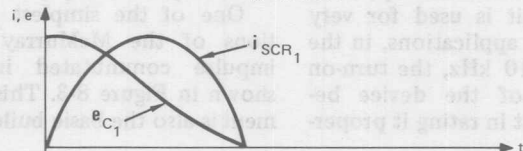
$$I_{PK} = E_{DC} \sqrt{\frac{C}{L}} \quad (8-A)$$

$$\frac{T}{2} = \pi \sqrt{LC} \quad (8-B)$$

The various waveshapes for SCR current and voltage, load current and voltage, capacitor current and voltage, and inductor current and voltage are shown in Figure 8-2(b). These waveshapes, of course, will vary with the Q of the circuit. As



(a) CIRCUIT



(b) WAVEFORMS

Figure 8-2. Series Inverter

the load increases, especially if it is of unity power factor, the waveshapes will vary somewhat from these ideal conditions. If the load is purely inductive, it can be lumped in the analysis into L_1 and L_2 and the waveshapes will be identical with those depicted. If it is capacitive in nature, it can be lumped into C_1 and C_2 and then again the waveshapes will be of this ideal nature.

If the period of oscillation of this type of inverter is long, the dv/dt on the SCR is low and the characteristics generally available in thyristors intended primarily for 60 Hz operation are satisfactory; however, if the unit is used for very high frequency applications, in the order of 5 to 10 kHz, the turn-on characteristics of the device becomes important in rating it proper-

ly so as to maintain junction temperatures below the maximum allowable value. Thus, the turn-on losses of the device become important. An ACE-type inverter SCR offers low turn-on losses and high frequency capability.

Although the series inverter has most of the disadvantages of the parallel inverter, it does not require a large dc reactor. Thus, it is quite widely used in high frequency applications where the commutating L and C are small and the load is relatively constant. [2],[3].

McMurray Inverter[4]

One of the simplest configurations of the McMurray auxiliary impulse commutated inverter is shown in Figure 8-3. This arrangement is also the basic building block

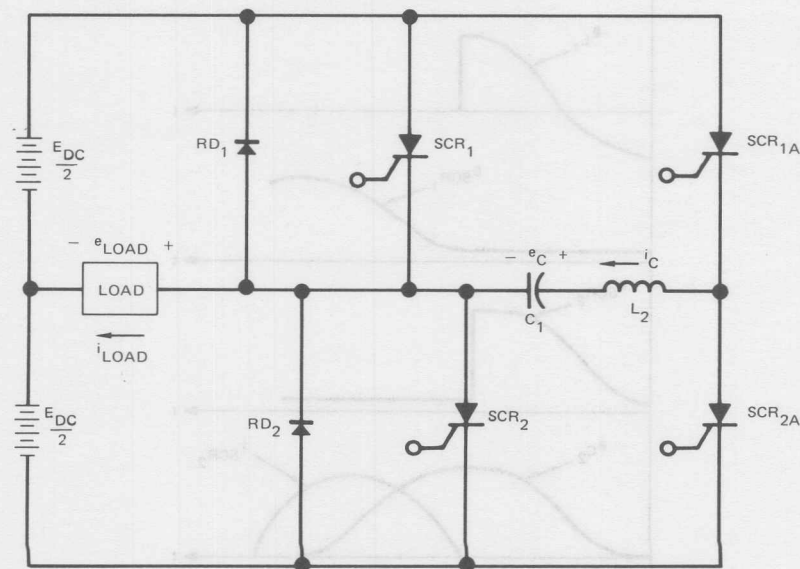


Figure 8-3. McMurray Inverter Circuit

in the single phase bridge and three phase versions of the McMurray inverter.

The basic operation of the circuit in Figure 8-3 is relatively uncomplicated. Assuming the correct initial capacitor voltage, a main SCR is commutated by gating the appropriate auxiliary SCR. When SCR_{1A} or SCR_{2A} are triggered, they cause a resonant pulse of current to flow in opposition to that being carried by the conducting main SCR. When the main SCR current has been reduced to zero, the commutating current pulse will continue to flow in the appropriate feedback or free-wheeling diode, thus providing a small reverse voltage on the main SCR for the time interval necessary for it to regain its off-state blocking capability.

Possibly the most advantageous feature of this inverter is that after a given main SCR is commutated, the capacitor voltage is left at the polarity required to commutate the next main SCR. This feature, combined with the pulsating nature of the commutating action, provides a highly efficient inverter for operation at normal power frequencies. In fact, an efficiency of over 90% can be attained, with SCR turn-off times in the 20 microsecond range, for circuit operating frequencies up to several kilohertz.

Another very advantageous feature of this inverter approach is that with the proper SCR triggering sequence, sufficient commutating capacitor voltage is assured for a wide range of load conditions.

Possibly the two most important additional configurations of the McMurray inverter are shown in Figure 8-4 and Figure 8-5. Figure 8-4 is the single phase bridge ar-

angement. This is essentially two circuits of the type shown in Figure 8-3. By using two half bridge circuits, it is not necessary to return the load to a center tap on the dc supply. The opposite leg of the bridge provides the load return path.

Figure 8-5 shows the basic three phase McMurray inverter. This contains three half bridge circuits. Thus, the circuit of Figure 8-3, is the basic building block for both the single phase bridge and the three phase McMurray inverter.

The commutating action in Figures 8-4 and 8-5 is the same as for the circuit of Figure 8-3. However, the load voltage waveforms are somewhat more involved. Possibly the simplest way to derive the load voltage waveforms is to first sketch the waveforms of the voltages of Figure 8-3. The voltages in Figure 8-5 may then be obtained by subtracting the appropriate half bridge output voltages.

Modified McMurray — Bedford Inverter [1],[5]

This circuit can best be analyzed by examining a single-phase version of this type of inverter, which is shown in Figure 8-6(a). Under steady-state conditions, assume that SCR_1 is conducting current to the load and that the capacitor C_1 is charged with a voltage equivalent to one half the supply voltage, with terminal A positive with respect to terminal B. In order to commutate SCR_1 , a gate signal is applied to SCR_2 , turning it on. At the same instant that SCR_2 is gated on, the gating signal is removed from SCR_1 , but because SCR_1 is conducting load current, it does not turn off at that instant. Thus, im-

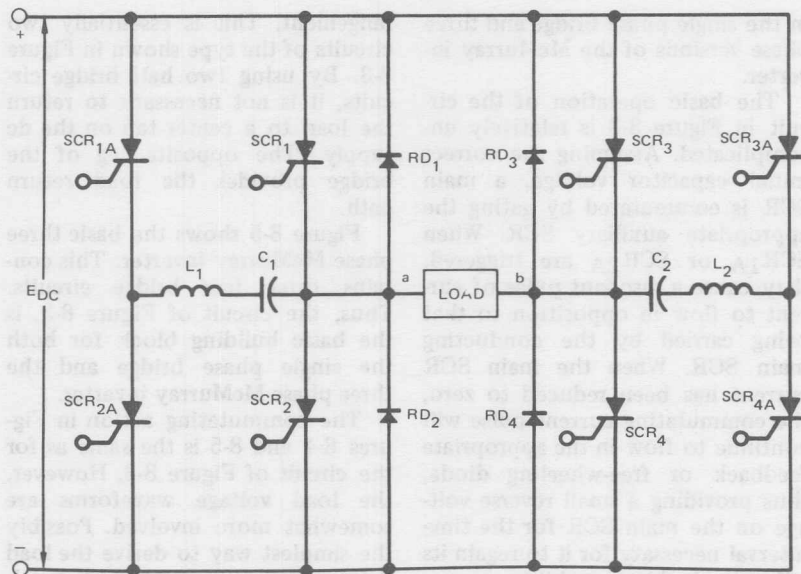


Figure 8-4. Single Phase Bridge McMurray Inverter Circuit

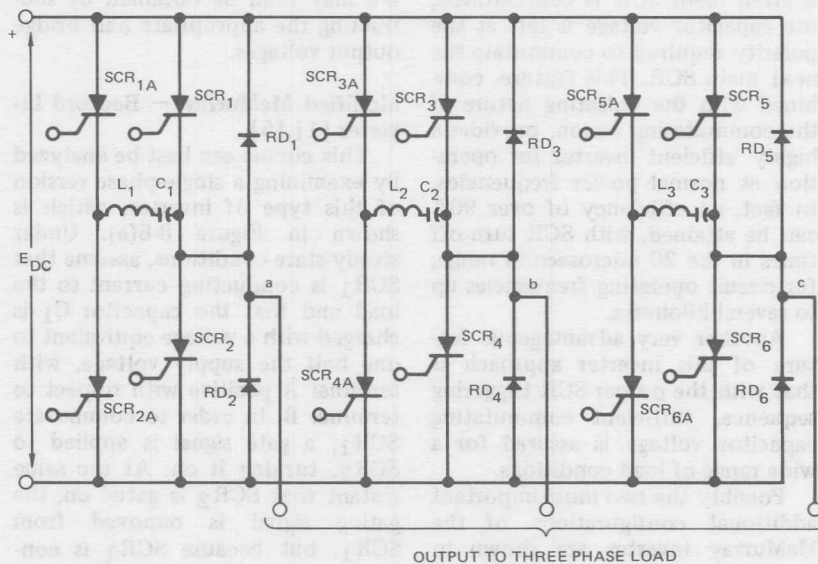


Figure 8-5. Three-Phase McMurray Inverter Circuit

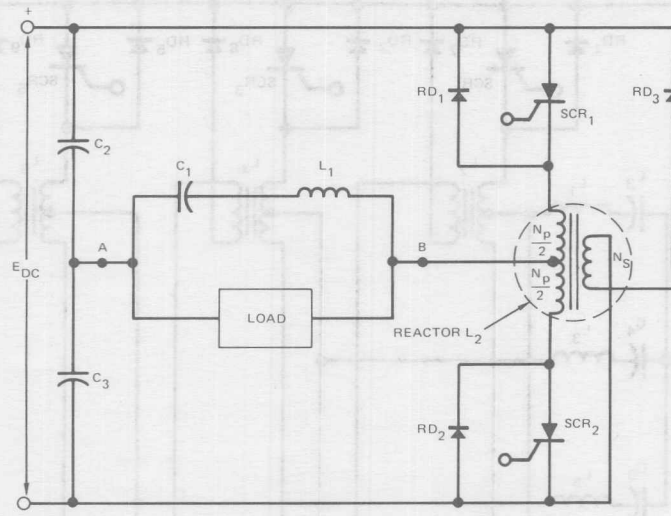


Figure 8-6(a). Single Phase Half Bridge Modified McMurray-Bedford Inverter Circuit

mediately after SCR_2 is turned on, both SCR s are conducting and the full dc supply voltage is impressed across the primary turns, N_p , of the reactor L_2 . Since the voltage across N_p is the supply voltage, E_{DC} , the center-tap point at this instant of time must be one half E_{DC} . Thus, the load voltage between A and B must be zero, since A is also at one half E_{DC} voltage. Hence, no current flows to a resistive load while both SCR s are conducting.

Just prior to the turn-on of SCR_2 , a current was flowing through the upper winding of the L_2 reactor. Immediately after turn-on of SCR_2 , the load current in SCR_1 drops to one half the load current and the current through SCR_2 jumps to one half the load current to satisfy the ampere turns of the L_2 reactor. The capacitor C_1 then begins to discharge through L_1

into the center-tap of L_2 where it divides. One half of the commutating current flows up through the upper windings of L_2 , decreasing the load current through SCR_1 , then flows back into capacitor C_1 through C_2 . The other half of the commutating current flows down through the lower half of L_2 , then back into C_1 , through C_3 . The commutating current builds up sinusoidally at a rate determined by the natural frequency of C_1 and L_1 . The current in the upper winding will build up and exceed the current to SCR_1 with the excess current flowing through diode RD_1 , back biasing SCR_1 and turning it off. The lower commutating current adds to the original lower winding current, thus maintaining the ampere turns in the L_2 reactor.

This type of circuit imposes considerably different reapplied dv/dt

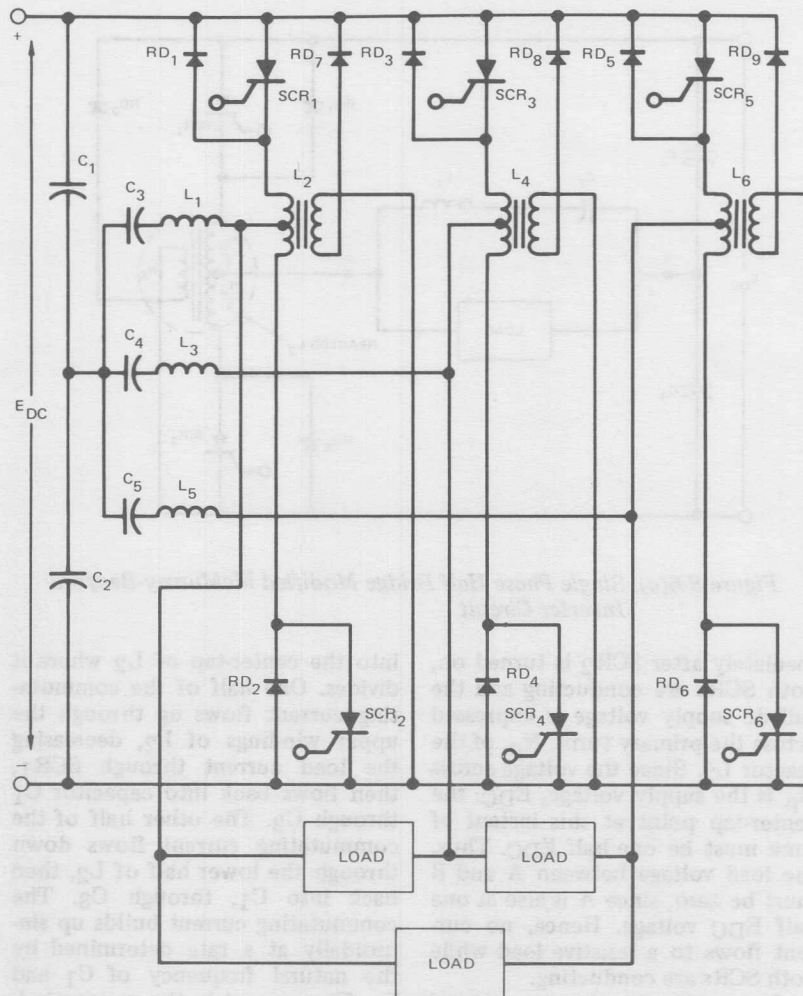


Figure 8-6(b). Three-Phase Bridge Modified McMurray-Bedford Inverter Circuit

conditions on the SCRs than was seen in a series inverter. It should also be noted that in this circuit, during turn-off of an SCR, the reverse bias on the device is simply

the forward drop of the diode which is connected in anti-parallel with it. This also imposes a different turn-off duty than was seen by the SCRs used in the previously mentioned series inverter case.

Current Source Inverter [6],[7]

A single phase version of the current source inverter circuit is shown in Figure 8-7. It is quite similar to the parallel inverter, except that the commutating capacitor is divided into two parts and diodes RD_1 and RD_4 are added. In a practical application, the circuit is driven from a rectified voltage with a large series reactor to provide low ripple in the dc bus current.

The waveforms shown in Figure 8-8 illustrate the operation with a purely resistive load R , and assuming ideal semiconductor components. At time t_0 it is assumed that SCR_1 and SCR_4 are triggered with some initial voltage on the capacitors.

A three phase version of the current source inverter circuit of Figure 8-7 is shown in Figure 8-9.

The most significant features of the current source inverter are:

- A. No commutating reactors are required.
- B. With a phase controlled rectifier supply to the dc bus and a large dc reactor in series to provide relatively constant dc current, the inverter can feed power back to the ac system since E_{DC} can have an average value of either polarity.
- C. The constant current dc provides an automatic current limit for the inverter output into a low impedance load. However, with a high impedance load, the capacitor voltage becomes large.
- D. The constant current system can provide very fast response to demanded speed changes when the inverter is supplying an ac motor. The change in speed is initiated by changing the frequency of the SCR gating oscillator and full torque is very quickly available to produce the required speed change.

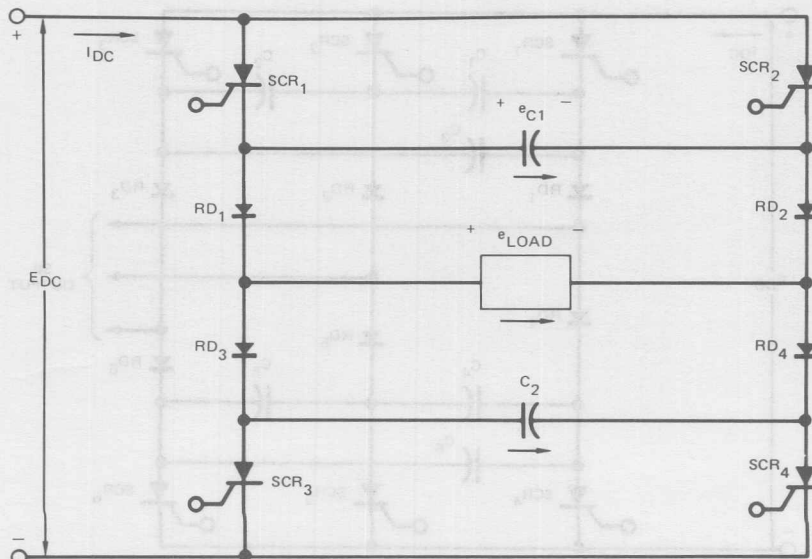


Figure 8-7. Single Phase Current Source Inverter Circuit

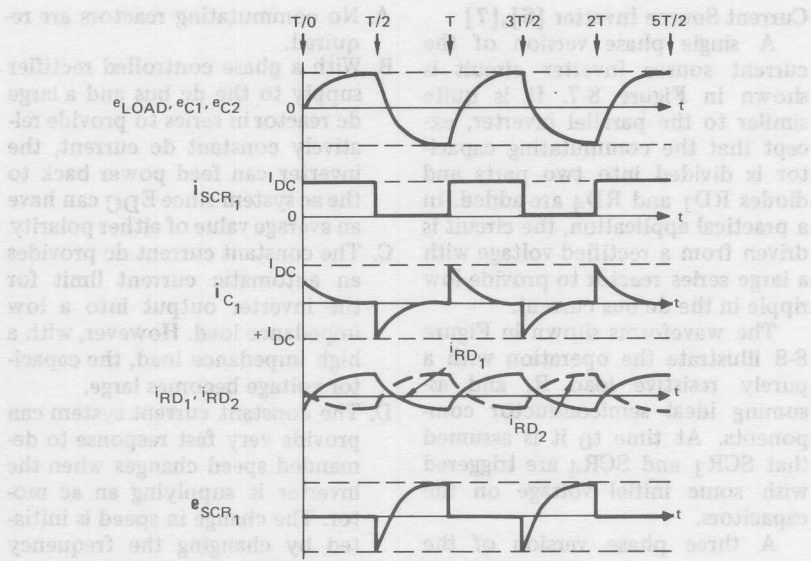


Figure 8-8. Single Phase Current Source Inverter Waveforms

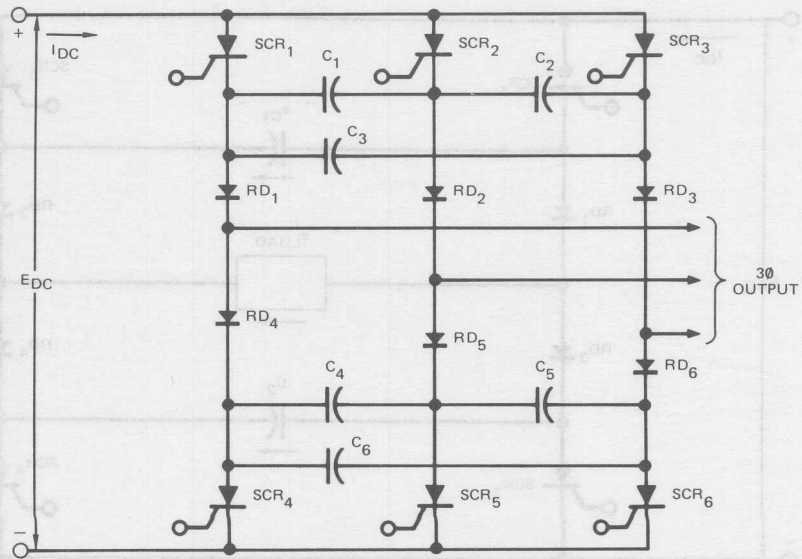


Figure 8-9. Three-Phase Current Source Inverter Circuit

Table VIII-I is a summary of forced commutated inverters. It lists the circuits discussed and compares their more important features.

FREQUENCY MULTIPLIER [8]

Thyristors are also used in frequency conversion equipment to provide power supplies for induction heating and melting applications. This system, known as a frequency multiplier, is shown in Figure 8-10. This cycloinverter uses a type of forced commutation. It has the capability of maintaining relatively constant power in the load independently of resistance changes during the work cycle. These changes can be as much as 5 per unit.

In the past, the low power factor of the loaded coil was compensated for by using series or parallel capacitance. For an output frequency

higher than 60 Hz the power supply generally used a magnetic frequency multiplier or motor generator set. The thyristor system does not have the limitations of the magnetic frequency multiplier and the m-g set systems.

The static system has high efficiency, high input power factor, small size, low maintenance, and the output frequency is variable; thus no variation in load compensating capacitance is required. A low-pass input filter provides a path for higher harmonics generated by the frequency converter, thus keeping the higher harmonics to a low level in the input lines.

A thyristor block consisting of two thyristors in an AC switch configuration is connected to each phase. The appropriate one of these thyristors can be rendered conductive when a positive or negative output voltage is desired. The posi-

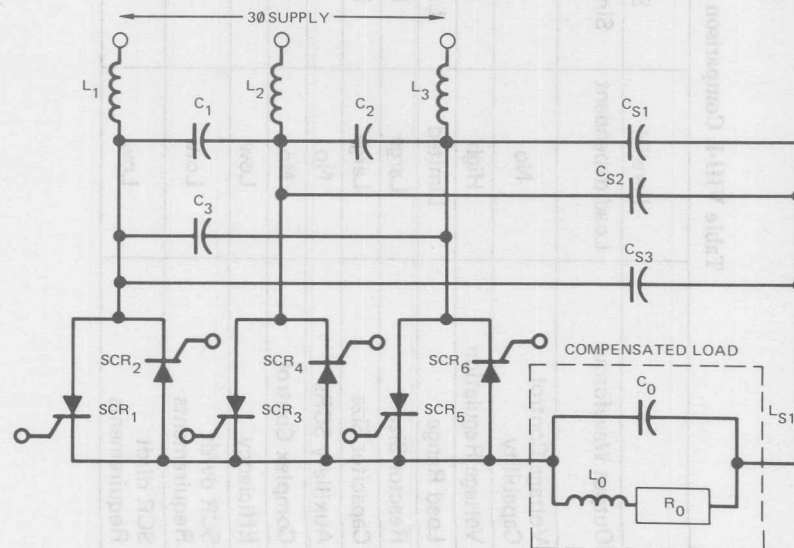


Figure 8-10. Frequency Multiplier or Cycloinverter Circuit

Table VIII-I. Comparison of Forced Commutated Inverters

	Parallel	Series	McMurray	Modified McMurray-Bedford	Current Source
Output Waveforms	Load dependent	Sinusoidal	Square	Square	Load dependent
Voltage Control Capability	No	No	Yes	No	No
Voltage Regulation	High	High	Low	Low	High
Load Range	Limited	Limited	Large	Large	Limited
Reactor Size	Large	Large	Small	Small	Large
Capacitor Size	Large	Large	Small	Small	Large
Auxiliary SCRs	No	No	Yes	No	No
Complex Control	No	No	Yes	No	No
Efficiency	Low	Low	Highest	Next Highest	Low
SCR dv/dt Requirements	Low	Low	Highest	Next Highest	Low
SCR di/dt Requirements	Low	Low	Highest	Next Highest	Low

tive and negative thyristor can be rendered conductive alternately at the desired output frequency. The parallel compensated induction heating melting load is shown connected to a ringing inductor-capacitance to achieve commutation of the thyristors. The ringing capacitors are wye connected and the wye point voltage varies at the output frequency with respect to the input supply neutral. These capacitors provide a path for the output frequency current preventing its appearance in the input lines.

The SCRs used in this type of application are, in general, required to be high voltage, fast turn-off devices, and considering the possible operating frequency for load compensation, should have extremely good turn-on capabilities and maintain high current capability at high frequency. For higher power systems, paralleling of devices might be advantageous for very large melting loads.

DC POWER SUPPLIES

Figure 8-11 is a circuit for conversion from 1,500 volt dc to 37.5 and 75 volt regulated dc for auxiliary power on a moving vehicle [9]. If it is assumed that all capacitors are charged initially, SCR₁ is turned-on, discharging C₂ through L₁ and L₂, and C₃ through L₂ at the same time that power is supplied to transformer T₁ through SCR₁. Both capacitors will charge negatively, thus shutting off SCR₁. C₅ and C₆ will, of course, reflect this charge in the opposite direction. R₁ is simply to suppress parasitic oscillations in the circuit. The bottom half of the converter will operate exactly as the top half.

It should be noted that C₂ and RD₃, and also RD₄ and C₅, act as dv/dt suppressors across SCR₁ and SCR₂ at the same time they form part of the commutation circuitry. Should the system be operated on a supply with high transient voltages, the gate and regulating circuitry can be equipped with a static high voltage interlock to stop trigger pulses during the transient condition, thus allowing SCR₁ and SCR₂ to form a series SCR pair to hold off the excess line voltage.

Figure 8-12 shows a high voltage inverter power supply. Triggering SCR₁ and SCR₄ simultaneously applies the input voltage E_{DC} to the load transformer T₁ and the commutation capacitor C₅. Turning on SCR₂ and SCR₃ on the opposite sides of the inverter causes the charge on C₅ to reverse bias SCR₁ and SCR₄, turning them off. Figure 8-12(b) shows the resulting trapezoidal voltage waveshape applied to the diode bridge RB₁. Figure 8-12(c) shows the current during the recovery period.

Since a square wave is applied to the diode bridge, the diodes will see a fast rising reverse voltage during their commutation interval. A high value of recovery current will result in a high instantaneous power dissipation. Therefore, fast recovery diodes should be utilized in the output bridge.

Figure 8-13 is an inverter dc power supply using soft commutation techniques [9]. This type of circuit has the capability of being designed, using high frequency SCRs, for extremely high repetition rates while maintaining relatively low dynamic stress on the devices and emitting low electrical noise.

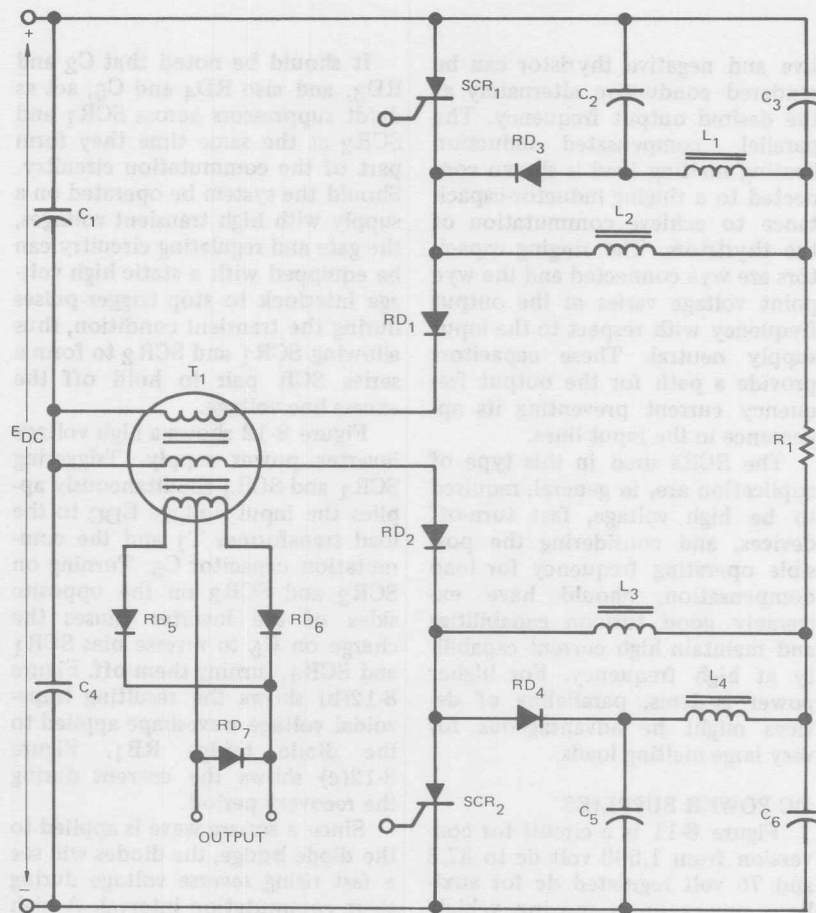


Figure 8-11. Vehicle Auxiliary Power DC Supply Circuit

The circuit waveforms are shown in Figure 8-14.

When SCR₁ is triggered on, at the beginning of time interval t_1 , with SCR₂ off, a series-resonant circuit is connected to the dc supply. The voltage across windings L₂ and L₃ will initially back bias SCR₂ and RD₁ respectively. The capacitor voltage sinusoidally charges up towards twice E_{DC} minus the ini-

tial voltage on the capacitor. The voltage across the transformer winding L₁ is the difference between the input voltage E_{DC} and the capacitor voltage. As the capacitor charges up to a value greater than the input voltage, the voltage across L₁ reverses polarity.

At some time after SCR₁ is triggered on and the magnitude of the voltage on the capacitor is larger

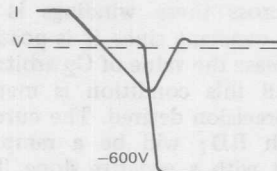
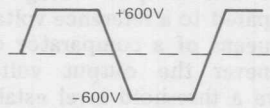
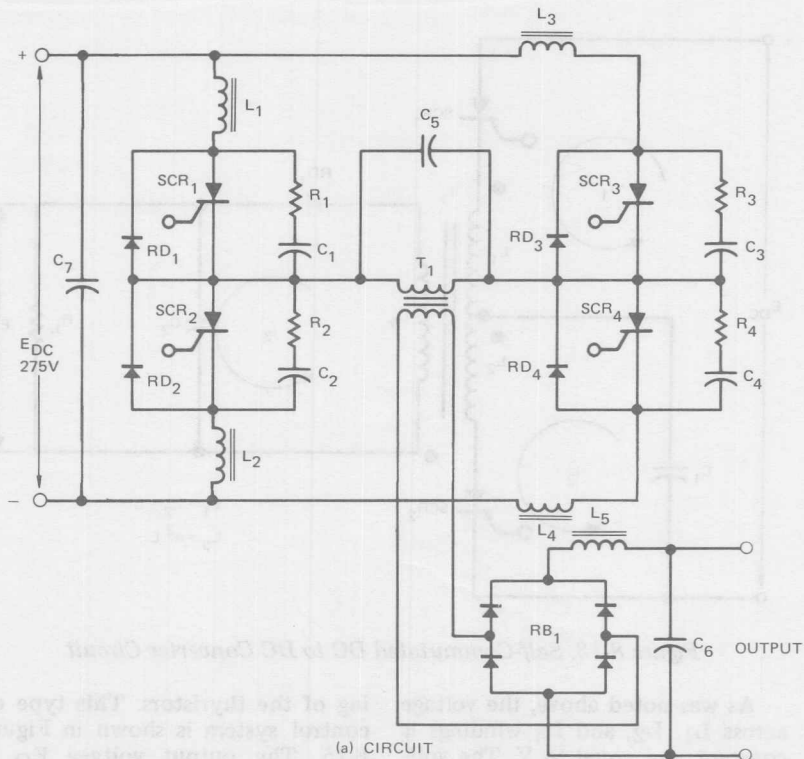


Figure 8-12. High Voltage Inverter Power Supply

than E_{DC} , the voltage across winding L_3 is of sufficient magnitude to forward bias RD_1 . At t_2 , when RD_1 conducts, the voltage of the windings will be clamped to the output voltage E_0 assuming that first $L_1 = L_2$; second, $L_3 = n^2L$; third, C_2 is much greater than C_1 ; and lastly, effects of leakage react-

ances are neglected. The current through SCR_1 will decrease to zero since any further current flow through SCR_1 will continue to charge capacitor C_1 and increase the reverse bias appearing across SCR_1 . SCR_1 then commutates off. The energy that has been stored in L_1 is now discharged to the load through RD_1 .

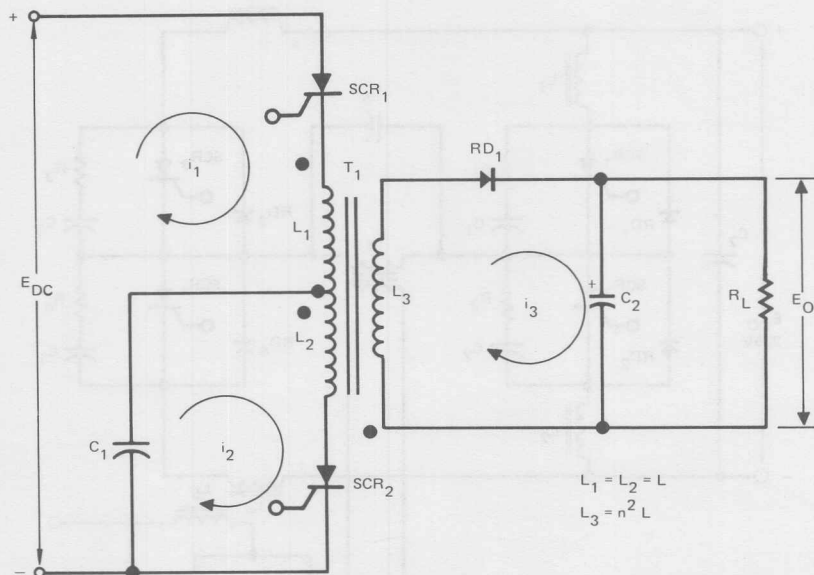


Figure 8-13. Self-Commutated DC to DC Converter Circuit

As was noted above, the voltage across L_1 , L_2 , and L_3 windings is constant and equal to V . The voltage across these windings is assumed constant since it is possible to increase the value of C_2 arbitrarily until this condition is met at with precision desired. The current through RD_1 will be a ramp of current with a negative slope. This current is allowed to relax to zero before SCR_2 is triggered on. SCR_2 is triggered at t_3 to repeat the cycle and reverse the voltage across C_1 . Energy is stored in L_2 ; SCR_2 commutates off and a ramp of current is discharged through RD_1 . The voltage across C_1 is now at its initial value. After the current through RD_1 has relaxed to zero, SCR_1 can now be retriggered.

The output voltage E_O can be regulated by controlling the trigger-

ing of the thyristors. This type of control system is shown in Figure 8-15. The output voltage E_O is compared to a reference voltage E_R by means of a comparator circuit. Whenever the output voltage is above a threshold level established by the reference, the comparator output biases the gate circuit in a manner to inhibit the free-running pulse generator. In addition, a signal is derived from the voltage appearing across L_3 , such that at any time RD_1 is conducting the gate circuit is biased to inhibit the blocking oscillator. The maximum frequency of the free-running pulse generator is equal to the maximum frequency of operation of the system. When the system is operating in a voltage regulated mode, the system frequency is less than maximum. Thus the output voltage is

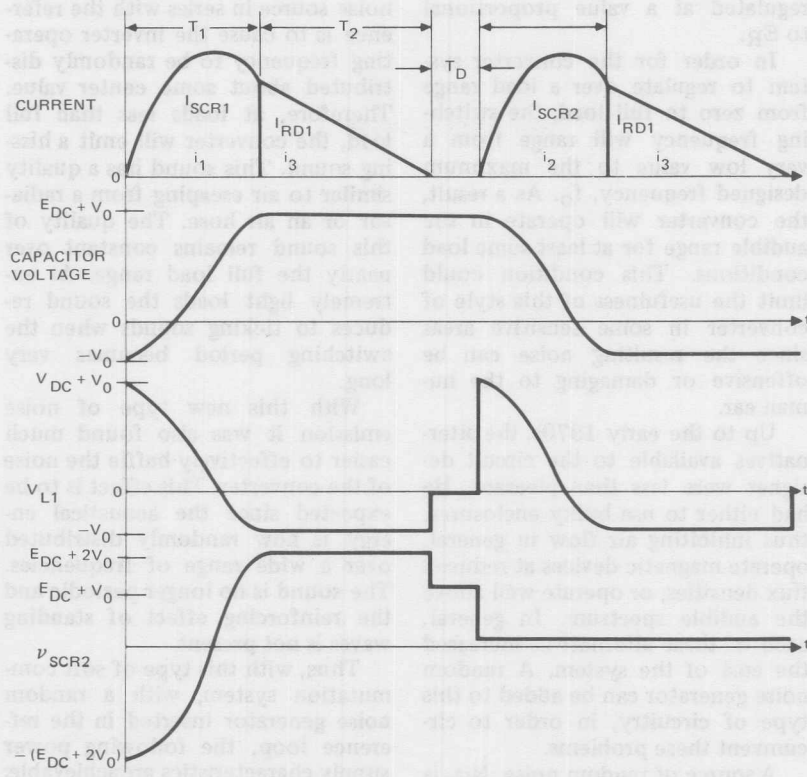


Figure 8-14. Circuit Waveforms for DC to DC Converter

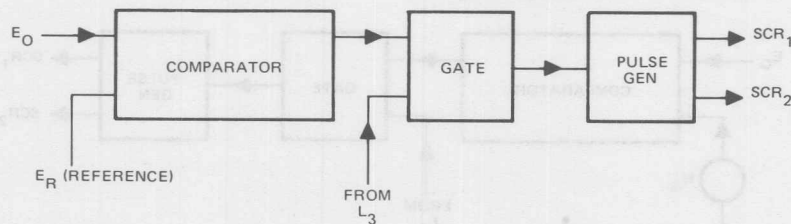


Figure 8-15. Diagram of DC to DC Converter

regulated at a value proportional to E_R .

In order for the converter system to regulate over a load range from zero to full load, the switching frequency will range from a very low value to the maximum designed frequency, f_O . As a result, the converter will operate in the audible range for at least some load conditions. This condition could limit the usefulness of this style of converter in some sensitive areas since the resulting noise can be offensive or damaging to the human ear.

Up to the early 1970s, the alternatives available to the circuit designer were less than pleasant. He had either to use bulky enclosures, thus inhibiting air flow in general, operate magnetic devices at reduced flux densities, or operate well above the audible spectrum. In general, each of these alternatives increased the cost of the system. A random noise generator can be added to this type of circuitry, in order to circumvent these problems.

A source of random noise, N_G , is connected in series with the reference voltage E_R as shown in Figure 8-16. The long-term average voltage of this source is zero, therefore the long-term average output voltage will not differ if the source is shorted out. The effect of putting this

noise source in series with the reference is to cause the inverter operating frequency to be randomly distributed about some center value. Therefore, at loads less than full load, the converter will emit a hissing sound. This sound has a quality similar to air escaping from a radiator or an air hose. The quality of this sound remains constant over nearly the full load range. At extremely light loads the sound reduces to ticking sounds when the switching period becomes very long.

With this new type of noise emission it was also found much easier to effectively baffle the noise of the converter. This effect is to be expected since the acoustical energy is now randomly distributed over a wide range of frequencies. The sound is no longer periodic and the reinforcing effect of standing waves is not present.

Thus, with this type of soft commutation system, with a random noise generator inserted in the reference loop, the following power supply characteristics are achievable:

- A. The rate of reapplied forward dv/dt and the rate of current rise during the turn-on di/dt , for the thyristor devices, are a function of L and C only and are independent of the load.

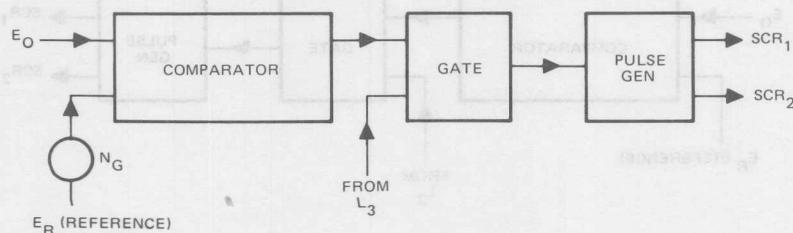


Figure 8-16. Diagram of DC to DC Converter with Random Noise Source

- B. The minimum turn-off time is independent of the load.
- C. The RF energy developed across the diode RD₁ can be minimized.
- D. The load impedance, R_L, can be varied from zero to infinity.
- E. High di/dt in the thyristors is avoided by permitting the current in the commutating inductances L₁ and L₂ to relax to zero, before triggering the thyristors.
- F. By decoupling the load from the main charging thyristors, the system results in being short circuit stable.
- G. Single frequency tones have been eliminated from the acoustical spectrum of the converter. The audible sound emitted by the converter is considerably altered by this procedure and results in a converter which produces less acoustical annoyance.

Induction Heating Supply Design Example [3],[11],[12]

Figure 8-17 shows the block diagram for a high frequency inverter for induction cooking. The main design constraints are the upper operating frequency, which is limited by present device technology, and the lower operating frequency which is set by the acoustic noise generated in the circuit. The present frequency limit on power semiconductor switching is approximately 50 kHz, and acoustic noise is obtained below 20 kHz. One other important constraint when considering a consumer product is cost. For this reason the minimum number of components must be selected while meeting the circuit requirements. Also, the system should be well shielded to prevent undesirable RFI.

The cooking unit uses induction heating principles. Thermal energy

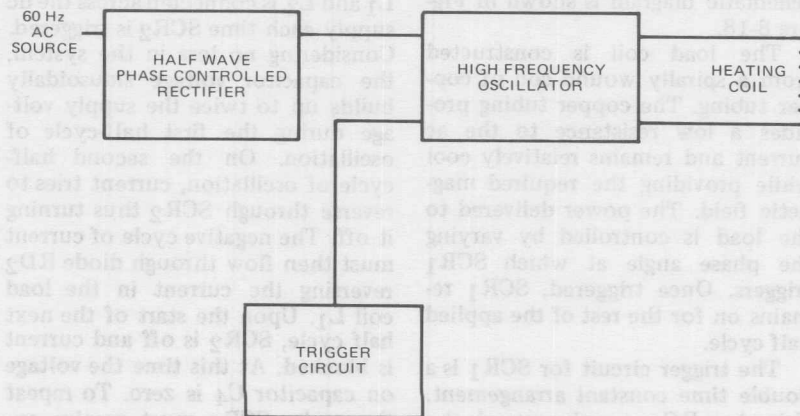


Figure 8-17. Induction Heating Cooking Unit Block Diagram

is generated within the metal of the cooking vessel by means of a strong high frequency magnetic field. The magnetic field sets up eddy currents that circulate within the vessel, heating its surface but not the circuit components. The magnetic field is produced by varying an electric current in a coil. This is accomplished by means of a series, single SCR inverter, which operates at a fixed resonant frequency. The amount of current flowing in the load coil is varied by changing the input dc voltage supplied to the series resonant circuit. This is accomplished using a half wave phase controlled rectifier circuit. The half wave circuit is sufficient to meet the necessary voltage requirements; thus it is used because of its simplicity and relatively low cost. However, half-wave loading of the power line may be undesirable.

The series inverter is triggered by a basic UJT relaxation oscillator with a frequency fixed just above the audio range, thus keeping acoustic noise to a minimum. The schematic diagram is shown in Figure 8-18.

The load coil is constructed from a spirally wound coil of copper tubing. The copper tubing provides a low resistance to the ac current and remains relatively cool while providing the required magnetic field. The power delivered to the load is controlled by varying the phase angle at which SCR₁ triggers. Once triggered, SCR₁ remains on for the rest of the applied half cycle.

The trigger circuit for SCR₁ is a double time constant arrangement. Using two RC networks extends the range of gating control to something greater than 90°. This allows

the voltage applied to the inverter to be reduced effectively to zero. Triggering capacitor C₁ is recharged by capacitor C₂ after every trigger pulse. The voltage on C₁ builds up to a value slightly less than the breakdown voltage of DIAC₁, resulting in a relatively constant positive reference voltage, from which C₁ is recharged again to the diac triggering point. The circuit components are chosen to produce a phase shift as close to 180° as possible while simultaneously maintaining the voltage across C₁ above the 32 volts required to trigger the diac. This output is then filtered by capacitor C₃ to obtain a usable dc. Wave forms for the half-wave, phase controlled rectifier are shown in Figure 8-19.

The series, single SCR inverter was chosen for its simplicity and relatively low cost. Its principle of operation is quite old but it works exceptionally well with today's power semiconductors.

A series resonant circuit, consisting of capacitor C₄, and inductors L₁ and L₂, is connected across the dc supply each time SCR₂ is triggered. Considering no loss in the system, the capacitor voltage sinusoidally builds up to twice the supply voltage during the first half-cycle of oscillation. On the second half-cycle of oscillation, current tries to reverse through SCR₂ thus turning it off. The negative cycle of current must then flow through diode RD₂ reversing the current in the load coil L₁. Upon the start of the next half cycle, SCR₂ is off and current is blocked. At this time the voltage on capacitor C₄ is zero. To repeat the cycle, SCR₂ must receive another trigger pulse from the trigger circuit. Therefore, for each pulse

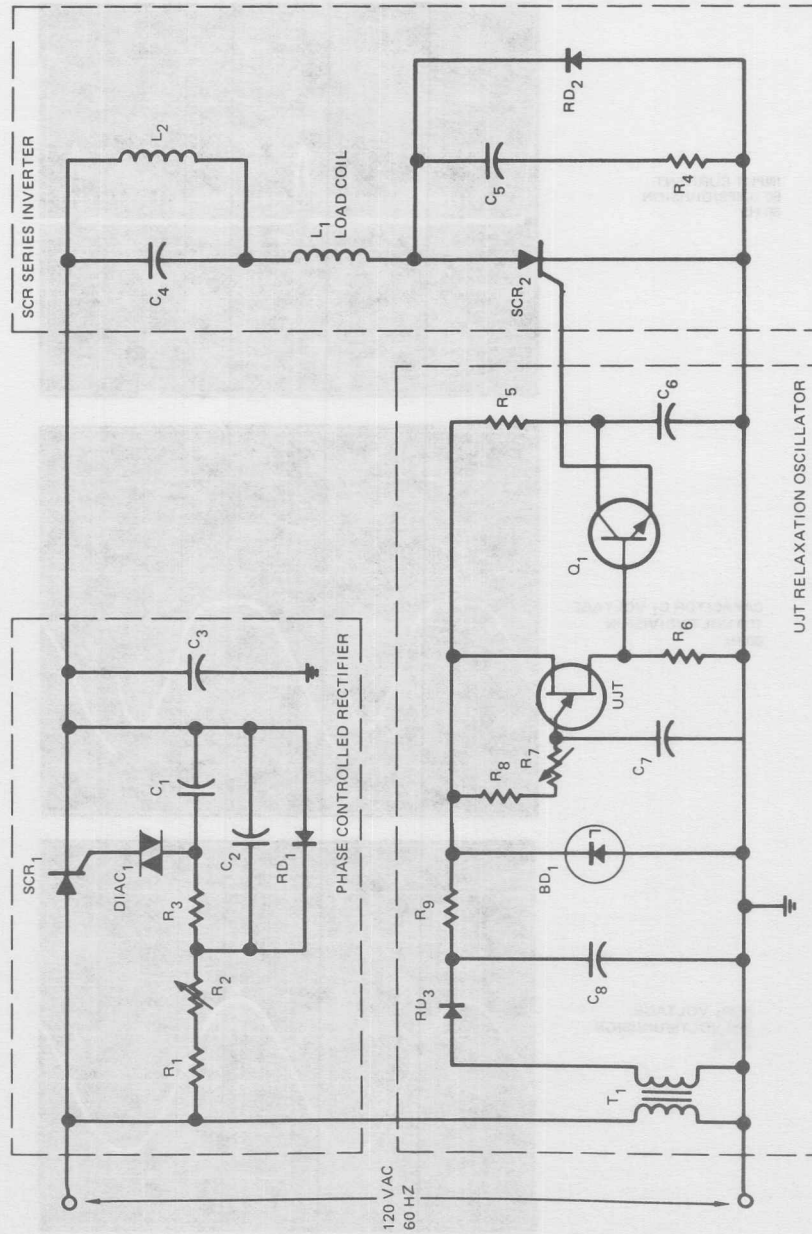


Figure 8-18. Induction Heating Cooking Unit Circuit

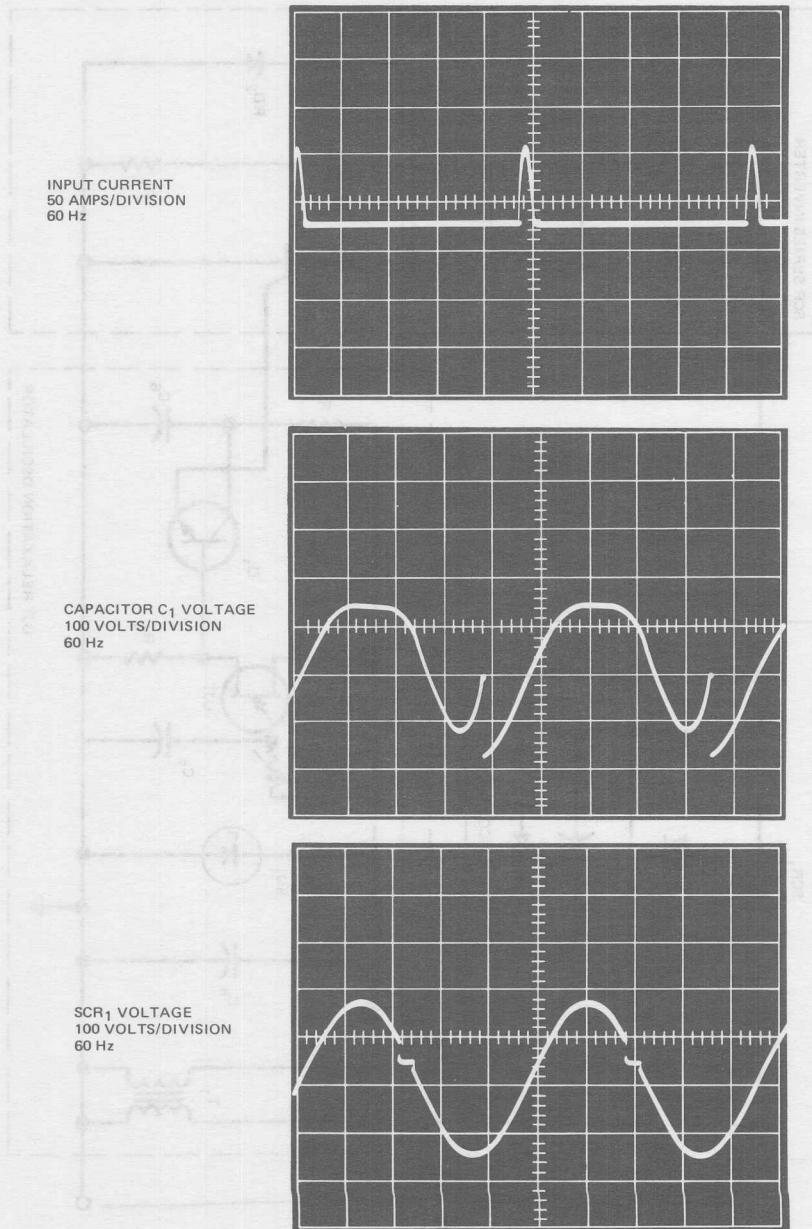


Figure 8-19. Induction Heating Phase Controlled Rectifier Waveforms

from the UJT oscillator, there is one complete cycle of current through the load coil.

With no cooking vessel near the load coil, the diode half-cycle average current I_{RD2} is nearly equal to SCR_2 's half-cycle average current I_{SCR2} . The total current is $I_{DC} = I_{SCR2} - I_{RD2}$. When a load is placed on the load coil the SCR current, I_{SCR2} , increases while the diode current, I_{RD2} , decreases and the total current from the dc supply increases.

The basic design parameters are:

- f_o = resonant frequency of capacitor C_4 with inductor L_1 .
- E_{DC} = dc supply voltage
- I_M = peak current through L_1
- f_t = frequency of the trigger circuit

The resonant frequency f_o was chosen equal to 35 kHz for which, from formula 8-C, time on equals 28.6 μ sec.

$$\tau = \frac{1}{f_o} = 28.6 \mu\text{sec} \quad (8-C)$$

The circuit will only operate properly when the current is less than zero for at least the turn-off time of the SCR. This is required for SCR_2 to regain its off-state blocking capability at the end of every other half-cycle. Therefore, the maximum turn-off time for SCR_2 has to be less than $\tau/2$ or approximately 14 μ sec.

The peak value of the SCR current is given in formula 8-D:

$$I_M = \sqrt{\frac{E_{DC}}{\frac{L_1}{C_4}}} \quad (8-D)$$

The circuit was designed to produce a peak current of 100 A. Thus, the greatest required value of the dc supply voltage is $E_{DC} = 100 \sqrt{L/C}$.

The resonant frequency determines the LC product as shown in formula 8-E:

$$f_o = \frac{1}{2\pi\sqrt{LC}} \quad (8-E)$$

$$LC = \left(\frac{0.159}{35 \times 10^3}\right)^2$$

With the heating coil L_1 equal to 6 μ H and thus $C_4 = 3.45 \mu$ F, the greatest value of the dc supply voltage is $E_{DC} = 100 [1.32] = 132$ volts. These values are assuming that the resistance of the circuit is approximately zero.

The choice of L_2/L_1 depends on several factors. If L_2/L_1 is low then the cost of L_2 will be low but the turn off time for SCR_2 will be reduced. An increase in L_2/L_1 will result in an increase in cost plus an increase in size. Therefore L_2/L_1 is selected at about 50. This is large enough so that L_2 does not affect the resonance of L_1 and C_4 at the present operating frequency.

Waveforms for the inverter are shown in Figure 8-20.

Many different triggering circuits could be used to produce the necessary 20 kHz pulse, capable of triggering SCR_2 . The relaxation UJT oscillator has been selected here for its reliability and simplicity. Q_1 is used as a current amplifier to drive the SCR gate circuit. Capacitor C_7 is charged through R_7 and R_8 until the emitter voltage of the UJT reaches V_p , at which time it turns on and discharges C_7 through R_6 . When the emitter voltage drops be-

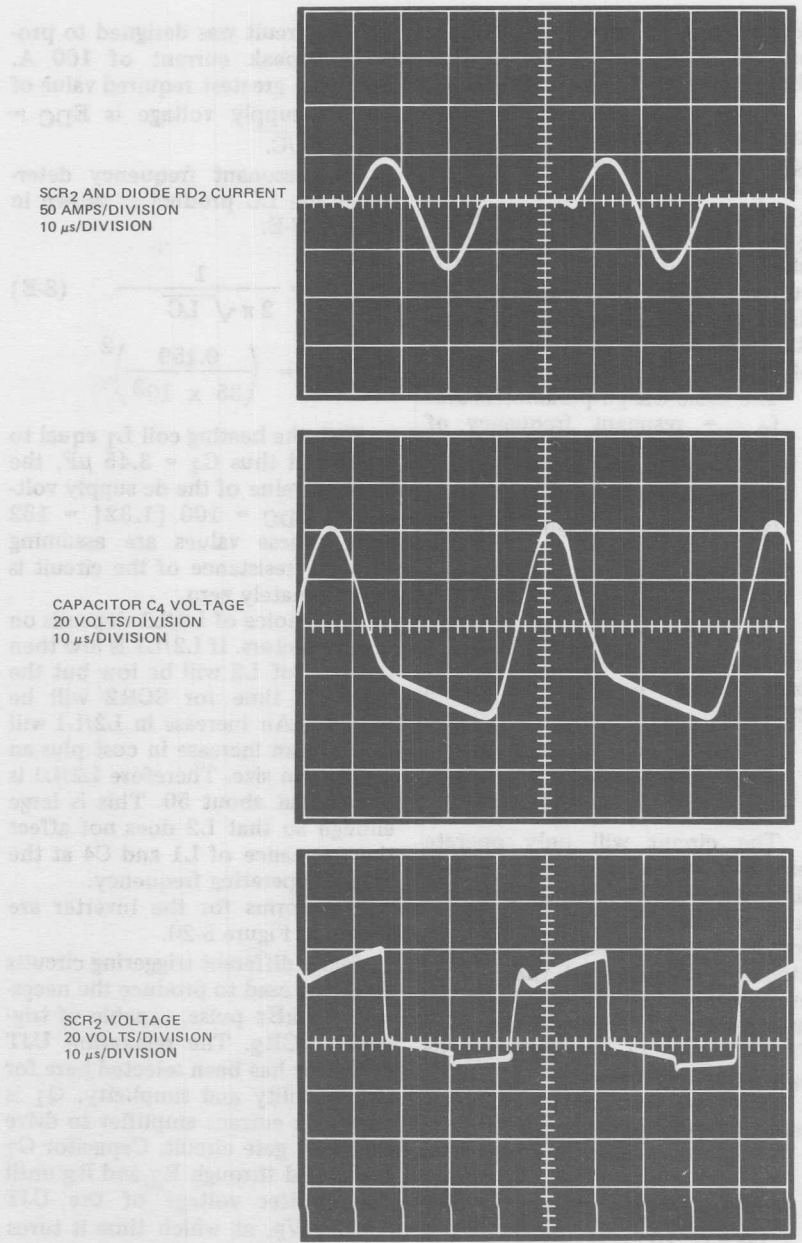


Figure 8-20. Induction Heating SCR Series Inverter Waveforms

low the holding value of the UJT emitter, it ceases to conduct and the cycle repeats. The period of oscillation, T , is given by Formula 8-F:

$$T = \frac{1}{f} = (R_7 + R_8)(C_7 \ln \frac{1}{1 - \eta}) \quad (8-F)$$

Where:

η = the intrinsic standoff ratio of the UJT.

The pulsed output, developed across R_6 , is coupled directly to the base of Q_1 . Q_1 turns on and C_6 then discharges through the gate of SCR_2 , providing a greater pulse of current for SCR_2 than that from UJT_1 . The dc that supplies the UJT oscillator is furnished from a 25 volt filament transformer, rectified through RD_3 and filtered by C_8 . BD_1 , a 25 volt zener voltage regulator, provides the necessary regulation for the UJT. Resistor R_9 limits the zener current.

Variable Frequency Motor Drives

The curve shown in Figure 8-21 is a comparison of cost of ac motors versus dc motors in various

horsepower sizes. With even a premium price for the ac system required to drive an ac motor, the overall ac drive should be less costly than the similar horsepower size using a dc motor.

The heart of the ac drive is the silicon controlled rectifier. Production of SCRs suitable for ac drives has historically been a matter of parameter trade-offs leading to the production of limited numbers (due to low yield factors) of suitable devices at relatively high prices. These problems have been solved so that SCR devices are now available with all of the parameters required by an ac drive system. Figure 8-22 shows curves of weight, inertia and efficiency, versus horsepower for dc and ac motors. With the inertia of the ac machine lower than that of a comparable dc machine, the response time of the control system can be reduced, thus increasing the achievable accuracy with a high gain, stable system. Moreover, the inherent weight savings (decreasing the necessary support structure in an installation) further reduces the initial system cost. The slightly bet-

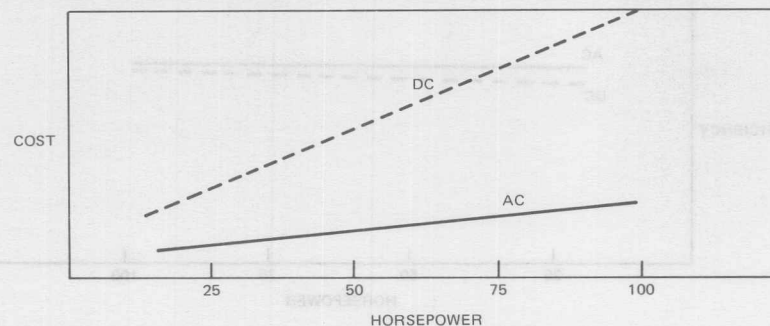


Figure 8-21. Horsepower versus Cost

ter efficiency of the ac machine proves to be an advantage over extended periods of operation in terms of power savings. In addition to these advantages there are savings in maintenance. The ac ma-

chine has no commutator and brushes, while in the dc machine these must be periodically replaced or overhauled, causing downtime in the installation. It is also possible to obtain an ac machine in an ex-

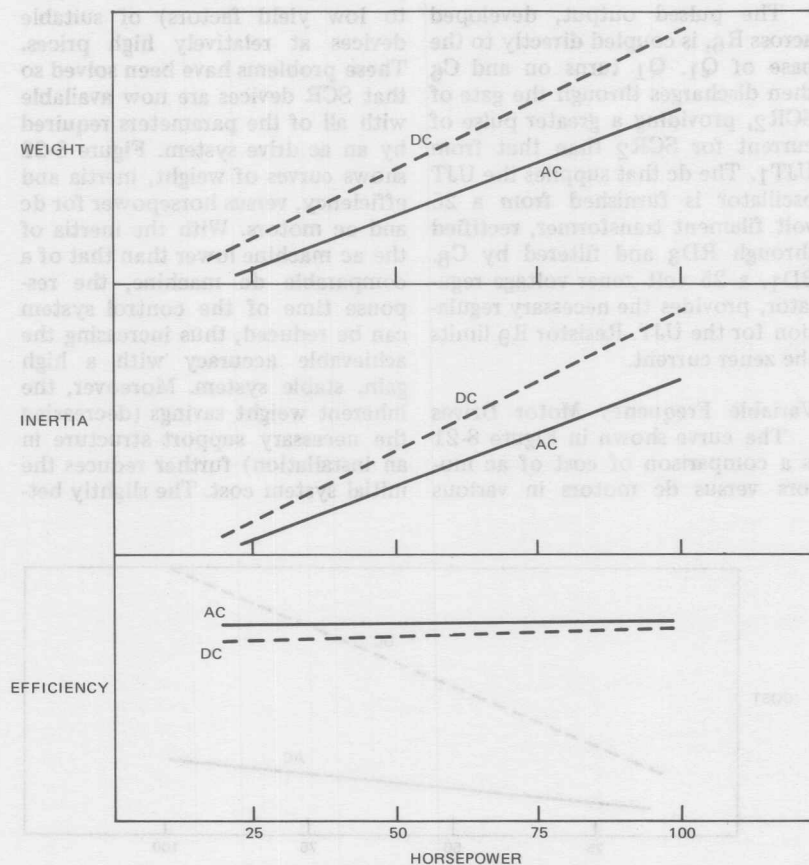


Figure 8-22. Motor Horsepower versus Pertinent Parameters

plosion-proof enclosure which is required in some volatile environments.

Using a pulse width modulated inverter it is possible to produce an ac motor drive system that can develop the full torque characteristics of dc machines. The phase shifted, fixed dc voltage inverter circuit approach found in the pulse width modulated inverter requires more sophisticated semiconductor devices than the variable voltage dc link inverter approach. Nevertheless, with an economical, high performance, high power SCR, the cost of the more advantageous (in terms of performance) pulse width modulated inverter becomes competitive to the dc system.

In the circuit arrangement shown in Figure 8-23(b), both voltage and frequency are controlled by a single set of SCRs, simplifying the necessary control and power circuitry and thus increasing the inherent reliability of the system. The triggering cir-

cuits needed to control the dc are completely eliminated, and the circuitry necessary to interlock these triggering circuits with the pulse system of the inverter is also eliminated (see Figure 8-23). If this drive system were applied to a moving vehicle, for instance, it would be possible to use a gas turbine prime mover directly coupled to a high speed alternator which in turn would supply the variable frequency inverter drive to power inductor motors coupled to the wheels. This system produces the ultimate in a high efficiency, high performance, light weight, and low operating cost electric transmission for large vehicle drives, with the added feature of making ac power available for auxiliary systems with a single power generating unit. The application of this concept to military vehicles, high speed rapid transit cars and large earth moving equipment is a technical reality. With the availability of low cost, sophisticated power thyristors it is an economic practicality.

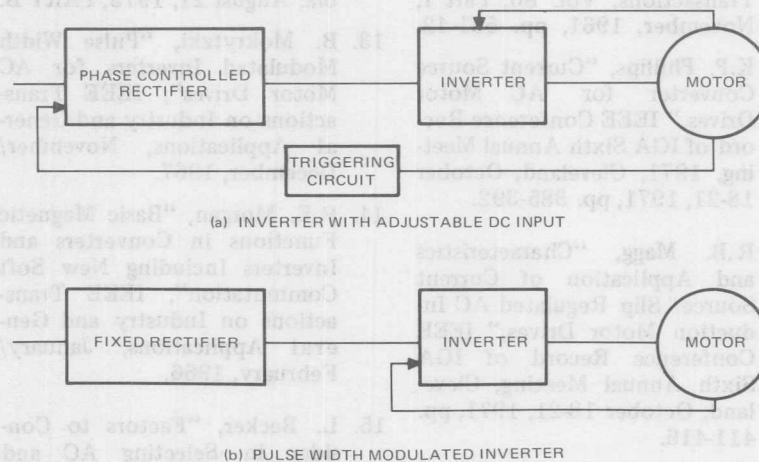


Figure 8-23. Block Diagram of DC Link Inverter Circuits

References

1. B.D. Bedford and R.G. Hoft, "Principles of Inverter Circuits," Wiley, 1964, pp. 48-53.
2. N. Mapham, "An SCR Inverter with Good Regulation and Sinewave Output," IEEE Transaction on Industry and General Applications, March/April, 1967, pp. 176-182.
3. N. Mapham, "A Low Cost Ultrasonic Inverter Using a Single SCR," IEEE/IGA Meeting, October 1966, pp. 451-472.
4. W. McMurray, "SCR Inverter Commutated by an Auxiliary Impulse," IEEE Transactions on Communications and Electronics, Vol. 83, No. 75, November, 1964, pp. 824-829.
5. W. McMurray and D.P. Shattuck, "A Silicon-Controlled Rectifier Inverter with Improved Commutation," AIEE Transactions, Vol. 80, Part I, November, 1961, pp. 531-42.
6. K.P. Phillips, "Current Source Converter for AC Motor Drives," IEEE Conference Record of IGA Sixth Annual Meeting, 1971, Cleveland, October 18-21, 1971, pp. 385-392.
7. R.B. Magg, "Characteristics and Application of Current Source/ Slip Regulated AC Induction Motor Drives," IEEE Conference Record of IGA Sixth Annual Meeting, Cleveland, October 18-21, 1971, pp. 411-416.
8. S. Dewan and G. Havas, "Solid State Supply for Induction Heating and Melting," IEEE Conference Record of IGA Third Annual Meeting, Publication 68C27-IGA.
9. D. Cooper, "The State of the Art in Power Thyristor Semiconductor Technology," International Rectifier.
10. "Fast Recovery Diodes — Calculating Recovery Losses," International Rectifier Application Note AN-B-6.
11. W.C. Moreland, II, "The Induction Range: Its Performance and Its Development Problems," IEEE Transactions on Industry Applications, Vol. IA-9, pp. 81-85, January/February 1973.
12. R.G. Hoft and G.M. Craig, "Solid-State Power Control Program Progress Report #2," University of Missouri, Columbia, August 21, 1973, PART B.
13. B. Mokrytzki, "Pulse Width Modulated Inverters for AC Motor Drives," IEEE Transactions on Industry and General Applications, November/December, 1967.
14. R.E. Morgan, "Basic Magnetic Functions in Converters and Inverters Including New Soft Commutation," IEEE Transactions on Industry and General Applications, January/February, 1966.
15. L. Becker, "Factors to Consider in Selecting AC and DC Adjustable Speed Drives," Automation, August 1968.

16. "Solid-state Controls Gain in AC as well as DC Drives," *Product Engineering* (January 1, 1968).
17. P.M. Espelage, J.A. Chiara, F.G. Turnbull, "A Wide-Range Static Inverter Suitable for AC Induction Motor Drives," *IEEE Transactions on Industry and General Applications*, Vol. IGA-5, No. 5, July/August, 1969, pp. 438-445.
18. C.W. Flairty, "A 50 KVA Adjustable Frequency 24-Phase Controlled Rectifier Inverter," *Direct Current*, December, 1961, pp. 278-282.
19. A.J. Humphrey, "Inverter Commutation Circuits," *IEEE Transactions on Industry and General Applications*, Vol. IGA-4, No. 1, January/February, 1968, pp. 104-110.
20. J.B. Forsythe and S.B. Dewan, "A Pulse Width Modulated Three Phase Complementary Commutated Inverter," *IEEE Conference Record of IGA 1971 Sixth Annual Meeting, Cleveland, October 18-21, 1971*, pp. 321-325.
21. F.G. Turnbull, "A Wide Range Impulse Commutated Static Inverter with a Fixed Commutation Circuit," *IEEE Conference Record of IGA First Annual Meeting, Chicago, October 3-6, 1966*, pp. 475-482.
22. S. Nonaka and H. Okada, "Three Phase SCR Inverter with a New Commutation Circuit," *IEEE Conference Record of IGA First Annual Meeting, Chicago, October 3-6, 1966*, pp. 483-498.
23. K. Heumann, "Development of Inverters with Forced Commutation for AC Motor Speed Control up to the Megawatt Range," *IEEE Transactions on Industry and General Applications*, January/February, 1969, pp. 61-67.



Automatic scribing systems employ a laser beam to cut chips from large SCR wafers in a "scribe and break technique." Computer programmed, the lasers provide high production capacity with accuracy. The chips, or junctions, are used for low power SCR's.

Choppers

Switching Principles [1]

If a switch is connected between a source of direct current and a load as in Figure 9-1(a), it is possible to energize or de-energize the load by simply closing or opening the switch. The voltage at the load terminals appears as in Figure 9-1(b) if the switch is opened and closed periodically.

The average voltage to the load is $E_{DC}/2$, if in Figure 9-1(b), t_1 is made equal to t_2 . This voltage can be varied by maintaining t_1 constant and varying t_2 (sometimes called pulsed rate modulation), by holding t_2 constant and varying t_1

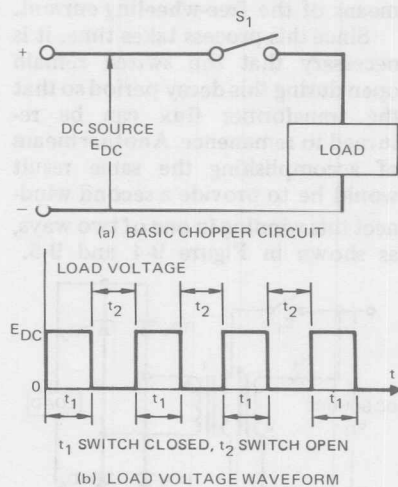


Figure 9-1. Basic Chopper Circuit and Output Voltage Waveform

(sometimes called pulse width modulation), or by varying both t_1 and t_2 .

It is easy to see how this system can be used to decrease the average voltage to the load, thus serving the purpose of a dc step-down transformer. Two basic techniques are available to provide a means of increasing the voltage from the supply to the load. The first of these, as shown in Figure 9-2, utilizes a transformer between the chopping switch S_1 and the load. Theoretically, as the switch is opened and closed in a periodic manner, the voltage to the load is again described by a chain of rectangular pulses, as in Figure 9-1(b), except that the maximum load voltage is now described in Formula 9-A and the maximum average load voltage is described in Formula 9-B:

$$E_{LOAD, MAX.} = E_{DC} \frac{N_2}{N_1} \quad (9-A)$$

Where:
 E_{DC} = DC source voltage
 N_1 = primary turns
 N_2 = secondary turns

$$E_{(AV)LOAD, MAX.} = E_{DC} \frac{N_2}{N_1} \cdot \frac{t_1}{t_1 + t_2} \quad (9-B)$$

Where:
 t_1 = time switch is closed
 t_2 = time switch is open

Although this system acts as a step-up transformer, the average

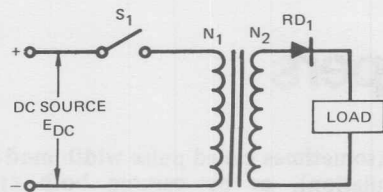


Figure 9-2. Transformer Load Switch

voltage to the load can still be varied by the means described for the basic Chopper Circuit (Figure 9-1(a)). When the switch is closed, the transformer and the load are energized. Then, as the switch is opened, the load is de-energized. The reactive nature of the transformer causes a voltage to be generated whose magnitude can be derived by Lenz' law, formula 9-C.

$$e = -N \frac{d\phi}{dt} \quad (9-C)$$

Where:

e = generated or induced voltage
 N = number of turns
 $d\phi/dt$ = rate of change of flux

If the switch were infinitely fast, the current in the transformer would try to cease instantaneously and the change in flux would also tend to be instantaneous.

This would result in a theoretically infinite voltage being generated by the transformer in a direction to continue the flow of current. The voltage measured across the switch would be $E + \infty$ and the diode would be required to block an infinite voltage.

Obviously, no physically realizable switch can operate (either open or closed) in zero time. However, the time can be sufficiently short to cause inordinately high

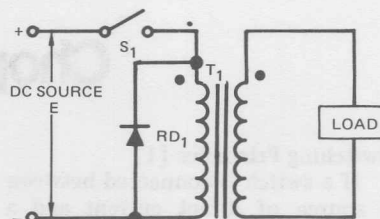


Figure 9-3. Transformer Load Switch with Free-wheeling Diode

voltages to be generated. One way to substantially reduce these voltages and yet continue the current in the transformer without continuing the load current is to connect diode RD_1 as shown in Figure 9-3. A diode in a configuration such as this is sometimes known as a "free-wheeling" or "by-pass" diode. This technique of obtaining slow flux decrease requires that the energy stored in the transformer be dissipated by means of the free-wheeling current.

Since this process takes time, it is necessary that the switch remain open during this decay period so that the transformer flux can be returned to remanence. Another means of accomplishing the same result would be to provide a second winding on the transformer and to connect this winding in one of two ways, as shown in Figure 9-4 and 9-5.

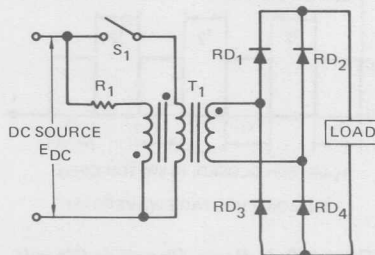


Figure 9-4. Transformer Load Switch with Reset Winding

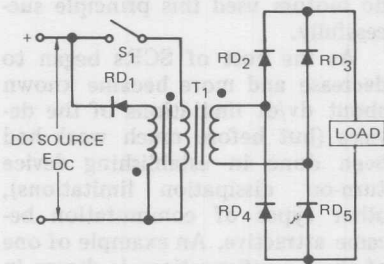


Figure 9-5. Transformer Load Switch with Clamped Reset Winding

In the case of Figure 9-4, the transformer flux is reset by means of the extra transformer winding being connected to the supply through limiting resistor R_1 . The resetting action in Figure 9-5 is provided by clamping the resetting winding through diode RD_1 to the supply. With the exception of the configuration in Figure 9-4, the transformer must be provided with an air gap in all of these schemes in order to avoid saturation.

Another method of constructing a step-up dc transformer is by means of the circuit shown in Figure 9-6. In this case, the reactive "kick" of an inductor, L_1 is used to generate very high voltages by means of a fast acting switch. While the switch is closed, energy is stored in the inductor L_1 . When the switch is open a voltage is generated across L_1 to keep the current flowing in the reactor. This voltage causes current to be conducted to the load and to charge capacitor C_1 . The diode, RD_1 , serves to block the capacitor from discharging into the switch while it is closed.

Each of these techniques is made practical by using thyristors, such

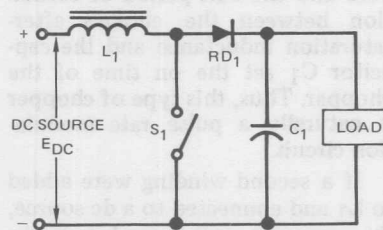


Figure 9-6. Step-Up Chopper

as SCRs or triacs, as the switch. However, since a thyristor is basically a latching device, a means must be provided to cause conduction to cease (open the switch). A circuit designed to accomplish this is called a commutating circuit. The function of the commutating circuit is to switch (or commutate) the load current away from the thyristor for a period sufficiently long for the thyristor to recover its blocking capability.

A discussion of various types of commutation circuits is appropriate in order to indicate some of the many techniques available to the circuit designer. These various methods of commutation are useful, not only for choppers, but also for inverters.

Commutation Circuits

The first type of commutation to be used is called the "Morgan" circuit, as shown in Figure 9-7, using a form of self-saturating choke, L_1 , in series with the commutation capacitor, C_1 , connected in parallel with the SCR, SCR_1 , to be commutated. The choke L_1 in this circuit is a self-saturating type using a square loop core material. The volt-second capacity of this

core and the half period of oscillation between the choke's after-saturation inductance and the capacitor C_1 set the on time of the chopper. Thus, this type of chopper is naturally a pulse rate modulation circuit.

If a second winding were added to L_1 and connected to a dc source, the apparent volt-second capacity of L_1 could be varied by varying the resulting flux setting current in the second winding. This then would make the circuit suitable for pulse width modulation. Recharging the commutation capacitor C_1 , in this circuit, takes place during the off time of SCR_1 . The discharge of C_1 through SCR_1 is limited by the after-saturation inductance of L_1 and thus is the determining factor (other than the load) of di/dt in the SCR.

This circuit was developed in the days when SCRs with guaranteed dynamic properties (turn-off time, dv/dt , di/dt , turn-on dissipation) were expensive and sometimes impossible to obtain. The advantages of this type of commutation are obvious in the light of these early drawbacks as compared to using a separate SCR to activate the commutation circuitry. Some of the early choppers for control of small

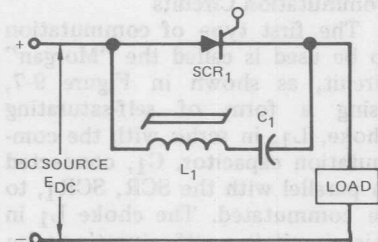


Figure 9-7. Morgan Circuit

dc motors used this principle successfully.

As the cost of SCRs began to decrease and more became known about dv/dt limitations of the devices (but before much work had been done in establishing device turn-on dissipation limitations), other types of commutation became attractive. An example of one of these configurations is shown in Figure 9-8.

As SCR_1 is turned on, it not only supplies the load, but also supplies energy to charge C_1 resonantly through RD_1 and L_1 . When C_1 is fully charged, RD_1 suddenly becomes back-biased. This then forward biases the gate to cathode junction of SCR_2 , turning SCR_2 on. The capacitor voltage is then impressed across the load (the capacitor in a high Q circuit can be charged nearly to $2E$) back biasing SCR_1 and supplying the load energy while SCR_1 turns off. The circuit as shown then is suitable for pulse rate modulation. If, however, the gate of SCR_2 were not connected as shown, but instead was supplied by a separate pulsing circuit with a varying, controllable pulse rate, the circuit could be used in the pulse width modulation mode.

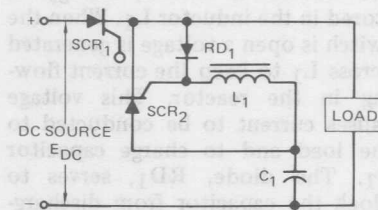


Figure 9-8. Pulse Rate Modulation Circuit

This circuit (Figure 9-8) has several disadvantages. First, the commutation charging current must be carried by SCR₁, thus decreasing its useful rating with respect to the load. Secondly, the di/dt through SCR₂ is inherently high and must be suppressed by added circuit reactance. And finally, the rise of commutation voltage at the beginning of the commutation interval is quite abrupt and can cause corona in the load, as well as extending the reverse recovery interval of SCR₁. This circuit has been used successfully on dc to dc converters for battery charging with and without transformer isolated loads on both low and high voltages. However, the disadvantages are considerable, and, in general, there are modern techniques which better suit the SCRs available today.

As has been seen, most commutation techniques have depended upon a resonant circuit to charge the commutation capacitor. The Morgan circuit was unique in that it combined the functions of the resonant circuit inductance, commutation switch and the pulse width timing device all into one component, the reactor. (Attributable to the clever use of magnetics usually in evidence in Morgan's work.) An analog for this circuit is shown in Figure 9-9.

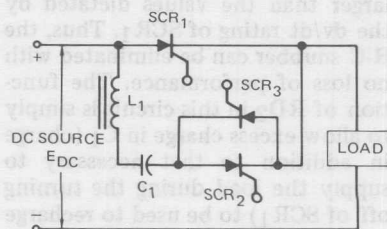


Figure 9-9. Modified Morgan Circuit

The operation of this circuit can be very similar to that of the Morgan chopper. SCR₂ is first turned on allowing capacitor C₁ to charge through the load and inductance L₁. When capacitor C₁ is fully charged, SCR₂ turns off from lack of anode current (assuming its gate signal has been removed). SCR₁ can then be turned on, energizing the load. Since SCR₃ is in a blocking state, capacitor C₁ remains charged. When SCR₃ is turned on, the capacitor will discharge resonantly with L₁ through SCR₁ and SCR₃ and the voltage on the capacitor will reverse polarity. When SCR₂ is once more turned on, capacitor C₁ will be discharged resonantly through L₁ and SCR₂ through the load. This will apply a back-bias to SCR₁ and allow it to turn off and regain its blocking capabilities. Thus, by controlling the triggering rates of SCR₁, SCR₂ and SCR₃, as well as the time relationships among their gating signals, either pulse width or pulse rate modulation or a combination of the two is possible with this circuit. The advantages of this type of circuit are obvious. The commutation pulse application can be made gradual, and the di/dt or switching losses in the various SCRs due to the commutation, are minimized by judiciously choosing the choke (L₁).

The disadvantages of the circuit are, of course, that SCR₁ is required to carry the commutation charging current and three SCRs are used to accomplish the logic. Of course, SCR₃ could be replaced by a diode (as shown in Figure 9-10). This eliminates the ability to control the timing between the inversion of voltage on C₁ and the triggering on SCR₁. Otherwise, the

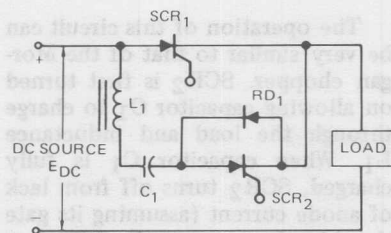


Figure 9-10. Modified Morgan Circuit — Diode Replacing one SCR

operation of the circuit is the same.

An interesting extension of this type of commutation is achieved by what is termed "delay line" commutation. By replacing the simple LC of Figure 9-10 with a "delay line" or pulse-forming network, some interesting effects can be achieved. A sample of this type of circuit is shown in Figure 9-11. The interesting characteristic of this type of commutation is that it concentrates the commutation energy in a trapezoidal current wave, thus providing excellent conditions for turning off SCR₁. For large power levels the commutation capacitor can be divided into several separate capacitors so that load sharing by the capacitors can be assured, due to the insertion of the network inductances. The waveshape of current through SCR₂ also tends to be trapezoidal, thus allowing it to be operated under more ideal conditions, especially for low frequency applications.

This type of commutation is especially useful in conjunction with the type of step-up chopper shown in Figure 9-6. The combination of the two circuits can be seen

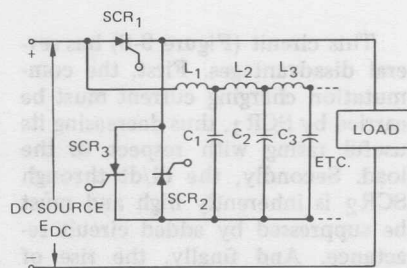


Figure 9-11. Modified Morgan Circuit — Delay Line Added

in Figure 9-12, the operation of this circuit being the same as described for Figure 9-6.

In order to minimize the probability of an SCR being triggered falsely by high rates of rise of line voltages or disturbances in the load, it has become common practice to use an R-C circuit (snubber) in parallel with the SCR to reduce the rates of rise of these voltages. It is possible, by arranging the commutation components properly, as shown in Figure 9-13, to combine the functions of the "snubber" and the commutation circuits. With a given load impedance, the dv/dt to which SCR₁ is subjected can be predicted by choosing C₁ properly. However, the size of C₁ as dictated by the turn-off time of SCR₁, is generally larger than the values dictated by the dv/dt rating of SCR₁. Thus, the R-C snubber can be eliminated with no loss of performance. The function of RD₂ in this circuit is simply to allow excess charge in C₁ (charge in addition to that necessary to supply the load during the turning off of SCR₁) to be used to recharge the capacitor, rather than dissipating it uselessly in the load.

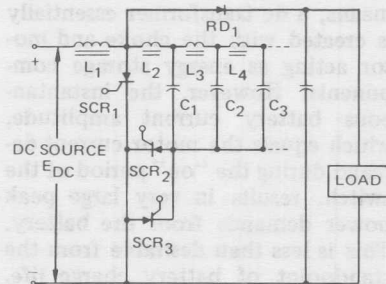


Figure 9-12. Step-Up Chopper With Delay Line

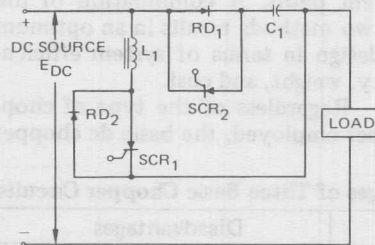


Figure 9-13. Chopper with Commutation Capacitor Functioning also as a Snubber Capacitor

An extension of this principle is shown in Figure 9-14. This circuit combines the functions of the snubber network with the delay line commutation circuit into a single set of components. In this case, RD_1 and C_1 act to suppress dv/dt across SCR_1 . C_1 also acts with L_1 , L_2 , and C_2 , as the commutation circuit tending to form a trapezoidal commutation current waveform. A diode in anti-parallel with SCR_1 , to recapture excess commutation energy, can also be added to this circuit.

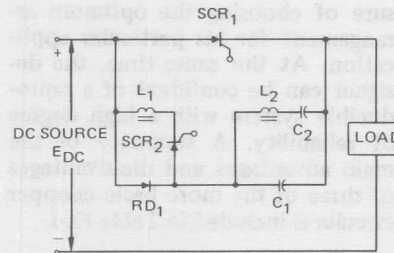


Figure 9-14. Chopper with Delay Line Type Commutation Capacitor Functioning also as a Snubber Capacitor

Each of these combinations has advantages and disadvantages as outlined, and, of course, there are an infinite number of combinations possible to achieve desired circuit characteristics. However, certain characteristics of such circuits, from the standpoint of properly commutating the SCR, must be considered by the design engineer. These are:

- A. High inrush current in the SCR
- B. Provide reverse bias to the SCR during commutation
- C. High voltage transients imposed on the SCR
- D. High rates of rise of reverse current causing increased SCR dissipation
- E. Re-applied rate of voltage rise on the SCR after the commutation period
- F. High rates of rise of forward voltage imposed on the SCR during its off-state

By observing these characteristics of the circuit carefully, and by properly coordinating with the SCR manufacturer, the designer can be

sure of choosing the optimum arrangement for his particular application. At the same time, the designer can be confident of a reproducible system with a high degree of reliability. A summary of the main advantages and disadvantages of three of the more basic chopper circuits is included in Table IX-I.

DC Motor Drives

A dc chopper type propulsion speed control is required to operate over a relatively wide range of speed, using a solid-state switch. The variable on-off duty cycle transfers a quantity of pulsed energy into the dc motor. The pulsed battery current is stored and expended within the motor and its series inductance during each period of SCR conduction and also during period when the free-wheeling diode is conducting. By this

means, a dc transformer essentially is created with the choke and motor acting as energy storage components. However, the instantaneous battery current amplitude, which equals the motor current demand during the "on" period of the switch, results in very large peak power demands from the battery. This is less than desirable from the standpoint of battery charge life. This may be corrected by one of two means, 1) inserting a means of energy storage between the battery source and the chopper, and 2) of sequentially switching a multi-phase chopper containing individual dc reactors and free-wheeling diode current paths. A combination of the two methods results in an optimum design in terms of system efficiency, weight, and cost.

Regardless of the type of chopper employed, the basic dc chopper

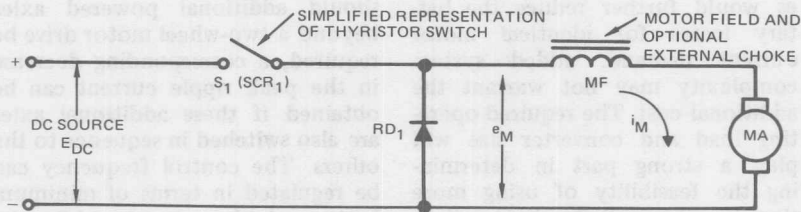
Table IX-I. Advantages and Disadvantages of Three Basic Chopper Circuits

	Advantages	Disadvantages
Morgan Circuit (Figure 9-7)	1. Simplicity — only one SCR needed	1. Approximately fixed on time so only useful for pulse rate modulation. 2. Requires saturable reactor 3. Current to reverse commutation capacitor charge increases rating required of SCR
Modified Morgan Circuit (Figure 9-9)	1. All types of pulse modulation control are possible	1. Requires three SCRs (or two if SCR ₃ replaced by diode) 2. Main SCR must carry current to reverse charge or commutation capacitor
Chopper with Snubber (Figures 9-13 and 9-14)	1. Includes dv/dt and di/dt limiting	1. Commutating reactor carries dc load current 2. Main SCR carries current to reverse charge on commutation capacitor

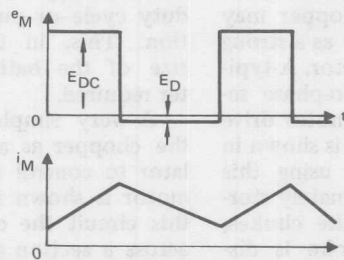
circuit can be represented as in Figure 9-15. The waveforms shown in the same figure assume negligible change in the motor back EMF. After interrupting the current flow in the switch, voltage is induced across the inductor which attempts to maintain the flow of current in the inductor. This current flows in the same direction but in decreasing magnitude through the motor and the free-wheeling diode, RD_1 .

Low speed motor operation for large drives requires large current amplitudes. Figure 9-16 shows a typical motor drive characteristic where maximum acceleration performance or torque capability is required to half speed, typically at about 50% chopper duty cycle. Using this, then, as a typical vehicle propulsion profile, and since this exhibits a low speed dc motor cur-

rent requirement of twice the full speed current to provide an acceptable acceleration characteristic or torque capability, it can be seen that low speed, high torque operation will result in the least efficient source power utilization. A typical battery bank, consisting of 110 cells delivering 142 volts no-load voltage and 34 ampere-hours capacity when fully charged, exhibits a source resistance of 135 milliohms. In terms of 500 ampere current pulses, this results in a 52% battery source utilization. This is poor performance, not only in terms of source efficiency, but also in RMS heating loss. Implementation of a two-phase sequentially switched chopper will increase battery efficiency to 75% by decreasing the battery surge pulse current to 50% of the current amplitude for the



(a) BASIC DC MOTOR CHOPPER CIRCUIT



(b) LOAD VOLTAGE AND CURRENT WAVEFORMS

Figure 9-15. Basic Chopper Type DC Motor Drive

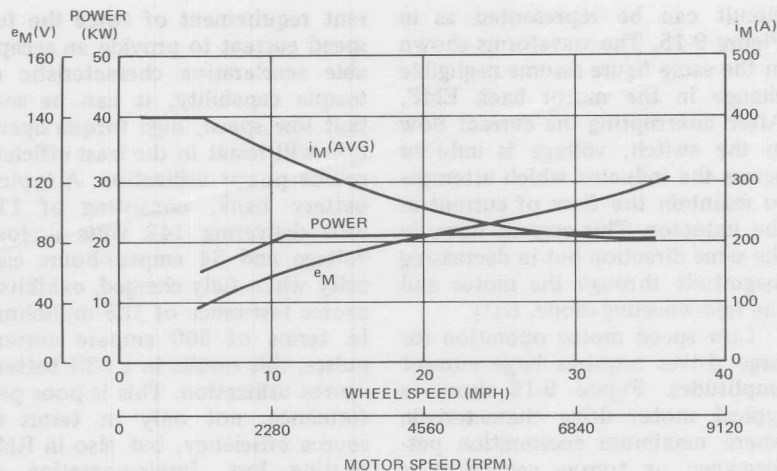


Figure 9-16. Typical Chopper Motor Drive Characteristics

single-phase chopper when operating at low duty cycle. Although additional sequentially phase switches would further reduce the battery losses for identical motor current demand, added system complexity may not warrant the additional cost. The required operating load and converter size will play a strong part in determining the feasibility of using more than two sequentially phase switches [17].

The addition of a filter between the source and the chopper may also come into the study as a strong primary determining factor. A typical schematic for a two-phase sequentially switched dc motor drive with L-C filter buffering is shown in Figure 9-17. Thus, by using this type of system and alternately storing energy in one of the chokes, while the opposite choke is discharging, the peak amplitude of the current drain from the motor is reduced by 50%, resulting in the

battery efficiency while discharging shown in Figure 9-18.

It is interesting to note that should additional powered axles beyond a two-wheel motor drive be required, a corresponding decrease in the peak ripple current can be obtained if these additional axles are also switched in sequence to the others. The control frequency can be regulated in terms of minimum battery ripple current, while the individual wheel speeds are still controlled by means of the chopper duty cycle or pulse width modulation. This, in turn, reduces the size of the battery capacitor filter required.

A very simple system utilizing the chopper as a resistance modulator to control the speed of a dc motor is shown in Figure 9-19. In this circuit the chopper is located across a section of current limiting resistance which is in series with the series motor. The method of operation is simply to increase the duty

OPERATING MODE	CONTACTOR CLOSED	
FORWARD	K ₂	K ₅
REVERSE	K ₃	K ₄
FULL SPEED	K ₆	
PLUG REVERSE	K ₁	

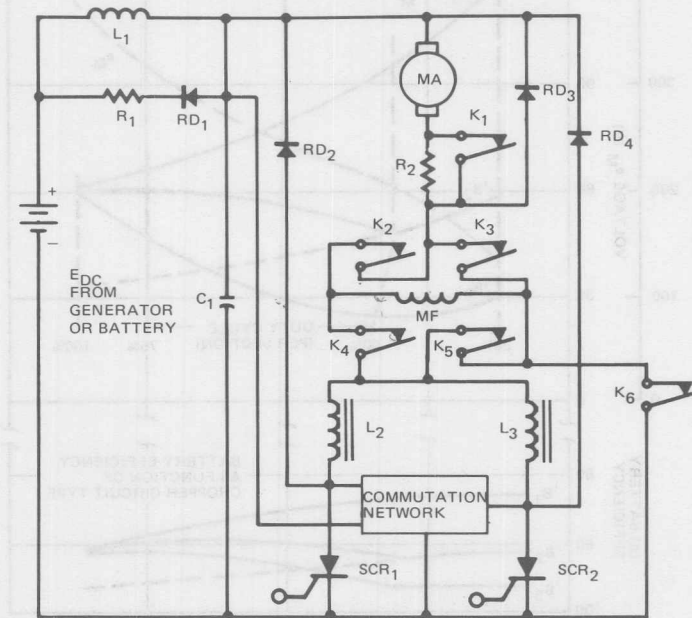


Figure 9-17. *Sequentially Switched Two-Phase Chopper*

cycle of the SCR until it is essentially full on, thus reducing the effective resistance in series with the dc motor by the amount of resistance across which the SCR is located. Then, by closing one of the mechanical contactors located across an equal segment of resistance in the propulsion circuit and by stopping the chopping action of the SCR circuit, the shunting action is transferred to the contactor. The chopper can then be increased in

duty cycle again until essentially a second section of the resistor has been shunted by it, at which time the second contactor can be closed, the chopper again reduced to zero duty cycle and the chopping action then repeated. By this means smooth acceleration can be obtained. It might be mentioned also that a similar means can be utilized for performing solid-state type motor field shunting, again using the chopper.

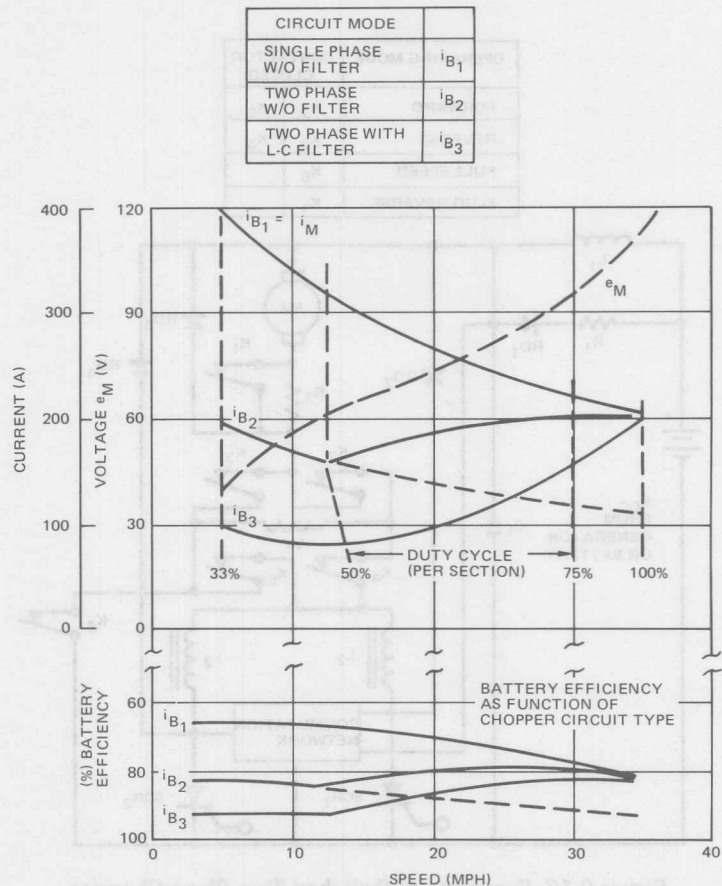


Figure 9-18. Discharge Characteristics of Two-Phase Chopper

DC Motor Step-Down Choppers

To control the power to a dc motor by means of a series chopper, it is preferable to provide a commutation system which is independent of the condition of the motor, to provide for stopping, and for reliable commutation. In the circuit in Figure 9-20, SCR₁ is the main power SCR supplying power directly from the source to the motor. C₁ is a large bank of capaci-

tors necessary to provide a low impedance source from which the chopper will operate. The action of the circuit is described as follows: SCR₂ is turned on, charging C₂ through L₁, RD₁; and SCR₂ through the smoothing reactance L₃ located in series with motor, MA and MF. Once capacitor C₂ becomes charged, SCR₂ turns off due to the cessation of current, at which time SCR₁ may be turned

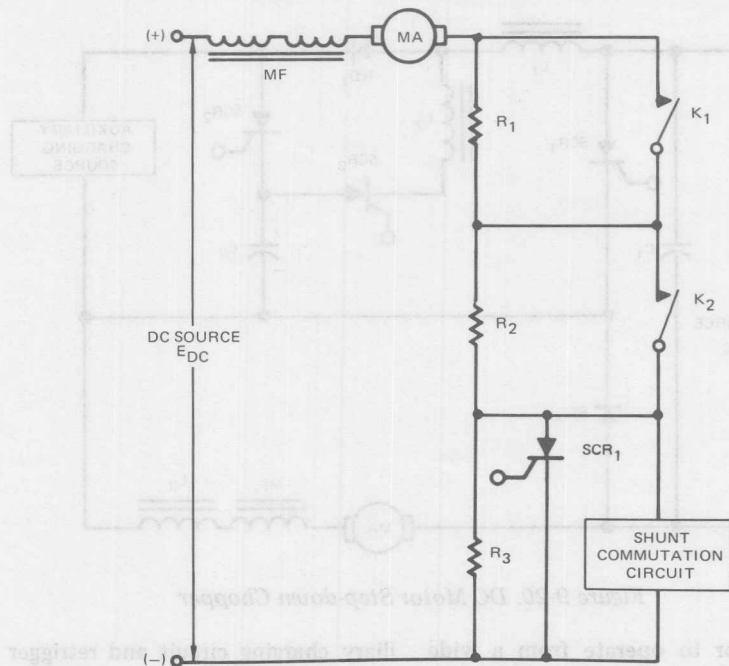


Figure 9-19. Resistance Modulator Chopper Circuit

on. C_2 remains charged in the polarity shown. After SCR_1 is turned on, SCR_3 may be turned on, which discharges C_2 through SCR_3 , L_2 , L_1 , and SCR_1 . C_2 then charges in the opposite direction to the polarity shown.

Reactor L_2 limits the additional peak current that SCR_1 is subjected to during the reversal of charge on C_2 when SCR_3 is triggered. This optimizes the utilization of SCR_1 for controlling the motor speed. Both RD_1 and RD_2 should be fast recovery diodes in order to minimize the transients caused by stored energy during the reverse recovery of these devices. RD_2 is simply to provide a by-pass for current from L_3 through the motor and helps smooth the motor cur-

rent. With this type of commutation scheme, as the motor builds in speed and the counter EMF rises, the available voltage to charge C_2 from the source, which is the source voltage minus the armature voltage of the motor, decreases. This in itself is not a limiting factor since any voltage on the capacitor in the order of ten or twenty volts would be sufficient to commutate SCR_1 in terms of providing negative bias, since this commutation scheme through SCR_3 provides a means for reversing the charge on the capacitor. However, it is required under those conditions for the capacitor to store enough energy to provide the required current by the motor during this commutation period. The need for the

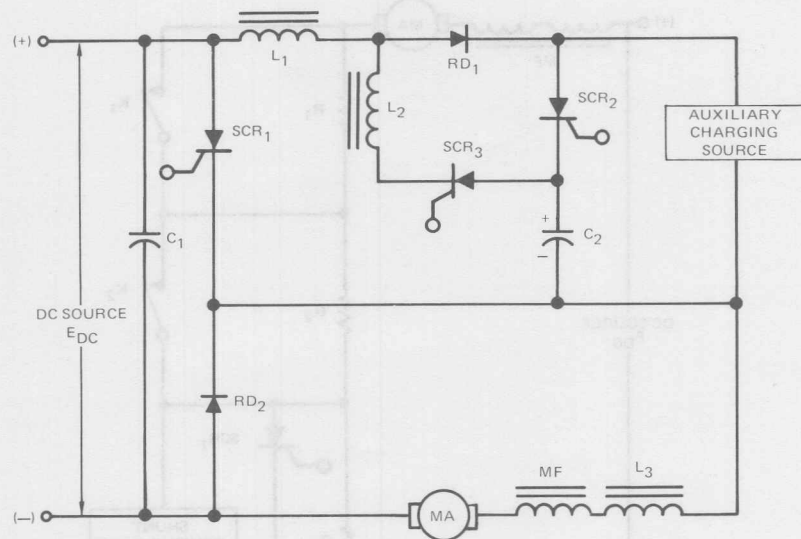


Figure 9-20. DC Motor Step-down Chopper

capacitor to operate from a wide range of operating voltages increases the energy storage requirement of the capacitor significantly.

Another characteristic with this type of commutation means is that should commutation not be achieved successfully, there is no longer any control over SCR₁. A method of correcting both these faults of the circuit is to provide an auxiliary charging source by which capacitor C₂ can be charged through SCR₂ even during the period that SCR₁ has been turned on. This is the reason for incorporating diode RD₁ in the circuit. RD₁ serves to block the auxiliary charging current from flowing through L₁ and SCR₁, thus isolating the auxiliary charging circuit from the main power circuit. Using this scheme it is now possible to have a mis-commutation of the system, recharge capacitor C₂ from the aux-

iliary charging circuit and retrigger the commutation system. This permits commutation of SCR₁ regardless of an intermittent fault in the system. Once C₂ has been charged negatively, (opposite to the polarity shown in Figure 9-20) SCR₂ can be triggered on at any time in order to cause commutation of SCR₁.

Reliable commutation without the necessity of an auxiliary voltage source is achieved by the practical chopper shown in Figure 9-21. The important current and voltage waveforms for this circuit are shown in Figure 9-22. These waveforms assume steady-state operation with a chopping frequency high enough so there is negligible ripple in the motor current. In addition to providing reliable commutation without the addition of an auxiliary commutating voltage source, the circuit of Figure 9-21 has several other advantages:

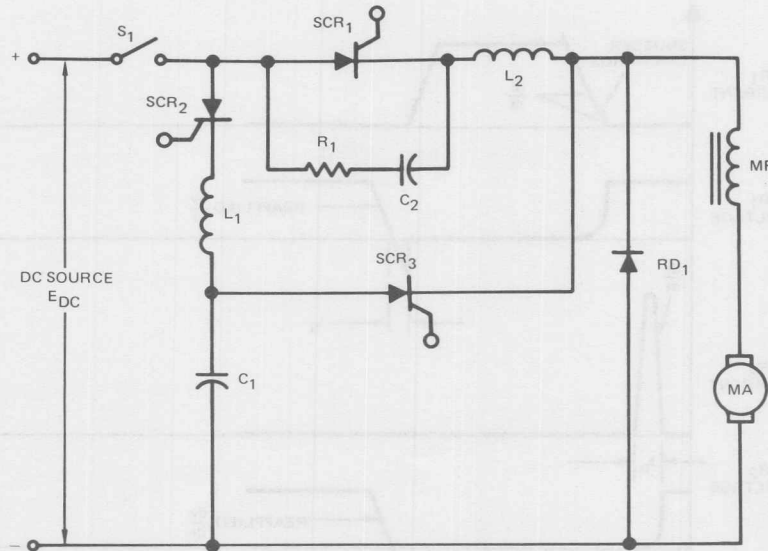


Figure 9-21. Modified Series DC Motor Chopper

- The di/dt is limited in each SCR due to the inductors L_1 and L_2 and the motor field inductance.
- The dv/dt reapplied to each SCR is limited.
- The commutating capacitor C_1 is reset to zero volts by discharging into the load after the end of each commutation. Assuming sufficient load for this to occur, the commutating voltage is then load independent.

Analysis of a Step-Up Chopper [15.16]

Figure 9-23 shows a diagram of a step-up chopper circuit. MF is the field winding of the motor and e_{C1} is the voltage across the armature taking into account the drop due to armature resistance; it is also the voltage across capacitor C_1 . SCR₁

is the main SCR and SCR₂, 3, 4, and 5 are the commutating SCRs. C_2 is the commutating capacitor and C_1 is a filter capacitor.

Ideally SCR₁, 2, 3, 4, and 5 and C_2 act together as a switch. This is represented in Figure 9-24. When the switch is closed, the supply voltage E_{DC} is impressed across the field winding and current i_F builds up linearly. When the switch is open, the current flows through diode RD₁ and into capacitor C_1 and the motor armature, MA.

When the circuit has reached steady-state operation, the average voltage across the inductor is zero, and the relationships in equation 9-D and 9-E hold true:

$$\frac{E_{DC} \cdot t_{on} + (E_{DC} - e_{C1}) t_{off}}{t_{on} + t_{off}} = 0 \quad (9-D)$$

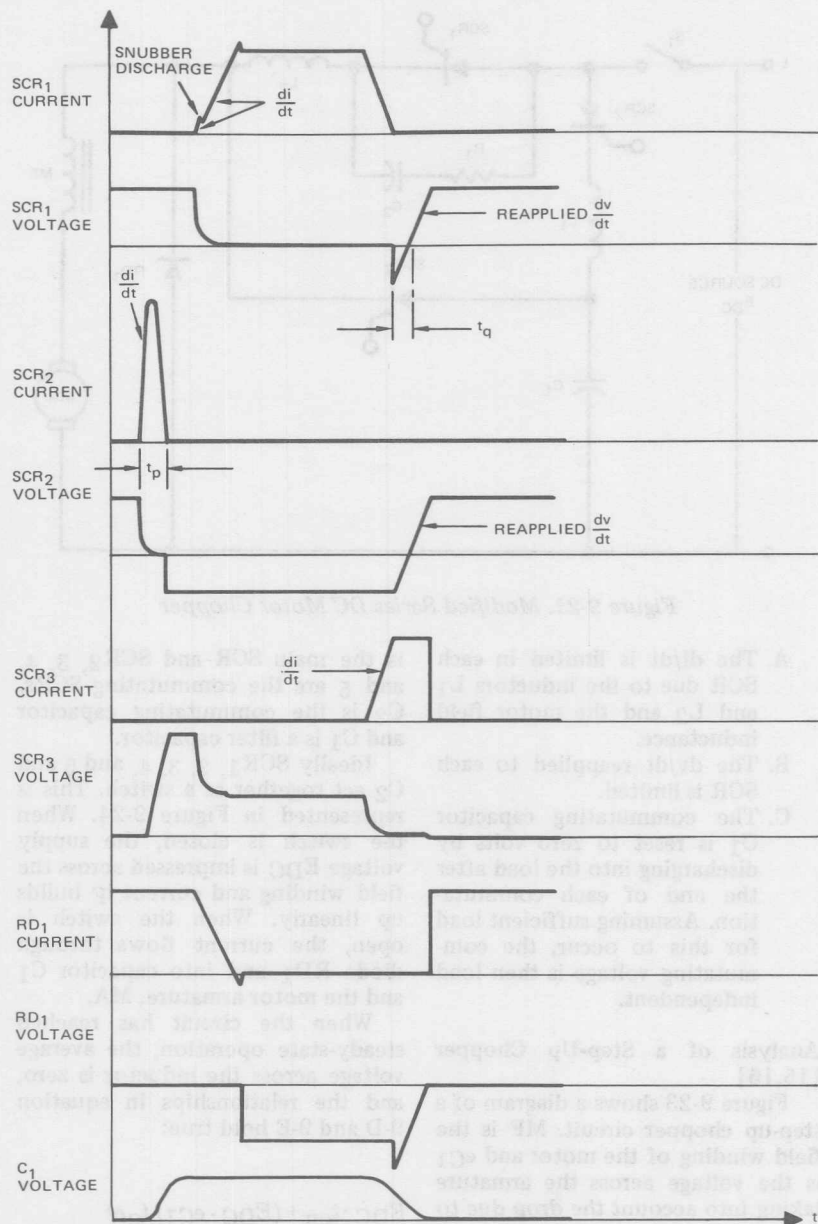


Figure 9-22. Waveforms for Modified Series DC Motor Chopper

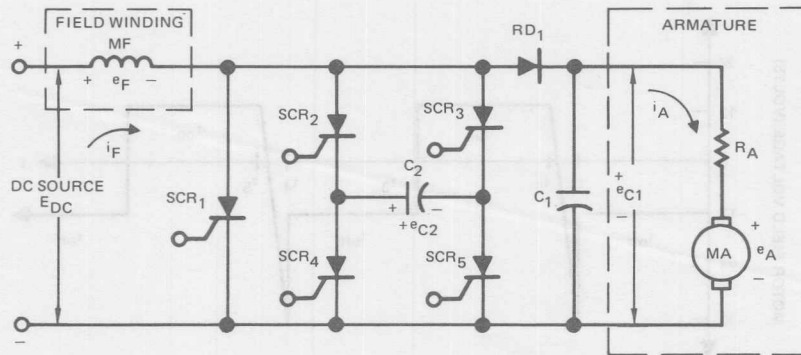


Figure 9-23. Step-Up Chopper Power Circuit

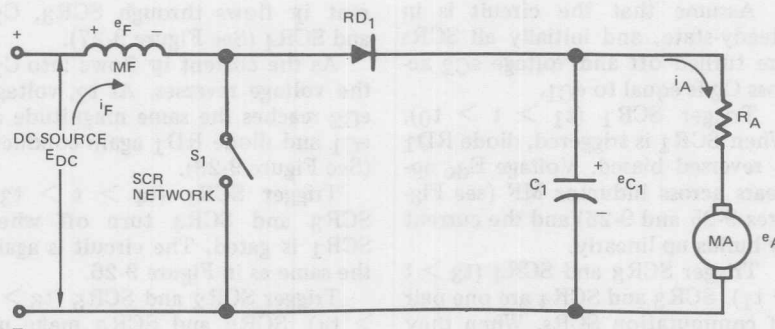


Figure 9-24. Equivalent Step-Up Chopper Power Circuit

Where:
 E_{DC} = supply voltage
 t_{on} = time on
 e_{C1} = voltage across armature
 t_{off} = time off
 OR

$$e_{C1} = \frac{t_{on} + t_{off}}{t_{off}} E_{DC} \quad (9-E)$$

$$= \frac{E_{DC}}{1 - \text{Duty Cycle}}$$

Where:
 $\text{Duty Cycle} = \frac{t_{on}}{t_{on} + t_{off}}$

Equation 9-E indicates the step-up feature of the circuit. When t_{on} is small compared to t_{off} , e_{C1} is nearly equal the supply voltage E_{DC} . As t_{on} increases relative to t_{off} the voltage e_{C1} becomes greater.

In order for SCR 1, 2, 3, 4, and 5 to act as the switch, they must be triggered in the proper sequence. The following is an analysis of the circuit at each step of its operation. A sketch of the voltage across the motor field at each time interval is shown in Figure 9-25. Note that the average voltage is ZERO.

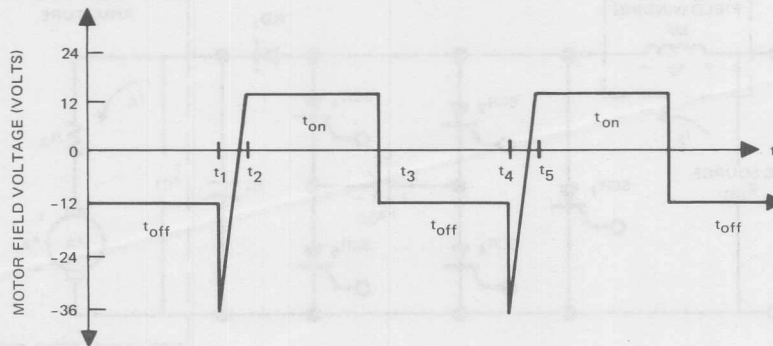


Figure 9-25. Voltage Across Motor Field in Step-Up Chopper Power Circuit

Assume that the circuit is in steady-state, and initially all SCRs are turned off and voltage e_{C2} across C_2 is equal to e_{C1} .

Trigger SCR_1 ($t_1 > t > t_0$). When SCR_1 is triggered, diode RD_1 is reverse biased. Voltage E_{dc} appears across inductor MF (see Figures 9-25 and 9-26) and the current i_F builds up linearly.

Trigger SCR_3 and SCR_4 ($t_3 > t > t_1$). SCR_3 and SCR_4 are one pair of commutation SCRs. When they are triggered, capacitor C_2 is placed in parallel with SCR_1 . From t_1 to t_2 , SCR_1 is reverse biased and cur-

rent i_F flows through SCR_3 , C_2 , and SCR_4 (See Figure 9-27).

As the current i_F flows into C_2 , the voltage reverses. At t_2 , voltage e_{C2} reaches the same magnitude as e_{C1} and diode RD_1 again conducts (See Figure 9-28).

Trigger SCR_1 ($t_4 > t > t_3$). SCR_3 and SCR_4 turn off when SCR_1 is gated. The circuit is again the same as in Figure 9-26.

Trigger SCR_2 and SCR_5 ($t_6 > t > t_4$). SCR_2 and SCR_5 make up the other pair of commutation SCRs. Note that when SCR_3 and SCR_4 were on, the capacitor volt-

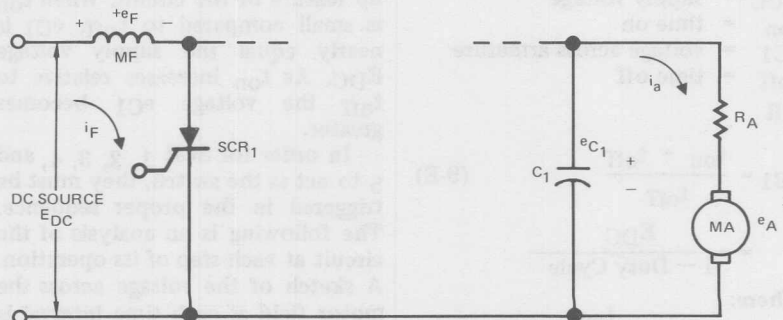


Figure 9-26. Step-Up Chopper Power Circuit — SCR_1 On

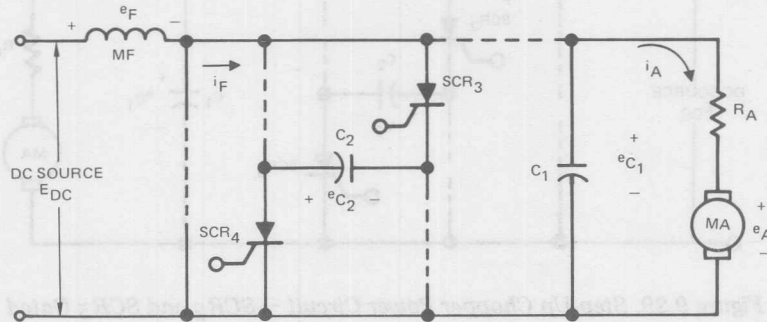


Figure 9-27. Step-Up Chopper Power Circuit — SCR_3 and SCR_4 Gated

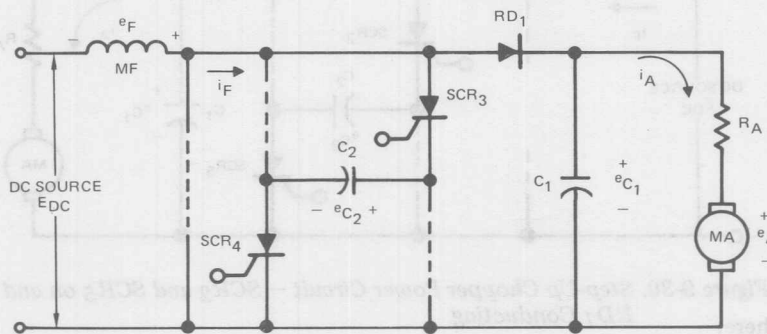


Figure 9-28. Step-Up Chopper Power Circuit — SCR_3 and SCR_4 On and RD_1 Conducting

age e_{C2} had reversed. When SCR_2 and SCR_5 are triggered, the polarity is such that SCR_1 is again reverse biased and current i_F flows into capacitor C_2 (See Figure 9-29). Again when e_{C2} reverses and builds up to e_{C1} (at $t = t_5$), diode RD_1 conducts (See Figure 9-30). At this point the cycle begins again.

Calculated torque vs. speed curves for this circuit are shown in Figure 9-31. These curves were plotted from Equation 9-F for the motor torque. It can be derived in a straight forward manner using the basic equations for dc motor operation.

$$T = \frac{K_t}{(1-D)(1-D)^2(R_A)^2 + 2(1-D)KV R_A W + (KV)^2 W^2} E_{DC}^2 \quad (9-F)$$

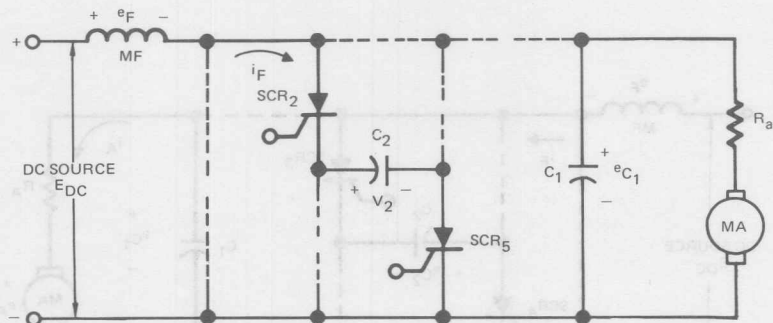


Figure 9-29. Step-Up Chopper Power Circuit — SCR₂ and SCR₅ Gated

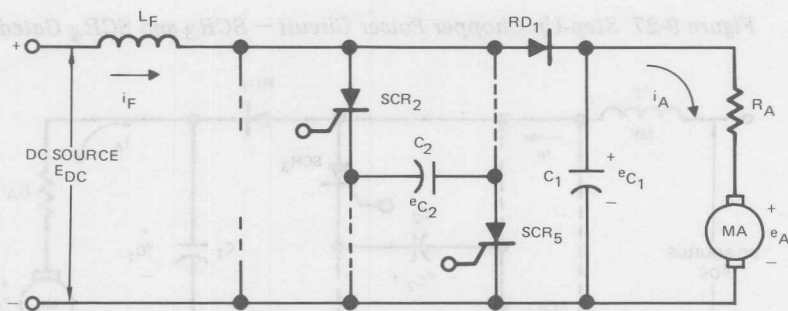


Figure 9-30. Step-Up Chopper Power Circuit — SCR₂ and SCR₅ on and RD₁ Conducting

Where:

K_t = torque constant

1-D = fraction of time off =

$$\frac{t_{\text{off}}}{t_{\text{off}} + t_{\text{on}}}$$

E_{DC} = dc supply voltage

R_A = motor armature resistance.

K_V = counter EMF constant

W = speed in radians/second

It is very interesting to note that the torque-speed characteristic for this modified series motor control is essentially the same as for a conventional dc series motor. Figure 9-32 shows the time relationships among the gate trigger pulses applied to SCR₁, 2, 3, 4 and 5.

The voltage waveform across SCR₁ appears as shown in Figures 9-33 and 9-34 along with the gating pulses to SCR₁. When SCR₁ is triggered, the voltage drops to zero and current builds up in the field. When a pair of commutating SCRs is gated, the negative voltage on the commutating capacitor instantly appears and the capacitor charges up fairly linearly to the output voltage on the filter capacitor. The waveform is very similar to the ideal waveform shown in Figure 9-25.

Figure 9-33 is with $\tau \approx 3/4$ where the output voltage should be

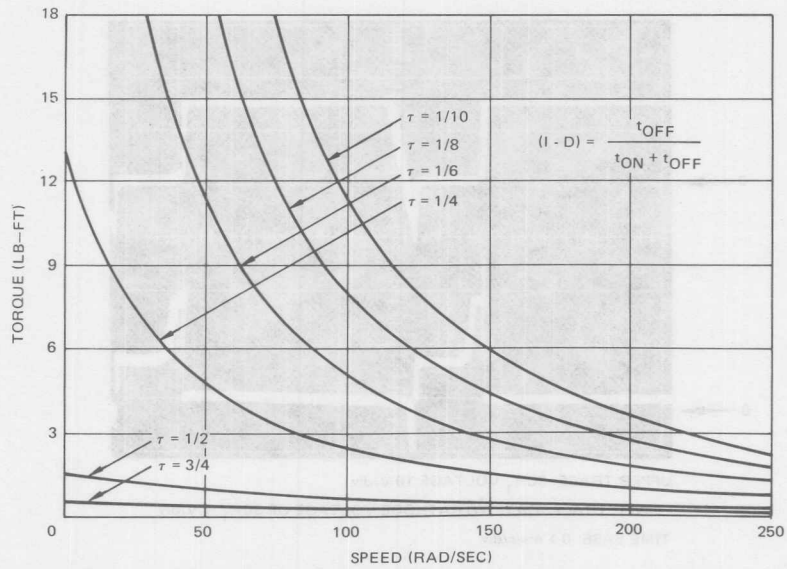


Figure 9-31. Step-Up Chopper — Torque Vs. Speed

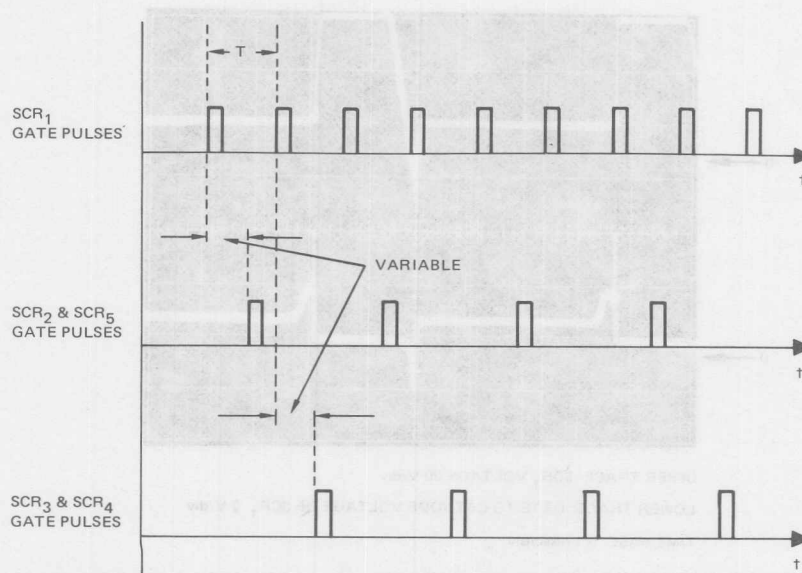


Figure 9-32. Step-Up Chopper — Gating Pulse Timing

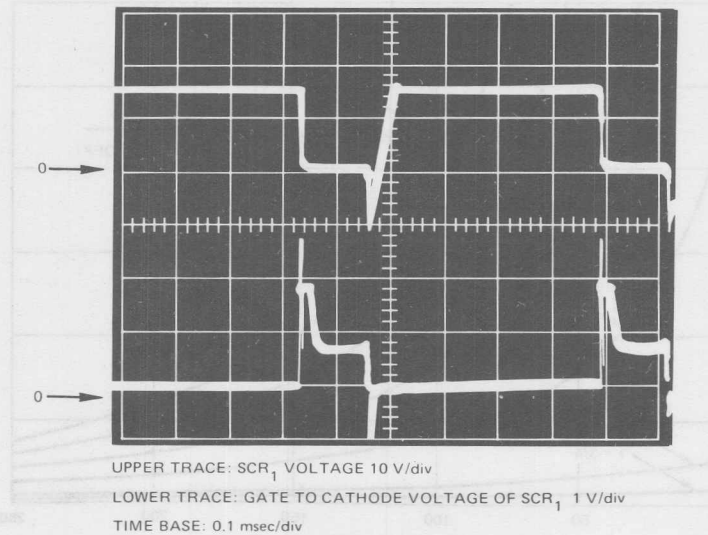


Figure 9-33. Step-Up Chopper—SCR₁ Anode and Gate Voltage Waveforms for $\tau \approx 3/4$

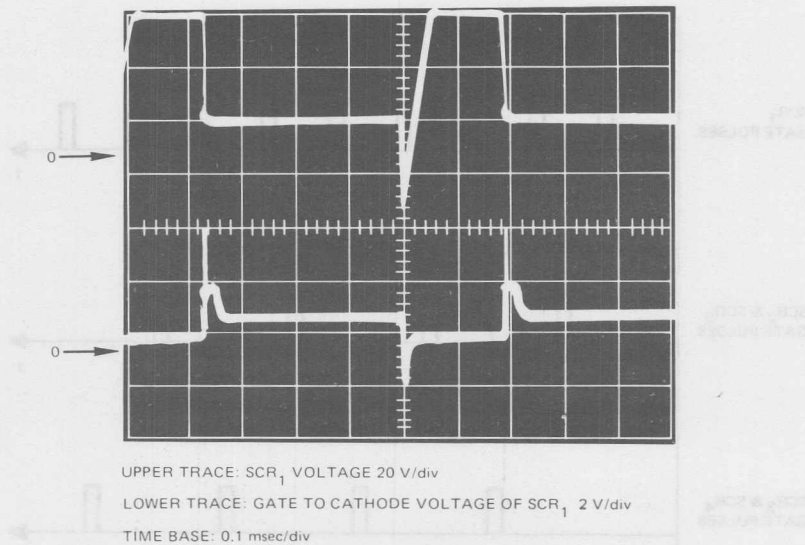


Figure 9-34. Step-Up Chopper—SCR₁ Anode and Gate Voltage Waveforms for $\tau \approx 1/3$

16 volts. The measured value was 15 volts. Figure 9-34 was taken with $\tau \approx 1/3$ and the measured output voltage was 40 volts. The theoretical voltage is 36 volts.

The motor armature voltage is quite smooth, as shown in Figure 9-35.

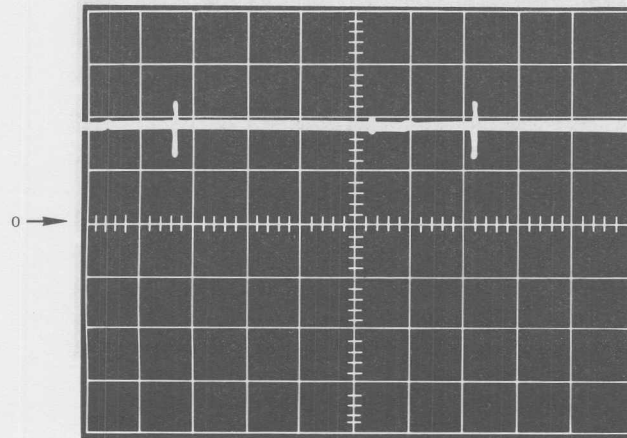
The current drawn from the source contains considerable ripple as shown in Figures 9-36 and 9-37. The voltage across SCR₁ appears in these figures as the top trace. When SCR₁ is triggered, the current builds up rapidly. At the point where a pair of commutating SCRs is triggered, the current rises sharply until the voltage on the commutating capacitor reverses to equal 12 volts. During the off time, the current decays as it is fed into the filter capacitor and motor armature.

Figure 9-36 was taken with minimum output voltage of about 15 volts. The current changes from 1 to 9 amps.

Figure 9-37 was taken with an output voltage of 50 volts. The current in this picture changes from about 20 amps to 50 amps.

The current supplied to the motor armature is very smooth as seen in Figure 9-38.

In summary, this rather novel modified series dc motor control has torque-speed characteristics essentially the same as a conventional series dc motor. The main advantage of the circuit is that it is possible to use reasonably standard motor armature voltage ratings even though the dc supply voltage is low. For the system discussed, the rated motor armature voltage is 100 volts with a dc source voltage of 12 volts. At least a 10:1 control range of motor speed and current is possible for a wide range of motor loads. However, the minimum current at low speed is limited by the nature of the motor load and the minimum on-time that is possible for SCR₁. A step-up ratio of at least



20 V/div, 0.1 msec/div

Figure 9-35. Step-Up Chopper — Armature Voltage Waveform

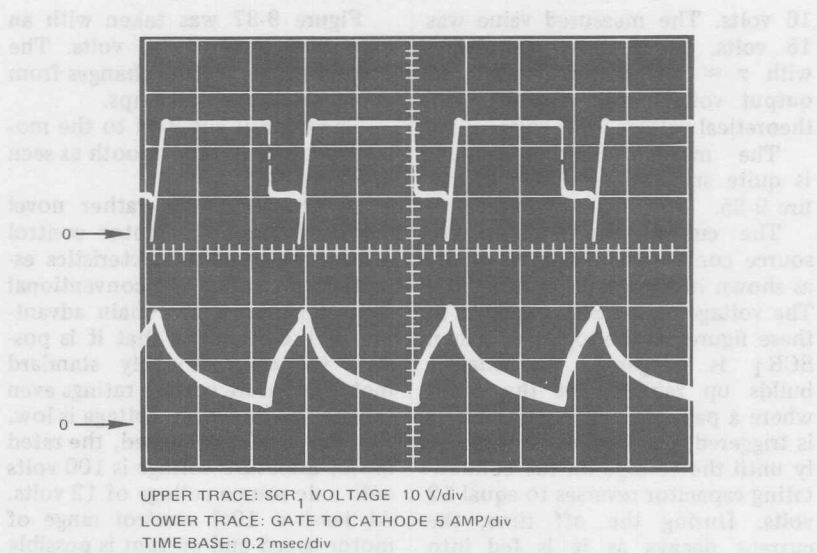


Figure 9-36. Step-Up Chopper — Source Current Waveform
 ($E_{DC} = 15V$)

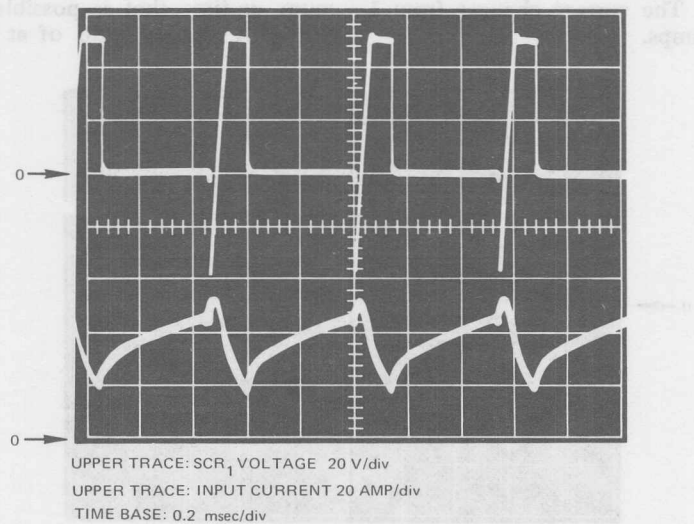


Figure 9-37. Step-Up Chopper — Source Current Waveform
 ($E_{DC} = 50V$)

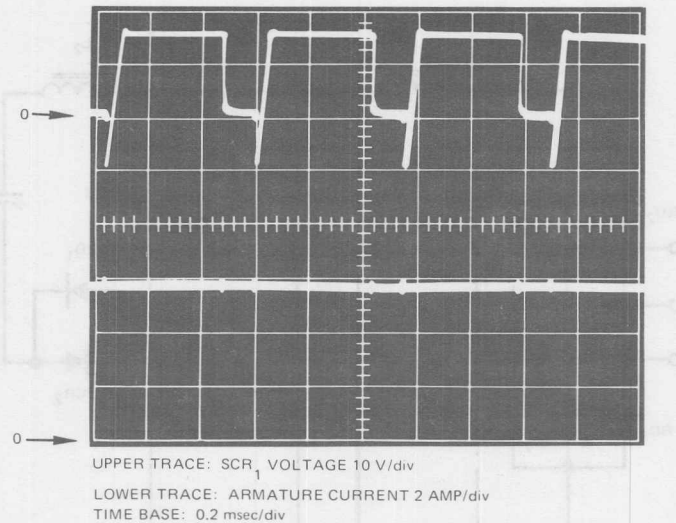


Figure 9-38. Step-Up Chopper — Waveform of Current into Armature

10:1 is easily attainable from rated load to a few percent of rated motor load.

With a 12 volt dc supply, the circuit efficiency is limited to about 70%. Also, nearly 100 amperes source current is required to deliver 10 amperes to the motor armature with a 10:1 voltage step-up ratio. Thus, with a 12 volt source, this motor control is most appropriate for motor ratings of 10 HP or less. The di/dt imposed on SCR₁ may be quite high, limited only by the inductance in the SCR₁, RD₁ and C₁ loop. However, the dv/dt on SCR₁ is limited by the commutating capacitor C₂ charging rate.

Wound Rotor Induction Motor Speed Control

One means of obtaining a variable-speed ac motor is to vary the rotor resistance of an induction motor [2]. This method of speed control provides speed-torque char-

acteristics similar to those of a dc shunt motor speed controlled by means of resistance in series with the armature.

Figure 9-39 is an interesting circuit which functions as a type of resistance modulator. The purpose of this circuit is to vary the average load on the filter L₁, C₁ and, therefore modulate the effective value of R₂ reflected to the rotor. The circuit operates as follows: with C₂ charged, SCR₁ is turned on, drawing current through R₁. At the same time, the charge on C₂ is reversed by the current flow through RD₁. Sometime later SCR₂ is turned on, back biasing and shutting off SCR₁ and recharging C₂ positive.

Figure 9-40 shows an equivalent circuit and theoretical waveforms. The relationships between the battery voltage (E_{DC}) and current (I_{DC}) to the motor parameters are shown in Formula 9-G.

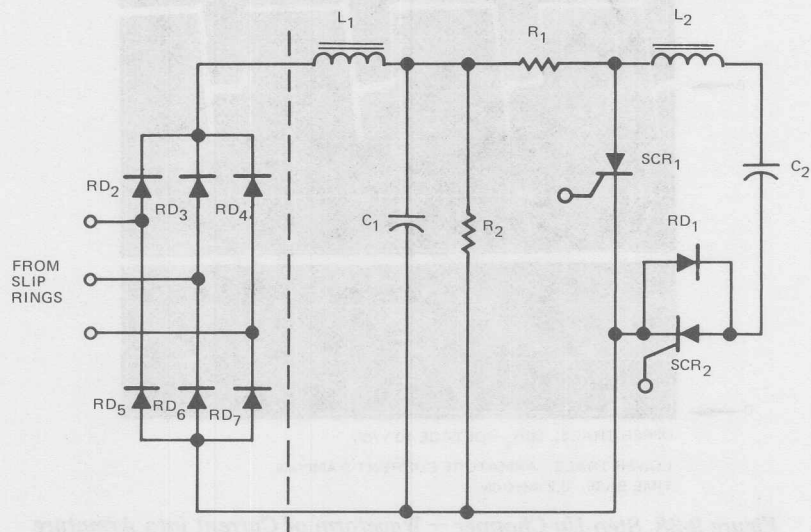


Figure 9-39. Wound Rotor Motor Chopper Speed Control

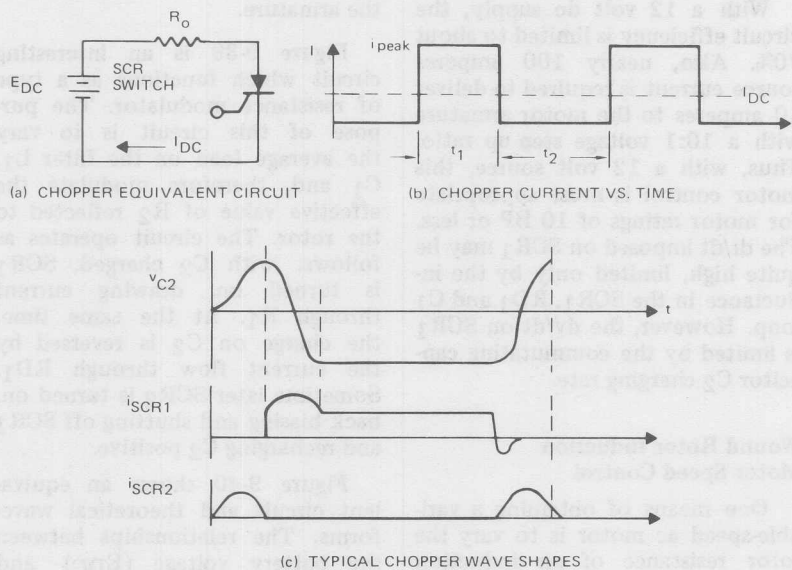


Figure 9-40. Wound Rotor Motor Chopper Speed Control Waveforms

$$E_{DC} = 1.35 E_{\text{line-to-line (rotor)}} \\ I_{DC} = 1.22 I_{\text{rotor}} \quad (9-G)$$

When the synchronous switch is turned on, I_{DC} will rise sharply to E_{DC}/R_o . The current will fall to zero when the switch is shut off. If we examine an idealized waveshape of I_{DC} shown in Figure 9-40, it is seen that Formula 9-H applies:

$$I_{DC} = \frac{(t_1)}{t_1 + t_2} \frac{E_{DC}}{R_o} \quad (9-H)$$

Resistor R_2 in Figure 9-39 is chosen to provide the minimum speed-torque characteristic. Resistor R_1 simply limits the current peaks to SCR_1 ; however, the relationship results in Formula 9-J.

$$S_{\text{min}} = \frac{R_1}{2\nu (100\% \text{ ohms})} \quad (9-J)$$

Where:

ν = maximum possible duty cycle of chopper

By using a pulse width modulated, pulse rate modulated chopper as in Figure 9-39, a duty cycle very close to 1 can be achieved giving the widest possible controllable speed range.

The importance of the filter approach shown in Figure 9-39 can be illustrated by understanding that excessive rotor ripple in the motor can obviously have a profound influence on machine temperature (therefore insulation life) and also perhaps less obviously on bearing life, due to sympathetic vibration.

High efficiency under normal running conditions requires a low rotor resistance; but a high resistance results in a high starting torque and low starting current at low starting power factor.

The motor control of Figure 9-39 provides a simple means of controlling the effective rotor resistance of a wound rotor motor. It also could be readily adapted to closed loop speed control systems, since the rotor resistance is controllable in response to the electrical signal for gating SCR_1 .

Battery Charger Design Example [16]

Figure 9-41 shows a chopper battery charging circuit. The main circuit is a series resonant dc-dc chopper; the input is half-wave rectified and filtered. When SCR_1 is triggered, the dc voltage is applied to the load through series inductor L_1 ; this also starts resonant charging of C_1 . This charges to a voltage approximately twice the applied dc voltage in the first half-cycle of the resonant interval, and the current returns to zero. In the second half-cycle, the current through L_2 - C_1 reverses. When it reaches the same magnitude as the load current, SCR_1 goes off and diode RD_2 conducts to permit current to flow back into the positive side of the dc source. When the current oscillates back to the load current value, the SCR_1 - RD_2 branch opens. Now C_1 discharges through the load. If L_1 is large compared to L_2 and the chopper frequency is relatively high, there is little decay in the load current during this interval; therefore, the voltage on C_1 decreases at an almost constant rate. When the voltage on C_1 reaches zero, diode RD_3 conducts and the load current decreases linearly with the battery load, until SCR_1 is triggered again. Capacitor C_1 and inductor L_2 start each cycle off from zero initial conditions due to the circuit configuration.

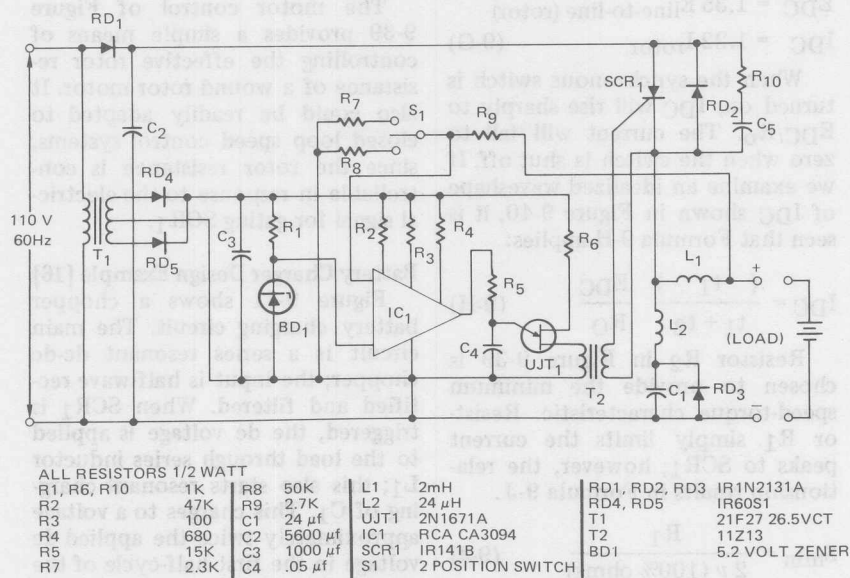


Figure 9-41. Chopper-Type Battery Charger

The triggering circuit utilizes a rectified center-tap transformer and a filter capacitor to provide a 20 volt dc power supply to drive IC₁ and UJT₁. The zener diode, BD₁, is used as a reference level for the differential amplifier; R₁ is a current limiter. The other input to the amplifier is connected to the positive terminal of the battery and is applied through a switch-controlled voltage divider to provide either a 6- or 12-volt charge. The output of the amplifier provides a variable voltage to trigger the emitter of UJT₁. UJT₁ is used to deliver a pulse through pulse transformer T₂ which triggers SCR₁.

Design factors for the dc-dc chopper battery charger are the amount of current desired, the frequency of the chopper, and the frequency of UJT₁.

To determine the value of the L-C series circuit, assume the amount of current desired and, depending on whether the circuit is half or full wave rectified, find the approximate dc voltage.

$$E_{DC} = \frac{E_{IN}}{\pi} \approx 50 \text{ volts} \quad (9-K)$$

With an assumed current of 25 amps,

$$\frac{E_{DC}}{\sqrt{L2/C1}} = 2 \times (\text{max. load current}) \quad (9-L)$$

$$= 2 \times 25 = 50 \text{ amps}$$

This implies that

$$\frac{L2}{C1} = 1 \quad (9-M)$$

Assume the turn-off time is 50 μsec, which is approximately 1/3

the period. Thus, a period is 150 μsec .

$$2\pi \sqrt{(L2)(C1)} = 150 \times 10^{-6} \quad (9-N)$$

$$\sqrt{(L2)(C1)} = 24 \times 10^{-6}$$

From equations 9-M and 9-L,

$$L2 = C1$$

$$(L2)(C1) = 576 \times 10^{-12}$$

$$(C1)^2 = 576 \times 10^{-12}$$

$$C1 = 24 \mu\text{F} \text{ and } L2 = 24 \mu\text{H}$$

To determine the oscillation frequency of UJT₁

$$\frac{50\text{V} \times t_{\text{on}}}{\tau} = 12\text{V}$$

$$\tau = 625 \mu\text{sec}$$

This indicates that the chopper frequency will be approximately 1.6 kHz to produce 12 volts output from the 50 volt dc source. The

maximum chopper frequency is approximately 6 kHz. Therefore, the UJT frequency range should be from 1 to 6 kHz.

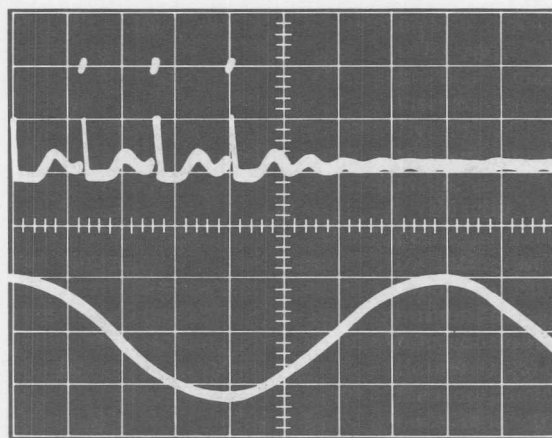
A rough calculation of the ripple current through the battery is provided by

$$\Delta i_{\text{ON TIME}} = \frac{(\Delta V)T}{L_1} = \quad (9-O)$$

$$\frac{(50 - 12)}{2 \times 10^{-3}} (150 \times 10^{-6}) = 2.85 \text{ amps}$$

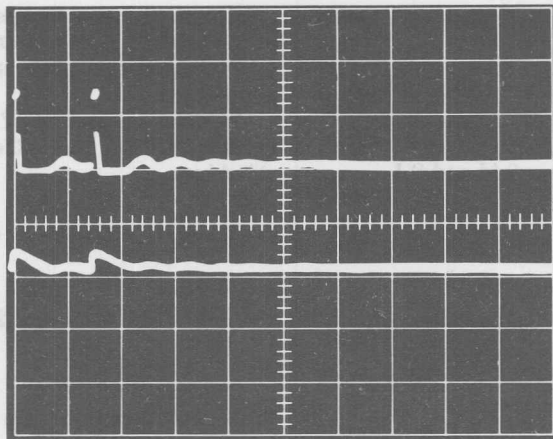
Figures 9-42, 9-43 and 9-44 show waveforms for the operating circuit.

The battery charger circuit of Figure 9-41 is considerably more complicated than a simple phase control type circuit. However, it provides an appreciable step-down voltage ratio without the need for a transformer. In addition, the filtering required is much smaller to



UPPER TRACE: VOLTAGE FROM SCR CATHODE TO
NEGATIVE BUS 50 V/div
LOWER TRACE: LINE VOLTAGE 100 V/div
TIME BASE: 2 msec/div

Figure 9-42. Waveforms for Chopper-Type Battery Charger



UPPER TRACE: VOLTAGE FROM SCR CATHODE TO
NEGATIVE BUS 100 V/div

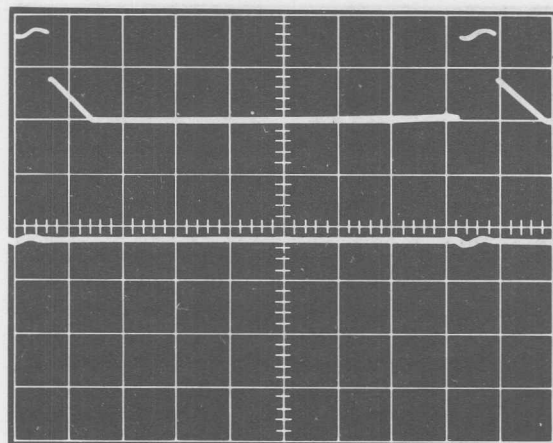
LOWER TRACE: BATTERY VOLTAGE 10 V/div

TIME BASE: 2 msec/div

Figure 9-43. Waveforms for Chopper-Type Battery Charger

achieve ripple-free charging current. Thus, where a power transformer is not desired or where a more com-

pact and lightweight charger may be required, this chopper charger is a feasible approach.



UPPER: VOLTAGE FROM SCR CATHODE TO NEGATIVE BUS 100 V/div

LOWER: FILTER CAPACITOR VOLTAGE 100V/div

TIME BASE : 2 msec/div

Figure 9-44. Waveforms for Chopper-Type Battery Charger

References

1. D. Cooper, "DC to DC Conversion with SCRs," International Rectifier News, Summer, 1968, pp 2-4.
2. A.E. Fitzgerald and C.E. Kingsley, "Electric Machinery," McGraw-Hill Book Co., 1952, pgs. 422-429.
3. K. Heumaun, "Pulse Control of D-C and A-C Motors by SCR," IEEE Trans. on Communications and Electronics, vol. 83, pp. 390-399, July 1964.
4. R.E. Morgan, "A New Magnetic-Controlled Rectifier Power Amplifier with a Saturable Reactor Controlling on Time," Trans. AIEE (Communications and Electronics), vol. 80, pp. 152-155, May 1961.
5. R.A. Colclaser and A.E. Relation, "A Fixed Frequency, Variable Pulse Width Silicon-Controlled Rectifier D-C Chopper Regulator," presented at the 1963 AIEE Winter General Meeting, New York, N.Y.
6. W. McMurray, "SCR D-C to D-C Power Converters," IEEE Trans. on Communications and Electronics, vol. 83, pp. 198-203, March 1964.
7. R.E. Morgan, "A New Control Amplifier Using a Saturable Current Transformer and a Switching Transistor," Trans. AIEE (Communications and Electronics), vol. 77, pp. 557-562, November 1958.
8. S.P. Jackson, "Design Considerations for the Transistor Saturable Current Transformer Amplifier (Morgan Circuit)," presented at the 1960 AIEE Fall General Meeting, Chicago, Ill.
9. R.A. Engelhardt and A.J. Papavasiliou, "A Study of the Morgan D-C to D-C Step-Down Circuit," 1963 Proc. INTER-MAG Conf. pp. 11-5-1-8. April 1963.
10. G. Sager, "A Magnetically Regulated DC to DC Converter Power Supply," Trans. AIEE (Communications and Electronics), vol. 80, pp. 513-514, November 1961.
11. F.G. Turnbull, "Controlled Rectifier D-C to D-C 30-HP Motor Drive," Trans. AIEE (Communications and Electronics), vol. 81, pp. 458-462, January 1963.
12. R.E. Morgan, "Time Ratio Control," IEEE Trans. on Communications and Electronics, vol. 83, pp. 366-371, July 1964.
13. R.G. Hoft, H.S. Patel, and Y. Dote, "Thyristor Series Resonant DC-DC Chopper," IEEE Transactions on Magnetics, September, 1972, pp. 286-288.
14. D.W. Borst, E.J. Diebold, and F.W. Parrish, "Voltage Control by Means of Power Thyristors," IEEE Transactions on Industry and General Applications, March/April 1966, pp. 102-124.
15. J.W. Finnell and R.G. Hoft, "Thyristor Chopper for Modified Series Motor," IFAC Conference on Control in Power

- Electronics and Electrical Drives, Dusseldorf, Germany, October, 1974.
16. R.G. Hoft and G.N. Vogelgesang, "Solid-State Power Control Program Progress Report #2," University of Missouri, Columbia, August 21, 1973.
 17. E. Reimers, "Design Analysis of Multi-Phase DC Chopper Motor Drive," IEEE/IGA Conference, 1970, pp. 587-595.

Fast Recovery Rectifiers

The need for fast recovery diodes has been considerably increased by the development of power control systems using SCRs. Proper use of fast recovery diodes reduces di/dt and accompanying stress levels on SCRs, thereby increasing reliability without necessitating additional complex circuitry.

With fast recovery diodes, power levels may be increased and costly power losses reduced. The primary advantage is that junction heating caused by recovery action is minimized.

Rectifier diodes with fast-recovery characteristics are becoming increasingly important in the design of high-power semiconductor equipment. Circuit designers are showing an increasing interest in these devices for such applications as free-wheeling diodes (also called by-pass diodes), high-frequency inverters, and high-frequency power rectifiers.

Fast-recovery diodes are available today with ratings upwards of 650A average, and 1300 PRV and higher. Specific devices in these higher current ratings may be obtained with recovery times as short as 1.5 μsec maximum when rated 1000V or less, and 2.0 μsec when rated 1100 through 1300V.

While rectifier diodes with higher voltage and current ratings and shorter recovery times are available, the general rule is that the higher the voltage rating, the longer the shortest recovery time that is available.

High-Frequency Power Rectification

The most obvious application for fast-recovery diodes is in converting high-frequency ac to dc. The upper frequency for efficient rectification with conventional alloy or diffused 250A diodes is about 1 kHz. By contrast, the upper frequency limit for efficient operation of the 100 to 650A fast-recovery diodes is about 10 kHz.

At any operating frequency, fast-recovery characteristics result in less power dissipation in the diode during recovery, thus more power may be dissipated during the passage of forward current without overheating the diode. The result is a more efficient circuit and a reduction in spurious diode heating.

Free-Wheeling Diodes in Rectifier Circuits

Large fast-recovery diodes function well as free-wheeling diodes or by-pass diodes, on the output of any single or three-phase SCR rectifier unit when the load is both resistive and inductive, and when the rectifier-unit output voltage is to be reduced by phase-controlling the SCRs. Failure to use free-wheeling diodes in rectifier units can result in problems when there is an inductive component to the applied load.

If the load is 100% inductive, and there is no free-wheeling diode, the inductance will cause current to flow continuously in the SCRs, and zero output voltage is obtained with 90° phase retard. When the

load includes a resistive as well as an inductive component, and large angles of phase-retard are employed, the load current becomes discontinuous. To obtain zero output voltage with this load, it is necessary to use a larger amount of phase retard; therefore, an abrupt change in the relationship between output voltage and phase retard occurs (at the phase retard angle where the output current becomes discontinuous). Essentially, there is a change in the transfer function of the rectifier unit when viewed as a part of a feedback-regulating system.

The change in operating mode experienced without the free-wheeling diode may therefore create severe instabilities in the operation of a closed-loop voltage or current-regulating system. With or without the free-wheeling diode, the same larger range of phase control is needed to obtain zero output voltage, but the abrupt change in transfer function, and the consequent system instability, are eliminated when the free-wheeling diode is used.

Another advantage of the free-wheeling diode is that at reduced output voltage from the rectifier unit current is carried only intermittently by the SCRs. This reduces heating in the SCRs and increases their reliability.

If a hybrid-bridge (semiconverter) circuit is used to feed a partially inductive load, a free-wheeling diode is recommended when near-zero output voltage from the bridge is desired. With the free-wheeling diode, the bridge circuit will feed an apparently resistive load and behave accordingly. Without it, the SCRs may fail to turn off (commutate) when operating with large an-

gles of phase control. This is similar to a failure in an inverter. The SCRs in a hybrid bridge actually function like inverters at very low output voltages, feeding energy from the diode portion of the bridge back into the ac line. A commutation failure in this inverter results in loss of control of output voltage from the hybrid-bridge rectifier unit.

Any rectifier diode can function as a free-wheeling diode; however, the advantages of using a type with fast-recovery characteristics include lower diode junction heating during recovery and reduced di/dt duty imposed on SCRs in the rectifier unit during diode recovery.

If a free-wheeling diode is conducting when an SCR begins to turn on, a high inrush current will flow during the recovery period of the diode; that is, during the flow of recombination current in the diode junction. If this happens, the SCR turns on into a virtual short circuit, resulting in a high di/dt in the SCR. Damage to both the SCR and the free-wheeling diode could result from this effect.

This circuit action is illustrated in Figure 10-1, where an SCR feeds half-wave power to an inductive load with a free-wheeling diode. A high spike of current is carried by the SCR when it is first triggered on, and this same current pulse passes in the reverse direction through the free-wheeling diode. To avoid overheating of the free-wheeling diode during recovery, a snubber network consisting of a resistor and capacitor in series could be placed across the free-wheeling diode. This will limit the rate-of-rise of reverse voltage across the diode while it is recovering, and reduce the heating of the junction during

the recovery period; however, this snubber network will increase the di/dt on the SCR in the rectifier circuit.

At 60 Hz, the di/dt stress level may not be inordinately high, but at higher-power frequencies, the SCR may be damaged by high localized junction temperatures during turn-on. To reduce the rate of current rise during turn-on, a limiting inductance could be placed in the circuit; however, when current ceases, this inductance induces a voltage in the circuit that could damage the free-wheeling diode or break over the SCR.

A better solution is an RC snubber network, placed across each SCR to provide a current path, and thereby reduce the voltage transients during recovery.

The large apparent stored charge of a conventional diode, which must be removed during recombination, is the basic problem in these

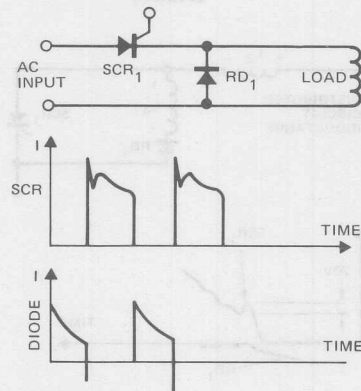


Figure 10-1. Free-wheeling Diode in Half-Wave Phase-Controlled Rectifier Circuit

cases. By using a fast-recovery diode, and thus minimizing the stored charge, snubber networks might be eliminated altogether. Or, if they are required, snubber-network capacitance may be minimized.

Free-Wheeling Diodes in DC Choppers

As SCR manufacturers have developed more controlled dynamic characteristics of thyristors, greater attention has been focused on inverter and dc chopper applications.

Figure 10-2 illustrates a typical early chopper circuit with some pertinent waveshapes. The circuit through which current flows while RD_1 is recovering, stores enough energy in lead inductances and elsewhere to cause a considerable voltage transient when RD_1 recovers. To suppress this transient, an RC

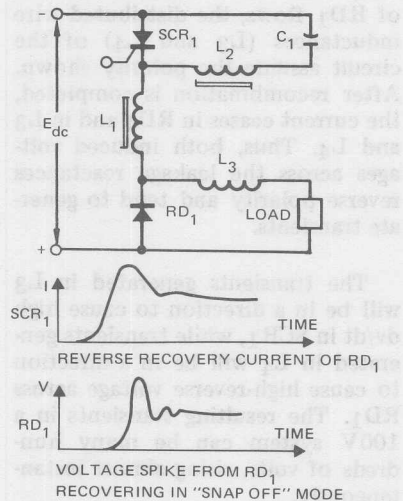


Figure 10-2. Time-Ratio Control with "Hard" Commutation

network could be inserted across both SCR_1 and RD_1 ; however, this causes higher circuit losses and more complexity. A far better solution is to use a fast-recovery diode for RD_1 .

Free-Wheeling Diodes in Inverters

An inverter using free-wheeling diodes connected in anti-parallel with the SCRs is shown in Figure 10-3. With minor modifications, this type of inverter can be made to generate either a sine or square wave. Similar circuits have been operated up to 25 kHz with an output power of 400W. The trace in Figure 10-3 is the voltage across one SCR.

Examining Figure 10-4, which shows a circuit equivalent to part of the circuit shown in Figure 10-3, it can be seen that fast-recovery devices are required for RD_1 and RD_2 . While the sweepout current of RD_1 flows, the distributed wire inductances (L_3 and L_4) of the circuit assume the polarity shown. After recombination is completed, the current ceases in RD_1 and in L_3 and L_4 . Thus, both induced voltages across the leakage reactances reverse polarity and tend to generate transients.

The transients generated in L_3 will be in a direction to cause high dv/dt in SCR_1 , while transients generated in L_4 will be in a direction to cause high-reverse voltage across RD_1 . The resulting transients in a 100V system can be many hundreds of volts, rising almost instantaneously.

As illustrated in Figure 10-4, operating conditions are considerably improved with a fast-recovery rectifier. The voltage generated

across SCR_1 when RD_1 recovers is typically 20V in a 125V circuit. A fast-recovery diode is also appropriate here to minimize the energy drawn from the dc supply when the diode is recovery, and to minimize junction heating caused by the recovery action.

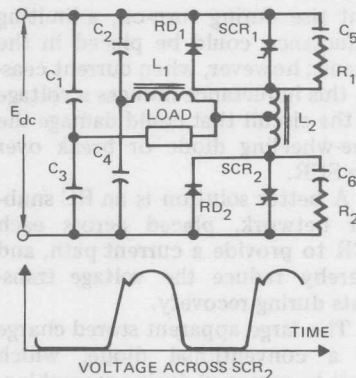


Figure 10-3. Inverter with Free-Wheeling Diodes

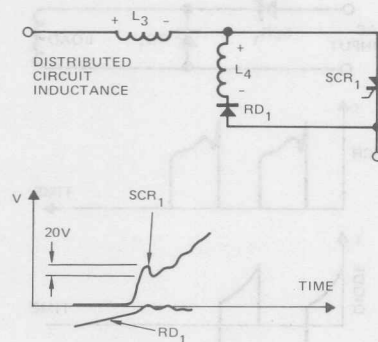


Figure 10-4. Equivalent Circuit During Rectifier Recovery

SCRs as Free-Wheeling Diodes in Inverters

The free-wheeling diodes of Figure 10-3 have the undesirable characteristic of clamping the reverse voltage applied to the companion controlled rectifiers, causing increased turn-off time. Hence SCRs with shorter turn-off time must be used. Where it is not possible to obtain an SCR fast enough to counteract the presence of the free-wheeling diode, it is possible to use an SCR in place of the diode.

The free-wheeling SCR should be triggered by connecting the gate to the anode via an appropriate resistor. When the voltage across the inverter SCR first starts to reverse, the clamping action of the free-wheeling SCR will not be felt until the free-wheeling SCR turns on. During the delay time of the free-wheeling SCR, the main SCR can be turning off with full available reverse voltage applied, thereby assuring fast turn-off action.

Soft Commutation

High-voltage, inverter-type power thyristors (e.g., V_{DRM} of 1200V) are being used in large installations, such as process control and vehicle drives. In these higher ratings, some of the early quick fixes for sweepout transients are not acceptable. Neither are the sharply rising waveshapes generated by the early types of inverters and choppers (because of the resultant low corona threshold of many components).

At operating frequencies of 5 to 10 kHz, losses in the snubber networks in these inverters, sometimes amounting to 10% of the load, became unacceptable. Therefore, as SCR applications have developed

and operating frequencies of thyristors have increased, the sharply rising waveshape circuits have become less popular, and "soft" waveshape circuits have gained favor.

Figure 10-5 illustrates a cushioned waveshape circuit that reduces the necessity for a fast-recovery rectifier for RD_1 . However, as the frequency of circuit operation increases, this circuit requires fast-recovery characteristics in the free-wheeling diode to hold the SCR stress to a minimum.

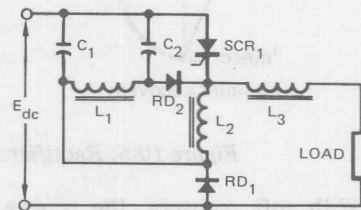


Figure 10-5. Time-Ratio Control with "Soft" Commutation

Recovery Characteristics

Figure 10-6 characterizes the four types of recovery characteristics of a rectifier. Figure 10-6(a) depicts a "normal" recovery for a diffused power rectifier. Figures 10-6(b) and 10-6(c) show recovery current of a snap-off rectifier. Figure 10-6(d) shows recovery current of a "soft" recovery rectifier. The snap-off diode characteristic has been found to be so rapid that some rather unique pulse-forming networks have been designed using the snap characteristics of certain rectifier diodes. It is generally found less than desirable to generate such pulses in a circuit that contains components which can be punched through by these transients.

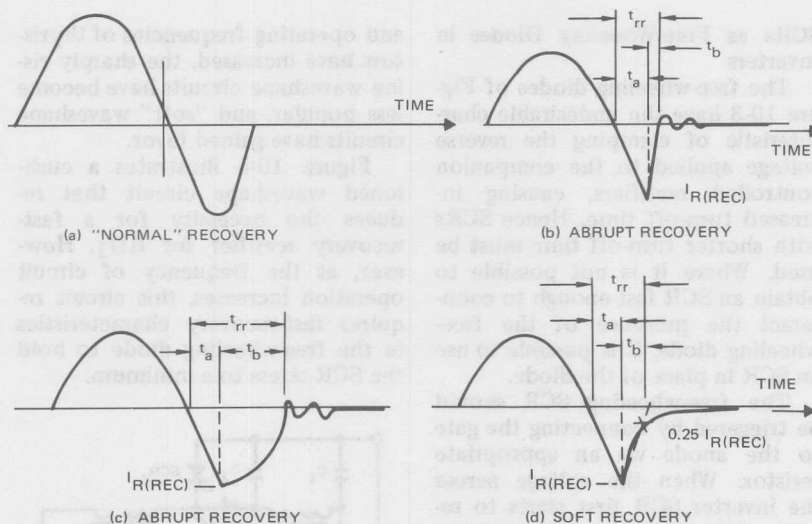


Figure 10-6. Rectifier Recovery Characteristics

With soft recovery, the reverse current trace gradually approaches normal leakage current. With abrupt recovery, the reverse current suddenly drops to zero, and inductance/capacitance current oscillates violently. More rapid minority carrier recombination in the silicon crystal can reduce recovery time (often accomplished by doping the crystal, creating dislocation centers in the lattice structure).

Measurement of Reverse Recovery Time

Several years ago, a circuit was devised for measuring reverse recovery time of a small rectifier diode rated about 5 amperes. It consists of a forward current supply which delivers one ampere, and a transistor to abruptly switch on a reverse voltage of 30 volts. This voltage causes the device under test to block the one ampere of forward

current. Later, the transistor was replaced by a mercury-wetted contact relay. These same circuit conditions were subsequently used when measuring the reverse recovery time of rectifier diodes rated as much as 35 amperes average.

Reverse recovery time is a strong function of the forward current, prior to the application of reverse voltage. A forward current of one ampere in a rectifier diode rated tens or hundreds of amperes is not a representative operating condition. Recovery times of the order of 200 nanoseconds, measured under this condition, are gratifyingly low, and perhaps can form a basis of comparison of one diode with another. However, these ratings are not indicative of the recovery time that will be observed when the diode is operated at its normal current level.

Recognizing the shortcomings of this early test method, JEDEC Committee JC-22 on Power Rectifiers, diodes, and thyristors has adopted a different circuit for recovery time measurements on power rectifier diodes. This circuit is shown in Figure 10-7.

The two most important test conditions are the rate of forward current reversal, di/dt , and the magnitude of the forward current. If the resistance of the power loop is kept very small; e.g., $2\sqrt{L_1/C_1} \gg R$, then the forward current trace is essentially sinusoidal. Typical waveforms are shown in Figures 10-6(b) and 10-6(d). Called I_{FM} , the peak forward test current is specified as π times the full cycle average (half sine wave) rated current of the device under test. The di/dt of this current should be linear as it crosses the zero axis. The slope of the current trace is to be measured

from $1/2 I_{FM}$ to $I_{FM} = 0$ and the JEDEC registration procedure states that this di/dt be 25 amperes/microseconds. Since the time for this measurement is 30 electrical degrees or $1/6$ of the pulse width (t_p) (assuming a true half sine wave), we can express pulse width in microseconds as $t_p = 0.12 I_{FM}$ when $di/dt = 25$. If high voltage oscillations above the peak reverse voltage rating of the diode under test (DUT) occur, adjust the value of C_1 , L_1 , or V (increase the value of C_1 for instance).

If this is not effective, apply the clamping circuit, shown in Figure 10-7, by closing SW_1 . Typical values for this circuit are $R_2 \approx 250\Omega$, $C_2 \approx 4$ mf.

Rectifier diode RD_2 and its circuit branch, should provide a very low inductance path around SCR_1 . If the reverse recovery time of SCR_1 is shorter than that of the

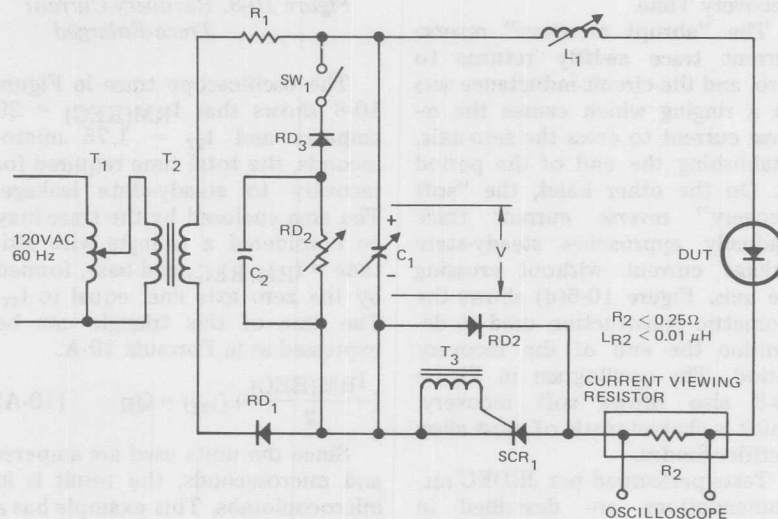


Figure 10-7. JEDEC Reverse Recovery Test Circuit

DUT, RD₂ will provide an alternate path for the reverse recovery current of the DUT. An external triggering source is to be connected to the primary of T₃.

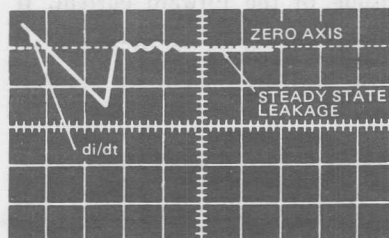
It is believed these test parameters represent typical operation of power rectifier diodes under commutating conditions. The earlier test method paid little heed to the commutating rate ($-di/dt$) and the measurements were considerably influenced by stray circuit inductance.

From the typical waveforms shown, it can be seen that two types of recovery action can occur: Figure 10-6(b) is abrupt recovery, and Figure 10-6(d) is soft recovery. Reverse recovery time, t_{rr} , is divided into two parts, t_a and t_b , the sum of these equals t_{rr} . The JEDEC committee did not name these parts, but it is suggested that t_a may aptly be named Junction Recovery Time and t_b named Bulk Recovery Time.

The "abrupt recovery" reverse current trace swiftly returns to zero, and the circuit inductance sets up a ringing which causes the reverse current to cross the zero axis, establishing the end of the period t_b . On the other hand, the "soft recovery" reverse current trace gradually approaches steady-state leakage current without crossing the axis. Figure 10-6(d) shows the geometric construction used to determine the end of the recovery period. The oscillogram in Figure 10-8 also shows soft recovery, which is characteristic of most alloy rectifier diodes.

Tests performed per JEDEC recommendations are described in terms of reverse recovery time in microseconds. However, some en-

gineers prefer to think of the recovery phenomenon in terms of recovered charge, called Q_R , and measured in microcoulombs. This recovered charge is proportional to the area of the approximate triangle formed as the reverse recovery current, $I_{RM(REC)}$, increases from zero to its maximum, then recedes to steady-state leakage.



V = 20 A/div H = 1 μ sec/div
 $t_{rr} = 1.75 \mu$ sec $I_{R(REC)} = 29$ A
 $di/dt = -25A/\mu$ sec $Q_R = 25.4 \mu$ coulombs
 $I_{FM} = 785A$

Figure 10-8. Recovery Current Trace-Enlarged

The oscilloscope trace in Figure 10-8 shows that $I_{RM(REC)} = 29$ amperes and $t_{rr} = 1.75$ microseconds, the total time required for recovery to steady-state leakage. The area enclosed by the trace may be considered a triangle with altitude = $I_{RM(REC)}$ and base, formed by the zero axis line, equal to t_{rr} . The area of this triangle can be expressed as in Formula 10-A.

$$\left(\frac{I_{RM(REC)}}{2}\right) (t_{rr}) = Q_R \quad (10-A)$$

Since the units used are amperes and microseconds, the result is in microcoulombs. This example has a recovered charge of $29 \times 1.75/2 = 25.4$ microcoulombs.

The slope of the current trace remains approximately constant as the current goes through zero and reverses, until the current nearly reaches $I_{RM}(REC)$. It is possible to write equations which approximately describe the relationship of reverse recovery time, recovered charge, and peak reverse recovery current to each other.

For IR's fast recovery rectifiers, the ratio of the recovery time periods t_a and t_b is approximately 3:1. Making this assumption, Formulas 10-B, 10-C and 10-D approximate these relationships:

$$Q_R \approx \frac{[I_{RM}(REC)] [t_{rr}]}{2} \quad (10-B)$$

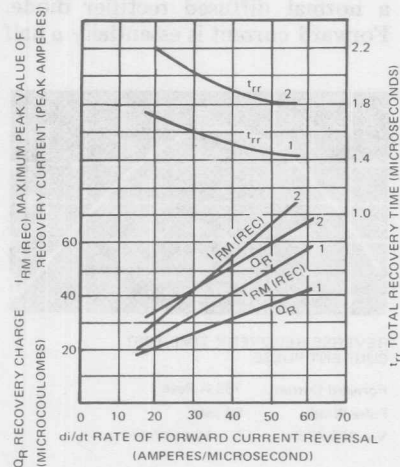
$$t_{rr} \approx \sqrt{\frac{2.67 Q_R}{di/dt}} \quad (10-C)$$

$$I_{RM}(REC) \approx \sqrt{1.5 Q_R (di/dt)} \quad (10-D)$$

The JEDEC registration procedure includes specifying maximum $I_{RM}(REC)$, as well as I_{FM} , di/dt , and maximum t_{rr} , so a comparison may be made between recovered charge and recovery time.

Most tests have been made at a specified slope of 25 amperes/microseconds as the test current reverses from the conducting to blocking mode. However, there is value in observing the relationship of the other variables when the test current slope is changed, but the peak forward current, I_{FM} , is maintained constant at the device rating. Figure 10-9 shows how the slope of the test current affects $I_{RM}(REC)$, t_{rr} and Q_R . This stresses the importance of defining test parameters when assigning a recovery time rating to any rectifier diode with

the fast recovery feature. These relationships are also of value when it is desired to estimate device performance under conditions which are not the same as the standard test conditions.



1. CHARACTERISTICS OF A FAST RECOVERY DIFFUSED 250 AMP RECTIFIER DIODE.
2. CHARACTERISTICS OF A MODERATE RECOVERY DIFFUSED 250 AMP RECTIFIER DIODE.

Figure 10-9. Effects of Slope of Test Current

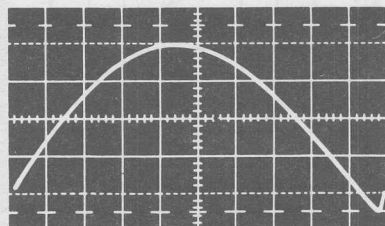
A 250 ampere, Fast Recovery Rectifier Diode

Reverse recovery time can be reduced by speeding up the recombination of minority carriers in the silicon crystal; in other words, by reducing the minority carrier lifetime. This can be done by creating dislocation centers in the crystal lattice structure.

Diffused junctions respond to physical changes used to speed up the recombination of minority carriers, which results in a decrease of recovery time. Several oscillograms

display the waveforms of a 250 ampere diode with various types of junction structure to produce changes in recovery type.

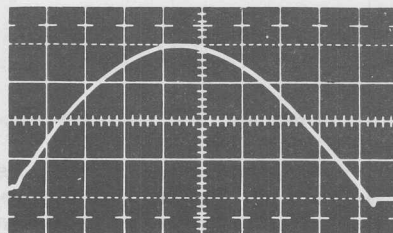
Figure 10-10 shows the forward and reverse current waveforms observed during recovery time tests on a normal diffused rectifier diode. Forward current is essentially a half



REVERSE RECOVERY TIME TEST
CURRENT PULSE

Forward Current: 785 A Peak
Pulse Width: 94 μ sec
V = 200 A/div H = 10 μ sec/div

Figure 10-10. Normal Diffused Rectifier Current Waveform



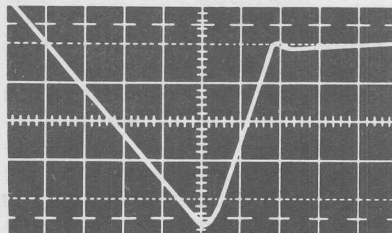
REVERSE RECOVERY TIME TEST
CURRENT PULSE

Forward Current: 785 A Peak
Pulse Width: 94 μ sec
V = 200 A/div H = 10 μ sec/div

Figure 10-11. Fast-Recovery Diffused Rectifier Current Waveform

sine wave with a peak value of π times 250 amperes (785A). The reverse recovery current trace is quite evident in the lower right-hand corner. Figure 10-11 shows the waveform when the same test conditions are applied to a similar diode which has been treated to provide fast recovery. The reverse recovery current trace is noticeably smaller.

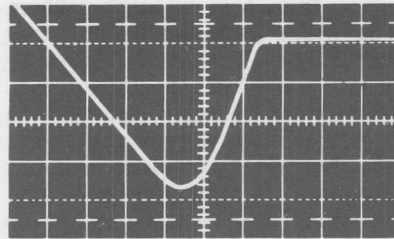
The next four figures show only the reverse recovery traces, but with scales enlarged. All have identical oscilloscope sensitivity. Figure 10-12 shows the normal diffused rectifier. It is interesting to compare this with Figure 10-13, the characteristics of an alloy rectifier of similar current rating. The recovery time and charge of the alloy rectifier are seen to be less than that of the diffused, also the recovery action is more gradual. Figures 10-14 and 10-15 are for diffused rectifiers of the same size



REVERSE RECOVERY CHARACTERISTICS

Forward Current: 785 A Peak
 di/dt : -25 A/ μ sec
 t_{rr} = 5.8 μ sec $I_{RM(REC)}$ = 95A
 t_a = 4.1 μ sec t_b = 1.7 μ sec
V = 20 A/div H = 1 μ sec/div

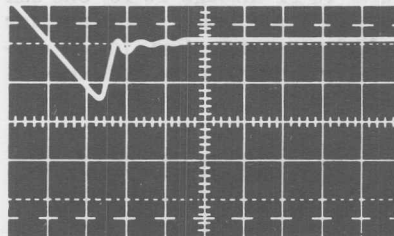
Figure 10-12. Normal Diffused Rectifier Reverse Recovery Detail



REVERSE RECOVERY CHARACTERISTICS

Forward Current: 785 A Peak
 di/dt : $-25 \text{ A}/\mu\text{sec}$
 $t_{rr} = 5.5 \mu\text{sec}$ $I_{RM}(\text{REC}) = 74 \text{ A}$
 $t_a = 3.5 \mu\text{sec}$ $t_b = 2.0 \mu\text{sec}$
 $V = 20 \text{ A}/\text{div}$ $H = 1 \mu\text{sec}/\text{div}$

*Figure 10-13. Alloy Rectifier
Reverse Recovery
Detail*



REVERSE RECOVERY CHARACTERISTICS

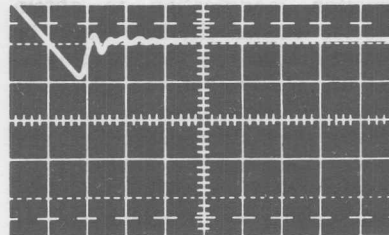
Forward Current: 785 A Peak
 di/dt : $25 \text{ A}/\mu\text{sec}$
 $t_{rr} = 1.75 \mu\text{sec}$ $I_{RM}(\text{REC}) = 29 \text{ A}$
 $t_a = 1.3 \mu\text{sec}$ $t_b = .45 \mu\text{sec}$
 $V = 20 \text{ A}/\text{div}$ $H = 1 \mu\text{sec}/\text{div}$

*Figure 10-14. Moderate Recovery
Rectifier Reverse
Recovery Detail*

which have been modified to give different values of recovery time.

The reductions in recovery time and charge are seen to be considerable. Table X-I summarizes the range of reverse recovery times observed in these four types of 250 ampere rectifier diodes. Similar

data is available for IR's other fast recovery diodes.



REVERSE RECOVERY CHARACTERISTICS

Forward Current: 785 A Peak
 di/dt : $-25 \text{ A}/\mu\text{sec}$
 $t_{rr} = 1.1 \mu\text{sec}$ $I_{RM}(\text{REC}) = 18 \text{ A}$
 $t_a = 0.8 \mu\text{sec}$ $t_b = 0.3 \mu\text{sec}$
 $V = 20 \text{ A}/\text{div}$ $H = 1 \mu\text{sec}/\text{div}$

*Figure 10-15. Very Fast Recovery
Diffused Rectifier
Reverse Recovery
Detail*

Table X-I. Rectifier Diode Recovery Times

	μsec
Alloy	4.3 - 5.0
Normal Diffused	4.8 - 6.5
Moderate Recovery Diffused	1.5 - 2.2
Very Fast Recovery Diffused	1.1 - 1.9
Test Conditions:	
$I_{FM} = 785 \text{ A}$, $di/dt = -25 \text{ A}/\mu\text{sec}$, $t_p = 94 \mu\text{sec}$	

Relationships as Recovery Time Change

Peak reverse voltage and avalanche voltage are closely related. Both vary directly with silicon resistivity. Forward voltage varies directly with silicon thickness and inversely with carrier lifetime, but is not appreciably affected by resistivity. Recovery time varies directly

with silicon thickness and directly with carrier lifetime. Usually reducing the recovery time results in an increase of forward voltage. The junction modification to obtain shorter carrier lifetime must be properly balanced with junction resistivity and thickness to achieve an optimum relationship between recovery time, forward voltage, and peak reverse voltage. Reducing recovery time by changing carrier lifetime results in increasing the diode's reverse leakage current, which becomes especially significant at elevated temperatures as shown in Figure 10-16.

The initial, or saturation leakage current at 150°C for the 900 volt avalanche normal diffused diode shown in Figure 10-16 is 0.6 mA. For the fast recovery diode, the saturation leakage current is 6 mA, and it is 9 mA for the very fast recovery diode. Normal diodes,

made from high resistivity silicon and which avalanche above 2,000 volts, show a saturation leakage current at 150°C of only about 2 mA. The greater leakage current and the higher forward voltage observed in the fast recovery diode make it necessary to limit the maximum operating junction temperature to 175°C in order to avoid excessive reverse power dissipation and resulting thermal run-away.

Calculation of Recovery Losses in Power Rectification

Converting high frequency ac power to dc is the most obvious application for a fast recovery diode in power circuitry. By using recovery waveshapes, shown in Figures 10-11 through 10-15, one can calculate the upper frequency for efficient rectification for a conventional alloy or conventional diffused diode.

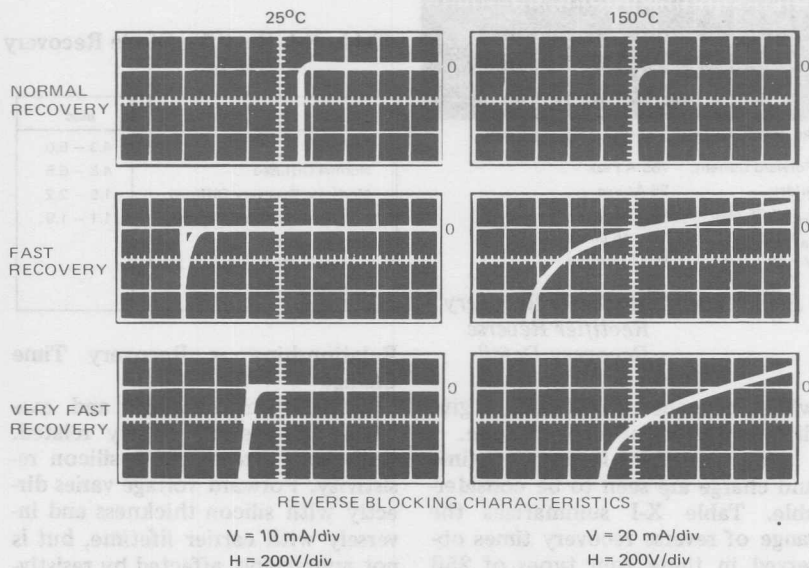


Figure 10-16. Reverse Leakage Current

Consider, for instance, the waveshape for the diode shown as a normal diffused rectifier in Figure 10-12. Let us assume we wish to apply the diode in a typical inverter power supply (Figure 10-17(a)). Triggering SCR₁ and SCR₄ simultaneously, applies the input voltage E_{DC} to the load transformer T₁ and the commutating capacitor C₅. Turning on SCR₂ and SCR₃ on the opposite sides of the inverter causes the charge on C₅ to reverse bias SCR₁ and SCR₄, turning them off. Figure 10-17(b) shows the resulting trapezoidal voltage waveshape applied to the diode bridge RD₅, RD₆, RD₇, and RD₈. The current and voltage waveforms pertaining to one of the diodes in this bridge during reverse recovery are shown in Figure 10-17(c). From these figures it can be shown that the average losses during recovery can be calculated using Formula 10-E.

Averaging this dissipation over the full cycle period for the inverter determines the contribution of the recovery losses to the total diode dissipation. This contribution is shown in Formula 10-F.

$$P_{R(AV)}(REC) = f P_R t_{rr} \quad (10-F)$$

Where:

$$P_{R(AV)}(REC) = \text{Average Recovery Power}$$

$$f = \text{Inverter operating frequency}$$

$$t_a = 4.1 \times 10^{-6} \text{ sec}$$

$$t_b = 1.7 \times 10^{-6} \text{ sec}$$

$$t_{rr} = t_a + t_b = 5.8 \times 10^{-6} \text{ sec}$$

Assume: $f = 1 \text{ kHz}$

Therefore: the average recovery losses,

$$P_{R(AV)}(REC) = 1 \text{ kHz} \cdot 28,500\text{W}$$

$$(4.1 \times 10^{-6} \text{ sec} + 1.7 \times 10^{-6} \text{ sec})$$

$$= 165.3\text{W}$$

At 3 kHz, this dissipation would be 495.9 watts. Therefore, high operating frequencies limit the application of normal recovery diodes.

Consider now the performance of a fast recovery diode, the waveform for which is shown in Figure 10-14. Since $I_{RM}(REC)$ for this diode is only 29A, the losses, P_R , are only 8700W. At 1 kHz, since t_a is only 1.3×10^{-6} sec and t_b is only 0.45×10^{-6} sec, this becomes an average dissipation of 15.23 watts.

Before the dissipation during recovery becomes as much as that, at 1 kHz, of the previously discussed

$$P_R(REC) = \frac{V_{RWM} \cdot Q_R(REC)}{t_{rr}} = \frac{V_{RWM} \cdot I_{RM}(REC)}{2} \quad (10-E)$$

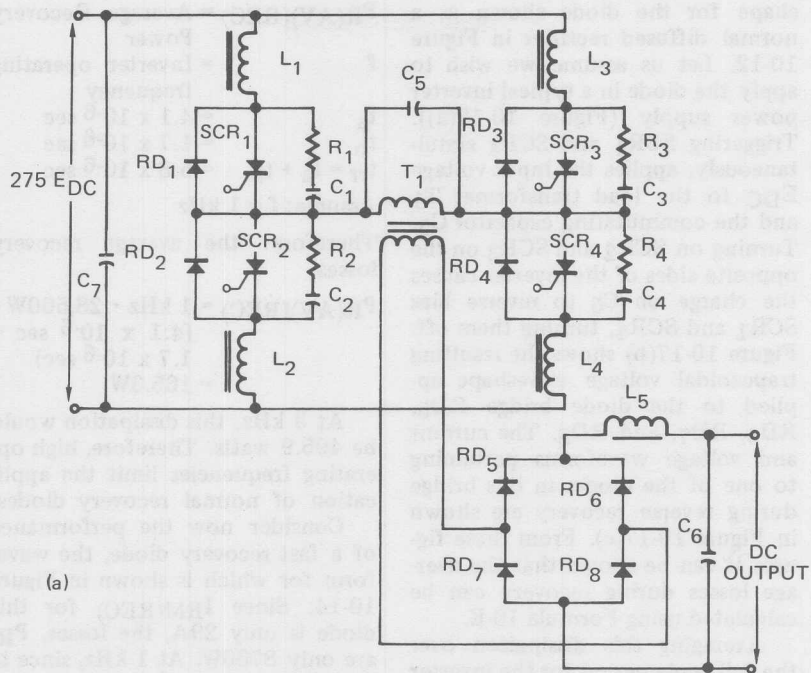
Where:

$P_R(REC)$ = Recovery power

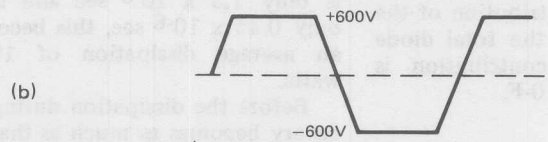
$I_{RM}(REC)$ = 95A

V_{RWM} = Peak reverse voltage applied to rectifier during operation

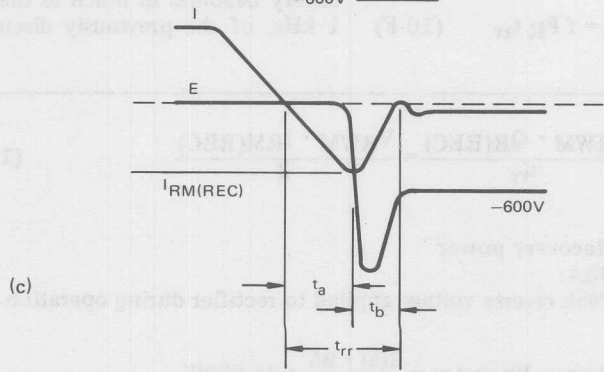
$$\text{therefore, the losses, } P_R(REC) = \frac{600 \cdot 95}{2} = 28,500\text{W}$$



(a)



(b)



(c)

Figure 10-17. High Frequency Inverter with Fast Recovery Rectifiers

diode, the operating frequency would have to be increased to 10.85 kHz.

Thus, by using a fast recovery diode at these higher operating frequencies, average power dissipation during recovery is reduced and rectification efficiency is improved. Furthermore, the diode can handle a larger forward current without overheating.

Schottky Barrier Diodes

The crystal rectifier or Schottky diode was used for many years as a laboratory detector for high frequencies, and as detector for radio broadcasts in the early days of radio.

Today, many uses have been found for Schottky diodes. One, in particular, is for power rectification using large area metal contacts.

In Figure 10-18, a large barrier exists for electron flow from the metal into the semiconductor; however, when the device is forward-biased, the energy level of the conduction band in the semiconductor is raised so that electrons can flow into the metal.

Since no holes (mobile positive charges) are present in the metal, none can be injected into the semiconductor. Thus, we have the concept of a "majority carrier device." That is, only electrons participate in the conduction mechanism which eliminates the minority carrier storage which slows down the recovery action of P-N junction devices.

The reverse voltage of the Schottky is limited by its structure, which is designed to minimize forward voltage drops. Figure 10-19 illustrates the Schottky diode structure. Extremely low contact resistance is required, and since the Schottky is a majority carrier device, the higher resistivity epitaxial layer must be very thin in order to reduce series resistance. The metal overlapping the insulator at the edge of the barrier region acts as a "guard-ring" and helps reduce the surface electric field and improves the reverse characteristics of the device.

Applications of Schottky Diodes

The diodes discussed in this sec-

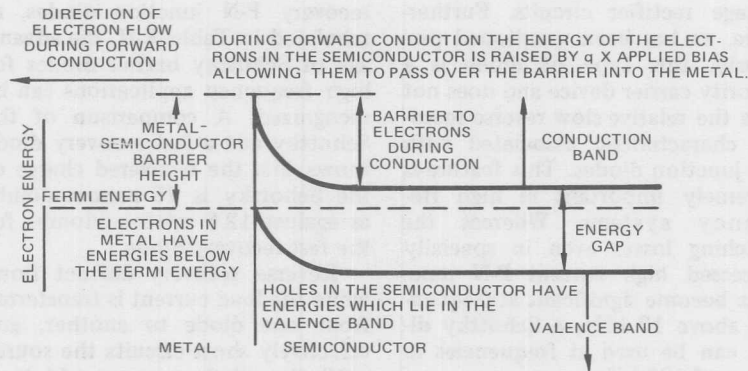


Figure 10-18. Schottky Barrier Band Diagram

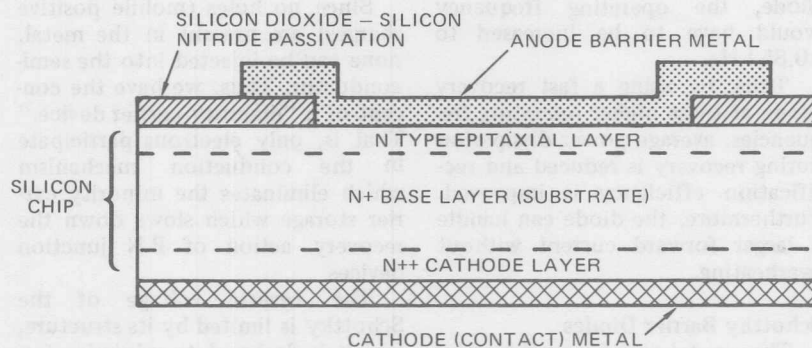


Figure 10-19. Schottky Barrier Structure

tion are classed as power Schottkys with a 50 ampere average rating and a repetitive peak reverse voltage rating of 20 volts. Devices rated up to 40V are available, also 25A devices over the same voltage range.

When the reverse voltage rating of 20 volts is first considered, it may seem to be too low to be practical; however, when this is considered in conjunction with the very low forward voltage (0.65 volts at 100 amps), it becomes obvious that this type of device will have very wide application in low voltage rectifier circuits. Furthermore, as has been mentioned previously, this type of diode is a majority carrier device and does not have the relative slow reverse recovery characteristic associated with P-N junction diodes. This feature is extremely important in high frequency systems. Whereas the switching losses even in specially processed high current P-N junctions become significant at frequencies above 10 kHz, a Schottky diode can be used at frequencies in excess of 100 kHz.

Figure 10-20 shows the basic electrical characteristics of a typical

power Schottky. This figure shows that the reverse characteristic is noticeably different from the standard P-N junction diode reverse characteristic. The Schottky diode has a flat reverse characteristic until the reverse voltage reaches 8 to 10 volts and then it takes a more resistive form.

The significance of the reverse recovery characteristic has been mentioned and oscillographs of this characteristic are shown in Figure 10-21. When these are compared with similar characteristics of fast recovery P-N junction diodes, as tabulated in Table X-II, the advantage of Schottky barrier diodes for high frequency applications can be recognized. A comparison of the Schottky and a fast recovery diode shows that the recovered charge of the Schottky is 75 nanocoulombs as against 12.6 microcoulombs for the fast recovery diode.

Reverse recovery current flows while the load current is transferred from one diode to another, and effectively short circuits the source until the diode recovers. If it is assumed that the source voltage is fixed at some voltage, V , then every

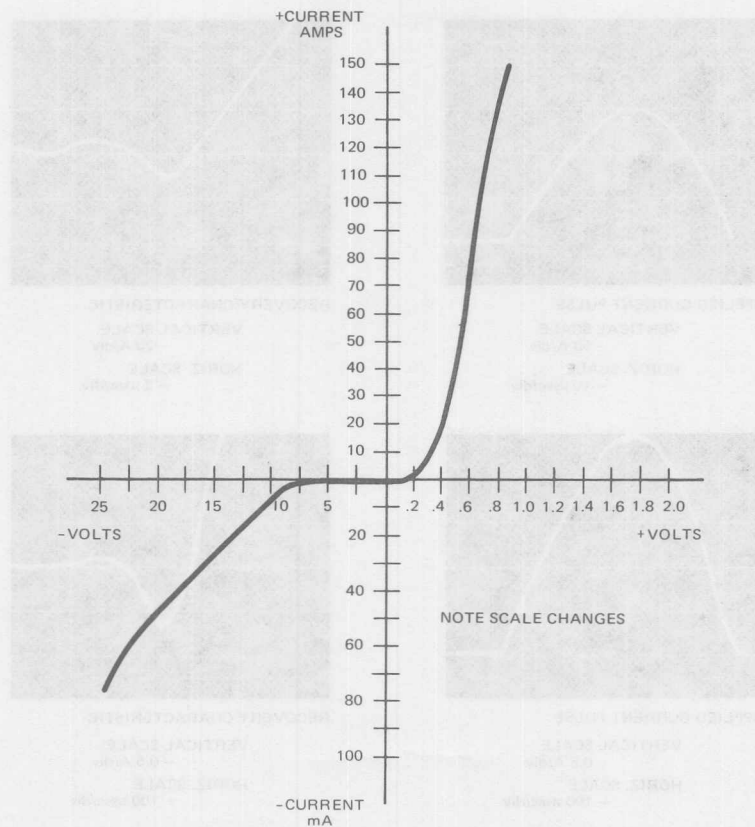
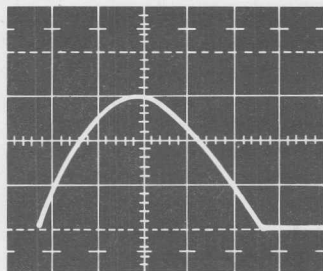


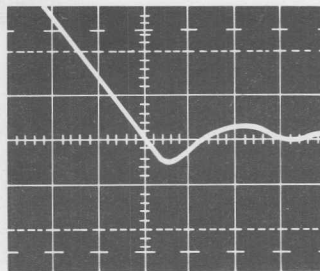
Figure 10-20. Schottky Diode Characteristics

Table X-II. Recovery Characteristics for Different Types of Diodes Rated Approximately 50 Amperes

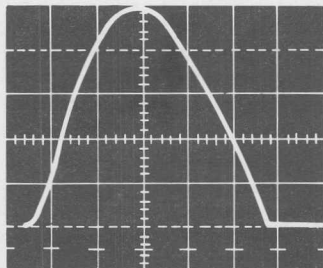
	RECOVERY TIME	PEAK REVERSE RECOVERY CURRENT	RE-COVERED CHANGE
Schottky Diode	150 nsec	1A	75 nCoulombs
Alloyed PN Junction	5 μ sec	50A	125 μ Coulombs
Diffused PN Junction	3 μ sec	40A	60 μ Coulombs
Fast Recovery PN Junction	1 μ sec	25A	12.5 μ Coulombs
Test conditions, forward current = 100A peak, half sine wave			
Negative di/dt of forward current = 25A/ μ sec			



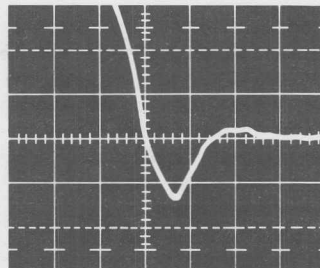
APPLIED CURRENT PULSE
 VERTICAL SCALE
 - 50 A/div
 HORIZ. SCALE
 - 10 μ sec/div



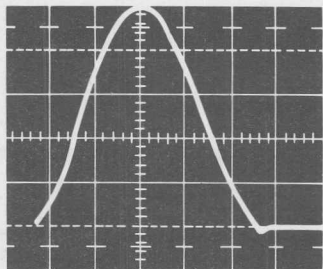
RECOVERY CHARACTERISTIC
 VERTICAL SCALE
 - 20 A/div
 HORIZ. SCALE
 - 2 μ sec/div



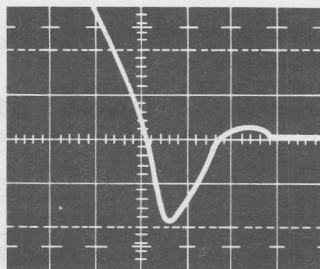
APPLIED CURRENT PULSE
 VERTICAL SCALE
 - 0.5 A/div
 HORIZ. SCALE
 - 100 nsec/div



RECOVERY CHARACTERISTIC
 VERTICAL SCALE
 - 0.5 A/div
 HORIZ. SCALE
 - 100 nsec/div



APPLIED CURRENT PULSE
 VERTICAL SCALE
 - 20 A/div
 HORIZ. SCALE
 - 0.5 μ sec/div



RECOVERY CHARACTERISTIC
 VERTICAL SCALE
 - 0.5 A/div
 HORIZ. SCALE
 - 100 nsec/div

Figure 10-21. Recovery Characteristics

time the supply reverses a certain amount of energy is lost, partly in the diode, and also in the wiring, the transformer, and the switching elements. The amount of energy lost is given by Formula 10-G.

Energy = $\int V \, idt$

$$= \frac{V \cdot i_{rr} \cdot t_{rr}}{2} \quad (10-G)$$

(Assuming the waveshape of the reverse recovery current is triangular), but

$$\frac{i_{rr} \cdot t_{rr}}{2} \quad \text{Is equal to the recovered charge}$$

Thus, Energy = V x recovered charge in Watt-sec/pulse

Power lost = Energy x Frequency

As an example of the power savings which can be obtained using a Schottky diode, compared with a fast recovery diode, consider a system with a 20 volt source, an average output voltage of 5 volts (obtained by pulse width modulation) and an output current of 100 amps.

The energy dissipated in a fast recovery diode is, from Equation 10-G, $20 \times 12.5 \times 10^{-6}$ watt seconds/pulse for each diode; for the Schottky diode, the energy lost is $20 \times 75 \times 10^{-9}$ watt seconds/pulse for each diode. The fast recovery diode will exhibit a forward voltage of approximately 1.15 volts at 100 amps whereas the Schottky diode will have a forward voltage of approximately 0.65 volts resulting in less power being lost in the Schottky during forward conduction also.

This comparison is shown in tabular form in Table X-III. Table X-

III(a) shows how the losses associated with the two types of diodes vary with frequency when operated under the circuit conditions shown. The static losses are simply the diode current multiplied by the diode voltage, assuming a square wave of current through each diode; one or the other diode is conducting at all times.

The switching losses per cycle are twice the losses per pulse derived from Formula 10-G, because one or the other diode conducts (and therefore recovers) once each half cycle.

Table X-III(b) shows how the efficiency of a system can be improved, even at low frequencies, by the use of a Schottky diode. At 1 kHz, the Schottky diode saves 50 watts, and at 100 kHz, the efficiency of the system, using Schottky diodes, changes by only 0.1 percent, whereas using fast recovery diodes, this change in system efficiency is 6 percent (49.7 watts more power required).

These data are shown in graphical form in Figure 10-22; here the Schottky diode losses below 1 kHz have been taken as a per unit base to compare the efficiency of Schottky diodes with fast recovery P-N junction diodes over a wide frequency range.

Circuit current	= 100 amps
Base Losses	= 65 watts (dc losses of the Schottky diode)
Per Unit Efficiency	= Losses at specified conditions

The high frequency efficiency of Schottky diodes has been verified by the operation of an experimental inverter at International Recti-

Table X-III. Schottky Diode and Fast Recovery Diode Rectification Losses

(a)

FREQUENCY OF OPERATION	FAST RECOVERY DIODE LOSSES (FOR 2 DIODES IN CENTER TAP CIRCUIT)				SCHOTTKY DIODE LOSSES (FOR 2 DIODES IN CENTER TAP CIRCUIT)			
	STATIC (W)	SWITCHING LOSSES		TOTAL LOSSES (W)	STATIC (W)	SWITCHING LOSSES		TOTAL LOSSES (W)
		PER CYCLE (W-SEC)	TOTAL (W)			PER CYCLE (W-SEC)	TOTAL (W)	
1 kHz	115	0.5×10^{-3}	0.5	115.5	65	3×10^{-6}	0.003	65.003
5 kHz	115	0.5×10^{-3}	2.5	117.5	65	3×10^{-6}	0.015	65.015
10 kHz	115	0.5×10^{-3}	5	120	65	3×10^{-6}	0.03	65.03
20 kHz	115	0.5×10^{-3}	10	125	65	3×10^{-6}	0.06	65.06
40 kHz	115	0.5×10^{-3}	20	135	65	3×10^{-6}	0.12	65.12
100 kHz	115	0.5×10^{-3}	50	165	65	3×10^{-6}	0.3	65.3

Circuit conditions — source voltage 20 volts, output voltage 5 volts, output current 100 amps.

(b)

FREQUENCY	OUTPUT POWER (WATTS)	RECTIFIER ASSOCIATED LOSSES (WATTS)		RECTIFICATION EFFICIENCY (%)	
		FAST RECOVERY	SCHOTTKY	FAST RECOVERY	SCHOTTKY
1 kHz	500	115.5	65.003	81.2	88.5
5 kHz	500	117.5	65.015	81.0	88.5
10 kHz	500	120	65.03	80.6	88.5
20 kHz	500	125	65.06	80.0	88.5
40 kHz	500	135	65.12	78.4	88.5
100 kHz	500	165	65.3	75.2	88.4

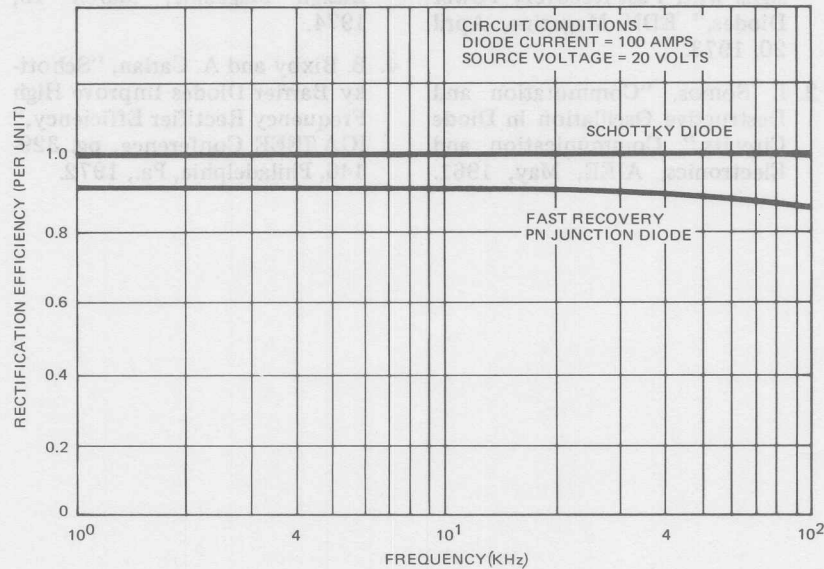


Figure 10-22. Diode Rectification Efficiency

fier. This inverter has been operated over a frequency range of 1.5 kHz to 20 kHz. When using Schottky diodes, no change in efficiency could be measured over the entire frequency range, whereas with standard and fast recovery diodes, a noticeable increase in the diode losses was measured.

The power loss measurements were made by carefully calibrating a particular heat dissipator in terms of temperature rise vs. power loss. The diode under test was then installed in this dissipator and the temperature rise of the dissipator was measured while maintaining a constant output (load) power at

several discrete switching frequencies. From the dissipator calibration curve, the actual power dissipated in the diode could be determined.

The advantages of power Schottky diodes over conventional P-N junction diodes can be summarized as being (1) lower forward voltage and (2) greatly reduced switching losses. Although the Schottky diode is only applicable in low voltage circuits, this is the area where the low forward voltage is most significant. In fact, the lower the circuit voltage, the more important becomes the rectifying element forward voltage characteristic.

References

1. D. Borst and D. Cooper, "Improve High-Power Circuit Designs with Fast-Recovery Power Diodes," EDN Magazine, April 20, 1973.
2. I. Somos, "Commutation and Destructive Oscillation in Diode Circuits," Communication and Electronics, AIEE, May, 1961.
3. D. Borst, "Protect Solid-State Power Rectifiers," Electronic Design Magazine, March 15, 1974.
4. B. Bixby and A. Carlan, "Schottky Barrier Diodes Improve High Frequency Rectifier Efficiency," IGA/IEEE Conference, pg. 329-446, Philadelphia, Pa., 1972.



Figure 1: Schottky Barrier Diode Rectifier Efficiency

Several factors affecting the diode efficiency are: (1) the diode's forward voltage drop, (2) the diode's reverse recovery time, (3) the diode's junction temperature, and (4) the diode's forward current density. The diode's forward voltage drop is the most important factor in determining the diode's efficiency. The diode's forward voltage drop is a function of the diode's forward current density and the diode's junction temperature. The diode's forward voltage drop is a function of the diode's forward current density and the diode's junction temperature.

The diode's reverse recovery time is a function of the diode's reverse current density and the diode's junction temperature. The diode's reverse recovery time is a function of the diode's reverse current density and the diode's junction temperature. The diode's reverse recovery time is a function of the diode's reverse current density and the diode's junction temperature. The diode's reverse recovery time is a function of the diode's reverse current density and the diode's junction temperature. The diode's reverse recovery time is a function of the diode's reverse current density and the diode's junction temperature. The diode's reverse recovery time is a function of the diode's reverse current density and the diode's junction temperature.

The diode's junction temperature is a function of the diode's forward current density and the diode's reverse current density. The diode's junction temperature is a function of the diode's forward current density and the diode's reverse current density. The diode's junction temperature is a function of the diode's forward current density and the diode's reverse current density. The diode's junction temperature is a function of the diode's forward current density and the diode's reverse current density. The diode's junction temperature is a function of the diode's forward current density and the diode's reverse current density.

The diode's forward current density is a function of the diode's forward current and the diode's junction area. The diode's forward current density is a function of the diode's forward current and the diode's junction area. The diode's forward current density is a function of the diode's forward current and the diode's junction area. The diode's forward current density is a function of the diode's forward current and the diode's junction area. The diode's forward current density is a function of the diode's forward current and the diode's junction area.

Protection

PROTECTING WITH FUSES

Fault currents in controlled rectifier applications may result from short circuits, either in the rectifier devices or in the external connections.

Silicon diodes and thyristors, due to their small mass, have a very limited overload capacity as compared to motors and transformers. This can be represented by an overload curve similar to the operating time/current characteristic curve of a fuse. Figures 11-1 and 11-2 indicate diagrammatically two alternative methods of using fuses alone or in combination with other protective devices to protect diodes or thyristors over the full range of

overloads. Figure 11-1 indicates how a fuse alone could be used to provide complete protection, but such applications are usually limited to low power installations, or installations where an excess of rectifying capacity is available. Figure 11-2 indicates the more commonly used system in which the fuse is used for short circuit protection only; normal overload protection is provided by a circuit breaker or other means, depending on the application.

In general, the elements employed in protective systems can be split into two groups:

1. Means to interrupt short circuits, such as:

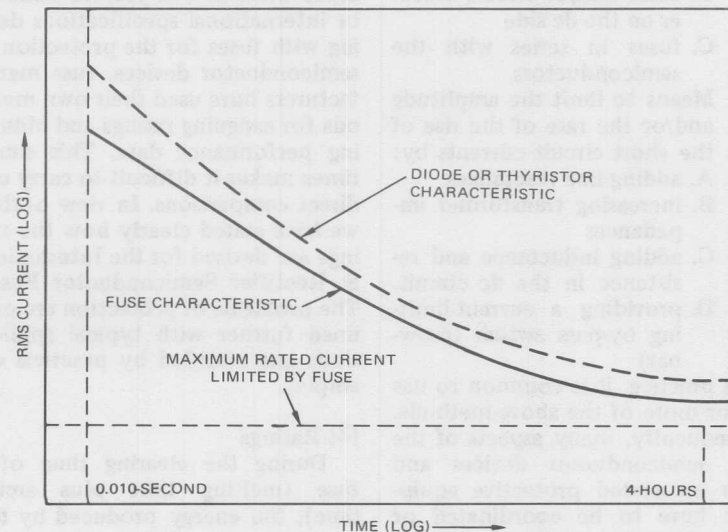


Figure 11-1. Complete Overload Protection by Fuse

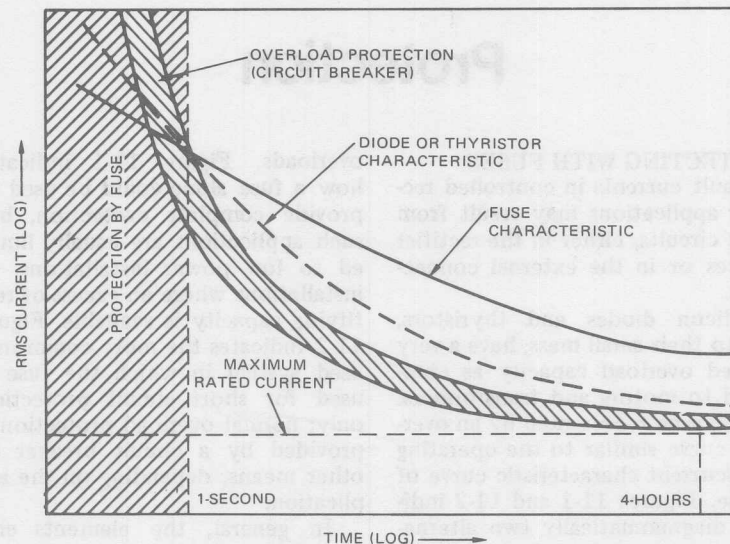


Figure 11-2. Fuse Used for Short Circuit Protection Only

- A. fuses and/or circuit breaker on the ac side
- B. fuses and/or circuit breaker on the dc side
- C. fuses in series with the semiconductors
2. Means to limit the amplitude and/or the rate of the rise of the short circuit currents by:
 - A. adding line reactances
 - B. increasing transformer impedances
 - C. adding inductance and resistance in the dc circuit.
 - D. providing a current-limiting by-pass switch (crowbar)

In practice, it is common to use one or more of the above methods. Consequently, many aspects of the fuse, semiconductor devices and other associated protective equipment have to be coordinated or matched to give reliable and economic protection for any scheme.

The various factors to be considered are listed in Table XI-I. Since there are, as yet, no national or international specifications dealing with fuses for the protection of semiconductor devices, fuse manufacturers have used their own methods for assigning ratings and obtaining performance data. This sometimes makes it difficult to carry out direct comparisons. In view of this, we have stated clearly how the ratings are devised for the International Rectifier Semiconductor Fuses. The problems of protection are outlined further with typical applications and clarified by practical examples.

I^2t Ratings

During the clearing time of a fuse (melting time plus arcing time), the energy produced by the power source and the energy stored in the inductive portion of the cir-

Table XI-I. Factors to Consider During Fuse Selection

PARAMETER	FACTORS AFFECTING PARAMETER		DATA PROVIDED	
	FUSE	DIODE OR THYRISTOR	FUSE	DIODE OR THYRISTOR
Steady State RMS Current	Ambient, attachment, proximity of other apparatus and other fuses, cooling employed	Ambient, type of circuit, parallel operation, cooling employed, heat sink	Maximum rated current under specified conditions, factors for ambient up-rating for forced cooling attachments	Comprehensive curves (average currents generally quoted)
Watts Dissipated for Steady State	As for current	As for current	Maximum quoted for specified conditions	Comprehensive data
Overload Curves	Pre-loading cyclic loading surges, manufacturing tolerances	Preloading, cyclic loading surges	Nominal time/current curves for initially cold fuse, pre-loaded fuse	Overload curves, also transient thermal impedances
Interrupting Voltages	ac or dc	Voltage rating	Maximum voltage specified	Voltage rating quoted
I^2t Ratings	Pre-loading; total I^2t dependent on: circuit impedance (X/R), applied voltage, point of initiation of short circuit, fault current, frequency	Pre-loading	For initially cold fuses; total I^2t curves for worst case conditions, variation with frequency, fault current, voltage, X/R, pre-arcing I^2t constant	Quoted value (minimum)

Table XI-I. Factors to Consider During Fuse Selection (Continued)

PARAMETER	FACTORS AFFECTING PARAMETER		DATA PROVIDED	
	FUSE	DIODE OR THYRISTOR	FUSE	DIODE OR THYRISTOR
Peak Current	Pre-loading; fault current (voltage second order effect), frequency	Pre-loading	Curves for worst conditions for initially cold fuses	Half cycle surge current
Arc Voltage	Peak value dependent on: applied voltage, circuit impedance point of initiation of short circuit	PRV voltage ratings, peak non-repetitive voltage ratings	Maximum peak arc voltages plotted against reapplied voltages	PRV voltage rating and/or peak non-repetitive voltage rating

cuit ($\frac{1}{2}Li^2$) are transformed into heat within the system. The total energy dissipated in the system is $\int i^2Rdt$, where R is the total circuit resistance. The $\int i^2dt$ is identical for all elements in a series system. And so the comparing of fuses to semiconductor devices is done on the basis of I^2t . The fuse will "let-through" an amount of I^2t based upon fuse design and circuit conditions. The semiconductor device has an ability to withstand an I^2t , usually stated for a specific sub-cycle time. To properly match a fuse with a semiconductor device requires that the let-through I^2t of the fuse never exceeds the I^2t capability of the semiconductor device under any set of operating circumstances.

Operation of the fuse is split into the melting (or prearcing) and arcing regions. The melting I^2t is basically a function of the element dimensions. For a given melting time, the melting I^2t is affected only by preloading. For subcycle operation, the fuse melting time is inversely proportional to the available symmetrical fault current.

There is considerable change in melting I^2t from 1.0 to 8.3 milliseconds because the condition of no heat loss from the restricted portion, required for I^2t to remain constant, is only achieved at very short melting times.

Figure 11-3 illustrates the variation in melting I^2t vs. melting time for a typical semiconductor fuse. For pre-arcing times less than approximately 5 milliseconds, the melting I^2t tends toward a definite minimum value. In this period there is insufficient time for the heat to be dissipated from the restricted portions of the fuse elements.

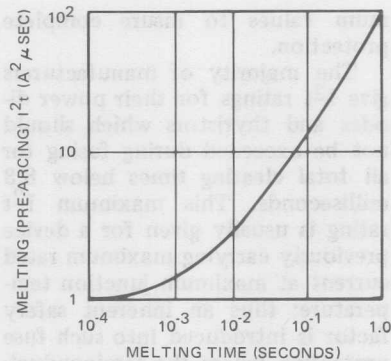


Figure 11-3. Typical Variation of Melting (Pre-Arcing) I^2t with Melting Time

During fuse operation over a number of cycles due to a heavy overload, and where the fuse melting time/current characteristic curves are utilized, the melting I^2t is essentially the total let-through I^2t of the fuse. During sub-cycle operation, however, the melting I^2t becomes a much smaller part of the total let-through I^2t . The remaining I^2t let-through is known as the arcing I^2t and this is a function of the circuit parameters, being greatly affected by the X/R ratio and the applied voltage.

The arcing I^2t varies with applied voltage, fault current level, power factor and the point on the voltage wave for the initiation of the short circuit. The total I^2t let-through figures quoted on fuse data sheets are for the worst of the above conditions with a given voltage and available prospective fault current. There will be a reduction in I^2t when the fuse carries load current prior to the fault (pre-loading), but it is better to use maxi-

imum values to insure complete protection.

The majority of manufacturers give I^2t ratings for their power diodes and thyristors which should not be exceeded during fusing for all total clearing times below 8.3 milliseconds. This maximum I^2t rating is usually given for a device previously carrying maximum rated current at maximum junction temperature; thus an inherent safety factor is introduced into such fuse protection where the semiconductor is operated at less than maximum junction temperature.

International Rectifier data sheets on diodes and thyristors show a value of I^2t for 5 milliseconds through 8.3 milliseconds and a lower value based on a derating factor of 55 to 60% for a time of 1.5 milliseconds.

The value of let-through I^2t of a particular fuse is dependent on available fault current and various other circuit operating conditions, as discussed in Reference [1]. Knowing this a circuit designer can determine the let-through I^2t of a particular fuse under his operating conditions.

To complete the analysis, the designer also should ascertain the clearing time of the fuse under the anticipated fault conditions. The I^2t capability of the semiconductor device being protected can then be determined for a current pulse of duration equal to the clearing time of the fuse. Interpolation between the published 5 msec and 1.5 msec I^2t values is generally required to obtain this value. The designer should be sure it is greater than the I^2 let-through by the fuse.

To assist the designer in ascertaining fuse clearing time, the

curves for maximum I^2t let-through by International Rectifier fuses include lines which indicate total clearing times of 5, 2 and 1.5 msec. In addition, the curves begin at the left-hand end at approximately 8.3 msec clearing time. By entering these curves at the magnitude of the available fault current, the designer can estimate the clearing time of the fuse he is considering, as well as determine the let-through I^2t under the same conditions.

Isolating Fuses

In large rectifier equipment, where a number of SCRs are operated in parallel in each arm of the rectifier circuit, a fuse may be connected in series with each thyristor simply to remove it from the circuit in the event it fails to properly block in the reverse direction. In this instance, the fuse characteristic is generally coordinated with other prospective devices so that the fuse only operates when there is a reverse breakdown of its associated SCR. Thus the fuse provides protection, not to its associated SCR, but to the other elements of the circuit which are subjected to the fault current caused by a reverse blocking failure of one SCR.

Operation of Fuses on DC

Current limiting fuses intended for the protection of semiconductor rectifying devices may be used in both ac and dc circuits. On the other hand, most of the published information for such fuses pertains to their performance in alternating current applications; very little published information pertains to operation on direct current. Yet, in an inverter or dc chopper, each SCR is in a dc circuit, and information on

fuse performance with dc applied is needed to make it possible to select a fuse which will adequately protect the semiconductor device and at the same time permit it to be operated at the highest possible current level.

DC operation of a fuse is different from ac operation because the applied voltage is at all times of one polarity. This in general makes it more difficult for the fuse to perform its intended function of current interruption following a current of sufficient magnitude to melt the fuse element because the current through the fuse is not inherently reduced to zero as it is when the applied voltage is ac. Whenever the voltage across the fuse reverses repetitively, the fuse can be considered to be operating on ac (except with very low frequency waveforms) even though the voltage waveform does not follow some regular pattern, such as a sinusoidal wave.

A special circumstance is met in the case of dc where the voltage drops to zero, or nearly to zero, in a cyclical manner. An example would be the output of a single phase, full-wave rectifier, where the load is non-inductive. In this instance, a fuse will perform as though connected to an ac source, because the current through the fuse will cease when the voltage reaches zero.

The major factor which determines how a fuse will operate in a dc circuit is the time constant (L/R) of the dc circuit. If the time constant is small, fault current will build up through the fuse rapidly, and this will cause a multiple arcing condition, one arc at each element restriction, giving essentially the

same type of fuse performance as occurs when the fuse clears a fault on an ac system. With a high rate-of-rise of current through the fuse, the peak current and also the energy let-through by the fuse (or I^2t let-through) during the melting and clearing periods will be much the same as for the same fuse when clearing a fault on an ac circuit.

The maximum voltage that can be applied to the fuse and still enable it to clear will be less in the case of dc operation; with many current limiting fuses designed for the protection of semiconductors, the dc voltage rating will be about 75 percent of the ac RMS voltage rating when the rate of rise of current through the fuse is high.

For low rates of rise of direct current (L/R of 20 msec or more), the maximum voltage the fuse can interrupt is less, and furthermore, the I^2t let-through becomes greater as L/R is made longer. This effect is brought about because the melting time of the fuse increases when the rate-of-rise of current through the fuse is low. If the rate-of-rise of current is low, it is possible for arcing to occur at only one point along the fuse element, thus reducing the dc voltage which the fuse can clear.

The maximum voltage rating that a given current limiting fuse can be given when operated in a dc circuit is therefore not a fixed value, but depends upon the L/R characteristic of the circuit to which the fuse is connected. This relationship, for one make of fuse rated 500 volts ac, is shown in Figure 11-4. The curves pertaining to fuses of other voltage ratings are similar.

The instantaneous peak let-through current for dc operation

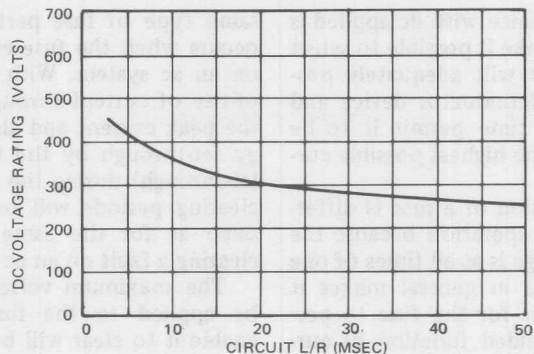


Figure 11-4. DC Voltage Rating of 500V Semiconductor Fuse

can be related to the value published for ac operation in a low power factor circuit and is dependent upon the dc circuit L/R as shown in Figure 11-5. This curve was calculated on the basis that the direct current pulse rises in an exponential manner. The let-through I^2t for dc operation can also be related to the value published for ac operation, and again shows a dependency upon the dc circuit L/R as shown in Figure 11-6, which is representative of the performance of many current limiting fuses.

From Figure 11-5, it can be seen that for dc circuits with values of L/R above 2.5 milliseconds, the peak let-through current is less than the peak current anticipated in an ac circuit. As an illustration of this, refer to Figure 11-7, where two circuits with similar voltages and currents are shown. In the case of the dc fault, the rate of current rise is much slower, and the melting time is far longer, as shown in Figure 11-8. The fuse requires a certain energy input (related to the melting I^2t) to melt the element. As the melting time is far greater on the dc fault, it follows that the

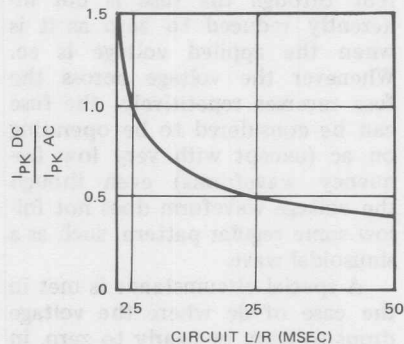


Figure 11-5. Instantaneous Peak Let-Through Current of AC Fuse in DC Circuit

current in the circuit at the time of melting will be less than the current at melting in the ac circuit. The reduction in melting current in the dc circuit is not as great as it would appear it should be, however, because during the long melting period, the element has time to lose considerable heat from the restricted portions and hence more energy is needed to melt the restrictions.

The simple case involving the interruption of a purely dc load,

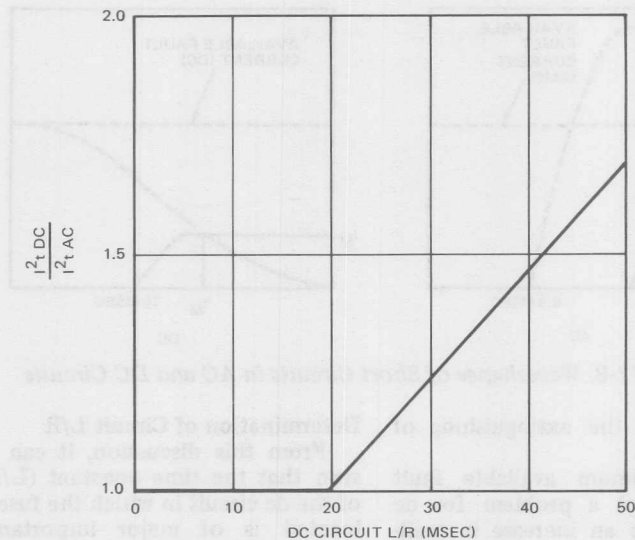


Figure 11-6. Let-Through I^2t in DC Circuit vs. AC Circuit

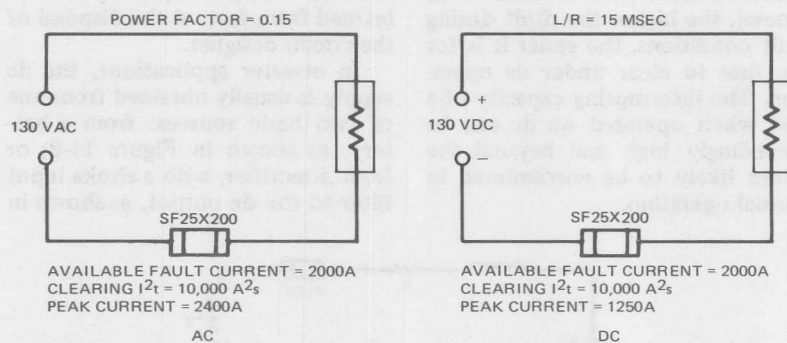


Figure 11-7. AC and DC Circuits under Short Circuit Conditions

such as on the output of a rectifier where the output is heavily filtered by a series inductance, generally results in a very long time constant for the short circuit current. In this case, the melting time of the fuse becomes very long, because of the very slow rate-of-rise of current.

When the fuse melts and begins arcing, the rate-of-rise of current is still very low, and hence the arc voltage produced by the fuse is low. This, in turn, makes the extinguishing of the arc very difficult. A further difficulty is the absence of any natural voltage zeros which

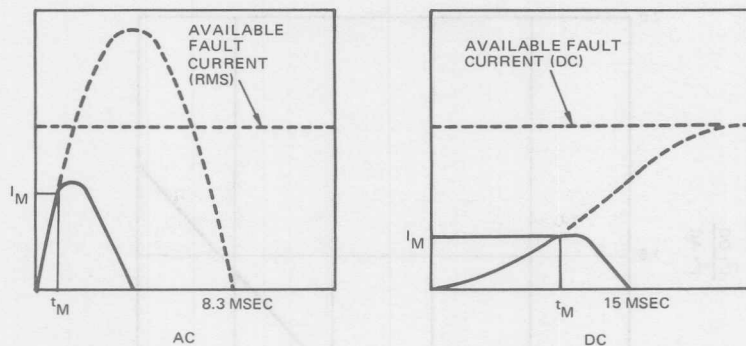


Figure 11-8. Waveshapes of Short Circuits in AC and DC Circuits

would make the extinguishing of the arc easier.

The maximum available fault current is not a problem for dc circuits. With an increase in available fault current, at a given value of L/R , the rate-of-rise of current increases and allows the fuse to clear in a more positive manner. In general, the higher the di/dt during fault conditions, the easier it is for the fuse to clear under dc operation. The interrupting capacity of a fuse when operated on dc can be exceedingly high and beyond the values likely to be encountered in normal operation.

Determination of Circuit L/R

From this discussion, it can be seen that the time constant (L/R) of the dc circuit in which the fuse is located is of major importance when selecting the fuse. At first glance, it may seem that values of L/R are not readily available for dc circuits, but, in fact, they can be learned from facts at the disposal of the circuit designer.

In inverter applications, the dc supply is usually obtained from one of two basic sources: from a battery, as shown in Figure 11-9; or from a rectifier, with a choke input filter to the dc output, as shown in

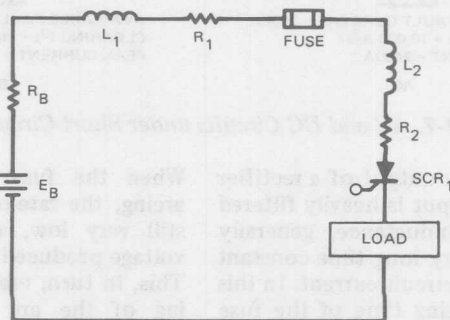


Figure 11-9. DC Circuit with Battery as a Source

Figure 11-10. A charger is often found connected to the battery in Figure 11-9, but current delivered by this charger will generally be limited to some relatively low level and therefore, is not a factor in fuse selection.

Referring to Figure 11-9, the battery voltage is known and the internal impedance of the battery, R_B , can be obtained either from the battery specification or by measurement. The circuit resistance, R_1 is more difficult to measure but can be calculated from the known parameters of the length and hence the resistance of the conductors in the power circuit, and also should include the effective on-state resistance of the thyristor at high current levels and the resistance of the fuse. The winding resistance of the di/dt choke, R_2 , should also be included. The maximum available fault current can then be calculated as shown in Formula 11-A.

$$E_B/R = E_B/(R_B + R_1 + R_2) \quad (11-A)$$

The total circuit inductance, $L_1 + L_2$, is a circuit parameter which the designer has to know for di/dt

protection of the thyristor. However, it must not be assumed that the di/dt choke inductance, L_2 , swamps the circuit lumped stray inductance, L_1 . In general, the only way to obtain an accurate indication of circuit inductance is to measure it. This measurement can be made very easily by measuring the di/dt of the thyristor current and from this measurement, the inductance is obtained from Formula 11-B.

$$L = \frac{E_B}{di/dt} \quad (11-B)$$

Therefore, if $E_B = 100$ volts and di/dt is measured to be $20A/\mu\text{sec}$, then,

$$L = \frac{100}{20} = 5 \mu\text{H}$$

With these inductance and resistance values, the circuit L/R can be calculated under load short circuit conditions.

We now have all the basic information necessary for proper fuse selection; E_B , the supply voltage, L/R , the circuit time constant, and E_B/R , the prospective (available) current through the fuse.

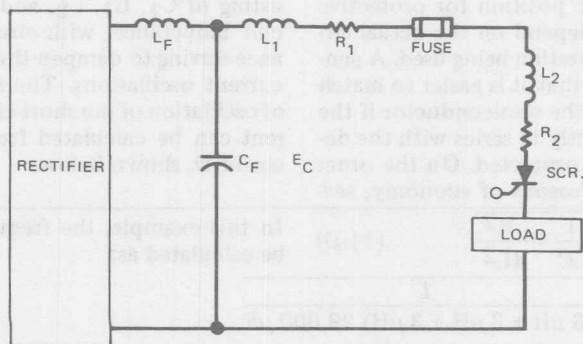


Figure 11-10. DC Circuit with Rectifier as a Source

The parameters of the circuit of Figure 11-10 are obtained in the same way; however, the source is now capacitor C_F , as under very short time conditions the rectifier supply is effectively decoupled from the thyristor circuit by the filter inductor L_F . If the natural period of C_F and $L_1 + L_2$ is very long compared with the clearing time of the fuse, then this circuit may be treated in the same manner as the circuit of Figure 11-9. However, if the natural period of C_F and $L_1 + L_2$ is comparable to the clearing time of the fuse, it must be recognized that the prospective (available) current will be greater than E_C/R because of the oscillatory nature of the current. The actual amplitude of the prospective current will depend on the damping factor of the circuit. The formula for calculating the peak prospective fault current is given as:

$$I_P = E_O \sqrt{C/L} e^{-\frac{125}{f/LR}} \quad (11-C)$$

Where:

$$L/R = \text{time constant of circuit} \\ (\mu\text{sec})$$

$$f = \text{frequency (Hz)}$$

Location of Protective Fuses

The best position for protective fuses will depend on the actual circuit configuration being used. A general rule is that it is easier to match the fuse to the semiconductor if the fuse is directly in series with the device to be protected. On the other hand, for reasons of economy, sev-

eral semiconductors may be protected by one fuse. In such a case, if all the semiconductors connected to the fuse do not have the same current rating, the fuse may not be able to protect the smaller ones in the event of an overload. In such a circumstance, the fuse may function solely as an isolating fuse to quickly interrupt the fault when there is a blocking failure of one of the smaller semiconductors.

Protection of Inverter Thyristors

To further explore the selection of a current limiting fuse to protect the main thyristors in an inverter, in the event that both thyristors do not block in the off-state direction and there is a shoot-through, a more detailed analysis will be given. Refer to Figure 11-11 for a frequently used three-phase inverter circuit (based on the popular McMurray circuit). The characteristics of the main SCRs in this example and the significant circuit parameters are given in the figure.

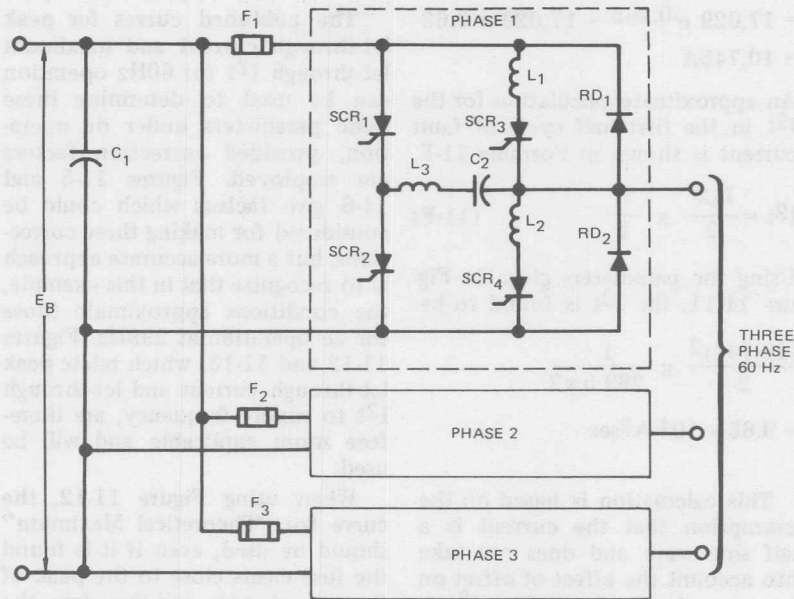
When a shoot-through occurs, both main thyristors (SCR₃ and SCR₄) are in the on-state, virtually short circuiting the dc supply. An oscillatory circuit is established consisting of C_1 , L_1 , L_2 , and stray circuit inductance, with circuit resistance serving to dampen the resulting current oscillations. The frequency of oscillation of the short circuit current can be calculated from Formula 11-D, shown below.

$$f = \frac{1}{2\pi} \sqrt{\frac{1}{LC} - \frac{R^2}{4L^2}} \quad (11-D)$$

$$f = \frac{1}{2\pi} \sqrt{\frac{1}{(3 \mu\text{H} + 3 \mu\text{H} + 3 \mu\text{H}) 29,000 \mu\text{F}}} \quad (11-Da)$$

$$= \frac{[2(7 \times 10^{-4} \Omega) + 7.8 \times 10^{-3} \Omega + 8 \times 10^{-4} \Omega]^2}{4(3 \mu\text{H} + 3 \mu\text{H} + 3 \mu\text{H})^2} = 299 \text{ Hz}$$

In this example, the frequency can be calculated as:

CIRCUIT PARAMETERS:

C_1	= 29,000 μF
L_1, L_2	= 3 μH
STRAY CIRCUIT INDUCTANCE	= 3 μH
R OF ONE SCR @ 10000A	=
	$\frac{7\text{V}}{10^4 \text{ A}} = 7 \times 10^{-4} \Omega$
INTERNAL R OF C_1	= $7.8 \times 10^{-3} \Omega$
STRAY CIRCUIT RESISTANCE	= $8 \times 10^{-4} \Omega$

SCR 3 & SCR 4 RATING

$I_{T(\text{RMS})}$	= 710A
I_{TSM}	= 8000A
I_t^2	= 265,000 A^2sec ($t = 5$ to 8.3 msec)
I_t^2	= 160,000 A^2sec ($t = 1.5$ msec)

Figure 11-11. Three-Phase Inverter Circuit

The circuit L/R is seen from the data in Figure 11-11 to be:

$$\frac{1}{2\pi} \sqrt{\frac{1}{LC} - \frac{R^2}{4L^2}}$$

The peak prospective fault current is the peak of the first half cycle of oscillatory current and can be calculated from Formula 11-E.

$$I_p = E_B \sqrt{\frac{C}{L}} e^{-\frac{125}{f L/R}} \quad (11-E)$$

Note that L/R is to be given in milliseconds. Using the values from Figure 11-11, the peak current can be calculated:

$$I_p = 300 \sqrt{\frac{29,000}{9}} e^{-\frac{125}{299 \times 9 \times 10^{-1}}}$$

$$= 17,029 e^{-0.465} = 17,029 \times 0.63$$

$$= 10,745A$$

An approximate calculation for the I^2t in the first half cycle of fault current is shown in Formula 11-F.

$$I^2t = \frac{I_p^2}{2} \times \frac{\tau}{2} \quad (11-F)$$

Using the parameters given in Figure 11-11, the I^2t is found to be:

$$\frac{(10,745)^2}{2} \times \frac{1}{299.5 \times 2}$$

$$= 9.65 \times 10^4 A^2sec$$

This calculation is based on the assumption that the current is a half sine wave and does not take into account the effect of offset on the current waveform. The I^2t is actually greater, and a more exact calculation shows it to be about 20 percent greater. Thus, the I^2t of the current during the first half cycle is close to $11.6 \times 10^4 A^2sec$.

It is now possible to select a particular fuse and determine how its performance compares with the capabilities of the main thyristors. From Figure 11-4, it is seen that this particular type of 500V fuse can be used; for a circuit L/R of 0.9, it is seen to have a dc voltage rating of nearly 500V.

Since the main thyristors are rated 710A RMS, it is desirable to select a fuse of nearly equal current rating. From the fuse product data sheet, it is found that a 700A fuse is not available, but 600A and 800A units are. In addition, it is seen that in a 35°C ambient, the 600A fuse can carry 500A, and the 800A unit is good for 700A.

The published curves for peak let-through current and maximum let-through I^2t for 60Hz operation can be used to determine these same parameters under dc operation, provided correction factors are employed. Figures 11-5 and 11-6 give factors which could be considered for making these corrections, but a more accurate approach is to recognize that in this example, the conditions approximate those for ac operation at 299Hz. Figures 11-12 and 11-13, which relate peak let-through current and let-through I^2t to supply frequency, are therefore more applicable and will be used.

When using Figure 11-12, the curve for "Theoretical Maximum" should be used, even if it is found the fuse clears close to the peak of the current wave, and therefore, the curve marked "for limit of current limiting condition" would appear to be the one to use. This is, again, the result of the effect of offset of the current waveform.

To use the published curves for peak let-through current and maximum let-through I^2t , it is necessary to convert the peak prospective fault current to the equivalent symmetrical RMS amperes; this relationship is shown in Formula 11-G.

Max. Symmetrical RMS Fault Current =

$$\frac{\text{Max. Peak Prospective Fault Current}}{2.35}$$

In the example discussed here, this becomes:

$$\text{Max. Symmetrical RMS Fault Current} = \frac{10,745}{2.35} = 4572A$$

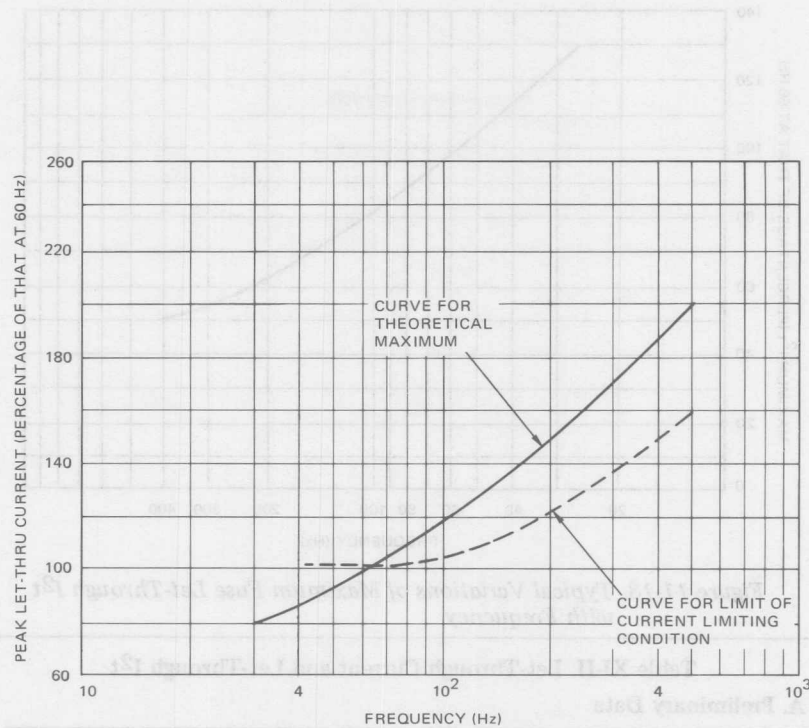


Figure 11-12. Typical Variation of Peak Let-Through Current with Frequency

Calculated values of peak let-through current and maximum let-through I^2t are found in Table XI-IIA.

The final column in Table XI-IIA is an interpolated value obtained from:

$$I^2t @ 300V = (I^2t @ 500V - I^2t @ 240V)$$

$$\frac{300V - 240V}{500V - 240V} + I^2t @ 240V$$

The preliminary values in Table XI-II can be corrected for operation at 299 Hz instead of 60 Hz by using Figures 11-12 (reading from "Curve for Theoretical Maximum") and 11-13, respectively, and are shown in Table IX-IIB.

Table XI-IIB also lists the melting I^2t of these fuses as given in IR's product data sheet, PD-8.003A.

From the previous calculations, the following additional conclusions can be drawn:

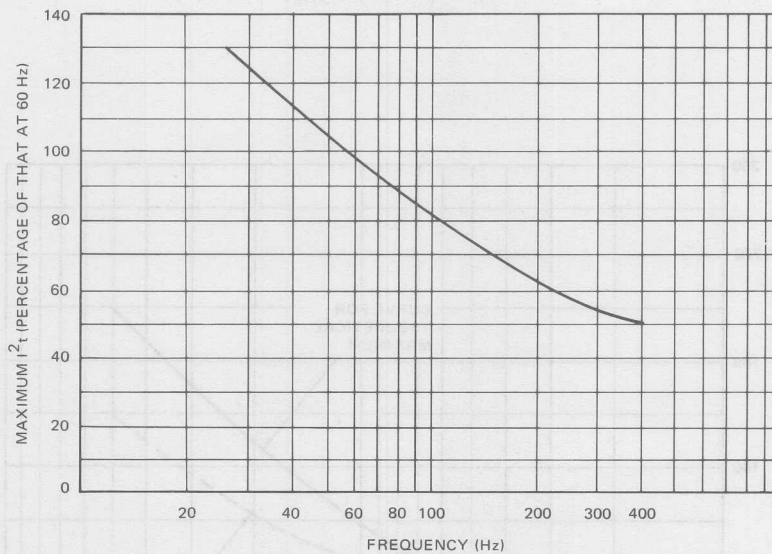


Figure 11-13. Typical Variations of Maximum Fuse Let-Through I^2t with Frequency

Table XI-II. Let-Through Current and Let-Through I^2t

A. Preliminary Data

FUSE RATING	PEAK LET-THROUGH CURRENT	LET-THROUGH I^2t		
		@ 500V	@ 240V	@ 300V
600A	6,300A	2.8×10^5	1.25×10^5	$1.60 \times 10^5 \text{ A}^2\text{sec}$
800A	7,900A	5.0×10^5	2.6×10^5	$3.15 \times 10^5 \text{ A}^2\text{sec}$

B. Detailed Data

FUSE	FUSE RATING	CORRECTED PEAK LET-THROUGH CURRENT	CORRECTED LET-THROUGH I^2t @ 300V	MELTING I^2t
SF50P600	600A	$6,300 \times 1.71$ 10,770A	$1.6 \times 10^5 \times$.53 = 8.5 $\times 10^4 \text{ A}^2\text{sec}$	4.3×10^4 A^2sec
SF50P800	800A	$7,900 \times 1.71$ = 13,510A	3.15×10^5 $\times .53 = 16.7$ $\times 10^4 \text{ A}^2\text{sec}$	8.3×10^4 A^2sec

A. For the 800A fuse, the peak let-through current of 13,510A is greater than the peak prospective fault current of 10,745A. On the other hand, the I^2t in the first half cycle of fault current ($11.6 \times 10^4 A^2 \text{sec}$) is greater than the melting I^2t for the fuse ($8.3 \times 10^4 A^2 \text{sec}$). Thus, the fuse will open during the first half cycle and the fault will be interrupted in $\tau/2$ or 1.67 msec.

Note that the fuse will not "current limit"; the I^2t let-through will be $11.6 \times 10^4 A^2 \text{sec}$, the total I^2t available from the circuit. However, this is less than the I^2t rating of the main thyristors at 1.5 msec ($16 \times 10^4 A^2 \text{sec}$) and so the fuse will protect the main thyristors.

B. For the 600A fuse, the peak let-through current of 10,770A is the same as the 10,745A peak prospective current. The $8.5 \times 10^4 I^2t$ let-through is less than $11.6 \times 10^4 I^2t$ available from the circuit. The fuse will just barely current limit and therefore interrupt the current in less than 1.67 msec. However, the fuse is seen to be not much faster than $\tau/2$, and so the 1.5 msec I^2t rating of the semiconductor can be used to coordinate with the $8.5 \times 10^4 A^2 \text{sec}$ let-through by the fuse. There is an even greater margin in this case between the semiconductor I^2t rating and the I^2t let-through by the fuse than for the 800A unit. If, because of other considerations, such as

the cooling conditions found in the inverter, the main SCRs will be operated at less than 500A RMS, the 600A fuse should be selected, since it offers a greater I^2t margin.

It is instructive to consider the consequences if the fuse fails to clear the fault within a few milliseconds after it occurs. As previously explained, a shoot-through results in a pulse of current (as the capacitor discharges through the relatively low circuit inductance) often of high magnitude and short duration. This is followed by a slower rising dc fault current from the rectifier, which may have a long time constant. The usual practice is to choose a fuse such that the I^2t in the current pulse causes the fuse to operate before the peak of the current is reached. This is usually a relatively easy task for the fuse, since the high di/dt has the same effect as a high frequency alternating current with a low associated circuit inductance.

If the fuse does not operate before the peak, current then flows around through the free-wheeling diodes RD_1 and RD_2 , while the fuse continues to carry only a slowly rising direct current from the supply. This is a more serious fault condition than the initial one, since it normally has a long time constant. If any possibility exists of the discharge current pulse not causing fuse operation, the fuse voltage rating must be chosen to be capable of clearing a fault on the dc supply. In this respect, it is important that stray circuit inductance and resistance, which have the effect of reducing the value of I^2t in the pulse, are taken into account.

In addition to protecting the main thyristors, the fuse, F_1 , in Figure 11-11 operates in the event of a blocking failure of a commutating thyristor, SCR_1 or SCR_2 , or of a free-wheeling diode, RD_1 or RD_2 . The current rating of F_1 is too large to enable it to operate at a low enough current level to protect these devices in the event of an injurious overload. But in the event of a blocking failure of any one of these devices, the fuse will operate during the ensuing short circuit, preventing damage to the main thyristors and also protecting the dc supply to the inverter section from a sustained fault which could damage it.

Discussion of Preceding Example

The preceding example presents a method of analysis which can be used with many different types of inverters and dc choppers. From this example, it is evident that a key factor in determining fuse performance is the L/R of the inverter power circuit under fault conditions. If some of the circuit inductance is found in an inductor which saturates during a fault, the calculation of peak prospective fault current may have to be done in two steps. The first step would be to obtain the initial fault current waveform based on full capacitor voltage and the L/R with maximum (unsaturated) circuit inductance. The second step is to determine the current waveform based on the voltage across the capacitor at the instant the inductor saturates and on a new (lower) L/R based on the minimum (saturated) circuit inductance. The waveform of the fault current is the composite of these two calculated waveforms.

PROTECTING BY LIMITING PEAK JUNCTION TEMPERATURES

To extend the life of semiconductor power rectifier diodes and thyristors, limit the junction temperature when designing the circuit.

Most engineers worry more about the maximum current ratings. Because power rectifiers and thyristors are not usually built to withstand moderate-to-severe current overloads, the average designer relies on control devices alone for protection. And, to some extent, this tactic is successful. You can prevent catastrophic damage with fuses and circuit breakers, true. But with every overload, there is some deterioration in the life of the devices.

If the circuit design limits device junction temperatures to the maximum specified by the manufacturer, most overloads can be accommodated safely without the clearing of fuses or tripping of circuit breakers. Moreover, overloads need not be limited in frequency of occurrence. The only restriction: allow the device temperature to return to the initial value before another overload is applied. Fortunately, since the thermal storage capacity of SCRs is small, they cool quickly following an overload condition.

Limiting temperatures to maximum ratings requires that the anticipated overloads be defined (in terms of duration and current magnitude) and that the peak junction temperature at the end of the overload be calculated. The peak temperature is determined by calculating the junction temperature rise caused by the load (or overload) current and adding this to the initial or ambient temperature.

Calculate Junction Temperature Above Case

The load current carried by rectifying devices usually has essentially a rectangular waveform (Figure 11-14). Some load inductance — almost always present — prevents the current from varying in direct proportion to the variations in output voltage. Hence, each device carries a current pulse equal in magnitude to the dc output of the rectifier unit. The pulse lasts one-third of a cycle (120 electrical degrees) in a three-phase bridge circuit (Figure

11-14(a)). In a double-wye circuit, the duration of the current pulses is the same, but the amplitude is only one-half the dc output of the rectifier unit.

When the rectifying devices are SCRs and phase retard is used to control output voltage, the current waveform remains essentially the same; it is shifted in time, however, by an amount that depends on the angle of retard, α (Figure 11-14(c)).

Because of the rectangular waveform, calculating junction-temperature rise is not difficult. The data

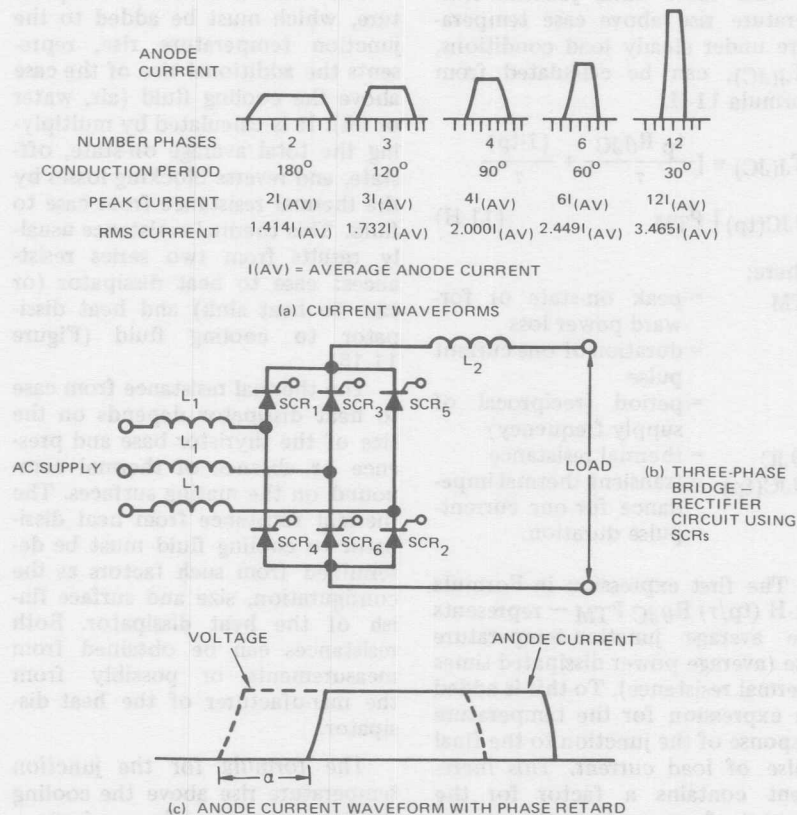


Figure 11-14. Three-Phase Bridge Rectifier Waveforms and Circuit

required are the following: the on-state (forward) voltage curve at maximum rated junction temperature, the transient thermal impedance curve for times between 1 and 10 msec (the time range for one current pulse) and the rated thermal resistance of the device from junction to case. If a curve of instantaneous on-state power loss vs. current is available, the calculation can be somewhat simplified: on-state power loss may then be read directly rather than calculated from the forward voltage curve.

With these data, junction-temperature rise above case temperature under steady load conditions, $\Delta T_{J(JC)}$, can be calculated from Formula 11-H.

$$\Delta T_{J(JC)} = \left[\frac{t_p R_{\theta JC}}{\tau} + \frac{(1-t_p)}{\tau} Z_{\theta JC}(t_p) \right] P_{TM} \quad (11-H)$$

Where;

- P_{TM} = peak on-state or forward power loss
 t_p = duration of one current pulse
 τ = period (reciprocal of supply frequency)
 $R_{\theta JC}$ = thermal resistance
 $Z_{\theta JC}(t_p)$ = transient thermal impedance for one current-pulse duration.

The first expression in Formula 11-H $(t_p/\tau) R_{\theta JC} P_{TM}$ — represents the average junction-temperature rise (average power dissipated times thermal resistance). To this is added an expression for the temperature response of the junction to the final pulse of load current. This increment contains a factor for the amount of power above the average power that is dissipated during the

final pulse: $-(1 - t_p/\tau) P_{TM}$ — multiplied by the transient thermal impedance.

For a more accurate version of Formula 11-H, the small heating effect of losses during the reverse and off-state (forward) periods should be included. However, in power semiconductors, these losses are only a few watts and are generally neglected. They cause only a small temperature rise of 1 or 2°C.

Include Case-to-Ambient Temperature Rise

The case-to-ambient temperature, which must be added to the junction temperature rise, represents the additional rise of the case above the cooling fluid (air, water or oil). It is calculated by multiplying the total average on-state, off-state, and reverse blocking losses by the thermal resistance from case to fluid. This thermal resistance usually results from two series resistances: case to heat dissipator (or case to heat sink) and heat dissipator to cooling fluid (Figure 11-15).

The thermal resistance from case to heat dissipator depends on the size of the thyristor base and presence or absence of thermal compound on the mating surfaces. The thermal resistance from heat dissipator to cooling fluid must be determined from such factors as the configuration, size and surface finish of the heat dissipator. Both resistances can be obtained from measurements or possibly from the manufacturer of the heat dissipator.

The formula for the junction temperature rise above the cooling fluid temperature, $\Delta T_{J(JA)}$, is given in Formula 11-J.

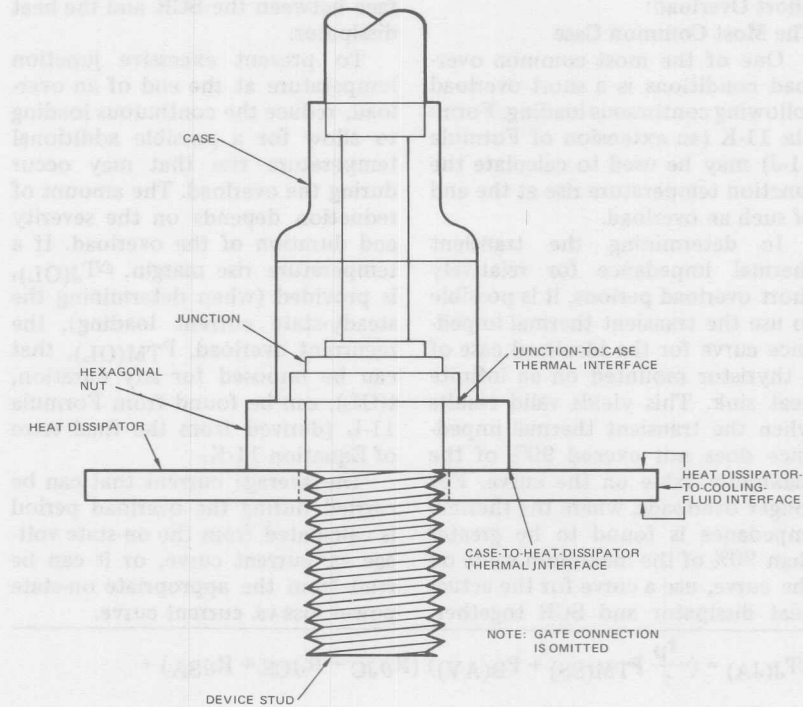


Figure 11-15. Thermal Interfaces of SCR

$$\Delta T_{J(JA)} = \left(\frac{t_p}{\tau} P_{TM} + P_B \right)$$

$$\left(R_{\theta JC} + R_{\theta CS} + R_{\theta SA} \right) + \left(1 - \frac{t_p}{\tau} \right) P_{TM} Z_{\theta JC}(t_p) \quad (11-J)$$

Where:

$R_{\theta CS}$ = case-to-heat dissipator thermal resistance;

$R_{\theta SA}$ = heat-dissipator-to-fluid thermal resistance;

$P_B(AV)$ = average power losses during reverse blocking and forward off-state periods.

Note that the heating caused by blocking losses $P_B(AV)$ (neglected in Formula 11-H) is included in Formula 11-J. For the calculation of

$\Delta T_{J(JA)}$, this heating becomes significant.

Finally the RMS value of the current found by the above procedure should not exceed the RMS current rating of the device.

Short Overload: The Most Common Case

One of the most common overload conditions is a short overload following continuous loading. Formula 11-K (an extension of Formula 11-J) may be used to calculate the junction temperature rise at the end of such an overload.

In determining the transient thermal impedance for relatively short overload periods, it is possible to use the transient thermal impedance curve for the idealized case of a thyristor mounted on an infinite heat sink. This yields valid results when the transient thermal impedance does not exceed 90% of the maximum value on the curve. For longer overloads, where the thermal impedance is found to be greater than 90% of the maximum value on the curve, use a curve for the actual heat dissipator and SCR together.

Such a curve can be drawn by forming a composite of the published transient thermal impedance curves for the rectifier device and the actual heat dissipator. Make certain to include the effect of the thermal resistance at the interface between the SCR and the heat dissipator.

To prevent excessive junction temperature at the end of an overload, reduce the continuous loading to allow for a possible additional temperature rise that may occur during the overload. The amount of reduction depends on the severity and duration of the overload. If a temperature rise margin, $\Delta T_{J(OL)}$, is provided (when determining the steady-state current loading), the recurrent overload, $P_{TM(OL)}$, that can be imposed for any duration, $t(OL)$, can be found from Formula 11-L (derived from the final term of Equation 11-K).

The average current that can be carried during the overload period is calculated from the on-state voltage vs. current curve, or it can be read from the appropriate on-state power loss vs. current curve.

$$\Delta T_{J(JA)} = \left(\frac{t_p}{\tau} P_{TM(SS)} + P_{B(AV)} \right) (R_{\theta JC} + R_{\theta CS} + R_{\theta SA}) + \left(1 - \frac{t_p}{\tau} \right) P_{TM(SS)} Z_{\theta JC}(t_p) + (P_{TM(OL)} - P_{TM(SS)}) \left[\frac{t_p}{\tau} Z_{\theta JA}(tOL) + \left(1 - \frac{t_p}{\tau} \right) Z_{\theta JC}(t_p) \right] \quad (11-K)$$

Where:

- $P_{TM(SS)}$ = peak steady on-state power loss (prior to overload)
- $P_{TM(OL)}$ = peak on-state power loss during overload
- $Z_{\theta JA}(tOL)$ = transient thermal impedance, junction to fluid, for the overload period.

$$P_t(OL) = \frac{\Delta T_{J(OL)} + P_{TM(SS)} \left[\frac{t_p}{\tau} Z_{\theta JA}(tOL) + \left(1 - \frac{t_p}{\tau} \right) Z_{\theta JC}(t_p) \right]}{\frac{t_p}{\tau} Z_{\theta JA}(tOL) + \left(1 - \frac{t_p}{\tau} \right) Z_{\theta JC}(t_p)} \quad (11-L)$$

Severe Overloads

Sometimes rectifying devices must accommodate severe overloads. In this case, operate the devices on a continuous basis well below their published continuous ratings. The penalty is particularly severe for controlled rectifiers, which usually have a maximum junction operating temperature of only 125°C.

Because of this limitation, some equipment designers permit the controlled rectifier junction temperature to exceed the maximum rated operating temperature during a severe overload. At the same time, steps are taken to make sure the SCR does not lose control when voltage is applied in the off-state direction during and immediately following such an overload. Two factors make such operation feasible:

- A. The repetitive peak off-state and reverse voltages impressed on an SCR during normal operating conditions are usually considerably lower than the maximum rated values for the part. These margins exist because the designer has provided for transients.
- B. When an SCR is supplied from a conventional 60 Hz power system, there is a time interval of about 8.3 msec between off-state voltage applications. During this time, the SCR junction is cooling, and since the junction has a short thermal time constant, it cools rapidly. Its temperature will approach, and may even drop to, less than the maximum rated operating temperature.

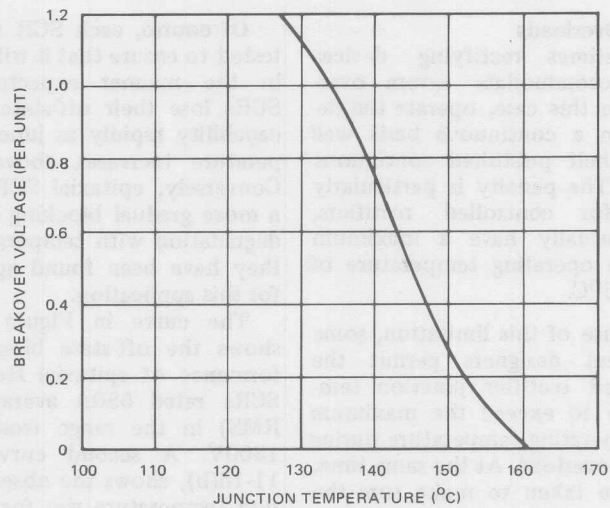
Of course, each SCR should be tested to ensure that it will perform in the manner expected. Some SCRs lose their off-state blocking capability rapidly as junction temperature increases above 125°C. Conversely, epitaxial SCRs exhibit a more gradual blocking capability degradation with temperature, and they have been found appropriate for this application.

The curve in Figure 11-16(a) shows the off-state blocking performance of epitaxial Hockey-Puk SCRs rated 550A average (860A RMS) in the range from 800 to 1300V. A second curve, Figure 11-16(b), shows the observed junction temperature rise for the same devices 8.3 msec after a half-sine-wave current surge. The curve is plotted for half sine waves up to 7000A peak.

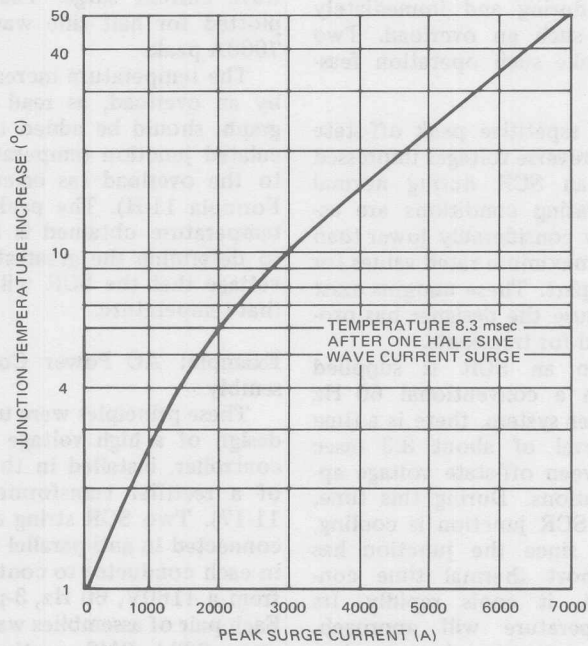
The temperature increase caused by an overload, as read from the graph, should be added to the calculated junction temperature prior to the overload (as calculated by Formula 11-H). The peak junction temperature obtained is then used to determine the greatest off-state voltage that the SCR will block at that temperature.

Example: AC Power Control Assembly

These principles were used in the design of a high voltage ac power controller, installed in the primary of a rectifier transformer (Figure 11-17). Two SCR string assemblies connected in anti-parallel were used in each conductor to control power from a 4160V, 60 Hz, 3-phase line. Each pair of assemblies was rated to carry 233A RMS continuously at an air flow rate of 350 cubic feet per minute in a maximum ambient



(a) BREAKOVER VOLTAGE ABOVE 100°C



(b) JUNCTION TEMPERATURE RISE VS SURGE CURRENT

Figure 11-16. Performance Above 125°C and Following Current Surge

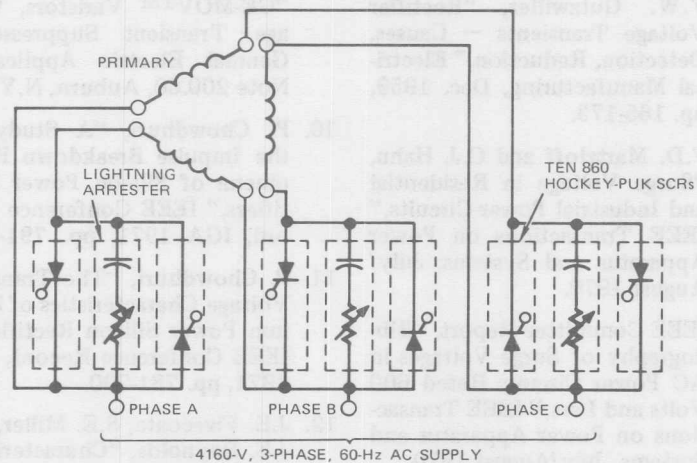


Figure 11-17. High Voltage Power Control Circuit

temperature of 75°C . The overload current rating of each assembly was 5200A peak for 0.2 second and 7000A peak for 0.0083 second. Following either overload, each string of SCRs in the controller was required to immediately block 4160V RMS.

The working peak reverse voltage that can be applied can be as much as 6500V under high-line voltage conditions. The string assembly consisted of ten 860A RMS Hockey-Puk SCRs in series, each device having a repetitive peak off-state and reverse voltage rating of 1300V.

Each device in Figure 11-17 was tested to be sure it did not self-trigger when a 1550V, 60 Hz half

sine wave was applied in the off-state direction at a junction temperature of 125°C . The aggregate repetitive peak off-state and reverse voltage rating was therefore 13,000V, two times the maximum working value, and the aggregate nonrepetitive peak reverse voltage rating was 15,500V, 2.38 times the maximum working value. These margins provided for nonuniform distribution of blocking voltage across the 10 devices and in addition for line voltage transients up to 2.5 times the normal working peak reverse voltage of 5883V. Tests showed that the power controller gave the required control under fault conditions.

References

1. G. Geissinger ed., "Semiconductor Fuse Applications Handbook," HB-50, International Rectifier, Oct. 1972, pg. 516-19.
2. F.W. Gutzwiller, "Rectifier Voltage Transients — Causes, Detection, Reduction," Electrical Manufacturing, Dec. 1959, pp. 165-173.
3. F.D. Martzloff and G.J. Hahn, "Surge Voltage in Residential and Industrial Power Circuits," IEEE Transactions on Power Apparatus and Systems, July/August 1970.
4. IEEE Committee Report, "Bibliography of Surge Voltages in AC Power Circuits Rated 600 Volts and Less," IEEE Transactions on Power Apparatus and Systems, July/August 1970.
5. T. Liao and T.H. Lee, "Surge Suppressors for the Protection of Solid State Devices," IEEE Transactions on Industry and General Applications, January/February 1966.
6. J.B. Rice and L.E. Nickols, "Commutation dv/dt Effects in Thyristor Three-Phase Bridge Converters," IEEE IGA Transactions, November/December 1968.
7. J. Merret, "Practical Transient Suppression Circuits for Thyristor Power Control Systems," Mullard Technical Communications, No. 104, March 1970.
8. W. McMurray, "Optimum Snubbers for Power Semiconductors," IEEE Transactions on Industry Applications, September/October 1972, pp. 593-600.
9. F.B. Golden and R.W. Fox, "GE-MOV™ Varistors, Voltage Transient Suppressors," General Electric Application Note 200.60, Auburn, N.Y.
10. P. Chowdhuri, "A Study on the Impulse Breakdown Phenomena of Silicon Power Rectifiers," IEEE Conference Record, IGA 1971, pp. 791-798.
11. P. Chowdhuri, "The Transient Voltage Characteristics of Medium Power Silicon Rectifiers," IEEE Conference Record, IGA 1971, pp. 781-790.
12. J.E. Fivecoate, S.E. Miller, and J.E. Reynolds, "Characteristics of a High Power Zener Diode," IEEE Conference Record, IGA 1970, pp. 437-442.
13. D.W. Borst and J.G. Leach, "Current Limiting Fuses for Protection of Thyristors in Inverters," IEEE Conference Record, IAS 1973, pp. 25-34.
14. Fuse Application Working Group Report, "Fuse Selection for Power Semiconductor Conversion Equipment," IEEE Transactions on Industry Applications, January/February, 1973.
15. D.W. Borst, G. Dydek, and G. Geissinger, "To Fuse or Not To Fuse Power Thyristors," IEEE Conference Record, IAS 1974.

Cooling

Thermal Considerations for Stud-Mounted Devices

Silicon rectifier devices (rectifier diodes, controlled rectifiers and triacs) have ratings which are based upon thermal considerations. Since it is inherent in the construction of silicon devices that the major losses must occur internally and within a very small volume of the device and that the heat generated by these losses must flow outward to some form of heat dissipator, the optimum cooling for silicon devices may be somewhat more critical than for some other electrical devices.

All three modes of heat transfer — conduction, radiation and convection — are always present and should be considered in all cases of cooling silicon devices. However, under some modes of operation, one or more of these heat transfer methods may be predominant to such an extent as to make the contribution of the other types negligible. For example, if the device is mounted directly on a liquid-cooled heat exchanger, the percentage of losses by natural convection and by radiation may be so small by comparison to the heat transfer by conduction as to be considered negligible. In extremely high altitude applications, conduction or convection heat transfer methods are much too inefficient, so that the major part of the cooling must come from radiation. However, for most industrial applications, either natural or forced convection cool-

ing in air will be used much more frequently than the other two methods.

General Cooling Theory

The losses within a silicon device occur in the thin wafer of silicon inside the primary component. The heat thus generated must first flow out through the case and/or the lead(s) of the device. By far the greatest proportion of this heat flows out through the case into some form of heat exchanger, and then through the heat exchanger into the cooling ambient, which may be air or a liquid. This thermal path, therefore, may be thought of as a group of thermal resistances all connected in series; analogous to a group of electrical resistors connected in series.

There will be a value of thermal resistance assigned to each resistor in series, the first of which is the internal thermal resistance from junction to case. This is given in the individual device specifications. The next resistance, in series, is the contact thermal resistance from the case to the heat exchanger. Following this is the thermal resistance of the heat exchanger, between the point where the device is mounted and the cooling medium. In normal practice, the heat exchanger internal thermal impedance and the surface to air thermal impedance are combined and experimentally determined as a composite value. Each of these thermal resistances must be considered in detail in or-

der to assure proper cooling of the device, since a temperature drop is associated with each of them.

The above-mentioned thermal resistances are steady-state values only, and are used to calculate the average temperature rise of the junction above the ambient of the cooling medium under steady-state operation.

In addition to continuous operation, there usually are transient heating conditions which may occur in a system and which must also be accounted for; e.g., there may be thermal overloads from rapid changes in the ambient temperature of the cooling medium, or electrical overloads due to varying current requirements which the device must supply. These electrical overloads may be either momentary process load variations or fault conditions, and each must also be considered as a function of its maximum time duration. The individual device specifications also contain curves of transient thermal resistance by which the electrical overload conditions can be translated into transient temperature changes occurring within the device. Only the system designer, however, can account for the transient thermal conditions of the ambient cooling medium.

In almost all systems there will be electrical transients which will create varying amounts of heat. Probably the one notable exception to this is when a unit must supply a large inductive load, such as a large electromagnet, and is coupled directly to the load in such manner that there is no switching between the device and the load. Under these conditions, only moderate variations in load current can occur, due to varying temperatures of the

windings in the electromagnet, or to variations in supply voltage. These are usually small, compared to the transient loading which can occur in most other applications.

Detailed Requirements

There are several items which should be carefully observed and considered when applying silicon devices in order to obtain optimum cooling conditions:

The device itself should be inspected to insure that the contact surface of the case is clean, smooth, flat, and specifically, that it has no projections from the case which would impair uniform total contact with the heat exchanger.

The heat exchanger for use with either the stud or Hockey-Puk package should be prepared to receive the device, and the contact area should be smooth, with no burrs, no projections, and preferably with no depressions in the surface. It should be flat, such that it can mate with the contact surface of the device case and achieve a maximum uniform contact between the two surfaces, and it should be clean, with no dirt, corrosion, and a minimum of surface oxides. The hole in the heat exchanger for the stud SCR should be accurately drilled perpendicularly to the mounting surface, and be no more than 0.015 ± 0.010 in. (0.38 ± 0.25 mm) larger in diameter than the nominal diameter of the stud. Buffing of mating surfaces to remove oxides prior to assembly will assure a low interface thermal resistance.

The two mating surfaces should be lubricated with a substance to improve the thermal heat transfer from the case of the device to the

heat exchanger, by filling any air spaces, and which will remain stable under wide variations of temperature and environmental conditions. In this way, the formation of corrosion products, galvanic products, or oxides between the two surfaces, will be prevented. For this purpose, a Dow Corning silicone grease (number DC-200) has been widely and effectively used. Another product, called "Penetrox A," which was developed for use on the contact surfaces of overlapping aluminum busbars, has also been successfully used in many places. This contains a heat conductive metal oxides to improve heat transfer. Thermal compounds containing filler particles have the disadvantage of indenting the mounting surface slightly, requiring a refinishing of the surfaces should reassembly become necessary. (See later sections of this chapter for mounting precaution for rotating members.)

It is very important to mount the device to the heat exchanger using the proper amount of torque, to obtain optimum pressure between the two mating surfaces. Individual device specifications list the correct torque to be used in these instance, and a torque wrench, accurate in the specified range, should be used in mounting all such devices in order to achieve optimum results.

Two notes of caution should also be added: (1) Excessive torque can damage the threads of the soft copper stud of the device and, in some cases, even mechanically stress the junction, causing a change in the electrical characteristics, and (2) The threads of the stud and nut should *not* be lubricated, since actual tensile stress on the stud can

double for the same measured torque with lubricated threads.

Care must also be exercised in the use of dissimilar metals in contact with each other when mounting devices to heat exchangers. Thyristors come with various plated metallic finishes to protect them from environmental conditions and to provide an acceptable material to be in contact with heat exchanger finishes. Some of the finishes applied to thyristors are: tin plating, cadmium plating, or nickel plating. When mounting devices with one or more of these finishes against a heat exchanger, care should be exercised either to choose a heat exchanger material which is compatible with the plated finish (which means near to this material in the galvanic series of metals), or to use a lubricating substance between the two metals which will inhibit galvanic action.

For a more comprehensive discussion of and listing of metal surfaces which are compatible with each other, refer to Military Specifications, MIL-F-14072 (Sig. C) and MIL-E-16400E (Navy). Both of these specifications offer excellent guidance in the selection of compatible metallic surfaces. When an aluminum heat exchanger is used, any anodizing should be removed from the contact surface, as it presents substantial thermal and electrical resistance. A light chromate treatment is often acceptable instead of anodizing, and it need not be removed.

Occasionally it is necessary to electrically insulate the case of the device from the surface of the heat exchanger. Under these conditions, usually a thin washer of mica or silicone rubber is placed between

the device and the heat exchanger surface (after lubricating all four mating surfaces with a thermal lubricant, as mentioned above). This practice is acceptable, when necessary, for small devices. It should rarely, or never, be used with high power devices, since the thermal resistance from the base, through the insulating washer, to the heat exchanger increases very rapidly and, in most cases, becomes prohibitively high for large power devices.

Rotating Rectifiers

Rotating fixtures mounting rectifier devices, such as found in ac motor and alternator exciters, demand special consideration to mounting techniques, thermal conditions, and potentially damaging centrifugal forces.

Special mounting techniques are needed with the large Hockey-Puk packages to avoid an increase in case-to-sink thermal impedance. Preferably, the total force will be greatest at whatever rotational speed demands the highest current. Care must be taken that mounting force plus centrifugal force at the highest rotational speed is uniform and does not result in damage to the silicon.

Thermal compound made with filler particles, such as ZnO, is not recommended for rotating applications, since lubricant will tend to be forced outward with filler particles left behind.

The top terminal of a stud device must have sufficient strength to withstand the high centrifugal forces. Special packages are available from IR for such applications. The 300 ampere diodes, 305U and 307U, are equipped with a stress

relief cone for use on rotating members.

Electrical Contact Resistance

For good (low) electrical contact resistance, the heat exchanger surfaces should be flat, smooth, and of low and stable resistivity. Clean base aluminum has a low surface resistivity but tends to oxidize easily and will have an increasing surface resistance with time unless it is suitably protected. An anodized finish is not conductive and therefore, where an electrical connection between the heat exchanger and semiconductor or where an external electrical connection is made, the affected areas must be masked before anodizing or spot faced after anodizing. Since the contact surface then will be bare aluminum, it is again necessary to be careful to avoid oxidation. A surface finish of thin chromate conversion, per MIL-C-5541, Type II, Class 3, offers a stable and low contact resistance only slightly higher than oxide-free bare aluminum.

Thermal Contact Resistance

For good heat exchanger contact thermal resistance surface finish over the areas where a semiconductor device is mounted should be flat (0.001 inches TIR) and very smooth. When a good thermal lubricant (plain or filled) is used on the mounting surface, acceptable results can be achieved with a surface finish of 64 microinches or less. In any event, a thermal lubricant should be used, since it results in substantial improvement of contact thermal resistance, and it provides long-term electrical and thermal resistance stability.

Thermal Resistance

Thermal resistance of a semiconductor device is defined as "the temperature difference between two specified points or regions divided by the power dissipated under conditions of thermal equilibrium." Thermal resistance values, as shown in Formula 12-A, are expressed in the units degrees C per watt.

$$R_{\theta} = \frac{\Delta T}{W} \quad (12-A)$$

Where:

ΔT is temperature difference between particular points, for example,

- A. Junction and case ($T_J - T_C$)
- B. Junction and heat exchanger (heat sink) ($T_C - T_S$)
- C. Heat exchanger and ambient ($T_S - T_A$)

R_{θ} = Thermal resistance between two particular points.

W = Power Dissipation

Thermal Considerations for Hockey-Puk Devices

In order to calculate the current rating of a Hockey-Puk device in a given mechanical assembly, it is necessary to know the thermal resistance from the Hockey-Puk case to ambient. This can be determined by referring to the published data for the heat exchangers (heat sinks) used in the assembly, or by measurement.

Analysis of the thermal resistance paths of the Hockey-Puk, shown in Figure 12-1, results in the thermal resistance schematic shown in Figure 12-2.

Using the junction as a starting point, it is obvious that two substantial thermal paths exist: anode-to-air and cathode-to-air. The thermal resistance, junction-to-air of each path, anode and cathode, is the sum of the series connected thermal resistances, as shown in Formulas 12-B and 12-C.

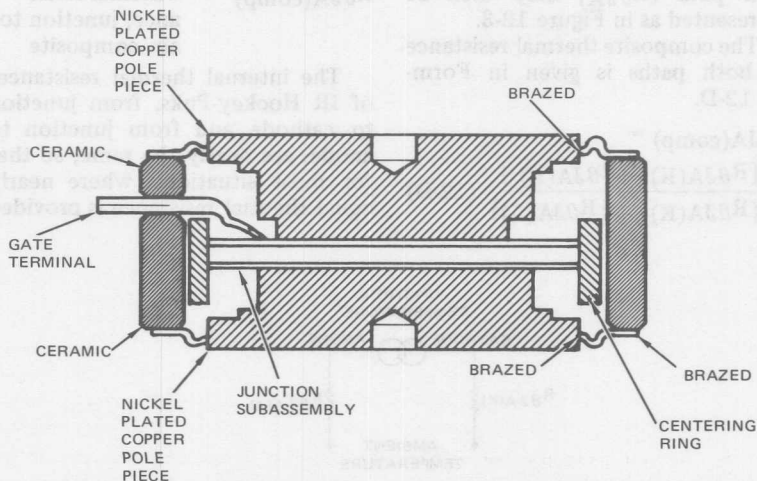


Figure 12-1. Typical Hockey-Puk Construction

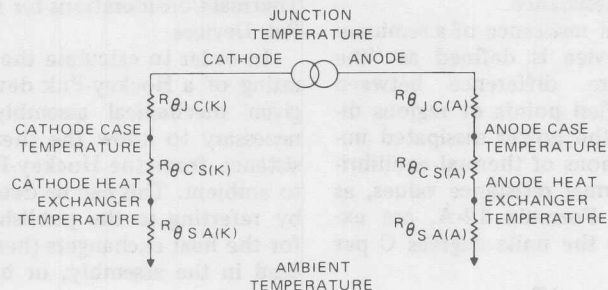


Figure 12-2. Thermal Resistance Schematic

$$R_{\theta JA(K)} = R_{\theta JC(K)} + R_{\theta CS(K)} + R_{\theta SA(K)} \quad (12-B)$$

$$R_{\theta JA(A)} = R_{\theta JC(A)} + R_{\theta CS(A)} + R_{\theta SA(A)} \quad (12-C)$$

Where:

Cathode Path	Anode Path	
$R_{\theta JC(K)}$	$R_{\theta JA(A)}$	= Thermal resistance, junction-to-air
$R_{\theta JC(K)}$	$R_{\theta JC(A)}$	= Thermal resistance, junction-to-case
$R_{\theta CS(K)}$	$R_{\theta CS(A)}$	= Thermal resistance, case-to-sink
$R_{\theta SA(K)}$	$R_{\theta SA(A)}$	= Thermal resistance, sink-to-air

The net thermal resistance in each path ($R_{\theta JA}$) may then be represented as in Figure 12-3.

The composite thermal resistance of both paths is given in Formula 12-D.

$$R_{\theta JA(comp)} = \frac{[R_{\theta JA(K)}] [R_{\theta JA(A)}]}{[R_{\theta JA(K)}] + [R_{\theta JA(A)}]} \quad (12-D)$$

Where:

$R_{\theta JA(comp)}$ = Thermal resistance, junction to air, composite

The internal thermal resistances of IR Hockey-Pucks, from junction to cathode and from junction to anode, are nearly the same, so that for most situations, where nearly equal thermal resistance is provided

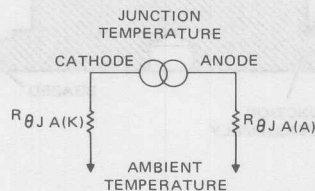


Figure 12-3. Simplified Thermal Resistance Schematic

from each pole piece to the cooling medium, a composite internal thermal resistance value may be used in place of the individual values. This composite value is found on the published ratings sheets for IR Hockey-Puks, and its use simplifies the calculation of the thermal resistance of Hockey-Puk assemblies.

When the Hockey-Puk is considered as having a single, composite, thermal resistance, the thermal paths in an assembly become those shown in Figure 12-4, and the composite thermal resistance, junction to ambient, of the assembly, can be calculated from Formula 12-E.

Quite frequently, identical heat exchangers will be used for cooling

a given Hockey-Puk. In this case, the thermal resistances in the anode and cathode paths external to the Hockey-Puk are identical, and the equation reduces to Formula 12-Eb.

To use the equations shown below, the thermal resistances of the heat exchangers in the Hockey-Puk assembly must be known. Thermal resistance data for IR heat exchangers are included in the heat exchanger data sheet, PD-7.001. Similar thermal design considerations are necessary for semiconductor packages other than the Hockey-Puk.

Thermal Resistance Measurements

If the heat exchangers are special ones, perhaps designed by the user.

$$R_{\theta JA(\text{comp})} = R_{\theta JC(\text{comp})} + \frac{[R_{\theta CS(K)} + R_{\theta SA(K)}] [R_{\theta CS(A)} + R_{\theta SA(A)}]}{[R_{\theta CS(K)} + R_{\theta SA(K)}] + [R_{\theta CS(A)} + R_{\theta SA(A)}]} \quad (12-E)$$

This can be written more simply as in Formula 12-E(a).

$$R_{\theta JA(\text{comp})} = R_{\theta JC(\text{comp})} + \frac{[R_{\theta CA(K)}] [R_{\theta CA(A)}]}{[R_{\theta CA(K)}] + [R_{\theta CA(A)}]} \quad (12-Ea)$$

Where:

$R_{\theta CA(K)}/R_{\theta CA(A)}$ = Thermal resistance, case-to-air

$$R_{\theta JA(\text{comp})} = R_{\theta JC} + \frac{R_{\theta CA}}{2} \quad (12-Eb)$$

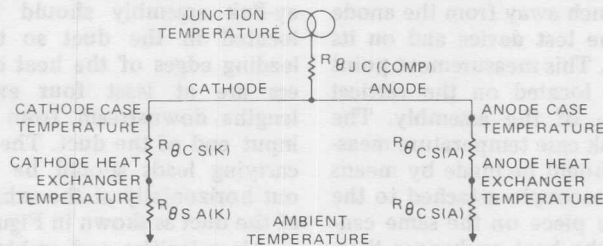


Figure 12-4. Thermal Resistance Schematic

it becomes necessary to measure the thermal resistance values. In making thermal resistance measurements on a Hockey-Puk assembly, the test puk should be mounted between the desired heat exchangers (heat sinks) with recommended lubrication and mounting pressures. Thermal resistance measurements of stud devices are covered in the NEMA-EIA standard RS-282[1].

Free Convection Air Measurements

The test assembly with its heat exchangers should be supported with the heat exchanger surfaces in a vertical plane in a cubic enclosure whose dimensions are a minimum of four times the heat exchanger length, so as to allow natural convection, air circulation. The enclosure should be so designed that the inside walls are approximately the same temperature as the inside ambient temperature. The inside ambient temperature should be measured by means of a thermocouple mounted a minimum of 2 inches directly below the center of the bottom edge of the assembly.

The heat exchanger temperature should be measured by means of a peened thermocouple attached to the particular heat exchanger which makes contact to the anode of the device. The thermocouple should be attached no more than one quarter of an inch away from the anode pole of the test device and on its upper side. This measurement point should be located on the vertical center line of the assembly. The Hockey-Puk case temperature measurement should be made by means of a thermocouple attached to the anode pole piece on the same centerline as the heat exchanger thermocouple.

The thermal resistance is determined by dividing the observed temperature rise above ambient (with input power held constant and all measured temperatures at equilibrium) by the average input power. This calculation will provide the composite thermal resistance case to ambient, and will be conservative when the two thermal paths external to the Hockey-Puk are essentially identical.

Forced Convection Air Measurements

The Hockey-Puk assembly should be firmly supported inside a rectangular air duct. It should be oriented in such a way that the heat exchanger fins are parallel to the air stream. The duct should have a height and width one inch greater than the test assembly. If the spacing between the Hockey-Puk assembly and the duct is less than one inch, proper air flow over all parts of the assembly may not occur during the test.

The length of the duct from air input end to air exhaust end should be a minimum of six times the assembly length (measured parallel to the cooling fins of the heat exchanger). A duct length of six times the assembly length is recommended so that the effect of turbulence will be minimized. The Hockey-Puk assembly should then be located in the duct so that the leading edges of the heat exchangers are at least four exchanger lengths downstream from the air input end of the duct. The current carrying leads should be brought out horizontally at the exhaust end of the duct as shown in Figure 12-5.

Air velocities and ambient temperature should be measured one

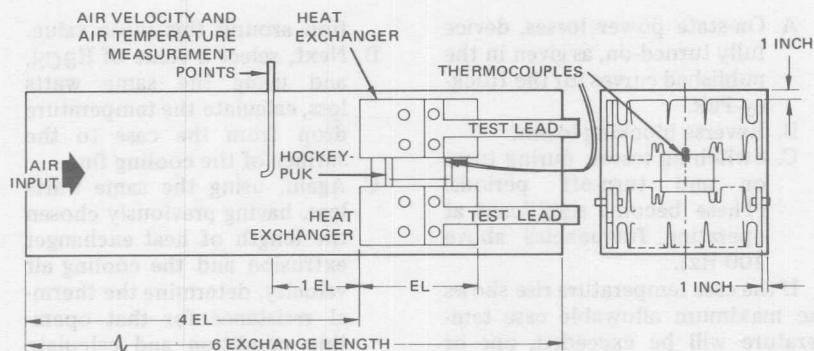


Figure 12-5. Recommended Heat Exchanger Test Set-Up

exchanger length upstream from the leading edge of the assembly. The test air velocity should be considered the average of all point velocities over the air stream cross section. Individual velocities should not vary with respect to each other by more than $\pm 10\%$.

The heat exchanger and case temperature test points should be the same as previously described for free convection thermal resistance measurements. The calculation of the composite thermal resistance, junction-to-case, is performed as described before.

Precautions

The following precautions should be observed when making temperature measurements using thermocouples. The thermocouple junction should be formed by welding rather than soldering or twisting. Welding makes a more reliable junction with increased accuracy. The thermocouple should be attached to the surface of the heat exchanger by inserting it into a drilled hole and peening the hole closed.

Case temperature measurements are made by inserting a thermocouple into a drilled hole in the side of the anode pole piece. Care should be taken to be sure that the surface of the pole is not distorted, to prevent incorrect test results. Five or ten mil. diameter thermocouple wire is recommended (No. 30 AWG wire is often specified).

Current Rating Calculations

The composite thermal resistance from Hockey-Puk case to ambient, when multiplied by the average power dissipated in the Hockey-Puk during operation, will give the temperature rise of the Hockey-Puk case above ambient temperature. This rise, when added to the maximum anticipated ambient temperature, should not exceed the maximum allowable Hockey-Puk case temperature, for the particular operating conditions to which the calculations pertain.

When calculating case temperature rise, all power dissipated in the Hockey-Puk must be considered. The power dissipated may be considered as falling into these categories:

- A. On-state power losses, device fully turned-on, as given in the published curves for the Hockey-Puk.
- B. Reverse blocking losses.
- C. Switching losses, during turn-on and turn-off periods. (These become significant at operating frequencies above 400 Hz).

If the case temperature rise shows the maximum allowable case temperature will be exceeded, one or more of the following steps can be taken to overcome this:

- A. Increase the cooling provided the Hockey-Puk by increasing the cooling fluid velocity or using larger heat exchangers.
- B. Switch to a different cooling method; use forced air cooling instead of free convection air, or water cooling instead of air.
- C. Reduce the ambient temperature.
- D. Switch to a larger Hockey-Puk or use two devices in parallel.

The above rating calculations are treated more fully in reference [3] and in other chapters of this book.

Cooling for Specific Applications

The basic procedure of the overall analysis of cooling for a specific application is outlined as follows:

- A. Determine the average watts loss developed in the component under steady-state operation. Using this value and the appropriate internal thermal resistance, determine the average temperature drop from junction-to-case for the device. For low duty cycles, the procedure described in steps E through H should be used to obtain the maximum junction temperature varia-

tion around this mean value.

- B. Next, select a value of $R_{\theta CS}$, and using the same watts loss, calculate the temperature drop from the case to the surface of the cooling fin.
- C. Again, using the same watts loss, having previously chosen the length of heat exchanger extrusion and the cooling air velocity, determine the thermal resistance for that operating condition and calculate the temperature drop from the heat exchanger surface where the device is mounted, to the ambient air.
- D. Total the three temperature drops, and add these to the maximum expected ambient air temperature to find the average junction temperature of the device under a steady-state operating condition.
- E. Calculations similar to A through D must now be made for all overload conditions which will be superimposed on the steady-state operation. Using the transient thermal impedance curves and the *additional* watts loss due to these overloads, the additional temperature rise caused by the overload condition should be calculated and added to the temperature rise previously calculated for the steady-state load.
- F. Compare this last total junction temperature with the maximum allowable junction temperature of the device as listed on the detailed specifications to determine if operation is still within the limits specified for the particular device under study.

- G. Note the time interval between the application of each overload. If there is sufficient time for the device to cool to its steady-state operating temperature, the calculation is complete. If other overloads are applied before cooling is complete, higher peak temperatures may be reached. Reference [2] indicates methods of calculation which can be used in cases such as this.
- H. Adjustments may be necessary either to increase or decrease the cooling obtained from the heat exchanger, or to change the semiconductor device or the number in parallel to achieve a satisfactory operating system depending upon the results obtained in steps E, F, and G.

If the electrical overload surges of medium and large power devices are of duration less than 0.5 second, the transient heat will not have time to flow from the device into the heat exchanger. In that case, the transient properties of the device and steady-state properties of the heat exchanger are of major importance. For overloads longer than 0.5 second, the thermal storage capacity of the heat exchanger becomes important.

Table XII-I shows the heat exchanger capabilities for some 12 metals. From these data, it is evident that if weight is of minor concern, nickel has the highest heat storage per cubic inch. However, where weight is important, aluminum has the highest heat storage per pound. It also has the highest thermal conductivity per pound

(given under conductivity density) which, coupled with a moderate material cost per pound, makes aluminum a very attractive choice for fabrication of heat exchangers.

Flat fin heat exchangers are sometimes used in low power applications for PACE/paks (hybrid assemblies) or discrete devices. Electrically isolated packages allow the system enclosure to be utilized as the heat sink. Figure 12-6 is a nomogram for determining sink to ambient thermal resistance, $R_{\theta SA}$, for a flat heat exchanger using natural convection. To use, select the heat sink area at left and draw a horizontal line across the chart from this value. Read the value of $R_{\theta SA}$ depending on the thickness of the material, type of material and mounting position.

Oil-Immersed Cooling

To apply semiconductor devices to oil-immersed power supply applications, use the curves shown on Figure 12-7, and the following recommended design procedure.

The basic steps in designing the cooling enclosure for the oil and rectifiers (and any other immersed equipment) are: (It is assumed that the rectifier devices are mounted on flat cooling fins.)

- A. Establish the maximum ambient air temperature and the maximum device case temperature. (For industrial use, the maximum device case temperature may be indicated by the class of insulating materials used, Class A or B.)
- B. Determine the losses in watts for all immersed components, i.e.,
 1. Watts loss per rectifier device

Table XII-I. Heat Exchanger Properties of Various Metals

MATERIAL	HEAT STORAGE CAPACITY		THERMAL CONDUCTIVITY (w/in.-°C)	DENSITY (POUND/ in. ³)	THERMAL CONDUCTIVITY (W-in. ² /°C-lb.)
	(JOULE/in. ³)	(JOULE/ POUND)			
Aluminum (6061)	40.5	413	4.35	0.098	44.4
Brass	50.5	165	2.94	0.306	9.6
Copper	57.5	178	9.93	0.323	32.4
Gold	41.3	59	7.48	0.698	10.7
Lead	24.2	59	0.88	0.41	2.15
Molybdenum	45.5	123	3.71	0.369	10.1
Nickel	67.0	208	1.54	0.322	4.8
Silver	40.5	107	10.55	0.380	27.8
Steel, Carbon	62.0	209	1.14	0.283	4.0
Steel, Stainless	65.0	224	0.413	0.29	1.4
Tin	28.6	110	1.54	0.261	5.9
Zinc	47.5	184	2.84	0.258	10.6

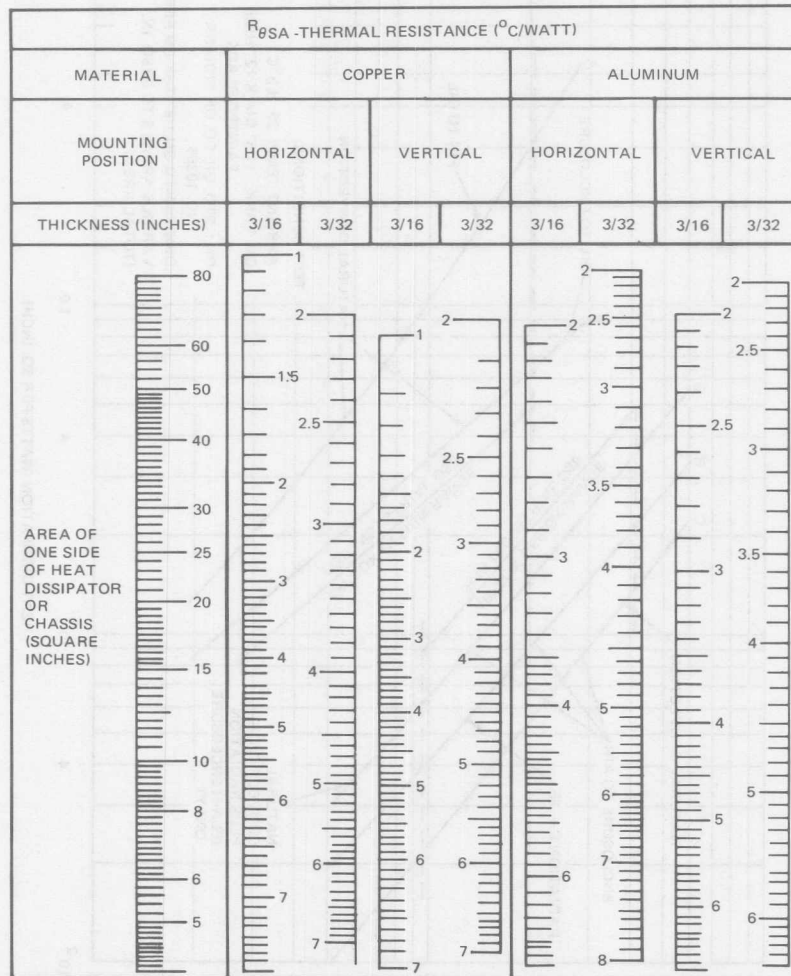


Figure 12-6. Thermal Resistance of Flat Fin Heat Exchanger

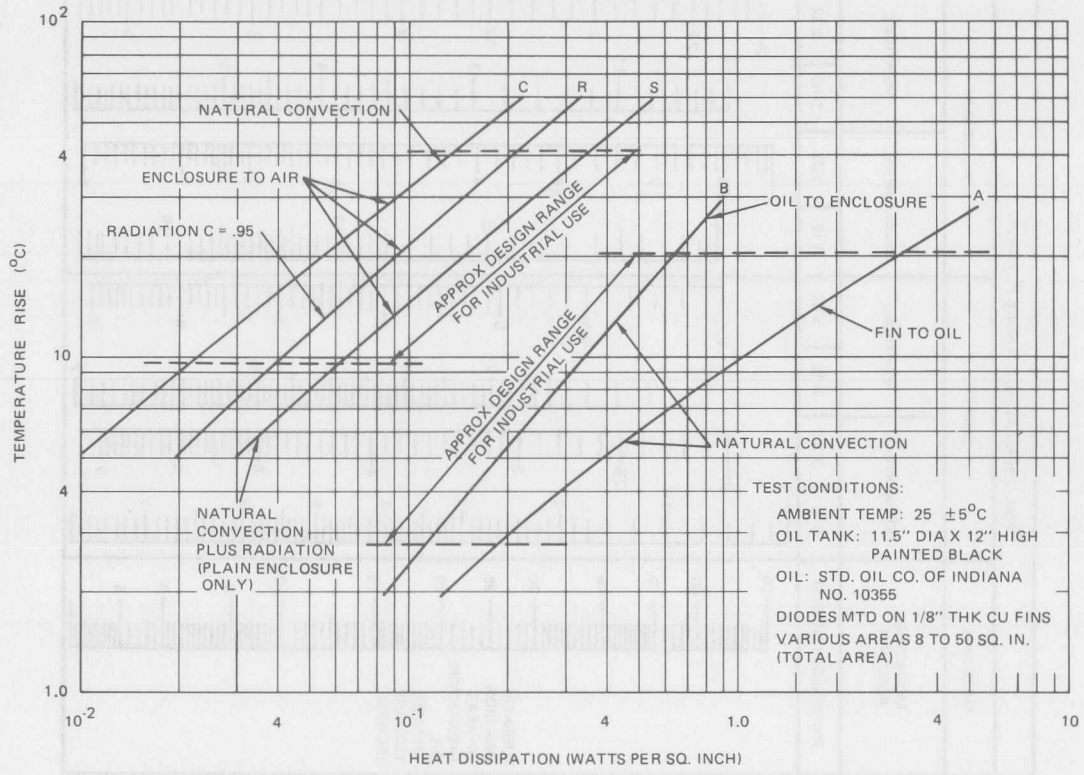


Figure 12-7. Temperature Rise of Oil-Immersed Rectifiers

2. Watts loss for complete assembly.
3. Watts loss for other immersed components (transformer, contactors, etc.)

C. From the above temperature and loss data, calculate:

1. Temperature drop from device case to fin center.
2. Temperature drop from mean fin temperature to oil (from Curve A on Figure 12-7).

NOTE: Fin thickness should be 1/8 inch minimum when using copper and 1/4 inch thickness for aluminum. Compute area using both sides of the fin. To obtain the temperature drop from center (hottest spot) to oil, multiply the temperature drop from mean fin temperature by a factor of 1.9 approximately.

3. Select an enclosure size and from total area of vertical sides, and total watts loss, determine temperature drop from enclosure to air (using Curve S, if a plain enclosure is used, or Curve R if cooling fins are used).
4. After enclosure dimensions have been fixed from 3. above, calculate the temperature drop from oil to enclosure, using Curve B internal area of enclosure, and total watts loss.
5. Total all of the temperature drop figures from 1. through 4. above and compare with temperature limits as established in A. above. (The sum of the individual temperature drops should always be 10 to 15

percent less than the total temperature difference to allow for hot spots and a small safety factor.)

D. The following notes concerning the curves may be of help:

1. The difference in location and slope between curves A and B is empirically adjusted to approximately compensate for the difference in oil temperature under various conditions and velocity in oil movement at the two surfaces.
2. If a plain enclosure is used (no fins or tubes) and is painted black, and where radiation is unrestricted, Curve S may be used to determine temperature drop from enclosure to air (Curve S is summation of Curves C and R).
3. If a finned tank or cooling tubes are used, it is necessary to use the total enclosure plus fin plus tube area, and Curve C to determine temperature drop by convection, but use only the envelope area and Curve R to determine the temperature drop by unrestricted radiation.

NOTE: If the tank is located in direct sunlight, or near a furnace or boiler or other source of radiant energy, the radiant cooling of the enclosure will be partially offset by radiant heating from the external heat source. It is advisable to reduce the temperature drop from Curve R by 50%, or sometimes not include it at all.

References

1. "NEMA-EIA Standards for Silicon Rectifier Diodes and Stacks," NEMA Pub. No. SK-60-1963 EIA Std. RS-282 (Par. 7.09, 7.13).
2. F.W. Gutzwiller & T.P. Sylvan, "Power Semiconductors under Transient and Intermittant Loads," AIEE Transactions, Part I, Communications and Electronics, 1960, pp. 699-706.
3. D.W. Borst, "Calculation of Rectangular Waveform Current Ratings," Rectifier News, Summer, 1967.
4. E.J. Diebold and W. Luft, "Thermal Impedance of Cooling Fins," AIEE Transactions, Vol. 77, Part 1 (1958), pp. 739-745.
5. E.J. Diebold and W. Luft, "Transient Thermal Impedance of Semiconductor Devices," AIEE Transactions, Vol. 79, Part 1 (1961), pp. 719-726.
6. J.L. Saiers, "Optimum Cooling by Use of Finned Dissipators," Electronic Packaging and Production, Feb. 1963, pp. 10 to 14.
7. W.H. McAdams, "Heat Transmission," McGraw-Hill Book Co., Inc., New York, N.Y. (1942).

Testing

In order to cover the area of testing SCRs, test circuit diagrams are presented with actual wave-shapes expected at various points in the circuit during operation. The systems presented are not necessarily the same circuits or systems used at IR during production and Quality Control inspection. The circuits presented here are designed for customer use to meet the same conditions and values established by IR's equipment.

International Rectifier has developed many specialized test systems. Some of these do use the circuits presented, while others use more extensive or multi-purpose circuits to meet the particular requirements of production and control procedures.

The test methods and circuits are generally those recommended by the EIA-NEMA standards for thyristors. EIA Standard RS-397 (NEMA Standard SK516-1972) as formulated by the JEDEC Solid-State Products Council in June, 1972.

Three tests which are usually performed on an SCR to ensure that it will meet the requirements of a specific application are:

1. Off-state (forward) and reverse blocking voltage.
2. On-state voltage during conduction (full-cycle average, instantaneous peak, or by a dc measurement).
3. DC triggering characteristics.

Other tests which may or may not be needed to verify that an SCR will adequately fill a particular application include:

4. Holding current
5. Latching current (as measured with a moderately long repetitive gate pulse).
6. Turn-on time into a resistive load (with or without distinction of delay and rise times).
7. Turn-on voltage in a resonant pulse circuit (often taken as an indirect measure of rate-of-rise of current capability).
8. Turn-off time under "standard" conditions (using properly gated dc supplies with a linear ramp of reapplied forward voltage).
9. Critical rate-of-rise of off-state voltage (dv/dt), with applied waveform approximating exponential as closely as possible.
10. Critical rate-of-rise of turned-on current (di/dt).
11. Thermal resistance from specified case point to "virtual junction," under steady-state dc equilibrium conditions.

Each of these parameters is discussed in relation to its test circuit on the following pages. In addition, a discussion on testing power triacs, trigger circuits, and additional comments are included at the end of this chapter.

Parameter 1: Blocking Voltage

"Blocking voltage" is discussed in Chapter 1. It is usually determined dynamically at a specified case temperature. Peak voltage, either off-state or reverse, is determined at a given peak or full-cycle average forward or reverse leakage current. An oscilloscopic presentation is usual, so sharpness of breakdown is noted.

Figure 13-1 shows a circuit suitable for this measurement. This circuit can test off-state and reverse blocking simultaneously, or it can show off-state or reverse characteristics alone. If the required reverse blocking capability should be appreciably different from forward, this feature is essential. Protective lamp bulbs, L_1 to L_4 , distort waveform to a minimum, but still protect meters and transformer in the event of breakover, or disappearance of forward or reverse blocking capability.

The oscilloscope may be grounded at one side for both the vertical and horizontal inputs, with the heat dissipator to which the anode is attached floating above ground only by the few millivolts across the current shunt. The voltage divider used to produce oscilloscope

horizontal deflection can be of relatively low impedance in order to stabilize the sinusoidal waveform as a bleeder.

Peak-reading voltmeters, M_1 and M_2 , should use high-sensitivity, taut-band microammeters; 1) to insure linear meter calibration, and 2) to allow use of small capacitors in the peak reading voltmeters, with resulting minimized clipping of peaks.

Steering diodes in series with leakage meters need not have high voltage ratings (because one meter circuit clamps the other at 3 volts or less), but, to avoid non-linearity of the leakage meters, two protective diodes, RD_4 and RD_6 , should be used across the meters instead of one, with the resistors, R_3 and R_4 , shown in series with the individual meters, adjusted for maximum protection of the movements with-

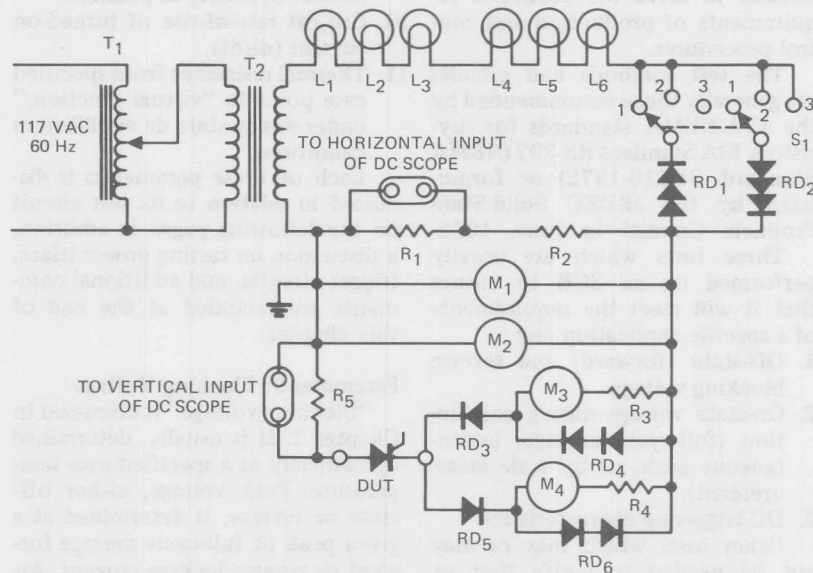


Figure 13-1. Blocking Voltage Test Circuit

L ₁ - L ₆	Lamp Bank	R ₃ , R ₄	Potentiometer
M ₁	Voltmeter, peak-reading, "Forward Positive"	RD ₁ , RD ₂	Rectifier, high voltage cartridges
M ₂	Voltmeter, peak-reading, "Reverse Negative"	RD ₃ , RD ₅	Rectifier
M ₃	Milliammeter, high-sensitivity, "Reverse Leakage"	RD ₄ , RD ₆	Rectifier, 2 each, 1 amp (IR10D)
M ₄	Milliammeter, high-sensitivity, "Forward Leakage"	S ₁	Switch, 2-pole, 3-throw
R ₁ , R ₂ , R ₅	Resistor	T ₁	Transformer, variable, auto
		T ₂	Transformer, step-up

Figure 13-1. Blocking Voltage Test Circuit

out clipping of peaks at full-scale deflection.

Oscilloscope leads must be short, and excessive capacitance should be avoided from lead to lead, or from lead to chassis, to prevent a loop within the scope pattern. A small amount of hysteresis still is possible if the junction of the unit under test is pushed far enough into breakdown for it to increase in temperature. Every precaution should be taken to avoid ground loops.

Parameter 2: On-state Voltage

"On-state voltage during conduction," is defined in Chapter 1. It is usually found by a half-wave test of brief duration, with the unit in a Kelvin (separate current and voltage contacts in a four-point configuration) jig of large thermal mass, to avoid excessive rise of case temperature during the test. Pulse techniques, with low pulse repetition rate and an oscilloscope readout of forward voltage versus forward current, require much less power and give forward voltages at a junction temperature quite close to the jig ambient.

Figure 13-2 shows a test circuit suitable for the usual half-wave test.

Full-cycle average on-state voltage can be read from meter M₁ at a specified value of full-cycle average on-state current, read on meter M₂ or peak on-state voltage can be read from a scope screen at a given peak on-state current.

The test unit must conduct for close to 180° to retain the usual relationship between full-cycle average values and peak values. This requires 1) that gate signal be present from a point close to 0° to a point almost at 180°, and 2) that peak supply voltage be much higher than the peak on-state voltage of the device under test.

Requirement 1) may be satisfied by a low impedance metered gate supply delivering ripple-free direct current, but this supply must be adjusted for each unit to insure nearly full half-cycle conduction without excessive gate dissipation. For gating without individual adjustment, this tester uses a 175° wide square wave, properly phased with respect to the transformer which supplies the anode current; the output to the gate is ten volts open-circuit and short-circuit current is limited to a safe value. To obtain this gate pulse, an ac supply

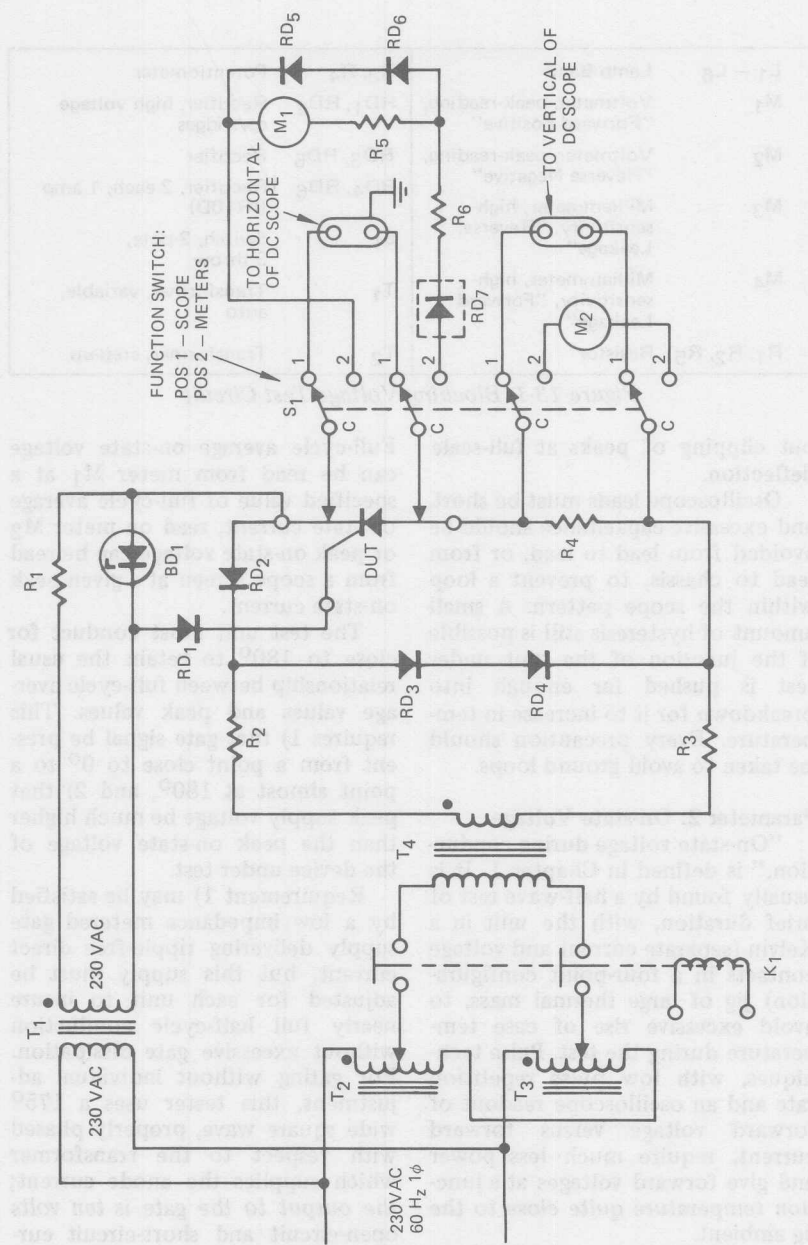


Figure 13-2. On-State Voltage Test Circuit

BD1	Voltage Regulator, 11V	R ₁ , R ₃	Resistor	RD7	Rectifier in a 70°C Crystal Oven
K1	Contactor, or Wetted Mercury	R ₄	Resistor, Low Inductance, 50 mV Shunt	T ₁	Transformer, Isolation
M1	Voltmeter, Special "FCA On-State Voltage"	RD1, RD2	Rectifier	T ₂ , T ₃	Autotransformer, Variable
M2	Ammeter, 50 mV DROP, "FCA On-State Current"	RD3, RD4	Rectifier	T ₄	Transformer, Step-down, 230V, 24V
		RD5, RD6	Rectifier		

Figure 13-2. On-State Voltage Test Circuit

of high voltage feeds a power zener voltage regulator through a large dropping resistor, R₁. An isolating diode, RD₁, is provided in series with the gate of the test unit.

Requirement 2) is satisfied by an ac on-state current supply of low impedance and of high enough output voltage to allow a voltage drop at peak of eight or more times the peak on-state voltage of the unit under test to appear across the series dropping resistors, R₂ and R₃. With conduction through a balancing rectifier string, RD₃ and RD₄, during the 180° to 360° interval, the transformer secondary sees a nearly resistive load. The rating of the transformers should be several times that dictated for calculated dissipation, to avoid problems of possible saturation.

Diode isolation, by rectifier RD₇, of the on-state voltage meter, M₁, is desirable, despite the working diode RD₂ in the on-state circuit, to avoid the effect of possible reverse recovery spikes. The desired high front-to-back ratio of the isolating diode calls for a silicon unit. To reduce forward drop across the diode and to minimize the effect of varying ambient upon final calibration of this meter, the isolating diode, RD₇, is housed in a 70°C crystal oven. The net result is a meter with a suppressed zero which reads from 0.5 volt full-cycle average to 2.0 volts and which must be hand-calibrated.

With this tester, physical layout of wiring is of prime importance. Poor layout leads to an excessive loop in the scope display and to more insidious errors. The shunt generally must be mounted directly upon the test jig. With the commonly used Hewlett Packard 120

oscilloscope, an internal ground exists at the horizontal input and the vertical input ground must not float by more than 100 millivolts. This means that the only true ground of the equipment must be at the horizontal input to the scope, although in the drawing, a ground is indicated at the scope jacks of the equipment itself. Ground shields may be used for scope connections, but the shield must not be a sensing lead (use a floating twisted pair through the shield).

Parameter 3: DC Triggering Characteristics

“DC triggering characteristics” is discussed in Chapter 1. It can be determined by a tester such as shown in Figure 13-2, if a suitable dc gating supply is substituted for the half-wave network. The power supply which is a part of Figure 13-3 is a suitable supply. The supply characteristics which are important are: 1) an extremely low internal impedance, 2) a low ripple voltage and 3) monitoring of gate current by a milliammeter of low constant impedance (to avoid excessive error occasioned by IR drop across the meter) and monitoring of gate voltage by a voltmeter of sufficiently high impedance so as not to draw appreciable current through the series milliammeter (if the voltmeter should be connected directly across the gate). The low impedance of the supply is necessary so the supply voltage does not drop when the unit triggers, and the low ripple of the supply output is necessary so the unit triggers at the dc voltage indicated by the meter, and not a peak ripple point not shown by the average-reading voltmeter.

This technique can be ambiguous. As voltage is increased to the gate, the unit will first trigger at the peak of the half-wave dc waveform, and the voltage to the gate must be increased until the voltage across the unit just before triggering is at a specified point. To avoid this ambiguity, many customers and some military specifications call out the application of dc voltage to the anode, with a specified series anode current limiting resistor and meter. This technique is slow, because if voltage is varied rapidly, an excessive voltage requirement may be read, and if high accuracy is required, several trials may be necessary, with the anode connection broken each time to interrupt current and reset the test unit. In production screening, this technique can be quite quick if gate voltage of a specified value is applied, with a "pass" bulb included as part of the anode current limiting resistor.

An anode voltage of either 6 or 12 volts dc is part of several industry standard specifications. The circuit shown in Figure 13-3 meets the requirements of a dc anode supply, but permits easy and exact adjustment, possibly with 60 Hz resetting, by use of a square anode pulse close to 180° wide. The basic square wave is formed by a power zener voltage regulator, BD₄, yielding a waveform which extends approximately 6.8 volts above (positive) zero baseline and about 0.8 volts below (negative). The diode, RD₁, which couples the zener voltage regulator output into a load resistor, R₈, drops the 6.8 volts to approximately 6.0 volts. Potentiometer R₉ is adjusted to 60 mA dc as read on a milliammeter short-

ing out the anode and cathode terminals. The lighting of lamp, L₁, is a positive indication of anode triggering. The series resistor, R₉, serves to adjust total anode load to a value (after triggering) which approximates that specified in MIL-S-19500/108D.

Parameter 4: Holding Current

"Holding current" is discussed in Chapter 1 and in Chapter 2. However, some stipulations on equipment are necessary. Certainly the supply voltage must have a value appreciably below the maximum which the device under test can normally block; for an apparatus to have general utility, this voltage must be low enough to handle all devices to be tested. In addition, the tester must provide a changing load rather than a changing supply voltage. To change the load smoothly, without generation of noise or interruption of current, even momentarily, is difficult with a commercial variable resistor, and an active element must be substituted.

Less obvious is the need for an initial anode current sufficient for full turn-on of the device. In MIL-S-19500/108B, a current of 500 milliamperes is specified. In IR production testing, a minimum current of 1 ampere is called out. Even at this level, however, high power units occasionally show evidence of incomplete turn-on.

This phenomenon generally is uncovered during a determination of dc thermal impedance. A prerequisite of this test is the determination of on-state voltage at a reference constant current (up to five amperes dc for the largest devices), with the case at a desired

maximum temperature (the assumption being that at relatively low dissipation, junction and stud temperatures are identical). Incomplete turn-on is evidenced by the fact that, as the initial turn-on current of the unit is increased, this reference on-state voltage will drop; an indication of lowered current density and thus of increased conducting cross section.

Figure 13-4 shows a circuit for a manual tester for holding current which, on the basis of complete turn-on at 0.5 ampere dc through the anode, can be used with any commercial controlled rectifier, and which meets the general requirements of MIL-S-19500/108D. The major portion of the tester is an extremely stable, hum or noise-free constant current supply, whose compliance voltage (with current regulation to a fraction of a percent) is fixed by a clamping zener voltage regulator, BD₂, (outside the current-sensing loop) to six volts dc. The current through the unit under test is measured on the basis of voltage drop across a power resistor, R₉, (working at a fraction of rating) connected in a Kelvin mode. While this technique of affording multiple range is deplorable in most applications, here it permits the meter range to be switched without interruption of load current. The rectifier under test is overgated to insure as complete turn-on as possible; the gate signal is the charging current of a Mylar capacitor C₃, connected between the positive supply and the gate. When the PRESS TO READOUT switch, S₃, is closed, after the unit under test just drops out, a small silicon diode, RD₁, is substituted for the controlled rectifier to read out the

constant current. The function of the clamping zener voltage regulator, BD₁, is to assure reasonably constant thermal loading of the constant current transistor.

Figure 13-5 illustrates the shift of emphasis which must be made when a test is to be performed by production, rather than quality assurance, personnel. The tester in Figure 13-4 requires strict adherence to a specific procedure as outlined in Table XIII-I and yields quantitative data. The tester in Figure 13-5 can be used for rapid routine screening, since the criterion is simply whether a pilot lamp remains lighted after the gating button is pressed.

In the production tester, Figure 13-5, two constant-current supplies are used, one of which is set permanently to one ampere dc, and the other is variable over any of four widespread ranges. Each supply is individually clamped by a zener voltage regulator. During gating, a minimum of one ampere anode current is supplied, which is abruptly, but smoothly, shifted down to the limit point when gate switch S₄ is open. Capacitor C₅ between gate connection and negative common is necessary in perhaps five cases of a hundred; its use was permitted only after extensive evaluation and intercomparison with testers of the type shown in Figure 13-4. Whatever the capacitor's role, its presence actually improves reproducibility of permanent known standards when the tester is used quantitatively for holding current readout, with no shift from established values for these standards.

Indicator lamp, L₂, intensity is consistent down to a current of a few milliamperes as a result of the

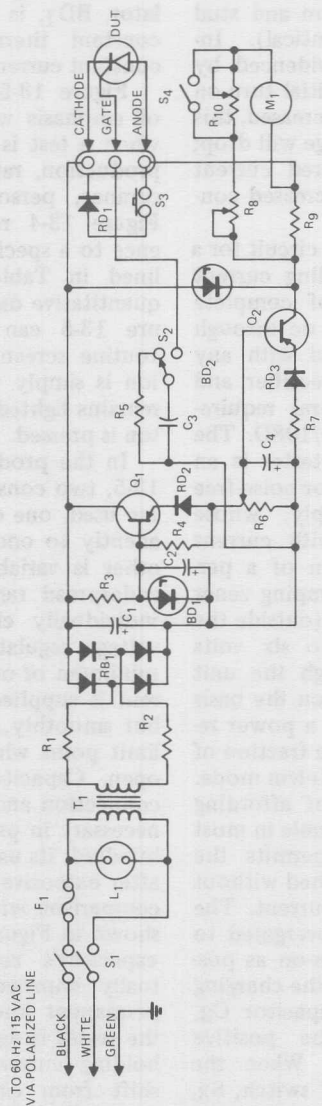


Figure 13-4. Holding Current Manual Test Circuit

BD ₁	Voltage Regulator, 12V, 10W (IR - 1N2976B)	R ₁ , R ₂	Resistor, 1 Ω , 10W	RD ₁	Rectifier, 1000V, 1A (IR - 10D10)
BD ₂	Voltage Regulator, 6.8 V, 10W (IR - 1N2970B)	R ₃	Resistor, 100 Ω , 10W	RD ₂ , RD ₃	Rectifier, 600V, 16A (IR - 16F60)
C ₁	Capacitor, 1500 μ F, 50 VDC	R ₄	Resistor, 470 Ω , 1W, 5%	S ₁	Switch, DPST, 3A, 125 VAC "Power"
C ₂ , C ₄	Capacitor, 1000 μ F, 15 VDC	R ₅	Resistor, 33 Ω , 1W, 10%	S ₂	Switch, SPDT, Push, Button, Snap Action, "Press to Trigger"
C ₃	Capacitor, 5 μ F, 100V, Mylar	R ₆	Potentiometer, 100 Ω , 10 Turn, "Current Adjust"	S ₃	Switch, SPST, No Push Button, Snap Action, "Press to Read Out"
F ₁	Fuse, 2AFB	R ₇	Resistor, 20 Ω , 50W	S ₄	Switch, SPST, 1A, 125 VAC, "Meter Range: Open 0-500 Closed 0-50"
L ₁	Lamp, Neon Pilot, 115 VAC	R ₈	Potentiometer, 200 Ω , "Calibration Trimmer"	T ₁	Transformer, 115 VAC/25.2 VAC @ 2A
M ₁	Meter, 0-50mV, 0-1 mADC Movement	R ₉	Resistor, 2 Ω , 10W, Shunt		
Q ₁ , Q ₂	Transistor (2N457A) On Insulated Heat Exchanger	R ₁₀	Potentiometer, 1000 Ω , "Calibration Trimmer"		
		RB ₁	Rectifier Bridge, 1.8 Amp, 600V (IR - 18DB6)		

Figure 13-4. Holding Current Manual Test Circuit

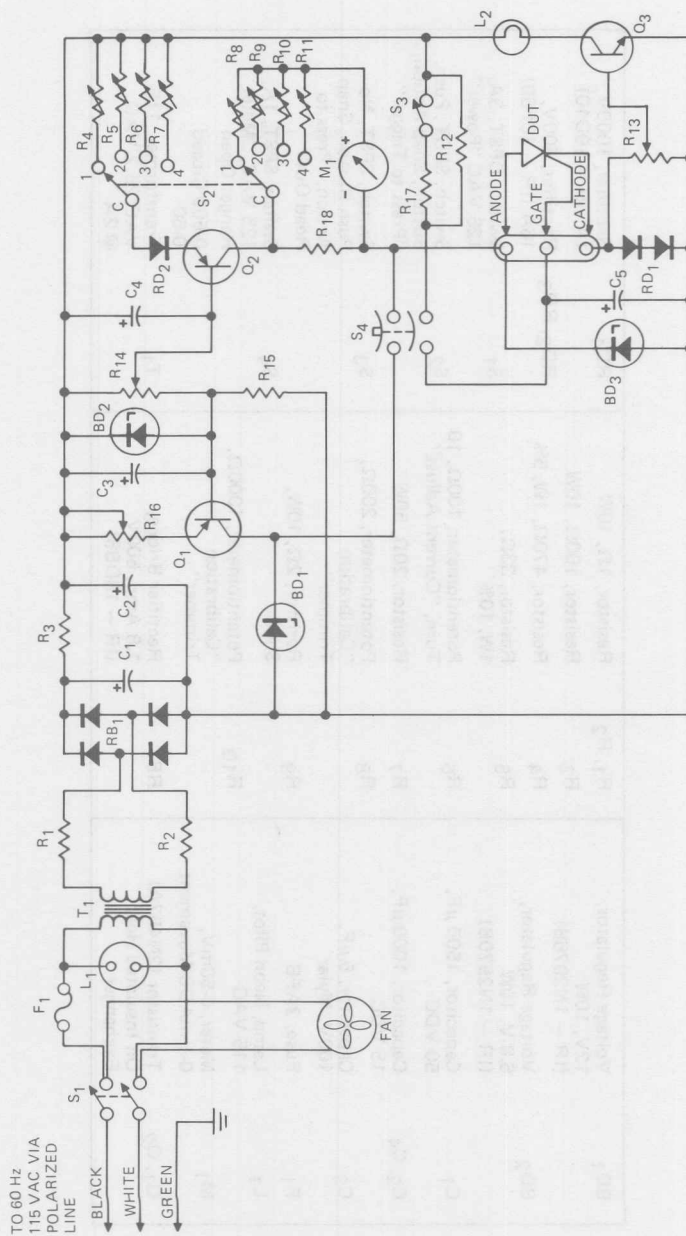


Figure 13-5. Holding Current Production Test Circuit

Figure 13-5. Holding Current Production Test Circuit

BD ₁ , BD ₃	Voltage Regulator, 6.8 V _Z , 10W (IR - 1N2970B) On Heat Exchanger	Q ₁ , Q ₂	Transistor, 2N458A, On Heat Exchanger	R ₁₇	Resistor, 55Ω, 10W
BD ₂	Voltage Regulator, 9.1 V _Z , 10W (IR - 1N2974B) On Heat Exchanger	Q ₃	Transistor, 2N339, Insulated	R ₁₈	Resistor, 2Ω, 10W
C ₁ , C ₂ , C ₃ , C ₄	Capacitor, 2000 MF, 50 VDC	R ₁ , R ₂	Resistor, 0.5Ω, 5W	RB ₁	Rectifier Bridge, 7.5 Amp Full Wave (IR-75JB3)
C ₅	Capacitor, 33 MF, 35 VDC, Tantalum	R ₃	Resistor, 5Ω, 25W	RD ₁	Rectifier, 2 each, Lamp, 100V, (IR-10D10)
F ₁	Fuse 2AFB	R ₄	Rheostat, 15Ω, 25W	RD ₂	Rectifier, 20 Amp
FAN	Muffin Fan, 115 VAC, 60 Hz, (Rotron)	R ₅	Rheostat, 50Ω, 25W	S ₁	Switch, DPST, 3A, 125 VAC "Power"
L ₁	Lamp, Neon, 115 VAC, "Line Pilot"	R ₆	Rhoestat, 150Ω, 25W	S ₂	Switch, 2-Pole, 4-Position Shorting, "Limit Range" Pos 1 = 100 mADC, Pos 2 = 0.250 mADC, Pos 3 = 0-100 mADC, Pos. 4 = 0.25 mADC
L ₂	Lamp, #57, "Unit Triggered"	R ₇	Rhoestat, 500Ω, 25W	S ₃	Switch, SPDT, 3A, 125 VAC, "Gate Range: Closed, 400 mA Max. Open, 100 mA Max.
M ₁	Meter, 50 MV, 1 mA Movement, Scale, 0.25-100-250-1000 mADC, "Holding Current"	R ₈	Trimmer, 2,000Ω Max.	S ₄	Switch, DPST, Snap Action Push Button, "Operate Gate"
		R ₉	Trimmer, 1,000Ω Max.	T ₁	Transformer, 117 VAC/ 25.2 VAC @ 2A
		R ₁₀	Trimmer, 500Ω Max.		
		R ₁₁	Trimmer 50Ω Max.		
		R ₁₂	Resistor, 225Ω, 10W		
		R ₁₃	Potentiometer, 1000Ω, 2W, "Adjust Lamp"		
		R ₁₄	Potentiometer, 200Ω, 10 Turn, "Adjust Current"		
		R ₁₅	Resistor, 20Ω, 10W		
		R ₁₆	Rheostat, 15Ω, 50V		

Table XIII-I. Holding Current Test Procedure

Lab Procedure (Refer to Figure 13-4)
<ul style="list-style-type: none"> A. Press "PRESS TO READOUT" button and hold. B. Adjust R₉ and R₁₀ to read 500 mA dc on Meter M₁. C. Release button. D. Press "PRESS TO GATE" button and release. E. Adjust "CURRENT ADJUST" potentiometer R₆ until dropout. F. Press "PRESS TO READOUT," and record reading.
Production Procedure (Refer to Figure 13-5)
<ul style="list-style-type: none"> A. Adjust "ADJUST CURRENT" potentiometer for maximum. B. Adjust Rheostats R₄ thru R₇ and trimmers R₈ thru R₁₁ for 10% overrange per range switch. Read on Meter M₁. C. Adjust Rheostat R₁₆ for 1A dc with standard meter across anode-cathode, with "OPERATE GATE" switch closed and "ADJUST CURRENT" potentiometer at minimum. D. Calibrate "HOLDING CURRENT" meter, M₁, at 80% of full scale. E. Turn "RANGE" switch S₂, to appropriate range. F. Insert device to be tested. G. Press and release "OPERATE GATE" button. H. Device passes if "UNIT TRIGGERED" lamp stays lit.

low dynamic impedance of the forward-biased rectifier, RD₁ in series with the unit under test and the negative common.

Meter M₁ at all times monitors the output current from the variable constant current supply. Whereas in the tester shown in Figure 13-4, and in the one ampere supply of this tester, the clamping zener voltage regulator is outside the current sensing loop, in this tester current passes from the variable supply either through the unit under test or through the clamping zener voltage regulator, BD₃, of this supply; the net result is barely perceptible momentary meter needle flicker when the unit under test shuts off.

Parameter 5: Latching Current

"Latching current" has been defined in Chapters 1 and 2 in this

book (refer to Index). There are major differences between holding current and latching current, as discussed in detail in other chapters.

In measuring holding current, the controlled rectifier is turned-on fully by over-gating to a relatively high anode current. The gate signal is called out specifically in measuring latching current. Not only may the unit not be turned-on fully, but conduction (for a minimal gate signal) may be confined strictly to the immediate vicinity of the gate, and di/dt stress (despite the low anode currents generally present), may be quite high. Dependent upon the specified gate signal, an order of magnitude spread between holding and latching current may be a signal of a faulty device design or a defective unit. (For dependable circuits, anode currents during gating should exceed latching current by a

wide margin.) In testing latching current, the gate signal should exist well beyond the usual turn-on time to insure spread of conduction.

Figure 13-6 shows simple tester with which a standard laboratory pulse generator, constant current generator, and oscilloscope may be used to determine latching current. The wetted contact mercury relay, K_1 , serves three purposes economically. It acts first as an adjustable and stable free-running relaxation oscillator to establish the basic repetition rate of the test. Secondly, it provides a means of shorting the unit under test periodically by a reproducible resistance of a few milliohms for a period of time sufficient to turn off any commercial unit. Thirdly, it provides an independent trigger output of fixed amplitude and shape which can trigger the external pulse generator reliably. Since this pulse starts when the mercury string contacts 3 and 5 of the wetted mercury relay collapses, and ceases when contact 3 first meets contact 5 (although the string between contacts 2 and 3 still shorts out the unit under test for 100 microseconds or more). The external pulse generator must be capable of variable delay of the output. While numerous other commercial equipments may be used, those specified in Figure 13-6 perform quite adequately.

The sequence of shorting out, re-arming, and gating evident from the anode waveforms of Figure 13-6, should be followed. With this arrangement, time t_A is typically 9-10 milliseconds. Time t_B is set by the delay of the pulse generator and is not critical past a certain minimum point. Time t_C (when the unit does not latch) is quite close to the

duration of the gate pulse. Within the limits of 1.7 pulses-per-second to 10 Hz obtained with this arrangement, time t_D (the reciprocal of the pulse repetition rate) is not critical. The current through 1) the short imposed by the mercury-wetted reed, 2) the clamping zener voltage regulator, BD_2 (which sets untriggered anode voltage at a nominal 6.8 volts dc), or 3) the triggered unit under test (during gating or later while latched) is constant and can be measured simply by a series milliammeter of desired accuracy.

The arrangement in Figure 13-6 is effective and is useful over a wide range of triggering and latching current requirements. The equipment required is costly and its operation requires a skillful technician. Figure 13-7 shows a tester which is suitable for both production screening and for quality assurance use and which yields test results consistent with those obtained with the laboratory equipment.

A point-to-point check shows the same basic elements. A stable constant current generator is provided which extends from two milliamperes to 100 milliamperes. The meter is rescaled for ranges 0-25 mA dc and 0-100 mA dc in black, and 0-50 mA dc and 0-10 V dc in red. Red is "Gate Pulse." Black is "Latching Current." Calibrate M_1 at 75% F.S. Use R_5 to adjust 0-25 mA scale; R_6 , 0-100 mA dc; R_{21} , 0-10 V dc; R_{25} , 0-50 mA dc. The basic mercury-wetted reed circuit, K_1 , is incorporated. When installing K_1 ; use #14 copper wire from 2 and 3 to DC, a hybrid circuit, using a second mercury-wetted reed and a controlled rectifier, completes an internal pulse generator triggering

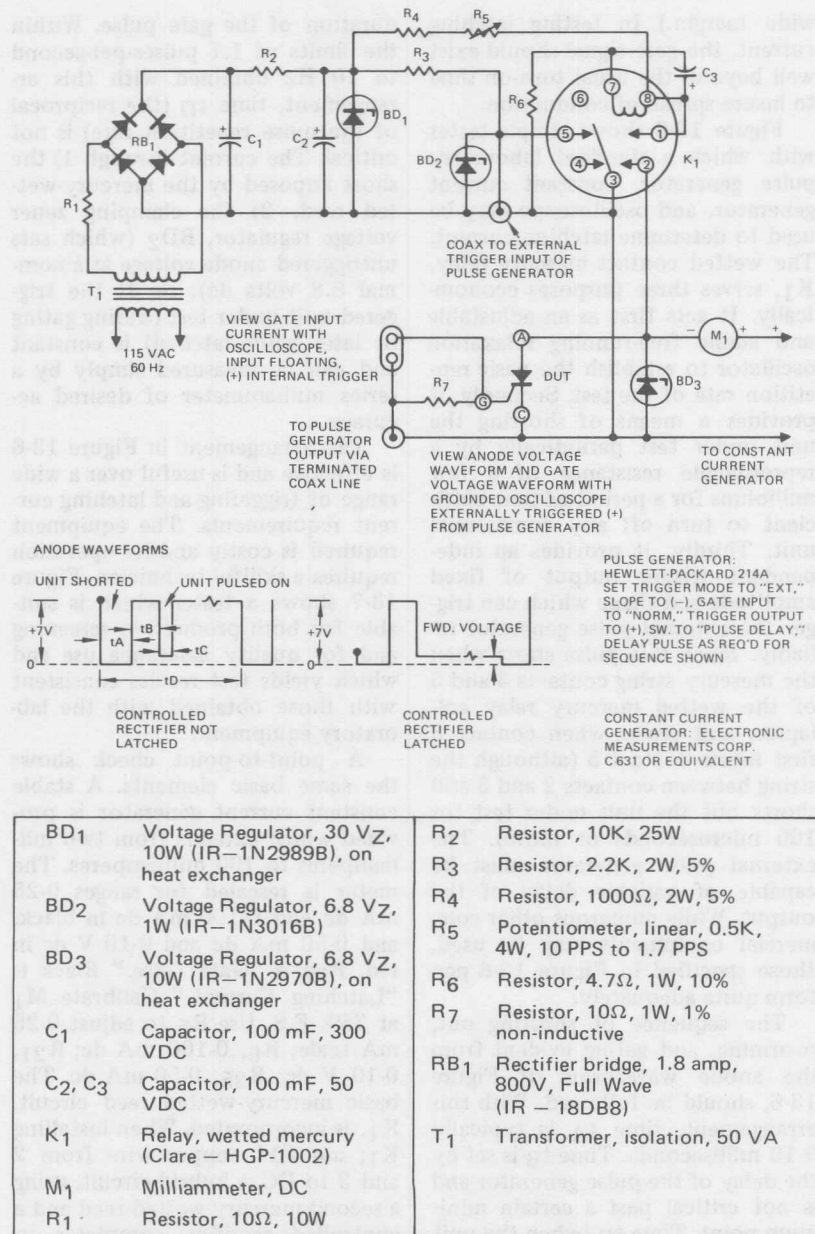
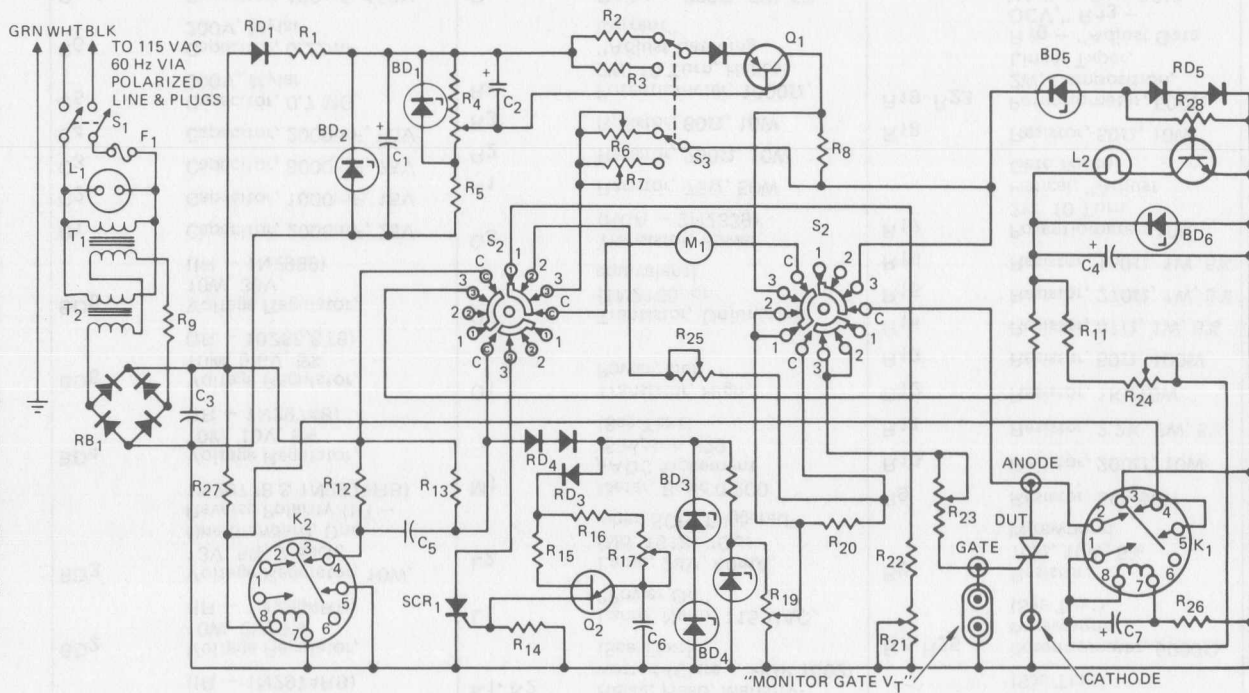


Figure 13-6. Latching Current Laboratory Test Circuit

Figure 13-7. Latching Current Production Test Circuit



BD ₁	Voltage Regulator, 10W, 10V, 5% (IR - 1N2974RB)	F ₁	Fuse, 2 Amp, Fast Blow	R ₆	Potentiometer, 500Ω, Wirewound (See Text)
BD ₂	Voltage Regulator, 10W, 2V, 5% (IR - 1N2984RB)	K ₁ , K ₂	Relay, Reed, Mercury-wetted (Clare - HGP 1002) (See Text)	R ₇ , R ₂₅	Potentiometer, 5000Ω, Wirewound (See Text)
BD ₃	Voltage Regulator, 10W, 13V, 5%, 2 Each, One Standard, One Reverse Polarity (IR - 1N2977B & 1N2977RB)	L ₁	Lamp, Neon, 115 VAC, "Power On"	R ₈	Resistor, 10Ω, 10W, 5% Wirewound
BD ₄	Voltage Regulator, 10W, 10V, 5% (IR - 1N2974B)	L ₂	Lamp, 28V, 40mA, (No. 1918) "Out when SCR Triggered"	R ₉	Resistor, 5Ω, 50W
BD ₅	Voltage Regulator, 10W, 5.6V, 5% (IR - 10ZS5,6T5)	M ₁	Meter, Basic 0.200 μADC Movement (Simpson #29) (See Text)	R ₁₀	Resistor, 200Ω, 10W
BD ₆	Voltage Regulator, 10W, 30V, (IR - 1N2989)	Q ₁	Transistor, High Power, Ger.	R ₁₁	Resistor, 2.2K, 2W, 5%
C ₁	Capacitor, 2000mF, 25V	Q ₂	Transistor, Unjunction (1N2160, or equivalent)	R ₁₂	Resistor, 1K, 10W
C ₂	Capacitor, 1000mF, 15V	Q ₃	Transistor, Power (RCA - 2N2339)	R ₁₃	Resistor, 50Ω, 100W
C ₃	Capacitor, 8000mF, 75V	R ₁	Resistor, 75Ω, 50W	R ₁₄	Resistor, 47Ω, 1W, 5%
C ₄	Capacitor, 2000mF, 50V	R ₂	Resistor, 250Ω, 10W	R ₁₅	Resistor, 270Ω, 1W, 5%
C ₅	Capacitor, 0.7 MG, 200V, Mylar	R ₃	Resistor, 60Ω, 10W	R ₁₆	Resistor, 150Ω, 1W, 5%
C ₆	Capacitor, 0.22mF, 200V, Mylar	R ₄	Potentiometer, 1000Ω, 2W, 10 Turn, Helical "Adjust Latching Current"	R ₁₇	Potentiometer, 10K, 2W, 10 Turn Helical, "Adjust Gate Width"
C ₇	Capacitor, 100mF, 150V	R ₅	Resistor, 220Ω, 5W, 5%	R ₁₈	Resistor, 50Ω, 10W
				R ₁₉ , R ₂₃	Potentiometer, 500Ω, 2W, Composition, Linear Taper, R ₁₉ - "Adjust Gate OCV," R ₂₃ - "Adjust Gate SCI"

Figure 13-7. Latching Current Production Test Circuit

R20	Resistor, 5 Ω , 10W, 5% Wirewound	RD ₁ , RD ₃	Rectifier, 1 Amp, 100V, (IR - 10D1)	S ₃	Switch, DPDT, 6A, 125 VAC, "Latching Current Range"
R21	Potentiometer, 10K, Wirewound (See Text)	RD ₂	Rectifier, 20 Amp, 200V, Mounted On Heat Exchanger (IR - 20F20)		R ₂ , R ₆ Pos = "0.25 mADC"; R ₃ , R ₇ , Pos. = "0-100 mADC"
R22	Resistor, 39K, 1W, 5%	RD ₄ , RD ₅	Rectifier, 2.1 Amp, 10V in Series (IR - 10D1)	SCR ₁	SCR, 7.4 Amp RMS, 400V, Mounted On Heat Exchanger (IR - 2N1777A)
R24	Potentiometer, 1K, 2W, Composition, Linear Taper, "Adjust PRR"	S ₁	Switch DPST, 6A, 125VAC, "Power"		
R26	Resistor, 4.7 Ω , 1W, 5%	S ₂	Switch, 2 Wafer 3 Pole, 4 Position (Centralab - 2515 or 2525) "Function," Pos. 1 = "Set OC Gate V", Pos 2 = "Set SC Gate I" Pos 3 = "Measure Latching I"	T ₁ , T ₂	Transformer, (Triad - F-41X) (See Text)
R27	Resistor, 10K, 2W, 5%				
RB ₁	Rectifier, Full Wave Bridge, 2.2 Amp, 200V, (IR - 22DB2)				

Figure 13-7. Latching Current Production Test Circuit

with proper sequence. The output pulse has a rise time (10-90 percent) of seven microseconds and a fall time of even less, with less than five percent ringing or undershoot. Droop is less than one percent. Pulse duration can be extended from 38 microseconds to 1.34 milliseconds (50% level). Time t_B is consistently 10-11 milliseconds.

Switch S_2 makes it possible to set open-circuit gate voltage (when called out) and short-circuit gate current (through the gate) on a dc basis, with meter instead of expensive oscilloscope viewing. In actual gate voltage, it may be monitored by an external 20,000 Ohms-per-Volt multimeter.

While an oscilloscope is needed initially to set gate pulse width, in performance of the test, it is not required. In place of viewing the anode waveform, a simple transistor amplifier gates a pilot lamp on when current passes through the clamp made up of zener voltage regulator BD_5 and forward-biased rectifier RD_5 . If the controlled rectifier under test latches, current through the lamp has a low duty cycle and the lamp lights but faintly; if it does not latch, the duty cycle exceeds perhaps 90% and the lamp lights brightly.

A relatively unskilled operator may thus set gate current and voltage by simple meter readings and read out latching current readily after rotating R_4 slowly to increase current until the lamp turns off.

Parameter 6: Turn-On Time

Turn-on time was defined in Chapters 1 and 2 in this book. The delay time portion of turn-on time is particularly important in the parallel operation of controlled recti-

fiers. If two devices operating in parallel exhibit large differences in delay time and the rate-of-rise of on-state current in the circuit is high, the device with the shorter delay time will carry a larger portion of the total current. The test circuit for measuring turn-on time is shown in Figure 13-8.

Capacitor C_1 is half-wave charged through RD_1 and R_1 . The peak voltage on C_1 should be equal to the voltage rating of the test device. R_3 is a non-inductive resistor whose value depends on the test current for the particular controlled rectifier.

Resistor R_2 is a low impedance, non-inductive shunt. The controlled rectifier under test should be triggered during the non-charging portion of the 60 Hertz ac input, so that there will be no current flow from the input through the controlled rectifier. Circuit configuration and wiring components can change the rise time of the controlled rectifier. The circuit wiring using heavy lines must be made short and low impedance to minimize its inductance and resistance. Parts values are not given in Figure 13-8, since these depend on ratings of thyristor under test.

Parameter 7: Turn-On Voltage

Turn-on voltage of controlled rectifiers is commonly used as an indirect measure of rate-of-rise of on-state current capability. The principle behind measuring the voltage across the SCR during turn-on under a resonant pulse condition is that the lower the V_{TQ} (turn-on voltage), the lower the power dissipation under these conditions, and, therefore, the greater the di/dt capability the device may have. The

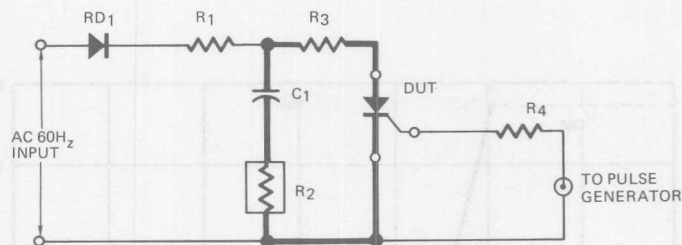


Figure 13-8. Turn-On Time Test Circuit

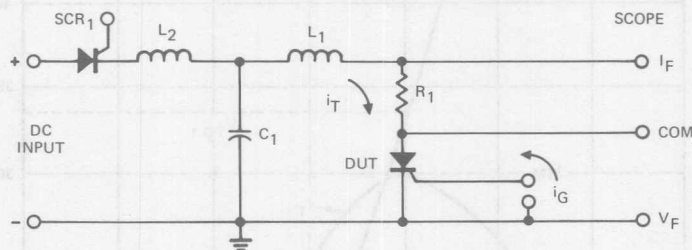


Figure 13-9. Turn-On Voltage Test Circuit

test circuit shown in Figure 13-9 is used for measuring the turn-on voltage of a controlled rectifier.

During operation, SCR₁ is triggered and charges Capacitor C₁ through inductor L₂. The inductance L₂ causes SCR₁ to resonantly commutate, therefore isolating the dc power supply from the test portion of the circuit. One millisecond after SCR₁ is triggered on, the device under test is triggered, discharging C₁ through L₁. (R₁ is a non-inductive shunt used to determine amplitude and waveshape of the on-state current pulse). Figure 13-10 shows a typical waveshape as seen on an oscilloscope and indicates at what instants to measure V_{TO1} and V_{TO2}. Table XIII-II lists typical parameters during the test. Because of the high rates-of-rise of current, good instrumentation prac-

tices must be adhered to. As always, ground loops must be avoided.

Parameter 8: Turn-Off Time

Turn-off time is defined in other chapters in this book. Figure 13-11 shows the waveshapes associated with this test. Figure 13-12 is a diagram showing the basic modules required to construct a turn-off time tester. The high current on-state and reverse module is used to supply principal current for the test device. The linear dv/dt module supplies a linear ramp of voltage to the test device at a variable time after the test device has been triggered. The sequential triggering module controls the duty cycle and time relationship between the high current on-state and reverse module and linear dv/dt module.

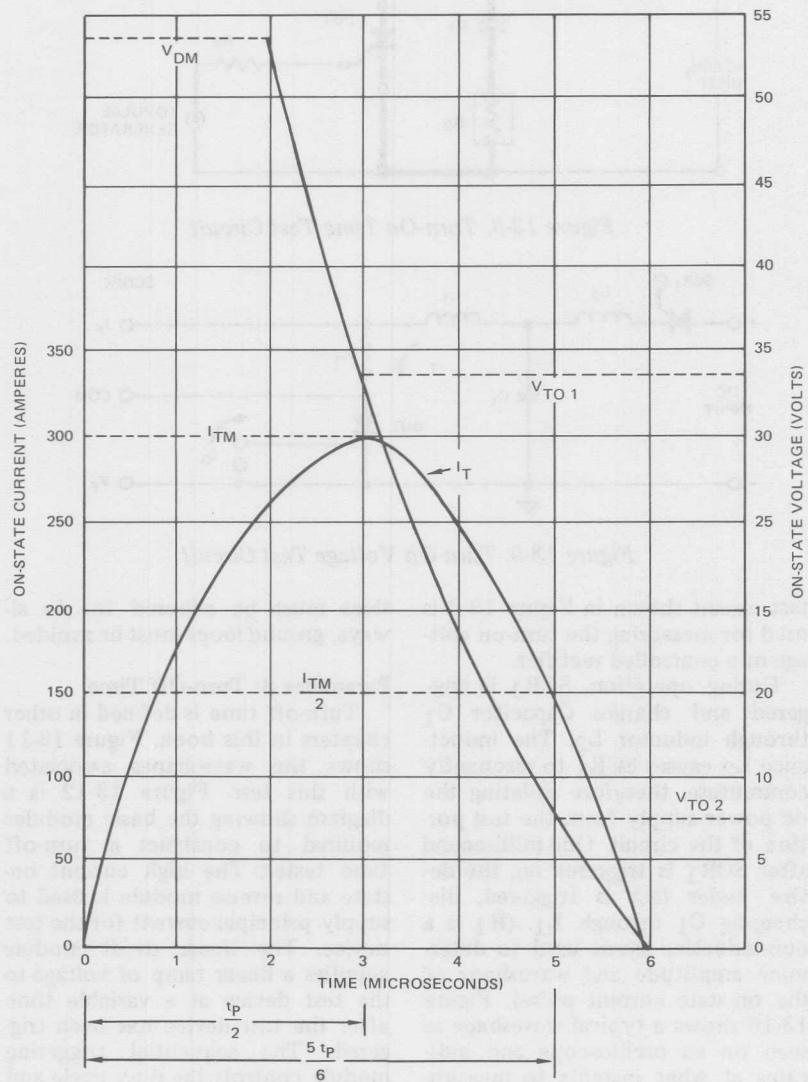


Figure 13-10. Typical Turn-On Voltage Waveform

Table XIII-II. Typical Turn-On Voltage Test Parameters (For 35A to 50A Thyristors)

I_{FM}	300A
t_p	6 μ sec
V_{DM}	200 volts maximum
C_1	5 to 7.0 μ F (Adjust to obtain symmetrical current pulse with minimum V_{DM})
L_1	0.64 μ Hy (air core approximately 1/4" diameter conductor)
R_1	0.01 Ohms (typical) (non-inductive viewing shunt) plus circuit and DUT resistance.
di/dt	157A/ μ sec
Repetition Rate: ≤ 60 Hz	
Gate Source (O.C.) Voltage = 20 Volts	
Gate Source short circuit current = 1.33A min.	
$t_r(\text{gate}) = 0.1 \mu\text{sec Max.}$	
$T_A = 25^\circ\text{C}$	
Gate pulse width = 6 μ sec min. under load.	
CAUTION: Always check device data sheets for specific parameters.	

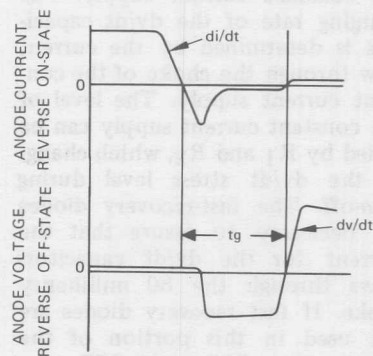


Figure 13-11. Turn-Off Test Waveforms

The on-state and reverse current supply is shown in Figure 13-13. Capacitors C_1 and C_2 are charged up to approximately 200 volts. Thyristors SCR_1 and SCR_2 control the pulse width of the on-state current. This is accomplished by changing the triggering of SCR_2 . In other words, triggering SCR_2 reverse biases the controlled rectifier under test causing SCR_1 to commutate off. Using this scheme, pulse widths from 10 microseconds to about 150 microseconds are available. The pulse width can be further increased if capacitors C_1 and C_2 are increased.

Turn-off time is affected by reverse recovery currents. By definition, the controlled rectifier under test should be reverse-biased until

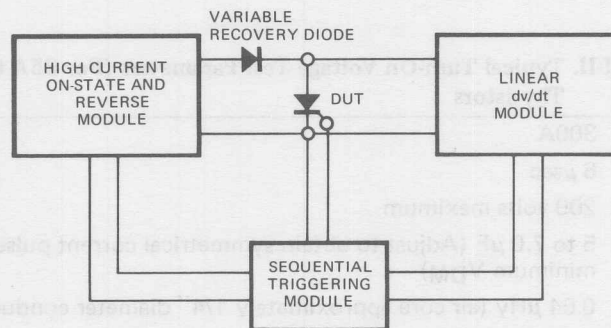


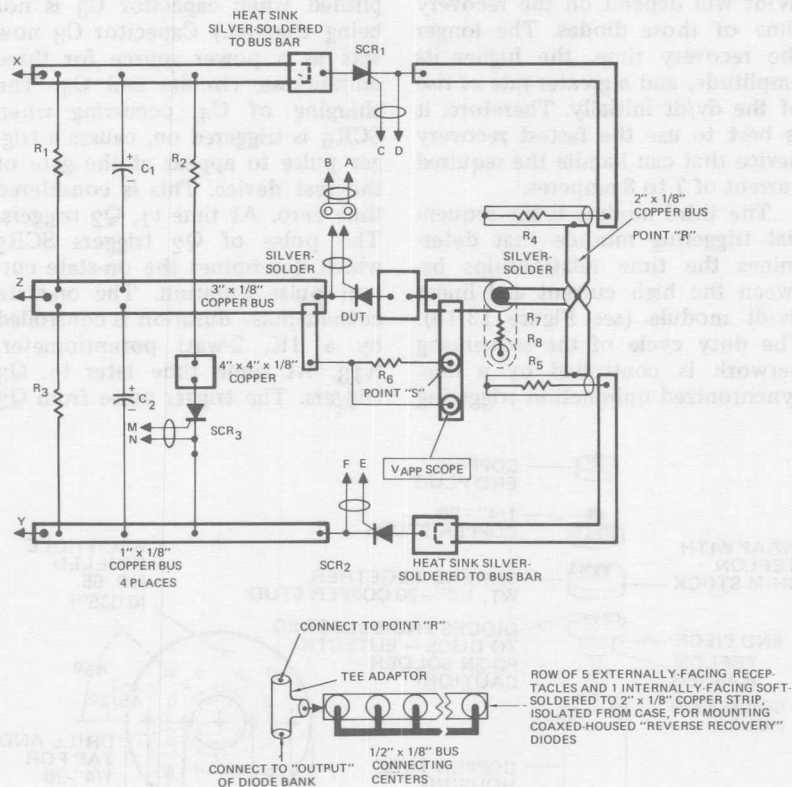
Figure 13-12. Turn-Off Tester — Block Diagram

the reapplication of forward blocking voltage occurs. To accomplish this, the reverse recovery time of the diode in series with the test device must be variable so that the diode reverse recovery characteristic can be matched to the turn-off time of the controlled rectifier under test. Figures 13-14 and 13-15 show a method to vary the reverse recovery characteristic of the circuit. Diodes having a wide range of recovery times are mounted in a coaxial configuration utilizing two devices in series per recovery diode. The recovery time of the circuit can be varied by switching in the discrete recovery diodes (A, B, C, D, E, or F) singly or in various parallel combinations, so that a configuration is obtained which more nearly matches the turn-off time of the test device.

The parallel combinations of recovery diodes provided by the two selector switches in Figure 13-14 are shown in Table XIII-III.

The circuit for the reapplied linear dv/dt is shown in Figures 13-16 and 13-17. The linear dv/dt section can be broken down into three parts. Figure 13-16 shows the con-

stant current and high voltage supply. Figure 13-17 shows the switching section, which is the most critical and must be designed in a non-inductive configuration. The linear dv/dt is generated by charging the dv/dt capacitors with a constant current. In this case, the dv/dt capacitors are charged up to the voltage rating of the device by the high voltage power supply (Figure 13-16) through half the full wave bridge and 80 millihenry choke of the constant current supply. The charging rate of the dv/dt capacitors is determined by the current flow through the choke of the constant current supply. The level of the constant current supply can be varied by R_1 and R_2 , which changes the dv/dt stress level during turn-off. The fast-recovery diodes are necessary to assure that the current for the dv/dt capacitors flows through the 80 millihenry choke. If fast recovery diodes are not used in this portion of the circuit, when SCR_4 and SCR_5 are switched on, current will flow through the diodes until the devices recover. At this time, there will appear across the test device a step



C1, C2	Capacitor, 1300 mF, 350V		minimum inductance configuration
R1, R3	Resistor, 1000Ω, 200W		
R2	Resistor, 0.5Ω, 1220W (GE - C5B50)	R7	Resistor, shunt, 0.01Ω, 50W, 1% (T&M Modified - F-500-2)
R4, R5	Resistor, variable, 0.25 to 12Ω, 2.250V (Allen-Bradley-Carbon Pile - Form SM), R4 "ADJ. I _{TM} ," R5 "ADJ. I _{REV} ."	R8	Resistor, Shunt, 0.01Ω, non-linear
R6	Resistor, 16 each, 100Ω, 2W, 5% (Magic 16)	SCR1, SCR2	SCR, 70 amp, 800V (IR - 72RA80)
		SCR3	SCR, 150 amp, 800V (IR - 150RA80)

Figure 13-13. Turn-Off Tester - On-State and Reverse Current Module

of voltage that is three or four times the dv/dt desired. This step of dv/dt will depend on the recovery time of those diodes. The longer the recovery time, the higher its amplitude, and a greater rate of rise of the dv/dt initially. Therefore, it is best to use the fastest recovery device that can handle the required current of 7 to 8 amperes.

The third module is the sequential triggering module that determines the time relationships between the high current and linear dv/dt module (see Figure 13-18). The duty cycle of the sequencing network is controlled by a line-synchronized unijunction triggering

circuit which triggers SCR₆. (The triggering of SCR₆ must be accomplished when capacitor C₃ is not being charged.) Capacitor C₃ now acts as a power source for three unijunction circuits and C₄. The charging of C₄, occurring when SCR₆ is triggered on, causes a trigger pulse to appear at the gate of the test device. This is considered time zero. At time t_1 , Q₂ triggers. The pulse of Q₂ triggers SCR₂ which determines the on-state current pulse duration. The on-state current pulse duration is controlled by a 1K, 2-watt potentiometer, R₁₃. At some time later t_2 , Q₃ triggers. The trigger pulse from Q₃

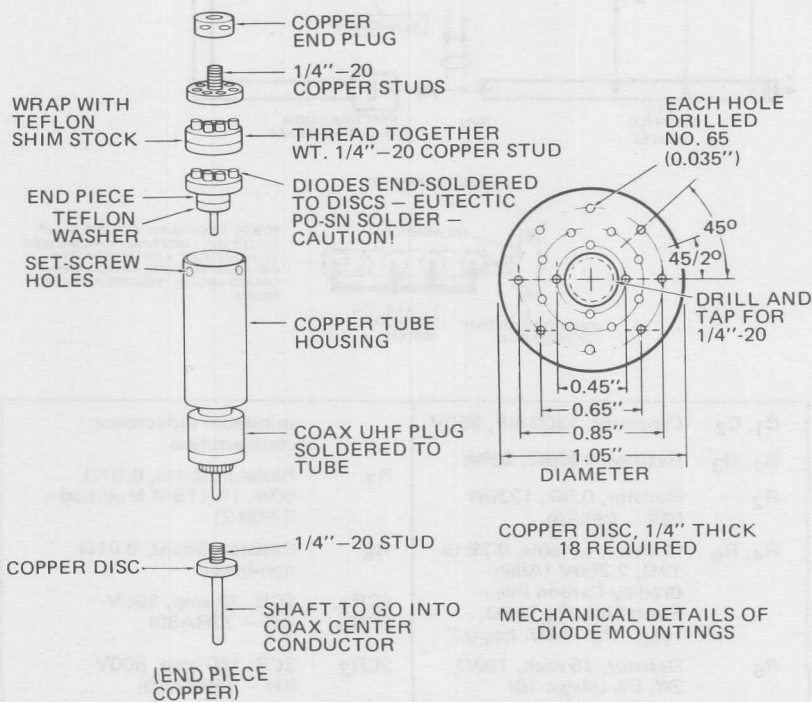
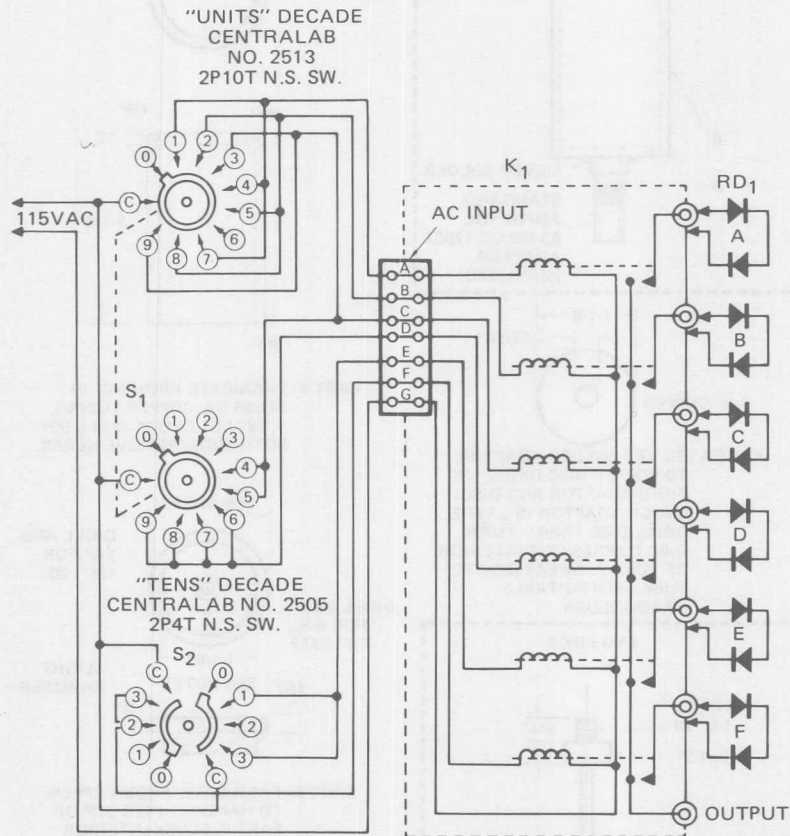


Figure 13-14(a). Turn-off Tester—On-State Module—Construction Techniques



K ₁	Relay Network, 110 VAC coils. UHF conductor (Dow-Key - DKC71-SP6T Rating)	S ₁	Rotary Switch, 10-position, 2 disc, "units" (Centralab - 2513, 2P10T N.S. SW)
RD ₁	Rectifiers, reverse recovery, bank of 6 series pairs	S ₂	Rotary Switch, 10-position, "tens" (Centralab - 2505, 2P4T N.S. SW)

Figure 13-14(b). Turn-Off Tester—On-State Module—Construction Techniques

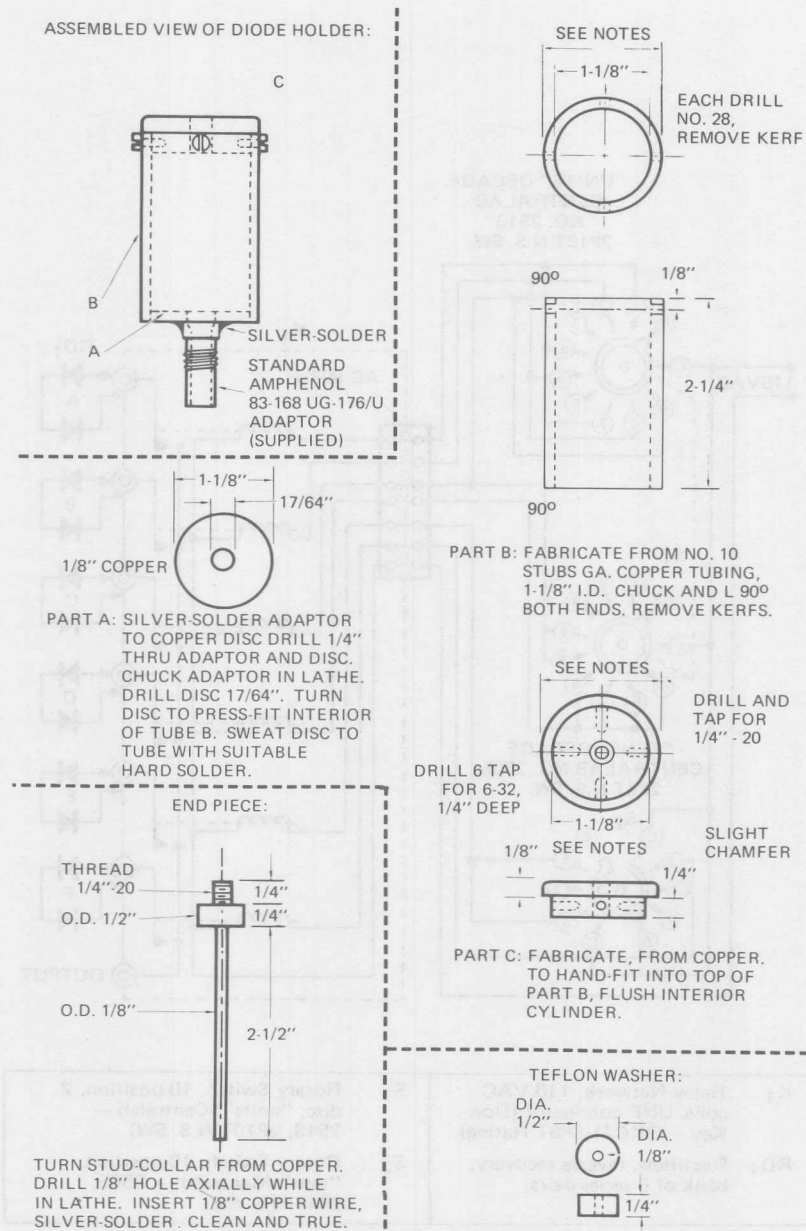
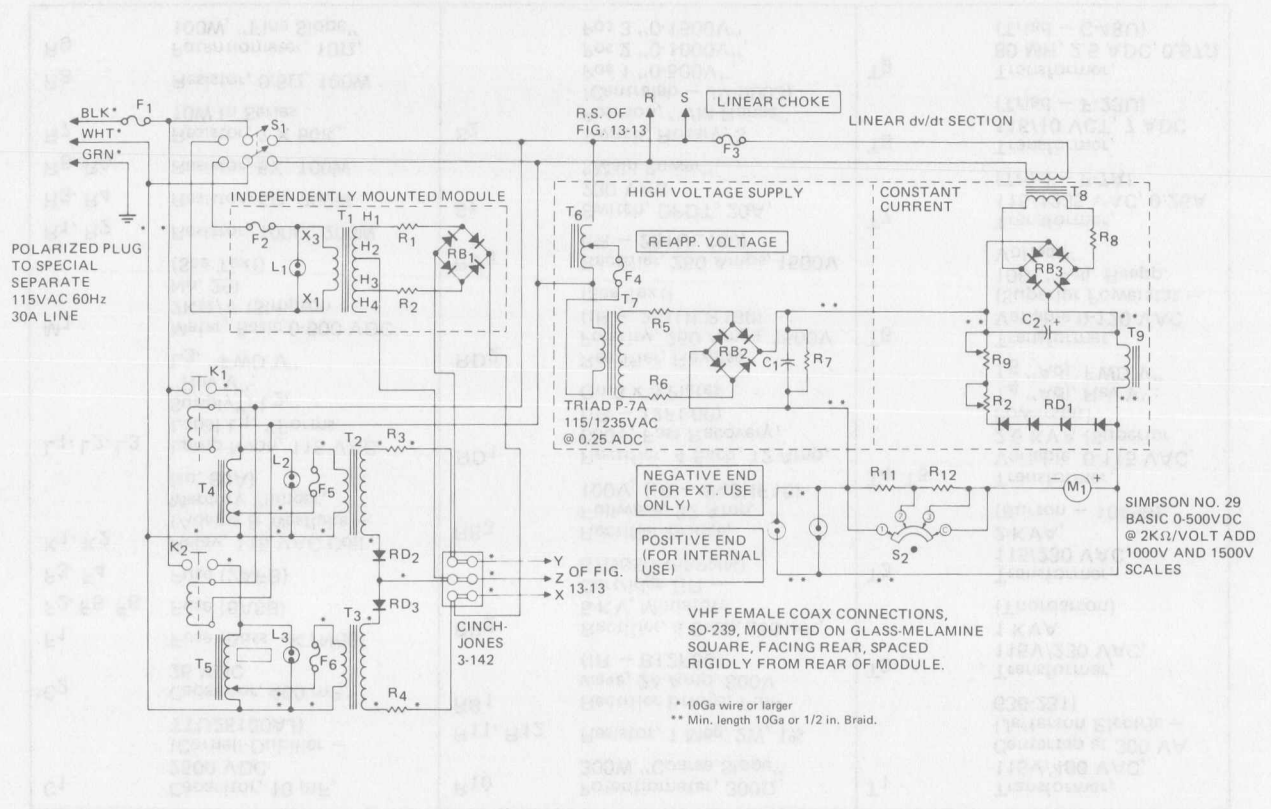


Figure 13-15. Turn-Off Tester—On-State Module—Construction Techniques

Figure 13-16. Turn-Off Tester — dv/dt Module



C1	Capacitor, 10 mF, 2500 VDC (Cornell-Dubilier – TTU25100AJ)	R10	Potentiometer, 300 Ω , 300W "Coarse Slope"	T1	Transformer, 115V/460 VAC, Centertap at 300 VA (Jefferson Electric – 636-231)
C2	Capacitor, 400 mF, 25 VDC	R11, R12	Resistor, 1 Meg, 2W, 1%	T2	Transformer, 115V/230 VAC, 1 KVA (Thordarson)
F1	Fuse (Buss – KTN60)	RB1	Rectifier Bridge, Full-wave, 24 Amp, 800V (IR – B12F80)	T3	Transformer, 115/230 VAC, 2 KVA, (Burton – 10459)
F2, F5, F6	Fuse (5ASB)	RB2	Rectifier, 4 Each, 250 mA, 5 KV, Miniature Cartridge (IR – 67D050H53PNN)	T4, T5	Transformer, Variable, 0-115 VAC, 2.6 KVA (Superior Powerstat) T4 "Adj. Rev V"; T5 "Adj. FWD V"
F3, F4	Fuse (2AFB)	RB3	Rectifier Bridge, Fullwave, 32 Amp, 100V, (IR – B40HF10)	T6	Transformer, Variable 0-120 VAC (Superior Powerstat – 10B) "Adj. Reapp. Voltage"
K1, K2	Relay, 115 VAC Coil (Adams & Westlake – Mercury Plunger, No. 50A)	RD1	Rectifier, 4 Each, 12 Amp, 600V, Fast Recovery, (IR – 12FL60) On 3 x 3 Plates	T7	Transformer, 115/1235 VAC, 0.25A (Triad – P-7A)
L1, L2, L3	Lamp Neon, 115 VAC Label L1, "Forms Supply"; L2, "Rev V"; L3, "FWD V"	RD2	Rectifier, Reverse Polarity, 250 Amps, 1500V (IR – 251ULR150) (See Text)	T8	Transformer, 115/10 VCT, 7 ADC (Triad – F-23U)
M1	Meter, Basic 0-500 VDC 2K Ω /V (Simpson No. 29) (See Text)	RD3	Rectifier, 250 Amps, 1500V (IR – 251UL150)	T9	Transformer, 80 MH, 2.5 ADC, 0.57 Ω (Triad – C-48U)
R1, R2	Resistor, 100 Ω , 200W	S1	Switch, DPDT, 20A, 230 VAC "Main Power"		
R3, R4	Resistor, 5 Ω , 200W	S2	Switch, Rotary, 3 Position, "VM Range" (Centralab – JV-9003) Pos 1 "0-500V", Pos 2 "0-1000V", Pos 3 "0-1500V"		
R5, R6	Resistor, 5K, 100W				
R7	Resistor, 7 X 50K, 10W In Series				
R8	Resistor, 0.5 Ω , 100W				
R9	Potentiometer, 10 Ω , 100W, "Fine Slope"				

Figure 13-16. Turn-Off Tester — du/dt Module

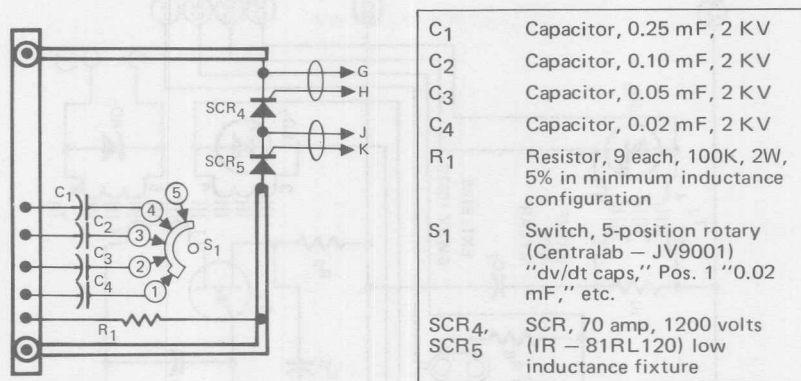
Figure 13-17. Turn-Off Tester — dv/dt Module — Switching Section

Table XIII-III. Switch Positions for Turn-Off Tester

SWITCH POSITION	RECOVERY DIODE SWITCHED FOR:	
	"UNITS" SWITCH	"TENS" SWITCH
0	Open	Open
1	A	E
2	B	F
3	C	E & F
4	C & A	
5	C & B	
6	D	
7	D & A	
8	D & B	
9	D & C	

triggers SCR₄ and SCR₅ (Figure 13-17), which are the reapplied dv/dt controlled rectifiers. The time relationship between Q₂ and Q₃ is determined by a 2.5K, 2-watt, single potentiometer, R₁₇, and a 500-Ohm, 10-turn current helipot, R₁₆. The 10-turn helipot is used so that very fine adjustments can be made between t_1 and t_2 . Q₄ triggers SCR₇ and completes the cycle. SCR₇ completely discharges C₃ so

that there is no longer a voltage supply for the other trigger circuits. The discharge pulse of C₃ triggers SCR₃ (Figure 13-13) which crowbars the high current on-state module and sets the conditions for the beginning of the next cycle.

The turn-off time tester is a complex piece of test equipment, and only by rigorously following schematics, can a tester be built that repeats turn-off time readings

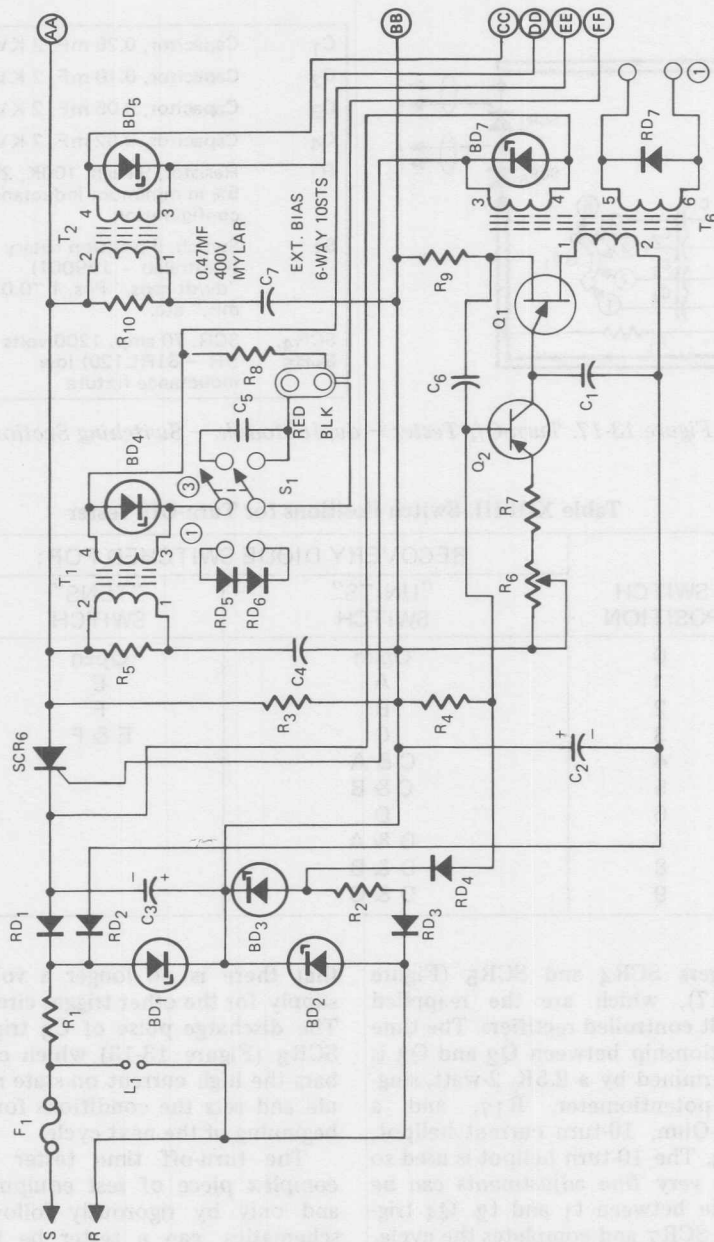


Figure 13-18(a). Turn-Off Tester—Sequential Triggering Module

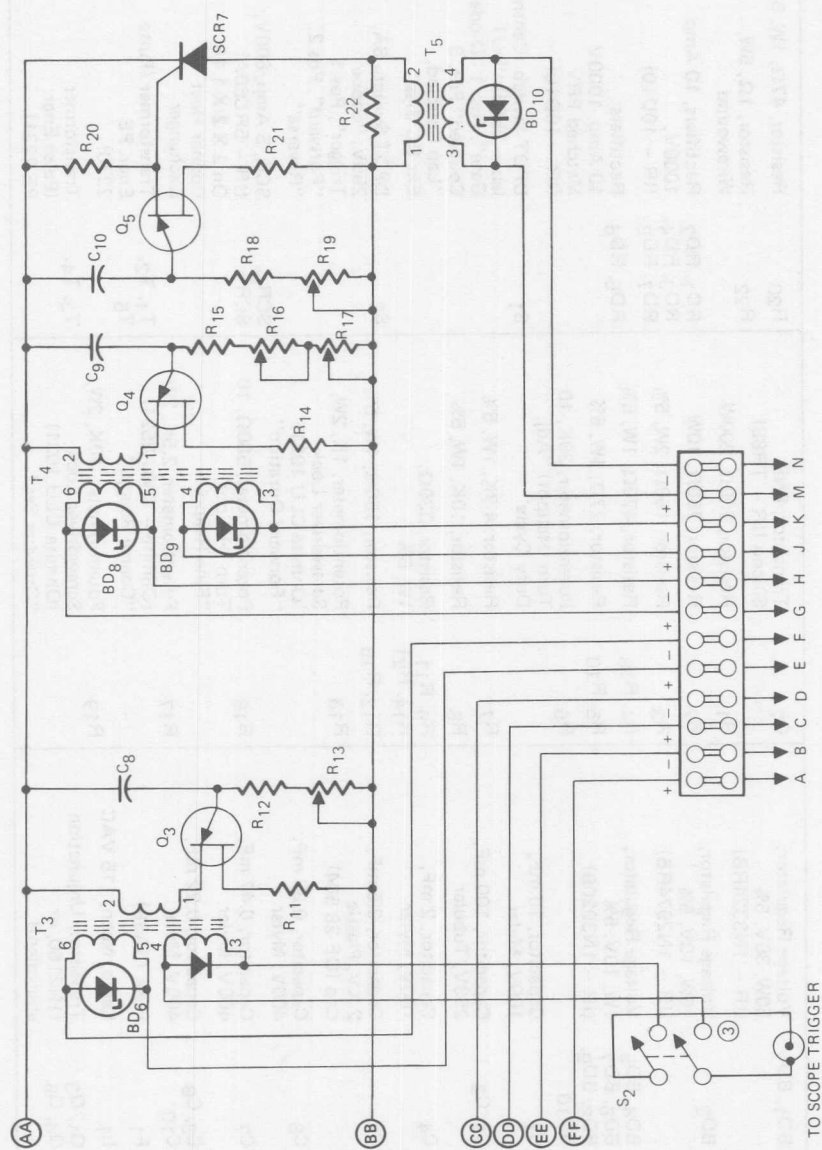


Figure 13-18(b). Turn-Off Tester — Sequential Triggering Module

BD ₁ , BD ₂	Voltage Regulator, 50W, 30V, 5% (IR - 1N3324RB)	Q ₂	Transistor, PNP Silicon (IR - TR88)	R ₂₀	Resistor, 47Ω, 1W, 5%
BD ₃	Voltage Regulator, 10W, 10V, 5% (IR - 1N2974RB)	R ₁	Resistor, 200Ω, 200W	R ₂₂	Resistor, 1Ω, 5W, Wirewound
BD ₄ , BD ₅ BD ₆ , BD ₇ BD ₈ , BD ₉ , BD ₁₀	Voltage Regulator, 1W, 10V, 5% (IR - 1N3020B)	R ₂	Resistor, 750Ω, 10W	RD ₁ , RD ₂ , RD ₃ , RD ₄ , RD ₇ , RD ₈	Rectifiers, 10 Amp 1000V, (IR - 10D10)
C ₁	Capacitor, 10 mF, 100V, Mylar	R ₃	Resistor, 150Ω, 2W, 5%	RD ₅ , RD ₆	Rectifiers, 10 Amp, 1000V Matched PRV (IR - 10D10)
C ₂ , C ₃	Capacitor, 100 mF, 250V, Tubular	R ₄ , R ₁₈	Resistor, 470Ω, 1W, 5%	S ₁	DPDT Switch (Centralab - 2505) "DUT Gate", Pos. 1 "Diode Coupled" Pos. 3 "Lap Coupled, Ext DC Bias"
C ₄	Capacitor, 2 mF, 100V, Mylar	R ₅ , R ₁₀	Resistor, 27Ω, 1W, 5%	S ₂	DPDT Switch, 6A, 250V, "Scope Trigger", Pos 1 "Forward", Pos 2 "Reverse"
C ₅	Capacitor, 0.5 mF, 2 KV, Plastic Cap (OF 28 504)	R ₆	Potentiometer, 30K, 10 Turn (Helipot) "Adj. Duty Cycle"	SCR ₆ , SCR ₇	SCR, 5 Amp, 600V, (IR - 5RC60A) On 2 X 2 X 1 16 Copper Heat Exchanger
C ₆	Capacitor, 0.33 mF, 400V, Mylar	R ₇	Resistor, 4.7K, 1W, 5%	T ₁ , T ₂ , T ₅	Transformer (Pulse Engr. PE 2230)
C ₇	Capacitor, 0.47 mF, 400V, Mylar	R ₈	Resistor, 10K, 1W, 5%	T ₃ , T ₄	Transformer (Pulse Engr. PE 2231)
C ₈ , C ₉ , C ₁₀	Capacitor, 0.22 mF, 400V, Mylar	R ₉ , R ₁₁ , R ₁₄ , R ₂₁	Resistor, 330Ω, 1W, 5%		
F ₁	Fuse (3ASB)	R ₁₂ , R ₁₅	Resistor, 150Ω, 1W, 5%		
L ₁	Lamp, Neon, 115 VAC	R ₁₃	Potentiometer, 1K, 2W, Screwdriver Lock (Ohmite CLU 1021) "Forward Duration"		
Q ₁ , Q ₃ Q ₄ , Q ₅	Transistor, Unjunction (1N2160, or equivalent)	R ₁₆	Potentiometer, 500Ω, 10 Turn (Helipot) "Fine Reapp."		
		R ₁₇	Potentiometer, 2.5K, 2W (Ohmite - CMU 2521) "Coarse Reapp."		
		R ₁₉	Potentiometer, 10K, 2W, Screwdriver Lock (Ohmite CLU 1031) "Crowbar Set"		

Figure 13-18. Turn-Off Tester — Sequential Triggering Module

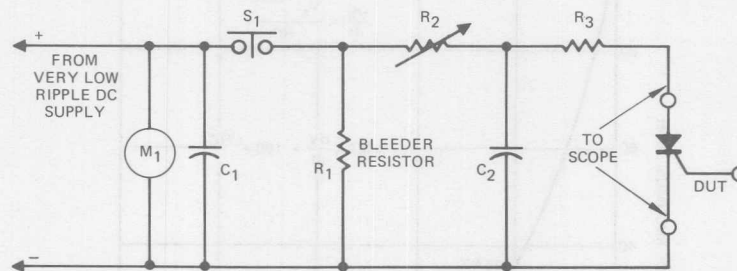
and correlates with users and manufacturers throughout the industry.

Parameter 9: Critical dv/dt

The term "critical rate-of-rise of forward voltage," or "critical dv/dt ," has been interpreted several ways by the industry. These are discussed in detail in Chapter 1 of this book. The actual dv/dt and at what fraction of peak applied off-state voltage it is measured is important to the designer and user of controlled rectifier circuits. The manufacturer can test dv/dt by one of two techniques: he can generate the applied dv/dt by a circuit which produces a linearly rising sawtooth, or a circuit which produces an exponentially rising sawtooth. At low rates of dv/dt , this latter is easy to produce; primarily for this reason, the industry standardized upon this waveform when only low dv/dt -re-

sistant controlled rectifiers could be made. Its use has remained to plague both manufacturer and user because of its inclusion in military specifications. In Figure 13-19(a), an idealized test circuit is shown which appears in several military specifications. Figure 13-19(b) shows the voltage curve which results when a capacitor is charged through a resistor from a constant voltage source. In graph (c), the instantaneous dv/dt present at any point of this voltage curve has been plotted as a fraction of the maximum dv/dt (which occurs at time zero).

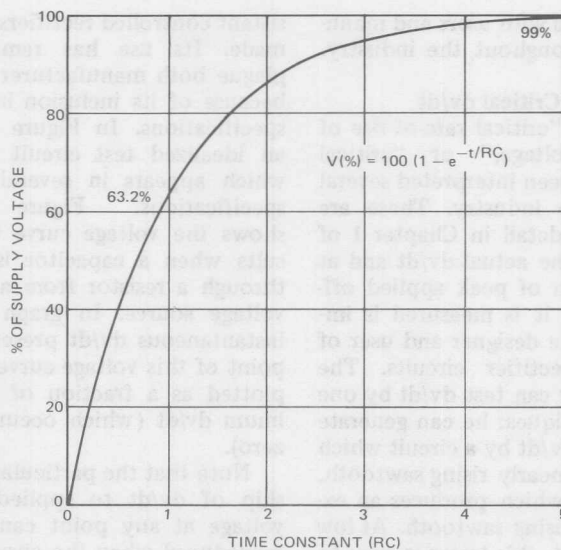
Note that the particular relationship of dv/dt to applied forward voltage at any point can only be reproduced when the curve is truly exponential and follows the equations shown in these two graphs. Correlation problems occur when



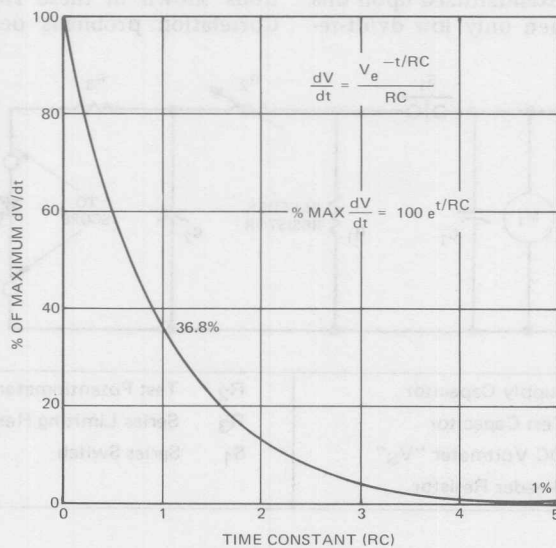
C_1	Supply Capacitor	R_2	Test Potentiometer
C_2	Test Capacitor	R_3	Series Limiting Resistor
M_1	DC Voltmeter " V_S "	S_1	Series Switch
R_1	Bleeder Resistor		

(a) Ideal Test Circuit

Figure 13-19. dv/dt Test Circuit and Waveforms



(b) VOLTAGE



(c) DV/DT

Figure 13-19. dv/dt Test Circuit and Waveforms

either the manufacturer or the user disregards a particular convention promulgated by both manufacturer and military. By this convention, dv/dt is defined for a true exponential waveform as given in Formula 13-A.

$$\text{"Critical } dv/dt\text{"} = \frac{0.632 V_{\text{supply}}}{R_{\text{test}} \times C_{\text{test}}} \quad (13-A)$$

This presumably was arrived at by assuming the exponential waveform to be linear from zero time to one time constant. Since the instantaneous dv/dt (that value which will determine capacitive charging current) varies from 157% of this "critical dv/dt " at zero time to 58% at one time constant, the designer can only use this figure as a relative order of merit when comparing two controlled rectifiers, and his incoming inspector must use equipment which satisfies all the requirements of the exponential waveform.

Requirements

In the test circuit of Figure 13-19, to obtain an exponential curve which does not show error when viewed upon a suitable laboratory oscilloscope,

- A. Capacitor C_1 must be a minimum of 99 times as great in capacitance as C_2 .
- B. The time constant $R_2 C_2$ must be at least 4.6 times the maximum test period (to achieve full V_s across C_2).
- C. Capacitor C_2 must have a value of at least 0.02 microfarad for the curve not to be influenced by the middle junction capacitance of the unit under test (appreciably higher values for C_2 make switch increments ex-

tremely difficult and for high dv/dt values require absurdly low values of R_2).

- D. Inductance within the capacitor charging loop (for extremely high values of dv/dt) must be kept to a very small fraction of a microhenry, to avoid distortion of the initial portion of the exponential curve.
- E. The series switch must operate instantaneously and with no appreciable voltage drop.

This last requirement rules out the use of controlled rectifiers for exponential dv/dt testers used at dv/dt s of above about 400 volts per microsecond. Such testers do check dv/dt but do not reproduce the exponential waveform, and results obtained must be corrected extensively. An error can also be introduced at low dv/dt s when an oscilloscope is used to adjust peak off-state voltage, which may not be equal to supply voltage because of dropout of the SCR switch when charging current reaches the holding current level. Supply voltage, and not peak off-state, is called out.

The detailed sketches and schematic of Figure 13-20 show how to make a true exponential dv/dt tester which has been used up to 1000 volts and a "critical dv/dt " of above 6000 volts per microsecond. It introduces some interesting techniques of field cancellation employed at International Rectifier. The pressure upon graphite discs within the cylindrical coaxially-coupled carbon resistor, R_4 , is increased until the series milliammeter, M_1 , shows consistent full-scale excursion; the pressure is then decreased gradually until meter fluctuations just cease and the time constant (the time from zero volts

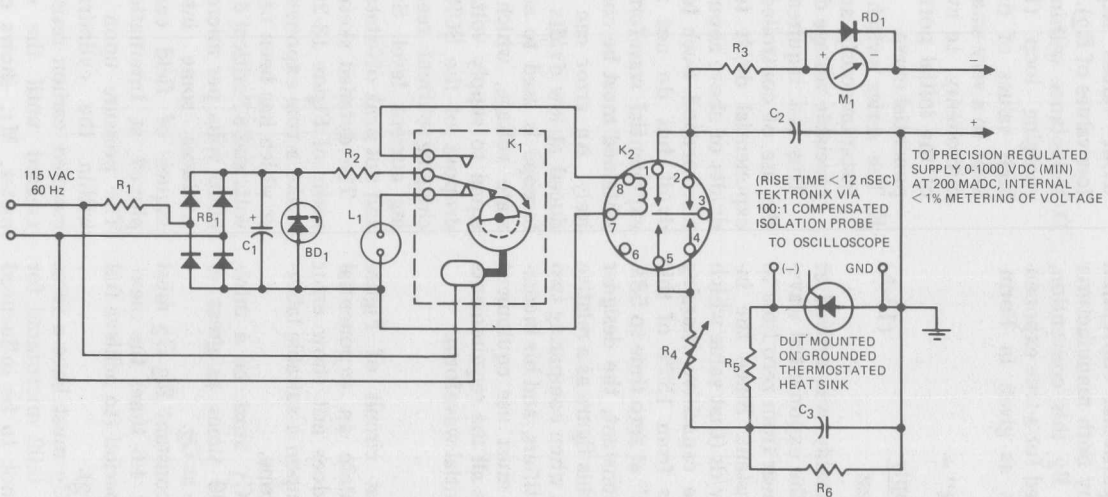
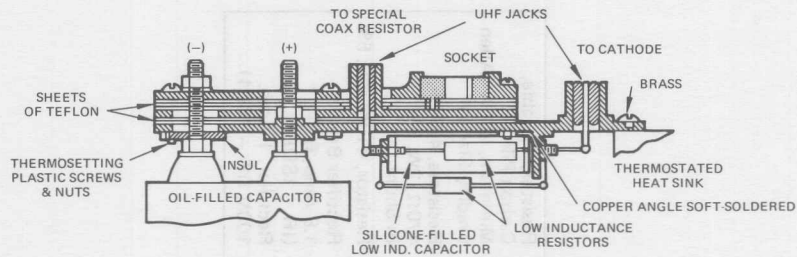


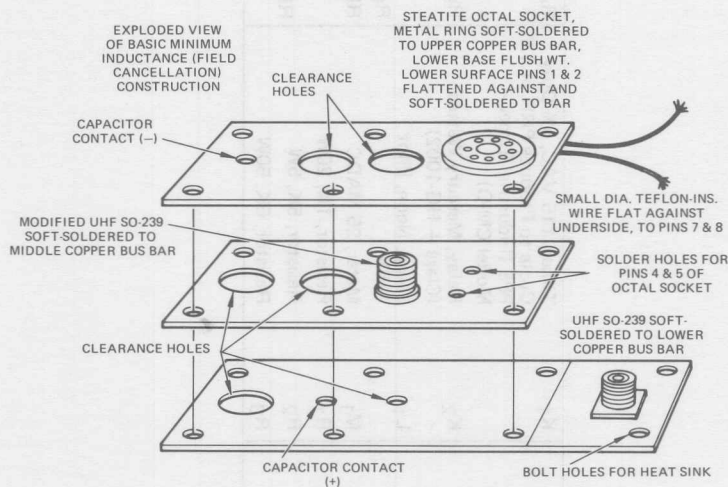
Figure 13-20. True Exponential dv/dt Test Circuit

BD ₁	Voltage Regulator, 120 V _Z , 10W, 5% On Heat Sink (IR – 1N3008B)	K ₁	Timer, 115 VAC, 5% Duty Cycle to Produce PRR of 1.2 PPS (Industrial Timer – Model CM-O)	R ₄	Resistor, Variable, Carbon Pile 5Ω Minimum, 250W (Allen Bradley Size 2)
C ₁	Capacitor, 50 mF, 150VDC	K ₂	Relay, Mercury Wetted (Clare – HG-1002)	R ₅	Resistors, 4 Each, 470Ω, 2W, 5% In Shunt
C ₂	Capacitor, Oil-Filled, 8 mF 1500 VDC	L ₁	Lamp, Neon, Pilot 115V	R ₆	Resistor, 410K, 2W, 5%
C ₃	Capacitor, 0.02 mF, 3,000 VDC (Plastic Cap, 30-203)	M ₁	Meter, 25 MADC	RB ₁	Rectifier Bridge, 1.8 Amp, 600V (IR – 18DB6)
		R ₁	Resistor, 1K, 20W	RD ₁	Rectifier, 1 Amp, 100V (IR – 10D1)
		R ₂	Resistor, 5K, 5W		
		R ₃	Resistor, 6K, 50W		

Figure 13-20. True Exponential dv/dt Test Circuit



SKETCH OF MECHANICAL CROSS-SECTION

Figure 13-20. True Exponential dv/dt Test Circuit

to a voltage 63.2% of the supply voltage) is read out by use of a very fast oscilloscope.

Peak currents through the mercury-wetted contact relay are several times greater than those recommended by the manufacturer. The applied voltages are also much higher than recommended. The connection of contacts is unorthodox. This relay is a make-before-break (Form D) unit, and in this circuit switching occurs only during bridg-

ing (when the coil is either energized or deenergized). This mode of operation has yielded rise times (with properly non-inductive external circuits) of a very few nanoseconds, with a closed switch duration of about 400 microseconds, and relays have lasted an average of six months.

Parameter 10: Critical di/dt

Critical di/dt is discussed in Chapter 1 (refer to Index). The

basic test circuit schematic and on-state current waveshapes are shown in Figure 13-21. The following conditions are specified:

- A. The time t_1 shall be ≥ 1 micro-second.
- B. I_{TM} shall be \geq twice the rated value of on-state current at T_3 . (The rated value of on-state current at T_3 will be an average [T_3 is case temperature where derating of average on-state current starts] value for ac rated devices and a dc value for dc rated devices.)
- C. The pulse repetition rate shall be 60 pps.
- D. The off-state voltage V_{DM} shall be equal to the rated value at T_5 (T_5 is maximum operating temperature).
- E. The temperature shall be 25°C .
- F. The gate trigger pulse shall be specified as to:
 - 1) Pulse width, t_w .

2) Rise time, t_r .

3) Gate source voltage and resistance.

G. The test duration shall be:

- 1) 1000 hours to establish the repetitive rating.
- 2) 300 on-state current pulses to establish the gate-triggered non-repetitive rating.

di/dt ratings given at power frequencies (50-60 Hz) do not necessarily reflect the inrush capabilities of the same device at high frequency (above 400 Hz), because of the greater cumulative effect of the turn-on losses at higher repetition rates. Thus, this is only a test of device capability to handle fast rising current pulses of short duration at power frequencies. It is a figure of merit and can be used to compare one device with another.

Current capabilities at specific repetitive values of di/dt and other concurrent test conditions are often

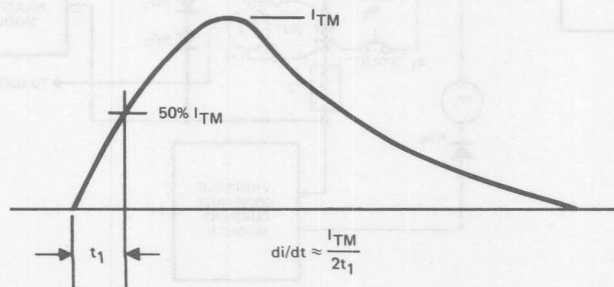
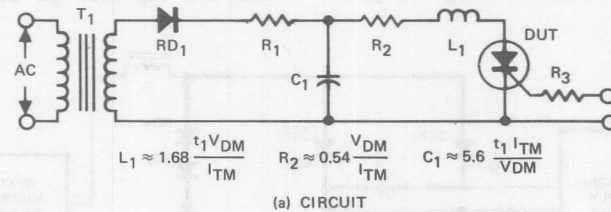


Figure 13-21. Critical di/dt Test Circuit and Waveform

included on data sheets for those SCRs intended for inverter applications.

Parameter 11: Thermal Resistance

Thermal resistance is discussed in detail in Chapter 1. A block diagram of the test circuit used for the measurement of thermal resistance is shown in Figure 13-22. The junction of the device under test is heated by a direct on-state current having an RMS ripple content of 5% or less, which is passed continuously through the device under test except for a 400 microsecond period every 0.167 seconds or more. During this 400 microsecond period, the junction temperature is measured by reducing the on-state current to a small fixed value and measuring the on-state voltage. Current and on-state voltage wave-shapes are shown in Figure 13-23.

A calibration point along the curve of on-state voltage vs. junc-

tion temperature is used to convert the on-state voltage reading to a junction temperature. In addition, the case temperature of the device under test is measured by a thermocouple. DC thermal resistance is calculated using the relationship in Formula 13-B.

$$R_{\theta JC} = \frac{T_{J(\text{MAX})} - T_C}{V_{TM} \times I_{HEAT}} \quad (13-B)$$

Where:

V_{TM} = On-state voltage

I_{HEAT} = Heating current

Control of the heating current through the device under test is accomplished by SCR₁ and SCR₂, which function as a dc flip-flop. Switching is at a 60 hertz repetition rate to facilitate oscillographic observations. Current is carried by SCR₁ only during the 400 microsecond periods that heating current is not flowing through the device

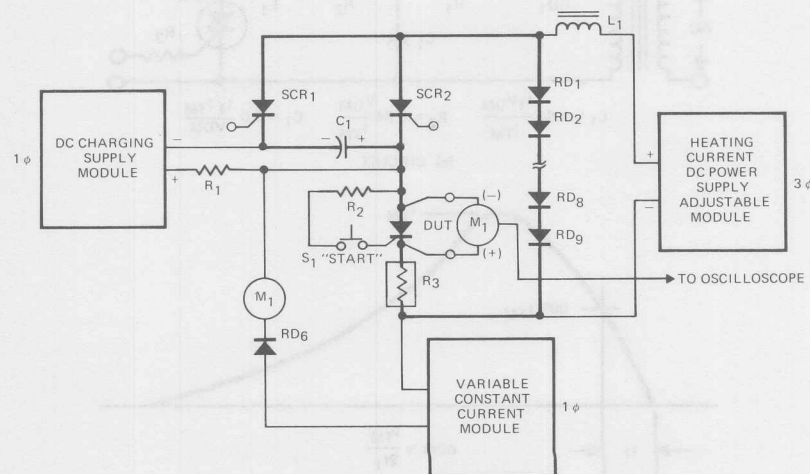


Figure 13-22. Thermal Resistance Test Circuit

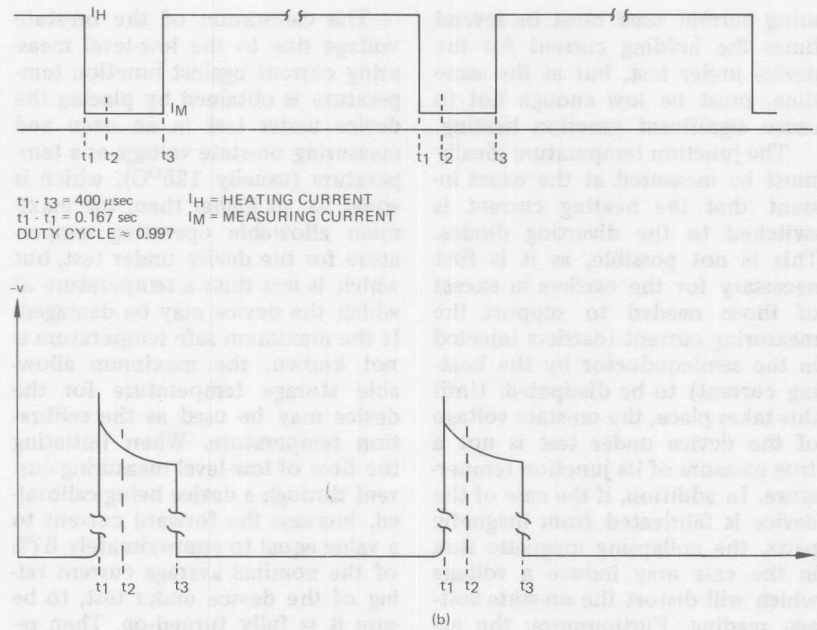


Figure 13-23. Thermal Resistance Test Waveforms

under test, and so SCR_1 may be considerably smaller than SCR_2 .

The value of heating current selected should be large enough to create significant heating in the device under test. Inductances in the heating current power supply and circuit wiring make it possible to abruptly turn this current off without creating transient voltages which interfere with the measurement being made.

Instead, a diverter circuit consisting of rectifier diodes RD_1 through RD_4 is provided so that the heating current is not interrupted by SCR_2 , but simply switched to a different path. The inductor, L_1 , is included to make it certain that the heating current is not varied while it is being switched from

one path to another. This inductor also serves to reduce to a negligible value undesired flow of current from C_1 through the device under test and the heating current power supply.

The measuring current which remains flowing through the device under test must be held at a fixed value during the 400 microsecond interval when the heating current is diverted by SCR_1 . During this measuring interval, the impedance of the controlled rectifier under test is not constant. To assure a constant measuring current, a low level constant-current supply is used. Fast recovery diode RD_6 prevents any voltage from capacitor C_1 from damaging the low level supply. In addition, the value of meas-

uring current used must be several times the holding current for the device under test, but at the same time, must be low enough not to cause significant junction heating.

The junction temperature ideally must be measured at the exact instant that the heating current is switched to the diverting diodes. This is not possible, as it is first necessary for the carriers in excess of those needed to support the measuring current (carriers injected in the semiconductor by the heating current) to be dissipated. Until this takes place, the on-state voltage of the device under test is not a true measure of its junction temperature. In addition, if the case of the device is fabricated from magnetic parts, the collapsing magnetic flux in the case may induce a voltage which will distort the on-state voltage reading. Furthermore, the action of the capacitor C_1 on turning off SCR₂ may influence the on-state voltage of the device under test. These spurious effects on the on-state voltage will disappear after a brief interval, in the order of 200 microseconds, t_2 in Figure 13-23. It is therefore possible to measure junction temperature at t_2 to t_3 and the value obtained at t_2 will be essentially the same as the junction temperature immediately after the flow of heating current ceases (t_1 in Figure 13-23).

In order to accurately read the on-state voltage at the items specified, a cathode ray oscilloscope is used as a null balance, and the forward voltage drop at any desired instant is balanced against the voltage fed from a potentiometer connected across a low voltage source. The voltage used to create this balance is then read by a voltmeter.

The calibration of the on-state voltage due to the low-level measuring current against junction temperature is obtained by placing the device under test in an oven and measuring on-state voltage at a temperature (usually 125°C), which is equal to, or higher than, the maximum allowable operating temperature for the device under test, but which is less than a temperature at which the device may be damaged. If the maximum safe temperature is not known, the maximum allowable storage temperature for the device may be used as the calibration temperature. When initiating the flow of low-level measuring current through a device being calibrated, increase the forward current to a value equal to approximately 67% of the nominal average current rating of the device under test, to be sure it is fully turned-on. Then reduce the current to the value of low-level measuring current being used.

A special jig, which accommodates a thermocouple is mounted to, or a small hole for the thermocouple is drilled in, the hex base of the device under test, or a hole is drilled in the side of one of the pole pieces if a Hockey-Puk type device is to be measured. This thermocouple is used to measure case temperature.

The magnitude of the heating current used should be sufficient to cause a substantial difference between the junction and case temperatures of the DUT. This will increase the accuracy of the test results, since a small error in reading either the case or junction temperature will have very little effect on the value obtained for the temperature rise of the junction above

the case. If the case of the DUT is cooled well (water cooling is recommended), it is possible to use a large value of heating current and hence obtain a large difference between junction temperature and case temperature without running the danger of overheating the junction of the DUT.

When measuring the temperature of the junction during the brief intervals, the DUT is conducting the low-level measuring current, it is not possible to make the measurement exactly when it is desirable to do so which is at the exact instant when the high-level forward current ceases. At that instant, the forward voltage of the DUT is abnormally low (which would indicate a junction temperature much higher than is actually the case), because recombination of minority carriers is taking place. In addition, some semiconductor devices exhibit inductance, and therefore produce, for a brief instant, a voltage which tries to prevent the current from decreasing. This voltage tends to cancel out the forward voltage of the DUT, again resulting in too low a forward voltage at the instant the high-level current ceases. After approximately 100 μ sec, these transient voltage effects disappear in most semiconductor devices, and the actual junction temperature is then able to be measured.

A small amount of cooling of the junction will take place during the interval when junction temperature cannot be read, and therefore, a refinement of the test method is to extrapolate the curve of forward voltage vs. time during the measuring interval back to the instant the high-level current ends. A straight line extrapolation is a close approx-

imate. The approximate junction temperature at exactly the end of conduction of high level current can then be obtained from the forward voltage determined by extrapolating back.

Further details on how to conduct this test for thermal resistance are found in JEDEC Publication No. 88, "Thermal Resistance and (Transient) Thermal Impedance Test Methods for Stud- and Base-Mounted Rectifier Diodes and Thyristors," which is available from the Electronic Industries Association, 2001 Eye St., N.W., Washington, D.C. 20006.

In building the test circuit shown in Figure 13-22, inductance must be minimized in those portions of the circuit drawn with heavy lines. Figures 13-24, 13-25, 13-26, and 13-27 are detailed schematics showing the power supply module and all the associated circuitry and systems.

Testing Power Triacs

The testing of a power triac as compared to that for a power controlled rectifier becomes somewhat more involved. Parameters of triacs are discussed in Chapter 1 (refer to Index). Since the triac must be tested bi-directionally under certain conditions, it is often more difficult to arrange the circuitry, especially in the case of large power triacs, to yield irrefutable data.

One of the basic tests, of course, is for current rating. Although a computer program can be (and is being) used to determine current ratings of power triacs, certain basic inputs are necessary for meaningful results. One must be able to measure thermal impedance accurately in order to properly calculate the

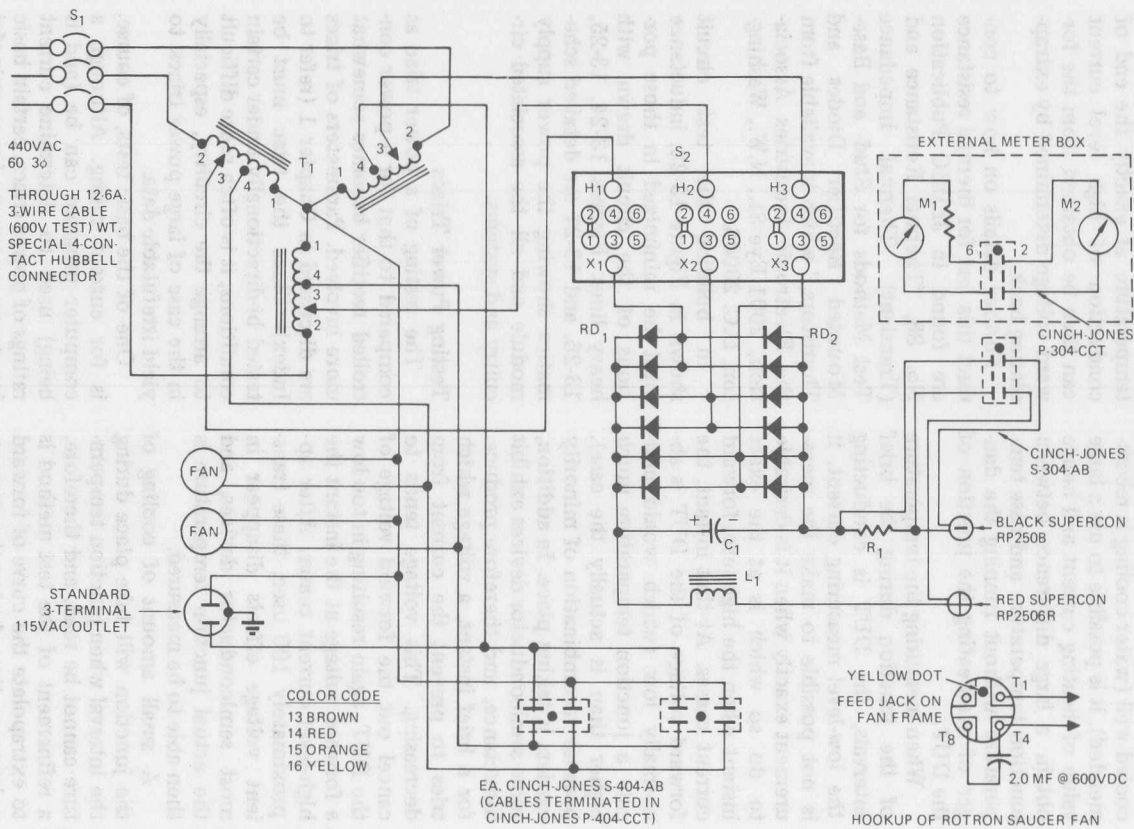
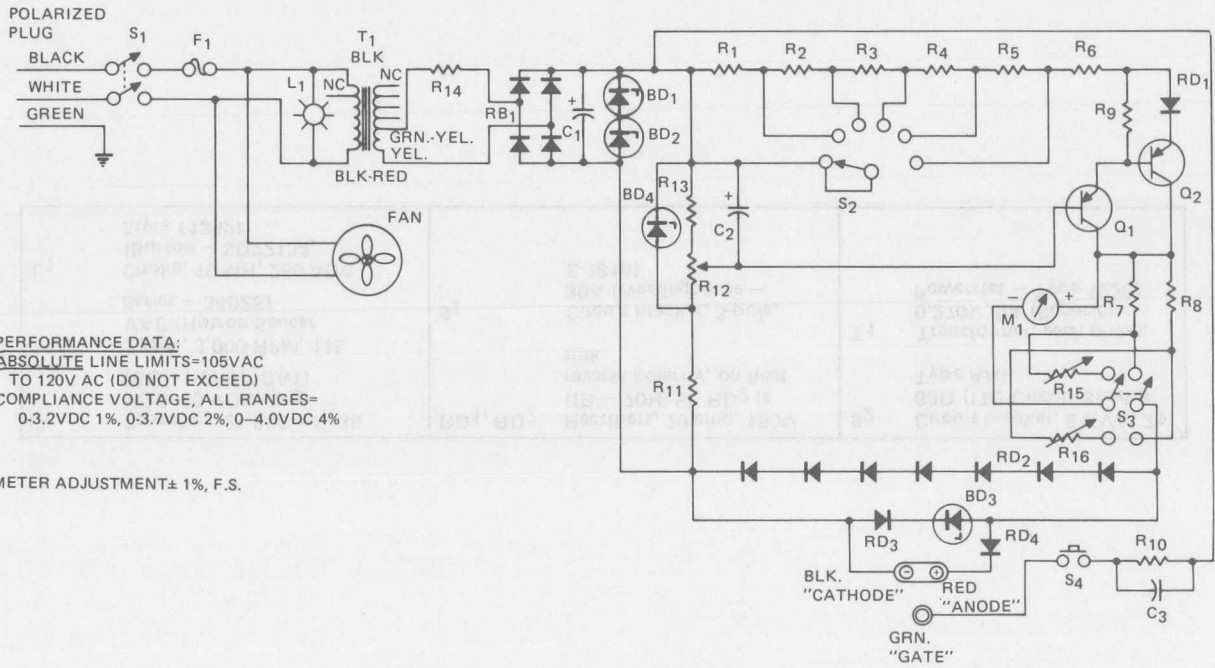


Figure 13-24. Thermal Resistance Tester—Heating Current DC Power Supply

Figure 13-24. Thermal Resistance Tester — Heating Current DC Power Supply

C ₁	Capacitor, 21,500 mF, 35 VDC, 40 VDC surge (GE — 43F877CA1)	RD ₁ , RD ₂	Rectifiers, 70 amp, 150V (IR — 70H15), RD ₂ is reverse polarity, on heat sink	S ₂	Circuit breaker, 5 KVA, 3 ϕ , 60 Ω (ITE Circuit Breaker — Type AA)
FAN	2 each, 3,000 RPM, 115 VAC (Rotron Saucer Series — 340ZS)	S ₁	Circuit breaker, 3-pole, 30A (Westinghouse — E-7819)	T ₁	Transformer, each phase, 0.270V, 9A (Superior Powerstat — Type 1226)
L ₁	Choke, 10 MH, 250 ADC (Burton — SD22134, Style 11392)				



PERFORMANCE DATA:
 ABSOLUTE LINE LIMITS=105VAC
 TO 120V AC (DO NOT EXCEED)
 COMPLIANCE VOLTAGE, ALL RANGES=
 0-3.2VDC 1%, 0-3.7VDC 2%, 0-4.0VDC 4%

METER ADJUSTMENT ± 1%, F.S.

Figure 13-25. Thermal Resistance Tester — Constant Current Reference Supply Circuit

BD ₁ , BD ₂	Voltage Regulator, 7.5 VZ, 50W (IR - 1N3306B) On Heat Sink	R ₁	Resistor, 20Ω, 25W (Dalohm - RH-25)	RD ₁	Rectifier, Bridge, 600V, 16 Amp (4 Each IR - 16F60) On Heat Sink
BD ₃	Voltage Regulator, 10 VZ, 10W (IR - 1N2974RB)	R ₂	Resistor, 10Ω, 50W (Dalohm - RH-50)	RD ₂	Rectifier, 600V, 16 Amp (IR - 16F60) On Heat Sink
BD ₄	Voltage Regulator, 6.8 VZ, 10W (IR - 1N2970B) On Heat Sink	R ₃	Resistor, Series, 2 Each, 2Ω, 20W, 2% (Truohm - RW20G2RG)	RD ₃	Rectifier, 7 in Series, 600V, 16 Amp (IR - 16F60) On Heat Sink
C ₁	Capacitor, 10,000 mF, 50 VDC (Sangamo - 539-2650-01)	R ₄ , R ₅	Resistor, Series, 2 Each, 0.8Ω, 68W (IRC - RW23VR80)	RD ₄ , RD ₅	Rectifier, 600V, 16 Amp (IR - 16F60) On Heat Sink
C ₂	Capacitor, 2,000 mF, 15 VDC (C.D. - BR-20001)	R ₆ , R ₁₄	Resistor, 0.8Ω, 68W (IRC - RW23VR80)	S ₁	Switch, DPDT, 6A, 250V Label "Power"
C ₃	Capacitor, 0.25 mF, 600 VDC	R ₇	Resistor, 0.1Ω, 10W, 1% (Ohmite)	S ₂	Switch, Rotary, 6A 250V (1P6T) Label "Coarse"
F ₁	Fuse	R ₈	Resistor, Manganin Strip, Adjusted to 0.01Ω, 1%	S ₃	Switch, DPDT, 6A, 250V Label "Meter Range", "0.500 mA", "0.5A"
Fan	Fan, Muffin (Rotran Gold Sealed)	R ₉	Resistor, 10Ω, 2W, 5%	S ₄	Switch, Pushbutton, SPST, N.O.
L ₁	Lamp, Neon, 115 VAC	R ₁₀	Resistor, 10K, 1W, 1%	T ₁	Transformer, 115V/36V @ 8A RMS (Triad - F67/U)
M ₁	Meter, 0-5 mA, Basic (Remove Internal Series Resistor)	R ₁₁	Resistor, 100Ω, 20W (Ohmite - 1808)		
Q ₁ , Q ₂	Transistor, 2N514A (Texas Instrument)	R ₁₂	Potentiometer, 100Ω (Ohmite - CMU1011) Label "Fine"		
		R ₁₃	Resistor, 82Ω, 2W, 5%		
		R ₁₅ , R ₁₆	Potentiometer, 10Ω (Bourns - 2605)		

Figure 13-25. Thermal Resistance Tester — Constant Current Reference Supply Circuit

Figure 13-26. Thermal Resistance Tester — DC Charging Supply

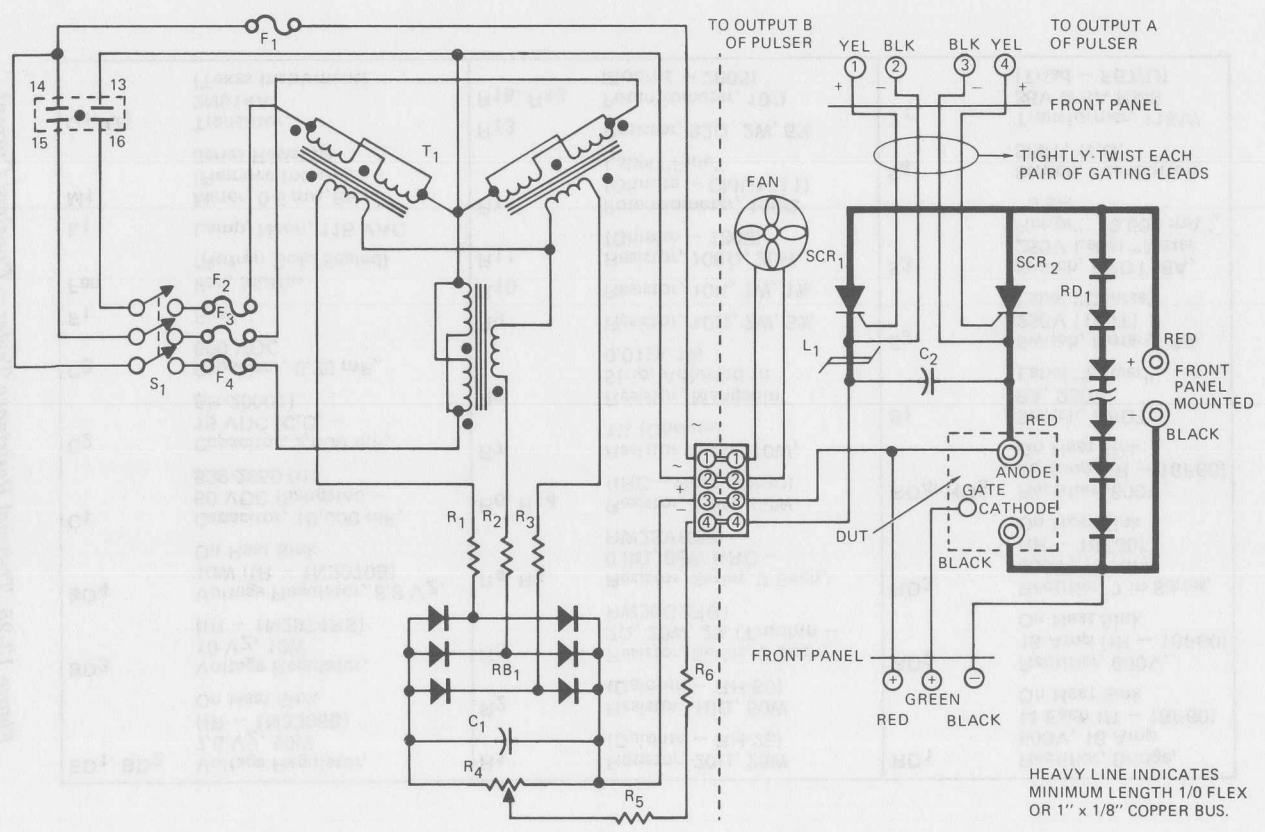


Figure 13-26. Thermal Resistance Tester — DC Charging Supply

C ₁	Capacitor, 7 Units in Shunt, 240 mF @ 450 VDC (Mallory — CG241T450D1)	L ₁	Inductor (Tape 2 Indiana General Ferramic Cores Type of 117-Matic H) Together, Pass Cathode Cable of SCR ₁ , thru Core Twice)	RD ₁	Rectifier Stack, 9 Series, 250 Amp, 100V (IR — 300U10A)
C ₂	Capacitor, 75 μ F, 600 VDC, 0.1 (GE — 23F102462)	R ₁ , R ₂ , R ₃	Resistor, 2 Ω , 25W	S ₁	Switch, 3PST, 6A @ 250V
F ₁	Fuse (1 AFB) in 110V Indicating Holder	R ₄	Potentiometer, 1200 Ω , 225W	SCR ₁	SCR, 235 Amps, 500V (IR — 161RM50) On Heat Sink
F ₂ , F ₃ , F ₄	Fuse (3 AFB) in 220V Indicating Holder	R ₅	Resistor, 500 Ω , 100W	SCR ₂	SCR, 470 Amps, 500V (IR — 300RA50) On Heat Sink
Fan	Saucer Fan (Rotron)	R ₆	Rheostat, 200 Ω , 100W, Turns Off @ Max. Cap. Voltage, Adjust 50 @ 300A	T ₁	Transformer, 3 Each 120/120 (Triad — M-66A)
		RB ₁	Rectifier Bridge, 30 (IR — 66A1T1A3DZ)		

PERFORMANCE DATA:

PULSE REP. RATE - CONTINUOUSLY VARIABLE, 10.9 P.P.S. TO 0.108 P.P.S.
 PULSE SEPARATION (WIDTH) - CONTINUOUSLY VARIABLE, 270 μSEC TO 8500 μSEC
 OUTPUT IMPEDANCES - 50Ω
 PULSE OUTPUT:
 RISE TIME - 1.2 μSEC
 WIDTH - 17-23 μSEC
 FALL TIME - 5-8 μSEC
 MAGNITUDE - 10 VOLTS

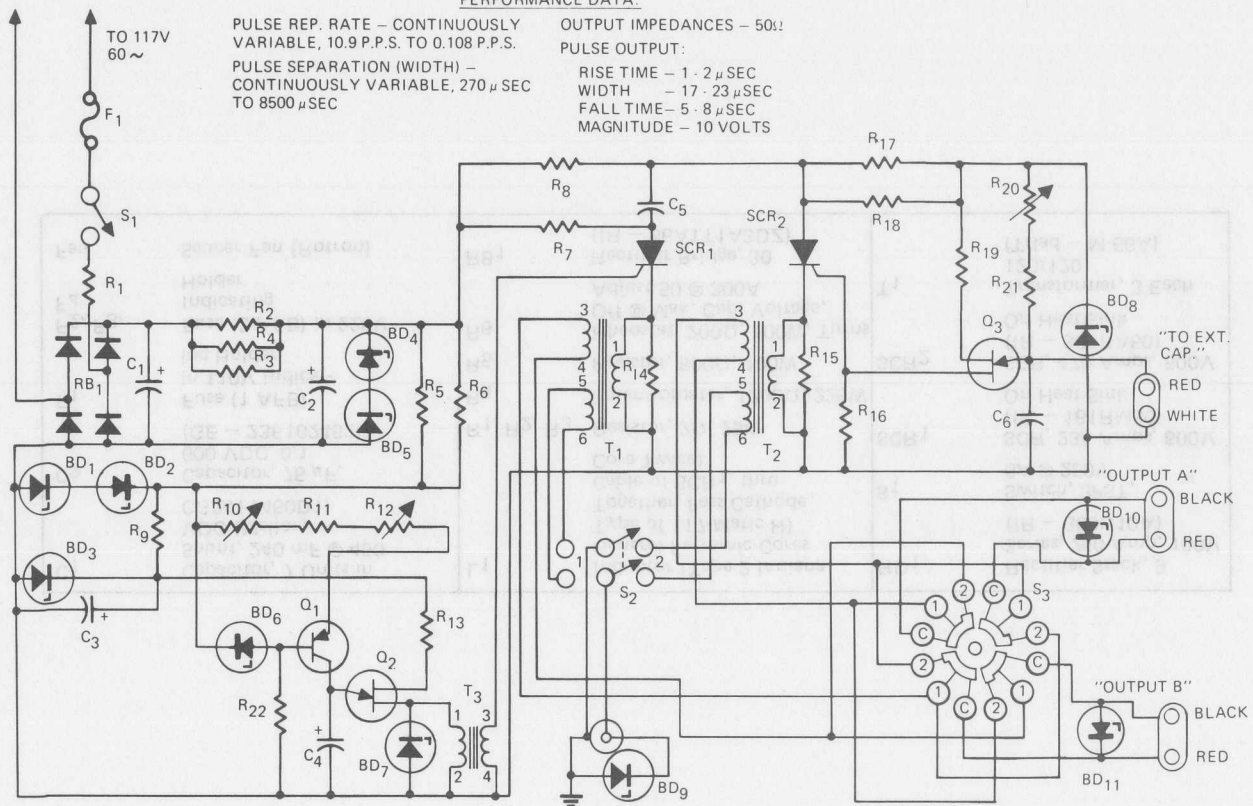


Figure 13-27. Thermal Resistance Tester - Pulsar Timing Circuit

Figure 13-27. Thermal Resistance Tester — Pulser Timing Circuit

BD ₁ , BD ₂ , BD ₃	Voltage Regulator, 30 VZ, 1W (IR — 1N3031B)	Q ₁	Transistor (2N1256)	R ₁₄ , R ₁₅	Resistor, 47Ω, 2W, 5%
BD ₄ , BD ₅	Voltage Regulator, 47 VZ, 10W (IR — 1N2994B)	Q ₂ , Q ₃	Unjunction Transistor (2N2160)	R ₁₆ , R ₂₂	Resistor, 47Ω, 1W, 5%
BD ₇ , BD ₉	Voltage Regulator, 10 VZ, 1W, (IR — 1N3020B)	R ₁	Resistor, 20Ω, 25W	R ₁₇	Resistor, 1.0K, 2W, 5%
BD ₁₀	Voltage Regulator	R ₂ , R ₃	Resistor, 500Ω, 20W	R ₂₁	Resistor, 300Ω, 2W, 5%
BD ₁₁	Voltage Regulator	R ₄	Resistor, 2000Ω, 10W	RB ₁	Rectifier Bridge, 4 Each, 1 Amp 1000V (IR — 10D10)
C ₁ , C ₂	Capacitor, 140 mF, 200 VDC (Sprague — 32D1121T)	R ₅ , R ₁₈	Resistor, 1.5K, 2W, 5%	S ₁	Switch SPST, 3A, 125V Labeled "Power"
C ₃ , C ₄	Capacitor, 50 mF, 50 VDC, (Sprague — TE-1307)	R ₆	Resistor, 2.0K, 2W, 5%	S ₂	Switch DPDT, 3A, 125V Labeled "Sync Pulse"
C ₅	Capacitor, 0.3 mF, 400V, Mylar	R ₇ , R ₈	Resistor, 500Ω, 50W	S ₃	Switch, Rotary (Centralab — 2515) Labeled "Type Pulse" 1 = "Off", 2 = "On"
C ₆	Capacitor, 0.2 mF, 400V, Mylar	R ₉	Resistor, 4.7K, 1W, 5%	SCR ₁ , SCR ₂	SCR, 7.4A, 500V (IR — 2N1778 — Specially Selected)
F ₁	Fuse (3AFB)	R ₁₀ , R ₂₀	Potentiometer, 30K, 10 Turn Labeled R ₁₀ = "Fine, R ₂₀ = "Pulse Width"	T ₁ , T ₂	Transformer (Sprague — 31Z286)
		R ₁₁	Resistor, 2.7K, 1W, 5%	T ₃	Transformer (Sprague — 3Z209)
		R ₁₂	Potentiometer, 9 Each, 27K, 1W, 10% Resistors Mounted On Switch (Centra- lab — 25021P11TSH)		
		R ₁₃ , R ₁₉	Resistor, 270Ω, 1W, 5%		

device rating. The ratings so calculated can then be verified by tests in order to establish the accuracy of the program. Since only a portion of the triac is dissipating heat during each conduction half cycle, and since the total silicon chip is a homogeneous thermal mass, accurate theoretical thermal impedance determinations are impossible. A test circuit was derived in order to measure this thermal impedance accurately using junction temperature and device base temperature measurements as absolute quantities. This circuit is shown in Figure 13-28.

By supplying three power sources to the test device, a single circuit can be used to obtain three ratings:

- A. Bi-directional thermal impedance.
- B. Dynamic current rating.
- C. Bi-directional surge current rating.

By substituting a source of low ampere level test current for the surge current source shown in Figure 13-28, the bi-directional apparent thermal impedance can be obtained. If the device is brought to a steady-state operating current with the power "current source" and the forward voltage of the device has been previously measured by interrupting the main current and gating on SCR₁ or SCR₂. (Interruption of the main current can be achieved by gating on SCR₆, thus removing the gate signal from SCR₄.) The current source of known magnitude then yields a forward voltage for the device under test during this test half cycle (which can be read on a differential input to an oscilloscope to give an accurate reading). Knowing, from previous calibration

what the device forward voltage vs. temperature is at this current level, will yield an accurate reading of junction temperature. By monitoring device base temperature, both effective thermal resistance and dynamic current rating can be calculated.

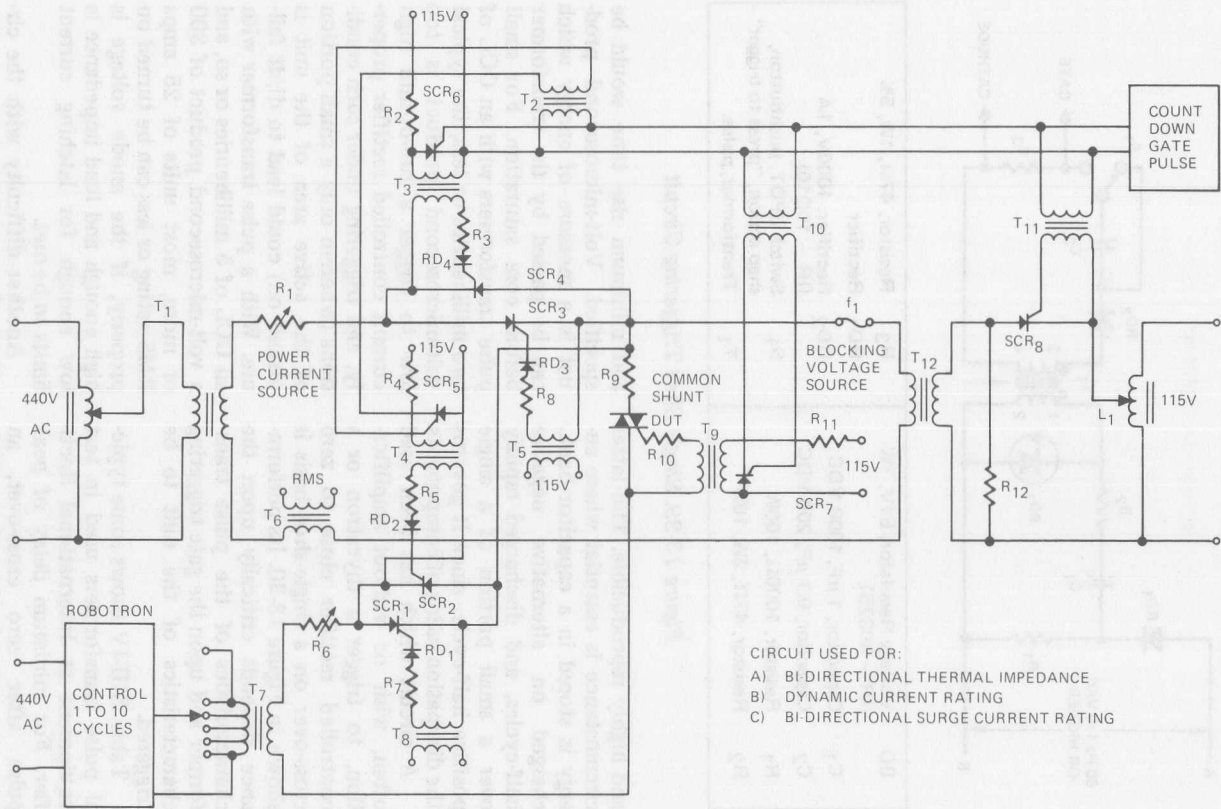
The same general test circuit can be used to determine surge current rating. By using the circuit shown in Figure 13-28, the device can be brought to maximum operating conditions by means of the power current source, a surge current can be superimposed at the desired time for a predetermined duration by means of the surge current source and at the end of this surge, the ability for the device to block voltage can be determined by turning on SCR₅ and SCR₆.

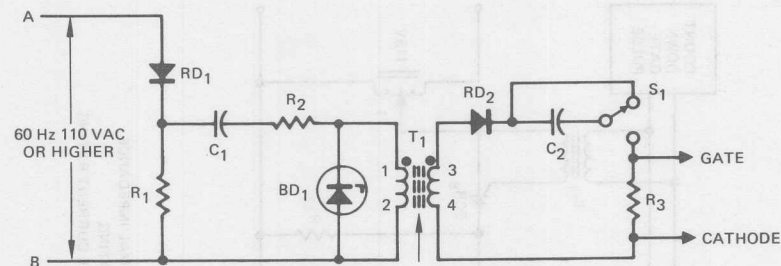
Triggering Circuits

Triggering thyristors is discussed in many places in this book (refer to Index for locations). Often it is desirable to trigger a controlled rectifier at a point within a very few degrees of the start of a 60 Hz sine wave. On a 60 Hz basis, this can be done readily by a sine wave from a high ac supply voltage, clipped by a zener voltage regulator fed from the supply through a large dropping resistor, with diode isolation of the gate. This technique is used in the circuit of Figure 13-29.

In many tests, however, this gating must be done on a single shot basis, with a gate pulse present for a portion of one positive half-cycle, within a very few degrees of the start of the cycle. In other tests, instead of a single shot basis, repeated manually at a low and random repetition rate, low repetition rate triggering must be automatic

Figure 13-28. Triac Test Circuit





BD	Voltage Regulator, 51V, 1W (IR - 3037B)	R3	Resistor, 47 Ω , 1W, 5%
C1	Capacitor, 1 μ F, 1000 VDC	RD1	Rectifier
C2	Capacitor, 0.1 μ F, 200 VDC	RD2	Rectifier, 1000V, 1A (IR - 10D10)
R1	Resistor, 1000 Ω , 100W	S1	Switch SPDT, pushbutton, snap action, "press to trigger"
R2	Resistor, 47 Ω , 2W, 10%	T1	Transformer, pulse.

Figure 13-29. Single Shot Triggering Circuit

and highly reproducible. This latter circumstance is essential where energy is stored in a capacitor bank, charged on alternative negative half-cycles, and discharged rapidly over a small portion of a single positive half-cycle, since it governs the dissipation rating of components.

A circuit which has been used often, with or without amplification, to trigger a thyristor or a controlled rectifier close to zero cross-over on a single-shot basis is shown in Figure 13-30. Its performance depends critically upon the characteristics of the pulse transformer and upon the gate triggering characteristics of the unit to be triggered.

Table XIII-IV shows some typical pulse transformers used in test equipment at International Rectifier. For minimum delay of peak pulse after zero cross-over, an otherwise suitable unit of low OCL (open-circuit primary inductance)

and minimum rise time would be specified. Volt-microsecond product is a measure of energy which can be passed by the transformer before core saturation. For small pulse transformers with an OCL of two millihenries or less, the typical volt-microsecond product is too low to trigger a run-of-mill high current controlled rectifier properly, and triggering under such conditions (wherein only a small portion of the active area of the unit is turned on) could lead to di/dt failure. With a pulse transformer with an OCL of 5 millihenries or so, and a volt-microsecond product of 300 or more, most units of 25 amps RMS rating or less can be turned on properly, if the anode voltage is high enough and load impedance is low enough for latching current limits to be met.

Another difficulty with the circuit in Figure 13-29 is the way by which successive gate triggering

Table XIII-IV. Pulse Transformers

MANUFACTURER AND TYPE	URNS RATIO	APPROX. OCL IN MILLIHENRIES	APPROX. MAXIMUM VOLT-MICROSECOND	APPROX. RISE TIME 10/90 IN MICROSECONDS	APPROX. 50% PULSE WIDTH, STEP INPUT IN MICROSECONDS
Sprague 31Z201 Sprague 35ZM300 Pulse Engineering PE-2228	1:1	1-2	100-250	0.04-0.08	4-8
Sprague 31Z281 Sprague 35ZM315 Pulse Engineering PE-2229	1:1:1	1-2	100-250	0.04-0.08	4-8
Sprague 31Z204 Sprague 35ZM904 Pulse Engineering PE-2230	1:1	4-7	200-400	0.07-0.11	17-22
Sprague 31Z286 Sprague 35ZM930 Pulse Engineering PE-2231	1:1:1	4-7	200-400	0.07-0.11	17-22
Sprague 31Z307 Sprague 43Z307 Pulse Engineering PE-2242	1:1	40-50	1000-1500	0.5-1.5	140-200
Sprague 31Z387 Pulse Engineering PE-2479	1:1:1	40-50	1000-1500	0.5-1.5	140-200

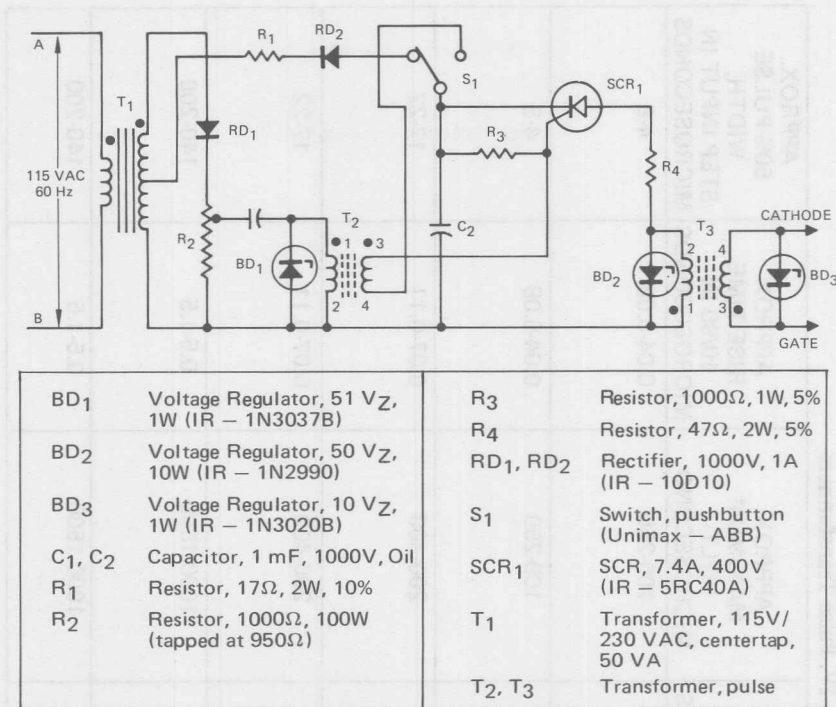


Figure 13-30. Zero Voltage, Single Shot Triggering Circuit

pulses after the first are blocked. The 0.1 Mfd capacitor charges up almost to peak positive output voltage from the transformer secondary on the first pulse, but enough difference between its charged voltage and unloaded source voltage exists to enable several more, much smaller pulses to be passed. Were sufficient output voltage available, alternate output configurations could be used to eliminate this effect, but with proximity to zero cross-over a must, output pulses are generally neither high enough or long enough.

The circuit shown in Figure 13-30 not only permits the use of a low OCL transformer, near-ideal for

differentiation, but also yields a nearly simultaneous pulse, which 1) can supply enough energy, either directly or through an overdriven pulse transformer, to trigger any size controlled rectifier, and 2) does not result in successive after pulses. With the pushbutton pressed down and held firmly, one and only one husky line-synchronized pulse is produced within three degrees of the zero cross-over point.

In both Figures 13-29 and 13-30, a fifty-volt zener voltage regulator is placed across the primary of the pulse transformer. A regular diode, such as IR's 10D6, could suffice, but the zener regulator also prevents overvolting of the primary

should line surges occur. The zener voltage regulator in the primary of the second pulse transformer also helps shape output pulse waveform and a non-zener should not be substituted.

The output pulse waveform of the circuit in Figure 13-30 is shown in Figure 13-31. For these oscilloscope photographs, T_2 was a PE-2231. The lack of droop and uniform output voltage is the reason for the zener voltage regulator in the circuit. A ten-volt zener voltage regulator could have been substituted for the 50 volt regulator, and a 47-ohm terminating resistor used, but the output pulse then would have been rounded and with a peak of but 7 to 8 volts, because of $I_x R$ drop through the transformer secondary. Without the zener regulator or a terminating resistor, high-frequency transients and excessive ringing are present.

Figure 13-32 shows a line-synchronized countdown triggering circuit developed at International Rectifier. It has been used at repetition rates of as high as 10 pulses per second and as low as 1 pulse per 10 minutes, with extremely high reliability and reproducibility. Output waveforms are shown in Figure 13-33. Again, the pulse transformer

used was a PE-2231, although the circuit has been used successfully with a PE-2479 to produce a pulse with a rise time (10-90%) of a microsecond, a pulse width (50%) of 170 microseconds, and a fall time (90-100%) of 170 microseconds. The top of the pulse shows little droop over a full 66-microsecond period.

In operation, the phasing of the pulse within a given positive half-cycle can be shifted but a small amount before the triggering rate increases or decreases by a cycle per second.

When supply line B is positive, the 100 μF capacitor, C_3 , charges to the zener regulator voltage of BD_2 (30V) less the on-state voltage of the rectifier, RD_3 . During this half cycle, the base voltage of Q_1 is zero, and no current passes through R_1 and Q_1 to charge C_1 . When supply line A is negative, a sharply rising square wave exists across BD_1 (10V) and a square wave pulse of about 8 volts occurs across the 1000-ohm load resistor, R_5 through the two diodes RD_1 and RD_2 . This biases Q_1 to charge capacitor C_1 from supply capacitor, C_3 . At the same time, it produces through capacitor C_2 by differentiation, a negative pulse at base 2 of the unijunc-

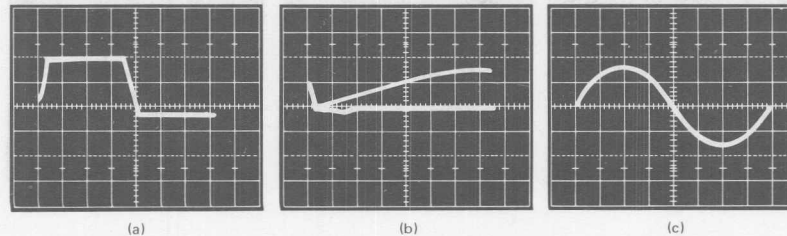
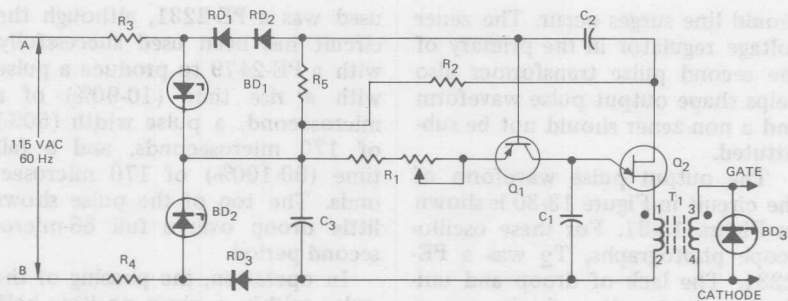


Figure 13-31. Output Waveforms for Zero Cross-over Trigger Circuit



BD1	Voltage Regulator, 10 VZ, 10W (IR - 1N2974RB)	Q1	Transistor (see text)
BD2	Voltage Regulator, 30 VZ, 10W (IR - 1N2989RB)	Q2	Transistor, unijunction (2N2160) selected
BD3	Voltage Regulator, 10 VZ, 1W (IR - 1N3020B)	R1	Resistor (see text)
C1	Capacitor (see text)	R2	Resistor, 330Ω, 1W, 5%
C2	Capacitor, 0.33 μF, 400 VDC, Mylar	R3, R4	Resistor, 500Ω, 50W
C3	Capacitor, 100 μF, 50 VDC	R5	Resistor, 1K, 1W, 5%
		RD1, RD2, RD3	Rectifier, 1000V, 1A (IR - 10D10)
		T1	Transformer, pulse (see text)

Figure 13-32. Countdown Triggering Circuit

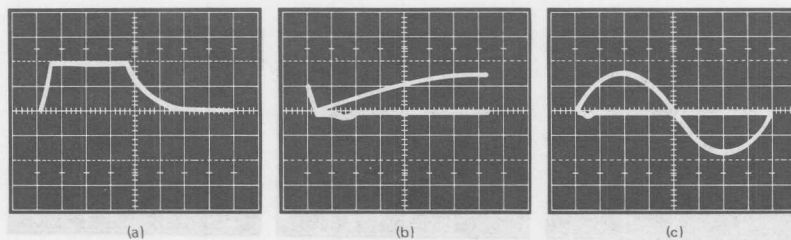


Figure 13-33. Output Waveforms for Countdown Trigger Circuit

tion transistor, Q_2 . At the start of this negative pulse, if the voltage across C_1 is high enough, the unijunction will trigger.

For proper operation of the circuit, a value of C_1 of one μfd or more should be used, even at fairly high repetition rates. This capacitor should be paper, oil, Mylar, or a tantalum electrolytic, for stability and proper discharge characteristics. If smaller values of C_1 are used, under some conditions multiple pulses may be produced.

The circuit has worked with a variety of silicon and germanium

PNP transistors, but best performance is possible with a silicon PNP high-frequency transistor such as mentioned, with a typical BV_{CEO} of 60V or above, and a small-signal beta of 100 or more at 5 mA dc.

In the circuit as shown, with C_1 a 10-mfd, 100 Vdc Mylar, a value for R_1 of 10 kilohms yielded a pulse repetition rate of 4.1 pulses per second, while a value of 20 kilohms yielded 1.9 pulses per second. Down to a certain minimum value for R_1 , different for each Q_1 , pulse repetition rate appears linearly inversely proportional to value of R_1 .

References

1. H.F. Haight, "Testing Procedures and Test Equipment for Controlled Rectifiers," Rectifier News, Summer 1966 and Spring 1966, International Rectifier.
2. F. Durnya, "Inrush Current Testing," Rectifier News, Fall 1968 International Rectifier.



Large diameter wafers of high-purity silicon are arranged in a glass "boat" and loaded into a diffusion furnace. The boat also contains a small amount of an additive element which will precisely change the electrical characteristics of the silicon. The two are heated together until the additive element gasifies into the lattice structure of the silicon.

Triggering Circuits

Gate Triggering Circuits

The simplest means for triggering a controlled rectifier is to apply a positive dc potential between the gate and cathode. This is the operating condition used to determine compliance with published specifications for maximum gate current and voltage required to trigger all units of a given type. The designer quickly learns that there are a number of considerations which require the application of greater current and voltage to the gate in order to achieve successful device operation in a practical piece of equipment. Fortunately, in modern devices the maximum gate current and voltage which may be applied greatly exceed the values required to trigger under dc conditions. This is illustrated in Figure 14-1, which shows the gate characteristics for a 70 ampere (average) device. It can be seen that the designer has a large region within which to operate where the gate can be driven harder than the amount barely required to turn the device on and yet not be driven beyond its maximum peak power rating. Care must be taken to avoid exceeding the maximum average power rating of the gate when applying a high peak signal.

Gate Triggering to Accommodate High Load Circuit di/dt

For applications using conventionally gated devices where the initial rate-of-rise of anode current is more than a few amperes per microsecond it becomes important to provide a considerably greater current pulse than that which will

barely turn the device on. A larger than minimum gate current pulse will cause a larger portion of the total cross section of the device to turn on initially, thus reducing the turn-on current density and minimizing the chance of a device failure due to the di/dt effect. In Figure 14-1, a region is shown where best results will be obtained when the device must accommodate a high di/dt . In addition, the gate pulse should have a fast rise time, in the order of 0.1 microseconds. The objective is to inject a significant charge into the gate region during the delay period.

ACE gated and Di-Vergence[®] gated devices in general require the above mentioned precautions except that di/dt and switching losses are less severe for fast rising anode currents.

Short Gate Triggering Pulses

For reasons of economy, both to reduce the size of components used to build the gate excitation circuit and the power consumed by this circuit, a relatively short pulse is often applied to the gate rather than a long pulse or a continuous dc signal. As pulse width is reduced it is found that the peak current and voltage required to trigger a given device becomes greater. This effect is most noticeable for pulse widths shorter than 10 microseconds, as shown in Figure 14-2. For such short pulses it can be seen that essentially a fixed electrical charge is required to trigger the controlled rectifier.

There is another problem which

is encountered with a lagging power factor load. In many inverter circuits, the power SCR may not be forward-biased until well into the half-cycle. At the same time, reactive current is flowing through the free-wheeling diodes. In this case a short pulse triggering scheme cannot be used. A relatively long cur-

rent pulse must be supplied to the gate to ensure that the device triggers when it becomes forward biased. This is often accomplished by providing, immediately after the initial gate pulse, a longer but lower amplitude pulse which is commonly called the "back porch" of the gate drive signal. See Figure 14-3.

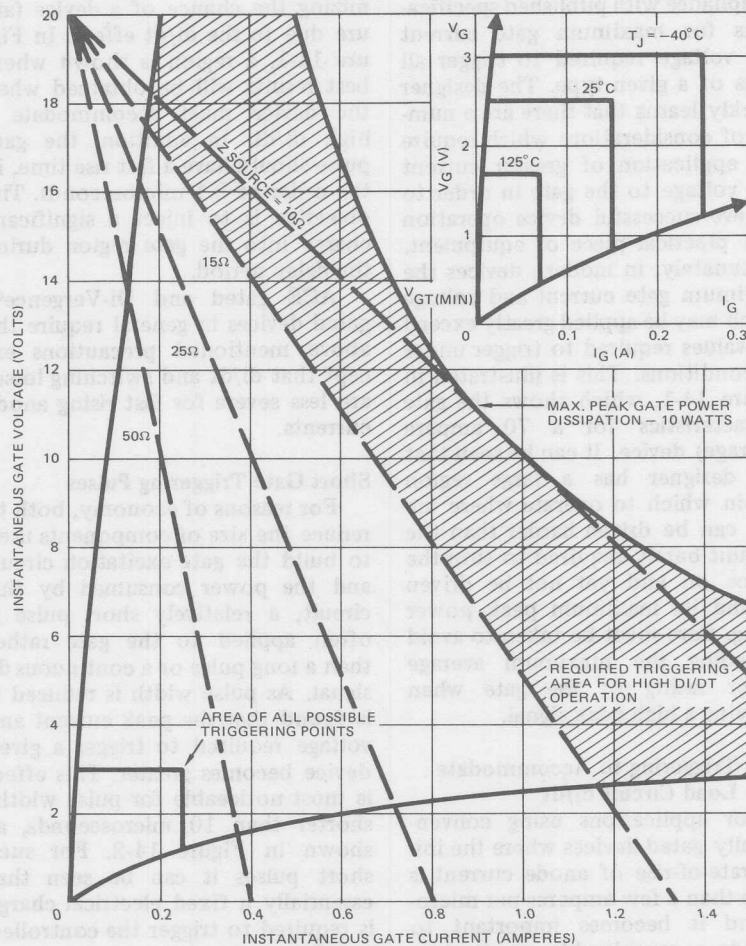


Figure 14-1. Gate characteristics for 70 A controlled rectifier

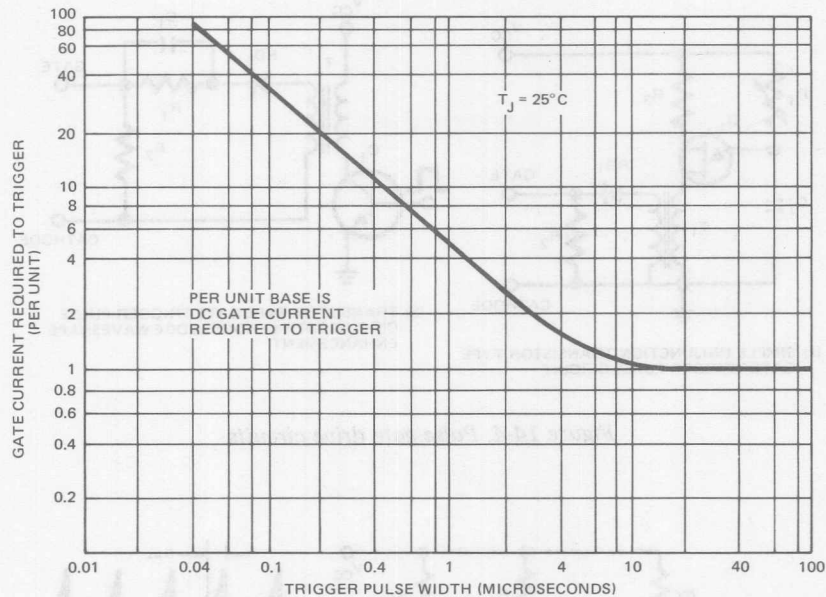


Figure 14-2. Gate current required to trigger controlled rectifier vs. gate trigger pulse width

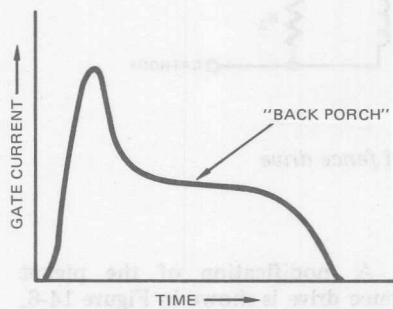


Figure 14-3. Generalized waveform of gate trigger pulse with back porch

Several circuits that can be used for pulse drive are shown in Figure 14-4.

The circuit shown in Figure 14-4(a) is a unijunction relaxation

oscillator circuit, timed by R_1 and C_1 with a pulse transformer coupling the energy to the gate. This rather simple circuit puts out a pulse with no back porch. The circuit shown in Figure 14-4(b) has a little more wave shaping by using a speed-up capacitor C_1 across R_1 to decrease the pulse rise time. R_2 in both circuits reduces the gate-cathode impedance, thus lowering the SCR's susceptibility to noise and dv/dt triggering. This resistor is usually in the order of 100 ohms and is mounted as close physically to the SCR as is practical. The diode RD_1 functions to block the reverse voltage kick produced when the pulse transformer resets, protecting the gate-cathode junction in the reverse direction.

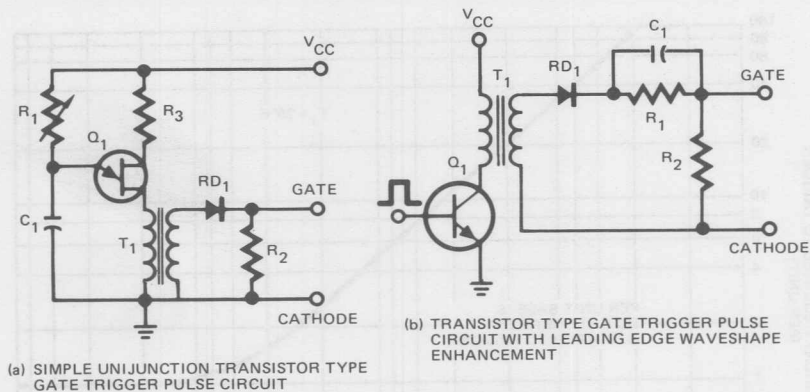


Figure 14-4. Pulse gate drive circuits.

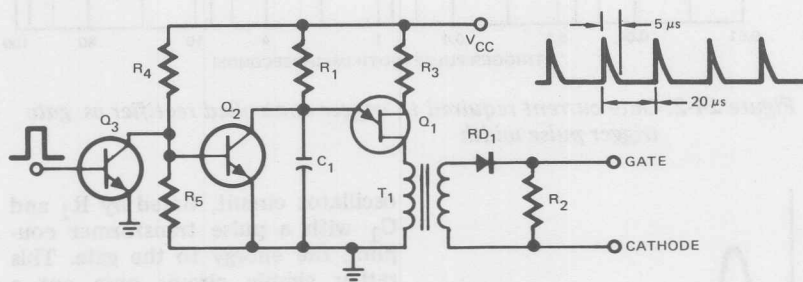


Figure 14-5. Picket fence drive

Picket Fence Drive

The Picket Fence Drive Circuit, shown in Figure 14-5, is a variation of pulse drive (using a small pulse transformer) but has the effect of putting pulses on the gate all through the conduction period. While Q_3 is turned on, unijunction Q_1 is allowed to cycle many times as set by R_1 and C_1 . The output would be typically as shown in Figure 14-5.

A modification of the picket fence drive is shown in Figure 14-6. In this circuit the pulse transformer is driven in both directions and the output is rectified to give a dc gate signal. This circuit has the added feature of requiring only one oscillator, which can be directed to any SCR by use of logic gates. This is useful for multi-device circuits.

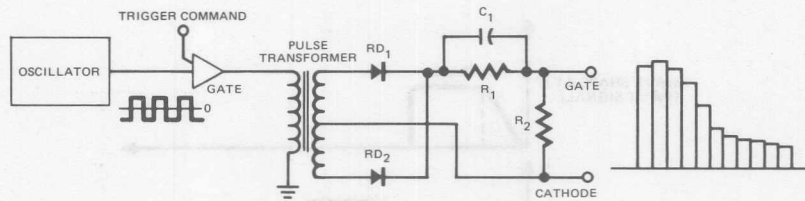


Figure 14-6. Rectified picket fence drive

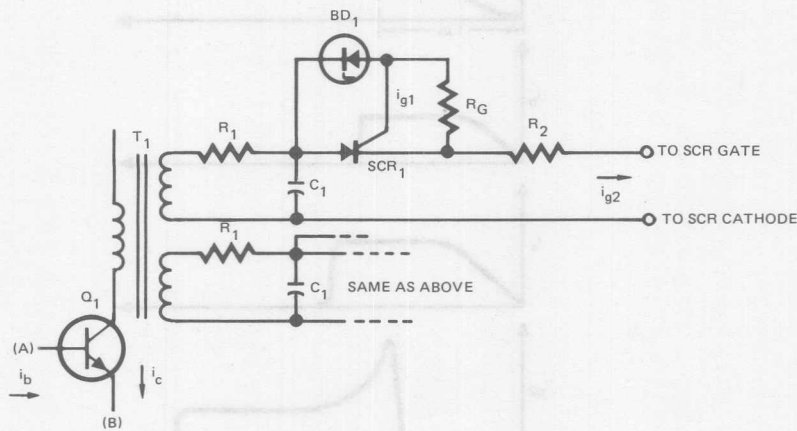


Figure 14-7(a). Local energy storage type gate trigger pulse circuit (for triggering two thyristors is shown)

Local Energy Storage Gate Triggering

Local energy storage gate trigger circuit design will be discussed briefly in order to give the circuit designer some tips on ways of achieving the rise times recommended above in a relatively inexpensive manner. The circuit shown in Figure 14-7(a) serves as a pulse sharpening circuit to give good voltage isolation without requiring the isolation transformer to have good high frequency characteristics. In this circuit, the combination of v_g and i_{g1} for SCR₁ and also R_G should be chosen to give a triggering characteristic which is uniform for all combinations of v_g , R_G , and

SCR₁ which are to be used in each of the SCR trigger circuits. Capacitors C_1 and resistors R_1 act not only as delay circuits to square up the collector (point B) vs. time characteristic shown in Figure 14-7(b), but also as noise suppressors to the gates of the SCRs which are connected in parallel. R_2 simply acts as a pulse stretcher to stretch out the discharge of the local energy storage capacitor C_1 and should be chosen so that there is no discontinuity in the SCR gate triggering current between the discharge of the capacitor and the follow-up of the slower current from the pulse transformer.

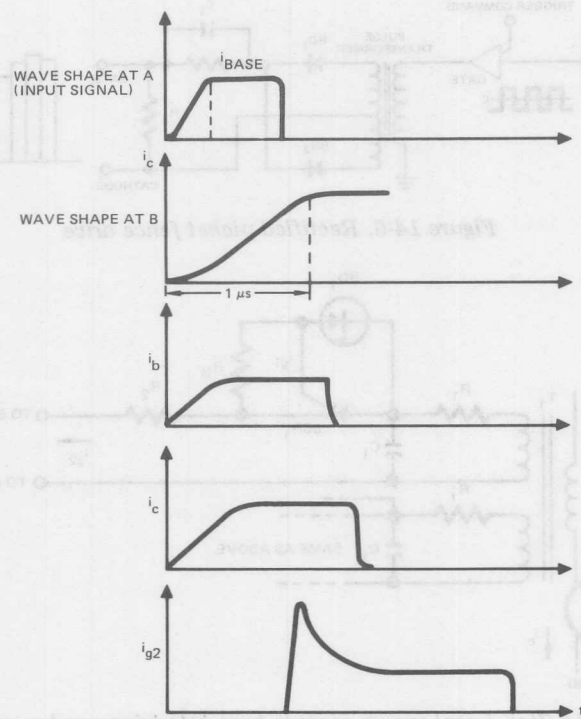


Figure 14-7(b). Waveforms pertaining to circuit in Figure 14-7(a)

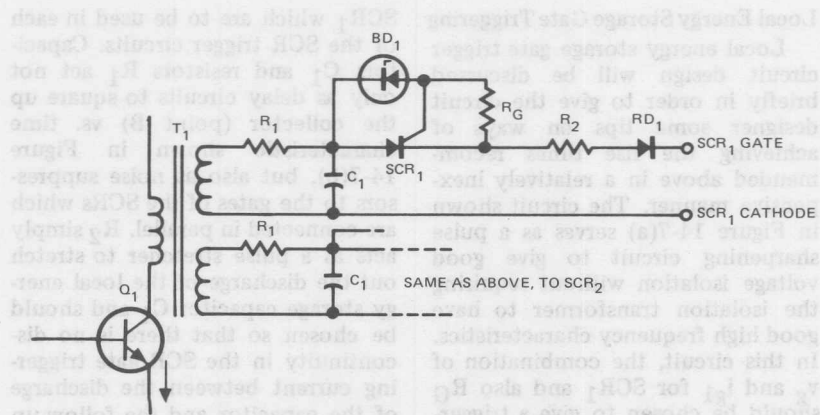


Figure 14-8(a). Local energy storage type gate trigger pulse circuit which provides DC gate trigger pulse

Figure 14-8(a) shows an alternate method of achieving voltage isolation and yet using pulse gating techniques with local energy storage where it may be important, because of a reactive load in the main power circuit, that the gate current will essentially be continuous. This can be achieved by supplying a series of gate pulses from two circuits operating alternately and connected through diodes to the same gate. These pulses (refer to Figure 14-8(b)) need not be overlapping or continuous as far as the gate is concerned. A ratio of time-on to time-between-pulses might be about 70% on, 30% off for large SCRs, as long as the 30% off time is well below the turn-off time of the SCR. In the case of devices of 300 ampere rat-

ing or more, the off-time should probably be kept below about 30 or 40 microseconds. It would not then be normal for the devices to achieve a great deal of recombination during the off-time.

If diodes RD_1 are used in the gate circuit for isolation, their turn-on characteristics should be studied by the circuit designer to be sure that they do not affect the gate current rise characteristic. Normally a diode doped for fast recovery characteristics will serve well in this type of application.

The gate circuit of Figure 14-9 combines the qualities of a fast rise time gate current to minimize delay time effects and a wide pulse for inductive loads.

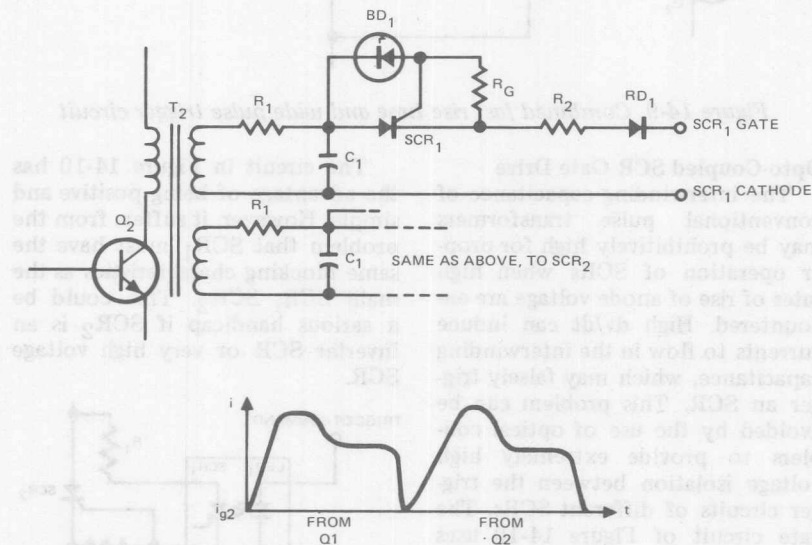


Figure 14-8(b). Gate current waveform pertaining to circuit in Figure 14-8(a)

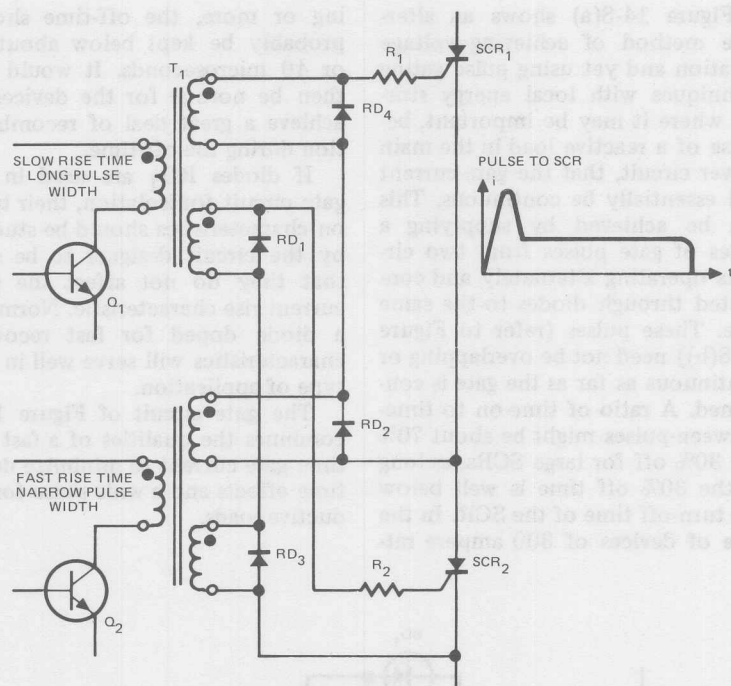


Figure 14-9. Combined fast rise time and wide pulse trigger circuit

Opto-Coupled SCR Gate Drive

The interwinding capacitance of conventional pulse transformers may be prohibitively high for proper operation of SCRs when high rates of rise of anode voltage are encountered. High dv/dt can induce currents to flow in the interwinding capacitance, which may falsely trigger an SCR. This problem can be avoided by the use of optical couplers to provide extremely high voltage isolation between the trigger circuits of different SCRs. The gate circuit of Figure 14-10 uses a light emitting diode (LED) and photo-sensitive SCR (SCR_1) to provide optical isolation for each main SCR (SCR_2).

The circuit in Figure 14-10 has the advantage of being positive and simple. However, it suffers from the problem that SCR_1 must have the same blocking characteristics as the main SCR, SCR_2 . This could be a serious handicap if SCR_2 is an inverter SCR or very high voltage SCR.

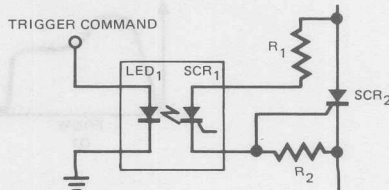


Figure 14-10. Optically coupled trigger circuit

Noise

There are general rules that can be followed to reduce false triggering from noise (some were mentioned above), whether generated in the circuit, or externally.

A. Introduce a gate-to-cathode resistor (mentioned above) near the device.

B. Add snubbing devices anode to cathode to reduce voltage spikes generated during device recovery.

C. Twist the auxiliary gate and cathode leads, especially when running any distance. This reduces inductive pick up.

D. Introduce a diode or zener diode in series with the gate to raise the effective threshold voltage of the device gate. If this method is used, a gate-cathode resistor must be used on the device, otherwise the impedance in the gate to cathode region will be very high and this will make the device more susceptible to noise.

E. Reverse gate-cathode bias has been used in the past, not only to act as a sink for circuit noise, but also to enhance the dv/dt characteristics of an SCR by bleeding off capacitive leakage from the anode circuit. However this is no longer needed with the emitter shorting used in modern devices. There is still some noise immunity achieved by this method but the amount is questionable when considered against the cost.

F. Capacitors have been placed from gate to cathode to reduce the effect of high frequency noise in the circuit. However, in most cases this is not recommended any longer because it also reduces the rise time

of the desired gate signal. There are a few cases where this may not be detrimental (i.e., low di/dt anode currents) and a capacitor can be safely used.

G. A great deal of noise immunity can be achieved by using a gate transformer with extremely low interwinding capacitance, in the order of 5 pf or less. This not only reduces the noise from the control circuit side of the transformer that gets to the devices, but reduces the noise from the power circuit that gets into and falsely triggers the control circuit.

H. Operate parallel and potentially interacting thyristor circuits from a stiff (low reactance) supply line. Notches in the voltages of power lines, particularly those tied to control circuits, can cause a false change of state in logic elements; one shot multivibrators are especially susceptible to this type of noise.

J. If the supply line is soft (high reactance), consider using separate transformers to feed the parallel branch circuits; each transformer should be rated no more than required by the rating of the branch circuit load.

K. Avoid purely resistive loads operating from stiff lines — they give highest rates of current rise on switching.

L. Keep both leads of each power circuit run together; avoid loops that encircle sensitive control circuitry.

M. Arrange magnetic components so as to avoid interacting stray fields.

References

1. General Electric SCR Manual, 4th Edition.
2. L.R. Carver, "How the Experts Use SCR Ratings," Machine Design, July 12, 1973.
3. D.W. Borst, "Turn-On Action in Large Controlled Rectifiers," Rectifier News, Fall 1966.

High Speed Thyristors

Comparing Gate Structures

A glance at Figure 15-1 clearly shows a major problem associated with the design of high frequency, high current thyristors; the equalization time (the time necessary to turn the thyristor fully on) increases with the current rating.

The solution is to use an interdigitated gate structure; i.e., a multiplicity of gate arms such that no point on the cathode is more than a few millimeters away from the gate. Combining this concept with the ACE gate construction yields a device which:

- A. Requires a relatively low external gate drive.
- B. Propagates rapidly and effi-

ciently over the main cathode.

C. Turns on the entire main cathode in less than 20 microseconds.

To illustrate the effect of the several gate structures, consider three thyristors* with a cathode diameter of 25 mm, differing only in gate structure. Figure 15-2 shows not only the advantage of the ACE and interdigitated gates, but also the trade-off in top (cathode) surface area.

A. The point gate thyristor uses 100% of the surface as cath-

*Calculations based on realistic designs and a constant $0.1 \text{ mm}/\mu\text{s}$ turn-on propagation velocity.

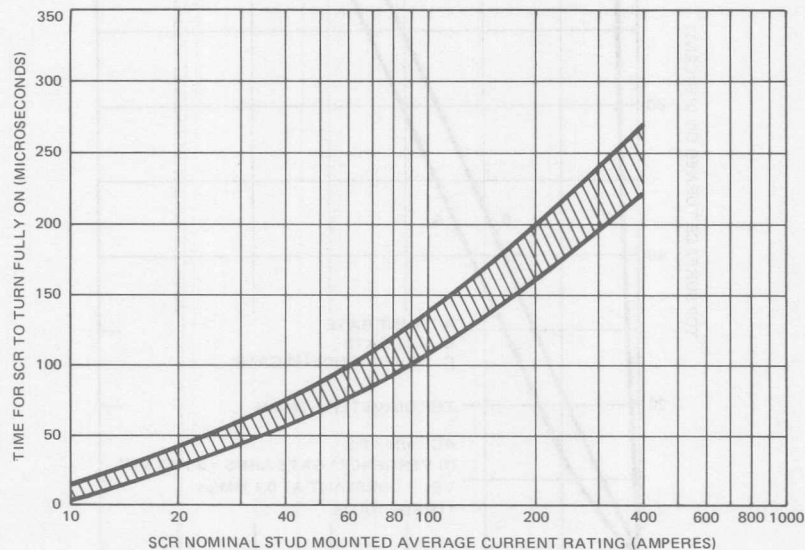


Figure 15-1. Typical time for SCRs of various average current ratings to turn on fully (conventional point gate devices, hard firing gate pulse)

ode, but takes $250 \mu\text{s}$ to turn on completely.

B. The ACE gate thyristor uses less than 91% of the surface as cathode, but always has significantly more area "on" until it is completely on in $215 \mu\text{s}$.

C. The interdigitated (Di-Vergence) gate thyristor uses approximately 82% of the surface, but is completely on in $13.2 \mu\text{s}$.

With a larger Di-Vergence gate thyristor, the length of each gate arm increases in proportion to the

area of the surface and the equalization time is relatively constant. The gate arm width remains about constant and so the percentage of surface area devoted to the gate is relatively constant.

The effect of incomplete turn-on is increased watts loss and therefore heating of the thyristor during the turn-on interval. This is true even at intermediate frequencies where the ACE gate device is completely turned on at the end of the current pulse.

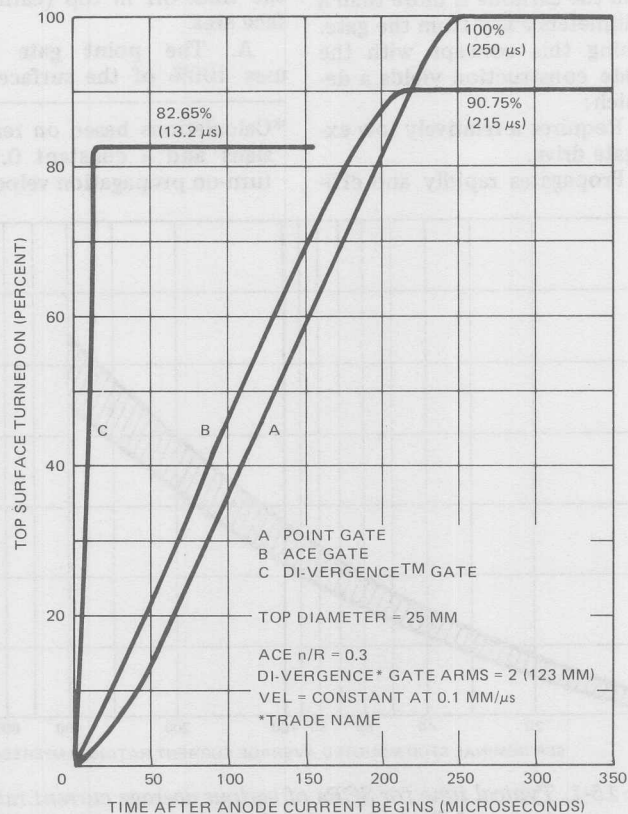


Figure 15-2. Typical turn-on characteristics of three gate structures

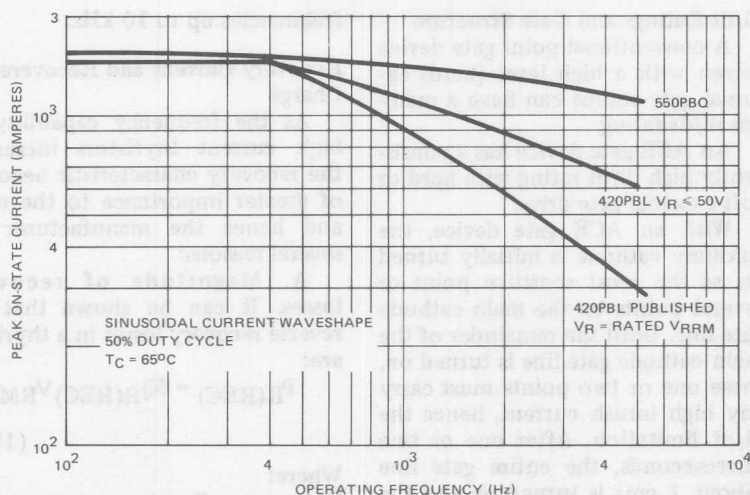


Figure 15-3. Maximum Allowable Peak On-State Current versus Frequency

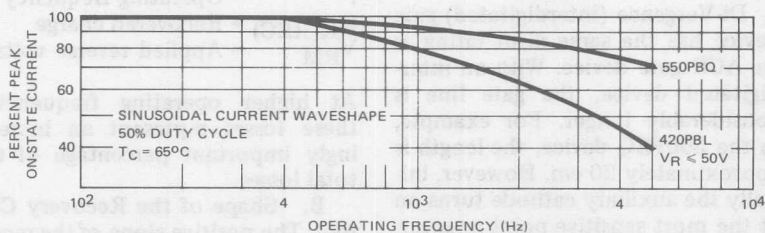


Figure 15-4. Maximum Allowable Peak On-State Current Rating as a Percent of Low Frequency Rating

Figure 15-3 shows the Maximum Allowable Peak On-State Current for sinusoidal waveforms and 50% duty cycle at a case temperature of 65° with $V_R \leq 50$ volts for the 420PBL ACE gate thyristor and the 550PBQ interdigitated gate thyristor. * Figure 15-4 shows the same information except that it is plotted as a percentage (%) of the low frequency rating.

As expected at 5 kHz, the 550PBQ is significantly better than the 420PBL. At frequencies below 3 kHz the 420PBL is completely

turned on at the end of each current pulse, yet the 550PBQ can handle more current (or conversely requires less cooling) than the 420PBL. For example, at 1.5 kHz the 550PBQ can carry up to 88% of its rated low frequency current but the 420PBL can carry only 70% of its rated low frequency current.

*These two particular thyristors were chosen because the low frequency ratings are approximately equal.

di/dt Ratings and Gate Structure

A conventional point gate device driven with a high level (hard) external gate source can have a medium di/dt rating.

An ACE gate device has a consistently high di/dt rating with hard or soft external gate drive.

With an ACE gate device, the auxiliary cathode is initially turned on at the most sensitive point or several points on the main cathode gate line. Until the remainder of the main cathode gate line is turned on, these one or two points must carry any high inrush current, hence the di/dt limitation. After one or two microseconds, the entire gate line (about 1 cm) is turned on and the current density propagates laterally across the main cathode.

Di-Vergence (interdigitated) gate device has the same di/dt rating as an ACE gate device. With an interdigitated device, the gate line is considerably longer. For example, in the 500PBQ device, the length is approximately 20 cm. However, initially the auxiliary cathode turns on at the most sensitive point or several points on the main cathode gate line and once again these one or two points must carry any high inrush currents for the first one or two microseconds. After one or two microseconds, the entire gate line is turned on, and the current density propagates laterally across the main cathode. After approximately 15 μ s the entire cathode is turned on.

With the introduction of interdigitated gate structures, thyristors can now be applied efficiently in high frequency power conversion systems and they are now being used in such applications as induction heating generators operating at

frequencies up to 10 kHz.

Recovery Current and Recovered Charge

As the frequency capability of high current thyristors increases, the recovery characteristic becomes of greater importance to the users and hence the manufacturer for several reasons:

A. **Magnitude of recovery losses.** It can be shown that the reverse recovery losses in a thyristor are:

$$P_{R(REC)} = fQ_{R(REC)}V_{RM} \quad (15-A)$$

Where:

$P_{R(REC)}$ = Reverse recovery power loss in watts
 f = Operating frequency
 $Q_{R(REC)}$ = Recovered charge
 V_{RM} = Applied reverse voltage

At higher operating frequencies, these losses represent an increasingly important percentage of the total losses.

B. **Shape of the Recovery Current.** The positive slope of the recovery current as the current decreases towards zero creates a self-induced voltage across the thyristor, which, when added to the supply voltage, may exceed the voltage rating of the device. If another thyristor is connected in anti-parallel, the dv/dt of this voltage may cause triggering of the other thyristor.

Each of these matters will be considered separately.

Magnitude of Recovery Losses

The recovered charge of a thyristor in any application is a combination of parameters controlled by the manufacturer and controlled by the circuit.

Keeping the circuit parameters constant, the recovered charge of a given thyristor type is:

$$Q_{R(REC)} = f(I, V, \& 1/\tau_{eff}) \quad (15-B)$$

Where:

- I = Current rating for which the type was designed
 V = Highest voltage rating for which the type was designed
 $1/\tau_{eff}$ = Reciprocal of the effective lifetime of minority carrier silicon used in the particular device type

For a given current and voltage rating, the only design freedom left to the device designer is lifetime control. Since high frequency thyristors must have short turn-off

times, the τ_{eff} of these types is already controlled and low. The effective lifetimes of these types can be lowered further by several additional means in order to lower the recovered charge. It must be remembered that lifetime control is a trade-off. As lifetime is lowered, the on-state voltage increases and the on-state current rating is decreased.

With a given device type:

$$Q_{R(REC)} = f(T_{JX}, I_{TM}, \& -di/dt) \quad (15-C)$$

Where:

- T_{JX} = Instantaneous junction temperature at the end of on-state current flow
 I_{TM} = Peak on-state current (see Figure 15-5)
 $-di/dt$ = Rate of change of on-state current (see Figure 15-6)

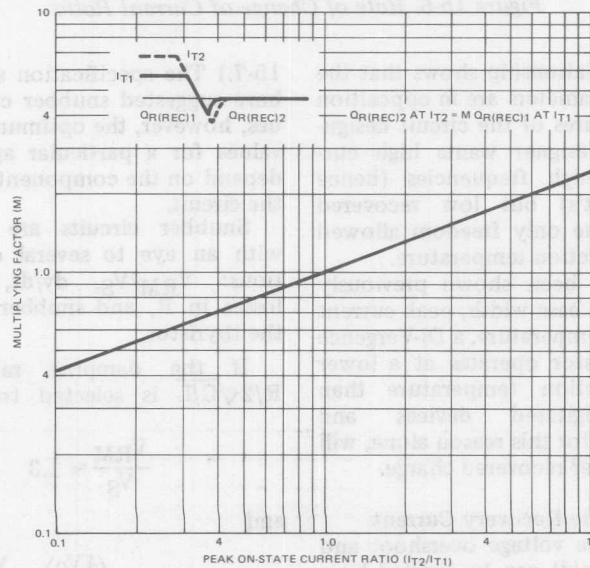


Figure 15-5. Peak On-State Current Ratio

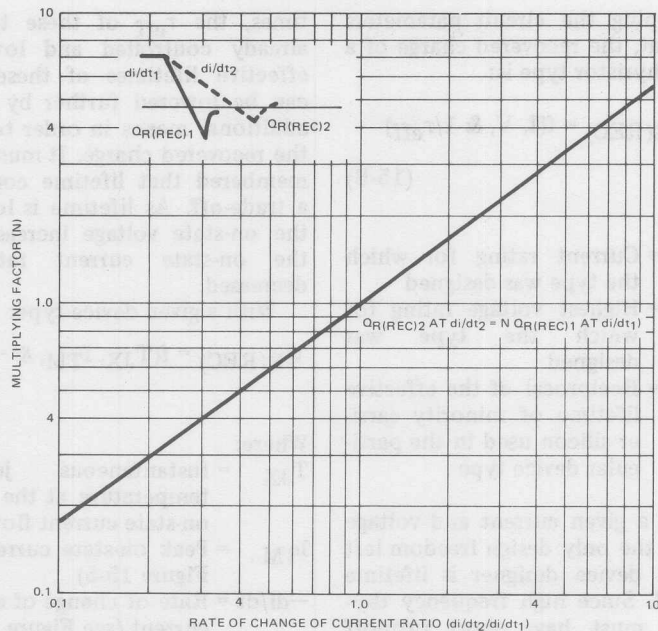


Figure 15-6. Rate of Change of Current Ratio

This relationship shows that the circuit parameters are in opposition to the desires of the circuit designer. The designer wants high currents at high frequencies (hence high di/dt 's) but low recovered charge. The only freedom allowed is peak junction temperature.

As has been shown previously for a given base width, peak current and case temperature, a Di-Vergence gate thyristor operates at a lower peak junction temperature than non-interdigitated devices and therefore, for this reason alone, will have a lower recovered charge.

Shape of the Recovery Current

Both the voltage overshoot and negative dv/dt can be limited by a snubber circuit. (Refer to Figure

15-7.) The specification sheet may have suggested snubber circuit values, however, the optimum snubber values for a particular application depend on the component values of the circuit.

Snubber circuits are designed with an eye to several considerations: V_{RM}/V_S , dv/dt , snubber losses in R , and snubber losses in the thyristor.

If the damping ratio $\zeta = R/2\sqrt{C/L}$ is selected to be 0.5:

$$\frac{V_{RM}}{V_S} \approx 1.3$$

and

$$dv/dt = \zeta \left(\frac{4V_S}{RC} \right) = \frac{V_S}{RC} \quad (15-D)$$

Where:

V_{RM} = Peak Reverse Voltage (V)
 V_S = Reverse Supply Voltage (V)
 C = Snubber Capacitance (μF)
 R = Snubber resistance (ohms)
 L = Effective circuit inductance (μH)

See Figure 15-7 for the snubber circuit and Figure 15-8 for wave-shapes.

If: $V_S = 600\text{V}$, $V_{SCR} = 1000\text{V}$,
 $dv/dt_{SCR} = 200\text{V}/\mu\text{s}$ and $L = 35\ \mu\text{H}$:

$$\zeta = 0.5 = \frac{R}{2} \sqrt{\frac{C}{L}} \quad \text{and} \quad \frac{200}{600} = \frac{1}{RC}$$

Hence:

$$R^2 C = 35 \quad \text{and} \quad RC = 3$$

$$R = 11.7\ \Omega \quad \text{and} \quad C = 0.257\ \mu\text{F}$$

Select 10 ohms and $0.25\ \mu\text{F}$.

Losses in Resistor during Recovery

This loss has been shown to be:

$$J_R = \frac{CV^2}{2} \left(1 + \frac{LI^2}{CV_S^2} \right) = \frac{CV^2}{2} (1 + \chi^2) \quad (15-E)$$

$$\chi^2 = \frac{LI^2}{CV_S^2} = \frac{4\zeta^2 I^2}{C \left(\frac{dv}{dt} \right)^2} \quad (15-F)$$

Where:

J_R = Energy dissipated in resistor during recovery

That is, these extra losses are proportional to the damping factor and inversely proportional to the dv/dt .

Losses during Turn-On

These have been shown as a first order approximation to be:

$$J_{THY} \approx \frac{CV^2}{2} \left(\frac{t_r}{t_r + t_s} \right) \quad (15-G)$$

$$J_{RES} \approx \frac{CV^2}{2} \left(\frac{t_s}{t_r + t_s} \right) \quad (15-H)$$

Where:

J_{THY} = Energy dissipated in thyristor during turn-on

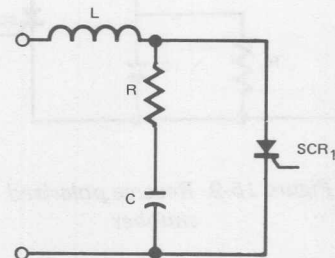
J_{RES} = Energy dissipated in resistor during turn-on

t_s = Snubber circuit time constant

= RC

t_r = Thyristor rise time

= $t_{on} - t_{delay}$



L = TOTAL EFFECTIVE CIRCUIT INDUCTANCE

Figure 15-7. Typical snubber circuit

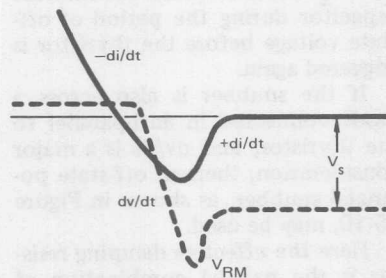


Figure 15-8. Recovery waveform

More simply, the loss is divided between the thyristor and resistor in proportion to their respective time constants.

If the thyristor loss at turn-on is found to be excessive, a polarized snubber may be considered to reduce the current supplied by the snubber during turn on.

If dv/dt is not a consideration, a reverse polarized snubber, as in Figure 15-9, may be used.

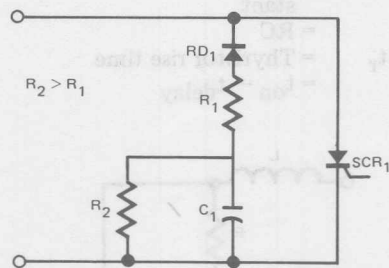


Figure 15-9. Reverse polarized snubber

Here the damping resistor R_1 is effective during reverse recovery and R_2 serves to bleed the snubber capacitor during the period of off-state voltage before the thyristor is triggered again.

If the snubber is also across a diode connected in anti-parallel to the thyristor, and dv/dt is a major consideration, then an off-state polarized snubber, as shown in Figure 15-10, may be used.

Here the effective damping resistor is the parallel combination of R_1 and R_2 , but the discharge resistor at turn-on is R_2 .

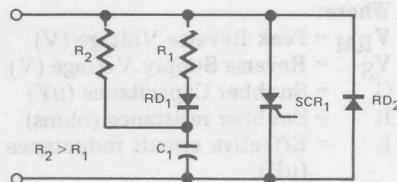


Figure 15-10. Off-state polarized snubber

There are two things to note: polarized snubbers do not reduce the turn-on losses, they only serve to reduce the loss in the resistor. It is not practical to design a polarized snubber across two thyristors connected in anti-parallel. A non-linear reactor may be used advantageously in this case to minimize the extra power loss resulting from the snubber during turn-on or reverse recovery. The arrangement is shown in Figure 15-11.

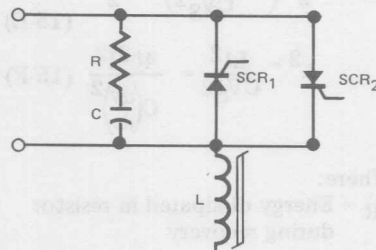


Figure 15-11. Unpolarized snubber with non-linear reactor

Symbols and Terms

The symbols and terms listed here are from EIA-NEMA Standard "Recommended Standards for Thyristors," June 1972 (EIA Standard RS-397 and NEMA Standard SK516-1972). Additional figures illustrating the symbols and some specific definitions are presented from International Rectifier's Application Note AN-313.

Classes of Thyristors

Thyristor

A bistable semiconductor device comprising three or more junctions, which can be switched from the off-state to the on-state or vice versa, such switching occurring within at least one quadrant of the principal voltage-current characteristic.

Reverse Blocking Diode Thyristor

A two-terminal thyristor which switches only for positive anode-to-cathode voltages and exhibits a reverse blocking state for negative anode-to-cathode voltages.

Reverse Blocking Triode Thyristor

A three-terminal thyristor which switches only for positive anode-to-cathode voltages and exhibits a reverse blocking state for negative anode-to-cathode voltages.

Reverse Conducting Diode Thyristor

A two-terminal thyristor which switches only for positive anode-to-cathode voltages and conducts large currents at negative anode-to-cathode voltages comparable to magnitude to the on-state voltages.

Reverse Conducting Triode Thyristor

A three-terminal thyristor which

switches only for positive anode-to-cathode voltages and conducts large currents at negative anode-to-cathode voltages comparable in magnitude to the on-state voltages.

Bidirectional Diode Thyristor

A two-terminal thyristor having substantially the same switching behavior in the first and third quadrants of the principal voltage-current characteristic.

Bidirectional Triode Thyristor

A three-terminal thyristor having substantially the same switching behavior in the first and third quadrants of the principal voltage-current characteristic.

Turn-Off Thyristor

A thyristor which can be switched from the on-state to the off-state and vice versa by applying control signals of appropriate polarities to the gate terminal, with the ratio of triggering power to triggered power appreciably less than one.

P-Gate Thyristor

A thyristor in which the gate terminal is connected to the P-region adjacent to the region to which the cathode terminal is connected and which is normally switched to the on-state by applying a positive signal between

the gate and cathode terminals. Standard production SCRs are P-gate thyristors.

N-Gate Thyristor

A thyristor in which the gate terminal is connected to the N-region adjacent to the region to which the anode terminal is connected and which is normally switched to the on-state by applying a negative signal between gate and anode terminals.

Semiconductor Controlled Rectifier (SCR)

An alternative name used for the reverse blocking triode thyristor.

Physical Structure Nomenclature

Electrode (of a semiconductor device)

An electric and mechanical contact to a region of a semiconductor device.

Anode

The electrode by which current enters the thyristor, when the thyristor is in the on-state with the gate open-circuited.

Note: This term does not apply to bidirectional thyristors.

Cathode

The electrode by which current leaves the thyristor, when the thyristor is in the on-state with the gate open-circuited.

Note: This term does not apply to bidirectional thyristors.

Gate

An electrode connected to one

of the semiconductor regions for introducing control current.

Junction (of a semiconductor device)

A region of transition between semiconductor regions of different electrical properties (e.g., n-n+, p-n, p-p+ semiconductors), or between a metal and a semiconductor.

Collector Junction

The junction across which the polarity of the voltage reverses when switching occurs.

Terminal (of a semiconductor device)

The externally available point of connection to one or more electrodes.

Main Terminals

The terminals through which the principal current flows.

Main Terminal 1 (of a bidirectional thyristor)

The main terminal which is named "1" by the device manufacturer.

Main Terminal 2 (of a bidirectional thyristor)

The main terminal which is named "2" by the device manufacturer.

Anode Terminal

The terminal which is connected to the anode.

Note: This term does not apply to bidirectional thyristors.

Cathode Terminal

The terminal which is connected to the cathode.

Note: This term does not apply to bidirectional thyristors.

Gate Terminal

A terminal which is connected to a gate.

Electrical Characteristic Terms

Principal Voltage-Current Characteristic (Principal Characteristic)

The function, usually represented graphically, relating the principal voltage to the principal current with gate current, where applicable, as a parameter.

Anode-to-Cathode Voltage-Current Characteristic (Anode Characteristic)

A function, usually represented graphically, relating the anode-to-cathode voltage to the principal current with gate current, where applicable, as a parameter.

Note: This term does not apply to bidirectional thyristors.

On-State

The condition of the thyristor corresponding to the low-resistance, low-voltage portion of the principal voltage-current characteristic in the switching quadrant(s).

Note: In the case of reverse conducting thyristors, this definition is applicable only for a positive anode-to-cathode voltage.

Off-State

The condition of the thyristor corresponding to the high-resistance, low-current portion of the principal voltage-current characteristic between the origin and the breakover point(s) in the switching quadrant(s).

Breakover Point

Any point on the principal voltage-current characteristic for which the differential resistance is zero and where the principal voltage reaches a maximum value.

Negative Differential Resistance Region

Any portion of the principal voltage-current characteristic in the switching quadrant(s) within which the differential resistance is negative.

Reverse Blocking State (of a reverse blocking thyristor)

The condition of a reverse blocking thyristor corresponding to the portion of the anode-to-cathode voltage-current characteristic for reverse currents of lower magnitude than the reverse breakdown current.

On-Impedance

The differential impedance between the terminals through which the principal current flows, when the thyristor is in the on-state at a stated operating point.

Principal Voltage

The voltage between the main terminals.

Notes:

1. In the case of the reverse blocking and reverse conducting thyristors, the principal voltage is called positive when the anode potential is higher than the cathode potential, and called negative when the anode potential is lower than the cathode potential.

2. For bidirectional thyristors, the polarity designation is arbitrary, and must be specified.

Anode-to-Cathode Voltage (Anode Voltage)

The voltage between the anode terminal and the cathode terminal.

Notes:

1. It is called a positive when the anode potential is higher than the cathode potential, and called negative when the anode potential is lower than the cathode potential.

2. This term does not apply to bidirectional thyristors.

Forward Voltage (of a reverse blocking or reverse conducting thyristor)

A positive anode-to-cathode voltage.

Off-State Voltage

The principal voltage when the thyristor is in the off-state.

Working Peak Off-State Voltage

The maximum instantaneous value of the off-state voltage which occurs across a thyristor, excluding all repetitive and nonrepetitive transient voltages.

Repetitive Peak Off-State Voltages

The maximum instantaneous value of the off-state voltage which occurs across a thyristor, including all repetitive transient voltages, but excluding all non-repetitive transient voltages.

Nonrepetitive Peak Off-State Voltage

The maximum instantaneous value of any nonrepetitive transient off-state voltage which occurs across the thyristor.

Critical Rate-of-Rise of Off-State Voltage

The minimum value of the rate-

of-rise of principal voltage which will cause switching from the off-state to the on-state.

Breakover Voltage

The principal voltage at the breakover point.

On-State Voltage

The principal voltage when the thyristor is in the on-state.

Minimum On-State Voltage

The minimum positive principal voltage for which the differential resistance is zero with the gate open-circuited.

Principal Current

A generic term for the current through the collector junction.

Note: It is the current through the main terminals.

On-State Current

The principal current when the thyristor is in the on-state.

Forward Current (of a reverse blocking or reverse conducting thyristor)

The principal current for a positive anode-to-cathode voltage.

Peak Repetitive On-State Current

The peak value of the on-state current including all repetitive transient currents.

Overload On-State Current

An on-state current of substantially the same waveshape as the normal on-state current and having a greater value than the normal on-state current.

Surge (Nonrepetitive) On-State Current

An on-state current of short-time duration and specified wave-shape.

Critical Rate-of-Rise of On-State Current

The maximum value of the rate-of-rise of on-state current which a thyristor can withstand without deleterious effect.

Off-State Current

The principal current when the thyristor is in the off-state.

Breakover Current

The principal current at the breakover point.

Holding Current

The minimum principal current required to maintain the thyristor in the on-state.

Reverse Voltage (of a reverse blocking or reverse conducting thyristor)

A negative anode-to-cathode voltage.

Working Peak Reverse Voltage (of a reverse blocking thyristor)

The maximum instantaneous value of the reverse voltage which occurs across the thyristor, excluding all repetitive and nonrepetitive transient voltages.

Repetitive Peak Reverse Voltage (of a reverse blocking thyristor)

The maximum instantaneous value of the reverse voltage which occurs across the thyristor, including all repetitive transient voltages, but excluding all nonrepetitive transient voltages.

Nonrepetitive Peak Reverse Voltage (of a reverse blocking thyristor)

The maximum instantaneous value of any nonrepetitive transient reverse voltage which occurs across a thyristor.

Reverse Breakdown Voltage (of a reverse blocking thyristor)

The value of negative anode-to-cathode voltage at which the differential resistance between the anode and cathode terminals changes from a high value to a substantially lower value.

Reverse Current (of a reverse blocking or reverse conducting thyristor)

The principal current for negative anode-to-cathode voltage.

Reverse Blocking Current (of a reverse blocking thyristor)

The reverse current when the thyristor is in the reverse blocking state.

Reverse Breakdown Current (of a reverse blocking thyristor)

The principal current at the reverse breakdown voltage.

Gate Voltage

The voltage between a gate terminal and a specified main terminal.

Gate Trigger Voltage

The gate voltage required to produce the gate trigger current.

Gate Nontrigger Voltage

The maximum gate voltage which will not cause the thyristor to switch from the off-state to the on-state.

Forward Gate Voltage

The voltage between the gate terminal and the terminal of an

adjacent region resulting from forward gate current.

Note: This term does not apply to bidirectional thyristors.

Reverse Gate Voltage

The voltage between the gate terminal and the terminal of an adjacent region resulting from reverse gate current.

Note: This term does not apply to bidirectional thyristors.

Gate Turn-Off Voltage (of a turn-off thyristor)

The gate voltage required to produce the gate turn-off current.

Gate Trigger Current

The minimum gate current required to switch a thyristor from the off-state to the on-state.

Gate Nontrigger Current

The maximum gate current which will not cause the thyristor to switch from the off-state to the on-state.

Forward Gate Current

The gate current when the junction between the gate region and the adjacent anode or cathode region is forward-biased.

Note: This term does not apply to bidirectional thyristors.

Reverse Gate Current

The gate current when the junction between the gate region and the adjacent anode or cathode region is reverse-biased.

Note: This term does not apply to bidirectional thyristors.

Gate Turn-Off Current (of a turn-off thyristor)

The minimum gate current re-

quired to switch a thyristor from the on-state to the off-state.

Thermal Resistance (of a semiconductor device)

The temperature difference between two specified points or regions divided by the power dissipation under conditions of thermal equilibrium.

Transient Thermal Impedance (of a semiconductor device)

The change of temperature difference between two specified points or regions at the end of a time interval divided by the step function change in power dissipation at the beginning of the same time interval causing the change of temperature difference.

Gate Controlled Turn-On Time

The time interval between a specified point at the beginning of the gate pulse and the instant when the principal voltage (current) has dropped (risen) to a specified low (high) value during switching of a thyristor from the off-state to the on-state by a gate pulse.

Gate Controlled Delay Time

The time interval between a specified point at the beginning of the gate pulse and the instant when the principal voltage (current) has dropped (risen) to a specified value near its initial value during switching of a thyristor from the off-state to the on-state by a gate pulse.

Gate Controlled Rise Time

The time interval between the instants at which the principal voltage (current) has dropped (risen) from a specified value near its initial value to a specified low (high)

Thyristor Letter Symbols*General Letter Symbols:*

Ambient Temperature . . .	T_A
Case Temperature	T_C
Virtual Junction Temperature	T_J
Storage Temperature . . .	T_{stg}
Thermal Resistance	R_θ
Junction-to-Ambient . .	$R_{\theta JA}$
Junction-to-Case	$R_{\theta JC}$
Case-to-Ambient	$R_{\theta CA}$
Transient Thermal Impedance	$Z_\theta(t)$
Junction-to-Ambient . .	$Z_{\theta JA}(t)$
Junction-to-Case	$Z_{\theta JC}(t)$
Delay Time	t_d
Rise Time	t_r
Fall Time	t_f
Reverse Recovery Time . .	t_{rr}
Gate-Controlled Turn-On Time	t_{gt}
Gate-Controlled Turn-Off Time	t_{gq}
Circuit-Commutated Turn-Off Time	t_q

Letter Symbol Subscripts

The following letters are used as qualifying subscripts for Thyristor Letter Symbols:

A-a	Anode
K-k	Cathode
G-g	Gate
R-r	Reverse or, as a Second Subscript, Repetitive
D-d	Off-State, Non-Trigger
T-t	On-State, Trigger
M-m	Maximum Value
MIN-min.	Minimum Value
AV-av	Average Value
RMS	Total RMS Value
W	Working
O-o	Open Circuit
S-s	Short Circuit, or as a Second Subscript, Non-Repetitive
X-x	Specified Circuit
H-h	Holding
(BR)	Breakdown
(BO)	Breakover
Q-q	Turn-Off, Recovery
(TO)	Threshold
(OV)	Overload

value during switching of a thyristor from the off-state to the on-state by a gate pulse.

Note: This time interval will be equal to the rise time of the on-state current only for pure resistive loads.

Gate Controlled Turn-Off Time (of a turn-off thyristor)

The time interval between a specified point at the beginning of the gate pulse and the instant when the principal current has decreased to a specified value during switching from the on-state to the off-state by a gate pulse.

Circuit-Commutated Turn-Off Time

The time interval between the instant when the principal current has decreased to zero after external switching of the principal voltage circuit, and the instant when the thyristor is capable of supporting a specified principal voltage without turning on.

Reverse Recovery Time (of a reverse blocking thyristor)

The time required for the principal current or voltage to recover to a specified value after instantaneous switching from an on-state to a reverse voltage or current.

Letter Symbol Table

QUANTITY	TOTAL RMS VALUE	DC VALUE, NO ALTERNATING COMPONENT	DC VALUE, WITH ALTERNATING COMPONENT	INSTANTANEOUS TOTAL VALUE	MAXIMUM (PEAK) TOTAL VALUE
On-State Current	$I_T(\text{RMS})$	I_T	$I_T(\text{AV})$	i_T	I_{TM}
Repetitive Peak On-State Current	—	—	—	—	I_{TRM}
Surge (Non-Repetitive) On-State Current	—	—	—	—	I_{TSM}
Overload On-State Current	—	—	—	—	$I_{T(OV)}$
Breakover Current	—	$I_{(BO)}$	—	$i_{(BO)}$	—
Off-State Current	$I_D(\text{RMS})$	I_D	$I_D(\text{AV})$	i_D	I_{DM}
Repetitive Peak Off-State Current	—	—	—	—	I_{DRM}
Reverse Current	$I_R(\text{RMS})$	I_R	$I_R(\text{AV})$	i_R	I_{RM}
Repetitive Peak Reverse Current	—	—	—	—	I_{RRM}
Reverse Breakdown Current	—	$I_{(BR)R}$	—	$i_{(BR)R}$	—
On-State Voltage	$V_T(\text{RMS})$	V_T	$V_T(\text{AV})$	v_T	V_{TM}
Breakover Voltage	—	$V_{(BO)}$	—	$v_{(BO)}$	—
Off-State Voltage	$V_D(\text{RMS})$	V_D	$V_D(\text{AV})$	v_D	V_{DM}

Letter Symbol Table (Continued)

QUANTITY	TOTAL RMS VALUE	DC VALUE, NO ALTERNATING COMPONENT	DC VALUE, WITH ALTERNATING COMPONENT	INSTANTANEOUS TOTAL VALUE	MAXIMUM (PEAK) TOTAL VALUE
Minimum On-State Voltage	—	$V_T(\text{MIN})$	—	—	—
Working Peak Off-State Voltage	—	—	—	—	V_{DWM}
Repetitive Peak Off-State Voltage	—	—	—	—	V_{DRM}
Non-Repetitive Peak Off-State Voltage	—	—	—	—	V_{DSM}
Reverse Voltage	$V_R(\text{RMS})$	V_R	$V_R(\text{AV})$	v_R	V_{RM}
Working Peak Reverse Voltage	—	—	—	—	V_{RWM}
Repetitive Peak Reverse Voltage	—	—	—	—	V_{RRM}
Non-Repetitive Peak Reverse Voltage	—	—	—	—	V_{RSM}
Reverse Breakdown Voltage	—	$V(\text{BR})R$	—	$v(\text{BR})R$	—
Holding Current	—	I_H	—	i_H	—
Latching Current	—	I_L	—	i_L	—
Gate Current	—	I_G	$I_G(\text{AV})$	i_G	I_{GM}

Letter Symbol Table (Continued)

QUANTITY	TOTAL RMS VALUE	DC VALUE, NO ALTERNATING COMPONENT	DC VALUE, WITH ALTERNATING COMPONENT	INSTANTANEOUS TOTAL VALUE	MAXIMUM (PEAK) TOTAL VALUE
Gate Trigger Current	—	I_{GT}	—	i_{GT}	I_{GTM}
Gate Non-Trigger Current	—	I_{GD}	—	i_{GQ}	I_{GDM}
Gate Turn-Off Current	—	I_{GQ}	—	i_{GQ}	I_{GQM}
Gate Voltage	—	V_G	$V_G(AV)$	v_G	V_{GM}
Gate Trigger Voltage	—	V_{GT}	—	v_{GT}	V_{GTM}
Gate Non-Trigger Voltage	—	V_{GD}	—	v_{GD}	V_{GDM}
Gate Turn-Off Voltage	—	V_{GQ}	—	v_{GQ}	V_{GQM}
Gate Power Dissipation	—	P_G	$P_G(AV)$	p_G	P_{GM}
Turn-On Dissipation	—	—	$P_{TT}(AV)$	p_{TT}	P_{TTM}
Turn-Off Dissipation	—	—	$P_{RO}(AV)$	p_{RO}	P_{ROM}

Specific Definitions Used in International Rectifier Data Sheets

ITSM *Peak One-Cycle Non-Recurrent Surge Current.* The maximum on-state current having a single half cycle (8.3 milliseconds) duration for a 60 Hz, single phase resistive load. The surge may be preceded and followed by maximum rated voltage, current, and junction temperature conditions and maximum allowable gate power may be concurrently dissipated. However, limitations with respect to on-state current during switching should not be exceeded.

I²t *I Squared t.* A measure of maximum on-state non-recurrent over-current capability for pulse durations between 1.5 and 8.3 milliseconds. I is in RMS amperes and t is pulse duration in seconds. (The same conditions as listed above for ITSM apply.)

IRQM *Peak Reverse Recovery Current.* The peak reverse current obtained when instantaneously switching from an on-state current to a reverse voltage in a given circuit.

VAM *Peak Anode Voltage.* The maximum instantaneous value of principal voltage which may be applied to the anode. If breakover occurs at this voltage or at some lower value, no damage to the SCR will result. If a higher voltage is applied and breakover occurs, the SCR may be damaged.

VTO *Turn-On Voltage.* The principal voltage at some specified principal current and at some specified time during the transition between the off-state and the on-state.

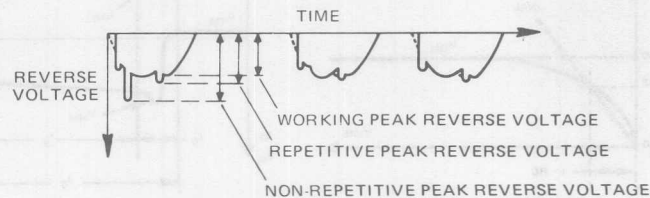


Figure 1. Reverse Voltage Symbols

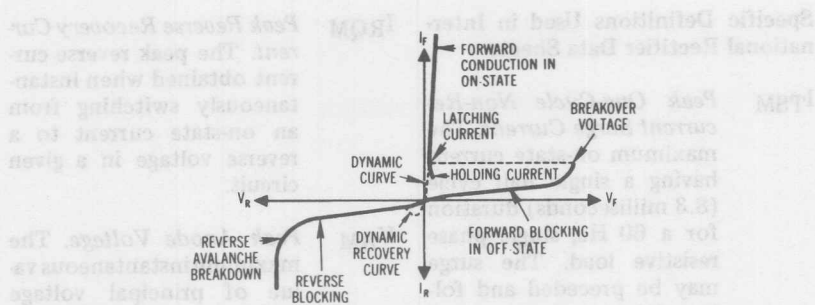


Figure 2. Instantaneous Forward and Reverse Characteristics (Reverse Blocking Thyristor)

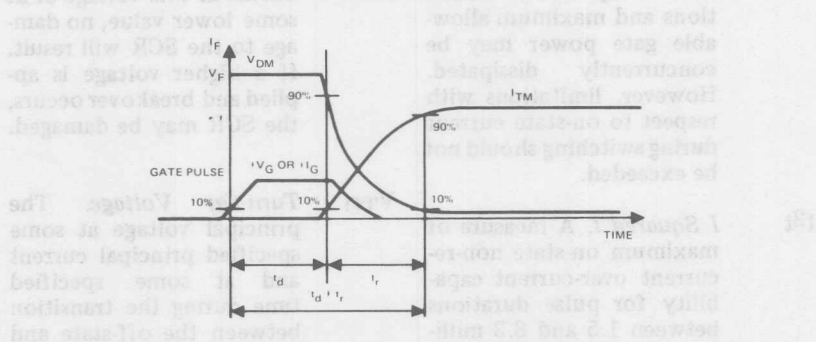


Figure 3. Anode Voltage and Current Waveforms During Turn-On Time Test

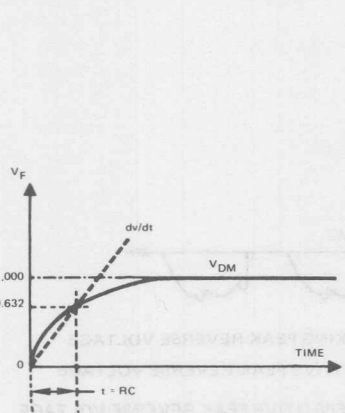


Figure 4. Anode Voltage Waveform During Critical dv/dt Test

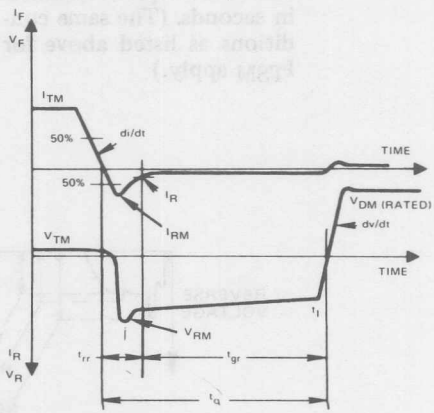
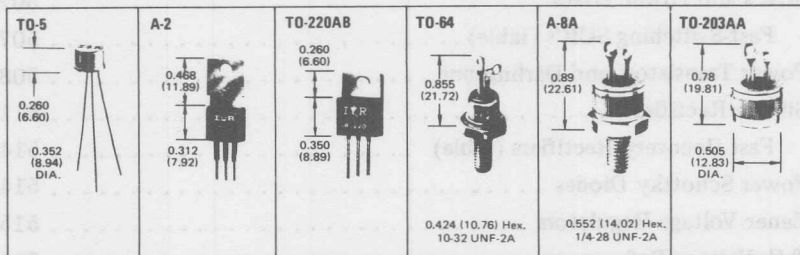


Figure 5. Anode Voltage and Current Waveforms During Turn-Off Time Test

Device Specifications

SCR's and Power Triacs	502
Fast-Switching SCR's (table)	507
Power Transistors and Darlingtons	508
Silicon Rectifiers	511
Fast Recovery Rectifiers (table)	514
Power Schottky Diodes	514
Zener Voltage Regulators	515
T.C. Voltage References	515
PACE/pak Circuits, AC Switches	519
Molded Circuit Assemblies	521
Selenium Rectifiers	524
Heat Exchangers, and Device Mounting Hardware	527
Opto-Electronic Devices	529
Semiconductor Protective Fuses	530

Silicon Controlled Rectifiers Power Triacs



International Rectifier offers a broad and growing range of SCR types and ratings to serve SCR users, with new series of SCRs being added to this edition for low, medium, high power and inverter applications.

INVERTER SERVICE SCRs are listed in a separate summary table on page 6, in addition to being defined by notes within the main tables.

POWER TRIACS are a series of high current triacs with the capability of AC or DC control.

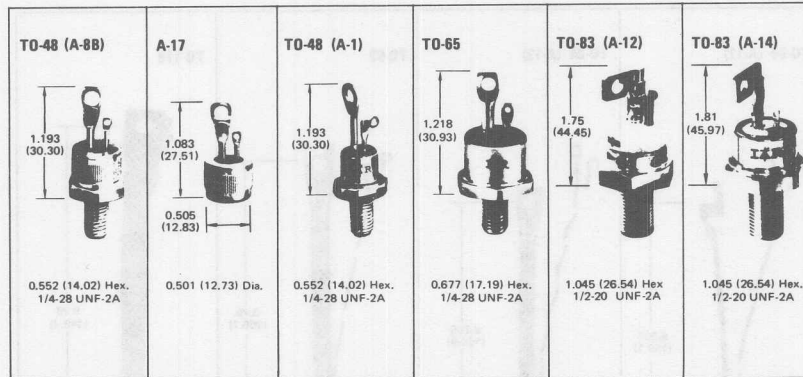
COMPANION SERIES are listed in the tables. They differ from the basic series only in case style and/or turn-off time.

BOLD FACE LISTINGS. Those series listed in heavier, bold face type are the more common International Rectifier series.

IT(RMS) (A)	1.8	1.8	1.8	1.8	1.8	1.8	4.0	4.7	4.7	7.4
IT(AV) (A) @ Max. T _C = (°C)	1.0 @ 80°	1.0 @ 80°	1.0 @ 85°	1.0 @ 85°	1.0 @ 85°	1.0 @ 85°	2.55 @ 80°	3.0 @ 80°	3.0 @ 105°	4.7 @ 80°
Max. I _{GT} @ 25°C (mA)	10	2	0.2	0.2	1	0.1	0.2	10	15	15
dv/dt (V/μs), typical	20	20	20	20	20	20	8	20	20	20
I _{TSM} (A)	15	15	15	15	10	15	25	25	40	60
Notes	①	①	①	①	①	①	①②	—	—	—
Case Style	T0-5	T0-5	T0-5	T0-5	T0-5	T0-5	A-2	T0-64	T0-64	T0-64
15 Volts	—	—	IR5U	2N2322	IR6U	2N4212	IR106D1	—	—	2N1770
25 Volts	—	—	—	—	—	—	—	—	—	—
30 Volts	—	—	—	—	—	—	IR106Y1	—	—	—
50 Volts	2N1595	2N1595A	IR5F	2N2323	IR6F	2N4213	IR106F1	2N1600	—	2N1771
100 Volts	2N1596	2N1596A	IR5A	2N2324	IR5A	2N4214	IR106A1	2N1601	3RC10A	2N1772
150 Volts	—	—	IR5G	2N2325	IR6G	2N4215	—	—	—	2N1773
200 Volts	2N1597	2N1597A	IR5B	2N2326	IR6B	2N4216	IR106B1	2N1602	3RC20A	2N1774
250 Volts	—	—	IR5H	2N2327	IR6H	2N4217	—	—	—	2N1775
300 Volts	2N1598	2N1598A	IR5C	2N2328	IR6C	2N4218	IR106C1	2N1603	3RC30A	2N1776
400 Volts	2N1599	2N1599A	IR5D	2N2329	IR6D	2N4219	IR106D1	2N1604	3RC40A	2N1777
500 Volts	—	—	—	—	—	—	—	—	3RC50A	2N1778
600 Volts	—	—	—	—	—	—	—	—	3RC60A	2N2619

IT(RMS) (A)	7.4	7.4	8.0	16	16	25	25	25	25	25
IT(AV) (A) @ Max. T _C = (°C)	4.7 @ 80°	4.7 @ 105°	5.1 @ 85°	10 @ 35°	10 @ 80°	16 @ 45°	16 @ 65°	16 @ 95°	16 @ 95°	16 @ 95°
Max. I _{GT} @ 25°C (mA)	15	15	25	90	75	90	40	25	25	25
dv/dt (V/μsec), typical	20	20	50 (min.)	20	20	10 (min.)	20	20	20	20
I _{TSM} (A)	75	60	80	125	125	200	150	250	250	250
Notes	—	①	—	—	—	—	†	—	—	—
Case Style	T0-64	T0-64	T0-200AB	T0-48	T0-48	T0-48	T0-48	A-8A	A-88	T0-203AA
25 Volts	—	2N1770A	—	2N1842	2N1842A	—	2N681	IR30U	IR30U2	IR32U
50 Volts	—	2N1771A	IR122F	2N1843	2N1843A	—	2N682	IR30F	IR30F2	IR32F
100 Volts	5RC10A	2N1772A	IR122A	2N1844	2N1844A	10RC10A	2N683	IR30A	IR30A2	IR32A
150 Volts	—	2N1773A	—	2N1845	2N1845A	—	2N684	—	—	—
200 Volts	5RC20A	2N1774A	IR122B	2N1846	2N1846A	10RC20A	2N685	IR30B	IR30B2	IR32B
250 Volts	—	—	—	2N1847	2N1847A	—	2N686	—	—	—
300 Volts	5RC30A	2N1775A	IR122C	2N1848	2N1848A	10RC30A	2N687	IR30C	IR30C2	IR32C
400 Volts	5RC40A	2N1776A	IR122D	2N1849	2N1849A	10RC40A	2N688	IR30D	IR30D2	IR32D
500 Volts	5RC50A	5RC50B	—	2N1850	2N1850A	10RC50A	2N689	IR30E	IR30E2	IR32E
600 Volts	5RC60A	5RC60B	—	—	—	10RC60A	2N690	—	—	—
700 Volts	—	—	—	—	—	10RC70A	2N691	—	—	—
800 Volts	—	—	—	—	—	10RC80A	—	—	—	—
1000 Volts	—	—	—	—	—	10RC100A	—	—	—	—
1100 Volts	—	—	—	—	—	10RC110A	—	—	—	—
1200 Volts	—	—	—	—	—	10RC120A	—	—	—	—

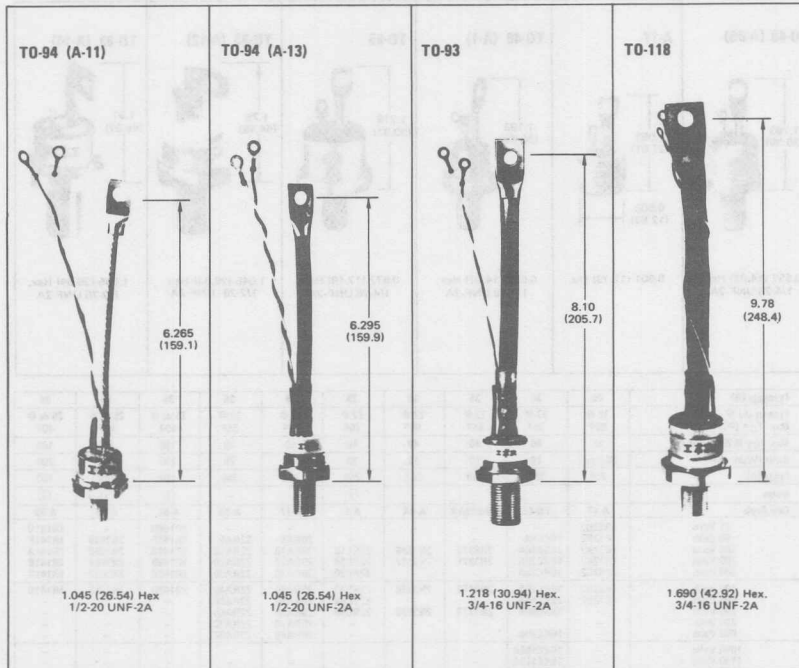
Silicon Controlled Rectifiers Power Triacs



I _T (RMS) (A)	25	35	35	35	35	35	35	35	35	35
I _T (AV) (A) @ Max. T _C = (°C)	16 @ 85°	22 @ 35°	22 @ 65°	22 @ 65°	22 @ 70°	22 @ 85°	22 @ 85°	25 dc @ 40°	25 dc @ 40°	25 dc @ 40°
Max. I _{GT} @ 25°C (mA)	25	40	40	40	40	40	40	180	180	180
dv/dt (V/μs), min.	20 (typ.)	10	10	10	20	20	20	200	200	200
I _{TSM} (A)	250	300	350	350	250	350	350	180	180	180
Notes	—	—	—	—	①	—	—	①	①	①
Case Style	A-17	TO-48	TO-203AA	A-8A	A-1	A-17	A-8B	A-8B	A-8B	A-8B
25 Volts	IR32U2	—	—	—	—	—	—	—	IR140U	—
50 Volts	IR32F2	16RC5A	—	—	—	20RA5	22RA5	IR140F	2N3649	IR141U
100 Volts	IR32A2	16RC10A	2N3870	2N3896	22RC10	20RA10	22RA10	IR140A	2N3650	IR141F
200 Volts	IR32B2	16RC20A	2N3871	2N3897	22RC20	20RA20	22RA20	IR140B	2N3651	IR141B
300 Volts	IR32C2	16RC30A	—	—	22RC30	20RA30	22RA30	IR140C	2N3652	IR141C
400 Volts	IR32D2	16RC40A	2N3872	2N3898	22RC40	20RA40	22RA40	IR140D	2N3653	IR141D
500 Volts	IR32E2	16RC50A	—	—	22RC50	20RA50	22RA50	—	—	—
600 Volts	—	16RC60A	2N3873	2N3899	—	20RA60	22RA60	—	—	—
700 Volts	—	—	—	—	—	20RA70	22RA70	—	—	—
800 Volts	—	16RC80A	—	—	—	20RA80	22RA80	—	—	—
1000 Volts	—	16RC100A	—	—	—	—	—	—	—	—
1100 Volts	—	16RC110A	—	—	—	—	—	—	—	—
1200 Volts	—	16RC120A	—	—	—	—	—	—	—	—

I _T (RMS) (A)	35	63	80	80	80	80	110	110	110	110
I _T (AV) (A) @ Max. T _C = (°C)	25 dc @ 40°	40 @ 87°	50 @ 75°	50 @ 75°	50 @ 80°	50 @ 105°	70 @ 62°	70 @ 62°	70 @ 62°	70 @ 65°
Max. I _{GT} @ 25°C (mA)	180	110	70	200	110	200	70	70	110	150
dv/dt (V/μs), min.	200	20	20	200	25	4	20	20 (typ.)	20	200
I _{TSM} (A)	180	1,000	1,000	1,200	1,200	1,000	1,200	1,000	1,000	1,200
Companion Series	—	—	37RC-A	37RA	—	37REH	72RC-A	—	—	72RB
Notes	①	—	④	③	—	⑤	④	†	†	③
Case Style	A-8B	TO-45	A-13	A-11	TO-65	A-11	A-13	A-13	A-11	A-11
25 Volts	—	—	—	—	—	—	—	—	—	—
50 Volts	2N3654	40RC55	—	—	50RC55	—	—	2N1909	—	—
100 Volts	2N3655	40RC10	36RC10A	—	50RC10	—	71RC10A	2N1910	—	—
150 Volts	—	—	—	—	—	—	—	2N1911	—	—
200 Volts	2N3656	40RC20	36RC20A	—	50RC20	—	71RC20A	2N1912	—	—
250 Volts	—	—	—	—	—	—	—	2N1913	—	—
300 Volts	—	—	—	—	—	—	—	2N1914	—	—
400 Volts	2N3657	40RC30	36RC30A	—	50RC30	—	71RC30A	2N1915	—	—
500 Volts	2N3658	40RC40	36RC40A	—	50RC40	—	71RC40A	2N1916	—	—
600 Volts	—	40RC50	36RC50A	36RA50	50RC50	—	71RC50A	2N1805	—	71RB50
700 Volts	—	40RC50	36RC60A	36RA60	50RC60	36REH60	71RC60A	2N1806	2N3091	71RB60
800 Volts	—	40RC70	—	—	50RC70	—	—	2N1807	2N3092	—
900 Volts	—	40RC80	36RC80A	36RA80	50RC80	36REH80	71RC80A	—	2N3093	71RB80
1000 Volts	—	—	—	—	50RC90	—	—	—	2N3094	—
1100 Volts	—	40RC100	—	36RA100	50RC100	36REH100	—	—	2N3095	71RB100
1200 Volts	—	40RC110	—	36RA110	50RC110	36REH110	—	—	2N3096	71RB110
1300 Volts	—	40RC120	—	36RA120	50RC120	36REH120	—	—	—	71RB120
1400 Volts	—	—	—	36RA130	—	36REH130	—	—	—	71RB130
1500 Volts	—	—	—	36RA140	—	—	—	—	—	71RB140
1600 Volts	—	—	—	36RA150	—	—	—	—	—	71RB150
1600 Volts	—	—	—	36RA160	—	—	—	—	—	71RB160

Silicon Controlled Rectifiers Power Triacs



I_T (RMS) (A)	110	110	110	110	110	125	125	125	150	160
I_T (AV) (A) @ Max. $T_C = 100^\circ\text{C}$	70 @ 65°	70 @ 80°	70 @ 85°	70 @ 85°	70 @ 105°	80 @ 70°	80 @ 70°	80 @ 85°	95 @ 65°	100 @ 80°
I_{GT} @ 25°C (mA)	70	150	70	70	150	150	150	150	150	250
dv/dt (V/μs), min.	20 (typ.)	200	20	20 (typ.)	50	200	200	200	200	200
I_{TSM} (A)	1,000	1,600	1,000	1,000	1,400	1,600	1,600	1,800	1,800	2,500
Companion Series	—	72RA	72RC-B	—	72REH	82RLB	82RM/8182RL	82RLA	S2RM/8182RL	—
Notes	†	①	① ①	① †	① †	① ① ①	① ① ① ①	① ①	① ① ①	—
Case Style	A-14	A-11	A-13	A-13	A-11	A-11	A-11	A-11	A-11	TO-93
25 Volts	—	—	71RC2B	2N2023	—	—	—	—	—	—
50 Volts	2N1792	—	71RC5B	2N2024	—	—	—	—	—	—
100 Volts	2N1793	—	71RC10B	2N2025	—	—	81RM10	—	91RM10	—
150 Volts	2N1794	—	71RC15B	2N2026	—	—	—	—	—	—
200 Volts	2N1795	—	71RC20B	2N2027	—	—	81RM20	—	91RM20	—
250 Volts	2N1796	—	71RC25B	2N2028	—	—	—	—	—	—
300 Volts	2N1797	—	71RC30B	2N2029	—	—	81RM30	—	91RM30	—
400 Volts	2N1798	—	71RC40B	2N2030	—	—	81RM40	—	91RM40	—
500 Volts	2N1799	71RA50	71RC50B	—	—	81RLB50	81RM50	81RLA50	91RM50	101RA50
600 Volts	2N1800	71RA60	71RC60B	—	71REH60	81RLB60	81RM60	81RLA60	91RM60	101RA60
700 Volts	2N1801	—	—	—	—	—	—	—	—	—
800 Volts	2N1802	71RA80	—	—	71REH80	81RLB80	81RM80	81RLA80	—	101RA80
900 Volts	2N1803	—	—	—	—	—	—	—	—	—
1000 Volts	2N1804	71RA100	—	—	71REH100	81RLB100	81RM100	81RLA100	—	101RA100
1100 Volts	—	71RA110	—	—	71REH110	81RLB110	—	81RLA110	—	101RA110
1200 Volts	—	71RA120	—	—	71REH120	81RLB120	—	81RLA120	—	101RA120
1300 Volts	—	71RA130	—	—	71REH130	—	—	—	—	101RA130
1400 Volts	—	71RA140	—	—	—	—	—	—	—	101RA140
1500 Volts	—	71RA150	—	—	—	—	—	—	—	101RA150
1600 Volts	—	71RA160	—	—	—	—	—	—	—	101RA160

Silicon Controlled Rectifiers Power Triacs

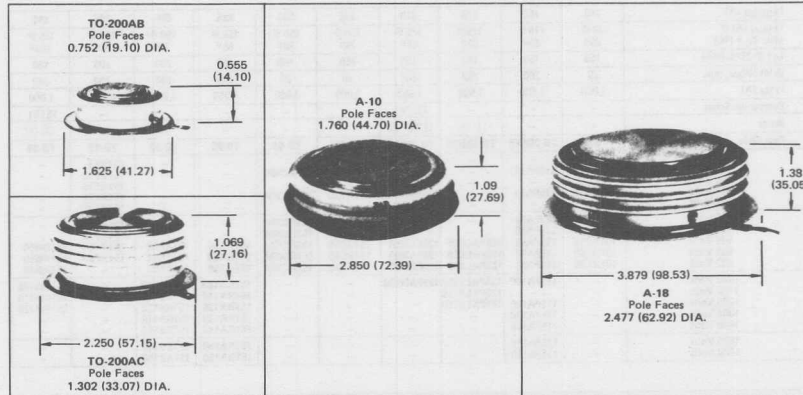
IT(RMS) (A)	160	180	210	210	235	235	235	235	235	245
IT(AV) (A) @ Max. T _C = (°C)	100 @ 80°	115 @ 85°	135 @ 85°	135 @ 85°	150 @ 70°	150 @ 80°	150 @ 85°	150 @ 75°	150 @ 90°	155 @ 180°
I _{GT} @ 25°C (mA)	150	150	150	150	150	150	150	200	200	150
dv/dt (V/μs), min.	20	200	200	200	20	20	200	200	200	200
ITSM (A)	2,000	1,600	1,600	1,600	3,000	3,500	4,250	3,300	4,250	4,000
Companion Series	—	—	—	12SPAL	—	—	—	—	—	151RL
Notes	—	—	① ④	① ④ ⑤	—	—	—	—	③	① ④
Case Style	TO-93	TO-200AB	TO-200AB	TO-200AB	TO-93	TO-93	TO-93	TO-93	TO-93	TO-93
50 Volts	—	—	—	—	—	—	—	—	—	—
100 Volts	101RC10	115PA10	—	125PAM10	151RC10	151RC10A	—	—	151RF5	—
150 Volts	—	—	—	—	—	—	—	—	151RF10	—
200 Volts	101RC20	115PA20	—	125PAM20	151RC20	151RC20A	—	—	151RF15	—
250 Volts	—	—	—	—	—	—	—	—	151RF20	—
300 Volts	101RC30	115PA30	—	125PAM30	151RC30	151RC30A	—	—	151RF30	—
400 Volts	101RC40	115PA40	—	—	151RC40	151RC40A	—	—	151RF40	—
500 Volts	101RC50	115PA50	125PALB50	125PAM50	151RC50	151RC50A	151RA50	151RB50	151RF50	151RM50
600 Volts	101RC60	115PA60	125PALB60	125PAM60	151RC60	151RC60A	151RA60	151RB60	151RF60	151RM60
800 Volts	101RC80	115PA80	125PALB80	125PAM80	151RC80	151RC80A	151RA80	151RB80	151RF80	151RM80
1000 Volts	—	115PA100	125PALB100	125PAM100	—	—	151RA100	151RB100	—	151RM100
1100 Volts	—	—	125PALB110	—	—	—	151RA110	151RB110	—	151RM110
1200 Volts	—	115PA120	125PALB120	—	—	—	151RA120	151RB120	—	151RM120
1300 Volts	—	115PA130	—	—	—	—	151RA130	151RB130	—	—
1400 Volts	—	115PA140	—	—	—	—	151RA140	151RB140	—	—
1500 Volts	—	115PA150	—	—	—	—	151RA150	151RB150	—	—
1600 Volts	—	115PA160	—	—	—	—	151RA160	151RB160	—	—

IT(RMS) (A)	250	275	275	285	400	400	400	400	450	455
IT(AV) (A) @ Max. T _C = (°C)	160 @ 65°	175 @ 85°	175 @ 90°	180 @ 75°	250 @ 65°	250 @ 75°	250 @ 70°	255 @ 65°	285 @ 70°	285 @ 65°
I _{GT} @ 25°C (mA)	150	200	150	150	150	150	150	150	150	150
dv/dt (V/μs), min.	200	200	200	200	20	100	200	200	200	200
ITSM (A)	1,800	3,300	5,000	4,500	4,000	6,500	4,250	4,000	8,000	4,500
Companion Series	140PAL	—	—	161RL	—	—	—	240PAL	250RL	250PAL
Notes	① ④	—	—	① ④	—	—	—	① ④	① ④	① ④
Case Style	TO-200AB	TO-200AB	TO-93	TO-93	TO-200AB	TO-118	TO-200AB	TO-200AB	TO-118	TO-200AB
100 Volts	140PAM10	—	—	161RM10	250PAC10	250RA10	—	240PAM10	—	250PAM10
200 Volts	140PAM20	—	—	161RM20	250PAC20	250RA20	—	240PAM20	—	250PAM20
300 Volts	140PAM30	—	—	161RM30	250PAC30	250RA30	—	240PAM30	—	250PAM30
400 Volts	140PAM40	—	—	161RM40	250PAC40	250RA40	—	240PAM40	—	250PAM40
500 Volts	140PAM50	175PA50	175RA50	161RM50	250PAC50	250RA50	250PA50	240PAM50	—	250PAM50
600 Volts	140PAM60	175PA60	175RA60	161RM60	250PAC60	250RA60	250PA60	240PAM60	250RM60	250PAM60
800 Volts	—	175PA80	175RA80	—	—	250RA80	250PA80	240PAM80	250RM80	—
1000 Volts	—	175PA100	175RA100	—	—	250RA100	250PA100	240PAM100	250RM100	—
1100 Volts	—	175PA110	175RA110	—	—	250RA110	250PA110	—	250RM110	—
1200 Volts	—	175PA120	175RA120	—	—	250RA120	250PA120	—	250RM120	—
1300 Volts	—	175PA130	—	—	—	250RA130	250PA130	—	—	—
1400 Volts	—	175PA140	—	—	—	250RA140	250PA140	—	—	—
1500 Volts	—	175PA150	—	—	—	250RA150	250PA150	—	—	—
1600 Volts	—	175PA160	—	—	—	250RA160	250PA160	—	—	—
1700 Volts	—	—	—	—	—	250RA170	—	—	—	—

IT(RMS) (A)	470	470	470	470	550	660	710	740	785	785
IT(AV) (A) @ Max. T _C = (°C)	300 @ 77°	300 @ 70°	300 @ 75°	300 @ 75°	350 @ 80°	420 @ 65°	450 @ 67°	470 @ 65°	500 @ 65°	500 @ 65°
I _{GT} @ 25°C (mA)	150	150	150	150	150	150	150	150	150	150
dv/dt (V/μs), min.	200	20	100	100	100	100	200	100	500	500
ITSM (A)	5,500	5,000	8,000	7,000	8,000	6,500	8,000	7,000	7,500	7,500
Companion Series	—	—	—	—	—	—	420PBL	—	—	—
Notes	—	—	—	—	—	—	① ④	—	① ④	① ④
Case Style	TO-200AB	TO-200AB	TO-118	TO-118	TO-118	TO-200AC	TO-200AC	TO-200AC	TO-200AC	TO-200AC
100 Volts	—	300PAC10	300RA10	300RB10	350RA10	—	—	—	—	—
200 Volts	—	300PAC20	300RA20	300RB20	350RA20	—	—	—	—	—
300 Volts	—	300PAC30	300RA30	300RB30	350RA30	—	—	—	—	—
400 Volts	—	300PAC40	300RA40	300RB40	350RA40	—	—	—	—	—
500 Volts	300PA50	300PAC50	300RA50	300RB50	350RA50	420PB50	420PB50	470PB50	500PB050	501PB050
600 Volts	300PA60	300PAC60	300RA60	300RB60	350RA60	420PB60	420PB60	470PB60	500PB060	501PB060
800 Volts	300PA80	—	300RA80	300RB80	350RA80	420PB80	420PB80	470PB80	500PB080	501PB080
1000 Volts	300PA100	—	300RA100	300RB100	350RA100	420PB100	420PB100	470PB100	500PB100	501PB100
1100 Volts	300PA110	—	300RA110	300RB110	350RA110	420PB110	420PB110	470PB110	500PB110	501PB110
1200 Volts	300PA120	—	300RA120	300RB120	350RA120	420PB120	420PB120	470PB120	500PB120	501PB120
1300 Volts	—	—	300RA130	300RB130	350RA130	420PB130	—	470PB130	—	—
1400 Volts	—	—	300RA140	300RB140	350RA140	420PB140	—	470PB140	—	—
1500 Volts	—	—	300RA150	300RB150	350RA150	420PB150	—	470PB150	—	—
1600 Volts	—	—	300RA160	300RB160	350RA160	420PB160	—	470PB160	—	—
1700 Volts	—	—	300RA170	300RB170	350RA170	420PB170	—	470PB170	—	—

Silicon Controlled Rectifiers

Power Triacs



I _T (RMS) (A)	785	865	950	1100	1180	1350	1420	1600	1875	2500
I _T (AV) (A) @ Max. T _C = (°C)	500 @ 65°	550 @ 65°	600 @ 75°	700 @ 75°	750 @ 72°	850 @ 75°	900 @ 72°	1000 @ 75°	1200 @ 75°	1600 @ 75°
I _{GT} @ 25°C (mA)	150	150	150	150	150	150	150	150	150	150
dv/dt (V/μs), min.	500	100	100	200	100	200	100	200	200	200
I _{TSM} (A)	7,500	8000	10,000	14,000	11,000	16,000	13,000	20,000	26,000	35,000
Companion Series	—	—	—	—	—	—	—	—	—	—
Notes	(3) ††	—	(6)	(6)	(6)	(6)	(6)	(6)	(6)	(6)
Case Style	TO-200AC	TO-200AC	TO-200AC	A-10	TO-200AC	A-10	TO-200AC	A-10	A-18	A-18
100 Volts	550PB010	—	—	—	—	—	—	—	—	—
200 Volts	550PB020	—	—	—	—	—	—	—	—	—
300 Volts	550PB030	—	—	—	—	—	—	—	—	—
400 Volts	550PB040	—	—	—	—	—	—	—	—	—
500 Volts	550PB050	550PB50	—	700PK50	—	850PK50	900PB50	1000PK50	1200PN50	1600PN50
600 Volts	550PB060	550PB60	—	700PK60	—	850PK60	900PB60	1000PK60	1200PN60	1600PN60
800 Volts	—	550PB80	—	700PK80	—	850PK80	900PB80	1000PK80	1200PN80	1600PN80
1000 Volts	—	550PB100	—	700PK100	—	850PK100	900PB100	1000PK100	1200PN100	1600PN100
1100 Volts	—	550PB110	—	700PK110	750PB110	850PK110	900PB110	1000PK110	1200PN110	1600PN110
1200 Volts	—	550PB120	—	700PK120	750PB120	850PK120	900PB120	1000PK120	1200PN120	1600PN120
1300 Volts	—	550PB130	—	700PK130	750PB130	850PK130	—	1000PK130	1200PN130	1600PN130
1400 Volts	—	550PB140	—	700PK140	750PB140	850PK140	—	1000PK140	1200PN140	1600PN140
1500 Volts	—	550PB150	—	700PK150	750PB150	850PK150	—	1000PK150	1200PN150	1600PN150
1600 Volts	—	550PB160	—	700PK160	750PB160	850PK160	—	1000PK160	1200PN160	1600PN160
1700 Volts	—	550PB170	600PB170	700PK170	750PB170	850PK170	—	1000PK170	1200PN170	—
1800 Volts	—	—	600PB180	700PK180	750PB180	850PK180	—	1000PK180	1200PN180	—
1900 Volts	—	—	600PB190	700PK190	—	850PK190	—	—	1200PN190	—
2000 Volts	—	—	600PB200	700PK200	—	850PK200	—	—	1200PN200	—
2100 Volts	—	—	600PB210	700PK210	—	—	—	—	1200PN210	—
2200 Volts	—	—	600PB220	700PK220	—	—	—	—	1200PN220	—
2300 Volts	—	—	600PB230	700PK230	—	—	—	—	1200PN230	—
2400 Volts	—	—	600PB240	700PK240	—	—	—	—	1200PN240	—
2500 Volts	—	—	600PB250	700PK250	—	—	—	—	1200PN250	—

NOTES:

- Current drawn by 1,000Ω shunt resistor not included in max. I_{GT} rating.
- Other bent and modified pin and tab configurations readily available.
- Inverter series. If shown, companion series ending with L has longer t_q.
- Companion series uses flag terminal case A-14.
- Companion series uses flag terminal case A-12.
- Has ACE gate construction for high di/dt.
- Dv/dt at higher T_J = 150°C.
- Companion series available to 1200 Volts.
- Companion series has sensitive 200 mA I_{GT}.
- IR's exclusive power logic triacs. AC or DC control available, depending on gate polarity.
- Has Di-Vergence gate for highest di/dt.
- JAN types available.

POWER TRIACS

I _T (RMS) (A)	50	60	100	200	200	
I _T (AV) (A) @ Max. T _C = (°C)	—	85°	85°	75°	65°	65°
I _{GT} @ 25°C (mA)	500	500	500	500	500	500
dv/dt (V/μs), min.	200	50	50	50	50	50
I _{TSM} (A)	400	700	900	1,300	1,300	1,300
Companion Series	50AC-A	61AC	101AC	—	—	—
Notes	(1)	(3)(6)	(6)	(6)	(6)	(6)
Case Style	TO-65	A-11	TO-94	TO-93	TO-93	TO-93
400 Volts	50AC40	60AC40	100AC40	200AC40	2N5257	2N5258
600 Volts	50AC60	60AC60	100AC60	200AC60	2N5258	2N5258
800 Volts	50AC80	60AC80	100AC80	200AC80	2N5259	2N5259
1000 Volts	50AC100	60AC100	100AC100	200AC100	2N5260	2N5260
1200 Volts	50AC120	—	—	—	—	—

Silicon Controlled Rectifiers Power Triacs

SCRs FOR INVERTER SERVICE

There is an ever-increasing number of inverter circuits which demand more sophisticated devices operating under more stringent dynamic circuit conditions. Many IR devices are designed, custom built, and tested to meet these demanding applications. In addition, units may be selected for specific parameters from standard product runs.

The table below includes IR series specifically designed for inverter service. In specific cases, the second letter of the part number code is changed to indicate a change in t_q rating.

For the best solution to your problems in standard, selected, or custom devices, contact your local IR Distributor, or local IR Field Office, or IR's El Segundo offices.

SILICON CONTROLLED RECTIFIERS FOR INVERTER SERVICE

MAX. CURRENT RMS (A)	VOLTAGE RANGE	MAX. TURN-OFF TIME $t_q = \mu s$	dv/dt (V/ μs)	CASE	IR SERIES
35	50-600	10	200	A-8B	IR141
35	50-400	10	200	A-8B	2N3654-58
35	50-600	15	200	A-8B	IR140
35	50-400	15	200	A-8B	2N3649-53
125	100-1000	20	200	TO-94 (A-11)	81/82RM
125	100-1200	30	200	TO-94 (A-11)	81/82RL
125	500-1200	40	200	TO-94 (A-11)	81/82RLB
150	100-600	10	200	TO-94 (A-11)	91/92RM
150	100-600	20	200	TO-94 (A-11)	91/92RL
160	100-1200	20	200	TO-200AB	100PAM
160	100-1200	30	200	TO-200AB	100PAL
210	100-1200	20	200	TO-200AB	125PAM
210	100-1200	30	200	TO-200AB	125PAL
210	500-1200	40	200	TO-200AB	125PALB
235	50-600	20	200	TO-93	151RF
245	100-1200	20	200	TO-93	151RM
245	100-1200	30	200	TO-93	151RL
250	100-600	10	200	TO-200AB	140PAM
250	100-600	20	200	TO-200AB	140PAL
285	100-600	10	200	TO-93	161RM
285	100-600	20	200	TO-93	161RL
400	100-1200	25	200	TO-200AB	240PAM
400	100-1200	30	200	TO-200AB	240PAL
450	600-1200	40	200	TO-118	250RM
450	600-1200	60	200	TO-118	250RL
455	100-600	10	200	TO-200AB	250PAM
455	100-600	20	200	TO-200AB	250PAL
660	600-1200	40	200	TO-200AC	420PBM
660	600-1200	60	200	TO-200AC	420PBL
785	100-600	15	500	TO-200AC	550PBQ
785	500-1200	30	500	TO-200AC	501PBQ
785	500-1200	40	500	TO-200AC	500PBQ

CROSS REFERENCE OF OBSOLETE PART NUMBERS TO NEW PART NUMBERS

The following part numbers have been discontinued since the previous edition of this Product Locator.

OLD PART NUMBER	REPLACED BY	MAJOR DIFFERENCES OF REPLACEMENT PART TO ORIGINAL	OLD PART NUMBER	REPLACED BY	MAJOR DIFFERENCES OF REPLACEMENT PART TO ORIGINAL
35RCS-A*	37RC-A	1/2-20 threaded stud, flag cathode terminal	420PA	420PB	None: Change of nomenclature
36RCS-A*	36RC-A	1/2-20 threaded stud	450PF	550PBQ-S52	Di-Vergence Gate (higher di/dt)
51RCG	61RM-S54	ACE gate (higher di/dt)	451PF	550PBQ-S52	Di-Vergence Gate, 1 inch thick ceramic case (higher di/dt)
52RCG	62RM-S54	ACE gate (higher di/dt)	470PA	550PB	None: Change of nomenclature
71RCG	91RL-S53	ACE gate (higher di/dt)	500PA	470PB	$I_{TSM} = 7000A$
72RCG	92RL-S53	ACE gate (higher di/dt)	501PA	470PB	$I_{TSM} = 7000A$, 1 inch thick ceramic case
70RCS-A*	72RC-A	1/2-20 threaded stud, flag terminal	550PA	550PB	$I_{TSM} = 8000A$
71RCS-A*	71RC-A	1/2-20 threaded stud	551PA	550PB	$I_{TSM} = 8000A$, 1 inch thick ceramic case
275RF	250RM-S53	ACE gate, $t_q = 15 \mu sec$ max. (higher di/dt)			
325RA	300RB	$I_{TSM} = 7000A$			ACE gate (higher di/dt)
375RA	350RA	$I_{TSM} = 8000A$	700PA*	700PK	ACE gate (higher di/dt)
420PM	420PBM	None: Change of nomenclature	850PA	850PK	ACE gate (higher di/dt)
			1000PA	1000PK	ACE gate (higher di/dt)

Power Transistors and Darlington

International Rectifier's Power Transistors and Power Darlington offer state-of-the-art processes and techniques in popular device ratings. IR's unique glass passivation ensures high reliability and exceptional stability. The triple-diffused process used offers high voltage, fast switching times, and low saturation voltages.

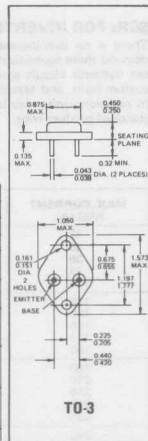
34 types of high voltage Silicon Power Transistors offer high power, high voltage, and high current ratings. Applications include inverters, choppers, deflection circuits, etc. In addition, there are **15 types of fast switching power transistors**.

25 types of high voltage Monolithic Darlington offer high power, high voltage, high current and high gain. Applications include inverters, choppers, switching regulators, ignition systems, etc. In addition, there are **9 types of fast-switching Darlington**.

HIGH VOLTAGE NPN POWER TRANSISTORS

T_C = 25°C unless otherwise specified

I _C Cont. (A)	1.0	2.0	3.0	3.0	3.0	3.0	3.0
I _C Peak (A)	4.0	5.0	5.0	5.0	5.0	7.0	7.0
V _{CE0} (V)	800	1,000	275	300	375	900	900
SERIES	IR701	IR801	2N5838	2N5839	2N5840	IR708	IR709
V _{CE0} (<i>t</i> _{st}) min. (V)	800	700	250	275	350	600	600
@ I _C (A)	0.10	0.10	0.20	0.20	0.20	0.50	0.50
I _{CE0} max. (mA)	0.5	0.5	2.0	2.0	2.0	0.25	0.25
@ V _{CE} (V)	800	800	200	250	250	900	900
I _{CEV} max. (mA)	—	—	5.0	2.0	2.0	0.25	0.25
@ V _{CE} (V)	—	—	265	290	360	900	900
@ V _{BE} (V)	—	—	-1.5	-1.5	-1.5	-1.5	-1.5
h _{FE} (min)	20	20	8	10	10	—	—
@ I _C (A)	0.150	0.200	3.0	2.0	2.0	—	—
@ V _{CE} (V)	5.0	5.0	2.0	3.0	3.0	—	—
V _{CE(sat)} max. (V)	—	—	1.0	1.5	1.5	2.0	1.0
@ I _C (A)	—	—	3.0	2.0	2.0	1.0	2.0
@ I _B (A)	—	—	0.375	0.20	0.20	0.20	0.80
P _d (W)	50	100	100	100	100	50	50



I _C Cont. (A)	3.0	3.0	3.5	3.5	3.5	3.5	3.5	5.0	5.0
I _C Peak (A)	7.0	—	10	10	10	—	—	7.0	7.0
V _{CE0} (V)	900	—	200	400	700	700	700	400	400
SERIES	IR710	IR721	IR660 (1)	IR663 (1)	IR665 (1)	2N3902	2N5157	IR401	IR413
V _{CE0} (<i>t</i> _{st}) min. (V)	800	800	200	325	400	325	400	300	325
@ I _C (A)	0.50	0.50	0.10	0.10	0.10	0.10	0.10	0.10	0.10
I _{CE0} max. (mA)	0.25	0.25	0.25	0.25	0.25	0.25	0.25	0.25	0.25
@ V _{CE} (V)	900	1,000	200	400	500	400	500	400	400
I _{CEV} max. (mA)	—	0.25	0.50 (2)	0.50 (2)	0.50 (2)	2.5	0.50	0.50 (2)	0.5 (2)
@ V _{CE} (V)	—	1,000	200	400	700	700	400	400	400
@ V _{BE} (V)	—	-1.5	-1.5	-1.5	-1.5	-1.5	-1.5	-1.5	-1.5
h _{FE} (min/max)	10/50	(3) 7	20/60	30/90	30/90	30/90	30/90	20/100	20/80
@ I _C (A)	0.15	1.0	0.150	1.0	1.0	1.0	1.0	0.5	0.5
@ V _{CE} (V)	5.0	5.0	5.0	5.0	5.0	5.0	5.0	5.0	5.0
V _{CE(sat)} max. (V)	—	—	0.8	0.8	0.8	0.8	0.8	0.8	0.8
@ I _C (A)	—	—	1.0	1.0	1.0	1.0	1.0	0.5	0.5
@ I _B (A)	—	—	0.10	0.10	0.10	0.10	0.10	0.05	0.05
P _d (W)	50	50	60	60	60	100	100	100	100

I _C Cont. (A)	5.0	5.0	5.0	5.0	7.0	7.0	7.0	7.0	7.0
I _C Peak (A)	15	15	—	10	10	10	10	10	10
V _{CE0} (V)	300	375	400	400	300	400	400	400	400
SERIES	2N5804	2N5805	2N5241	IR410	IR411	IR430	IR431	IR409	IR423
V _{CE0} (<i>t</i> _{st}) min. (V)	225	300	325	200	300	300	325	325	325
@ I _C (A)	0.20	0.20	0.10	0.10	0.10	0.10	0.10	0.10	0.10
I _{CE0} max. (mA)	15.0	5.0	2.5	0.25	0.25	2.5	2.5	0.25	0.25
@ V _{CE} (V)	15.0	150	400	300	300	400	400	400	400
I _{CEV} max. (mA)	5.0	5.0	0.5	0.50 (2)	0.5 (2)	5.0 (2)	5.0 (2)	0.5 (2)	0.5 (2)
@ V _{CE} (V)	270	340	400	200	300	400	400	400	400
@ V _{BE} (V)	-1.5	-1.5	-1.5	-1.5	-1.5	0	0	-1.5	-1.5
h _{FE} (min/max)	10/100	10/100	15/35	30/90	30/90	15/45	15/35	15 (1)	30/90
@ I _C (A)	5.0	5.0	2.5	1.0	1.0	2.5	2.5	1.0	1.0
@ V _{CE} (V)	4.0	4.0	5.0	5.0	5.0	5.0	5.0	5.0	5.0
V _{CE(sat)} max. (V)	2.0	2.0	0.7	0.8	0.8	0.9	0.7	1.2	0.8
@ I _C (A)	5.0	5.0	2.5	1.0	1.0	2.5	2.5	1.0	1.0
@ I _B (A)	0.50	0.50	0.50	0.10	0.10	0.50	0.50	0.167	0.10
P _d (W)	110	110	125	100	100	125	125	125	125

Power Transistors and Darlingtontons

TO-66



HIGH VOLTAGE NPN POWER TRANSISTORS (Continued)

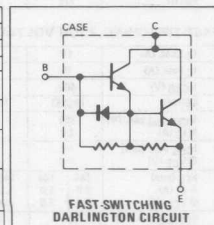
 $T_C = 25^\circ\text{C}$ unless otherwise specified

I_C Cont. (A)	7	7	7	7	10	10	10	10	10	
I_C Peak (A)	10	10	10	10	15	15	15	15	15	
V_{CB0} (V)	400	700	700	700	300	400	500	600	700	
SERIES	IR403	IR402	IR424	IR425	IR515	IR516	IR517	IR518	IR519	
V_{CE0} (sat) min. (V) @ I_C (A)	325 0.10	325 0.10	350 0.10	400 0.10	250 0.10	250 0.10	250 0.10	275 0.10	275 0.10	
I_{CE0} max. (mA) @ V_{CE} (V)	0.5 400	0.25 400	0.25 500	0.25 500	0.5 300	0.5 400	0.5 500	0.5 600	0.5 700	
I_{CEV} max. (mA) @ V_{CE} (V)	0.5 (2)	0.5 (2)	0.5 (2)	0.5 (2)	—	—	—	—	—	
@ V_{CE} (V)	400	700	700	700	—	—	—	—	—	
@ V_{CE} (V)	-1.5	-1.5	-1.5	-1.5	—	—	—	—	—	
h_{FE} (min/max) @ I_C (A) @ V_{CE} (V)	— — —	— — —	30/80 1.0 5.0	30/90 1.0 5.0	15/80 (3) 3.0 5.0	20/80 (3) 4.0 5.0	20/80 (3) 5.0 5.0	25/75 (3) 5.0 5.0	25/75 (3) 5.0 5.0	25/75 (3) 5.0 5.0
V_{CE} (sat) max. (V) @ I_C (A) @ I_B (A)	1.1 3.5 0.8	2.0 3.0 0.6	0.8 1.0 0.10	0.8 1.0 0.10	1.8 3.0 0.30	5.0 7.0 1.4	1.5 3.0 0.3	1.9 7.0 1.4	1.2 3.0 0.3	1.6 7.0 1.4
P_d (W)	125	125	125	125	125	125	125	125	125	

FAST-SWITCHING, HIGH VOLTAGE NPN POWER TRANSISTORS

I_C Cont. (A)	5.0	5.0	8.0	8.0	8.0	8.0	8.0	10	10			
I_C Peak (A)	—	—	16	16	—	16	—	15	15			
V_{CB0} (V)	650	850	500	600	650	700	850	500	600			
SERIES	2N6542	2N6543	2N6306	2N6307	2N6544	2N6308	2N6545	2N6573	2N6574			
V_{CE0} (sat) min. (V) @ I_C (A)	300 0.10	400 0.10	250 0.10	300 0.10	300 0.10	350 0.10	400 0.10	250 0.10	275 0.10			
I_{CE0} max. (mA) @ V_{CE} (V)	— —	— —	0.5 250	0.5 300	— —	0.5 350	— —	— —	— —			
I_{CEV} max. (mA) @ V_{CE} (V)	0.5 650	0.5 850	0.5 500	0.5 600	0.5 650	0.5 700	0.5 850	0.5 500	0.5 600			
@ V_{CE} (V)	—	—	—	—	—	—	—	—	—			
@ V_{CE} (V)	—	—	—	—	—	—	—	—	—			
h_{FE} (min/max) @ I_C (A) @ V_{CE} (V)	12/60 1.5 2.0	7/35 3.0 2.0	12/60 1.5 2.0	7/35 3.0 2.0	5/75 (3) 4.0 5.0 5.0	15/75 (3) 4.0 3.0 5.0	12/60 (3) 3.0 2.5 3.0	7/35 5.0 5.0	12/60 (3) 3.0 2.5 3.0	15/60 (3) 5.0 3.0 3.0	20/60 (3) 5.0 10 3.0	20/60 (3) 5.0 3.0 3.0
V_{CE} (sat) max. (V) @ I_C (A) @ I_B (A)	5.0 5.0 1.0	5.0 5.0 1.0	5.0 5.0 2.0	5.0 5.0 2.0	5.0 8.0 2.0	5.0 8.0 2.0	5.0 8.0 2.67	5.0 8.0 2.0	1.2 8.0 0.3	5.0 8.0 2.0	1.0 3.0 0.3	5.0 3.0 0.3
P_d (W)	100	100	125	125	125	125	125	125	125			
t_{tr}/t_{rr} max. (μ s) @ I_C (A)	0.7/4.0/0.8 3.0	0.7/4.0/0.8 3.0	0.6/1.6/0.4 3.0	0.6/1.6/0.4 3.0	1.0/4.0/1.0 5.0	0.6/1.6/0.4 3.0	1.0/4.0/1.0 5.0	0.9/2.5/0.7 7.0	0.9/2.5/0.7 7.0			

I_C Cont. (A)	10	10	10	10	15	15	
I_C Peak (A)	15	30	30	30	30	30	
V_{CB0} (V)	700	300	375	450	650	850	
SERIES	2N6575	2N6249	2N6250	2N6251	2N6546	2N6547	
V_{CE0} (sat) min. (V) @ I_C (A)	300 0.10	200 0.20	275 0.20	350 0.20	300 0.10	400 0.10	
I_{CE0} max. (mA) @ V_{CE} (V)	— —	5.0 150	5.0 225	5.0 300	— —	— —	
I_{CEV} max. (mA) @ V_{CE} (V)	0.5 700	5.0 225	5.0 300	5.0 375	1.0 650	1.0 850	
@ V_{CE} (V)	—	—	—	—	—	—	
@ V_{CE} (V)	—	—	—	—	—	—	
h_{FE} (min/max) @ I_C (A) @ V_{CE} (V)	20/60 3.0 3.0	5 (3) 10 5.0	10/50 10 3.0	8/50 10 3.0	6/50 10 2.0	12/60 5.0 2.0	6/30 10 2.0
V_{CE} (sat) max. (V) @ I_C (A) @ I_B (A)	1.0 3.0 0.3	5.0 10 2.0	1.5 10 1.0	1.5 10 1.67	1.5 10 2.0	5.0 15 3.0	1.5 10 3.0
P_d (W)	125	175	175	175	175	175	
t_{tr}/t_{rr} max. (μ s) @ I_C (A)	0.9/2.5/0.7 7.0	2.0/3.5/1.0 10	2.0/3.5/1.0 10	2.0/3.5/1.0 10	0.7/4.0/0.8 10	0.7/4.0/0.8 10	



NOTES:

(1) TO-66 Case. (All others are TO-3 Case)

(2) $T_C = 125^\circ\text{C}$

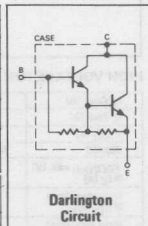
(3) Min.

Power Transistors and Darlington

HIGH VOLTAGE NPN POWER DARLINGTONS

T_C = 25°C unless otherwise specified

I _C Cont. (A)	10	10	10	10	10	15	15
I _C Peak (A)	15	15	15	15	15	20	20
V _{CE0} (V)	120	120	400	450	500	400	400
SERIES	IR1010	IR1020	IR5251	IR5252	IR5253	IR4039	IR4041
V _{CE(sat)} min. (V) @ I _C (A)	80 0.50	80 0.50	350 2.0	400 2.0	450 2.0	300 1.0	300 1.0
I _{CEO} max. (mA) @ V _{CE} (V)	0.10 120	0.10 120	1.0 400	1.0 450	1.0 500	0.25 400	0.25 400
h _{FE} (min.) @ I _C (A) @ V _{CE} (V)	500 3.0 1.5	200 10 1.5	1,000 500 5.0	140 10 5.0	140 10 5.0	140 10 5.0	200 5 5.0
V _{CE(sat)} max. (V) @ I _C (A) @ I _B (A)	1.8 5.0 0.02	1.5 5.0 0.02	2.0 10 2.0	2.0 10 2.0	2.0 10 2.0	5.0 15 3.0	2.2 15 3.0
P _D (W)	100	100	100	100	100	100	100



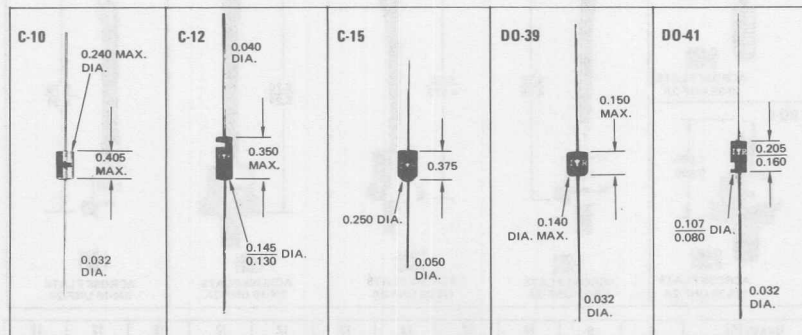
I _C Cont. (A)	15	15	15	15	15	15	15
I _C Peak (A)	20	20	20	20	20	20	20
V _{CE0} (V)	400	400	400	450	500	600	600
SERIES	IR5000	IR4040	IR4045	IR5001	IR4050	IR4055	IR4059
V _{CE(sat)} min. (V) @ I _C (A)	300 2.0	325 1.0	325 1.0	350 2.0	350 1.0	350 1.0	350 1.0
I _{CEO} max. (mA) @ V _{CE} (V)	1.0 400	0.25 400	0.25 400	1.0 450	0.25 500	0.25 500	0.25 600
h _{FE} (min.) @ I _C (A) @ V _{CE} (V)	15 15 5.0	140 5.0 5.0	250 3.0 5.0	8 15 5.0	150 15 5.0	250 15 5.0	8 5 5.0
V _{CE(sat)} max. (V) @ I _C (A) @ I _B (A)	1.8 15 3.0	2.0 15 3.0	2.0 15 3.0	1.2 15 3.0	1.8 15 3.0	2.0 15 3.0	1.8 15 3.0
P _D (W)	125	125	125	125	125	125	100

I _C Cont. (A)	15	15	15	15	15	15	20	20	20
I _C Peak (A)	20	20	20	20	20	20	25	25	25
V _{CE0} (V)	600	600	600	700	850	1,000	350	400	450
SERIES	IR4060	IR4065	IR5063	IR5064	IR5065	IR5066	IR5060	IR5061	IR5062
V _{CE(sat)} min. (V) @ I _C (A)	400 1.0	400 1.0	500 2.0	600 2.0	750 2.0	900 2.0	300 2.0	350 2.0	400 2.0
I _{CEO} max. (mA) @ V _{CE} (V)	0.25 600	0.25 600	1.0 500	1.0 600	1.0 750	1.0 900	1.0 350	1.0 400	1.0 450
h _{FE} (min.) @ I _C (A) @ V _{CE} (V)	250 3.0 5.0	8 15 5.0	500 3.0 5.0	15 20 5.0	14 10 5.0	8 15 5.0	4 10 5.0	8 10 5.0	5 10 5.0
V _{CE(sat)} max. (V) @ I _C (A) @ I _B (A)	2.0 15 3.0	1.8 15 3.0	2.0 15 3.0	2.0 10 1.6	2.0 10 1.2	2.0 10 1.4	2.0 10 1.6	2.0 10 2.0	2.0 10 2.0
P _D (W)	125	125	125	125	125	125	125	125	125

FAST-SWITCHING, HIGH VOLTAGE NPN POWER DARLINGTONS *

I _C Cont. (A)	10	10	10	15	15	15	20	20	20
I _C Peak (A)	15	15	15	20	20	20	25	25	25
V _{CE0} (V)	400	450	500	400	450	500	350	400	450
SERIES	IR6251	IR6252	IR6253	IR6000	IR6001	IR6002	IR6060	IR6061	IR6062
V _{CE(sat)} min. (V) @ I _C (A)	350 2.0	400 2.0	450 2.0	300 2.0	350 2.0	400 2.0	300 2.0	350 2.0	400 2.0
I _{CEO} max. (mA) @ V _{CE} (V)	1.0 400	1.0 450	1.0 500	1.0 400	1.0 450	1.0 500	1.0 350	1.0 400	1.0 450
h _{FE} (min.) @ I _C (A) @ V _{CE} (V)	140 3.0 5.0	100 5.0 5.0	140 3.0 5.0	100 5.0 5.0	150 5.0 5.0	60 10 5.0	150 5.0 5.0	60 10 5.0	100 10 5.0
V _{CE(sat)} max. (V) @ I _C (A) @ I _B (A)	2.0 10 2.0	2.0 10 2.0	2.0 10 2.0	1.8 10 3.0	1.8 10 3.0	1.8 10 3.0	2.0 10 2.0	2.0 10 2.0	2.0 10 2.0
P _D (W)	100	100	100	125	125	125	125	125	125
I _B /I _C max. (sat) @ I _C (A)	0.25/2.5/1.0 5.0	0.25/2.5/1.0 5.0	0.25/2.5/1.0 5.0	0.4/2.5/1.0 10	0.4/2.5/1.0 10	0.4/2.5/1.0 10	0.4/2.5/1.0 10	0.4/2.5/1.0 10	0.4/2.5/1.0 10

Silicon Rectifiers



IR has been a major producer of low-current, low-voltage silicon rectifier diodes for many years. Through continuous improvements in engineering and manufacturing techniques, IR is now producing standard rectifiers with current handling capacities from 400 mA to 3000 amps in a wide array of lead-mounted, stud-mounted, and Hockey-Puk packages.

Fast Recovery Rectifiers. The growing demand for high frequency rectification, free-wheeling diodes, and inverters has

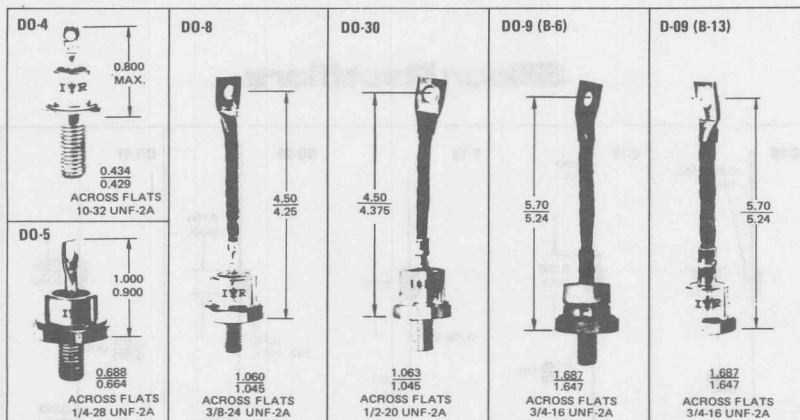
increased the need for high-speed, low-loss rectifiers. To satisfy this need, IR now lists 15 series of fast recovery rectifiers in a separate table.

Power Schottky Rectifiers. IR now offers six series of Schottky barrier rectifiers from 20 to 50 amps. Included are two JEDEC series.

Bold Face Listings. Those series listed in heavier, bold face type are the more common international Rectifier series.

IF(AV) (A) @ Max. T _C (°C)	750mA @ 25°	750mA @ 25°	750mA @ 25°	750mA @ 75°	1 @ 75°	1 @ 75°	1 @ 75°	1.5 @ 40°	2 @ 100°	3 @ 50°	3 @ 140°
I _{FSM} (A)	10	22	22	40	30	40	50	50	50	25	40
Notes	(1)	(1)	(1)	(1)(2)	(1)	(1)	(1)		(2)(3)	(4)(5)	(5)
Case Style	C-10	D0-39	D0-39	C-10	D0-41	C-10	D0-39	D0-39	D0-39	D0-4	D0-4
PRV	PART NUMBERS										
50 Volts	1N2103	-	-	-	1N4001	-	10005	1N4816	20005	1N2348	-
100 Volts	1N2104	-	-	-	1N4002	-	10C1	1N4817	20D1	1N2349	3F10
150 Volts	-	-	-	-	-	-	-	-	-	1N2350	-
200 Volts	1N2105	1N2069	1N2069A	1N3193	1N4003	10C2	1002	1N4818	20D2	1N1124	3F20
300 Volts	1N2106	-	-	-	-	10C3	1003	1N4819	20D3	1N1125	3F50
400 Volts	1N2107	1N2070	1N2070A	1N3194	1N4004	10C4	1004	1N4820	20D4	1N1126	3F40
500 Volts	1N2108	-	-	-	-	10C5	1005	1N4821	20D5	1N1127	3F50
600 Volts	-	1N2071	1N2071A	1N3195	1N4005	10C6	1006	1N4822	20D6	1N1128	3F60
700 Volts	-	-	-	-	-	-	-	1N5052	-	-	-
800 Volts	-	-	-	-	1N4006	10C8	1008	1N5053	20D8	-	3F80
1000 Volts	-	-	-	1N3563	1N4007	10C10	10010	1N5054	20D10	-	3F100
IF(AV) (A) @ Max. T _C (°C)	3 @ 125°	3.3 @ 50°	3.5 @ 85°	6 @ 95°	6 @ 95°	6 100°	6 100°	6 100°	6 100°	6 @ 150°	6 @ 150°
I _{FSM} (A)	150	25	35	150	400	75	75	75	75	150	150
Notes	(2)	(4)	(4)	(3)	(2)	(3)(4)	(3)(4)	(3)(4)	(3)(4)	(1)	(3)
Case Style	C-12	D0-4	D0-4	D0-4	C-15	D0-4	D0-4	D0-4	D0-4	D0-4	D0-4
PRV	PART NUMBERS										
50 Volts	-	-	-	1N1341	60S05	1N3879	6FL5	6FT5	6FV5	1N1341A	1N1341B
100 Volts	30S1	-	-	1N1342	60S1	1N3880	6FL10	6FT10	6FV10	1N1342A	1N1342B
150 Volts	-	-	-	1N1343	-	-	-	-	-	1N1343A	1N1343B
200 Volts	30S2	1N1124A	1N3570	1N1344	60S2	1N3881	6FL20	6FT20	6FV20	1N1344A	1N1344B
300 Volts	30S3	1N1125A	1N3571	1N1345	60S3	1N3882	6FL30	6FT30	6FV30	1N1345A	1N1345B
400 Volts	30S4	1N1126A	1N3572	1N1346	60S4	1N3883	6FL40	6FT40	6FV40	1N1346A	1N1346B
500 Volts	30S5	1N1127A	1N3573	1N1347	60S5	-	6FL50	6FT50	6FV50	1N1347A	1N1347B
600 Volts	30S6	1N1128A	1N3574	1N1348	60S6	-	6FL60	6FT60	6FV60	1N1348A	1N1348B
700 Volts	-	1N3645	-	-	-	-	-	6FT70	6FV70	1N3887	-
800 Volts	30S8	1N3650	-	-	60S8	-	-	6FT80	6FV80	1N3888	-
900 Volts	-	-	-	-	-	-	-	6FT90	6FV90	1N3889	-
1000 Volts	30S10	-	-	-	60S10	-	-	6FT100	6FV100	1N3900	-

Silicon Rectifiers



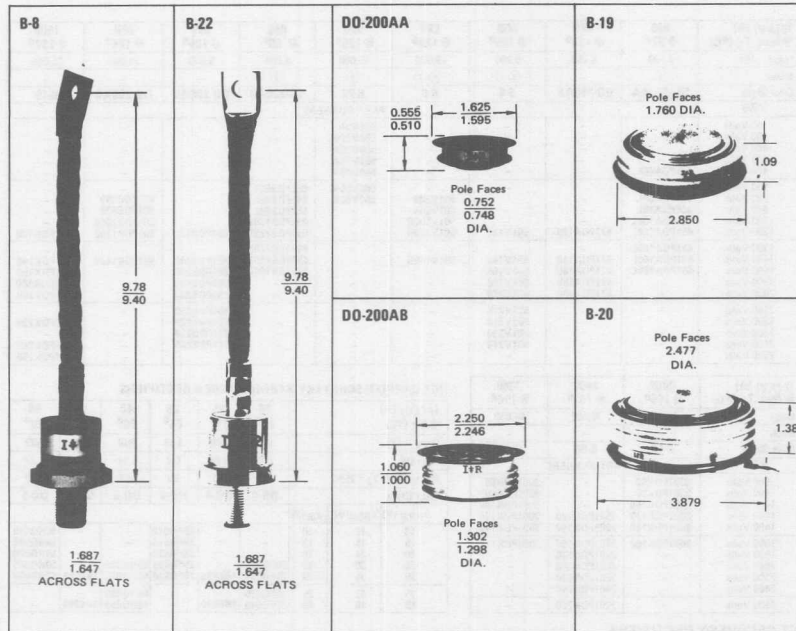
I_F (A) @ Max. T_C (°C)	6 @ 150°	6 @ 150°	12 100°	12 100°	12 100°	12 100°	12 @ 150°	12 @ 150°	12 @ 150°	12 @ 150°	12 150°
I_{FSM} (A)	150	160	150	150	150	150	200	240	250	240	250
Notes	(1)	(1)	(1) (4)	(1) (4)	(1) (4)	(1) (4)	(1)	(1) (1)	(1) (1)	(1)	(1) (1)
Case Style	D0-4	D0-4	D0-4	D0-4	D0-4	D0-4	D0-4	D0-4	D0-4	D0-4	D0-4
PRV	PART NUMBERS										
50 Volts	6F5A	6F58	1N3889	12FL5	12FT5	12FV5	1N1199	1N1199A	1N1199B	12F5A	12F58
100 Volts	6F10A	6F10B	1N3890	12FL10	12FT10	12FV10	1N1200	1N1200A	1N1200B	12F10A	12F10B
150 Volts	6F15A	6F15B	—	—	—	—	1N1201	1N1201A	1N1201B	12F15A	12F15B
200 Volts	6F20A	6F20B	1N3891	12FL20	12FT20	12FV20	1N1202	1N1202A	1N1202B	12F20A	12F20B
300 Volts	6F30A	6F30B	1N3892	12FL30	12FT30	12FV30	1N1203	1N1203A	1N1203B	12F30A	12F30B
400 Volts	6F40A	6F40B	1N3893	12FL40	12FT40	12FV40	1N1204	1N1204A	1N1204B	12F40A	12F40B
500 Volts	6F50A	6F50B	—	12FL50	12FT50	12FV50	1N1205	1N1205A	1N1205B	12F50A	12F50B
600 Volts	6F60A	6F60B	—	12FL60	12FT60	12FV60	1N1206	1N1206A	1N1206B	12F60A	12F60B
700 Volts	6F70A	6F70B	—	—	12FT70	12FV70	1N3670	1N3670A	—	—	—
800 Volts	6F80A	6F80B	—	—	12FT80	12FV80	1N3671	1N3671A	—	12F80A	12F80B
900 Volts	6F90A	6F90B	—	—	12FT90	12FV90	1N3672	1N3672A	—	—	—
1000 Volts	6F100A	6F100B	—	—	12FT100	12FV100	1N3673	1N3673A	—	12F100A	12F100B

I_F (A) @ Max. T_C (°C)	15 @ 150°	16 @ 150°	16 @ 150°	20 @ 150°	35 @ 140°	40 @ 140°	40 @ 150°	60 @ 115°	60 @ 140°	60 @ 125°	100 @ 140°
I_{FSM} (A)	250	300	300	400	500	500	800	700	900	1,200	1,600
Notes	(1)	(1)	(1)	(1)	(1)	(1)	(1)	(1)	(1)	(1)	(1)
Case Style	D0-5	D0-4	D0-4	D0-4	D0-5	D0-5	D0-5	D0-5	D0-5	D0-5	D0-8
PRV	PART NUMBERS										
50 Volts	1N3208	16F5	1N3615	—	1N1183	40HF5	1N1183A	1N2128	1N2128A	—	—
100 Volts	1N3209	16F10	1N3616	20F10	1N1184	40HF10	1N1184A	1N2129	1N2129A	70H10A	1N3288
150 Volts	—	16F15	1N3617	—	1N1185	40HF15	1N1185A	1N2130	1N2130A	70H15A	—
200 Volts	1N3210	16F20	1N3618	20F20	1N1186	40HF20	1N1186A	1N2131	1N2131A	70H20A	1N3289
250 Volts	—	—	—	—	—	—	—	1N2132	1N2132A	70H25A	—
300 Volts	1N3211	16F30	1N3619	20F30	1N1187	40HF30	1N1187A	1N2133	1N2133A	70H30A	1N3290
350 Volts	—	—	—	—	—	—	—	1N2134	1N2134A	—	—
400 Volts	1N3212	16F40	1N3620	20F40	1N1188	40HF40	1N1188A	1N2135	1N2135A	70H40A	1N3291
450 Volts	—	—	—	—	—	—	—	1N2136	1N2136A	—	—
500 Volts	1N3213	16F50	1N3621	—	1N1189	40HF50	1N1189A	1N2137	1N2137A	70H50A	1N3292
600 Volts	1N3214	16F60	1N3622	—	1N1190	40HF60	1N1190A	1N2138	1N2138A	70H60A	1N3293
700 Volts	—	—	—	—	1N3765	40HF70	—	—	—	70H70A	—
800 Volts	—	16F80	1N3623	—	1N3766	40HF80	—	—	—	70H80A	1N3294
900 Volts	—	—	—	—	1N3767	40HF90	—	—	—	70H90A	—
1000 Volts	—	16F100	1N3624	—	1N3768	40HF100	—	—	—	70H100A	1N3295
1200 Volts	—	—	—	—	—	—	—	—	—	70H120*	1N3296

- ① Ambient temperature.
- ② Lead temperature, measured 3/8-inch from body.
- ③ 20A Series also available.
- ④ Cathode-to-Stud only.
- ⑤ Cathode-to-Stud. For anode-to-stud, add "R" to base number (2F110, 1N3569R).
- ⑥ Fast recovery rectifiers, see table on page 10.

- ⑦ Note that thermal resistance is lower and operating temperatures higher on "Reverse Polarity" devices.
- † J&N types available.
- ⑧ I_2 = Current Rating. 1N3196 = 500 mA; 1N3563 = 400 mA.
- ⑨ t_{rr} = 5 μ s max.
- ⑩ IN2348 series has 15A surge rating.
- * For "A" series at this voltage, contact factory.

Silicon Rectifiers



$I_F(AV)$ (A) @ Max. T_C (°C)	100 @ 110°	100 @ 140°	150 @ 150°	150 @ 150°	150 @ 150°	250 @ 105°	250 @ 130°	250 @ 135°	275 @ 120°	300 @ 120°	300 @ 120°
I_{FSM} (A)	2,500	2,300	3,000	3,000	3,000	3,500	4,500	4,500	5,000	5,000	6,250
Notes	(1) (2) (7)	(1)	(1)	(1)	(1)	(1) (2) (7)	(1)	(1)	(1)	(1)	(1) (7)
Case Style	DO-8	DO-8	DO-30	DO-8	DO-30	B-6	B-13	B-13	B-13	B-13	B-6
PRV	PART NUMBERS										
50 Volts	-	-	1N3111	-	-	-	-	1N2054	1N4044	-	-
100 Volts	-	1N3288A	1N3085	150K10A	150L10A	-	1N3735	1N2055	1N4045	300U10A	-
150 Volts	-	-	-	150K15A	150L15A	-	-	1N2056	1N4046	300U15A	-
200 Volts	-	1N3289A	1N3086	150K20A	150L20A	-	1N3736	1N2057	1N4047	300U20A	-
250 Volts	-	-	-	150K25A	150L25A	-	-	1N2058	1N4048	300U25A	-
300 Volts	-	1N3290A	1N3087	150K30A	150L30A	-	1N3737	1N2059	1N4049	300U30A	-
350 Volts	-	-	-	-	-	-	-	1N2060	-	-	-
400 Volts	101KL40	1N3291A	1N3088	150K40A	150L40A	251UL40	1N3738	1N2061	1N4050	300U40A	-
450 Volts	-	-	-	-	-	-	-	1N2062	-	-	-
500 Volts	-	1N3292B	1N3089	150K50A	150L50A	-	1N3739	1N2063	1N4051	300U50A	-
600 Volts	101KL60	1N3293A	1N3090	150K60A	150L60A	251UL60	1N3740	1N2064	1N4052	300U60A	-
700 Volts	-	-	-	150K70A	150L70A	-	-	1N2065	1N4053	300U70A	-
800 Volts	101KL80	1N3294A	1N3091	150K80A	150L80A	251UL80	1N3741	1N2066	1N4054	300U80A	301U80
900 Volts	-	-	-	150K90A	150L90A	-	-	1N2067	1N4055	300U90A	-
1000 Volts	101KL100	1N3295A	1N3092	150K100A	150L100A	251UL100	1N3742	1N2068	1N4056	300U100A	301U100
1200 Volts	101KL120	1N3296A	1N5162	150K120*	150L120*	251UL120	1N3743	-	-	300U120*	301U120
1300 Volts	101KL130	-	-	-	-	251UL130	-	-	-	-	-
1400 Volts	101KL140	-	-	-	-	251UL140	1N3744	-	-	-	301U140
1500 Volts	101KL150	-	-	-	-	251UL150	-	-	-	-	-
1600 Volts	101KL160	-	-	-	-	251UL160	-	-	-	-	301U160
1800 Volts	-	-	-	-	-	-	-	-	-	-	301U180
2000 Volts	-	-	-	-	-	-	-	-	-	-	301U200
2100 Volts	-	-	-	-	-	-	-	-	-	-	301U210
2200 Volts	-	-	-	-	-	-	-	-	-	-	301U220
2300 Volts	-	-	-	-	-	-	-	-	-	-	301U230
2400 Volts	-	-	-	-	-	-	-	-	-	-	301U240
2500 Volts	-	-	-	-	-	-	-	-	-	-	301U250

Silicon Rectifiers

IF(AV) (A) @ Max. Tc (°C)	400 @ 97°	470 @ 105°	500 @ 105°	500 @ 120°	500 @ 125°	650 @ 80°	800 @ 105°	800 @ 125°	1600 @ 107°
IFSM (A)	3,500	6,250	8,000	10,000	10,000	8,000	8,000	10,000	25,000
Notes	(6)	—	(3) (7)	(4) (7)	(5)	(6)	—	—	—
Case Style	DO-200AA	DO-200AA	B-8	B-8	B-22	DO-200AB	DO-200AB	DO-200AB	B-19
PRV	PART NUMBERS								
50 Volts	—	—	—	—	500V5A	—	—	—	—
100 Volts	—	—	—	—	500V10A	—	—	—	—
200 Volts	—	—	—	—	500V20A	—	—	—	—
300 Volts	—	—	—	—	500V30A	—	—	—	—
400 Volts	401PDA40L	—	—	—	500V40A	—	—	—	—
500 Volts	401PDA60L	—	—	—	500V50A	651PDB50L	—	—	—
600 Volts	401PDA80L	—	—	501V60B	500V60A	651PDB60L	—	801PDB60B	—
800 Volts	401PDA100L	—	—	501V80B	—	651PDB80L	—	801PDB80B	—
1000 Volts	401PDA120L	471PDA120	501V120	501V100B	—	651PDB100L	—	801PDB100B	—
1200 Volts	401PDA120L	—	—	501V120B	—	651PDB120L	801PDB120	801PDB120B	1601PDK120
1300 Volts	401PDA130L	471PDA140	501V140	501V140B	—	651PDB130L	801PDB140	801PDB140B	1601PDK140
1400 Volts	401PDA140L	471PDA160	501V160	—	—	651PDB140L	801PDB160	—	1601PDK160
1600 Volts	401PDA160L	471PDA180	501V180	—	—	651PDB160L	801PDB180	—	1601PDK180
1800 Volts	—	471PDA200	501V200	—	—	—	801PDB200	—	1601PDK200
2000 Volts	—	—	—	—	—	—	—	—	—
2100 Volts	—	—	501V210	—	—	—	801PDB210	—	1601PDK220
2200 Volts	—	—	501V220	—	—	—	801PDB220	—	—
2300 Volts	—	—	501V230	—	—	—	801PDB230	—	1601PDK240
2400 Volts	—	—	501V240	—	—	—	801PDB240	—	1601PDK250
2500 Volts	—	—	—	—	—	—	—	—	—

IF(AV) (A) @ Max. Tc (°C)	2000 @ 105°	2400 @ 107°	3000 @ 108°
IFSM (A)	30,000	39,000	45,000
Notes	—	—	—
Case Style	B-19	B-20	B-20
PRV	PART NUMBERS		
600 Volts	2001PDK60	—	3001PDN60
800 Volts	2001PDK80	—	3001PDN80
1000 Volts	2001PDK100	—	3001PDN100
1200 Volts	2001PDK120	2601PDN120	3001PDN120
1400 Volts	2001PDK140	2601PDN140	3001PDN140
1600 Volts	2001PDK160	2601PDN160	3001PDN160
1800 Volts	—	2601PDN180	—
2000 Volts	—	2601PDN200	—
2200 Volts	—	2601PDN220	—
2400 Volts	—	2601PDN240	—
2500 Volts	—	2601PDN250	—

HOT CARRIER SCHOTTKY BARRIER POWER RECTIFIERS

IF(AV) (A) @ Tc (°C)	20 85°	25 70°	25 85°	40 80°	50 80°	50 80°
IFSM (A)	800	400	800	800	800	800
VFM (V)	0.8	0.86	0.7	0.97	0.86	0.87
@ IFM (A) @ Tj = 25°C	80	80	80	160	160	160
Case Style	DO-4	DO-4	DO-4	DO-5	DO-5	DO-5
VRRM (V) VRSM (V) Vg (V)						
10	12	10	—	—	25F0010	—
15	18	15	—	—	25F0015	—
20	24	20	—	—	25F0020	—
25	30	25	20F0025	—	25F0025	40H0025
30	36	30	20F0030	1N6095	25F0030	40H0030
35	42	35	20F0035	—	—	40H0040
40	48	40	20F0040	1N6096	—	40H0050

FAST RECOVERY RECTIFIERS

International Rectifier fast recovery diodes are similar to conventional diffused diodes of comparable current and voltage rating, but they have been specially processed so that the peak recovery current is lower and recovery time is shorter.

The three major uses for fast recovery rectifier diodes are:

1. *Rectifiers for high frequency AC.* The largest IR fast recovery rectifiers are capable of efficient rectification up to 10 kHz, smaller devices at even higher frequencies.

2. *By-pass (free-wheeling) diodes on the output of a phase-controlled rectifier unit.* They substantially reduce the momentary high load and junction heating on SCRs during reverse recovery of the by-pass diode.

3. *By-pass diodes in a DC chopper or inverter.* In addition to the benefits described above, in #2, IR fast recovery rectifiers for this application also make a significant reduction in potentially damaging transient voltages generated during recovery.

MAX. CONTINUOUS CURRENT (A)	VOLTAGE RANGE (V)	trr - RECOVERY TIME (µsec)	IRM(REC) - RECOVERY CURRENT (A)	CASE STYLE	IR SERIES
6	50-400	0.20 MAX.	2 MAX.	DO-4	1N3879
6	500-600	0.20 MAX.	2 MAX.	DO-4	6FL
6	50-1000	0.35 MAX.	3 MAX.	DO-4	6FT
6	50-1000	0.50 MAX.	4 MAX.	DO-4	6FV
12	50-400	0.20 MAX.	2 MAX.	DO-4	1N3889
12	500-600	0.20 MAX.	2 MAX.	DO-4	12FL
12	50-1000	0.35 MAX.	2 MAX.	DO-4	12FT
12	50-1000	0.50 MAX.	4 MAX.	DO-4	12FV
100	400-1000	1.5 MAX.	25 MAX.	DO-8	101KL-S15
100	400-1200	2.0 MAX.	33 MAX.	DO-8	101KL-S20
100	1000-1600	3.0 MAX.	50 MAX.	DO-8	101KL-S30
250	400-1000	1.5 MAX.	25 MAX.	DO-8	251UL-S15
250	400-1200	2.0 MAX.	33 MAX.	DO-8	251UL-S20
250	1000-1600	3.0 MAX.	50 MAX.	DO-8	251UL-S30
400	400-800	1.5 MAX.	30 MAX.	DO-200AA	401PDA-L15
400	400-1200	2.0 MAX.	35 MAX.	DO-200AA	401PDA-L20
400	1000-1600	3.0 MAX.	50 MAX.	DO-200AA	401PDA-L30
450	400-800	2.0 MAX.	33 MAX.	DO-200AB	651PDB-L20
450	400-1200	2.5 MAX.	41 MAX.	DO-200AB	651PDB-L25
650	800-1600	3.0 MAX.	49 MAX.	DO-200AB	651PDB-L30

Zener Voltage Regulators T.C. Voltage References

TEMPERATURE COMPENSATED VOLTAGE REFERENCES

Power Rating (mW)	V _Z - Zener Voltage (V)	I _{ZT} - Test Current (mA)	Z _Z - Zener Impedance (Ω) @ I _{ZT}	Case Style	Nom. Temp. Coefficient (%/°C)	IR Part No.
250	5.9 - 6.5	7.5	15	DO-7	0.005	1N3496
					0.002	1N3497
					0.001	1N3498
					0.0005	1N3499
250	8.0 - 8.8	10.0	15	C-5	0.002	1N1530
					0.001	1N1530A
400	5.9 - 6.5	7.5	15	DO-7	0.01	1N821 (1)
					0.005	1N823†
					0.002	1N825
					0.001	1N827
400	6.2 - 6.9	7.5	15	DO-7	0.0005	1N829
					0.002	1N826
					0.001	1N828
400	5.9 - 6.5	7.5	20	C-1	0.01	1N429
					0.002	1N826
400	6.3 - 6.7	7.5	10	DO-7	0.015	1N3779
					0.01	1N3780
					0.005	1N3781
					0.002	1N3782
					0.001	1N3783
					0.0005	1N3784
400	6.4±5%	0.5	200	DO-7	0.01	1N4555 (2)
					0.005	1N4556
400	6.4±5%	1.0	100	DO-7	0.01	1N4570 (2)
					0.005	1N4571
					0.002	1N4572
					0.001	1N4573
					0.0005	1N4574
400	6.4±5%	2.0	50	DO-7	0.01	1N4575 (3)
					0.005	1N4576
					0.002	1N4577
					0.001	1N4578
					0.0005	1N4579
400	6.4±5%	4.0	25	DO-7	0.01	1N4580 (3)
					0.005	1N4581
					0.002	1N4582
					0.001	1N4583
					0.0005	1N4584
400	8.0 - 8.8	10.0	15	C-4	0.002	1N430 (3)
					0.001	1N430
400	8.0 - 8.8	10.0	15	DO-7	0.01	1N3154 (3)
					0.005	1N3155
					0.002	1N3156
					0.001	1N3157
500	8.95 - 9.45	7.5	20	DO-7	0.01	1N935 (3)
					0.005	1N936†
					0.002	1N937
					0.001	1N938
					0.0005	1N939
Special Outline Series						
200	6.2	7.5	20	C-6	0.01	1N1735
400	12.4	40	40			1N1736 (4)
600	18.6	60	60			1N1737
800	24.8	80	80			1N1738
1000	31.0	100	100			1N1739
1200	37.2	120	120			1N1740
1400	43.4	140	140	1N1741		
1600	49.6	160	160	1N1742		
Time Stable Devices						
250	6.2 - 6.5	7.5	12	DO-7	0.0013	1N3501 (1)
					0.00065	1N3502
					0.0013	1N3503
					0.0013	1N3504
400	5.9 - 6.5	7.5	15	DO-7	0.01	6.2SR1
					0.005	6.2SR2
					0.002	6.2SR3
					0.001	6.2SR4

International Rectifier has long been recognized as a leader in the development and production of standard, selected, and special order Zener Voltage Regulators.

Temperature Compensated Voltage References are specially constructed Zeners which offer predictable variations in voltage with respect to temperature. These conditions are stable for any given set of parameters specified.

These regulators and references are complementary to IR's power-oriented line of quality semiconductors.

ZENER VOLTAGE REGULATORS

Power Rating	150mW	250mW	250mW			
Max. Op. Temp. (°C)	200 ⁽¹⁾	150 ⁽¹⁾	200 ⁽¹⁾			
Tolerance (%)	—	5, 10%	—			
Notes	(1)	(2)	(3)			
Case	C-1	DO-7	DO-7			
Nominal Values (V _Z)	Part No.	I _{ZT} (mA)	Part No.	I _{ZT} (mA)	Part No.	I _{ZT} (mA)
(2.6)	1N465	5	—	—	1N702	5
(3.5)	1N466	5	—	—	1N703	5
(4.1)	1N467	5	—	—	1N704	5
(4.8)	1N468	5	1N761	10	1N705	5
(5.8)	1N469	5	1N762	10	1N706	5
(7.1)	1N470	5	1N763	10	1N707	5
(8.7)	1N1313	0.20	1N764	10	—	—
(10.5)	1N1314	0.20	1N765	10	—	—
(12.7)	1N1315	0.20	1N766	5	—	—
(15.7)	1N1316	0.20	1N767	5	—	—
(19.0)	1N1317	0.20	1N768	5	—	—
(23.5)	1N1318	0.20	1N769	5	—	—
(28.5)	1N1319	0.20	—	—	—	—
(34.5)	1N1320	0.20	—	—	—	—

() V_Z ratings in parenthesis (2.6) are nominal values.

(1) For Z_Z = 10Ω, add "A" suffix.

(2) ΔBV Temperature Range = 0° to 75°C. Add "A" suffix for -55° to 25°C, 25° to 100°C.

(3) For 0.001 Temp. Coef., add "A" suffix.

(4) ΔBV Temperature Range = -55° to 25°, 25° to 100°C. Add "A" suffix for -55° to 25°, 25° to 150°C.

(5) ΔBV Temperature Range = 0° to 75°C. Add "A" suffix for -55° to 25°C, 25° to 100°C. Add "B" suffix for -55° to 25°, 25° to 150°C.

(6) For Nom. Temp. Coef. = 0.005%°C, add "A" suffix.

(7) Each device has time stability measured @ 40°C for 1,000 hours @ 7.5 mA.

(8) For 1N1313 thru 1N1320, max. temp. = 150°C.

(9) Add "A" for 5% tolerances.

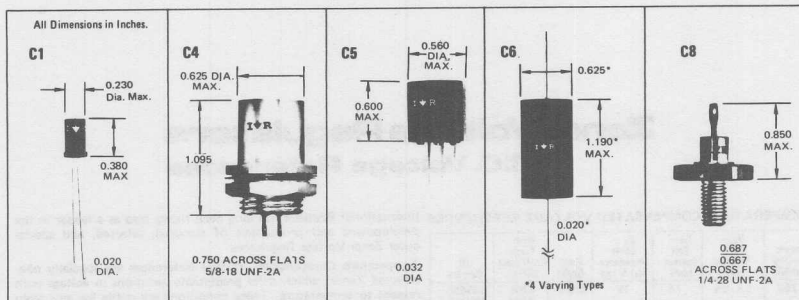
(10) "A" version offers tighter tolerances.

(11) Add "A" for 10% tolerances.

| (12) Add "A" for 10% tolerance; "B" for 5%. |
| (13) Add "T5" for 5% tolerance; "T10" for 10%; "T20" for 20%. |
| (14) Polarity - Cathode-to-stud only. |
| (15) Polarity - Anode-to-stud; add "R" for cathode-to-stud. |
| (16) Polarity - 1N3993 Series: cathode-to-stud only. 1N2498 Series, 1N1816 Series, and 1N2008 Series: anode-to-stud, for cathode-to-stud, add "R". |

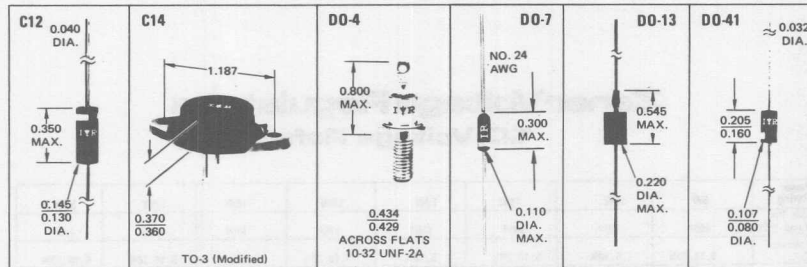
† JAN types available.

Zener Voltage Regulators T.C. Voltage References



Power Rating	250mW		400mW		400mW		400mW		400mW		500mW		1W		1W	
Max Op. Temp (°C)	200°		175°		175°		150°		200°		200°		165°		165°	
Tolerance (%)	5, 10%		5, 10%		5, 10, 20%		5, 10%		15%		5, 10, 20%		5, 10%		5, 10, 20%	
Notes	(1)		(1)		(1)		(1)		(1)		(1)		(1)		(1)	
Case Style	D0-7		D0-7		D0-7		D0-7		D0-7		D0-7		D0-13		D0-13	
V_Z	Part No.	I_{ZT} (mA)	Part No.	I_{ZT} (mA)	Part No.	I_{ZT} (mA)	Part No.	I_{ZT} (mA)	Part No.	I_{ZT} (mA)	Part No.	I_{ZT} (mA)	Part No.	I_{ZT} (mA)	Part No.	I_{ZT} (mA)
2.4	--	--	1N4370	20	--	--	--	--	--	--	1N5221	20	--	--	--	--
(2.5)	--	--	--	--	--	--	--	--	--	--	1N5222	20	--	--	--	--
2.7	--	--	1N4371	20	--	--	--	--	--	--	1N5223	20	--	--	--	--
(2.8)	--	--	--	--	--	--	--	--	--	--	1N5224	20	--	--	--	--
3.0	--	--	1N4372	20	--	--	--	--	--	--	1N5225	20	--	--	--	--
3.3	--	--	1N746	20	--	--	--	--	--	--	1N5226	20	--	--	--	--
3.6	--	--	1N747	20	--	--	--	--	--	--	1N5227	20	--	--	--	--
3.9	--	--	1N748	20	--	--	--	--	--	--	1N5228	20	1N1518	50	123.9	50
4.3	--	--	1N749	20	--	--	--	--	--	--	1N5229	20	--	--	124.3	50
4.7	--	--	1N750	20	--	--	--	1N3510	20	1N5230	20	1N1519	40	124.7	40	--
5.1	--	--	1N751	20	--	--	--	1N3511	20	1N5231	20	--	--	125.1	40	--
5.6	1N708	25	1N752	20	--	--	1N1956	5	1N3512	20	1N5232	20	1N1520	35	125.6	35
(6.0)	--	--	--	--	--	--	--	--	--	--	1N5233	20	--	--	--	--
6.2	1N709	25	1N753	20	--	--	--	1N3513	20	1N5234	20	--	--	126.2	35	--
6.8	1N710	25	1N754	20	1N957	18.5	1N1957	5	1N3514	20	1N5235	20	1N1521	30	126.8	30
7.5	1N711	25	1N755	20	1N958	16.5	--	1N3515	10	1N5236	20	--	--	127.5	30	--
8.2	1N712	25	1N756	20	1N959	15.0	1N1958	5	1N3516	10	1N5237	20	1N1522	25	128.2	25
(8.7)	--	--	--	--	--	--	--	--	--	--	1N5238	20	--	--	--	--
9.1	1N713	12	1N757	20	1N960	14.0	--	1N3517	10	1N5239	20	--	--	129.1	25	--
10	1N714	12	1N758	20	1N961	12.5	1N1959	5	1N3518	10	1N5240	20	1N1523	20	1210	20
11	1N715	12	--	--	1N962	11.5	--	1N3519	10	1N5241	20	--	--	1211	20	--
12	1N716	12	1N759	20	1N963	10.5	1N1960	1	1N3520	10	1N5242	20	1N1524	15	1212	15
13	1N717	12	--	--	1N964	9.5	--	1N3521	5	1N5243	9.5	--	--	1213	15	--
(14)	--	--	--	--	--	--	1N1961	1	--	1N5244	9.0	--	--	--	--	--
15	1N718	12	--	--	1N965	8.5	--	1N3522	5	1N5245	8.5	1N1525	13	1215	13	--
16	1N719	12	--	--	1N966	7.8	--	1N3523	5	1N5246	7.8	--	--	1216	13	--
(17)	--	--	--	--	--	--	--	--	--	1N5247	7.4	--	--	--	--	--
18	1N720	12	--	--	1N967	7.0	1N1962	1	1N3524	5	1N5248	7.0	1N1526	10	1218	10
(19)	--	--	--	--	--	--	--	--	--	1N5249	6.6	--	--	--	--	--
20	1N721	4	--	--	1N968	6.2	--	1N3525	5	1N5250	6.2	--	--	1220	10	--
22	1N722	4	--	--	1N969	5.6	1N1963	1	1N3526	5	1N5251	5.6	1N1527	9	1222	9
24	1N723	4	--	--	1N970	5.2	--	1N3527	5	1N5252	5.2	--	--	1224	9	--
(25)	--	--	--	--	--	--	--	--	--	1N5253	5.0	--	--	--	--	--
27	1N724	4	--	--	1N971	4.6	1N1964	1	1N3528	4	1N5254	4.6	1N1528	7	1227	7
(28)	--	--	--	--	--	--	--	--	--	1N5255	4.5	--	--	--	--	--
30	1N725	4	--	--	1N972	4.2	--	1N3529	4	1N5256	4.2	--	--	1230	7	--
33	--	--	--	--	1N973	3.8	1N1965	0.2	1N3530	3	1N5257	3.8	--	--	--	--
36	--	--	--	--	1N974	3.4	--	--	--	1N5258	3.4	--	--	--	--	--
39	--	--	--	--	1N975	3.2	--	--	--	1N5259	3.2	--	--	--	--	--
43	--	--	--	--	1N976	3.0	--	--	--	1N5260	3.0	--	--	--	--	--
47	--	--	--	--	1N977	2.7	--	--	--	1N5261	2.7	--	--	--	--	--
51	--	--	--	--	1N978	2.5	--	--	--	1N5262	2.5	--	--	--	--	--
56	--	--	--	--	1N979	2.2	--	--	--	1N5263	2.2	--	--	--	--	--
(58)	--	--	--	--	--	--	--	--	--	1N5264	2.1	--	--	--	--	--
62	--	--	--	--	1N980	2.0	--	--	--	1N5265	2.0	--	--	--	--	--
68	--	--	--	--	1N981	1.8	--	--	--	1N5266	1.8	--	--	--	--	--
75	--	--	--	--	1N982	1.7	--	--	--	1N5267	1.7	--	--	--	--	--
82	--	--	--	--	1N983	1.5	--	--	--	1N5268	1.5	--	--	--	--	--
(87)	--	--	--	--	--	--	--	--	--	1N5269	1.4	--	--	--	--	--
91	--	--	--	--	1N984	1.4	--	--	--	1N5270	1.4	--	--	--	--	--
100	--	--	--	--	1N985	1.3	--	--	--	1N5271	1.3	--	--	--	--	--

Zener Voltage Regulators T.C. Voltage References



Power Rating	1W		1W		1W		1W		1W		3.5W		3.5W		5W	
Max. Op. Temp. (°C)	175°		175°		175°		200°		200°		165°		165°		200°	
Tolerance (%)	5, 10, 20%		5, 10%		5, 10, 20%		5, 10%		5, 10%		5, 10%		5, 10, 20%		5, 10, 20%	
Notes	(5), (1)		(5)		(2), (1)		(5)		(5), (4)		(5), (4)		(1), (4)		(1)	
Case Style	D0-13		D0-13		D0-13		D0-41		D0-41		D0-41		D0-41		C-12	
V _Z	Part No.	I _{ZT} (mA)	Part No.	I _{ZT} (mA)	Part No.	I _{ZT} (mA)	Part No.	I _{ZT} (mA)	Part No.	I _{ZT} (mA)	Part No.	I _{ZT} (mA)	Part No.	I _{ZT} (mA)	Part No.	I _{ZT} (mA)
3.3	1N3821	76	--	--	--	--	1N4728	76	1ZS3.3	76	--	--	--	--	1N5333	380
3.6	1N3822	69	--	--	--	--	1N4729	69	1ZS3.6	69	--	--	--	--	1N5334	350
3.9	1N3823	64	--	--	--	--	1N4730	64	1ZS3.9	64	1N1588	150	3Z3.9	150	1N5335	320
4.3	1N3824	58	--	--	--	--	1N4731	58	1ZS4.3	58	--	--	3Z4.3	150	1N5336	290
4.7	1N3825	53	--	--	--	--	1N4732	53	1ZS4.7	53	1N1589	125	3Z4.7	125	1N5337	260
5.1	1N3826	49	--	--	--	--	1N4733	49	1ZS5.1	49	--	--	3Z5.1	125	1N5338	240
5.6 (6.0)	1N3827	45	1N1765	100	--	--	1N4734	45	1ZS5.6	45	1N1590	110	3Z5.6	110	1N5339	220
6.2	1N3828	41	1N1766	100	--	--	1N4735	41	1ZS6.2	41	--	--	3Z6.2	110	1N5341	200
6.8	1N3829	37	1N1767	100	1N3016	37	1N4736	37	1ZS6.8	37	1N1591	100	3Z6.8	100	1N5342	175
7.5	--	--	1N1768	100	1N3017	34	1N4737	34	1ZS7.5	34	--	--	3Z7.5	100	1N5343	175
8.2 (8.7)	--	--	1N1769	100	1N3018	31	1N4738	31	1ZS8.2	31	1N1592	80	3Z8.2	80	1N5344	150
9.1	--	--	1N1770	50	1N3019	28	1N4739	28	1ZS9.1	28	--	--	3Z9.1	80	1N5346	150
10	--	--	1N1771	50	1N3020	25	1N4740	25	1ZS10	25	1N1593	70	3Z10	70	1N5347	125
11	--	--	1N1772	50	1N3021	23	1N4741	23	1ZS11	23	--	--	3Z11	70	1N5348	125
12	--	--	1N1773	50	1N3022	21	1N4742	21	1ZS12	21	1N1594	50	3Z12	50	1N5349	100
13 (14)	--	--	1N1774	50	1N3023	19	1N4743	19	1ZS13	19	--	--	3Z13	50	1N5350	100
15	--	--	1N1775	50	1N3024	17	1N4744	17	1ZS15	17	1N1595	40	3Z15	40	1N5352	75
16 (17)	--	--	1N1776	50	1N3025	15.5	1N4745	15.5	1ZS16	15.5	--	--	3Z16	40	1N5353	75
18 (19)	--	--	1N1777	50	1N3026	14.0	1N4746	14.0	1ZS18	14.0	1N1596	35	3Z18	35	1N5354	70
20	--	--	1N1778	15	1N3027	12.5	1N4747	12.5	1ZS20	12.5	--	--	3Z20	35	1N5355	65
22	--	--	1N1779	15	1N3028	11.5	1N4748	11.5	1ZS22	11.5	1N1597	30	3Z22	30	1N5358	50
24 (25)	--	--	1N1780	15	1N3029	10.5	1N4749	10.5	1ZS24	10.5	--	--	3Z24	30	1N5359	50
27 (28)	--	--	1N1781	15	1N3030	9.5	1N4750	9.5	1ZS27	9.5	1N1598	25	3Z27	25	1N5360	50
30	--	--	--	--	--	--	--	--	--	--	--	--	--	--	1N5362	50
33	--	--	1N1782	15	1N3031	8.5	1N4751	8.5	1ZS30	8.5	--	--	3Z30	25	1N5363	40
36	--	--	1N1783	15	1N3032	7.5	1N4752	7.5	1ZS33	7.5	--	--	--	--	1N5364	40
39	--	--	1N1784	15	1N3033	7.0	1N4753	7.0	1ZS36	7.0	--	--	--	--	1N5365	30
43	--	--	1N1785	15	1N3034	6.5	1N4754	6.5	1ZS39	6.5	--	--	--	--	1N5366	30
47	--	--	1N1786	15	1N3035	6.0	1N4755	6.0	1ZS43	6.0	--	--	--	--	1N5367	30
51	--	--	1N1787	15	1N3036	5.5	1N4756	5.5	1ZS47	5.5	--	--	--	--	1N5368	25
56 (60)	--	--	1N1788	15	1N3037	5.0	1N4757	5.0	1ZS51	5.0	--	--	--	--	1N5369	25
62	--	--	1N1789	15	1N3038	4.5	1N4758	4.5	1ZS56	4.5	--	--	--	--	1N5370	20
68	--	--	1N1790	5	1N3039	4.0	1N4759	4.0	1ZS62	4.0	--	--	--	--	1N5372	20
75	--	--	1N1791	5	1N3040	3.7	1N4760	3.7	1ZS68	3.7	--	--	--	--	1N5373	20
82 (87)	--	--	1N1792	5	1N3041	3.3	1N4761	3.3	1ZS75	3.3	--	--	--	--	1N5374	20
91	--	--	1N1793	5	1N3042	3.0	1N4762	3.0	1ZS82	3.0	--	--	--	--	1N5375	15
100	--	--	1N1794	5	1N3043	2.8	1N4763	2.8	1ZS91	2.8	--	--	--	--	1N5377	15
110	--	--	1N1795	5	1N3044	2.5	1N4764	2.5	1ZS100	2.5	--	--	--	--	1N5378	12
120	--	--	1N1796	5	1N3045	2.3	1ZT110	2.3	1ZS110	2.3	--	--	--	--	--	--
130	--	--	1N1797	5	1N3046	2.0	1ZT130	2.0	1ZS120	2.0	--	--	--	--	--	--
150	--	--	1N1798	5	1N3047	1.9	1ZT150	1.9	1ZS130	1.9	--	--	--	--	--	--
180	--	--	1N1799	5	1N3048	1.7	1ZT180	1.7	1ZS150	1.7	--	--	--	--	--	--
200	--	--	1N1800	5	1N3049	1.6	1ZT180	1.6	1ZS160	1.6	--	--	--	--	--	--
	--	--	1N1801	5	1N3050	1.4	1ZT180	1.4	1ZS180	1.4	--	--	--	--	--	--
	--	--	1N1802	5	1N3051	1.2	1ZT200	1.2	1ZS200	1.2	--	--	--	--	--	--

Zener Voltage Regulators T.C. Voltage References

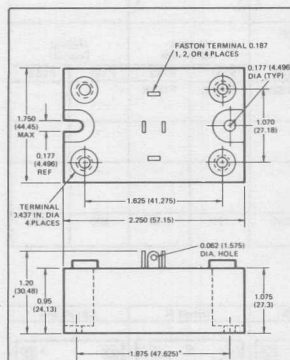
Power Rating	5W		10W		10W		10W		10W		10W		50W		50W		
Max. Op. Temp. (°C)	200°		165°		165°		175°		175°		175°		175°		175°		
Tolerance (%)	5, 10, 20%		5, 10%		5, 10, 20%		5, 10%		5, 10, 20%		5, 10%		5, 10, 20%		5, 10, 20%		
Notes	(d)		(e)		(f) (4)		(g) (5) †		(h) (5)		(i) (5) †		(j) (5)		(k)		
Case Style	C-12		D0-4		D0-4		D0-4		D0-4		D0-4		C-8		C-14		
V _Z	Part No.	I _{ZT} (mA)	Part No.	I _{ZT} (mA)	Part No.	I _{ZT} (mA)	Part No.	I _{ZT} (mA)	Part No.	I _{ZT} (mA)	Part No.	I _{ZT} (mA)	Part No.	I _{ZT} (mA)	Part No.	I _{ZT} (mA)	
3.3	5ZS3.3	380	—	—	—	—	—	—	—	—	—	—	—	—	—	—	
3.6	5ZS3.6	350	—	—	—	—	—	—	—	—	—	—	—	—	—	—	
3.9	5ZS3.9	320	1N1599	500	10Z3.9	500	1N3993	640	—	—	—	—	1N4549	3200	1N4557	3200	
4.3	5ZS4.3	290	—	—	10Z4.3	400	1N3994	580	—	—	—	—	1N4550	2900	1N4558	2900	
4.7	5ZS4.7	260	1N1600	400	10Z4.7	400	1N3995	530	—	—	—	—	1N4551	2650	1N4559	2650	
5.1	5ZS5.1	240	—	—	10Z5.1	400	1N3996	490	—	—	—	—	—	1N4552	2450	1N4560	2450
5.6	5ZS5.6	220	1N1601	350	10Z5.6	350	1N3997	445	—	—	—	—	—	1N4553	2250	1N4561	2250
(6.0)	5ZS6.0	200	—	—	10Z6.0	350	—	—	—	—	—	—	—	—	—	—	
6.2	5ZS6.2	200	—	—	10Z6.2	350	1N3998	405	—	—	—	—	1N4554	2000	1N4562	2000	
6.8	5ZS6.8	175	1N1602	300	10Z6.8	300	1N3999	370	1N1805	1000	1N2970	370	1N3305	1850	1N2804	1850	
6.8	—	—	—	—	—	—	—	—	—	—	—	—	—	1N4555	1850	1N4563	1850
7.5	5ZS7.5	175	—	—	10Z7.5	300	1N4000	335	1N1806	1000	1N2971	335	1N3306	1700	1N2805	1700	
8.2	5ZS8.2	150	1N1603	250	10Z8.2	250	—	—	1N1807	1000	1N2972	305	1N3307	1500	1N2806	1500	
(8.7)	5ZS8.7	150	—	—	—	—	—	—	—	—	—	—	—	—	—	—	
9.1	5ZS9.1	150	—	—	10Z9.1	250	—	—	1N1808	500	1N2973	275	1N3308	1370	1N2807	1370	
10	5ZS10	125	1N1604	200	10Z10	200	1N2498	500	1N1351	500	1N2974	250	1N3309	1200	1N2808	1200	
11	5ZS11	125	—	—	10Z11	200	1N2499	500	1N1352	500	1N2975	230	1N3310	1100	1N2809	1100	
12	5ZS12	100	1N1605	170	10Z12	170	1N2500	500	1N1353	500	1N2976	210	1N3311	1000	1N2810	1000	
13	5ZS13	100	—	—	10Z13	170	1N1816	500	1N1354	500	1N2977	190	1N3312	960	1N2811	960	
(14)	5ZS14	100	—	—	—	—	—	—	—	—	—	—	—	—	—	—	
15	5ZS15	75	1N1606	140	10Z15	140	1N1817	500	1N1355	500	1N2978	180	1N3313	890	1N2812	890	
16	5ZS16	75	—	—	10Z16	140	1N1818	500	1N1356	500	1N2980	155	1N3315	780	1N2814	780	
(17)	5ZS17	70	—	—	—	—	—	—	—	—	—	—	—	—	—	—	
18	5ZS18	65	1N1607	110	10Z18	110	1N1819	500	1N1357	150	1N2982	140	1N3317	700	1N2816	700	
(19)	5ZS19	65	—	—	—	—	—	—	—	—	1N2983	130	1N3318	660	1N2817	660	
20	5ZS20	65	—	—	10Z20	110	1N1820	250	1N1358	150	1N2984	125	1N3319	630	1N2818	630	
22	5ZS22	50	1N1608	90	10Z22	90	1N1821	250	1N1359	150	1N2985	115	1N3320	570	1N2819	570	
24	5ZS24	50	—	—	10Z24	90	1N1822	250	1N1360	150	1N2986	105	1N3321	520	1N2820	520	
(25)	5ZS25	50	—	—	—	—	—	—	—	—	1N2987	100	1N3322	500	1N2821	500	
27	5ZS27	50	1N1609	70	10Z27	70	1N1823	250	1N1361	150	1N2988	95	1N3323	460	1N2822	460	
(28)	5ZS28	50	—	—	—	—	—	—	—	—	—	—	—	—	—	—	
30	5ZS30	40	—	—	10Z30	70	1N1824	250	1N1362	150	1N2989	85	1N3324	420	1N2823	420	
33	5ZS33	30	—	—	—	—	1N1825	150	1N1363	150	1N2990	85	1N3325	380	1N2824	380	
36	5ZS36	30	—	—	—	—	1N1826	150	1N1364	150	1N2991	70	1N3326	350	1N2825	350	
39	5ZS39	30	—	—	—	—	1N1827	150	1N1365	150	1N2992	65	1N3327	320	1N2826	320	
43	5ZS43	30	—	—	—	—	1N1828	150	1N1366	150	1N2993	60	1N3328	290	1N2827	290	
45	—	—	—	—	—	—	—	—	—	—	1N2994	55	1N3329	280	1N2828	280	
47	5ZS47	25	—	—	—	—	1N1829	150	1N1367	150	1N2995	55	1N3330	270	1N2829	270	
50	—	—	—	—	—	—	—	—	—	—	1N2996	50	1N3331	250	1N2830	250	
51	5ZS51	25	—	—	—	—	1N1830	150	1N1368	150	1N2997	50	1N3332	245	1N2831	245	
52	—	—	—	—	—	—	—	—	—	—	1N2998	50	1N3333	240	—	—	
56	5ZS56	20	—	—	—	—	1N1831	150	1N1369	150	1N2999	45	1N3334	220	1N2832	220	
(60)	5ZS60	20	—	—	—	—	—	—	—	—	—	—	—	—	—	—	
62	5ZS62	20	—	—	—	—	1N1832	50	1N1370	50	1N3000	40	1N3335	200	1N2833	200	
68	5ZS68	20	—	—	—	—	1N1833	50	1N1371	50	1N3001	37	1N3336	180	1N2834	180	
75	5ZS75	20	—	—	—	—	1N1834	50	1N1372	50	1N3002	33	1N3337	170	1N2835	170	
82	5ZS82	15	—	—	—	—	1N1035	50	1N1373	50	1N3003	30	1N3338	150	1N2836	150	
(87)	5ZS87	15	—	—	—	—	—	—	—	—	—	—	—	—	—	—	
91	5ZS91	15	—	—	—	—	1N1836	50	1N1374	50	1N3004	28	1N3339	140	1N2837	140	
100	5ZS100	12	—	—	—	—	1N2008	50	1N1375	50	1N3005	25	1N3340	120	1N2838	120	
105	—	—	—	—	—	—	—	—	—	—	1N3006	25	—	—	—	—	
110	—	—	—	—	—	—	1N2009	50	1N1809	50	1N3007	23	—	—	—	—	
120	—	—	—	—	—	—	1N2010	50	1N1810	50	1N3008	20	—	—	—	—	
130	—	—	—	—	—	—	1N2011	50	1N1811	50	1N3009	19	—	—	—	—	
(140)	—	—	—	—	—	—	—	—	—	—	—	—	—	—	—	—	
150	—	—	—	—	—	—	—	—	—	—	—	—	—	—	—	—	
160	—	—	—	—	—	—	1N2012	50	1N1812	50	1N3011	18	—	—	—	—	
175	—	—	—	—	—	—	—	—	1N1813	50	1N3012	16	—	—	—	—	
180	—	—	—	—	—	—	—	—	—	—	—	—	—	—	—	—	
180	—	—	—	—	—	—	—	—	1N1814	50	1N3014	14	—	—	—	—	
200	—	—	—	—	—	—	—	—	1N1815	50	1N3015	12	—	—	—	—	

Power Circuits: PACE/paks

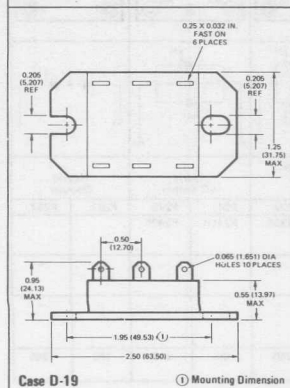
PACE/paks are IR's family of electrically isolated, solid-state power assemblies, which provide complete control functions. They offer a wide variety of advantages over conventional methods of fabricating power supplies, control circuits, battery chargers, and choppers, including reduced costs, more efficient heat-sinking, greater reliability, and a sharp reduction in total package size.

They are now available in both 25 Amp and 42.5 Amp current ratings in seven circuit configurations. All are available in both 120V and 230V RMS ratings.

Additional savings can be made using PACE/paks in an AC-switch configuration, as replacements for conventionally assembled switches. They are presently available in 50, 60, and 100 Amp (rms) series.



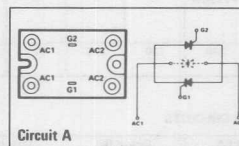
Case D-20



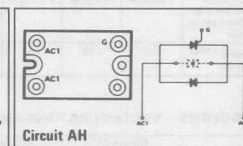
Case D-19

AC SWITCHES

VRRM and VDRM Max. Repetitive Peak Reverse Voltage and Off-State Voltage	50 Amps Circuits		60 Amps Circuits		100 Amps Circuits	
	A	AH	A	AH	A	AH
300	P241	P251	P641	P651	P341	P351
600	P242	P252	P642	P652	P342	P352
800	P243		P643		P343	
1000	P245		P645		P345	



Circuit A



Circuit AH

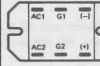
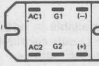
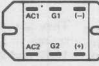
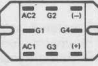
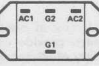
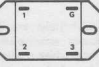
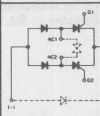
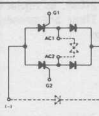
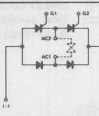
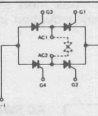
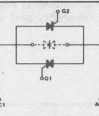
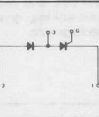
SPECIFICATIONS FOR PACE/pak CIRCUITS AND PACE/pak AC SWITCHES

CASE	PACE/pak Circuits		PACE/pak AC Switches		
	P100	P200	P240	P640	P340
I_d	max. dc output current @ 75°C T _C (A)	25	42.5	—	—
I_T (RMS)	max. output current @ 75°C base plate	—	—	50	60
V_{RMS}	AC input voltage (V)	120, 240	120, 240, 480	120, 240, 480	120, 240, 480
I_{TSM}	max. non-repetitive surge current (A)	250	600	600	1000
I^2t	max. I^2t for fusing, t = 5 to 8.3 msec (A ² -sec)	260	1500	1500	4000
di/dt	max. rate of rise of turned-on current (A/ μ sec)	100	100	100	100
dv/dt	min. critical rate of rise of turned-on current (A/ μ sec) (1)	20	20	20	20
I_{GT}	max. required gate current to trigger, 25°C (mA)	40	110	110	110
V_{GT}	max. required gate voltage to trigger, 25°C (V)	2.5	3.0	3.0	3.0
$R_{\theta cs}$	thermal resistance, case to sink (°C/W)	0.10	0.10	0.10	0.10

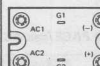
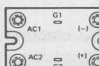
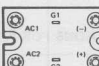
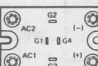
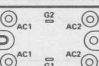
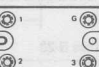
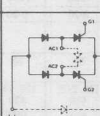
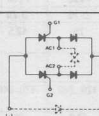
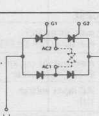
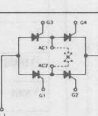
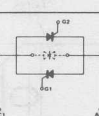
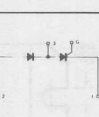
(1) Higher dv/dt available.

Power Circuits: PACE/paks

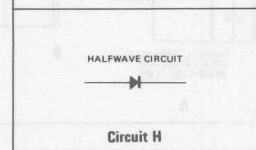
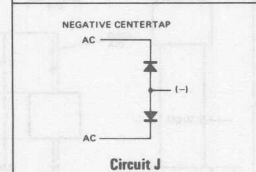
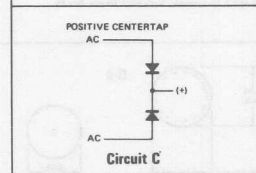
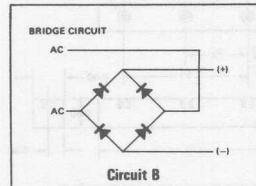
P100 SERIES – VOLTAGE RATINGS AND CIRCUITS

	Circuit BC		Circuit BA		Circuit BD		Circuit BS		Circuit A		Circuit DA	
Terminal Positions												
Schematic Diagram												
	Single Phase Hybrid Bridge, Common Cathode		Single Phase Hybrid Bridge, Common Anode		Single Phase Hybrid Bridge Doubler Connection		Single Phase, All SCR Bridge		Hybrid AC Switch		Hybrid Doubler	
Basic series	P101	P102	P111	P112	P121	P122	P131	P132	P141	P142	P161	P162
With Klip-Sel voltage suppression	P101K	P102K	P111K	P112K	P121K	P122K	P131K	P132K	P141K	P142K		
With free-wheeling diode	P101W	P102W	P111W	P112W	—	—	—	—	—	—	—	—
With both Klip-Sel and free-wheeling diode	P101KW	P102KW	P111KW	P112KW	—	—	—	—	—	—	—	—
V_{RMS} – Max. Voltage	120	240	120	240	120	240	120	240	120	240	120	240

P200 SERIES – VOLTAGE RATINGS AND CIRCUITS

	Circuit BC		Circuit BA		Circuit BD		Circuit BS		Circuit A		Circuit DA	
Terminal Positions												
Schematic Diagram												
	Single Phase Hybrid Bridge, Common Cathode		Single Phase Hybrid Bridge, Common Anode		Single Phase Hybrid Bridge Doubler Connection		Single Phase, All SCR Bridge		Hybrid AC Switch		Hybrid Doubler	
Basic series	P201	P202	P211	P212	P221	P222	P231	P232	P241	P242	P261	P262
With Klip-Sel voltage suppression	P201K	P202K	P211K	P212K	P221K	P222K	P231K	P232K	P241K	P242K		
With free-wheeling diode	P201W	P202W	P211W	P212W	—	—	—	—	—	—	—	—
With both Klip-Sel and free-wheeling diode	P201KW	P202KW	P211KW	P212KW	—	—	—	—	—	—	—	—
V_{RMS} – Max. Voltage	120	240	120	240	120	240	120	240	120	240	120	240

Power Circuits: Molded Circuit Assemblies



MOLDED CIRCUIT ASSEMBLIES

International Rectifier manufactures a wide range of compact, easy to handle, molded circuit assemblies. These include halfwave, doubler, and bridge-type circuits in a wide variety of mechanical configurations, as outlined on the following pages.

DIODE CENTERTAPS

I_{dc} - DC Output Current (A)	15	15	30	30
@ $T_C = 0^\circ\text{C}$	75	75	75	75
I_{FSM} - Surge Current (A)	150	150	300	300
Circuit	C	J	C	J
Case Style	D-27	D-27	D-27	D-27
V_{RRM}		PART NUMBERS		
50 Volts	-	-	-	-
100 Volts	150VC1L	150VJ1L	300WC1L	300WJ1L
200 Volts	150VC2L	150VJ2L	300WC2L	300WJ2L
300 Volts	150VC3L	150VJ3L	300WC3L	300WJ3L
400 Volts	150VC4L	150VJ4L	300WC4L	300WJ4L
600 Volts	150VC6L	150VJ6L	300WC6L	300WJ6L
800 Volts	150VC8L	150VJ8L	300WC8L	300WJ8L
1000 Volts	150VC10L	150VJ10L	300WC10L	300WJ10L

FUSE-CLIP RECTIFIERS

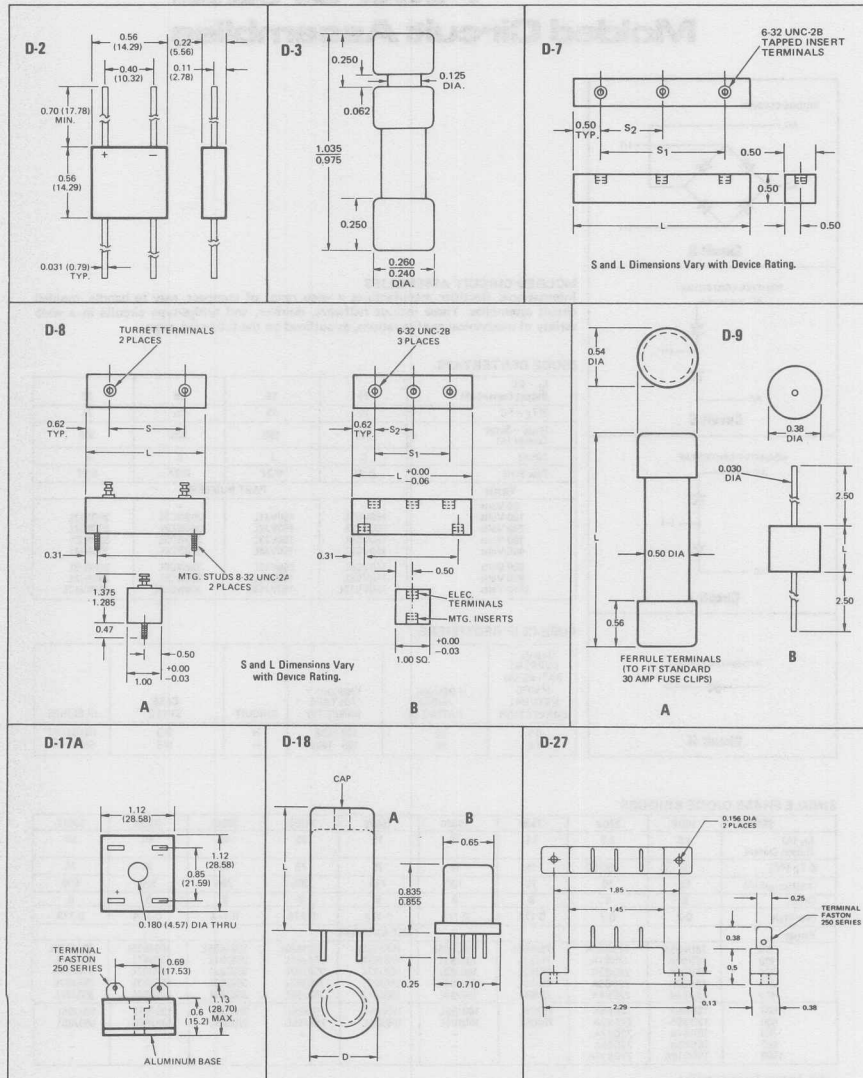
I_{FAV} - CURRENT RATING (A) @ 50°C NATURAL CONVECTION	I_{FM} (Surge) - SURGE RATING (A)	$V_{RM(rep)}$ - VOLTAGE RANGE (V)	CIRCUIT	CASE STYLE	IR SERIES
0.5	30	100 - 400	H	D-3	1N1081-84
1.0	50	100 - 1000	H	D-3	5MA1-10

SINGLE PHASE DIODE BRIDGES

SERIES	18DB	22DB	75JB	100JB	150JB	250JB	300JB	400JB	500JB
I_{dc} (A) Output Current	1.8	2.2	7.5	10	15	25	30	40	50
@ T_C (°C)	50 ①	50 ①	75	75	75	75	75	75	75
I_{FSM} (surge) (A)	50	50	75	100	150	300	350	500	600
Circuit	B	B	B	B	B	B	B	B	B
Case Style	D-2	D-2	D-17A	D-17A	D-17A	D-17A	D-17A	D-17A	D-17A
V_{RRM}		PART NUMBERS							
50	18DB05A	22DB05A	75JB05L	100JB05L	150JB05L	250JB05L	300JB05L	400JB05L	500JB05L
100	18DB1A	22DB1A	75JB1L	100JB1L	150JB1L	250JB1L	300JB1L	400JB1L	500JB1L
200	18DB2A	22DB2A	75JB2L	100JB2L	150JB2L	250JB2L	300JB2L	400JB2L	500JB2L
300	18DB3A	22DB3A	75JB3L	100JB3L	150JB3L	250JB3L	300JB3L	400JB3L	500JB3L
400	18DB4A	22DB4A	75JB4L	100JB4L	150JB4L	250JB4L	300JB4L	400JB4L	500JB4L
500	18DB5A	22DB5A	75JB5L	100JB5L	150JB5L	250JB5L	300JB5L	400JB5L	500JB5L
600	18DB6A	22DB6A	75JB6L	100JB6L	150JB6L	250JB6L	300JB6L	400JB6L	500JB6L
700	18DB7A	22DB7A	-	-	-	-	-	-	-
800	18DB8A	22DB8A	-	-	-	-	-	-	-
1000	18DB10A	22DB10A	-	-	-	-	-	-	-

① Ambient Temperature (T_A)

Power Circuits: Molded Circuit Assemblies



Power Circuits: Molded Circuit Assemblies

HIGH POWER CARTRIDGE RECTIFIERS

I _{F(AV)} - CURRENT RATING (A) @ 50°C NATURAL CONVECTION	I _{FM(Surge)} - SURGE RATING (A)	V _{RM(rep)} - VOLTAGE RANGE (V)	CIRCUIT	CASE STYLE	IR SERIES	COMMENTS
75mA to 250mA @ 25°C 25mA to 100mA @ 100°C	50	0.6 - 10KV	H	D-9B	1N2373-84 & 1N2399	Miniature Cartridges.
75mA to 250mA @ 25°C 25mA to 100mA @ 100°C	50	0.6 - 30KV	H	D-9B	67D060H-53PMN to 67D300H	Miniature Cartridges.
45mA to 100mA @ 75°C	50	1.5 - 16KV	H	D-9A	1N1133-49 & 1N2139	Ferrule mounted.
250mA @ 50°C	50	1.5 - 50KV	H	D-9A	67D015H-55FNN to 67D500HFNN	Ferrule mounted.
250mA to 440mA @ 75°C Oil 220mA to 360mA @ 75°C, 200LFM	50	1.5 - 16KV	H	D-9A	1N1745-62	High current type
375mA to 500mA @ 50°C Oil or 200LFM	50	1.5 - 50KV	H	D-9A	67D015H-55FNN to 67D500HFNN	High current type

HIGH VOLTAGE MOLDED ASSEMBLIES

250mA	50	5 - 40KV	H ①	D-7	67D050H0-4TNN to 67D400H	Avalanche selected devices
350mA	50	5 - 75KV	H	D-8A D-8B ②	67D050H-20TTS to 67D750H	RC compensated for system reliability.
1.25	90	1.5 - 75KV	H ①	D-8A	1N4865-77 & 1N4867	RC compensated
1.25	90	1.5 - 75KV	H ①	D-8A D-8B ②	67S015H-20LSS to 67S750H	RC compensated

① Standard circuit is halfwave. To order as doubler, change "H" to "D". (Ex.: 67D015H20TTS becomes 67D015D20TTS)

② D-8A is halfwave. D-8B is doubler.

SOLID-STATE TUBE REPLACEMENTS

International Rectifier's solid-state tube replacement line provides retrofit capabilities for mercury-vapor and vacuum rectifier tubes. These offer the following advantages; no filament require-

ment, no warm-up, long life, and high mechanical shock resistance.

For detailed information on pre-engineered assemblies or special designs, please contact your local IR Office.

IR PART NUMBER	V _{RM(rep)} - PER LEG (V)	I _{FM(AV)} - MAX. DC OUTPUT CURRENT @ 70°C (mA)	V _{FM} - VDC PER LEG (Vdc) @ 0.5 ADC @ 25°C	MAX. DIMENSIONS (Case D-18A) (In.)		REPLACES TUBES
				L	D	
1N570 (ST-1A)	1,500	75	1.8	Case D-18B		MIL-6X4, MIL-12X4, 5Z3, 80, 82, 83, 83V, 0Z4, 5X4, 5Y4, 6AX5, 6X5 5AV4, 5AW4, 5AZ4, 5T4, 5U4, 5V4, 5W4, 5Y3, 5Z4.
1N1150A	1,500	750 ①	3.0	2.65	1.25	
1N1237	1,500	750 ①	3.0	2.65	1.25	
1N1238	1,500	750 ①	3.0	2.65	1.25	
1N1239	2,800	500 ①	6.0	3.75	1.38	5R4 6AU4, 6AX4, 6BL4, 6W4, 12AX4, 17AX4, 25W4 5AY4, 5AW4, 5AX4, 5T4, 5U4, 5V4, 5W4, 5Y3, 5Z4, 6004
1N1262 (ST-7)	4,500	250 ①	4.5	2.65	1.25	
1N2389	1,600	600	5.3 ①	1.50	1.44	
1N2490	1,600	500 ①	3.0	1.50	0.87	6AX4 6X4, 12X4 5AW4, 5AX4, 5AZ4, 5T4, 5U4, 5Y3, 6004
1N2630 (ST-1)	1,500	85	1.8	1.81	0.88	
1N2631 (ST-2)	1,600	600	1.8	2.65	1.25	
1N2632	2,800	200	2.7	2.65	1.25	5R4, 5R4W
1N2633 (ST-3)	1,600	600	1.8	2.65	1.25	0Z4, 5X4, 6AX5, 6W5, 6X5, 6ZY5, 5839, 5852
1N2634 (ST-4)	1,600	600	3.6	2.65	1.28	5Z3, 80, 82, 83, 83V
1N2635 (ST-5)	1,500	85	3.6	1.81	0.88	High Altitude 6X4 and 12X4
1N2636 (ST-6)	1,500	85	3.6	2.45	1.19	84, 8Z4
1N2637 (ST-7A)	10,400	250	11.0	5.05	1.38	3B28, 2458, 866, 866A
ST-8 ①	1,250	80	6.2 ②	1.10	1.40	0Z4, 6X5
ST-9 ①	10,000	1,250	14.0	8.05	2.31	8008
ST-10 ②	10,000	1,250	14.0	8.05	2.31	872A
ST-11 ②	7,500	125	8.1	4.20	1.20	816
ST-12 ③	40,000	100	54.0	7.90	2.40	8020
ST-13	1,275	130	1.8	2.00	0.82	6BW4, 12BW4
ST-14	1,600	600	5.3 ①	1.50	1.44	5AV4, 5AW4, 5AX4, 5T4, 5U4, 5Y4, 5W4, 5Y3, 5Z4, 6004
ST-15 ③	15,000	1,750	15.0	9.65	3.88	673
ST-16 ③	15,000	1,750	15.0	9.65	3.88	575A

Notes

① @ 100°C. ② Including internal current limiting resistor. ③ Incorporates compensating R-C networks. ④ Surge ratings: ST-1 thru ST-14 = 50A; ST-15 & ST-16 = 200A.

Selenium Rectifiers

Fig. 1 All Dimensions in Inches.

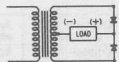


Fig. 2

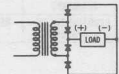


Fig. 3

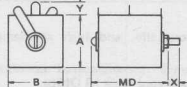


Fig. 4

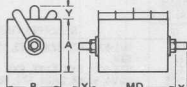


Fig. 5

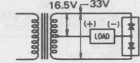


Fig. 6

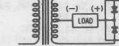
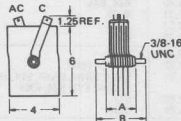


Fig. 7



Listed are the basic specifications for selected IR selenium rectifiers. IR offers an extensive selection of standard and special order selenium devices including: power stacks, cartridges, miniature stacks, diodes, loose cell kits, voltage suppressors (Klip-Sels) and contact protectors.

Your local IR Distributor, or IR Field Office, will gladly supply you with complete specifications, ordering assistance, price, and delivery quotations.

STANDARD STACKS

OUTPUT		AC VOLTS	CIRCUIT & CONNECTING DIAG. FIG.	IR PART NO.	FIG.	DIMENSIONS (Inches)					
DC VOLTS	DC AMP					A	B	MD	X	Y	STUD
0	0.5	36	1	J14C04	3	1.0	1.0	1.12	.38	.44	8-32
	1.5	36	1	J14C1	3	1.5	1.5	1.12	.38	.44	8-32
to	5.0	36	1	J14C5	3	3.0	3.0	1.12	.75	.63	3/8-16
	10.0	36	1	J14C8	3	4.0	4.0	1.88	.75	1.12	3/8-16
14	20.0	36	1	J14C17	3	6.0	5.0	2.12	.75	1.25	3/8-16
0	0.5	36	2	J29B04	4	1.0	1.0	1.5	.38	.44	8-32
	1.5	36	2	J29B1	4	1.5	1.5	1.5	.38	.44	8-32
to	5.0	36	2	J29B5	4	3.0	3.0	2.63	.75	.63	3/8-16
	10.0	36	2	J29B8	4	4.0	4.0	2.63	.75	1.12	3/8-16
29	20.0	36	2	J29B17	4	6.0	5.0	3.25	.75	1.25	3/8-16
0	0.5	72	2	J58B04	4	1.0	1.0	2.25	.38	.44	8-32
	1.5	72	2	J58B1	4	1.5	1.5	2.25	.38	.44	8-32
to	5.0	72	2	J58B5	4	3.0	3.0	4.19	.75	.63	3/8-16
	10.0	72	2	J58B8	4	4.0	4.0	4.19	.75	1.12	3/8-16
58	20.0	72	2	J58B17	4	6.0	5.0	5.63	.75	1.25	3/8-16
0	0.5	144	2	J116B04	4	1.0	1.0	3.81	.38	.44	8-32
	1.5	144	2	J116B1	4	1.5	1.5	3.81	.38	.44	8-32
to	5.0	144	2	J116B5	4	3.0	3.0	7.19	.75	.63	3/8-16
	10.0	144	2	J116B8	4	4.0	4.0	7.19	.75	1.12	3/8-16
116	20.0	144	2	J116B17	4	6.0	5.0	10.25	.75	1.25	3/8-16
0	0.5	180	2	J135B04	4	1.0	1.0	4.56	.38	.44	8-32
	1.5	180	2	J135B1	4	1.5	1.5	4.56	.38	.44	8-32
to	5.0	180	2	J135B5	4	3.0	3.0	8.69	.75	.63	3/8-16
	10.0	180	2	J135B8	4	4.0	4.0	8.69	.75	1.12	3/8-16
135	20.0	180	2	J135B17	4	6.0	5.0	12.56	.75	1.25	3/8-16

UNIVERSAL QUICK CHARGER STACKS

Maximum AC voltage input is 33 volts line-to-line (see figures 5 & 6). DC output is 6 to 12 volts. All ratings are based on forced convection cooling.

Stack Ratings and Dimensions

OUTPUT	CIRCUIT DIAGRAM FIG.	IR PART NO.	DIMENSIONS (Inches) (See Fig. 7)		
			A	B	C
50 - 100	5	BCR100	3.88	5.64	Neg (-)
30 - 60	5	BCR60	2.44	3.94	Neg (-)
50 - 100	6	BCF100	3.88	5.64	Pos (+)
30 - 60	6	BCF60	2.44	3.94	Pos (+)

Selenium Rectifiers

Replacement stacks — Often a standard IR stack with custom brackets, will meet the needs of a custom stack replacement. IR can also design and produce custom stacks to meet your requirements.

MINIATURE STACKS

MAX. AC INPUT (VOLTS RMS)	MAX. DC OUTPUT (mA)	PEAK REVERSE VOLTAGE (V)	MIN. SERIES RESISTANCE (Ω)	IR PART NO.	FIG.	DIMENSIONS (Inches)	
						A SQ.	B
ENTERTAINMENT POWER SUPPLY REPLACEMENT RECTIFIERS							
Half Wave Rectifiers for AC to DC Conversion							
130	75	380	—	E075L	8	0.66	0.75
130	150	380	—	E150L	8	1.0	1.0
130	300	380	—	E300L	8	1.2	1.25
130	500	380	—	E500L	8	1.5	1.25
130	650	380	—	E650L	8	2.0	1.25
HALF WAVE RECTIFIERS							
36	65	—	47	Q1H	8	0.67	0.44
36	100	—	22	A1H	8	1.0	0.44
36	150	—	15	B1H	8	1.2	0.44
36	250	—	5	C1H	8	1.5	0.44
36	500	—	5	M1H	8	2.0	0.44
FULL WAVE RECTIFIER BRIDGES							
36	100	—	—	O1B	9A	0.67	0.81
130	100	—	—	O4B	9A	0.67	1.25
260	100	—	—	O8B	9A	0.67	1.75
36	180	—	—	A1B	9A	1.0	0.81
130	180	—	—	A4B	9A	1.0	1.25
36	300	—	—	B1B	9A	1.2	0.81
36	600	—	—	C1B	9A	1.5	0.81
36	1200	—	—	M1B	9A	2.0	0.81
MAGNETIC-AMPLIFIER BRIDGE, SINGLE PHASE							
130	100	—	—	O4M	9B	0.67	1.25
260	100	—	—	O8M	9B	0.67	1.75
VOLTAGE DOUBLER, SINGLE PHASE (1)							
260	100	—	—	O8D	9C	0.67	1.25

(1) Ratings for 2 units connected as single phase bridge.

CARTRIDGE RECTIFIERS — A complete line of selenium cartridge rectifiers is available from IR with peak reverse voltages ranging from 63.5 to 30,000 volts. Four cell sizes (1/8 to 1/2 inch nominal diameter) and lengths from 1 inch to 7-7/8 inches.

TV REPLACEMENT CARTRIDGES

APPLICATION	OUTPUT VOLTAGE (V)	DC OUTPUT CURRENT (mA)	IR PART NO.	L — LENGTH (SEE FIGURE 10)
TV Boost	800	2	US17HFP	0.690 in. max.
TV Focus	6500	2	US144HFP	2.5 in. max.

KLIP-SELS (AC Types)

SOLID STATE DEVICE	SUPPRESSOR		FOR INDIVIDUAL RECTIFIER RATED THRU 3 AMP	FOR INDIVIDUAL RECTIFIER RATED THRU 60 AMP	FOR INDIVIDUAL RECTIFIER RATED THRU 80 AMP	FOR INDIVIDUAL RECTIFIER RATED THRU 250 AMP
	VOLTAGE RATING (VRRM)	TRANSIENT VOLTAGE RATING* (VRRM)	PEAK CURRENT 0.25A	PEAK CURRENT 1.0A	PEAK CURRENT 3.0A	PEAK CURRENT 15A
			Fig. 11 (A = .57" max. dia.)	Fig. 11 (A = .70" max. dia.)	Fig. 12 (A = 1" Sq.)	Fig. 12 (A = 2" Sq. Cells)
100	150	52	KV2DPF 0.63"	KZ2DPF 0.63"	KSA2DAF 1.50"	KSL2DAF 1.75"
150	250	78	KV2DPF 0.63"	KZ3DPF 0.63"	KSA3DAF 1.62"	KSL3DAF 1.93"
200	300	104	KY4DPF 0.63"	KZ4DPF 0.63"	KSA4DAF 1.75"	KSL4DAF 2.06"
250	350	130	KV5DPF 0.63"	KZ5DPF 0.63"	KSA5DAF 1.87"	KSL5DAF 2.25"
300	425	156	KV6DPF 0.88"	KZ6DPF 0.88"	KSA6DAF 2.00"	KSL6DAF 2.37"
400	525	182	490 KY7DPF 0.88"	KZ7DPF 0.88"	KSA7DAF 2.12"	KSL7DAF 2.53"
500	650	224	630 KY9DPF 0.88"	KZ9DPF 0.88"	KSA9DAF 2.34"	KSL9DAF 2.81"
600	800	260	700 KY10DPF 0.88"	KZ10DPF 0.88"	KSA10DAF 2.46"	KSL10DAF 2.96"
700	925	312	840 KY12DPF 0.88"	KZ12DPF 0.88"	KSA12DAF 2.71"	KSL12DAF 3.28"
800	1050	364	980 KY14DPF 1.63"	KZ14DPF 1.63"	KSA14DAF 2.93"	KSL14DAF 3.56"
900	1175	416	1120 KY16DPF 1.63"	KZ16DPF 1.63"	KSA16DAF 3.18"	KSL16DAF 3.87"
1000	1300	468	1260 KY18DPF 1.63"	KZ18DPF 1.63"	KSA18DAF 3.43"	KSL18DAF 4.15"
1200	1600	520	1400 KY20DPF 1.63"	KZ20DPF 1.63"	KSA20DAF 3.65"	KSL20DAF 4.46"

*Not standardized. Check device specifications.

All Dimensions in Inches.

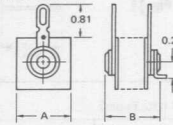


Fig. 8 — Half Wave Stacks

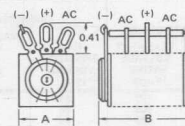


Fig. 9A — Full Wave Stacks

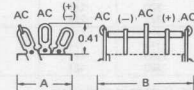


Fig. 9B — Magnetic Amplifier Stacks

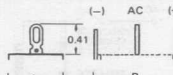


Fig. 9C — Doubler Stacks

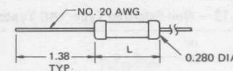
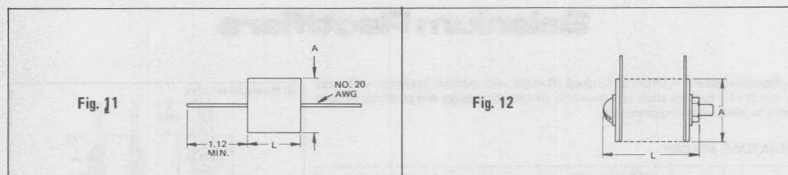


Fig. 10 — Cartridge Rectifiers

Selenium Rectifiers



KLIP-SELS (DC Types)

SOLID STATE DEVICE		SUPPRESSOR		FOR INDIVIDUAL RECTIFIER RATED THRU 3 AMP	FOR INDIVIDUAL RECTIFIER RATED THRU 15 AMP	FOR INDIVIDUAL RECTIFIER RATED THRU 60 AMP	FOR INDIVIDUAL RECTIFIER RATED THRU 250 AMP
VOLTAGE RATING (VRRM)	TRANSIENT VOLTAGE RATING* (VRSM)	MAX. OPERATING VOLTAGE (V _{OC})	MAX. CLAMPING VOLTAGE @ PEAK CURRENT (V _{PK})	PEAK CURRENT	PEAK CURRENT	PEAK CURRENT	PEAK CURRENT
				0.25A	1.0A	3.0A	15A
				Fig. 11 (A = .57" max. dia.)	Fig. 11 (A = .70" max. dia.)	Fig. 12 (A = 1" Sq.)	Fig. 12 (A = 2" Sq. Cells)
				IR PART NO.	IR PART NO.	IR PART NO.	IR PART NO.
				L Dim. (max.)	L Dim. (max.)	L Dim. (max.)	L Dim. (max.)
100	150	44	132	KYP2DPF 0.63"	KZP2DPF 0.63"	KSAP2DAF 1.28"	KSLP2DAF 1.50"
150	250	66	198	KYP3DPF 0.63"	KZP3DPF 0.63"	KSAP3DAF 1.34"	KSLP3DAF 1.56"
200	300	88	264	KYP4DPF 0.63"	KZP4DPF 0.63"	KSAP4DAF 1.40"	KSLP4DAF 1.62"
250	350	110	330	KYP5DPF 0.63"	KZP5DPF 0.63"	KSAP5DAF 1.46"	KSLP5DAF 1.71"
300	420	132	396	KYP6DPF 0.63"	KZP6DPF 0.63"	KSAP6DAF 1.50"	KSLP6DAF 1.78"
400	525	154	462	KYP7DPF 0.63"	KZP7DPF 0.63"	KSAP7DAF 1.58"	KSLP7DAF 1.87"
500	650	198	594	KYP9DPF 0.63"	KZP9DPF 0.63"	KSAP9DAF 1.68"	KSLP9DAF 2.00"
600	800	220	660	KYP10DPF 0.63"	KZP10DPF 0.63"	KSAP10DAF 1.75"	KSLP10DAF 2.09"
600	800	264	792	KYP12DPF 0.88"	KZP12DPF 0.88"	KSAP12DAF 1.87"	KSLP12DAF 2.25"
700	925	286	858	KYP13DPF 0.88"	KZP13DPF 0.88"	KSAP13DAF 1.93"	KSLP13DAF 2.31"
800	1050	330	990	KYP15DPF 0.88"	KZP15DPF 0.88"	KSAP15DAF 2.06"	KSLP15DAF 2.46"
900	1175	374	1122	KYP17DPF 0.88"	KZP17DPF 0.88"	KSAP17DAF 2.18"	KSLP17DAF 2.62"
1000	1300	418	1254	KYP19DPF 0.88"	KZP19DPF 0.88"	KSAP19DAF 2.28"	KSLP19DAF 2.75"
1200	1600	484	1452	KYP22DPF 0.88"	KZP22DPF 0.88"	KSAP22DAF 2.46"	KSLP22DAF 3.00"

*Not Standardized. Check device specifications.

All Dimensions in Inches.

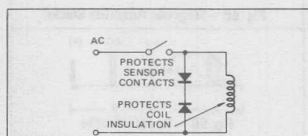


Fig. 13 - Non-Polarized Types (AC Types)

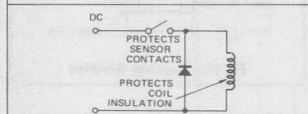


Fig. 14 - Polarized Protection (DC Types)

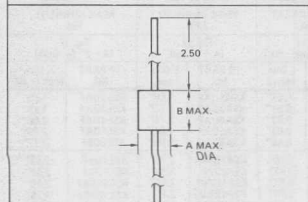


Fig. 15 - Cartridge Type

CONTACT PROTECTORS

AC TYPE (See Fig. 13)

DC TYPE (See Fig. 14)

WORKING VOLTS (VAC)	MAX. COIL CURR. (AMP)	IR PART NO.	DIMENSION FIG. 15		MIN.	MAX.	MAX. COIL CURR. (AMP)	IR PART NO.	DIMENSION FIG. 15	
			A (MAX)	B (MAX)					A (MAX)	B (MAX)
26	.20	S1V1P	.380	.620	15	22	.25	S1V1P	.380	.620
52	.20	S2V2P	.380	.620	23	44	.25	S2V2P	.380	.620
78	.20	S3V3P	.380	.620	45	66	.25	S3V3P	.380	.620
104	.20	S4V4P	.380	.620	67	88	.25	S4V4P	.380	.620
130	.20	S5V5P	.380	.620	89	110	.25	S5V5P	.380	.620
156	.20	S6V6P	.380	.990	111	132	.25	S6V2P	.380	.620
					133	154	.25	S7V2P	.380	.620
26	.40	S1Y1P	.500	.620	15	22	.60	S1Y1P	.500	.620
52	.40	S2Y2P	.500	.620	23	44	.60	S2Y2P	.500	.620
78	.40	S3Y3P	.500	.620	45	66	.60	S3Y2P	.500	.620
104	.40	S4Y4P	.500	.620	67	88	.60	S4Y2P	.500	.620
130	.40	S5Y5P	.500	.620	89	110	.60	S5Y2P	.500	.620
156	.40	S6Y6P	.500	.990	111	132	.60	S6Y2P	.500	.620
					133	154	.60	S7Y2P	.500	.620
26	.60	S1Z1P	.640	.754	15	22	.90	S1Z1P	.640	.754
52	.60	S2Z2P	.640	.754	23	44	.90	S2Z1P	.640	.754
78	.60	S3Z3P	.640	.754	45	66	.90	S3Z2P	.640	.754
104	.60	S4Z4P	.640	.754	67	88	.90	S4Z2P	.640	.754
130	.60	S5Z5P	.640	.754	89	110	.90	S5Z2P	.640	.754
156	.60	S6Z6P	.640	.990	111	132	.90	S6Z2P	.640	.754
					133	154	.90	S7Z2P	.640	.754
26	.90	S1X1P	1.050	.620	15	22	1.4	S1X1P	1.050	.620
52	.90	S2X2P	1.050	.620	23	44	1.4	S2X1P	1.050	.620
78	.90	S3X3P	1.050	.620	45	66	1.4	S3X2P	1.050	.620
104	.90	S4X4P	1.050	.620	67	88	1.4	S4X2P	1.050	.620
130	.90	S5X5P	1.050	.620	89	110	1.4	S5X2P	1.050	.620
156	.90	S6X6P	1.050	.990	111	132	1.4	S6X2P	1.050	.620
					133	154	1.4	S7X2P	1.050	.620
26	1.2	S1W1P	1.380	.620	15	22	2.0	S1W1P	1.380	.620
52	1.2	S2W2P	1.380	.620	23	44	2.0	S2W1P	1.380	.620
78	1.2	S3W3P	1.380	.620	45	66	2.0	S3W2P	1.380	.620
104	1.2	S4W4P	1.380	.620	67	88	2.0	S4W2P	1.380	.620
130	1.2	S5W5P	1.380	.620	89	110	2.0	S5W2P	1.380	.620
156	1.2	S6W6P	1.380	.990	111	132	2.0	S6W2P	1.380	.620
					133	154	2.0	S7W2P	1.380	.620

1 When connecting dc contact protectors, the terminal marked in red, or the end with polarity marking, should be connected to the positive side of the circuit.

Heat Exchangers and Hardware

HEAT EXCHANGERS AND HARDWARE

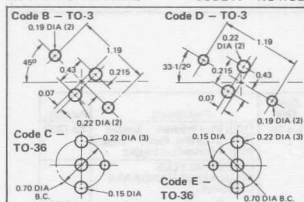
International Rectifier offers a wide variety of heat exchangers for large and small semiconductors. These were designed by power semiconductor specialists to maximize semiconductor operation and facilitate assembly. Specific units offer unique channels for the mounting of accessories and terminals. IR also offers an extensive selection of liquid-cooled Heat Exchangers for both stud-mounted and Hockey-Puk type devices. Contact your local IR Distributor, local IR Field Office, or IR's El Segundo Offices for further information. IR also offers two types of yokes for mounting Hockey-Puk type devices. These are used in conjunction with Heat Exchangers HE72 and HE75. It should be noted that there is a definite cost savings, without sacrificing thermal dissipation properties, in using an irridite finish.

HEAT EXCHANGER CODE

Example: HE 80 6 A 3
 HE - indicates heat exchanger.
 80 - two-digit extrusion number.
 6 - length in inches and decimals.
 A - indicates no-hole mounting pattern (see below).
 3 - finish (3 indicates gold irridite) (see below).

FINISH: 1 - no finish. 2 - black anodize. 3 - gold irridite.

MOUNTING PATTERNS CODE A - NO HOLE



CLEAR HOLES d - hole dia. d' - dia. free of anodize. (Type No. 2 finish)

d	d'	d	d'
K - 0.200	0.500	N - 0.330	1.000
L - 0.270	0.750	P - 0.390	1.125
H - 0.4975		Q - 0.520	1.125
M - 0.765	1.812	R - 1.030	1.812
		W - 0.765	2.250

Y - 2 holes for C3 yoke mounting.
 I - HE75, 4-hole pattern.
 Z - 2 holes for C4 yoke mounting.

TAPPED HOLES		
F - 10-32	U - 1/2-20	
G - 1/4-28	V - 5/16-24	
S - 8-32	X - 3/4-16	
T - 3/8-24		

HOLE REQUIREMENTS			
JEDEC		IR	
DD-4	K TO-48	Q	50IV W
DD-5	L TO-64	K	40RCS L
DD-8	P TO-83	Q	250PA Y
DD-9	M TO-93	M	471PD Y
DD-30	Q TO-94	Q	470PA Z
TO-48	L TO-118	W	801PD Z
	TO-203AA	H	

NOTE: Not all patterns are available in every type heat exchanger.

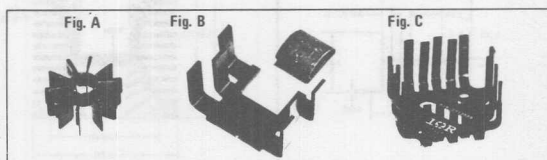
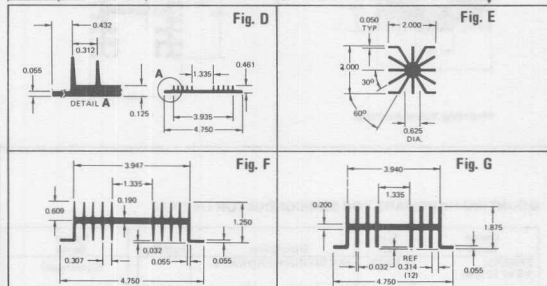


FIGURE	IR PART NUMBER	APPLICATION	LENGTH (INCHES)
A	HE101	For TO-18, 24, 28, 40, TO-4	OD = 11/16 x 3/8" long
A	HE102	For TO-5, 9, 11, 12, 15, 26, 29, 33, 39, 42, 43, 45	OD = 3/4 x 3/8 long
B	HE106	For tab plastic transistors, SCRs, Triacs, etc.	
C	HE223	For TO-3, 6, 36, 66.	



HEAT EXCHANGER SPECIFICATIONS

FIGURE	IR PART NUMBER	THERMAL RESISTANCE R _{θSA} (°C/W)		LENGTH (INCHES)
		NATURAL CONVECTION	FORCED CONVECTION (1000fpm)	
D	HE32-1.5A3	3.3	1.1	1.5
D	HE32-3A3	2.0	0.65	3.0
E	HE40-75A3	3.4	1.2	0.75
E	HE40-1.5A3	2.7	0.7	1.5
E	HE40-3A3	1.85	0.6	3.0
F	HE50-1.5A3	1.85	0.65	1.5
F	HE50-3A3	1.5	0.4	3.0
G	HE52-3A3	0.9	0.3	3.0
H	HE53-3A3	0.7	0.19	3.0
H	HE53-5.5A3	0.58	0.16	5.5
J	HE63-6A3	0.27	0.11	6.0
J	HE63-9A3	0.25	0.105	9.0
K	HE72-5A3	0.23*	0.10*	5.0
K	HE72-8A3	0.18*	0.08*	8.0
L	HE75-4A3	0.85*	0.09*	4.0
L	HE75-5A3	0.85*	0.08*	5.0
M	HE80-4A3	0.66	0.23	4.0
M	HE80-5A3	0.6	0.21	5.0
M	HE80-6A3	0.55	0.19	6.0
N	HE81-5A3	0.8	0.14	5.0
P	HE85-2A3	2.0	0.48	2.0
P	HE85-4A3	1.5	0.35	4.0

*Double-sided cooling (two heat exchangers).

All Dimensions in Inches.

Semiconductor Fuses

International Rectifier's fast-acting semiconductor protective fuses employ a high-grade alumina ceramic body to prevent charring and arcing under operating conditions. All-welded construction rather than soldering is used to prevent internal fatigue from changing fuse parameters. These quality fast-acting fuses are competitively priced.

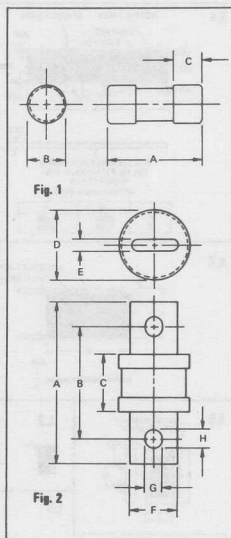
A complete range of European-style semiconductor fuses is also available.

Max. V _{RMS} (V)	130	250	500	600	600	700
Max. Arc Voltage (V)	220	410	850	1,050	1,050	1,200
Nominal RMS Current (A)						
5	SF13X5	SF25X5	—	SF60C5	SF60X5	—
10	SF13X10	SF25X10	—	SF60C10	SF60X10	SF70P10
15	SF13X15	SF25X15	—	SF60C15	SF60X15	SF70P15
20	SF13X20	SF25X20	—	SF60C20	SF60X20	SF70P20
25	SF13X25	SF25X25	—	SF60C25	SF60X25	SF70P25
30	SF13X30	SF25X30	—	SF60C30	SF60X30	SF70P30
35	SF13X35	—	SF50P35	SF60C35	SF60X35	SF70P35
40	SF13X40	SF25X40	SF50P40	SF60C40	SF60X40	SF70P40
45	—	—	SF50P45	SF60C45	—	—
50	SF13X50	SF25X50	SF50P50	SF60C50	SF60X50	SF70P50
60	SF13X60	SF25X60	SF50P60	SF60C60	SF60X60	SF70P60
70	SF13X70	SF25X70	SF50P70	SF60C70	SF60X70	SF70P70
80	SF13X80	SF25X80	SF50P80	SF60C80	SF60X80	SF70P80
90	—	—	SF50P90	SF60C90	SF60X90	SF70P90
100	SF13X100	SF25X100	SF50P100	SF60C100	SF60X100	SF70P100
125	SF13X125	SF25X125	SF50P125	SF60C125	SF60X125	SF70P125
150	SF13X150	SF25X150	SF50P150	SF60C150	SF60X150	SF70P150
175	—	SF25X175	SF50P175	SF60C175	SF60X175	SF70P175
200	SF13X200	SF25X200	SF50P200	SF60C200	SF60X200	SF70P200
225	—	SF25X225	—	SF60C225	—	—
250	SF13X250	SF25X250	SF50P250	SF60C250	SF60X250	SF70P250
300	SF13X300	SF25X300	SF50P300	SF60C300	SF60X300	SF70P300
350	SF13X350	SF25X350	SF50P350	SF60C350	SF60X350	—
400	SF13X400	SF25X400	SF50P400	SF60C400	SF60X400	SF70P400
450	—	SF25X450	SF50P450	SF60C450	SF60X450	—
500	SF13X500	SF25X500	SF50P500	SF60C500	SF60X500	SF70P500
550	—	—	SF50P550	—	—	—
600	SF13X600	SF25X600	SF50P600	SF60C600	SF60X600	SF70P600
700	—	—	SF50P700	SF60C700	—	SF70P700
800	SF13X800	—	SF50P800	SF60C800	—	SF70P800

NOTE: For maximum D.C. voltage, refer to individual data sheets.

SEMICONDUCTOR FUSE DIMENSIONS All Dimensions in Inches.

PART NUMBER	FIG.	A	B	C	D	E	F	G	H
SF13X5 to 30	1	1.500	0.406	0.375	—	—	—	—	—
SF13X35 to 60	1	2.00	0.812	0.594	—	—	—	—	—
SF13X70 to 400	2	2.656	2.062	1.156	1.000	0.125	0.750	0.312	0.438
SF13X500 to 800	2	3.500	2.438	1.250	1.500	0.250	1.000	0.406	0.406
SF25X5 to 30	1	2.000	0.562	0.500	—	—	—	—	—
SF25X40 to 60	2	3.188	2.438	1.562	0.812	0.125	0.719	0.344	0.406
SF25X70 to 200	2	3.125	2.375	1.625	1.218	0.188	1.000	0.344	0.406
SF25X225 to 600	2	3.944	2.781	1.578	1.531	0.250	1.000	0.406	0.469
SF50P35 to 60	2	3.188	2.438	1.563	0.818	0.125	0.719	0.344	0.406
SF50P70 to 100	2	3.625	2.875	2.125	0.947	0.125	0.750	0.313	0.375
SF50P125 to 200	2	3.625	2.875	2.125	1.218	0.188	1.000	0.344	0.406
SF50P250 to 400	2	4.344	3.281	2.084	1.525	0.245	1.000	0.406	0.469
SF50P450 to 600	2	4.469	3.406	2.219	2.000	0.250	1.500	0.406	0.500
SF50P700 to 800	2	6.469	4.469	2.219	2.500	0.375	2.000	0.531	0.720
SF60C5 to 30	2	2.875	2.500	1.875	0.563	0.063	0.406	0.250	0.250
SF60C35 to 60	2	4.375	3.625	2.734	0.812	0.125	0.719	0.344	0.406
SF60C70 to 100	2	5.000	3.875	2.875	0.938	0.125	0.750	0.406	0.625
SF60C125 to 200	2	5.500	4.000	2.906	1.531	0.250	1.000	0.406	0.781
SF60C225 to 400	2	6.250	4.750	3.000	2.000	0.250	1.500	0.563	0.625
SF60C450 to 600	2	6.250	4.750	3.063	2.500	0.250	2.000	0.563	0.625
SF60X5 to 30	1	5.000	0.813	0.625	—	—	—	—	—
SF60X35 to 60	2	4.375	3.625	2.750	0.813	0.125	0.719	0.344	0.406
SF60X70 to 100	2	4.406	3.656	2.906	1.000	0.125	0.750	0.313	0.375
SF60X125 to 200	2	4.406	3.656	2.906	1.219	0.188	1.000	0.344	0.406
SF60X250 to 400	2	5.094	4.032	2.844	1.532	0.250	1.000	0.406	0.469
SF60X450 to 600	2	5.094	4.032	2.844	2.000	0.250	1.500	0.406	0.500
SF70P10 to 30	1	2.000	0.563	0.500	—	—	—	—	—
SF70P35 to 60	2	4.325	3.625	2.750	0.818	0.125	0.719	0.344	0.406
SF70P70 to 100	2	4.406	3.656	2.906	1.000	0.125	0.750	0.313	0.375
SF70P125 to 200	2	5.063	4.032	2.844	1.525	0.245	1.000	0.406	0.469
SF70P250 to 400	2	5.063	4.032	2.844	2.000	0.250	1.500	0.406	0.500
SF70P500 to 600	2	7.094	5.094	2.844	2.500	0.375	2.000	0.531	0.720



COMPETITIVE PART NO.	SUGGESTED IR REPLACEMENT	COMPETITIVE PART NO.	SUGGESTED IR REPLACEMENT	COMPETITIVE PART NO.	SUGGESTED IR REPLACEMENT	COMPETITIVE PART NO.	SUGGESTED IR REPLACEMENT
C11M	2N2619	C37F	10RC5A	C55A	91RL10	C107A2	IR106A2
C11U	2N1770	C37M	10RC60A	C55B	91RL20	C107A3	IR106A3
C15A	5RC10A	C37N	10RC60A	C55C	91RL30	C107A4	IR106A4
C15B	5RC20A	C37S	10RC70A	C55D	91RL40	C107B1	IR106B1
C15C	5RC30A	C37U	10RC2A	C55E	91RL50	C107B2	IR106B2
C15D	5RC40A	C38A	22RC10	C55M	91RL60	C107B3	IR106B3
C15E	5RC50A	C38B	22RC20	C56A	92RM10	C107B4	IR106B4
C15F	5RC5A	C38C	22RC30	C56B	92RM20	C107C1	IR106C1
C15G	5RC15A	C38D	22RC40	C56C	92RM30	C107C2	IR106C2
C15M	5RC60A	C38E	22RC50	C56D	92RM40	C107C3	IR106C3
C15U	5RC2A	C38F	22RC5	C56E	92RM50	C107C4	IR106C4
C20A	IR30A	C38G	22RC15	C56M	92RM60	C107D1	IR106D1
C20B	IR30B	C38H	22RC25	C60A	71RC10B	C107D2	IR106D2
C20C	IR30C	C38U	22RC2	C60B	71RC20B	C107D3	IR106D3
C20D	IR30D	C40A	IR140A	C60C	71RC30B	C107D4	IR106D4
C20F	IR30F	C40B	IR140B	C60D	71RC40B	C107F1	IR106F1
C20U	IR30U	C40C	IR140C	C60E	71RC50B	C107F2	IR106F2
C22A	IR32A	C40D	IR140D	C60F	71RC5B	C107F3	IR106F3
C22B	IR32B	C40E	IR140E	C60G	71RC15B	C107F4	IR106F4
C22C	IR32C	C40F	IR140F	C60H	71RC25B	C107Q1	IR106Q1
C22D	IR32D	C40G	IR140G	C60M	71RC60B	C107Q2	IR106Q2
C22F	IR32F	C40H	IR140H	C60U	71RC2B	C107Q3	IR106Q3
C22U	IR32U	C40J	IR140J	C61A	72RC10B	C107Q4	IR106Q4
C30A	IR30A	C45A	37RC10A	C61B	72RC20B	C107U1	IR106U1
C30B	IR30B	C45B	37RC20A	C61C	72RC30B	C107U2	IR106U2
C30C	IR30C	C45C	37RC30A	C61D	72RC40B	C107U3	IR106U3
C30D	IR30D	C45D	37RC40A	C61E	72RC50B	C107U4	IR106U4
C30F	IR30F	C45E	37RC50A	C61F	72RC5B	C122A1	IR122A1
C30U	IR30U	C45F	37RC5A	C61G	72RC15B	C122B1	IR122B1
C31A	IR31A	C45G	37RC15A	C61H	72RC25B	C122C1	IR122C1
C31B	IR31B	C45H	37RC25A	C61M	72RC60B	C122D1	IR122D1
C31C	IR31C	C45M	37RC60A	C61U	72RC2B	C122F1	IR122F1
C31D	IR31D	C45N	37RC80A	C62A	72RC10B	C122Q1	IR122Q1
C31F	IR31F	C45S	37RC70A	C62B	72RC20B	C135A	16RC10A
C31U	IR31U	C45T	37RC90A	C62C	72RC30B	C135B	16RC20A
C32A	IR32A	C45U	37RC2A	C62D	72RC40B	C135C	16RC30A
C32B	IR32B	C46A	36RC10A	C62E	72RC50B	C135D	16RC40A
C32C	IR32C	C46B	36RC20A	C62F	72RC5B	C135E	16RC50A
C32D	IR32D	C46C	36RC30A	C62M	72RC60B	C135F	16RC5A
C32F	IR32F	C46D	36RC40A	C80A	151RC10A	C135M	16RC60A
C32U	IR32U	C46E	36RC50A	C80C	151RC30A	C135N	16RC80A
C33A	IR33A	C46F	36RC5A	C80D	151RC40A	C135S	16RC70A
C33B	IR33B	C46G	36RC15A	C80E	151RC50A	C137E	16RC60AS50
C33C	IR33C	C46H	36RC25A	C80F	151RC5A	C137M	16RC60AS50
C33D	IR33D	C46M	36RC60A	C80M	151RC50A	C137N	16RC80AS50
C33F	IR33F	C46N	36RC80A	C106A1	IR106A1	C137P	16RC100AS50
C33U	IR33U	C46S	36RC70A	C106A2	IR106A2	C137PA	16RC110AS50
C35A	16RC10A	C46T	36RC90A	C106A3	IR106A3	C137PB	16RC120AS50
C35B	16RC20A	C46U	36RC2A	C106A4	IR106A4	C137S	16RC70AS50
C35C	16RC30A	C50A	71RC10A	C106B1	IR106B1	C137T	16RC90AS50
C35D	16RC40A	C50B	71RC20A	C106B2	IR106B2	C140A	IR140A
C35E	16RC50A	C50C	71RC30A	C106B3	IR106B3	C140B	IR140B
C35F	16RC5A	C50D	71RC40A	C106B4	IR106B4	C140C	IR140C
C35G	16RC15A	C50E	71RC50A	C106C1	IR106C1	C140D	IR140D
C35H	16RC25A	C50F	71RC5A	C106C2	IR106C2	C140F	IR140F
C35M	16RC60A	C50G	71RC15A	C106C3	IR106C3	C141A	IR141A
C35N	16RC80A	C50H	71RC25A	C106C4	IR106C4	C141B	IR141B
C35S	16RC70A	C50M	71RC60A	C106C4	IR106C4	C141C	IR141C
C36A	10RC10A	C50N	71RC80A	C106D1	IR106D1	C141D	IR141D
C36B	10RC20A	C50S	71RC70A	C106D2	IR106D2	C141F	IR141F
C36C	10RC30A	C50T	71RC90A	C106D3	IR106D3	C145A	50RCS10S60
C36D	10RC40A	C50U	71RC2A	C106D4	IR106D4	C145B	50RCS20S60
C36E	10RC50A	C52A	72RC10A	C106F1	IR106F1	C145C	50RCS30S60
C36F	10RC5A	C52B	72RC20A	C106F2	IR106F2	C145D	50RCS40S60
C36G	10RC15A	C52C	72RC30A	C106F3	IR106F3	C145E	50RCS50S60
C36H	10RC25A	C52D	72RC40A	C106F4	IR106F4	C145F	50RCS5S60
C36M	10RC60A	C52E	72RC50A	C106Q1	IR106Q1	C145M	50RCS60S60
C36N	10RC80A	C52F	72RC5A	C106Q2	IR106Q2	C145N	50RCS80S60
C36S	10RC70A	C52G	72RC15A	C106Q3	IR106Q3	C145P	50RCS100S60
C36U	10RC2A	C52H	72RC25A	C106Q4	IR106Q4	C145Q	50RCS110S60
C37A	10RC10A	C52M	72RC60A	C106U1	IR106U1	C145PA	50RCS120S60
C37B	10RC20A	C52N	72RC80A	C106U2	IR106U2	C145PB	50RCS120S60
C37C	10RC30A	C52S	72RC70A	C106U3	IR106U3	C145S	50RCS70S60
C37D	10RC40A	C52T	72RC90A	C106U4	IR106U4	C145T	50RCS90S60
C37E	10RC50A	C52U	72RC2A	C107A1	IR106A1	C147A	50RCS10S60

APPENDIX III

COMPETITIVE PART NO.	SUGGESTED IR REPLACEMENT	COMPETITIVE PART NO.	SUGGESTED IR REPLACEMENT	COMPETITIVE PART NO.	SUGGESTED IR REPLACEMENT	COMPETITIVE PART NO.	SUGGESTED IR REPLACEMENT
C147B	50RCS20S60	C158D	81RLB40	C185E	151RF50	C358A	125PAL810
C147C	50RCS30S60	C158E	81RLB50	C185M	151RF60	C358B	125PAL820
C147D	50RCS40S60	C158M	81RLB60	C186N	151RL80	C358C	125PAL830
C147E	50RCS50S60	C158N	81RLB80	C186P	151RL100	C358D	125PAL840
C147F	50RCS55S60	C158P	81RLB100	C186PA	151RL110	C358E	125PAL850
C147M	50RCS60S60	C158PA	81RLB110	C186PB	151RL120	C358M	125PAL860
C147N	50RCS80S60	C158PB	81RLB120	C186S	151RL70	C358N	125PAL880
C147P	50RCS100S60	C158S	81RLB70	C186T	151RL90	C358P	125PAL100
C147PA	50RCS110S60	C158T	81RLB90	C280N	250RA80	C358PA	125PAL110
C147PB	50RCS120S60	C159A	82RLB10	C280P	250RA100	C358PB	125PAL120
C147S	50RCS70S60	C159B	82RLB20	C280PA	250RA110	C358S	125PAL170
C147T	50RCS90S60	C159C	82RLB30	C280PB	250RA120	C358T	125PAL890
C150E	71RA50	C159D	82RLB40	C280PC	250RA130	C364A	140PAM10
C150M	71RA60	C159E	82RLB50	C280PD	250RA140	C364B	140PAM20
C150N	71RA80	C159M	82RLB60	C280PE	250RA150	C364C	140PAM30
C150P	71RA100	C159N	82RLB80	C280PM	250RA160	C364D	140PAM40
C150PA	71RA110	C159P	82RLB100	C280PS	250RA170	C364E	140PAM50
C150PB	71RA120	C159PA	82RLB110	C280S	250RA70	C364M	140PAM60
C150PC	71RA130	C159PB	82RLB120	C280T	250RA90	C365A	140PAL10
C150S	71RA70	C159S	82RLB70	C281N	253RA80	C365B	140PAL20
C150T	71RA90	C159T	82RLB90	C281P	253RA100	C365C	140PAL30
C151E	81RL50	C164A	91RM10	C281PA	253RA110	C365D	140PAL40
C151M	81RL60	C164B	91RM20	C281PB	253RA120	C365E	140PAL50
C151N	81RL80	C164C	91RM30	C281PC	253RA130	C365M	140PAL60
C151P	81RL100	C164D	91RM40	C281S	253RA70	C380A	250PA10
C151PA	81RL110	C164E	91RM50	C281T	253RA90	C380B	250PA20
C151PB	81RL120	C164M	91RM60	C290A	300RA10	C380C	250PA30
C151PC	81RL130	C165A	91RL10	C290B	300RA20	C380D	250PA40
C151S	81RL70	C165B	91RL20	C290C	300RA30	C380E	250PA50
C151T	81RL90	C165C	91RL30	C290D	300RA40	C380M	250PA60
C152E	72RA50	C165D	91RL40	C290E	300RA50	C380N	250PA80
C152M	72RA60	C165E	91RL50	C290M	300RA60	C380P	250PA100
C152N	72RA80	C165M	91RL60	C290N	300RA80	C380PA	250PA110
C152P	72RA100	C178A	151RB10	C290P	300RA100	C380PB	250PA120
C152PA	72RA110	C178B	151RB20	C290PA	300RA110	C380PC	250PA130
C152PB	72RA120	C178C	151RB30	C290PB	300RA120	C380S	250PA70
C152PC	72RA130	C178D	151RB40	C290S	300RA70	C380T	250PA90
C152S	72RA70	C178E	151RB50	C290T	300RA90	C385A	250PAL10
C152T	72RA90	C178M	151RB60	C291A	303RA10	C385B	250PAL20
C153E	82RL50	C178N	151RB80	C291B	303RA20	C385C	250PAL30
C153M	82RL60	C178P	151RB100	C291C	303RA30	C385D	250PAL40
C153N	82RL80	C178PA	151RB110	C291D	303RA40	C385E	250PAL50
C153P	82RL100	C178PB	151RB120	C291E	303RA50	C385M	250PAL60
C153PA	82RL110	C178S	151RB70	C291M	303RA60	C387M	420PBM60
C153PB	82RL120	C178T	151RB90	C291N	303RA80	C387N	420PBM80
C153PC	82RL130	C180A	151RA10	C291P	303RA100	C387P	420PBM100
C153S	82RL70	C180B	151RA20	C291PA	303RA110	C387PA	420PBM110
C153T	82RL90	C180C	151RA30	C291PB	303RA120	C387PB	420PBM120
C154A	91RM10	C180D	151RA40	C291S	303RA70	C387S	420PBM70
C154B	91RM20	C180E	151RA50	C291T	303RA90	C387T	420PBM90
C154C	91RM30	C180M	151RA60	C350A	115PA10	C388M	420PBMM0S66
C154D	91RM40	C180N	151RA80	C350B	115PA20	C388N	420PBMM0S66
C154E	91RM50	C180P	151RA100	C350C	115PA30	C388P	420PBMM100S66
C154M	91RM60	C180PA	151RA110	C350D	115PA40	C388PA	420PBMM105S66
C155A	91RL10	C180PB	151RA120	C350E	115PA50	C388PB	420PBMM120S66
C155B	91RL20	C180PC	151RA130	C350M	115PA60	C388S	420PBMM70S66
C155C	91RL30	C180S	151RA70	C350N	115PA80	C388T	420PBMM90S66
C155D	91RL40	C180T	151RA90	C350P	115PA100	C390E	550PB50
C155E	91RL60	C181M	151RB10	C350PA	115PA110	C390M	550PB60
C155M	91RL80	C181B	151RB20	C350PB	115PA120	C390N	550PB80
C156A	92RM10	C181C	151RB30	C350PC	115PA130	C390P	550PB100
C156B	92RM20	C181D	151RB40	C350S	115PA70	C390PA	550PB110
C156C	92RM30	C181E	151RB50	C350T	115PA90	C390PB	550PB120
C156M	92RM40	C181M	151RB60	C354A	140PAM10	C390PC	550PB130
C156E	92RM50	C181N	151RB80	C354B	140PAM20	C390S	550PB70
C156M	92RM60	C181P	151RB100	C354C	140PAM30	C390T	550PB90
C157A	92RL10	C181PA	151RB110	C354D	140PAM40	C392A	550PBQ10
C157B	92RL20	C181PB	151RB120	C354E	140PAM50	C392B	550PBQ20
C157C	92RL30	C181PC	151RB130	C354M	140PAM60	C392C	550PBQ30
C157D	92RL40	C181S	151RB70	C355A	140PAL10	C392D	550PBQ40
C157E	92RL50	C181T	151RB90	C355B	140PAL20	C392E	550PBQ50
C157M	92RL60	C185A	151RF10	C355C	140PAL30	C392M	550PBQ60
C158A	81RL810	C185B	151RF20	C355D	140PAL40	C394A	550PBQ10
C158B	81RL820	C185E	151RF30	C355E	140PAL50	C394B	550PBQ20
C158C	81RL830	C185D	151RF40	C355M	140PAL60	C394C	550PBQ30

COMPETITIVE PART NO.	SUGGESTED IR REPLACEMENT	COMPETITIVE PART NO.	SUGGESTED IR REPLACEMENT	COMPETITIVE PART NO.	SUGGESTED IR REPLACEMENT	COMPETITIVE PART NO.	SUGGESTED IR REPLACEMENT
C394D	550PB040	C506E	470PB50S57	C28120PC	254RA130	E220-4	250PA40
C394E	550PB050	C506M	470PB60S57	C28120S	254RA70	E220-6	250PA60
C394M	550PB060	C507A	550PB10	C28120T	254RA90	E220-8	250PA80
C395A	550PB010564	C507B	550PB20	C29120E	304RA50	E220-10	250PA100
C395B	550PB020564	C507C	550PB30	C29120M	304RA80	E220-12	250PA120
C395C	550PB030564	C507D	550PB40	C29120N	304RA80	E220-14	250PA140
C395D	550PB040564	C507E	550PB50	C29120P	304RA100	E220-16	250PA160
C395E	550PB050564	C507M	550PB60	C29120PA	304RA110	E241A	16RC5A
C395M	550PB060564	C507N	550PB80	C29120PB	304RA120	E241B	16RC10A
C398E	420PM50	C507T	550PB100	C29120S	304RA120	E241C	16RC15A
C398M	420PM60	C507FA	550PB110	C29010T	304RA90	E241D	16RC20A
C398N	420PM80	C507FB	550PB120	CS3-02	IR122B	E241E	16RC25A
C398P	420PM100	C507FC	550PB130	CS3-03	IR122C	E241F	16RC30A
C398PA	420PM110	C507PD	550PB140	CS3-04	IR122D	E241H	16RC40A
C398PB	420PM120	C507S	550PB170	CS3-05	IR122E	E241K	15RC50A
C398S	420PM70	C507T	550PB90	CS3-06	IR122M	E241M	16RC60A
C398T	420PM90	C509M	500PB060	CS5-02	10RC20A	E241P	16RC70A
C440E	900PB50	C509N	500PB080	CS5-04	10RC40A	E241S	16RC80A
C440M	900PB60	C509P	500PBQ100	CS5-06	10RC80A	E241V	16RC90A
C440N	900PB80	C509PA	500PBQ110	CS5-08	10RC80A	E241Z	16RC100A
C440P	900PB100	C509PB	500PBQ120	CS5-10	10RC100A	E241ZB	16RC110A
C440PA	900PB110	C509S	500PBQ70	CS5-12	10RC120A	E241ZD	16RC120A
C440PB	900PB120	C509T	500PBQ90	CS220-08	250PA80	E351A	22RC5
C440PC	900PB130	C510A	550PBQ10	CS220-10	250PA100	E351B	22RC10
C440S	900PB70	C510B	550PBQ20	CS220-12	250PA120	E351C	22RC15
C440T	900PB90	C510C	550PBQ30	CS220-14	250PA140	E351D	22RC20
C441PA	750PB110	C510D	550PBQ40	CS220-16	250PA160	E351E	22RC25
C441PB	750PB120	C510E	550PBQ50	CS250-08	250PA80	E351F	22RC30
C441PC	750PB130	C510M	550PBQ60	CS250-10	250PA100	E351H	22RC40
C441PD	750PB140	C600P	900PB120	CS250-12	250PA120	E351K	22RC50
C441PE	750PB150	C600M	900PB60	CS250-14	250PA140	E351M	22RC60
C441PM	750PB160	C600N	900PB80	CS250-16	250PA160	E351P	22RC70
C441PS	750PB170	C600P	900PB100	CS400-08	550PB80	E352A	22RC5
C444A	701PB010	C600PA	900PB110	CS400-10	550PB100	E352B	22RC10
C444B	701PB020	C600PB	900PB120	CS400-12	550PB120	E352C	22RC15
C444C	701PB030	C600S	900PB70	CS400-14	550PB140	E352D	22RC20
C444D	701PB040	C600T	900PB90	CS400-16	550PB160	E352E	22RC25
C444E	701PB050	C601PA	750PB110	CS401-18	600PB180	E352F	22RC30
C444M	701PB060	C601PB	750PB120	CS401-20	600PB200	E352H	22RC40
C445A	700PB010	C601PC	750PB130	CS401-21	600PB210	E352K	22RC50
C445B	700PB020	C601PD	750PB140	CS401-22	600PB220	E352M	22RC60
C445C	700PB030	C601PE	750PB150	CS401-23	600PB230	E352P	22RC70
C445D	700PB040	C601PM	750PB160	CS401-24	600PB240	F400-2	420PB20
C445E	700PB050	C601PS	750PB170	CS401-25	600PB250	F400-4	420PB40
C445M	700PB060	C602L	600PB200	CS550-08	750PB80	F400-6	420PB60
C447E	650PB050	C602LA	600PB210	CS550-10	750PB100	F400-8	420PB80
C447M	650PB060	C602LB	600PB220	CS550-12	750PB120	F400-10	420PB100
C447N	650PB080	C602LC	600PB230	CS550-14	750PB140	F400-12	420PB120
C447P	650PB100	C602LD	600PB240	CS601-16	750PB160	F400-14	420PB140
C447PA	650PB0110	CS602L	600PB250	E151A	10RC5A	F400-16	420PB160
C447PB	650PB0120	C602PN	600PB180	E151B	10RC10A	F500-2	420PB20
C447S	650PB070	C602PS	600PB170	E151C	10RC15A	F500-4	420PB40
C447T	650PB090	C602PT	600PB190	E151D	10RC20A	F500-6	420PB60
C448E	651PB050	C609M	750PB060	E151E	10RC25A	F500-8	420PB80
C448M	651PB060	C609N	750PB080	E151F	10RC30A	F500-10	420PB100
C448N	651PB080	C609P	750PBQ100	E151H	10RC40A	F500-12	420PB120
C448P	651PBQ100	C609PA	750PBQ110	E151K	10RC50A	F500-14	420PB140
C448PA	651PBQ110	C609PB	750PBQ120	E151M	10RC60A	F500-16	420PB160
C448PB	651PBQ120	C609S	750PB070	E151P	10RC70A	F600-2	420PB20
C448S	651PBQ70	C609T	750PBQ90	E151S	10RC80A	F600-4	420PB40
C448T	651PBQ90	C701PA	1000PK110	E151V	10RC90A	F600-6	420PB60
C501N	550PB80	C701PB	1000PK120	E161A	10RC5A	F600-8	420PB80
C501P	550PB100	C701PC	1000PK130	E161B	10RC10A	F600-10	420PB100
C501PA	550PB110	C701PD	1000PK140	E161C	10RC15A	F600-12	420PB120
C501PB	550PB120	C701PE	1000PK150	E161D	10RC20A	F600-14	420PB140
C501PC	550PB130	C701PM	1000PK160	E161E	10RC25A	F600-16	420PB160
C501PD	550PB140	C702L	700PK200	E180-2	250PA20	G400-2	420PB20
C501PE	550PB150	C702LA	700PK210	E180-4	250PA40	G400-4	420PB40
C501PM	550PB160	C702LB	700PK220	E180-6	250PA60	G400-6	420PB60
C501PS	550PB170	C702LC	700PK230	E180-8	250PA80	G400-8	420PB80
C501S	550PB70	C702LD	700PK240	E180-10	250PA100	G400-10	420PB100
C501T	550PB90	C28120N	254RA80	E180-12	250PA120	G400-12	420PB120
C506A	470PB10S57	C28120P	254RA100	E180-14	250PA140	G400-14	420PB140
C506C	470PB30S57	C28120PA	254RA110	E180-16	250PA160	G400-16	420PB160
C506D	470PB40S57	C28120PB	254RA120	E220-2	250PA20	G500-2	470PB20

APPENDIX III

COMPETITIVE PART NO.	SUGGESTED IR REPLACEMENT	COMPETITIVE PART NO.	SUGGESTED IR REPLACEMENT	COMPETITIVE PART NO.	SUGGESTED IR REPLACEMENT	COMPETITIVE PART NO.	SUGGESTED IR REPLACEMENT
G500-4	470P840	H1800-10	1000PK100	MCR2935-6	IR30D	NLC36A	10RC10
G500-6	470P860	H1800-12	1000PK120	MCR3818-1	IR30U	NLC36B	10RC20
G500-8	470P880	MCR106-1	IR106Y1	MCR3818-2	IR32F	NLC36C	10RC30
G500-10	470PB100	MCR106-2	IR106F1	MCR3818-3	IR32A	NLC36D	10RC40
G500-12	470PB120	MCR106-3	IR106A1	MCR3818-4	IR32B	NLC36E	10RC50
G500-14	470PB140	MCR106-4	IR106B1	MCR3818-5	IR32C	NLC36M	10RC60
G500-16	470PB160	MCR106-5	IR106C1	MCR3818-6	IR32D	NLC36N	10RC80
G650-2	470PB20	MCR106-6	IR106D1	MCR3918-1	IR30U	NLC36S	10RC70
G650-4	470PB40	MCR406-1	IR106Y1	MCR3918-2	IR30F	NLC37A	10RC10A
G650-6	470PB60	MCR406-2	IR106F1	MCR406-2	IR30A	NLC37B	10RC20A
G650-8	470PB80	MCR406-3	IR106A1	MCR3918-4	IR30B	NLC37C	10RC30A
G650-10	470PB100	MCR406-4	IR106B1	MCR3918-5	IR30D	NLC37D	10RC40A
G650-12	470PB120	MCR406-5	IR106C1	MCR3818-6	IR30D	NLC37E	10RC50A
G650-14	470PB140	MCR406-6	IR106D1	MCR3935-1	22RA2	NLC37M	10RC60A
G650-16	470PB160	MCR407-1	IR106Y1	MCR3935-2	22RA5	NLC37N	10RC80A
G850-2	550PB20	MCR407-2	IR106F1	MCR3935-3	22RA10	NLC37S	10RC70A
G850-4	550PB40	MCR407-3	IR106A1	MCR3935-4	22RA20	NLC38A	22RC10
G850-6	550PB60	MCR407-4	IR106B1	MCR3935-5	22RA30	NLC38B	22RC20
G850-8	550PB80	MCR407-5	IR106C1	MCR3935-6	22RA40	NLC38C	22RC30
G850-10	550PB100	MCR407-6	IR106D1	MCR3935-7	22RA50	NLC38D	22RC40
G850-12	550PB120	MCR846-1	3RC2A	MCR3935-8	22RA60	NLC38E	22RC50
G850-14	550PB140	MCR846-2	3RC10A	NL511A	16RC10AS60	NLC38G	22RC15
G850-16	550PB160	MCR846-3	3RC10A	NL511B	16RC20AS60	NLC38H	22RC25
G950-2	550PB20	MCR846-4	3RC20A	NL511C	16RC30AS60	NLC45A	37RC10A
G950-4	550PB40	MCR1308-1	10RC2A	NL511D	16RC40AS60	NLC45B	37RC20A
G950-6	550PB60	MCR1308-2	10RC5A	NL511E	16RC50AS60	NLC45C	37RC30A
G950-8	550PB80	MCR1308-3	10RC10A	NL511M	16RC80AS60	NLC45D	37RC40A
G950-10	550PB100	MCR1308-4	10RC20A	NL511N	16RC80AS60	NLC45E	37RC50A
G950-12	550PB120	MCR1308-5	10RC30A	NL511P	16RC100AS60	NLC45G	37RC15A
G950-14	550PB140	MCR1308-6	10RC40A	NL511PA	16RC10AS60	NLC45H	37RC25A
G950-16	550PB160	MCR1907-1	IR141F	NL511PB	16RC120AS60	NLC45M	37RC60A
H800-2	700PK20	MCR1907-2	IR141F	NL511S	16RC70AS60	NLC45N	37RC70A
H800-4	700PK40	MCR1907-3	IR141A	NL511T	16RC90AS60	NLC45S	37RC70A
H800-6	700PK60	MCR1907-4	IR141B	NL555A	36RC10A	NLC45T	37RC90A
H800-8	700PK80	MCR1907-5	IR141C	NL555B	36RC20A	NLC46A	36RC10A
H800-10	700PK100	MCR1907-6	IR141D	NL555C	36RC30A	NLC46B	36RC20A
H800-12	700PK120	MCR2304-1	IR32U	NL555D	36RC40A	NLC46C	36RC30A
H800-14	700PK140	MCR2304-2	IR32F	NL555E	36RC50A	NLC46D	36RC40A
H800-16	700PK160	MCR2304-3	IR32A	NL555M	36RC60A	NLC46E	36RC50A
H1000-2	700PK20	MCR2304-4	IR32B	NL555N	36RA80	NLC46G	36RC15A
H1000-4	700PK40	MCR2304-5	IR32C	NL555P	36RA100	NLC46H	36RC25A
H1000-6	700PK60	MCR2304-6	IR32D	NL555PA	36RA110	NLC46M	36RC60A
H1000-8	700PK80	MCR2305-1	IR30U	NL555PB	36RA120	NLC46N	36RC80A
H1000-10	700PK100	MCR2305-2	IR30F	NL555PC	36RA130	NLC46S	36RC70A
H1000-12	700PK120	MCR2305-3	IR30A	NL555PD	36RA140	NLC46T	36RC90A
H1000-14	700PK140	MCR2305-4	IR30B	NL555PE	36RA150	NLC50A	71RC10A
H1000-16	700PK160	MCR2305-5	IR30C	NL555PM	36RA160	NLC50B	71RC20A
H1200-2	850PK20	MCR2305-6	IR30D	NL555S	36RA70	NLC50C	71RC30A
H1200-4	850PK40	MCR2604-1	5RC2A	NL555T	36RA90	NLC50D	71RC40A
H1200-6	850PK60	MCR2604-2	5RC5A	NL555A	37RC10A	NLC50E	71RC50A
H1200-8	850PK80	MCR2604-3	5RC10A	NL555B	37RC20A	NLC50G	71RC15A
H1200-10	850PK100	MCR2604-4	5RC20A	NL555C	37RC30A	NLC50H	71RC25A
H1200-12	850PK120	MCR2604-5	5RC30A	NL555D	37RC40A	NLC50M	71RC80A
H1200-14	850PK140	MCR2604-6	5RC40A	NL555E	37RC50A	NLC50N	71RC80A
H1200-16	850PK160	MCR2604-7	5RC50A	NL555M	37RC60A	NLC50S	71RC70A
H1400-2	1000PK20	MCR2604-8	5RC60A	NL555N	37RA80	NLC50T	71RC90A
H1400-4	1000PK40	MCR2605-1	5RC2A	NL555P	37RA100	NLC52A	72RC10A
H1400-6	1000PK60	MCR2605-2	5RC5A	NL555PA	37RA110	NLC52B	72RC20A
H1400-8	1000PK80	MCR2605-3	5RC10A	NL555PB	37RA120	NLC52C	72RC30A
H1400-10	1000PK100	MCR2605-4	5RC20A	NL555PD	37RA130	NLC52D	72RC40A
H1400-12	1000PK120	MCR2605-5	5RC30A	NL555PE	37RA140	NLC52E	72RC50A
H1400-14	1000PK140	MCR2605-6	5RC40A	NL555PE	37RA150	NLC52G	72RC15A
H1400-16	1000PK160	MCR2605-7	5RC50A	NL555PM	37RA160	NLC52H	72RC25A
H1600-2	1000PK20	MCR2605-8	5RC60A	NL555S	37RA70	NLC52M	72RC80A
H1600-4	1000PK40	MCR2835-1	IR32U	NL555T	37RA90	NLC52N	72RC80A
H1600-6	1000PK60	MCR2835-2	IR32F	NLC35A	16RC10A	NLC35S	72RC70A
H1600-8	1000PK80	MCR2835-3	IR32A	NLC35B	16RC20A	NLC52T	72RC90A
H1600-10	1000PK100	MCR2835-4	IR32B	NLC35C	16RC30A	NLC150E	71RA50
H1600-12	1000PK120	MCR2835-5	IR32C	NLC35D	16RC40A	NLC150M	71RA60
H1600-14	1000PK140	MCR2835-6	IR32D	NLC35E	16RC50A	NLC150N	71RA80
H1600-16	1000PK160	MCR2835-1	IR30U	NLC35M	16RC60A	NLC150P	71RA90
H1800-2	1000PK20	MCR2935-2	IR30F	NLC35N	16RC80A	NLC150PA	71RA110
H1800-4	1000PK40	MCR2935-3	IR30A	NLC35P	16RC100A	NLC150PB	71RA120
H1800-6	1000PK60	MCR2935-4	IR30B	NLC35S	16RC70A	NLC150PC	71RA130
H1800-8	1000PK80	MCR2935-5	IR30C	NLC35T	16RC90A	NLC150S	71RA70

COMPETITIVE PART NO.	SUGGESTED IR REPLACEMENT	COMPETITIVE PART NO.	SUGGESTED IR REPLACEMENT	COMPETITIVE PART NO.	SUGGESTED IR REPLACEMENT	COMPETITIVE PART NO.	SUGGESTED IR REPLACEMENT
NLC150T	71RA90	NLC185E	151RF50	NLC501P	550PB100	NLF158M	81RL860
NLC151E	81RL50	NLC185M	151RF60	NLC501PA	550PB110	NLF158N	81RL880
NLC151M	81RL60	NLC290A	300RA10	NLC501PB	550PB120	NLF159P	81RL8100
NLC151N	81RL80	NLC290B	300RA20	NLC501PC	550PB130	NLF158S	81RL870
NLC151P	81RL100	NLC290C	300RA30	NLC501PD	550PB140	NLF158T	81RL890
NLC151S	81RL70	NLC290D	300RA40	NLC501PE	550PB150	NLF159A	82RL810
NLC151T	81RL90	NLC290E	300RA50	NLC501PM	550PB160	NLF159B	82RL820
NLC152E	72RA50	NLC290G	300RA15	NLC501PS	550PB170	NLF159C	82RL830
NLC152M	72RA60	NLC290H	300RA25	NLC501S	550PB70	NLF159D	82RL840
NLC152N	72RA80	NLC290M	300RA60	NLC501T	550PB90	NLF159E	82RL850
NLC152P	72RA100	NLC290N	300RA80	NLF150B	81RLA20	NLF159M	82RL860
NLC152PA	72RA110	NLC290P	300RA100	NLF150C	81RLA30	NLF159N	82RL880
NLC152PB	72RA120	NLC290PA	300RA110	NLF150D	81RLA40	NLF159P	82RL8100
NLC152PC	72RA130	NLC290PB	300RA120	NLF150E	81RLA50	NLF159S	82RL870
NLC152S	72RA70	NLC290S	300RA70	NLF150M	81RLA60	NLF159T	82RL890
NLC152T	72RA90	NLC290T	300RA90	NLF150N	81RLA80	NLF159A	161RL10
NLC153E	82RL50	NLC291A	303RA10	NLF150P	81RLA100	NLF159B	161RL20
NLC153M	82RL60	NLC291B	303RA20	NLF150S	81RLA70	NLF159C	151RL30
NLC153N	82RL80	NLC291C	303RA30	NLF150T	81RLA90	NLF159D	151RL40
NLC153P	82RL100	NLC291D	303RA40	NLF151B	81RL20	NLF159E	151RL50
NLC153S	82RL70	NLC291E	303RA50	NLF151C	81RL30	NLF159M	161RL60
NLC153T	82RL90	NLC291G	303RA15	NLF151D	81RL40	NLF355A	140PAL10
NLC154A	91RM10	NLC291H	303RA25	NLF151E	81RL50	NLF355B	140PAL20
NLC154B	91RM20	NLC291M	303RA60	NLF151M	81RL60	NLF355C	140PAL30
NLC154C	91RM30	NLC291N	303RA80	NLF151N	81RL80	NLF355D	140PAL40
NLC154D	91RM40	NLC291P	303RA100	NLF151P	81RL100	NLF355E	140PAL50
NLC154E	91RM50	NLC291PA	303RA110	NLF151S	81RL70	NLF355M	140PAL60
NLC154M	91RM60	NLC291PB	303RA120	NLF151T	81RL90	NLF358A	125PALB10
NLC155A	91RL10	NLC291S	303RA70	NLF152B	82RLA20	NLF358B	125PALB20
NLC155B	91RL20	NLC291T	303RA90	NLF152C	82RLA30	NLF358C	125PALB30
NLC155C	91RL30	NLC350A	115PA10	NLF152D	82RLA40	NLF358D	125PALB40
NLC155D	91RL40	NLC350B	115PA20	NLF152E	82RLA50	NLF358E	125PALB50
NLC155E	91RL50	NLC350C	115PA30	NLF152M	82RLA60	NLF358M	125PALB60
NLC155M	91RL60	NLC350D	115PA40	NLF152N	82RLA80	NLF358N	125PALB80
NLC155A	92RM10	NLC350E	115PA50	NLF152P	82RLA100	NLF358P	125PALB100
NLC155B	92RM20	NLC350M	115PA60	NLF152S	82RLA70	NLF358PA	125PALB110
NLC156C	92RM30	NLC350N	115PA80	NLF152T	82RLA90	NLF358PB	125PALB120
NLC156D	92RM40	NLC350P	115PA100	NLF153B	82RL20	NLF358S	125PALB70
NLC156E	92RM50	NLC350PA	115PA110	NLF153C	82RL30	NLF358T	125PALB90
NLC156M	92RM60	NLC350PB	115PA120	NLF153D	82RL40	PS200	IR32F
NLC157A	92RL10	NLC350PC	115PA130	NLF153E	82RL50	PS120	IR32A
NLC157B	92RL20	NLC350S	115PA70	NLF153M	82RL60	PS220	IR32B
NLC157C	92RL30	NLC350T	115PA90	NLF153N	82RL80	PS320	IR32C
NLC157D	92RL40	NLC354A	140PAM10	NLF153P	82RL100	PS420	IR32D
NLC157E	92RL50	NLC354B	140PAM20	NLF153S	82RL70	S0301JS2	IR106Y1
NLC157M	92RL60	NLC354C	140PAM30	NLF153T	82RL90	S0301JS3	IR106Y1
NLC178A	151RB10	NLC354D	140PAM40	NLF154A	91RM10	S0301MS1	IR5F
NLC178B	151RB20	NLC354E	140PAM50	NLF154B	91RM20	S0301MS2	IR5F
NLC178C	151RB30	NLC354M	140PAM60	NLF154C	91RM30	S0301MS3	IR6F
NLC178D	151RB40	NLC355A	140PAL10	NLF154D	91RM40	S0303RS2	IR106Y1
NLC178E	151RB50	NLC355B	140PAL20	NLF154E	91RM50	S0303RS3	IR106Y1
NLC178F	151RB60	NLC355C	140PAL30	NLF154M	91RM60	S0306RS2	IR122Y
NLC178G	151RB70	NLC355D	140PAL40	NLF155A	91RL10	S0306RS3	IR122Y
NLC178H	151RB80	NLC355E	140PAL50	NLF155B	91RL20	S0308RS2	IR122Y
NLC178P	151RB100	NLC355M	140PAL60	NLF155C	91RL30	S0308RS3	IR122Y
NLC178PA	151RB110	NLC380A	250PA10	NLF155D	91RL40	S0525G	IR30F
NLC178PB	151RB120	NLC380B	250PA20	NLF155E	91RL50	S0601JS2	IR106Y1
NLC178S	151RB70	NLC380C	250PA30	NLF155M	91RL60	S0601JS3	IR106Y1
NLC178T	151RB90	NLC380D	250PA40	NLF156A	92RM10	S0601MS1	IR5F
NLC180A	151RA10	NLC380E	250PA50	NLF156B	92RM20	S0601MS2	IR5F
NLC180B	151RA20	NLC380M	250PA60	NLF156C	92RM30	S0601MS3	IR6F
NLC180D	151RA30	NLC380N	250PA80	NLF156D	92RM40	S0603RS2	IR106F1
NLC180E	151RA40	NLC380P	250PA100	NLF156E	92RM50	S0603RS3	IR106F1
NLC180M	151RA60	NLC380PA	250PA110	NLF156M	92RM60	S0606RS2	IR122F
NLC180N	151RA80	NLC380PB	250PA120	NLF157A	92RL10	S0606RS3	IR122F
NLC180P	151RA100	NLC380PC	150PA130	NLF157B	92RL20	S0608RS2	IR122F
NLC180PA	151RA110	NLC380S	250PA70	NLF157C	92RL30	S0608RS3	IR122F
NLC180PB	151RA120	NLC380T	250PA90	NLF157D	92RL40	S0525G	IR30F
NLC180PC	151RA130	NLC385A	250PAL10	NLF157E	92RL50	S1001JS2	IR106A1
NLC180S	151RA70	NLC385B	250PAL20	NLF157M	92RL60	S1001JS3	IR106A1
NLC180T	151RA90	NLC385C	250PAL30	NLF158A	81RL810	S1001MS1	IR5A
NLC185A	151RF10	NLC385D	250PAL40	NLF158B	81RL820	S1001MS2	IR5A
NLC185B	151RF20	NLC385E	250PAL50	NLF158C	81RL830	S1001MS3	IR6A
NLC185C	151RF30	NLC385M	250PAL60	NLF158D	81RL840	S1003RS2	IR106A1
NLC185D	151RF40	NLC501N	550PB80	NLF158E	81RL850	S1003RS3	IR106A1

APPENDIX III

COMPETITIVE PART NO.	SUGGESTED IR REPLACEMENT	COMPETITIVE PART NO.	SUGGESTED IR REPLACEMENT	COMPETITIVE PART NO.	SUGGESTED IR REPLACEMENT	COMPETITIVE PART NO.	SUGGESTED IR REPLACEMENT
S100RS2	IR122A	T4040322	IR140C	T5020890	81RLB80	T505078005AQ	71REH70
S100RS3	IR122A	T4040422	IR140D	T50210X70	81RLB100	T505084005AA	37REH80
S2001RS2	IR122A	T4050122	22RC10	T5021080	81RLB100	T505084005AQ	36REH80
S100RS3	IR122A	T4050222	22RC20	T50211X70	81RLB110	T505088005AA	72REH80
S1025G	IR30A	T4050322	22RC30	T5021180	81RLB110	T505088005AQ	71REH80
S2001JS2	IR106B1	T4050422	22RC40	T50212X10	81RLB120	T505094005AA	37REH90
S2001JS3	IR106B1	T4050522	22RC50	T5021280	81RLB120	T505094005AQ	36REH90
S2001MS1	IR5B	T4050522	22RC60	T502-X70B20	81RM20S66	T505098005AA	72REH90
S2001MS2	IR5B	T4070022	IR141F	T502-X70B30	81RM30S66	T505098005AQ	71REH90
S2001MS3	IR5B	T4070122	IR141A	T502-X70B40	81RM40S66	T505104005AA	37REH100
S2003RS2	IR106B1	T4070222	IR141B	T502-X70B50	81RM50S66	T505104005AQ	36REH100
S2003RS3	IR106B1	T4070322	IR141C	T502-X70B60	81RM60S66	T505108005AA	72REH100
S2006RS2	IR122B	T4070422	IR141D	T502-X70B70	81RM70S66	T505108005AQ	71REH100
S2006RS3	IR122B	T4080016	10RC5A	T502-X70B80	81RM80S66	T507018064AA	82RM10
S2006RS2	IR122B	T4080116	10RC10A	T502-X70B90	81RM90S66	T507018064AQ	81RM10
S2006RS3	IR122B	T4080216	10RC20A	T502-X70C10	81RM100S66	T507028064AA	82RM20
S2025G	IR30B	T4080316	10RC30A	T502-X70C11	81RLB110S66	T507028064AQ	81RM20
S4001JS2	IR106D1	T4080416	10RC40A	T502-X70C12	81RLB120S66	T507038064AA	82RM30
S4001JS3	IR106D1	T4080516	10RC50A	T504017074AA	82RM10	T507038064AQ	81RM30
S4001MS1	IR5D	T500014005AA	37RA10	T504017074AQ	81RM10	T507048064AA	82RM40
S4001MS2	IR5D	T500014005AQ	36RA10	T504024064AA	82RM20	T507048064AA	81RM40
S4001MS3	IR5D	T500024005AA	37RA20	T504024064AQ	81RM20	T507058064AA	82RM50
S4003RS2	IR106D1	T500034005AA	37RA30	T504027074AA	82RM20	T507058064AQ	81RM50
S4003RS3	IR106D1	T500034005AQ	36RA30	T504027074AQ	81RM20	T507068064AA	82RM60
S4006RS2	IR122D	T500044005AA	37RA40	T504034064AA	82RM30	T507068064AQ	81RM60
S4006RS3	IR122D	T500044005AQ	36RA40	T504034064AQ	81RM30	T50707064AA	81RM70
S4008RS2	IR122D	T500054005AA	37RA50	T504037074AA	82RM30	T50707064AA	81RM70
S4008RS3	IR122D	T500054005AQ	36RA50	T504037074AQ	81RM30	T507088064AA	82RM80
S4025G	IR30D	T500058005AA	72RA50	T504044064AA	82RM40	T507088064AQ	81RM80
SP528	2N1J71A	T500062005AQ	71RA50	T504044064AQ	81RM40	T507098064AA	82RM90
SP529	IR30F	T500064005AA	37RA60	T504047074AA	82RM40	T507098064AQ	81RM90
SP535	16RC5A	T500064005AQ	36RA60	T504047074AQ	81RM40	T507108064AA	82RM100
SP518	2N1772A	T500068005AA	72RA60	T504054064AA	82RM50	T507109064AQ	81RM100
SP528	2N1774A	T500068005AQ	71RA60	T504054054AQ	82RM50	T50711804AA	81RLB110
SP538	2N1776A	T500074005AA	37RA70	T504057074AA	82RM50	T50711804AQ	81RLB110
SP548	2N1777A	T500074005AQ	36RA70	T504057074AQ	81RM50	T50712804AA	82RLB20
SP558	2N1778A	T500078005AA	72RA70	T504064064AA	82RM60	T50712804AQ	81RLB20
SP568	2N2619A	T500078005AQ	71RA70	T504064064AQ	81RM60	T520011305DN	115PA10
SP5120	IR30A	T500084005AA	37RA80	T504067074AA	82RM60	T520021305DN	115PA20
SP5135	16RC10A	T500084005AQ	36RA80	T504067074AQ	81RM60	T520031305DN	115PA30
SP5220	IR30B	T500088005AA	72RA80	T504074064AA	82RM70	T520041305DN	115PA40
SP5235	16RC20A	T500088005AQ	71RA80	T504074064AQ	81RM70	T520051305DN	115PA50
SP5320	IR30C	T500094005AA	37RA90	T504077074AA	82RM70	T520061305DN	115PA60
SP5335	16RC30A	T500094005AQ	36RA90	T504077074AQ	81RM70	T520071305DN	115PA70
SP5470	IR30D	T500098005AA	72RA90	T504084064AA	82RM80	T520081305DN	115PA80
SP5435	16RC40A	T500098005AQ	71RA90	T504084064AA	81RM80	T520091305DN	115PA90
SP5535	16RC50A	T500104005AA	37RA100	T504087074AA	82RM80	T520101305DN	115PA100
SP5635	16RC60A	T500104005AQ	36RA100	T504087074AQ	81RM80	T52011305DN	115PA110
T1C106A1	IR106A1	T500108005AA	72RA100	T504094064AA	82RLB30	T52012305DN	115PA120
T1C106B1	IR106B1	T500108005AQ	71RA100	T504094054AQ	81RLB30	T520201305DN	115PA30
T1C106C1	IR106C1	T500114005AA	37RA110	T504097044AA	82RLB80	T52021305DN	115PA40
T1C106D1	IR106D1	T500114005AQ	36RA110	T504097044AQ	81RLB80	T520141305DN	115PA120
T1C106F1	IR106F1	T500118005AA	72RA110	T504104054AA	82RL100	T520151305DN	115PA150
T1C106G1	IR106G1	T500118005AQ	71RA110	T504104054AQ	81RL100	T520171364DN	125PAM20
T1C106U1	IR106U1	T500124005AA	37RA120	T504107044AA	82RLB90	T520213054DN	125PAM30
T400002208	16RC5A	T500124005AQ	36RA120	T504107044AQ	81RLB90	T520213054DN	125PAM40
T400011008	10RC10	T500128005AA	72RA120	T504114034AA	37RA110T60	T520251364DN	125PAM50
T400011608	10RC10A	T500128005AQ	71RA120	T504114034AQ	36RA110T60	T520261364DN	125PAM60
T400012208	16RC10A	T500134005AA	37RA130	T504117034AA	72RB110T60	T520271364DN	125PAM70
T400021008	10RC20A	T500134005AQ	36RA130	T504117034AQ	71RB110T60	T520281364DN	125PAM80
T400021608	10RC20A	T500138005AA	72RA130	T504124034AA	37RA120T60	T520291364DN	125PAM90
T400022208	16RC20A	T500138005AQ	71RA130	T504124034AQ	36RA120T60	T52031364DN	125PAM100
T400031008	10RC30A	T500144005AA	37RA140	T504127034AA	72RB120T60	T52031364DN	125PAM110
T400031608	10RC30A	T500144005AQ	36RA140	T504127034AQ	71RB120T60	T52031364DN	125PAM120
T400032208	16RC30A	T500148005AA	72RA140	T505054005AA	37REH50	T52031364DN	125PAM130
T400041608	10RC40A	T500148005AQ	71RA140	T505054005AA	36REH50	T600011504BT	151RA10
T400041608	10RC40A	T500154005AA	37RA150	T505058005AA	72REH50	T600011804BT	151RA10
T400042208	16RC40A	T500154005AQ	36RA150	T505058005AQ	71REH50	T600021304BT	151RB20
T400051008	10RC50A	T500158005AA	72RA150	T505074005AA	37REH70	T600021504BT	151RA20
T400051608	10RC50A	T500158005AQ	71RA150	T505074005AQ	36REH70	T600021804BT	151RA20
T400052208	16RC50A	T50205X70	81RLB80	T505084005AQ	36REH80	T600031304BT	151RB30
T400062208	16RC60A	T5020580	81RLB50	T505088005AA	72REH80	T600031504BT	151RA30
T4040022	IR140F	T50206X70	81RLB80	T505088005AQ	71REH70	T600031804BT	151RA30
T4040122	IR140A	T5020680	81RLB60	T505074005AQ	36REH70	T600041304BT	151RA40
T4040222	IR140B	T50206X70	81RLB80	T505078005AA	72REH70	T600041504BT	151RA40

COMPETITIVE PART NO.	SUGGESTED IR REPLACEMENT	COMPETITIVE PART NO.	SUGGESTED IR REPLACEMENT	COMPETITIVE PART NO.	SUGGESTED IR REPLACEMENT	COMPETITIVE PART NO.	SUGGESTED IR REPLACEMENT
T60041804BT	175RA40	T620123004DN	300PA120	T707072044BY	250RM70	T7601330	304RA130
T600051304BT	151RB50	T620131304DN	175PA130	T707072544BY	250RM70	T7601430	304RA140
T600051504BT	151RA50	T620132004DN	250PA130	T707082044BY	250RM80	T7601530	304RA150
T600051804BT	175RA50	T620141304DN	175PA140	T707082544BY	250RM80	T7601630	304RA160
T600061304BT	151RB60	T620142004DN	250PA140	T707092044BY	250RM90	T7601730	304RA170
T600061504BT	151RA60	T620151304DN	175PA150	T707092544BY	250RM90	T9200506	700PK50
T600061804BT	175RA60	T620152004DN	250PA150	T707102044BY	250RM100	T9200507	700PK50
T600071304BT	151RB70	T624041564DN	250PAL40	T707102544BY	250RM100	T9200508	850PK50
T600071504BT	151RA70	T624051564DN	250PAL50	T707112044BY	250RM110	T9200509	850PK50
T600071804BT	175RA70	T624061564DN	250PAL60	T707112544BY	250RM110	T9200510	1000PK50
T600081304BT	151RB80	T624071554DN	240PAL70	T707122044BY	250RM120	T9200606	700PK60
T600081504BT	151RA80	T524081554DN	240PAL80	T707122544BY	250RM120	T9200607	700PK60
T600081804BT	175RA80	T624091544DN	240PAL90S68	T7200535	420PB50	T9200608	850PK60
T600091304BT	151RB90	T624101544DN	240PAL100S68	T7200545	470PB50	T9200609	850PK60
T600091504BT	151RA90	T624111524DN	240PAL110T62	T7200555	550PB50	T9200610	1000PK60
T600091804BT	175RA90	T624121524DN	240PAL120T62	T7200635	420PB60	T9200806	700PK80
T600101304BT	151RB100	T62701156	250PAL10	T7200645	470PB60	T9200807	700PK80
T600101504BT	151RA100	T62701158	250PAM10	T7200655	550PB60	T9200808	850PK80
T600101804BT	175RA100	T62702156	250PAL20	T7200665	420PB80	T9200809	850PK80
T600111304BT	151RB110	T62702158	250PAM20	T7200845	470PB80	T9200810	1000PK80
T600111504BT	151RA110	T62703156	250PAL30	T7200855	550PB80	T9201006	700PK100
T600111804BT	175RA110	T62703158	250PAM30	T7201035	420PB100	T9201007	700PK100
T600121304BT	151RB120	T62704156	250PAL40	T7201045	470PB100	T9201008	850PK100
T600121504BT	151RA120	T62704158	250PAM40	T7201055	550PB100	T9201009	850PK100
T600121804BT	175RA120	T62705156	250PAL50	T7201135	420PB110	T9201010	1000PK100
T600131304BT	151RB130	T62705158	250PAM50	T7201145	470PB110	T9201106	700PK110
T600131504BT	151RA130	T62706156	250PAL60	T7201155	550PB110	T9201107	700PK110
T600141304BT	151RB140	T62706158	250PAM60	T7201235	420PB120	T9201108	850PK110
T600141504BT	151RA140	T6600530	303RA50	T7201245	470PB120	T9201109	850PK110
T600151304BT	151RB150	T6600630	303RA60	T7201255	550PB120	T9201110	1000PK110
T600151504BT	151RA150	T6600830	303RA80	T7201335	420PB130	T9201206	700PK120
T604011564BT	151RF10	T6601030	303RA100	T7201345	470PB130	T9201207	700PK120
T604021564BT	151RF20	T6601130	303RA110	T7201355	550PB130	T9201208	850PK120
T604031564BT	151RF30	T6601230	303RA120	T7201435	420PB140	T9201209	850PK120
T604041364BT	151RF40	T6601330	303RA130	T7201445	470PB140	T9201210	1000PK120
T604041564BT	151RF40	T6601430	303RA140	T7201455	550PB140	T9201306	700PK130
T604051364BT	151RF50	T6601530	303RA150	T7201545	470PB150	T9201307	700PK130
T604051564BT	151RF50	T6600530	303RB50	T7201555	550PB150	T9201308	850PK130
T604061364BT	151RF60	T6600630	303RB60	T7201635	420PB160	T9201309	850PK130
T604061564BT	151RF60	T6600830	303RB80	T7201645	470PB160	T9201406	700PK140
T604071354BT	151RL70	T6801030	303RB100	T7201655	550PB160	T9201407	700PK140
T604081354BT	151RL80	T6801130	303RB110	T7201735	420PB170	T9201408	850PK140
T604091344BT	151RL90S68	T6801230	303RB120	T7201745	470PB170	T9201409	850PK140
T604101344BT	151RL100S68	T6801330	303RB130	T7201755	550PB170	T9201506	700PK150
T620051304DN	175PA50	T6801430	303RB140	T7201755	550PB170	T9201507	700PK150
T620052004DN	250PA50	T6801530	303RB150	T727012574DN	550PBQ10	T9201508	850PK150
T6200530	300PA50	T7000525	250RA50	T727013574DN	550PBQ10	T9201509	850PK150
T620053004DN	300PA50	T7000530	300RA50	T727022574DN	550PBQ20	T9201606	700PK160
T620061304DN	175PA60	T7000535	350RA50	T727032574DN	550PBQ30	T9201607	700PK160
T620062004DN	250PA60	T7000625	250RA60	T727032574DN	550PBQ30	T9201608	850PK160
T6200630	300PA60	T7000630	300RA60	T727033574DN	550PBQ30	T9201609	850PK160
T620063004DN	300PA60	T7000635	350RA60	T727042574DN	550PBQ40	TC106A1	IR106A1
T620071304DN	175PA70	T7000825	250RA80	T727043574DN	550PBQ40	TC106B1	IR106B1
T620072004DN	250PA70	T7000830	300RA80	T727052574DN	550PBQ50	TC106C1	IR106C1
T6200730	300PA70	T7000835	350RA80	T727052574DN	550PBQ50	TC106D1	IR106D1
T620073004DN	300PA70	T7001025	250RA100	T727062574DN	550PBQ60	TC106F1	IR106F1
T620081304DN	175PA80	T7001030	300RA100	T727063574DN	550PBQ60	TC106G1	IR106G1
T620082004DN	250PA80	T7001035	350RA100	T727072544DN	420PBM70	TC106U1	IR106U1
T6200830	300PA80	T7001125	250RA110	T727073544DN	420PBM70		
T620083004DN	300PA80	T7001130	300RA110	T727082544DN	420PBM80		
T620091304DN	175PA90	T7001135	350RA110	T727083544DN	420PBM80		
T620092004DN	250PA90	T7001225	250RA120	T727092544DN	420PBM90		
T6200930	300PA90	T7001230	300RA120	T727093544DN	420PBM90		
T620093004DN	300PA90	T7001235	350RA120	T727102544DN	420PBM100		
T620101304DN	175PA100	T7001325	250RA130	T727103544DN	420PBM100		
T620102004DN	250PA100	T7001330	300RA130	T727112544DN	420PBM110		
T6201030	300PA100	T7001335	350RA130	T727113544DN	420PBM110		
T620103004DN	300PA100	T7001425	250RA140	T727122544DN	420PBM120		
T620111304DN	175PA110	T7001430	300RA140	T727123544DN	420PBM120		
T620112004DN	250PA110	T7001435	350RA140	T7600530	304RA50		
T6201130	300PA110	T7001525	250RA150	T7600630	304RA60		
T620113004DN	300PA110	T7001530	300RA150	T7600830	304RA80		
T620121304DN	175PA120	T7001535	350RA150	T7601030	304RA100		
T620122004DN	250PA120	T7001630	300RA160	T7601130	304RA110		
T6201230	300PA120	T7001730	300RA170	T7601230	304RA120		
						3RC10	3RC10A
						3RC20	3RC20A
						3RC30	3RC30A
						3RC40	3RC40A
						3RC50	3RC50A
						3RC60	3RC60A
						5RC10	5RC10A
						5RC20	5RC20A
						5RC30	5RC30A
						5RC40	5RC40A
						5RC50	5RC50A
						5RC60	5RC60A

APPENDIX III

COMPETITIVE PART NO.	SUGGESTED IR REPLACEMENT	COMPETITIVE PART NO.	SUGGESTED IR REPLACEMENT	COMPETITIVE PART NO.	SUGGESTED IR REPLACEMENT	COMPETITIVE PART NO.	SUGGESTED IR REPLACEMENT
10RC10	10RC10A	36RE50	36RA50	70C40F	72RC40A	72RE130	72RA130
10RC20	10RC20A	36RE60	36RA60	70C50	71RC50A	72RE150	72RA150
10RC30	10RC30A	36RE80	36RA80	70C50F	72RC50A	72RE160	72RA60
10RC40	10RC40A	36RE100	36RA100	70C60	71RC60A	72RE180	72RA80
10RC50	10RC50A	36RE110	36RA110	70C60F	72RC60A	72RE100	72RA100
10RC60	10RC60A	36RE120	36RA120	70C80	71RC80A	72RE110	72RA110
10RC20A	IR140C	36RE130	36RA130	70C80F	72RC80A	72RE120	72RA120
10RC100	10RC100A	37RCF5A	82RM5	70C100	71RA100	72RE130	72RA130
10RC110	10RC110A	37RCF10A	82RM10	70C100F	72RA100	72REB50	72RB50
10RC120	10RC120A	37RCF15A	82RM15	70C110	71RA110	72REB60	72RB60
10RCF10A	IR140A	37RCF20A	82RM20	70C110F	72RA110	72REB80	72RB80
10RCF20A	IR140C	37RCF25A	82RM25	70C120	71RA120	72REB100	72RB100
10RCF30A	IR140C	37RCF30A	82RM30	70C120F	72RA120	72REB110	72RB110
10RCF40A	IR140D	37RCF40A	82RM40	70C130	71RA130	72REB120	72RB120
10RCF50A	IR140E	37RCF50A	82RM50	70C130F	72RA130	100C10	101RC10
10RCF60A	IR140M	37RCF60A	82RM60	70C140	71RA140	100C20	101RC20
16C025	22RA2	37RCF70A	82RM70	70C140F	71RA140	100C40	101RC40
16C050	22RA5	37RCF80A	82RM80	70C150	71RA150	100C60	101RC60
16C10	22RA10	37RE50	37RA50	70C150F	72RA150	100C80	101RC80
16C20	22RA20	37RE60	37RA60	70C160	71RA160	100C100	101RA100
16C30	22RA30	37RE80	37RA80	70C160F	72RA160	100C110	101RA110
16C40	22RA40	37RE100	37RA100	71RCF10	81RM10	100C120	101RA120
16C50	22RA50	37RE110	37RA110	71RCF20	81RM20	100C140	101RA140
16C60	22RA60	37RE120	37RA120	71RCF30	81RM30	100C160	101RA160
16C80	16RC80A	37RE130	37RA130	71RCF40	81RM40	101RE50	101RA50
16C100	16RC100A	40C050	40RC55	71RCF50	81RM50	101RE60	101RA60
16C110	16RC110A	40C10	40RC10	71RCF60	81RM60	101RE80	101RA80
16C120	16RC120A	40C20	40RC20	71RCG5	81RM5	101RE100	101RA100
16RC10	16RC10A	40C30	40RC30	71RCG10	81RM10	101RE110	101RA110
16RC20	16RC20A	40C40	40RC40	71RCG15	81RM15	101RE120	101RA120
16RC30	16RC30A	40C50	40RC50	71RCG20	81RM20	125PL10	125PAL10
16RC40	16RC40A	40C60	40RC60	71RCG25	81RM25	125PL20	125PAL20
16RC50	16RC50A	40C80	40RC80	71RCG30	81RM30	125PL30	125PAL30
16RC60	16RC60A	40C100	40RC100	71RCG40	81RM40	125PL40	125PAL40
16RC80	16RC80A	40C110	40RC110	71RCG50	81RM50	125PL50	125PAL50
16RC100	16RC100A	40C120	40RC120	71RCG60	81RM60	125PL60	125PAL60
16RC110	16RC110A	55C050	36RC5A	71RE60	71RA60	125PL80	125PAL80
16RC120	16RC120A	55C050F	37RC5A	71RE70	71RA70	125PL100	125PAL100
16RCF10	IR140A	55C10	36RC10A	71RE80	71RA80	125PL120	125PAL120
16RCF20	IR140B	55C10F	37RC10A	71RE90	71RA90	125PM10	125PAM10
16RCF30	IR140C	55C20	36RC20A	71RE100	71RA100	125PM20	125PAM20
16RCF40	IR140D	55C20F	37RC20A	71RE110	71RA110	125PM30	125PAM30
16RCF50	IR140E	55C30	36RC30A	71RE120	71RA120	125PM50	125PAM50
16RCF60	IR140M	55C30F	37RC30A	71RE130	71RA130	125PM60	125PAM60
18RC10	16RC10A	55C40	36RC40A	71RE150	71RA150	125PM80	125PAM80
18RC20	16RC20A	55C40F	37RC40A	71RE160	71RA60	125PM100	125PAM100
18RC30	16RC30A	55C50	36RC50A	71RE180	71RA80	140PL10	140PAL10
18RC40	16RC40A	55C50F	37RC50A	71RE100	71RA100	140PL20	140PAL20
18RC50	16RC50A	55C60	36RC60A	71RE110	71RA110	140PL30	140PAL30
18RC60	16RC60A	55C60F	37RC60A	71RE120	71RA120	140PL40	140PAL40
18RC80	16RC80A	55C80	36RC80A	71RE130	71RA130	140PL50	140PAL50
18RC100	16RC100A	55C80F	37RC80A	71REB50	71RB50	140PL60	140PAL60
23C025	22RA2	55C100	36RA100	71REB60	71RB60	140PM10	140PAM10
23C050	22RA5	55C100F	37RA100	71REB80	71RB80	140PM20	140PAM20
23C10	22RA10	55C110	36RA110	71REB100	71RB100	140PM30	140PAM30
23C20	22RA20	55C110F	37RA110	71REB110	71RB110	140PM40	140PAM40
23C30	22RA30	55C120	36RA120	71REB120	71RB120	140PM50	140PAM50
23C40	22RA40	55C120F	37RA120	72RCF5A	82RM5	140PM60	140PAM60
23C50	22RA50	55C130	36RA130	72RCF10A	82RM10	150C10	151RC10A
23C60	22RA60	55C130F	37RA130	72RCF15A	82RM15	150C20	151RC20A
23C80	16RC80A	55C140	36RA140	72RCF20A	82RM20	150C40	151RC40A
23C100	16RC100A	55C140F	37RA140	72RCF25A	82RM25	150C60	151RC60A
23C110	16RC110A	55C150	36RA150	72RCF30A	82RM30	150C80	151RC80A
23C120	16RC120A	55C150F	37RA150	72RCF40A	82RM40	150C100	151RA100
36RCF5A	81RM5	55C160	36RA160	72RCF50A	82RM50	150C110	151RA110
36RCF10A	81RM10	55C160F	37RA160	72RCF60A	82RM60	150C120	151RC120
36RCF15A	81RM15	70C050	71RC5A	72RCF70A	82RM70	150C140	151RA140
36RCF20A	81RM20	70C050F	72RC5A	72RCF80A	82RM80	151C160	151RA160
36RCF25A	81RM25	70C10	71RC10A	72RE60	72RA60	150RC10	151RC10
36RCF30A	81RM30	70C10F	72RC10A	72RE70	72RA70	150RC20	151RC20
36RCF40A	81RM40	70C20	71RC20A	72RE80	72RA80	150RC30	151RC30
36RCF50A	81RM50	70C20F	72RC20A	72RE90	72RA90	150RC40	151RC40
36RCF60A	81RM60	70C30	71RC30A	72RE100	72RA100	150RC50	151RC50
36RCF70A	81RM70	70C30F	72RC30A	72RE110	72RA110	150RC60	151RC60
36RCF80A	81RM80	70C40	71RC40A	72RE120	72RA120	150RC70	151RC70

COMPETITIVE PART NO.	SUGGESTED IR REPLACEMENT	COMPETITIVE PART NO.	SUGGESTED IR REPLACEMENT	COMPETITIVE PART NO.	SUGGESTED IR REPLACEMENT	COMPETITIVE PART NO.	SUGGESTED IR REPLACEMENT
150RC80	151RC80	202U	10RC2A	218F	151RC30AS50	224ZF	303RA130
150RC10A	151RC10A	203B	10RC10A	218H	151RC40AS50	224ZH	303RA140
150RC20A	151RC20A	203D	10RC20A	218K	151RA50	224ZK	303RA150
150RC30A	151RC30A	203F	10RC30A	218M	151RA60	224ZM	303RA160
150RC40A	151RC40A	203H	10RC40A	218S	151RA80	224ZP	303RA170
150RC50A	151RC50A	203K	10RC50A	218Z	151RA100	227K	115PA50
150RC60A	151RC60A	203M	10RC60A	218ZB	151RA110	227M	115PA60
150RC70A	151RC70A	203S	10RC80A	218ZD	151RA120	227S	115PA80
150RC80A	151RC80A	203Z	10RC100A	218ZF	151RA130	227Z	115PA100
150RE50	151RA50	203ZD	10RC120A	218ZH	151RA140	227ZB	115PA110
150RE60	151RA60	204B	IR141A	218ZK	151RA150	227ZD	115PA120
150RE80	150RA80	204D	IR141B	218ZM	151RA160	227ZF	115PA130
150RE100	151RA100	204F	IR141C	219B	36RC10AS50	227ZH	115PA140
150RE110	151RA110	204H	IR141D	219D	36RC20AS50	227ZM	115PA150
150RE120	151RA120	204K	IR141E	219F	36RC30AS50	228K	175PA50
151RCF5A	151RF5	204M	IR141M	219H	36RC40AS50	228M	175PA60
151RCF10A	151RF10	206B	3RC10A	219K	36RA50	228S	175PA80
151RCF20A	151RF20	206D	3RC20A	219M	36RA60	228Z	175PA100
151RCF30A	151RF30	206F	3RC30A	219S	36RA80	228ZB	175PA110
151RCF40A	151RF40	205H	3RC40A	219Z	36RA100	228ZD	175PA120
151RCF50A	151RF50	206K	3RC50A	219ZB	36RA110	228ZF	175PA130
151RE50	151RA50	206M	3RC60A	219ZD	36RA120	228ZH	175PA140
151RE60	151RA60	207B	5RC10A	219ZF	36RA130	228ZM	175PA150
151RE80	151RA80	207D	5RC20A	219ZH	36RA140	229K	250PA50
151RE100	151RA100	207F	5RC30A	219ZK	36RA150	229M	250PA60
151RE110	151RA110	207H	5RC40A	219ZM	36RA160	229S	250PA80
151RE120	151RA120	207K	5RC50A	220K	175PA50	229Z	250PA100
151REA50	151RA50	207M	5RC60A	220Z	175PA60	241C10	250PA110
151REB50	151RB50	208A	2N1771	220S	175PA80	241C20	250PA120
151REB80	151RB80	208B	2N1772	220Z	175PA100	241C40	250PA140
151REB100	151RB100	208C	2N1773	220ZB	175PA110	241C50	250PA150
151REB110	151RB110	208D	2N1774	220ZD	175PA120	241C60	250PA160
151REB120	151RB120	208E	2N1775	220ZM	175PA130	241PC80	250PA180
151REB50	151RB50	208F	2N1776	220ZH	175PA140	241C100	250PA100
151REB60	151RB60	208H	2N1777	220ZK	175PA150	241C110	250PA110
151REB80	151RB80	208K	2N1778	220ZM	175PA160	241C120	250PA120
151REB100	151RB100	208U	2N1770	221K	301RB50	241C140	250PA140
151REB110	151RB110	208B	37RC10A	221M	301RB60	250K	71RA50
151REB120	151RB120	209D	37RC20A	221S	301RB80	250M	71RA60
171C10B	175PA10	209F	37RC30A	221Z	301RB100	250S	71RA80
171C20B	175PA20	209H	37RC40A	221ZB	301RB110	250Z	71RA100
171C40B	175PA40	209K	37RC50A	221ZD	301RB120	250ZB	71RA110
171C60B	175PA60	209M	37RC60A	221ZF	301RB130	250ZD	71RA120
171C80B	175PA80	209S	37RC80A	221ZH	301RB140	250ZF	71RA130
171C100B	175PA100	211B	36RC10A	221ZK	301RB150	250ZH	71RA140
171C110B	175PA110	211D	36RC20A	221ZM	301RB160	250ZK	71RA150
171C120B	175PA120	211F	36RC30A	221ZP	301RB170	250ZM	71RA160
171C140B	175PA140	211H	36RC40A	222K	304RA50	251K	36RA50
171C160B	175PA160	211K	35RC50A	222M	304RA60	251M	36RA60
200B	151RC10A	211M	35RC60A	222S	304RA80	251S	36RA80
200D	151RC20A	211S	36RC80A	222Z	304RA100	251Z	36RA100
200F	151RC30A	212A	81RM5	222ZB	304RA110	251ZB	36RA110
200H	151RC40A	212B	81RM10	222ZD	304RA120	251ZD	36RA120
200K	151RC50A	212C	81RM15	222ZF	304RA130	251ZF	36RA130
200M	151RC60A	212D	81RM20	222ZH	304RA140	251ZH	36RA140
200S	151RC80A	212E	81RM25	222ZK	304RA150	251ZK	36RA150
201A	16RC5A	212F	81RM30	222ZM	304RA160	251ZM	36RA160
201B	16RC10A	212H	81RM40	222ZP	304RA170	252K	115PA50
201D	16RC20A	212K	81RM50	223K	354RA50	252M	115PA60
201F	16RC30A	212M	81RM60	223M	354RA60	252S	115PA80
201H	16RC40A	212P	81RM70	223S	354RA80	252Z	115PA100
201K	16RC50A	212S	81RM80	223Z	354RA100	252ZB	115PA110
201M	16RC60A	213A	81RM5	223ZB	354RA110	252ZD	115PA120
201S	16RC80A	213B	81RM10	223ZD	354RA120	252ZF	115PA130
201Z	16RC100A	213C	81RM15	223ZF	354RA130	252ZH	115PA140
201ZB	16RC110A	213D	81RM20	223ZH	354RA140	252ZK	115PA150
201ZD	16RC120A	213E	81RM25	223ZK	354RA150	252ZM	115PA160
202A	10RC5A	213F	81RM30	223ZM	354RA160	254K	71RA50
202B	10RC10A	213H	81RM40	223ZP	354RA170	254M	71RA60
202C	10RC15A	213K	81RM50	224K	303RA50	254S	71RA80
202D	10RC20A	213M	81RM60	224M	303RA60	254Z	71RA100
202E	10RC25A	213P	81RM70	224S	303RA80	254ZB	71RA110
202F	10RC30A	213S	81RM80	224Z	303RA100	254ZD	71RA120
202H	10RC40A	218B	151RC10AS50	224ZB	303RA110	254ZF	71RA130
202M	10RC60A	218D	151RC20AS50	224ZD	303RA120	254ZH	71RA140

APPENDIX III

COMPETITIVE PART NO.	SUGGESTED IR REPLACEMENT	COMPETITIVE PART NO.	SUGGESTED IR REPLACEMENT	COMPETITIVE PART NO.	SUGGESTED IR REPLACEMENT	COMPETITIVE PART NO.	SUGGESTED IR REPLACEMENT
254ZK	71RA150	273ZF	175PA130	286-Y30C12	304RA120	850PA110	850PK110
254ZM	71RA160	273ZH	175PA140	286-Y30C13	304RA130	850PA120	850PK120
260K	175RA50	273ZK	175PA150	286-Y30C14	304RA140	850PA130	850PK130
260M	175RA60	273ZM	175PA160	286-Y30C15	304RA150	850PA140	850PK140
260P	175RA70	276K	300RA50	286-Y30C16	304RA160	850PA150	850PK150
260S	175RA80	276M	300RA60	286-Y30C17	304RA170	850PA160	850PK160
260V	175RA90	276S	300RA80	288B	303RA10	850PA170	850PK170
260Z	175RA100	276Z	300RA100	288D	303RA20	1000PA50	1000PK50
260ZB	175RA110	276ZB	300RA110	288F	303RA30	1000PA60	1000PK60
260ZD	175RA120	276ZD	300RA120	288H	303RA40	1000PA80	1000PK80
261K	151RA50	276ZF	300RA130	288K	303RA50	1000PA100	1000PK100
261M	151RA60	276ZH	300RA140	288M	303RA60	1000PA110	1000PK110
261S	151RA80	276ZK	300RA150	288P	303RA70	1000PA120	1000PK120
261Z	151RA100	276ZM	300RA160	288S	303RA80	1000PA130	1000PK130
261ZB	151RA110	276ZP	300RA170	288V	303RA90	1000PA140	1000PK140
261ZD	151RA120	278K	303RB50	288Z	303RA100	1000PA150	1000PK150
261ZF	151RA130	278M	303RB60	288ZB	303RA110	1000PA160	1000PK160
261ZH	151RA140	278P	303RB70	288ZD	303RA120	1000PA170	1000PK170
261ZK	151RA150	278S	303RB80	288ZF	303RA130	1600PA50	1600PK50
261ZM	151RA160	278V	303RB90	288ZH	303RA140	1600PA60	1600PK60
262K	175PA50	278Z	303RB100	288ZK	303RA150	1600PA80	1600PK80
262M	175PA60	278ZB	303RB110	288ZM	303RA160	1600PA100	1600PK100
262S	175PA80	278ZD	303RB120	301C10	300PA100	1600PA110	1600PK110
262Z	175PA100	282K	550PB50	301C20	300PA200	1600PA120	1600PK120
262ZB	175PA110	282M	550PB60	301C30	300PA300	2181K	151RF50
262ZD	175PA120	282S	550PB80	301C40	300PA400	2181M	151RF60
262ZF	175PA130	282Z	550PB100	301C50	300PA500	2182K	151RL50
262ZH	175PA140	282ZB	550PB110	301C60	300PA600	2182M	151RL60
262ZK	175PA150	282ZD	550PB120	301C80	300PA800	2182S	151RL80
262ZM	175PA160	282ZF	550PB130	301C100	300PA1000	2182Z	151RL100
263K	115PA50	282ZH	550PB140	301C110	300PA1100	2182ZB	151RL110
263M	115PA60	282ZK	550PB150	301C120	300PA1200	2182ZD	151RL120
263S	115PA80	282ZM	550PB160	420PL60	420PB160	2191K	91RM50
263Z	115PA100	282ZP	550PB170	420PL80	420PB180	2191M	91RM60
263ZB	115PA110	282-Y40B60	420PB60	420PL100	420PB100	2192K	81RM50
263ZD	115PA120	282-Y40B70	420PB70	420PL110	420PB110	2192M	81RM60
263ZF	115PA130	282-Y40B80	420PB80	420PL120	420PB120	2201K	250RM50
263ZH	115PA140	282-Y40B90	420PB90	420PM60	420PB600	2201M	250RM60
263ZK	115PA150	282-Y40C10	420PB100	420PM80	420PB800	2201S	250RM80
263ZM	115PA160	282-Y40C11	420PB110	420PM100	420PB1000	2201Z	250RM100
270K	350RA50	282-Y40C12	420PB120	420PM110	420PB1100	2201ZB	250RM110
270M	350RA60	282-Y40C13	420PB130	420PM120	420PB1200	2201ZD	250RM120
270S	350RA80	282-Y40C14	420PB140	470PA50	550PB50	2202K	250RM50
270Z	350RA100	282-Y40C15	420PB150	470PA60	550PB60	2202M	250RM60
270ZB	350RA110	282-Y40C16	420PB160	470PA80	550PB80	2202S	250RM80
270ZD	350RA120	282-Y40C17	420PB170	470PA100	550PB100	2202Z	250RM100
270ZF	350RA130	283H	470PB40	470PA110	550PB110	2202ZB	250RM110
270ZH	350RA140	283K	470PB50	470PA120	550PB120	2202ZD	250RM120
270ZK	350RA150	283M	470PB60	470PA130	550PB130	2248K	303RB50
270ZM	350RA160	283S	470PB80	470PA140	550PB140	2248M	303RB60
270ZP	350RA170	283Z	470PB100	470PA150	550PB150	2248S	303RB80
270-Y30B60	300RA60	283ZB	470PB110	470PA160	550PB160	2248Z	303RB100
270-Y30B70	300RA70	283ZD	470PB120	470PA170	550PB170	2248ZB	303RB120
270-Y30B80	300RA80	283ZF	470PB130	700PA50	700PK50	2248ZD	303RB140
270-Y30B90	300RA90	283ZH	470PB140	700PA60	700PK60	2248ZF	303RB130
270-Y30C10	300RA100	283ZK	470PB150	700PA80	700PK80	2248ZH	303RB140
270-Y30C11	300RA110	283ZM	470PB160	700PA100	700PK100	2248ZK	303RB150
270-Y30C12	300RA120	283ZP	470PB170	700PA110	700PK110	2248ZM	303RB160
270-Y30C13	300RA130	286K	304RA50	700PA120	700PK120	2248ZP	303RB170
270-Y30C14	300RA140	286M	304RA60	700PA130	700PK130	2451K	81RM50
270-Y30C15	300RA150	286S	304RA80	700PA140	700PK140	2451M	81RM60
270-Y30C16	300RA160	286Z	304RA100	700PA150	700PK150	2451S	81RM80
270-Y30C17	300RA170	286ZB	304RA110	700PK160	700PK160	2451Z	81RM100
272K	300PA50	286ZD	304RA120	700PK170	700PK170	2452K	81RM50
272M	300PA60	286ZF	304RA130	809B	71RC10A	2452M	81RM60
272S	300PA80	286ZH	304RA140	809D	71RC20A	2452S	81RM80
272Z	300PA100	286ZK	304RA150	809F	71RC30A	2452Z	81RM100
272ZB	300PA110	286ZM	304RA160	809H	71RC40A	2505K	71REH50
272ZD	300PA120	286ZP	304RA170	809K	71RC50A	2505M	71REH60
273K	175PA50	286-Y30B60	304RA60	809M	71RC60A	2505P	71REH70
273M	175PA60	286-Y30B70	304RA70	809S	71RC80A	2505S	71REH80
273S	175PA80	286-Y30B80	304RA80	850PA50	850PK50	2505V	71REH90
273Z	175PA100	286-Y30B90	304RA90	850PA60	850PK60	2505Z	71REH100
273ZB	175PA110	286-Y30C10	304RA100	850PA80	850PK80	2515K	36REH50
273ZD	175PA120	286-Y30C11	304RA110	850PA100	850PA100	2515M	36REH60

(Faint, illegible text from the reverse side of the page is visible through the paper.)

COMPETITIVE PART NO.	SUGGESTED IR REPLACEMENT	COMPETITIVE PART NO.	SUGGESTED IR REPLACEMENT	COMPETITIVE PART NO.	SUGGESTED IR REPLACEMENT	COMPETITIVE PART NO.	SUGGESTED IR REPLACEMENT
2515P	36REH70	2541Z	81RM100	2543D	91RM20	40743	IR30D
2515S	36REH80	2542A	81RM5	2543F	91RM30	40744	10RC60A
2515V	36REH90	2542B	81RM10	2543H	91RM40	40749	IR32A
2515Z	36REH100	2542D	81RM20	2543K	91RM50	40750	IR32B
2541A	81RM5	2542F	81RM30	2543M	91RM60	40751	IR32D
2541B	81RM10	2542H	81RM40	40735	10RC60A	40752	10RC60A
2541D	81RM20	2542K	81RM50	40737	IR32A	40753	IR30A
2541F	81RM30	2542M	81RM60	40738	IR32B	40754	IR30B
2541H	81RM40	2542S	81RM80	40739	IR32D	40755	IR30D
2541K	81RM50	2542Z	81RM100	40740	10RC60A	40756	10RC60A
2541M	81RM60	2543A	91RM5	40741	IR30A		
2541S	81RM80	2543B	91RM10	40742	IR30B		

① MECHANICAL DIFFERENCE

TYPICAL VOLTAGE CODE SUFFIXES

Peak Repetitive Reverse Voltage	GE NATL	W	IR	Peak Repetitive Reverse Voltage	GE NATL	W	IR
15	Q	—	—	1500	PE	ZK	C15
25	U	—	2	1600	PM	ZM	C16
30	Y	—	—	1700	PS	ZP	C17
50	F	A	5	1800	PN	ZS	—
100	A	B	10	2000	L	—	—
150	G	C	15	2100	LA	—	—
200	B	D	20	2200	LB	—	—
250	H	E	25	2300	LC	—	—
300	C	F	30	2400	LD	—	—
400	D	H	40	2500	LE	—	—
500	E	K	50	2600	—	—	—
600	M	N	60	2700	—	—	—
700	S	P	70	2800	—	—	—
800	N	S	80	2900	—	—	—
900	T	V	90	3000	—	—	—
1000	P	Z	100				
1100	PA	ZB	C11				
1200	PB	ZD	C12				
1300	PC	ZE	C13				
1400	PD	ZH	C14				

IR replacement numbers indicate the nearest IR equivalent, and in most instances are exact replacements. Occasionally, however, devices differ in size, electrical parameter, or manufacturing method. For this reason, IR cannot guarantee that the suggested type will, in every instance, serve as an exact replacement, and therefore assumes no responsibility for any consequences in the use of the replacements.

IR further suggests that examining the application may reveal that the qualities of another IR device may better fit the needs of the circuit than the simple replacement of a competitive device.

Index

— A —

- AC Controller 149, 157, 164
- AC Switch 149, 254
- AC Motor Control 193
- ACE Geometry 79
- Aircraft Power
 - Switch 223
 - System 218
- Alternating Current (See AC)
- Angle of Overlap 235
- Anti-parallel Diode 347
- Application Hints 102

— B —

- Battery
 - Charger 237, 339
 - Efficiency 324
- Bibliography (See reference at end of each chapter)
- Blocking
 - Current 34
 - Voltage, Test 410
- Breakover 31
- Bridge
 - Circuits 106, 231, 240, 242, 250, 253, 258
 - DC 231, 232, 234, 236, 238, 239, 240, 241, 243
- Brushless Motor 262, 263, 265, 266

— C —

- Case Temperature 401
- Characteristics
 - Dynamic 51
 - Gate 51, 414, 471, 481
 - Static 32
- Charger, Battery 237, 339
- Chopper Circuits 313, 320, 323, 325, 327, 329, 338, 340
- Circuit
 - Hints 161
 - L/R 376
 - Parallel 126

Circuits

- AC
 - Controller 164
 - Switch 217, 254
- Aircraft 223
- Battery Charger 237, 339
- Biphase 231
- Bridge 106, 231, 240, 242, 250, 253, 258
- Brushless Motor Control 263, 265, 266
- Chopper 313, 315, 320, 323, 325, 329, 338, 340
- Control 169, 250, 347, 349
- Converter 298
- Current Source Inverter 291, 292
- Cycloconverter 267, 271, 277
- Cycloinverter 293
- DC
 - Loads 232
 - Motor Control 244, 248, 321, 326
 - Power Supply 296
- Dual Converter 261
- Electric Vehicle 296
- Equalization 132, 133, 137
- Ferroresonant 186, 187, 189
- Frequency Multiplier 293
- Full Wave 231, 234, 249
- Gate (See Triggering)
- Half Wave 347
- Heating 169, 303
- High Frequency Inverter 358
- High Voltage Inverter 297
- Hybrid Bridge 242
- Impulse Commutated Inverter 8
- Induction Heating 303
- Inverse Voltage Protection 167
- Inverter 8, 255, 283, 285, 286, 288, 290, 291, 292, 296, 297, 298, 303, 348, 358

Circuits (con't.)

Light Dimmer 179, 180
Light Flasher 183
Line Voltage Compensator 184
Load Switch 344
McMurray Inverter 288
McMurray-Bedford 289
Morgan Chopper 316, 318
Motor Control 194, 195, 244,
248, 263, 264, 265, 266,
321, 326, 338
Motor Starter 194, 195, 215
Optical Coupled 143, 277, 478
PACE/pak 98, 101, 102, 103,
251, 253
Parallel Inverter 288
Phase Control 149
Protective 167, 367
Pulse Rate Modulation 316
Resistance Modulator 325
Reverse Recovery, JEDEC 351
Series Inverter 205
Solid State Contactor 215
Step-up Chopper 315, 319, 329
Switch 217, 254, 314
Test
Blocking Voltage 410
Critical de/dt 449
Critical dv/dt 443, 446
Gate Characteristics 414
Holding Current 418, 420
Inverter SCR 12
Latching Current 424, 425
Off-State Voltage 410
On-State Voltage 412
Thermal Resistance 450, 454,
456, 458, 460
Triacs 402
Triggering 415
Turn-Off Time 432, 433,
435, 437, 439, 440
Turn-On Time 429
Turn-On Voltage 429
Triac 165, 169, 249, 250
Time-Ratio Control 347, 349
Transformer Load Switch 314
Triggering 55, 56, 119, 121,
122, 139, 140, 141, 142,

Triggering (con't.)

143, 144, 145, 173, 174,
175, 464, 466, 468, 471, 478
Vehicle 296
Welding 197
Conduction Angle 43
Contact
Bounce 206
Resistance 396
Control
Circuits 253
RFI 207
Time-Ratio 347, 349
Controller 149, 157, 250
Motor 244, 248, 263, 265, 266,
320, 321, 326, 337, 338
Converter 7, 149, 231, 261, 295,
297
Cooling 393
Hockey Puks 397
Oil 403, 406
Specific Applications 402
Critical di/dt 53, 448
Critical dv/dt 64, 443
Cross Reference 531
Current
Blocking 34
Detector 280
Overload 388, 389
Peak Let-Thru 371
Rating 37
Recovery 484, 486
Sharing 126
Source Inverter 291
Cycloconverter 267, 271
Logic 278
Optical Isolation 277
Single Phase 271
Three Phase 280
Cycloinverter 293
— D —
DC
Bridge 231, 232, 236, 239, 240
Hybrid 241
Inductive Load 234
Poly Phase 238
Precautions 243

DC (con't.)

- Resistive Load 231
- Converter 295, 297
- Link 309
- Load 237
- Motor Control 244, 248, 250, 313, 320
- Power Supply 295
- Delay Time 114, 139
- Device Specifications 501
- di/dt 53, 109, 448
- Diode (Also See Rectifier)
 - Fast Recovery 10, 345, 353
 - Free Wheeling 10, 314, 345, 347
 - Recovery Test 351
 - Soft Recovery 10
- Direct Current (See DC)
- Dissimilar Metals 395
- Dual Converter 261
- dv/dt 61, 64, 443
 - Improvement 20, 23
 - Triac 86

— E —

- Electrical Vehicle 295, 296
 - Speed Control 320, 324, 337
- Emitter Shorting 23
- Epitaxial SCR 113
- Equalization 131, 132, 135, 137

— F —

- Fast Recovery Diodes 10, 345, 353
- Fast Rise Time 142
- Fault Protection 367
- Ferroresonant Regulator 182, 184, 186, 187, 189
- Finger Voltage 123, 124
- Flat Fin Heat Sink 405
- Form Factor 103
- Free-Wheeling Diode 10, 314, 346, 347
- Frequency Multiplier 293
- Full Wave Bridge 231, 234, 249
- Fuse 367
 - Arcing Time 371
 - Coordination 367
 - DC Operation 372
 - Isolating 372
 - Melting Time 371

— G —

- Gate (Also See Triggering)
 - Characteristics 51, 414, 471, 481
 - Circuits 119, 121, 122, 464, 466, 468, 471, 478
 - Hints 105, 471
 - Pulse 141, 152
 - Structures 481
- Geometry, ACE 60, 481

— H —

- Halfwave Circuit 347
- Heat Sink 393, 405
- Heater
 - Control 168, 208
 - Induction 301, 303
- High Frequency Inverter 358
- High Speed SCRs 481
- High Voltage Inverter 297
- Hints 102
- Hockey-Puk 90, 197, 397
- Holding Current 35, 125, 416
- Horsepower 307, 308
- Hybrid
 - Bridge 95, 105, 242, 253
 - Ripple 242
 - Module (See PACE/paks)

— I —

- I² Ratings 40, 368
- Impulse Commutated Inverter 8
- Induction Heating 301, 303
- Inductive
 - Load 155, 234
 - Energy Inversion 243
- Inverter SCR
 - Protecting 378
 - Testing 12
- Inverters 255, 283, 295, 301, 348
 - Comparison 294
 - Current Source 291
 - Electric Vehicle 296
 - Forced Commutated 283
 - High Frequency 358
 - High Voltage 295, 297
 - Impulse Commutated 8
 - Line-Commutated 257

Inverters (con't.)

- McMurray 284, 286
- McMurray-Bedford 285, 287
- Parallel 281
- Series 282, 283
- Three-Phase 286

- Inverse Voltage Protection 167
- Isolating Fuses 372

— J —

- JEDEC Reverse Recovery Test 351
- Junction Temperature 385

— L —

- Latching Current 125, 155, 422
- Light
 - Dimmer 179
 - Flasher 183
- Let-Thru Current 371
- Line Commutated Inverters 257
- Linear Motor Control 216
- Link, DC 237
- Load
 - DC 237
 - Switch 314
- Logic Triac (All See Triac)
 - 82, 169

— M —

- McMurray Inverter 286, 288
- McMurray-Bedford Inverter 287, 289
- Morgan Chopper 316, 318
- Motor Control 192, 216, 244, 248, 262, 263, 265, 296, 307, 313, 321, 326, 337, 338
- Starter 194, 210
- Mounting Hockey Puks 92

— N —

- Noise 300, 479

— O —

- Off-State Voltage Test 409
- Oil-Immersed Cooling 403, 406
- On-State Voltage 125, 411
- Optical
 - Coupling 143, 478
 - Isolation 277
- Overload Current 388, 389

— P —

- PACE/pak 95, 250
- Parameter Trade-Off 79
- Parallel
 - Inverter 283
 - SCRs 113
- Peak Let-Thru Current 371
- Phase Control 149
- Poly Phase, DC Bridge 238
- Power
 - Conversion 7, 149, 231
 - Dissipation 89
 - Module (See PACE/paks)
 - Supply, DC 295, 296
 - Switch 223
 - System, Aircraft 218
- Precautions, DC Bridge 243
- Protection
 - Fuses 367
 - Inverse Voltage 167
 - Junction Temperature 384
- Pulse
 - Burst Modulation 161, 208
 - Local Energy Storage 475
 - Picket Fence 474
 - Rate Modulation 316
 - Sharpener 140
 - Short Gate 471
 - Train Triggering 52, 141
 - Transformer 139

— R —

- Radiation Cooling 393
- Random Noise Generator 300
- RC Snubber 165, 347
- Recovered Charge 135, 138, 484
- Recovery
 - Characteristics, Test 350
 - Current 484, 486
 - Losses 356, 484, 487
- Rectifier
 - Fast Recovery 10, 345
 - Free-Wheeling 10, 314, 345, 347
 - Soft Recovery 10
- Rectangular Wave Form 40
- Regenerative Braking 257
- Regulator, Ferroresonant 182, 185 186, 187, 189, 190, 191

Resistance
 Modulator 325
 Welder 197
Resistive Load, DC Bridge 231
Reverse Recovery Time 106, 350,
 355
RFI, Control 207
Ripple 242
RMS Valve 37, 168
Rotating Fixtures 396

— S —

Saturating Transformer 185
SCR (Also See Specific Items) 27
 ACE-type 12
 Free-Wheeling Diode 349
 Geometry 79
 Operation 28
 Vs Triac 163
Sequential Switching 322
Series
 Inverter 284
 SCRs 131
 Triggering 139
Schottky Diode 359
Shoot-Through 270
Short Circuit Protection 368
Silicon Controlled Rectifier
 (See SCR)
Six Phase Double Y Rectifier
 Circuit 240
Slave Triggering 143
Snubber 104, 165, 209, 319
Soft
 Commutation 349
 Recovery 10
Solid-State Contactor 210, 215
Solid-State Relays 203, 208
Solid-State Switches 203, 213
Squirrel Cage Motor 162
State of the Art 5
Static Characteristics 32
Step-up Chopper 327
Switch, AC
 Aircraft 149, 223
 Load 314
Switching
 Losses 71

Switching (con't.)

 Principles 313

 Symbols 489

— T —

Tap changer 183
Temperature
 Dependent 34
 Rise 45
Terms 471
Test 409
 Circuits
 Blocking Voltage 410
 Critical di/dt 449
 Critical dv/dt 443, 446
 Gate Characteristics 414
 Holding Current 418, 420
 Inverter SCR 12
 Latching Current 424, 425
 Off-State Voltage 410
 On-State Voltage 412
 Thermal Resistance 450, 454,
 456, 458, 460
 Triacs 462
 Triggering 415
 Turn-Off Time 432, 433,
 435, 437, 439, 440
 Turn-On Time 429
 Turn-On Voltage 429
 Precautions 411, 412
 Thermal Resistance 45, 46, 397
 399, 400, 450
 Time-Ratio Control 347, 349
 Toroidal Transformer 123
 t_q -Improvement 18
 Transformer Load Switch 314
 Triacs 82, 163, 169, 195, 249, 250
 Testing 453
 Vs SCRs 163
 Triggering
 Characteristics 414, 471
 Circuits 55, 56, 119, 121, 122,
 139, 140, 141, 142, 143,
 144, 145, 173, 174, 175,
 464, 466, 468, 471, 478
 Local Energy Storage 475
 Noise 479
 Opto-Coupled 478

- Triggering (con't.)
 - Pulses 243, 471, 473, 474
- Turn-Off Time 68
 - Test Circuit 429
- Triacs 85
- Turn-On
 - Power Loss 58, 487
- Turn-On (con't.)
 - Sensitivity 114
 - Time 428
 - Voltage 428
- Two Phase Chopper 323
 - U —
- UJT Gate Circuit 303, 305
 - V —
- Variable Motor Drive 307
- Variable Counter 275, 276
- Vehicle Electric 295, 296, 320, 337
- Voltage
 - Blocking 409
- Voltage (con't.)
 - Finger 123, 124
 - Off-State 409
 - On-State 125, 411
 - Rating 36
 - W —
- Waveforms, Analyzing 40
- Welding Rating Curves 195, 197, 198, 199
- Wound Rotor Induction Motor 337
 - Z —
- Zero Voltage Control 169, 171, 207